Università degli Studi di Napoli Federico II
Facoltà di Ingegneria

Dottorato di Ricerca XX ciclo in Ingegneria dei Sistemi Idraulici, di Trasporto e Territoriali

A procedure to store and access the stratigraphy of non – cohesive deposits and its validation with laboratory and field data.

RELATORE
Prof. Giacomo Rasulo

CORRELATORE
Prof. Gary Parker

CANDIDATA
Enrica Viparelli

CONTRORELATORE
Prof. Guelfo Pulci Doria

COORDINATORE
Prof. Bruno Montella

INDEX

1 DYNAMIC EQUILIBRIUM

Features of rivers are the result of complex phenomena characterized by the mutual interaction of numerous parameters. Some of them such as climate, geology and vegetation are independent from the channel itself and are related to the regional environment only, others are also related to the movement of water and sediment in the channel network. In the present work the former group of parameters will be named ‘Environmental’ and the latter ‘Hydraulic’.

Hydraulic parameters can be divided in two groups:

- parameters whose values directly depend the environment: water discharge, sediment supply and grain size distribution of the alluvial material;
- parameters that are essentially functions of the action by or within the channel and that are only indirectly dependent on the environment: channel slope, water depth, friction coefficient, channel width and flow velocity.

It has been observed that equations expressing average relations among hydraulic parameters in stable irrigation channels are similar to those describing the average geometry of a river system. These relations generally express channel width, water depth and mean velocity of the flow as a power law of the effective water discharge. The effective water discharge is, generally, a pick flow whose recurrence interval depends on the climate and on the characteristic of the river. Even if graphs of width, depth and velocity for canals usually show a smaller scatter than those for rivers, the similar behaviour suggests that some natural river channels adjusted themselves to a stable or equilibrium form to the available discharge and to the character and quantity of the sediment supplied.

In the equilibrium state the sediment is moving and it implies both the adjustability of the channel to changes in independent variables and a stability in form and longitudinal profile. If we assume that just one hydraulic parameter varies, the others can change in two different directions:

- they tend to carry the varied parameter back to its original value. This behaviour is typical of a condition of equilibrium where all the hydraulic parameters oscillate around a mean value, that can be considered constant in time for practical purposes;
- they change in order to reach a condition of equilibrium in a longer time. This behaviour is typical of fluvial reaches that are not in equilibrium or that were

in equilibrium but, for an imposed change in flow regime, they tend to a different condition of equilibrium.

The concept of stability in form and profile is a delicate aspect of the problem because the unit of time plays an important role. Channel scour and fill are short – lived changes whose can happen in rivers in equilibrium. They refer to bed cutting and sedimentation during relatively short periods of time - from minutes to seasons. Aggradation and degradation, on the contrary, are terms that apply to persistent changes in mean bed elevation and they involve periods of time measured in years and decades (Leopold et al., 1964). In a river that reached conditions of equilibrium short – time scale phenomena such as scour and fill may happen but, on a reasonably long period of time, nor net erosion nor deposition can be observed or, in other words, the average bed elevation does not change.

From its headwater to its mouth a river can be described as a system in which potential energy, provided by quantities of water at a given elevation is converted in kinetic energy of flowing water (Leopold et al., 1964). This kinetic energy is dissipated in mechanical work to win resistance at the boundaries and to carry the sediment supplied from upstream. If the available energy is insufficient, part of the load is deposited and the channel slope increases (aggradation). On the contrary, when there is an excess of energy the flow erodes material from the bank and the bed and the channel slope decreases: the bed degrades. In a river in equilibrium the available kinetic energy is equal to the required mechanical work to win the friction and to carry the load contributed from upstream. According to the introduced energetic approach a classification of rivers in equilibrium can be proposed (C. Viparelli, 1972):

- rivers that reached equilibrium after a phase of aggradation;
- rivers that reached equilibrium after a phase of degradation.

Consequently rivers that are not in equilibrium can be classified as:

- rivers whose bed is aggrading;
- rivers whose bed is degrading.

In a river that reached equilibrium after a phase of aggradation the bed material is generally coarser than that characterizing reaches that reached equilibrium after degradation. At low and medium flow, the cross section is not properly incised in the

alluvial valley: the flow erodes and deposits material form bed and banks and so the mainstem continuously migrates in the floodplain. There are reaches where the valley is wide enough and the mainstem stays in a narrower area, generally close to a bank, called active – bed and the rest of the valley is not inundated even during high flows. Some of these configurations are quite stable but in other reaches after a major flood the active bed migrates to the other bank and the old mainstem is filled up with sediment.

Based on the valley width a river that reached equilibrium after a phase of aggradation can be divided in narrow and wide reaches:

- in a narrow reach hydraulic parameters even during frequent floods are affected by valley width. Channel slopes are generally smaller than in wide reaches;
- in a wide reach hydraulic parameters, even during major flood are independent from the valley width. In these reaches the active bed is narrower than the valley even at the pick of a major flood. During a flood the active bed may not coincide with the pre – flood bed because the flow incises one or more canals in the gravel following the direction it had upstream. After the flood these canals are at least partially filled up with sediment.

During floods, either in narrow or in wide reaches, the flow incises one or more canals in the alluvial valley. The number of canals increases with the active – bed width and with the channel slope. On the other hand, as the number of canals increases the transport capacity of the reach decreases. Therefore the value of hydraulic parameters and the number of incised canals are interrelated variables that varies from a reach to the other in order to carry the load contributed from the basin upstream. The prediction of the number of canals that a flood incises in the gravel bed and consequently the calculation of hydraulic parameters is still a matter of debate because the physics of the problem is not completely clear and so relations between the hydraulic parameters have not been derived yet.

A perusal of the literature on the subject shows that several criteria have been proposed to distinguish reaches where the discharge flows in a single channel from reaches where it flows in multiple channels. Very few indications have been given to compute the number of canals that a flood incises in the alluvial valley.

In rivers that reached equilibrium after a phase of aggradation the effective discharge is a pick flood with a recurrence interval exceeding 10 – 20 years and

morphodynamic processes depend on bedload only. The action of the suspended load is negligible because fine material is carried downstream with almost no interaction with the boundaries (Trush et a., 2000).

In rivers that reached equilibrium after a phase of degradation the cross section is well incised in the valley bed made of sand, silt and clay. For these rivers it is possible to define a bankfull discharge that controls the river morphology. Lower discharges are too small to cause significant changes in channel slope and higher discharges inundate the floodplain. In the inundated areas flow velocities and water depths are too low to move sediment and the fine particles in suspension deposit promoting riparian vegetation regeneration and growth.
In these reaches, that are not object of the present study, the bankfull discharge is a pick flow with a recurrence interval of 1 – 5 years and morphodynamic processes depend either on bedload and suspended load (Trush et a., 2000).

Conditions of equilibrium in a river can not be easily predicted because they depend on several parameters that varies from a basin to the other and it is fairly impossible to study the effect of each single parameter (C. Viparelli, 1972). Important tools to predict conditions of equilibrium in a river and how they depend on different parameters are models of river morphodynamics, based on known equations to compute flow parameters, sediment transport and bed evolution in space and time (Wrigth et al., 2005 and Bloom et al., 2006a). All the models mentioned in this Chapter are based on the following assumption: "in a reach, where the effective discharge flows in N channels, the active bed width B is equal to the sum of the N active bed widths b_i and the reach can be modelled as if the discharge flows in a single channel whose active bed width is equal to B".
The eight hydraulic parameters are interrelated and involved in the downstream changes in river slope and channel forms. Three of them depend on the environment and they have to be determined with specialized studies. To determine the other five parameters a closure relation is generally necessary because there are less equations than unknowns, therefore at least a closure relation is necessary to solve the problem. All the models mentioned in the present thesis are based on the following equations:

- mass conservation for water;
- momentum conservation for water;

- load relation (see Chapter 2).

Some models neglect the heterogeneity of the bed material, others consider the sediment as a mixture of different grain sizes. The former are based on the assumption that sediment transport, deposition and erosion can be described referring to a characteristic diameter of the bed material that can be a central parameter of the grain size distribution of the bed surface or of the substrate or it can also be a coarse diameter of the substrate (D_{84} or D_{90}) to approximate the median diameter of the coarser surface layer. The latter are more complex because the interaction between bed and bedload has to be considered and sediment transport, erosion and deposition have to be computed with a grain size based formulation.

To describe the interaction between bed and bedload the active layer approximation is introduced and the bed is divided in two regions, the substrate, whose particles can not be entrained into bedload, and the active or surface layer, whose grain size distribution may vary in the streamwise direction and in time and it is generally coarser than the substrate. The bedload transport rate and its grain size distribution are usually computed as a function of the grain size distribution of the surface layer and a grain size based equation of sediment conservation is implemented.

The first model that is described was defined in 1972 in the elaboration of the "Piano Regolatore Generale delle Acque per la Regione Basilicata" (C. Viparelli, 1972). Its unique feature is that hydraulic parameters are computed with different procedures in narrow and wide reaches. In all the other numerical models mentioned in the present Chapter there is no distinction between narrow and wide reaches in rivers that reached equilibrium after a phase of aggradation. Equations are: mass and momentum conservation for water, Manning – Strickler resistance relation, a 'modelling equation' and a load relation for narrow reaches. The normal flow approximation is introduced to compute water depth and the sediment is modelled as uniform and is characterized by the D_{90} of the substrate grain size distribution.

The modelling equation is necessary to close the problem. Its numerical expression does not have general validity because was derived from field data but its structure can be considered of general validity:

$$K = \frac{B}{\sqrt{Q}} = K(p, D_{90}) \tag{1}$$

where Q is the water discharge, p is the ratio between the sediment transport rate and the water discharge ($p = G_s/\gamma Q$, where γ is the specific weight of water) and D_{90} is the diameter of the substrate such that the 90% of the sediment is finer.

Input parameters in the 1972 model are:

- water discharge, equal to the pick flood with a 20 year recurrence interval;
- D_{90} of the bed material;
- channel slope;
- channel width for narrow reaches.

In narrow reaches water depths and flow velocities are computed with equations of momentum and mass balance for water and the sediment transport rate is evaluated with the load relation of Meyer – Peter and Muller. Assuming that the sediment transport rate in narrow reaches in equilibrium is equal to the sediment transport rate in neighbour wide reaches (either upstream or downstream) in equilibrium, the unknowns in wide reaches are flow velocities, water depths, active bed widths and flow resistance. These parameters can be determined with mass and momentum conservation for water, equation (1) and the Manning – Strickler resistance relation.

More recent models have been derived to describe rivers that are not in equilibrium or that tend to a different condition of equilibrium for imposed changes in flow regime. Assuming that sediment transport rates are always much smaller than water discharges so that the quasi – steady approximation holds, water depth is computed either with a uniform flow or with a backwater formulation and an equation of mass conservation for sediment has been introduced to describe the variation of the longitudinal profile (see Chapter 3). The closure relation in these models is necessary to evaluate the shear stress.

In 1978 Parker proposed the following relation at bankfull or effective flow:

$$\begin{aligned} \tau_b^* &= 0.049 \quad \text{in gravel – bed rivers} \\ \tau_b^* &= 1.86 \quad \text{in sand – bed rivers} \end{aligned} \tag{2}$$

Example of models where this relation was implemented are those of Parker to predict the condition of equilibrium of a river reach (Parker, 2004) and to describe the evolution of the Wax Lake delta (Parker et al., 2006)

In other models the shear stress is evaluated as a function of flow parameters (see Chapter 3). Example of these models for uniform sediment are those of Parker (Parker et al., 1998) to describe alluvial fans formed by channelized fluvial and sheet

flow or to describe the evolution of a gravel bed river for an imposed hydrograph (Parker 2004 and see Chapter 7), Cantelli (Cantelli et al., 2007) to describe the evolution of channels created by dam removal, Wong (Wong et al., 2007) to describe the dispersion of tracer stones under lower – regime plane bed equilibrium bedload transport. Models for sediment mixtures that compute the shear stress a function of flow parameters are those of Parker (1991 a and b), Hoey and Ferguson (1994) and Wright and Parker (2005 a and b) for downstream fining, Bloom (2006a) for vertical sorting in bed - form dominated rivers and the series of DREAM models on dam removal (Cui et al., 2006). The mentioned models for sediment mixtures can properly work for the case of simple aggradation or degradation in a substrate with no vertical stratigraphy, as discussed in Chapter 3.

Input parameters for the mentioned numerical models are water discharge, sediment yield contributed from the basin, active bed width, channel slope and a characteristic diameter of the bed material, when sediment is considered uniform, or the grain size distributions of bed surface, substrate and sediment yield for sediment mixtures. These parameters can be easily evaluated for a laboratory flume but for a river system their estimate is not trivial because they strictly depend on environmental parameters and their physical meaning is still a matter of debate. Their order of magnitude can be sometimes predicted with highly specialized studies or field campaigns, that are very expensive and so these data are generally unavailable when practical problems have to be solved.

A rough evaluation of the sediment yield averaged on a reasonably long period of time (decades) in a river reach in equilibrium can be done computing the transport capacity of the reach as a function of the effective discharge and the channel slope with a load relations. In that reach there is nor net erosion nor deposition and so, on a reasonably long period of time, the flow transports downstream all the sediment contributed from the basin. In the 1972 model for narrow reaches the sediment yield is computed with this system. The main limitation of the proposed procedure is that the majority of the load relations have a very limited applicability because they are derived from sets of field or laboratory data and so they can hardly be generalized to face with a different problem. Moreover, many laboratory experiments represent conditions of sediment transport in narrow reaches because the flow occupies the whole cross section and consequently the derived relations can not be applied to wide

reaches that reached equilibrium after a phase of aggradation. The evaluation of hydraulic parameters in these wide reaches is extremely important in mountainous regions like Southern Italy where plains are narrow and small and the economic activities must develop close to rivers where the active bed is narrower than the valley.

The definition of the grain size distribution of bed material in a river that reached equilibrium after a phase of aggradation is another basic problem in modeling alluvial rivers because it varies in the vertical, in the streamwise direction and also in the cross section if the mainstem is free to migrate in the alluvial valley. When sediment is modeled as a mixture of different grain sizes the uncertainty on input parameters increases because grain size distributions of substrate, surface and bedload for the effective discharge have to be specified. Grain size distributions of surface layers and bedload vary with the discharge and they can not be measured at effective flows because it is fairly impossible to access the active bed during floods.

All the uncertainties described above for the definition of input parameters for morphodynamic models made these tools too complex to solve practical problems but they are still extremely useful to study the mutual interaction of hydraulic parameters to have a description of the effect that an imposed change in flow conditions may have on alluvial rivers. In other words, these tools give a necessary description of the evolution of a river system.

In the present thesis a procedure to store and access the vertical stratigraphy of non cohesive deposits is described and its validation against laboratory data is presented. Stratigraphy is stored in a grid whose number of rows and columns are user specified parameters, therefore the described procedure can be employed to describe problems with different time and spatial scales. The above mentioned procedure was implemented in a novel version of a numerical model of a water – feed flume, whose original version for uniform sediment was derived by Parker in 2003.

Flume experiments were performed in the Hydrosystems Laboratory at the University of Illinois at Urbana – Champaign to compare measured longitudinal profiles, water depths, sediment transport rates and grain size distribution of the bedload, the bed surface and the substrate with numerical results. In order to test the procedure to store and access the stratigraphy a new version of the bedload relation of Ashida and Michiue (1972) was derived to fit the data.

In the last Chapter of the thesis the presented procedure was applied to a large scale problem to reproduce the variation in grain size distribution of the surface layer on the Trinity River in Northern California after the closure of a system of dams. This application shows that the presented procedure, tested against laboratory data and implemented in a laboratory scale model, can be also implemented in tools with much larger spatial and temporal scales to describe the evolution of a river system for an imposed change in flow regime.

2 LOAD RELATIONS

Bedload relations for uniform material generally compute sediment transport rates as a function of flow parameters, such as the mean flow velocity and the shear stress. Many bedload relations have a limited applicability because they empirically relate the Einstein parameter q_b^*, a non – dimensional bedload transport rate per unit width, with the Shields parameter τ_b^*, that is a non – dimensional shear stress. Their general form for uniform material is:

$$q_b^* = fn(\tau_b^*) \tag{3}$$

$$q_b^* = fn(\tau_b^* - \tau_c^*) \tag{4}$$

Relation expressed in the form of equation (4) computes the bedload transport rate as a function of the excess of shear stress above a critical value that can be defined either to fit the data or to define a lower limit for significant transport (Parker, 2004 and Montuori, 1997).

When sediment is modeled as a mixture of different grain sizes, the interaction between bed and bedload has to be considered. Even if it has been shown that this process has a stochastic nature (Wong et al., 2007) because the probability for a particle to be entrained into bedload decreases when its depth in the bed or its diameter increases, the probabilistic formulation can not yet be implemented (Parker et al., 2000) and the active layer approximation, proposed by Hirano in 1971, has to be introduced. The active or surface layer is a thin region in the upper part of the bed where sediment grains have an equal and finite probability in time to be entrained into bedload and the grain size distribution, that is generally coarser than the substrate does not vary in the vertical direction. The substrate is the whole bed under the active layer where sediment particles have a vertical structure and their probability to be entrained into bedload is zero. Bed material is divided in M classes characterized by a diameter D_i and the bedload transport rate in each class, q_{bi}, is computed. The total bedload transport rate q_{bT} is defined as

$$q_{bT} = \sum_{i=1}^{M} q_{bi} \tag{5}$$

and the fraction of bedload material in each grain size range is computer as

$$p_i = \frac{q_{bi}}{q_{bT}} \tag{6}$$

For each grain size range a Shields and an Einstein parameters can be defined and a functional relation like equation (3) or (4)is assumed:

$$\tau_{bi}^{*} = \frac{\tau_b}{\rho R g D_i} \tag{7}$$

$$q_{bi}^{*} = \frac{q_{bi}}{\sqrt{RgD_i} \cdot D_i \cdot F_i} \tag{8}$$

$$q_{bi}^{*} = f\left(\tau_i^{*}\right) \quad ; \quad q_{bi}^{*} = f\left(\tau_i^{*} - \tau_{ci}^{*}\right) \tag{3)(4}$$

where F_i represents the fraction of material of the surface layer in the i-th grain size range. Combining equations (3) or (4) and (8) a surface – based bedload relation is defined because it is assumed that a size range that is not in the surface layer can not be transported as bedload.

The critical value of the Shields number is computed with particular functions – hiding/exposure functions - that consider the different mobility of coarse and fine particles. Finer surface grains protrude less into the flow than coarser particles, that protect their small neighbors. As a result, finer surface grains are less mobile when they are in a mixture then when they are surrounded by particles of similar size. The isolated protrusion offered by coarser surface grains in a mixture increases their mobility compared to a uniform sediment of the coarse size in question. This phenomenon is named ‘microscopic hiding’ and it reduces the difference in mobility between coarser and finer surface grains (Parker et al., 1982b).

Streams with mostly gravel or coarser material are usually characterized by a thin surface layer that is often coarser than the substrate. This layer is generally named ‘pavement’ because it differs from the static armor, made of particles that never move. At low and medium flow in a gravel – bed stream the pavement is visible and during floods the bed is mobilized and all or nearly all sizes are often found in motion.

In gravel – bed streams, even during flood events, the bed shear stress often exceeds its critical value to mobilize the pavement only moderately and even during unusually severe floods it is rarely more than two or three times that critical value. At such low

ambient shear stress, motion becomes sporadic and even though grains of all sizes are in motion, only a small fraction of surface grains of a given size move and the vast majority of surface grains stay in place as pavement. Pavement can be therefore considered as a regulator that enables streams to transport the coarse half and the fine half of its bedload supply at equal rates. Coarser grains, that are less mobile, are concentrated in relatively larger quantities in the pavement and they are directly exposed to the flow so that the increased availability for motion can balance the smaller mobility of coarser particles. This fact and the typically poor sorted bed material are associated with the absence of dunes.

The definition of the pavement as a buffer between the flow and the subpavement, which is the bulk of material temporarily stored in a reach (Parker et al., 1982a), is the results of laboratory experiments designed to model two gravel rivers: the Oak Creek in Oregon and the Elbow River in Canada. Two hypothesis have been proposed to describe this behavior:

- pavement is washed out during floods and it reforms when the flow wanes;
- pavement is present even during floods but its structure differs a little from that at low flow.

and the experiments showed that the latter hypothesis is more realistic because during transport events pavement formed readily and could be maintained indefinitely under constant flows, even though all the grain sizes were represented in the bedload. In other words, pavement is a mobile bed phenomenon.

To explain the reason for pavement and to show why it provides a structural mechanism to regulate the different mobility of finer and coarser grains, a formal definition of relative mobility is necessary. Lets consider two different uniform materials A and B subjected to the same shear stress and that move solely as bedload. These materials are characterized by the diameters D_A and D_B and are transported at the volumetric rates q_{BA} and q_{BB}. The relative mobility of the material A with respect to the material B can be defined considering the ratio r_{AB}:

$$r_{AB} = \frac{q_{bA}}{q_{bB}} \tag{9}$$

if r_{AB} is smaller than 1, the material B is more mobile than material A.

Finer grains are generally more mobile than coarser grains of the same specific gravity. This simple observation can be formally defined as follows: finer grains are

more mobile than coarser grains if and only if $r_{AB} > 1$ when $D_A/D_B < 1$ or when $\tau_{bA}^*/\tau_{bB}^* > 1$. Considering that bedload transport rates can be computed with equations (4) and that the transport rate increases monotonically with the Shields parameter, for the range of stresses typical of gravel bed streams, uniform coarser material is significantly less mobile than uniform fine material at the same shear stress. For higher values of the Shields parameter the excess of shear stress becomes almost independent from the diameter. equal mobility is attained.

The concept of relative mobility of different grain sizes can be generalized to mixtures of different grain sizes in terms of bedload rate per fraction of material either in the pavement or in the substrate. The relative mobility r_{ij} of grain size D_i in comparison with grain size D_j can be defined as:

$$r_{ij} = \frac{q_{bi}}{fi} \cdot \frac{f_j}{q_{bj}} \tag{10}$$

where the fraction of material in the i - th and in the j – th size ranges can be referred either to the pavement or the substrate. If $r_{ij} > 1$, grain size D_i is more mobile than grain size D_j.

A less formal definition of relative mobility for sediment mixtures has its origin in the work of Egiazaroff (1965) and it is based on the critical value of the shear stress in equation (4). A grain size D_i is more mobile than grain size D_j if it has a lower critical bed shear stress. However, critical stresses are very difficult to estimate and they are usually substituted with a reference stresses defined such that at this stress the ratio q_{bi}/f_i takes the same value for all the grain sizes. All grain sizes are of equal mobility if the reference shear stress is constant.

The analysis of the laboratory experiments mentioned above showed that pavement and substrate size ranges are not mutually exclusive because they are parts of the gravel and sand stored in the bed of the stream. Pavement is a thin surface layer and the substrate represents the material stored in the bed, which is the supply for the bedload. Thus the bedload and the substrate should approximately have the same grain size distribution.

If a reach is in equilibrium, the coarse half of the bedload should be transported through the reach at the same rate as the fine half and this condition has to be satisfied even though finer grains are easier to mobilize. In a gravel bed stream the coarse pavement regulates the availability of substrate grains to the bedload: even if the coarser half of the substrate is more difficult to move than the fine half. In order to

maintain equilibrium, the surface layer must inevitably coarsen into a pavement until the increased availability counteracts the lower mobility of coarser grains, leading to a net equalization of mobility with an effect called 'macroscopic hiding'.

In the following paragraphs three load relations defined either for uniform sediment or mixtures are described: the relation of Ashida and Michiue (1972), that will be discussed in Chapter 5 and a new version is presented, the relation of Parker (1990) and that of Wilcock and Crowe (2003), characterized by hiding functions with an expression different from the classic relation proposed by Egiazaroff in 1965. These load relations and the new version of the load relation of Ashida and Michiue that is presented in Chapter 5, are implemented in the numerical model described in Chapter 3 and validated in Chapter 5.

2.1 RELATION OF ASHIDA AND MICHIUE (1972)

The bedload relation of Ashida and Michiue was determined from laboratory data for sand and small gravel.

For uniform sediment it expression is:

$$q_{bT}^{*} = 17\left(\tau_b^{*} - 0.05\right)\left(\sqrt{\tau_b^{*}} - \sqrt{0.05}\right) \tag{11}$$

The Shields parameter in the original model was a function of the arithmetic mean diameter of the substrate. In the surface based version due to Parker (Parker, 2004) it depends on the geometric mean diameter of the surface layer.

For gravel mixture the relation has the same structure of equation (4) and the surface grain size distributions measured at equilibrium was used to compute q_{bi} from equation (8):

$$q_{bi}^{*} = 17\left(\tau_i^{*} - \tau_{ci}^{*}\right)\left(\sqrt{\tau_i^{*}} - \sqrt{\tau_{ci}^{*}}\right) \tag{12}$$

In the surface based version the critical value of the Shields parameter for each grain size range is evaluated with the following hiding function:

$$\frac{\tau_{ci}^{*}}{\tau_{scg}^{*}} = \begin{cases} 0.834 \cdot \left(\dfrac{D_i}{D_{sg}}\right)^{-1} & for\ \dfrac{D_i}{D_{sg}} \le 0.4 \\ \left[\dfrac{log(19)}{log\left(19\dfrac{D_i}{D_{sg}}\right)}\right]^{2} & for\ \dfrac{D_i}{D_{sg}} > 0.4 \end{cases} \tag{13}$$

where D_{sg} is the geometric mean diameter of the grain size distribution of the surface layer and τ_{scg} is the critical Shields number for the surface geometric mean diameter equal to 0.05. In the 1972 version the model referred to the arithmetic mean diameter and the grain size distribution of the substrate.

2.2 RELATION OF PARKER (1990)

The bedload relations of Parker was derived from field data from the Oak Creek, Oregon (Parker et al., 1982c and Parker, 1990). It has to be used only for computation of gavel bedload transport rate therefore the sand fraction has to be removed and the grain size distribution has to be renormalized to compute its geometric mean size.
The non – dimensional parameter to describe the bedload transport rate is not the Einstein number but the specific bedload transport rate W^* defined as

$$W^* = \frac{q_b^*}{\left(\tau_b^*\right)^{3/2}} \tag{14}$$

The total bedload volume transport rate is computed with the relation:

$$q_{bT} = \frac{u_{*b}^3}{Rg} \cdot W^* \tag{15}$$

For uniform material the specific bedload transport rate W^* is

$$W^* = 0.00218 \cdot G(\phi) \tag{16}$$

where G is the hiding function defined as

$$G(\phi) = \begin{cases} 5475\left(1 - \dfrac{0.853}{\phi}\right)^{4.5} & if \quad \phi > 1.59 \\ exp\left[14.2(1-\phi) - 9.28(1-\phi)^2\right] & if \quad 1 \le \phi \le 1.59 \\ \phi^{14.2} & if \quad \phi < 1 \end{cases} \tag{17}$$

and ϕ is the parameter

$$\phi = \phi_{sgo} = \frac{\tau_{bg}^*}{\tau_{ssrg}^*} = \frac{\tau_{bg}^*}{0.0386} \tag{18}$$

where the subscript ‘g’ means that if sediment is considered uniform, it has to be characterized by the geometric mean diameter of the surface layer.
When sediment is modeled as a mixture of different grain sizes, the specific bedload transport rate of sediment in each grain size range is defined as

$$W_i^* = \frac{q_{bi}^*}{\left(\tau_{sbi}^*\right)^{1.5}} = \frac{Rgq_{bi}}{u_{*sb}^3 \cdot F_i} \tag{19}$$

and it can still be computed with equations (16) and (17) as a function of the parameter

$$\phi_i = \omega \cdot \phi_{sgo} \cdot \left(\frac{D_{si}}{D_{sg}}\right)^{-0.0951} \tag{20}$$

where ϕ_{sgo} is still defined by (18) and ω is a function of the grain size distribution geometric standard deviation σ_s

$$\omega = 1 + \frac{\sigma_s}{\sigma_o}\left[\omega_o - 1\right] \tag{21}$$

and σ_o and ω_o are the strain functions defined in Figure 1.

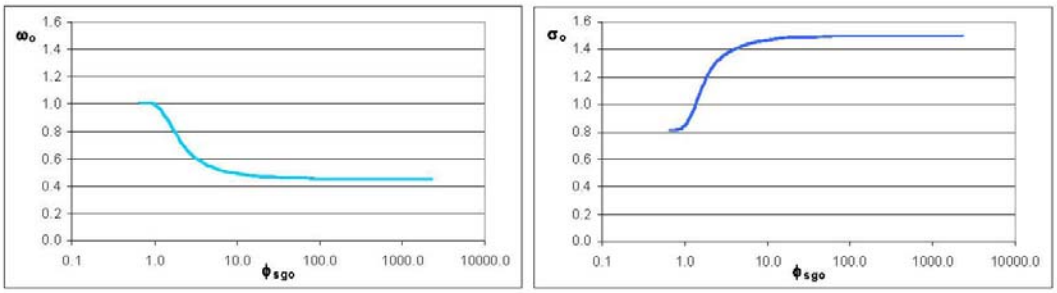

Figure 1 Strain functions for the bedload relation of Parker (1990)

The total bedload volume transport rate per unit width is evaluated as

$$q_{bT} = \sum_{i=1}^{M} q_{bi} = \frac{u_{*sb}^3}{Rg} \sum F_i \cdot W_i^* \tag{22}$$

2.3 RELATION OF WILCOCK AND CROWE (2003)

The bedload relation of Wilcock and Crowe can be used for gravel and sand-gravel mixtures. and it has been derived from laboratory experiments in a recirculating flume. As the above described relation of Parker the non dimensional parameter to express the sediment transport rate is the specific bedload transport rate W^*.

For uniform material the bedload relation of Wilcock and Crowe can be expressed as

$$W^* = G(\phi) \tag{23}$$

where the hiding function G is defined as

$$G(\phi)=\begin{cases} 0.002\cdot\phi^{7.5} & if \quad \phi<1.35 \\ 14\cdot\left(1-\dfrac{0.894}{\phi^{0.5}}\right)^{4.5} & if \quad \phi\geq 1.35 \end{cases} \tag{24}$$

and the parameter ϕ is still defined by equation (18) but the value of τ_{ssrg}^{*} is computed as

$$\tau_{ssrg}^{*}=0.021+0.015\cdot exp(-20\cdot Fs) \tag{25}$$

where Fs is the fraction of sand in the mixtures.

For sediment mixtures the specific bedload transport rate is still computed with (24) and (25) but the parameter ϕ has to be defined for each characteristic grain size:

$$\phi_i=\phi_{sgo}\left(\frac{D_{si}}{D_{sg}}\right)^{-b} \tag{26}$$

and

$$b=\frac{0.67}{1+exp\left(1.5-\dfrac{D_{si}}{D_{sg}}\right)} \tag{27}$$

3 NUMERICAL MODEL OF A WATER – FEED LABORATORY FLUME

The model is based on the physical principles of mass and momentum conservation for water and mass conservation for sediment but it is more straightforward than previous models because it is applied to a laboratory flume, an easier system than a river. Few assumptions and a closure relation for the shear stress are necessary to solve equations of mass balance for water and sediment and momentum balance for water. The assumptions are:

a) The flume has constant width B;
b) The flume is long enough so that entrance and exit regions can be neglected;
c) The flow in the flume is always subcritical;
d) The sediment is not cohesive and suspended load is considered negligible;
e) The volume transport rate of sediment is always much smaller than that of water
f) Lower regime plane bed.

The closure relation to evaluate the shear stress is

$$\tau = \rho \cdot C_f \cdot U^2 \tag{28}$$

where ρ is the water density, C_f is the friction coefficient and U is the mean flow velocity.

Hypothesis (e) and the closure relation (28) are necessary to introduce the quasi-steady approximation and to reduce mass and momentum balance for water to the classical backwater form. Hypothesis (c) is necessary to compute backwater curve. Hypothesis (a), (b), (d) (e) and (f) could be removed to address a more general case but they strongly help to simplify the problem.

In the present model the equation of mass conservation for sediment in each grain size range has been solved with the active layer approximation, whose thickness, L_a, in absence of small scale bedforms – hypothesis (f) - is defined as a linear function of D_{s90} , the grain size in the surface layer such that 90% of sediment is finer

$$L_a = n_a \cdot D_{s90} \tag{29}$$

where n_a is a user specified parameter that usually varies between 1 and 2 (Parker, 2004).

The substrate is the whole bed under the active layer where sediment particles have a vertical structure and their probability to be entrained into bedload is zero. Its grain size distribution varies in space and time when the bed aggrades or degrades: if the bed aggrades part of the active layer becomes new substrate and if the bed degrades the upper part of the substrate becomes active layer. The system of differential equations is solved with the finite difference method and the numerical scheme has a first order accuracy, that could be easily upgraded to second order accuracy.

3.1 BACKWATER EQUATION

The classical backwater equation can be written as

$$\frac{\partial H}{\partial x} = \frac{S - C_f \cdot Fr^2}{1 - Fr^2} \tag{30}$$

where H is the water depth, x is a streamwise coordinate, S is the channel slope, Fr is the Froude number and C_f is the friction coefficient evaluated with a Manning – Strickler resistance relation expressed as (Parker, 2004):

$$C_f^{-1/2} = \alpha_r \left(\frac{R_H}{k_s} \right)^{1/6} \qquad k_s = n_k \cdot D_{s90} \tag{31}$$

where R_H is the hydraulic radius k_s is the roughness height, α_r and n_k are two user specified parameters.

Different roughness between bed and walls in flumes causes the shear stresses on the bed to be higher than those computed with resistance relations commonly used and so the friction slope was evaluated with a slightly modified version of the procedure to remove wall effects from known data proposed by Vanoni and Brooks in 1957. The basic difference between the procedure implemented in the model and that to remove wall effects from measured data is that in the former water depth is unknown. Under the assumptions that

- - the cross section can be divided in two regions: the bed region and the wall region, as shown in Figure 2, where the flow velocity and the energy gradient are assumed to be the same;
- - the Darcy – Weisbach resistance relation can be applied to each region and to the entire cross section,

the friction coefficient for the whole cross section can be divided in two terms, one for the bed region C_{fb} and one for the wall region C_{fw}, as is normally done for a composite cross section (Vanoni, 1975).

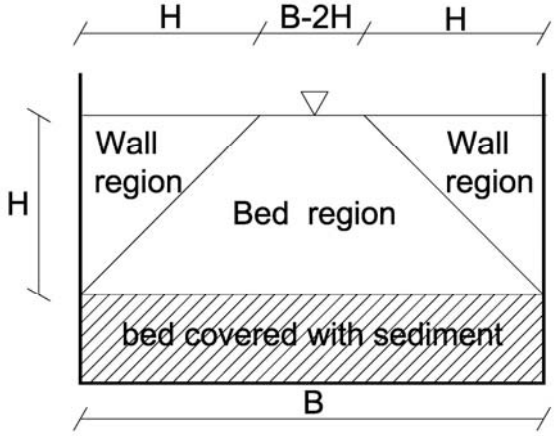

Figure 2 Division of the cross section to compute the shear stress on the bed

Momentum balance for water can be written as

$$\frac{\partial\left(U^2 HB\right)}{\partial x} = -\frac{1}{2} gB \frac{\partial H^2}{\partial x} + gBHS - \frac{1}{\rho}\left(\tau_b B + 2\tau_w H\right) \tag{32}$$

where subscript 'b' denotes the bed region and 'w' denotes the wall region. Substituting mass conservation equation for water, equation (32) can be reduced to backwater form:

$$\frac{\partial H}{\partial x} = \frac{\frac{\partial \eta}{\partial x} - \left(C_{f,b} + \frac{2H}{B} C_{f,w}\right) \cdot Fr^2}{1 - Fr^2} \tag{33}$$

where $C_{f,b}$ is the friction coefficient for the bed region and $C_{f,w}$ is for the wall region. The coefficient $C_{f,b}$ is still computed with the Manning – Strickler resistance relation substituting the hydraulic radius of the whole cross section with the hydraulic radius of the bed region. Considering that walls are generally much smoother than the bed, $C_{f,w}$ is iteratively evaluated with the relation of Nikuradse for smooth pipes:

$$\frac{1}{\sqrt{f_w}} = 0.86\, ln\left(Re_w \cdot \sqrt{f_w}\right) - 0.8 \tag{34}$$

where f_w is the Darcy – Weisbach friction coefficient ($f_w = 8\ C_{f,w}$), Re_w is the Reynolds number of the wall region defined as

$$Re_w = \frac{4UR_w}{\nu} \tag{35}$$

where U is the mean flow velocity, ν is the kinematic viscosity of water and R_w is the hydraulic radius of the wall region defined as ratio between the area of the wall region, A_p, and the wetted perimeter of the same region, χ_p:

$$R_w = \frac{A_w}{\chi_w} = 2\frac{H^2}{2}\cdot\frac{1}{2H} = \frac{H}{2} \tag{36}$$

The shear stress in the bed region can be easily computed because it is the only unknown in equation (72).

3.2 CONSERVATION OF MASS FOR BED SEDIMENT (EXNER EQUATION)

Exner equation expresses mass conservation of sediment. When suspended load is negligible – hypothesis (d) – there is no term for entrainment and deposition and its standard one – dimensional form is

$$\left(1-\lambda_p\right)\frac{\partial \eta}{\partial t} = -\frac{\partial q_{bT}}{\partial x} \tag{37}$$

where q_{bT} is the total bedload volume transport rate per unit width, λ_p is the sediment porosity and η is the bed elevation above a datum. When the bedload volume transport rate per unit width increases in the streamwise direction, the flow is eroding material from the bed and so the channel degrades. On the contrary, if the volume transport rate per unit width decreases, the flow is depositing material and the channel aggrades. The main problem in using the standard Exner equation is related to the evaluation of the total bedload volume transport rate per unit width because there are many empirical relations available but all of them have a limited applicability. (Wong, 2003).

3.3 LOAD RELATIONS

Load relations compute the total bedload transport rate as function of the shear stress, evaluated with equation (28). If wall effects can not be neglected the bedload transport rate is function of the shear stress in the bed region only, τ_b. The user can choose a bedload relation considering its particular problem. Load relations implemented in the numerical model are those of Ashida and Michiue (1972), Parker (1990), Wilcock and Crowe (2003) and the new version of the load relation of Ashida and Michiue described in Chapter 5.

3.4 GRAIN SIZE BASED EXNER EQUATION

When sediment is modeled as a mixture, the grain size distribution of the bed changes in space and time and the mass balance has to be verified for each grain size range. Mass conservation for bed material in each grain size range can be written as

$$\left(1-\lambda_p\right)\frac{\partial}{\partial t}\int_0^{\eta} f_i^{'}\,dz = -\frac{\partial q_{bi}}{\partial x};\ \sum_{i=1}^{M} f_i^{'} = 1 \tag{38}$$

where f'_i is the fraction of sediment in the i-th grain size range (Figure 3), q_{bi} is the volume bedload per unit width of sediment in the i-th grain size range and z is a coordinate in the vertical direction.

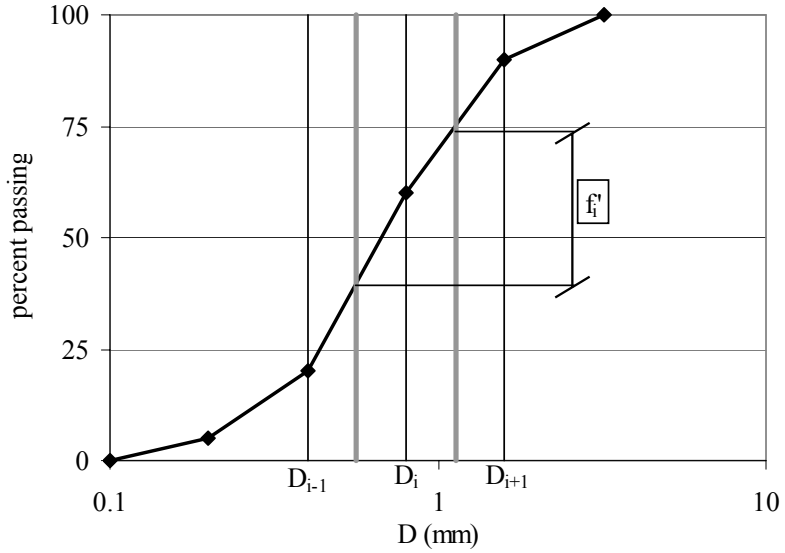

Figure 3 Description of $f_i^{'}$;

Equation (38) can not be immediately solved because f'_i varies in the vertical, in the streamwise direction and in time. According to the active layer approximation, f'_i can be written as (Parker et al., 2004)

$$f_i^{'}(x,z,t) = \begin{cases} F_i(x,t) & for \quad \eta - L_a < z \le \eta \\ f_i(x,z) & for \quad z \le \eta - L_a \end{cases} \tag{39}$$

where F_i is the fraction of material of active layer in the i-th grain size range – that does not vary in the vertical direction - and f_i is the fraction of material of the substrate in the same range – that does not vary in time – (Figure 4).

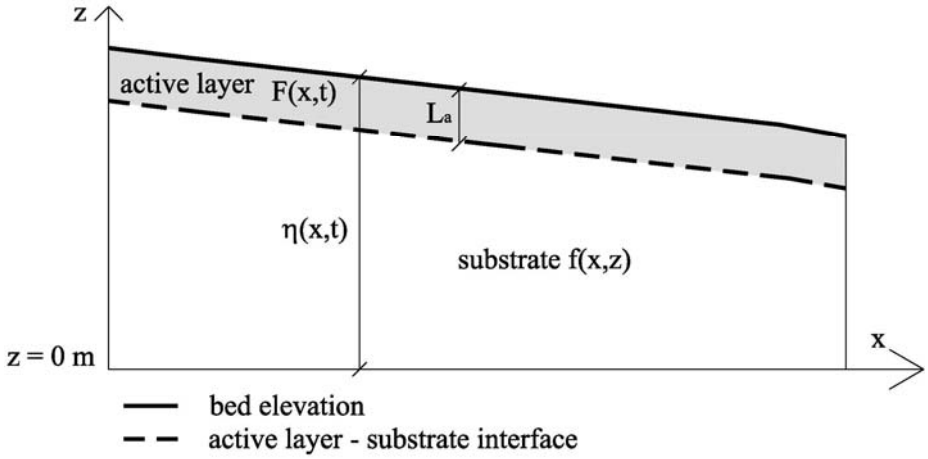

Figure 4 Grain size distribution in the active layer and in the substrate

Substituting (39) into (38) the time derivative can be written as sum of two terms: the first describes how the mass of sediment in the i-th grain size range changes in the upper part of the substrate while the bed aggrades or degrades and the second describes how it changes in the active layer:

$$\frac{\partial}{\partial t}\int_0^{\eta} f_i' \, dz = f_{li}\frac{\partial(\eta - L_a)}{\partial t} + \frac{\partial(F_i \cdot L_a)}{\partial t} \tag{40}$$

where f_{li} is f'_i at the active layer- substrate interface and describes how sediment is exchanged between the two regions and it is defined as (Hoey et al., 1994).

$$f_{li} = \begin{cases} f_i\big|_{z=\eta-L_a} & if \quad \dfrac{\partial \eta}{\partial t} < 0 \\ \alpha \cdot F_i + (1-\alpha)\cdot p_i & if \quad \dfrac{\partial \eta}{\partial t} > 0 \end{cases} \tag{41}$$

where p_i is the fraction of bedload in the i-th grain size range and α is a user specified parameter that varies between 0 and 1 and it describes how sediment is exchanged between bed and bedload. If α is equal to 1, the surface material is directly transferred to the substrate and so the difference between the coarser surface layer and the finer substrate, that characterize several gravel – bed streams, can not be reproduced. If α is equal to 0, bedload material is directly deposited in the substrate and the downstream fining, generally observed in gravel bed rivers, can not be modeled Therefore, when the bed aggrades, the material transferred from the active layer to the substrate should have a grain size distribution obtained averaging the grain size distributions of the active layer and of the bedload (Toro – Escobar et al., 1996).

If sediment transport rates and deposition are slow, the deposited material may be mixed in the surface layer before releasing the portion thicker than L_a to the substrate. In this hypothesis the material transferred to the substrate should have the same grain size distribution than the surface. On the contrary, under conditions of active transport the deposited bedload is directly transferred to the substrate and it is likely that the transferred material has a grain size distribution equal to the bedload (Parker, 1991 a). When the bed degrades the fraction of material in each grain size range at the active layer – substrate interface and in the upper layer of the substrate are the same. If the bed aggrades, the fraction of material in the i-th grain size range at the interface depends on how sediment is exchanged between bedload and active layer (Figure 5).

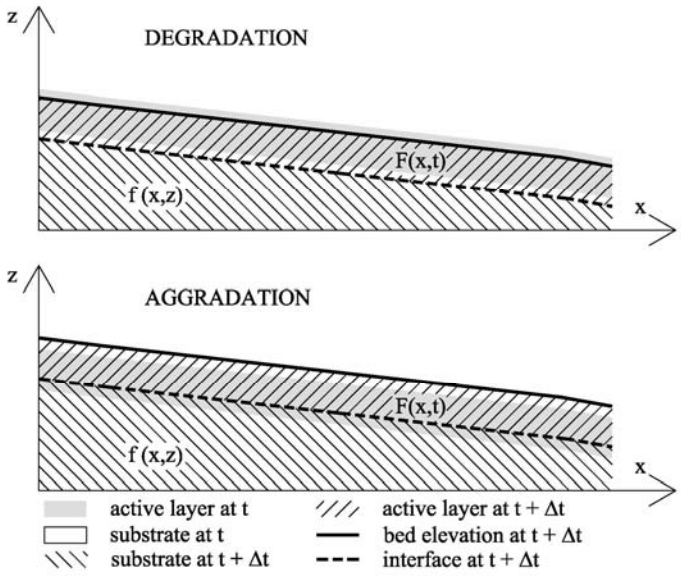

Figure 5 Grain size distribution at the interface changes when the bed aggrades or it degrades;

Substituting (40) and (37) in (38), the equation to describe the variation in time of the active layer grain size distribution is obtained:

$$\left(1-\lambda_p\right)\left[L_a\frac{\partial F_i}{\partial t}+\left(F_i-f_{li}\right)\frac{\partial L_a}{\partial t}\right]=-\frac{\partial\left(q_{bT}\cdot p_i\right)}{\partial x}+f_{li}\frac{\partial q_{bT}}{\partial x} \tag{42}$$

With equation (42) the problem is solved.

Water depth in the channel is computed with equation (30) or (33), then the bedload transport rate can be estimated with a load relation, the new bed profile is calculated with equation (37) and with equation (42) the active layer grain size distribution is updated everywhere. If we consider simple conditions of aggradation or degradation everywhere in the channel f_{li} can always be properly computed with (41). However when the flow builds and then it erodes a deposit, f_{li} can be properly computed only if the stratigraphy of the deposit is known.

3.5 PROCEDURE TO STORE AND ACCESS THE STRATIGRAPHY

The channel in the streamwise direction is divided in N_{node} nodes where water depth, bed elevation, active layer grain size distribution and bedload transport rate are computed.

When the bed aggrades at node j a layer will be deposited and its thickness can be evaluated as

$$\Delta\eta\big|_{j,t} = \eta\big|_{j,t} - \eta\big|_{j,t-\Delta t} \tag{43}$$

According to the active layer approximation, When the bed aggrades the lower part of the active layer becomes new substrate, as shown in Figure 5, and the new active layer–substrate interface elevation will be

$$\eta_{int}\big|_{j,t} = \left(\eta - L_a\right)\big|_{j,t} \tag{44}$$

Stratigraphy of deposits is stored in a grid with N_{node} vertical lines and a number of points on each vertical, N, that depends on the active layer – substrate interface elevation above a datum and on the row thickness, L_s, that is a user specified parameter. A simplified drawing of the grid is shown in Figure 6 where at point k the grain size distribution is characterized by the layer between point k-1 and point k.

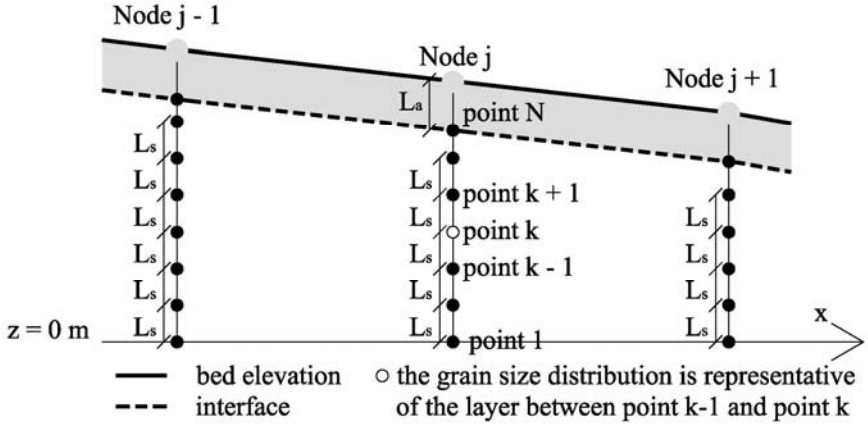

Figure 6 Grid to build the stratigraphy;

Having defined the initial longitudinal profile, the initial number of points for the node j will be computed as

$$N\big|_{j,0} = Int\left(\left.\frac{\eta - L_a}{L_s}\right|_{j,0}\right) + 2 \tag{45}$$

where Int is a function to round to the smaller integer because the lowest point will be on the datum and the highest will be on the active layer – substrate interface.
The elevation of the k-th point of the grid will be

$$z_k\big|_{j,0} = (k-1)\cdot L_s \tag{46}$$

During the computation the grid will be modified: new points might be added when the bed aggrades and some points might be removed when it degrades.

3.5.1 PROCEDURE FOR AGGRADATION

The grain size distribution changes only in the highest point of the old grid, located at the active layer – substrate interface. When the number of points in the vertical increases, the grain size distribution associated to the new points is computed with equation (41), as shown in Figure 7.

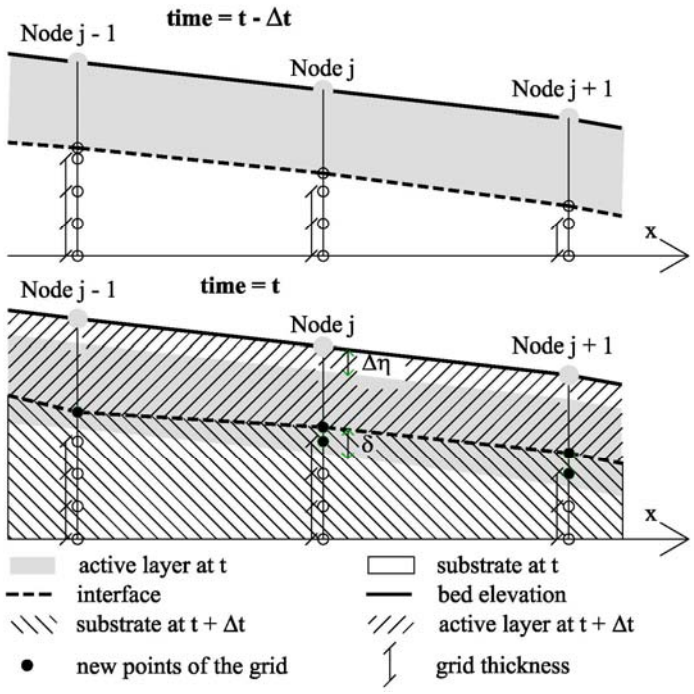

Figure 7 How the grid changes when the bed aggrades: blue points will be moved on the new interface. The number of points at nodes j and j+1 increases;

If the number of points at node j does not increase, it means that the new interface is in the same row of the grid than the interface computed at the previous time step

$$\eta_{int}\big|_{j,t} \le \left(N\big|_{j,t-\Delta t} - 1\right)\cdot L_s = \left(N\big|_{j,t} - 1\right)\cdot L_s \tag{47}$$

and so the highest point will have a new elevation

$$z_N\big|_{j,t} = \eta_{int}\big|_{j,t} \tag{48}$$

and a new associated grain size distribution computed as a weighted average on the deposit thickness with the equation

$$f_i\big|_{j,t,N} = \frac{\left\{f_i \cdot \left[\eta_{\text{int}} - (N-1)\cdot L_s\right]\right\}\big|_{j,t-\Delta t,N} + \left(\delta \cdot f_{li}\right)\big|_{j,t}}{\left[\eta_{\text{int}} - (N-1)\cdot L_s\right]_{j,t-\Delta t,N} + \delta\big|_{j,t}} \tag{49}$$

where f_{li} is computed with equation (41) and δ is the parameter

$$\delta\big|_{j,t} = \eta_{int}\big|_{j,t} - \eta_{int}\big|_{j,t-\Delta t} = \left(\eta - n_a \cdot D_{s,90}\right)\big|_{j,t} - \left(\eta - n_a \cdot D_{s,90}\right)\big|_{j,t-\Delta t} \tag{50}$$

that considers the variation in time of bed elevation and active layer thickness. In the present model the material transferred to the substrate has the same grain size distribution of the surface layer, therefore phenomena characterize by active transport can not be properly modeled.

When condition (47) is not verified the number of points in the vertical increases. The grain size distribution in the highest point of the old grid will be computed as

$$f_i\big|_{j,t,N} = \frac{\left\{f_i \cdot \left[\eta_{\text{int}} - (N-1)\cdot L_s\right]\right\}\big|_{j,t-\Delta t,N} + \left(N \cdot L_s - \eta_{\text{int}}\right)\big|_{j,t-\Delta t} \cdot f_{li}\big|_{j,t}}{\left[\eta_{\text{int}} - (N-1)\cdot L_s\right]_{j,t-\Delta t,N} + \left(N \cdot L_s - \eta_{\text{int}}\right)\big|_{j,t-\Delta t}} \tag{51}$$

where $N = N\big|_{j,t-\Delta t}$ and its new elevation will be $N\big|_{j,t-\Delta t} \cdot L_s$.

The new number of points on the vertical will be compute as

$$N\big|_{j,t} = Int\left(\frac{\eta - L_a}{L_s}\right)\Bigg|_{j,t} + 2 \tag{52}$$

and the highest point of the new grid will be the same elevation of the active layer – substrate interface.

3.5.2 PROCEDURE FOR DEGRADATION

When the flow erodes material from the bed, the substrate grain size distribution does not change and so the procedure to update the grid is much easier, as shown in Figure 8.

The point of the grid that satisfies the condition

$$z_k\big|_{j,t} \geq \eta_{int}\big|_{j,t} \tag{53}$$

has to be determined because, when k is known, the new number of points can be computed

$$N\big|_{j,t} = N\big|_{j,t-\Delta t} - \left(N\big|_{j,t-\Delta t} - k\right) \tag{54}$$

and the grain size distribution of the new highest point of the grid will be equal the same of the k-th node of the old grid.

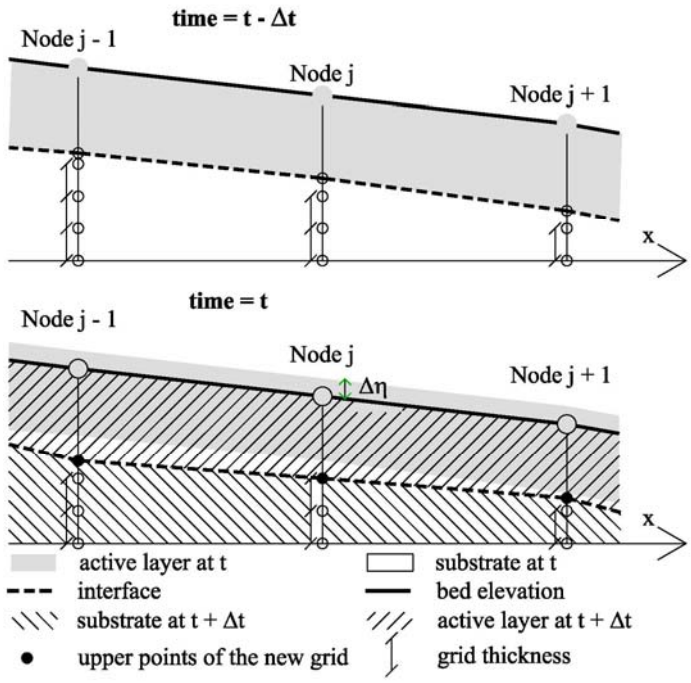

Figure 8 How the grid changes when the bed degrades

3.6 INITIAL AND BOUNDARY CONDITIONS

Bed elevation has to be given in each node to solve both Exner and the backwater equation (channel slope in each node). In the present model the initial longitudinal profile is computed as linear function of the average bed elevation and channel slope

$$\eta_j\big|_{t=0} = \overline{\eta}\big|_{t=0} + \left(x - \frac{L}{2}\right) \cdot S\big|_{t=0} \tag{55}$$

where x is the streamwise coordinate, L is the length of the flume and S is the slope. To solve equation (42) it is necessary to give the grain size distribution of active layer and substrate in each node, that is assumed to be the same for the whole flume length. Initial conditions can also be given reading the longitudinal profile and the grain size distributions of the bed at the end of a previous run, if the number of nodes in the streamwise direction does not change.

Backwater equation requires two boundary conditions: water discharge set by the pump (upstream boundary condition) and water level set by the tailgate (downstream

boundary condition). Downstream boundary condition is necessary because of hypothesis (c) – the flow is always Froude subcritical.

The boundary condition to solve the standard Exner equation (37) is the total bedload volume transport rate per unit width in the upstream ghost node (extra node at the upstream end of the flume where the sediment is feeded and neither water elevation nor bed elevation are computed). For a sediment – feed flume this is a user specified parameter while for a sediment recirculating flume the total bedload volume per unit width at the ghost node and at the downstream end of the channel is the same (cyclic boundary condition), if the amount of sediment stored in the recirculating line can be neglected.

The boundary condition for the grain size based equation of mass conservation for sediment (42) is the grain size distribution of the bedload at the ghost node. For a sediment – feed flume this is a user specified parameter while for a sediment recirculating flume the cyclic boundary condition applies and so the fraction of bed load in each grain size range will be the same at the downstream end of the channel and at the ghost node (Parker, 2003).

3.7 EQUILIBRIUM

Conditions of equilibrium in a flume or in a river can be defined in different ways because they depend on which measurements are available. If some parameters can be reasonably considered constant in a fairly long period, that depends on the time scale of the problem, it can be assumed that the flow and the sediment transport have reached equilibrium.

In this model, it is assumed that the flow and the sediment transport reach equilibrium when the total bedload volume transport rate per unit width is almost constant along the flume and so there is neither net erosion nor deposition. The condition of constant bedload volume transport rate can be expressed as a function of the ratio between the standard deviation and the mean value of the computed transport rate

$$\gamma_{q_{bT}} = \frac{\sigma_{q_{bT}}}{\mu_{q_{bT}}} \leq a \tag{56}$$

where ‘a’ is a user specified tolerance

The total bedload transport rate averaged over the flume length is computed as

$$\mu_{q_{bT}} = \frac{1}{N_{max}} \sum_{j=1}^{N_{max}} q_{bT,j} \tag{57}$$

and the standard deviation is

$$\sigma_{q_{bT}} = \sqrt{\frac{1}{(N_{max}-1)} \sum_{j=1}^{N_{max}} \left(q_{bT,j} - \mu_{q_{bT}}\right)^2} \tag{58}$$

4 CONDITION OF COURANT FOR UNIFORM SEDIMENT

Courant condition is necessary to define the maximum time step length for a stable numerical scheme. The velocity of perturbations has to be smaller than the ratio between spatial and temporal step lengths, otherwise the numerical scheme can not follow the evolution of the system and it becomes unstable. The condition can be expressed as

$$c\frac{\Delta t}{\Delta x} \le 1 \tag{59}$$

where c is the velocity of perturbation.

When sediment is modeled as uniform and the channel is wide enough to neglect wall effects and to approximate the hydraulic radius with the water depth, two differential equations – (30) and (37) – govern the problem and the celerity, c, is a function of H only, because water discharge and sediment characteristic diameters are constant in space and time.

The problem is characterized by two dependent variables – water depth and bed elevation that are function of space and time – and two independent variables – space and time.

Total bedload transport rate is function of water depth, therefore equation (37) can be written as

$$M(H)\frac{\partial H}{\partial x} + (1-\lambda_p)\frac{\partial \eta}{\partial t} = 0 \tag{60}$$

where M(H) is a function that varies with the load relation.

Equation (30) can be written as

$$(1 - Fr^2)\frac{\partial H}{\partial x} + \frac{\partial \eta}{\partial x} = -S_f \tag{61}$$

and two more independent equations are required to solve the problem.

These equations are given by the definition of the two total differentials:

$$dH = \frac{\partial H}{\partial x}dx + \frac{\partial H}{\partial t}dt \quad ; \quad d\eta = \frac{\partial \eta}{\partial x}dx + \frac{\partial \eta}{\partial t}dt \tag{62}$$

Equations (60), (61) and (62) can be considered as linear system whose matrix of coefficients is

$$A=\begin{bmatrix}\left(1-Fr^2\right) & 0 & 1 & 0\\ M(H) & 0 & 0 & \left(1-\lambda_p\right)\\ dx & dt & 0 & 0\\ 0 & 0 & dx & dt\end{bmatrix} \tag{63}$$

Velocity of perturbation can be found computing the characteristics curves of the systems, defined by equation

$$\det(A)=0 \tag{64}$$

whose solution is

$$\frac{dx}{dt}=c=-\frac{M(H)}{\left(1-Fr^2\right)\left(1-\lambda_p\right)} \tag{65}$$

Condition for numerical stability (59) can be rewritten as

$$\Delta t\le-\frac{\left(1-Fr^2\right)\cdot\left(1-\lambda_p\right)}{M(H)}\Delta x \tag{66}$$

and equation M(H) has to be derived for the different load relations, assuming that the cross section is wide (66) enough to neglect wall effects and to approximate the hydraulic radius with the water depth.

4.1 FUNCTIONS M(H) FOR THE LOAD RELATIONS IMPLEMENTED IN THE NUMERICAL MODEL

The general form of a load relation for uniform sediment as a function of the excess shear stress above a critical value is expressed by equation (4), where the function is a power law with the form:

$$q_b^*=\alpha_s\cdot\left(\tau_b^*-\tau_c^*\right)^{nt} \tag{67}$$

where α_s, n_t and τ_c^* are parameters that vary from a relation to the other. For these relations the function M(H) is

$$M(H)=-\frac{7}{3}\sqrt{RgD_{50}}\cdot D_{50}\cdot\alpha_s\cdot n_t\cdot\left(\tau_b^*-\tau_c^*\right)^{(n_t-1)}\frac{k_s^{1/3}q_w^2}{\alpha_r RgD_{50}}\cdot\frac{1}{H^{10/3}} \tag{68}$$

For the load relation of Ashida and Michiue (1972), equation (11) the function M(H) is

$$M(H)=-\frac{119}{3}\cdot\frac{D_g}{\sqrt{RgD_g}}\cdot\frac{q_w^2\cdot k_s^{1/3}}{\alpha_r^2}\cdot\frac{1}{H^{10/3}}\cdot\left[\frac{3}{2}\cdot\left(\tau_b^*\right)^{1/2}-\sqrt{0.05}-\frac{0.05}{2\cdot\sqrt{\tau_b^*}}\right] \tag{69}$$

For the proposed modified version the function M(H) has the same form but the 119 is substituted by 32 (32 = 0.27·119).

For the load relation of Parker (1990), equation (15), the function M(H) is

$$\text{If } \phi < 1 \quad H > \left(\frac{q_w^2 \cdot k_s^{1/3}}{\alpha_r^2} \cdot \frac{1}{0.0386 \cdot RgD_g} \right)^{3/7}$$

$$M(H) = -\frac{0.08}{(Rg)^{15.2}} \cdot \cdot \left(\frac{q_w \cdot k_s^{1/6}}{\alpha_r} \right)^{31.4} \cdot \left(\frac{1}{0.0386 \cdot D_g} \right)^{14.2} \cdot \frac{1}{H^{1129/30}}$$

If $1 \le \phi \le 1.59$

$$\left(\frac{q_w^2 \cdot k_s^{1/3}}{1.59 \cdot \alpha_r^2} \cdot \frac{1}{0.0386 \cdot RgD_g} \right)^{3/7} \le H \le \left(\frac{q_w^2 \cdot k_s^{1/3}}{\alpha_r^2} \cdot \frac{1}{0.0386 \cdot RgD_g} \right)^{3/7}$$

$$M(H) = -\frac{0.01526}{Rg} \cdot \frac{q_w^3 \cdot k_s^{1/2}}{\alpha_r^3} \cdot \exp\left\{ 14.2\left(1 - \frac{\tau_b^*}{0.0386} \right) - 9.28\left(1 - \frac{\tau_b^*}{0.0386} \right)^2 \right\} \cdot \left\{ \frac{1}{2} - \frac{\tau_b^*}{0.1158} \cdot \left[18.56\left(1 - \frac{\tau_b^*}{0.0386} \right) - 14.2 \right] \right\} \tag{70}$$

$$\text{If } \phi > 1.59 \quad H < \left(\frac{q_w^2 \cdot k_s^{1/3}}{1.59 \cdot \alpha_r^2} \cdot \frac{1}{0.0386 \cdot RgD_g} \right)^{3/7}$$

$$M(H) = -\frac{41.77}{Rg} \cdot \frac{q_w^3 \cdot k_s^{1/2}}{\alpha_r^3} \cdot \left(1 - \frac{0.0329}{\tau_b^*} \right)^{7/2} \cdot \frac{1}{H^{13/6}} \cdot \left[\frac{1}{H^{7/3}} + 0.0658 \frac{\alpha_r^2 \cdot RgD_g}{q_w^2 \cdot k_s^{1/3}} \right]$$

For the relation of Wilcock and Crowe (2003), equation (23), the function M(H) is

$$\text{If } \phi < 1.35 \quad H > \left(\frac{q_w^2 \cdot k_s^{1/3}}{\alpha_r^2} \cdot \frac{1}{0.021 \cdot RgD_g} \cdot \frac{1}{1.35} \right)^{3/7}$$

$$M(H) = -\frac{0.042}{Rg} \cdot \frac{q_w^3 \cdot k_s^{1/2}}{\alpha_r^3} \left(\frac{\tau_b^*}{0.021} \right)^{15/2} \cdot \frac{1}{H^{9/2}} \tag{71}$$

$$\text{If } \phi \ge 1.35 \quad H \le \left(\frac{q_w^2 \cdot k_s^{1/3}}{\alpha_r^2} \cdot \frac{1}{0.021 \cdot RgD_g} \cdot \frac{1}{1.35} \right)^{3/7}$$

$$M(H) = -\frac{49}{Rg} \cdot \frac{q_w^3 \cdot k_s^{1/2}}{\alpha_r^3} \cdot \left(1 - 0.894\sqrt{\frac{0.021}{\tau_b^*}}\right)^{7/2} \cdot \frac{1}{H^{9/2}} \cdot \left[1 + \frac{5}{2} \cdot 0.894\sqrt{\frac{0.021}{\tau_b^*}}\right]$$

5 VALIDATION OF THE NUMERICAL MODEL WITH LABORATORY DATA

Laboratory experiments were conducted under conditions of lower – regime plane bed at the Hydrosystems Laboratory of the University of Illinois at Urbana – Champaign in a water – feed and sediment – recirculating flume to derive a load relation for the validation of the numerical model presented in Chapter 3 and to compare numerical prediction of conditions of mobile bed equilibrium with measured data.

During the experiments longitudinal profiles and water elevations were periodically measured. When the bed elevation was reasonably constant in time, it was assumed that the flow and the sediment transport reached equilibrium and the run ended. The definition of equilibrium in a river or in a flume is a very delicate matter because it depends on the particular scale of the problem and on the available measurements. It can be generally defined as a situation where all the hydraulic parameters, such as channel slope and sediment transport rate, vary around a mean value (Bloom et al., 2006a), that can be considered constant in time.

Nine different runs were performed for different values of water discharge and water elevation at the downstream end of the flume, boundary conditions that affect the condition of equilibrium in a water – feed and sediment – recirculating flume (Parker et al., 1993). When the flow and the sediment transport reached equilibrium, the sediment transport rate and its grain size distribution were measured and the surface of the bed was sampled and sieved in different locations. At the end of the ninth run core samples were taken in ten different cross sections to measure the grain size distribution of the deposits. Experimental data have been recorded in Appendix 1: Laboratory data.

The derivation of a bedload relation for sediment mixtures is the first fundamental step in the validation of a numerical model. Even if several load relations have been derived, a universal formulation of the problem has not yet been found (Wong, 2003). Moreover the majority of the proposed relations are based on empirical data and so they are limited to particular experimental conditions such as the grain size range and the sediment transport rate. The proposed relation has the same structure of the equation of Ashida and Michiue (1972) for gravel mixtures: the bedload transport rate

of each grain size range is computed as a function of the excess of shear stress above a critical value that varies for each grain size range. The main difference between the novel and the old bedload relation is the hiding function because the original relation, as shown in the following paragraphs, predicted a sediment transport rate considerably finer than the measured.

5.1 EXPERIMENTAL SET-UP

Experiments were performed in a water – feed and sediment – recirculating flume that it is more convenient than a sediment – feed flume to run experiments with poorly – sorted sediment because the mixture can be prepared and put in the flume just once (Parker et al., 1982a).

For the described experiments the horizontal bottom of the flume was covered with a 18.5 cm thick layer of the poorly sorted mixture of gravel and sand represented in Figure 9.

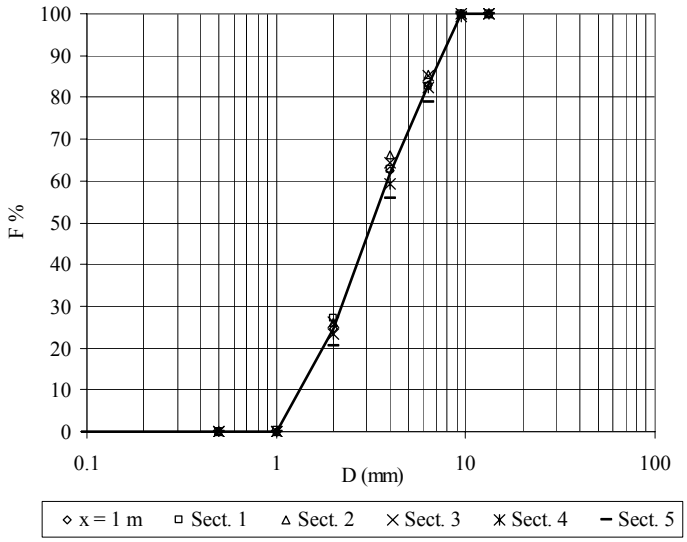

Figure 9 Grain size distribution of the sediment used during the experiments

The initial grain size distribution was measured in 6 sections of the flume at the beginning of the experiments. The first sample was taken at x = 1 m and the others in the 5 test sections: Sect.1 at x = 2.5 m, Sect. 2 at x = 4.3 m, Sect. 3 at x = 6.5 m, Sect. 4 at x = 8.5 m and Sect. 5 at x = 10.5 m, where distances are measured from the upstream end of the flume and x is a streamwise coordinate. The geometric mean diameter is 3.39 mm, the median diameter is 3.44 mm, the D_{90}, diameter such that the 90% of sediment is finer, is 7.83 mm and the geometric standard deviation is 1.79. The density of the sediment ρ_s has been measured and it is equal to 2580 kg/m^3.

The flume is straight with a rectangular cross section and plexiglas walls. It is 11.8 m long - from the end of the recirculating line to the wooden sediment trap - and 91 cm (3 feet) wide but the cross section was narrowed with a wooden wall on the left side of the channel to have a cross section 61 cm (2 feet) wide.

Water elevation was controlled by a rectangular tail gate at the downstream end of the flume. Particles coarser than 6.5 mm were manually recirculated because the diaphragm pump on the recirculating line could not work with such a coarse material. Water discharge was measured with two electromagnetic flowmeters: one on the recirculating line and the other on the pipe coming from the head tank. A sketch of the flume is drawn in Figure 10.

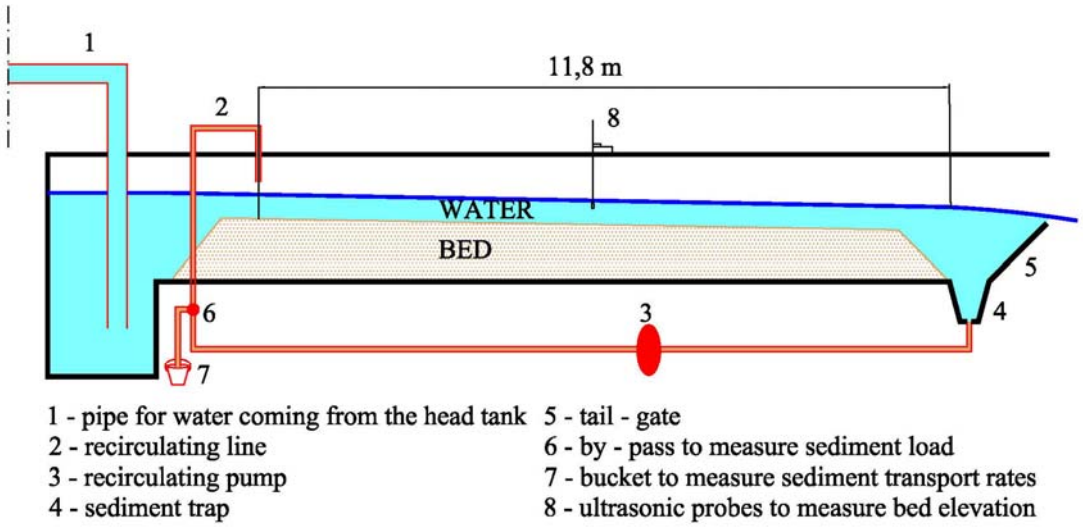

Figure 10 The laboratory flume

The test reach is 8 m (from x = 2.5 m to x = 10.5 m) long. Water elevation was measured in the test sections with piezometers. Longitudinal profiles were measured with the ultrasonic transducer probes described by Wong (2007): four probes were placed on the same cart and four longitudinal profiles were simultaneously recorded measuring bed elevation every 40 cm for 30 seconds.

5.2 EXPERIMENTAL PROCEDURE

The channel was backfilled with a hose and, when the bed was saturated, water was introduced from the head tank. The recirculating pump was turned on and the discharge from the head tank was adjusted to the desired value. The tail gate was lowered to fix the water elevation at the downstream end of the flume. Water surface

and bed elevation were measured every one or two hours. In these runs it was assumed that the flow and the sediment transport reached equilibrium when the longitudinal profiles was almost constant for two or three consecutive measurements. In Figure 11 some of the longitudinal profiles recorded during Run 4 are reported; the first profile was the bed at equilibrium at the end of Run 3 and, after a phase of aggradation, the longitudinal profile does not change much in time (see profiles recorded after 3 hours and 45 minutes and after 6 hours and 15 minutes).

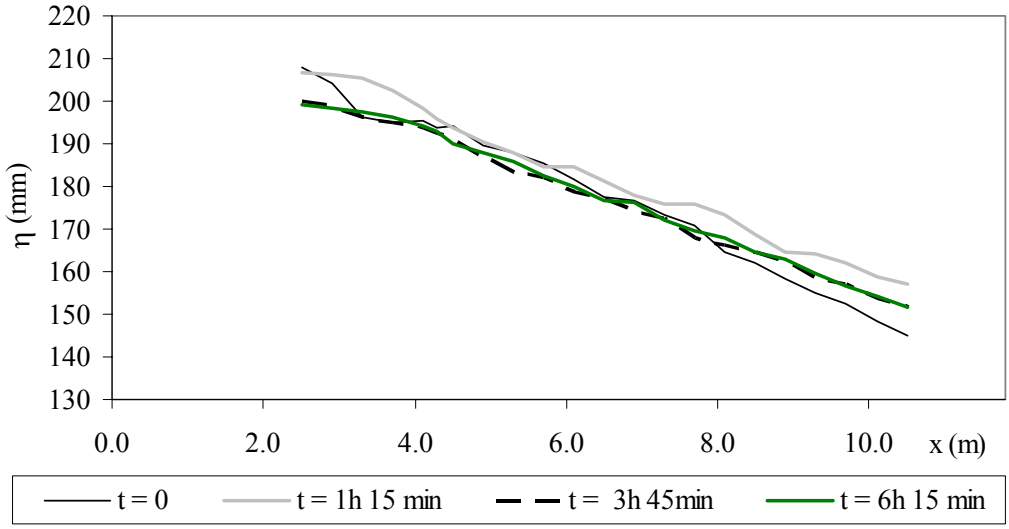

Figure 11 Longitudinal profiles recorded during Run 4.

When the flow and the sediment transport reached equilibrium, the sediment transport rate was measured: the by-pass on the recirculating line was open (see Figure 10) and the discharge from the head tank was adjusted because the water of the recirculating line was diverted to the big bucket where the sediment was collected. Coarse sediment was manually removed from the sediment trap.

After a 5 - 15 minutes interval depending on the sediment transport rate, the by-pass on the recirculating line was closed and the experiment ended. The collected sediment was dried in the oven, weighted and sieved. A final longitudinal profile was measured and the bed was drained.

Surface samples were collected with the Klingeman sampling method for bed surface in the five measuring sections. A rectangular area approximately 20 cm long (in the streamwise direction) and 30 cm wide (in the cross section), represented in Figure 12, was selected and the coarsest exposed particle was removed.

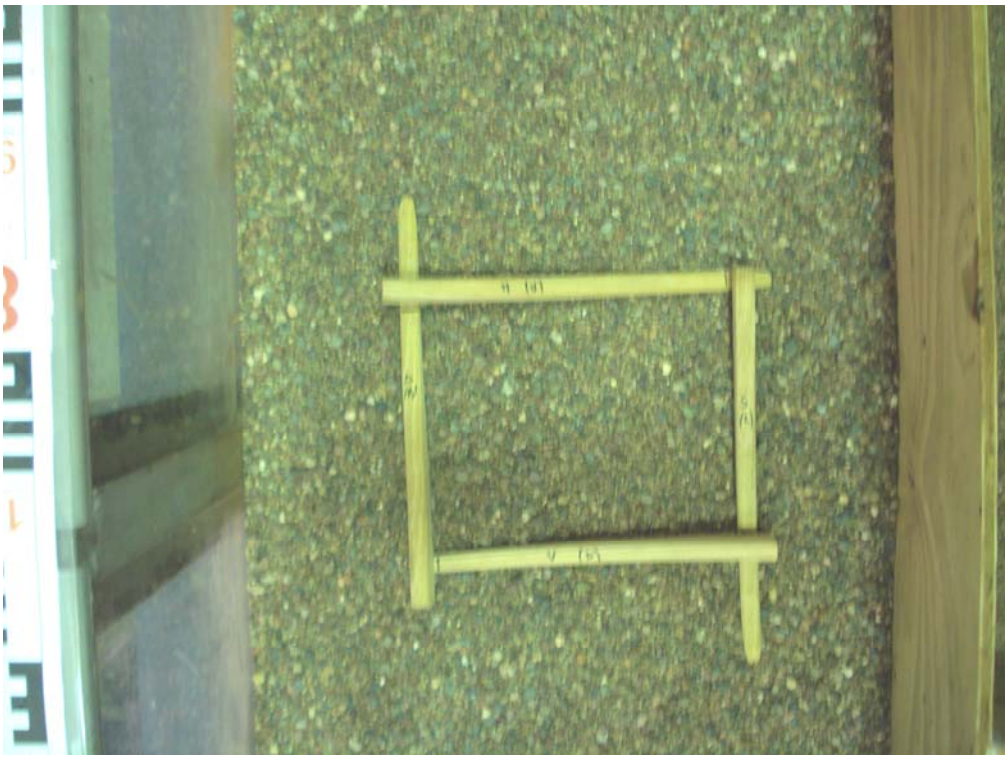

Figure 12 Area for surface samples.

The surface was spooned down to a level corresponding roughly to the bottom of the hole created removing the big particles (Parker, 1990). Samples were then oven – dried and sieved. They were then replaced and a new run started.

At the end of the ninth run the bed was sampled with the same metallic box (30 cm high with a rectangular basis 15 cm long and 10 cm wide) used by Bloom (2003). The flume was backfilled with a hose and the metallic box was driven into the bed. A metallic plate was then pushed under the box and the box and the plate were simultaneously removed. Considering that experiments were conducted in a water – feed and sediment - recirculating flume, where the total amount of sediment is a constant, vertical sorting can be mainly observed in the upstream part of the flume (Viparelli et al, 2007). The bed was sampled every 50 cm from x = 0.5 m to x = 3 m, then every meter at x = 4 m and x = 5 m and finally every two meters at x = 7 m and x = 9 m, as shown in Figure 13.

In each section a core sample was taken in the left side and another in the right side and they were cut in layers of 1 cm with a metallic plate. Each layer was oven - dried and sieved. To represent the vertical stratigraphy in a cross section, the grain size distributions of the same layer in left and in the right sample were averaged.

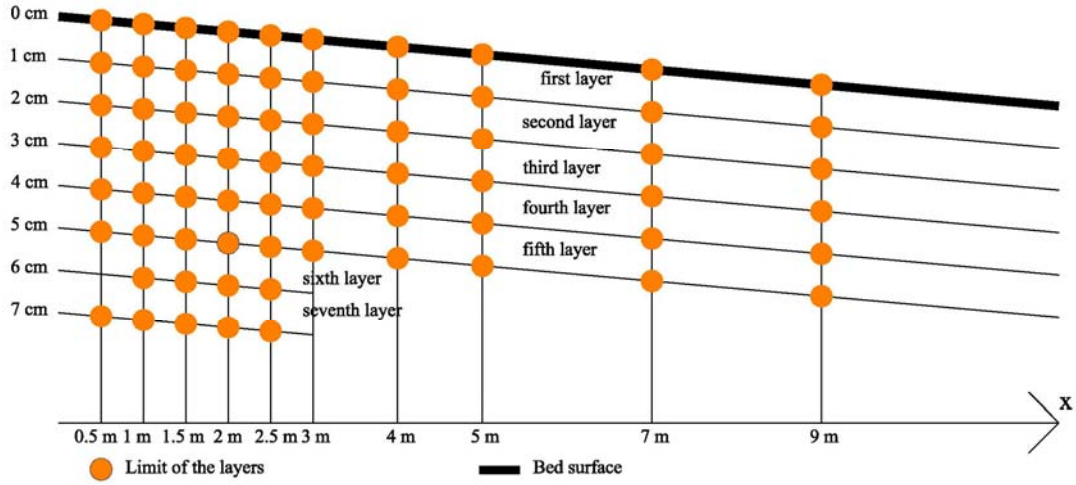

Figure 13 Grid to sample the bed at the end of the experiments

5.3 EXPERIMENTAL RESULTS

Experimental runs, reported in Table 1, are described in terms of water discharge and water elevation at the downstream end of the flume because in a water – feed and sediment – recirculating flume equilibrium depends on these two parameters and on the grain size distribution of the bed (Parker et al., 1993).

Table 1: Description of the runs; Q is the water discharge set by the pump and ξ_d is the water elevation at the downstream end of the flume set by the tail gate.

Run	Q (l/s)	ξ_d (cm)
1	30	22
2	25	21
3	20	19
4	35	23
5	20	21
6	30	24
7	30	23
8	35	24.8
9	35	22.5

The bed at the beginning of Run 1 was horizontal with no vertical stratigraphy, while initial conditions for Runs from 2 to 9 were the longitudinal profile and the grain size distribution of the bed at the end of the previous run

In a water – feed and sediment – recirculating flume, where the total amount of sediment in the system is constant, the bed surface and the substrate are segregated from the same mixture (Parker et al., 1982a), therefore if the thin bed surface results

much coarser than the initial mixture and the thick substrate should be slightly finer the initial mixture.

The sieve analysis of surface samples showed a systematic coarsening of the bed surface for the whole length of the flume and at the end of each run, as shown in Table 2, where the geometric mean diameter of the bed surface is reported. This coarse surface protects smaller grains that become harder to move. In the comparison between the initial mixture and the grain size distribution of the bed surface at the end of Run 1 in Section 4 (x = 8.5 m) is shown.

Table 2: Geometric mean diameter of the bed surface in millimetres

	Run 1	Run 2	Run 3	Run 4	Run 5	Run 6	Run 7	Run 8	Run 9
Section 1	4.13	3.56	4.74	4.69	4.11	4.89	4.33	4.44	4.19
Section 2	4.47	3.73	3.87	4.40	4.68	4.86	4.45	3.81	4.33
Section 3	4.08	3.80	4.23	4.00	4.77	4.62	4.53	4.49	4.09
Section 4	3.93	4.05	4.32	4.45	4.79	4.60	4.44	4.10	4.31
Section 5	4.06	4.06	4.21	4.55	5.08	4.69	4.47	4.85	4.19

The sieve analysis of core samples revealed a substrate with a grain size distribution equal or slightly coarser (mainly in the upper layers) than the original mixture, as shown in Figure 14.

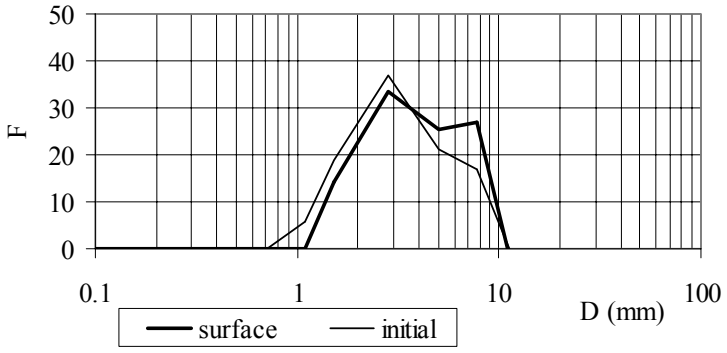

Figure 14 | Comparison between the initial mixture and the bed surface at the end of Run 1 in Section 4.

This unexpected result can be explained considering two different phenomena:

1) at the end of each run the bed was drained to sample the surface and then it was saturated again. These procedure, necessary to sample the surface, might have caused a reworking of the bed and the fining of its upper part of the substrate became negligible;
2) the initial bed was horizontal and at beginning of the experiments a front migrating downstream was observed. When a front migrates, the grain size

distribution of deposits depends on the slides of the material deposited on the top pf the front. After a slide, heavier particles (or coarser particles) will be placed at the front toe and finer particles will deposit on this coarser layer. As the front moves downstream part of the deposited material is remixed and a thin coarse lens remains at the bottom of the deposit, as shown in Figure 15.

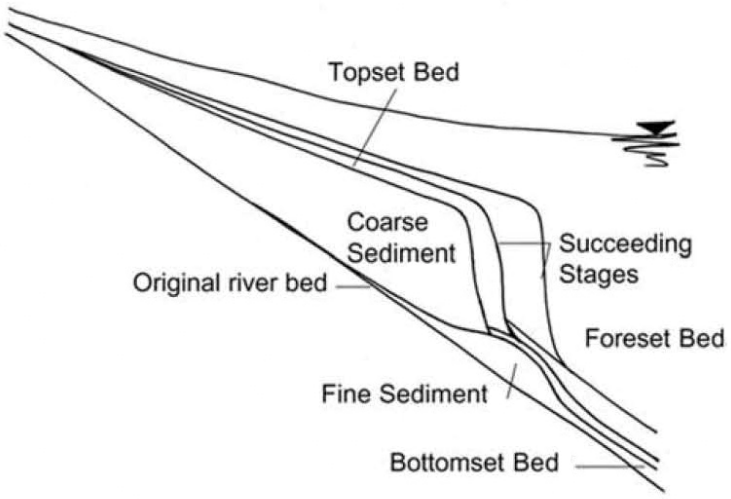

Figure 15 | Vertical stratigraphy of deposits due to a front migration from Cantelli et al., 2004.

In Figure 16 grain size distributions of the bed surface in Section 2 (x = 4.3 m) at the end of Run 9 and of the first layer of the core sample at x = 4 m are compared.

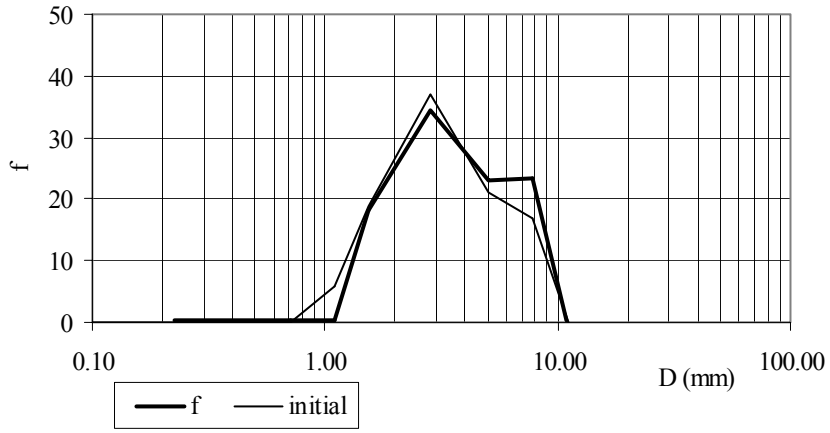

Figure 16 | Comparison between the initial mixture and the second layer of the substrate at x = 2.5 m.

The coarsening of the surface is always evident but the surface sample is much coarser than the first layer of the core sample. This difference can be ascribed to the different sampling technique because the first layers of core samples (Figure 13) were made of sediment from the surface and from the upper part of the substrate.

In Table 3 the sediment transport rates at equilibrium and some characteristic diameters of the bedload are reported. The sieve analysis of bedload samples showed that the bedload had a grain size distribution similar to the initial mixture except during Run 5 and Run 8 that were characterized by a low sediment transport rate (respectively 54 and 151 grams per minute).

Table 3: Bedload transport rates and characteristic diameters at equilibrium. G_s is the sediment transport rate in grams per minute, D_{lg} is the geometric mean diameter of the bedload, σ_{lg} is the geometric standard deviation of the bedload, D_{l50} is the median diameter of the bedload and D_{l90} is the diameter such that the 90% of the bedload is finer.

Run	G_s (gr/min)	D_{lg} (mm)	σ_{lg}	D_{l50} (mm)	D_{l90} (mm)
1	731	3.31	1.75	3.31	7.43
2	491	3.78	1.71	3.88	7.93
3	458	3.51	1.76	3.69	7.62
4	1432	3.70	1.68	3.73	7.74
5	54	2.85	1.74	2.70	6.79
6	64	3.36	1.76	3.3	7.69
7	371	3.89	1.64	3.98	7.83
8	151	2.99	1.84	2.78	7.58
9	1068	3.66	1.75	3.74	7.93

The bedload measured during Run 6, that was also characterized by a low sediment transport rate (64 grams per minute), had a grain size distribution similar to the initial mixture.

5.4 SHEAR STRESS IN THE BED REGION

Water depths and channel slopes averaged on the flume length to compute a single value of the bed shear stress for each condition of equilibrium are reported in Table 4. A complete description of the data is reported in Appendix 1: Laboratory data.

Table 4: Parameters at equilibrium. H is the water depth averaged on the flume length, S is the bed slope averaged on the flume length, Gs is the bedload transport rate and □b is the computed shear stress in the bed region.

Run	H (cm)	S (m/m)	Gs (g/min)	τ_b (Pa)
1	7.6	0.0069	731	4.90
2	6.8	0.0073	491	4.68
3	5.9	0.0079	412	4.42
4	8.3	0.0069	1432	5.33
5	6.1	0.0063	54	3.62
6	8.2	0.0046	64	3.48
7	8	0.0060	371	4.48
8	8.7	0.0052	151	4.16
9	8.2	0.0069	1068	5.26

The average shear stress on the bed was computed with the procedure presented by Vanoni and Brooks (Vanoni, 1975) to remove wall effects from measured values of water depth and channel slope described in Chapter 3.

Conservation of downstream momentum can be expressed as:

$$B\tau_b + 2H\tau_w = \rho g SBH \tag{72}$$

where B is the channel width, H is the water depth, S is the channel slope, g is the acceleration of gravity, ρ is the density of water and τ is the shear stress. Subscripts 'b' and 'w' respectively denote the bed and the wall region, see Figure 2. The shear stress in the wall region can be evaluated with the closure relation (28) for the wall region.

In the presented flume experiments side walls were made of plexiglas (hydraulic right) and plywood (hydraulic left) and so they were much smoother than the bed and the friction coefficient for the wall region was evaluated with the Nikuradse resistance relation for smooth pipes (34).

5.5 BEDLOAD RELATION

In order to verify the numerical model described in Chapter 3, the surface – based version of the relation of Ashida and Michiue for sediment mixtures (Parker, 2004) was tested against laboratory data. To compute the effective value of the Shields parameter and the volume bedload transport rate for unit width for each grain size range, grain size distributions of the surface layer measured at the end of each Run were averaged on the flume length to have a single value of the surface geometric mean diameter and a single grain size distribution for each condition of equilibrium. The comparison between measured and predicted sediment transport rates shows that relation (12) significantly overestimates the measured values. A better agreement between measured and predicted values can be obtained lowering the coefficient of the original relation. The modified version of equation (12) can be written as

$$q_{bi}^* = \beta \cdot 17\left(\tau_i^* - \tau_{ci}^*\right)\left(\sqrt{\tau_i^*} - \sqrt{\tau_{ci}^*}\right) \tag{73}$$

In Figure 17 measured sediment transport rate at equilibrium are plotted against sediment load predicted with equation (73) for β = 0.4 to state that the relation of Ashida and Michiue fits the data if its coefficient is lowered.

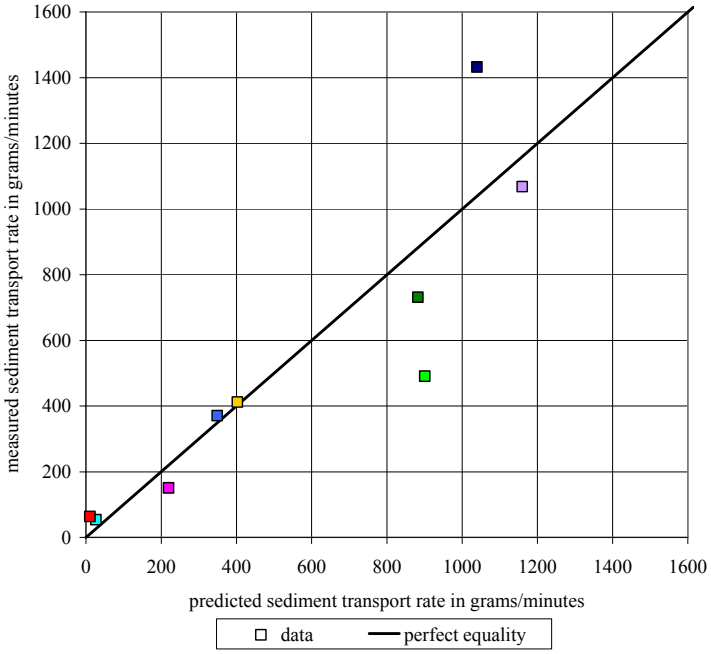

Figure 17

Comparison between predicted and measured sediment transport rate for equation (73) with $\beta = 0.4$.

In Figure 18 predicted geometric mean diameters of the sediment load, D_{lp}, are compared with measured values, D_{lm}, and it is evident that the computed sediment load is finer than the measured transport rates. A more detailed comparison between predicted and measured grain size distributions of the bedload is reported in Appendix 2: Validation of the bedload relation.

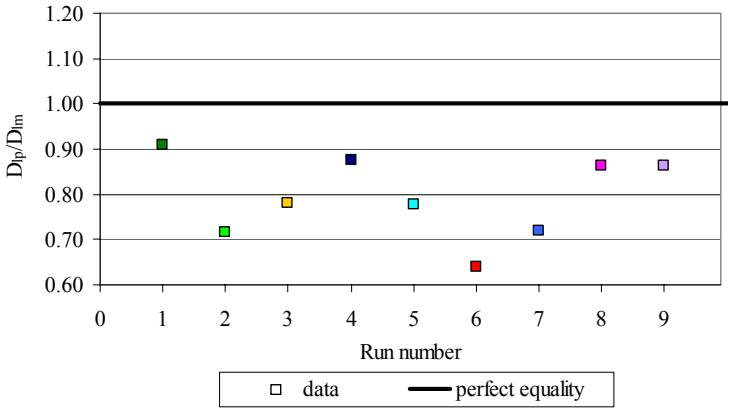

Figure 18

Comparison between predicted and measured geometric mean diameter in the sediment load for equation (73) with $\beta = 0.4$.

The difference in bedload grain size distributions can be ascribed to the hiding function (13). For coarse particles ($D_i/D_{sg} > 0.4$) the hiding function of Ashida and Michiue has the same expression of the function defined by Egiazaroff (1965) but, as

shown in Figure 19, for fine grains ($D_i/D_{sg} \leq 0.4$) the original relation was modified because it predicts a smaller mobility as the grain size decreases.

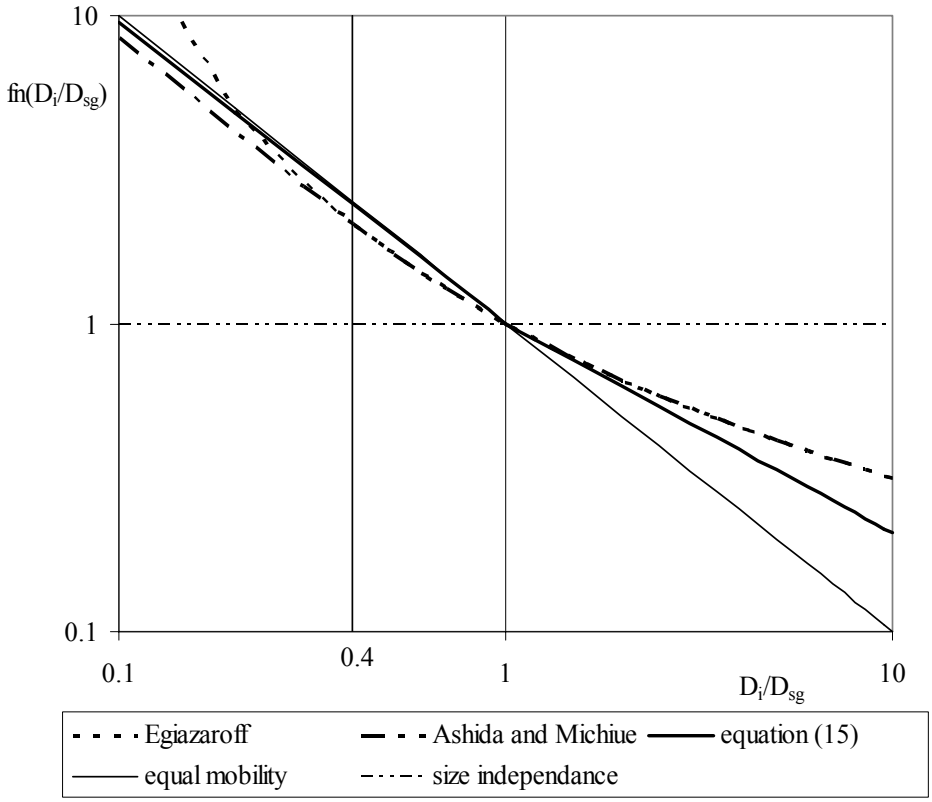

Figure 19 Hiding functions

A power law form for the hiding function was derived by Parker and Klingeman (1982 b):

$$\frac{\tau^*_{ci}}{\tau^*_{c50}} = \left(\frac{D_i}{D_{50}} \right)^{-m} \tag{74}$$

where D_{50} is the median diameter of the grain size distribution either of the substrate or of the surface layer. The exponent 'm' is a real number that varies from 0 to 1: m equal 0 corresponds to the limiting case called 'size – independence' where all particles are mobilized at the same Shields number. In this hypothesis the hiding effect is absent and the beginning of motion is highly dependent of the grain size. The other limiting case, m equal to 1, is called 'equal – mobility': the critical Shields number linearly varies with the grain size and all the particles are mobilized at the same shear stress. Fields and laboratory data are closer to the case of equal – mobility than to size – independence, therefore m is closer to 1 than 0, but it is still smaller than 1 (Parker, 2003).

In the present analysis the hiding function that fits the experimental data is expressed in terms of geometric mean diameter of the surface layer and has two different relations with the same form of equation (75) for coarse ($D_i/D_{sg} > 1$) and fine particles ($D_i/D_{sg} \leq 1$):

$$\frac{\tau^*_{ci}}{\tau^*_{scg}} = \begin{cases} \left(\frac{D_i}{D_{sg}}\right)^{-0.98} & for \ \frac{D_i}{D_{sg}} \leq 1 \\ \left(\frac{D_i}{D_{sg}}\right)^{-0.68} & for \ \frac{D_i}{D_{sg}} > 1 \end{cases} \tag{75}$$

The load relation for mixtures expressed by equations (73) and (75) was tested against the bedload data. For $\beta = 0.48$ in equation (73) there is a good agreement between measured and computed sediment transport rates. In Figure 20 measured and predicted geometric mean diameters of the sediment load are compared to show that the proposed hiding function gives a better description of the bedload grain size distribution than equation (12), neglecting runs 5 and 6 where the sediment transport rate was very low and the excess shear stress above its critical value can not always be properly computed.

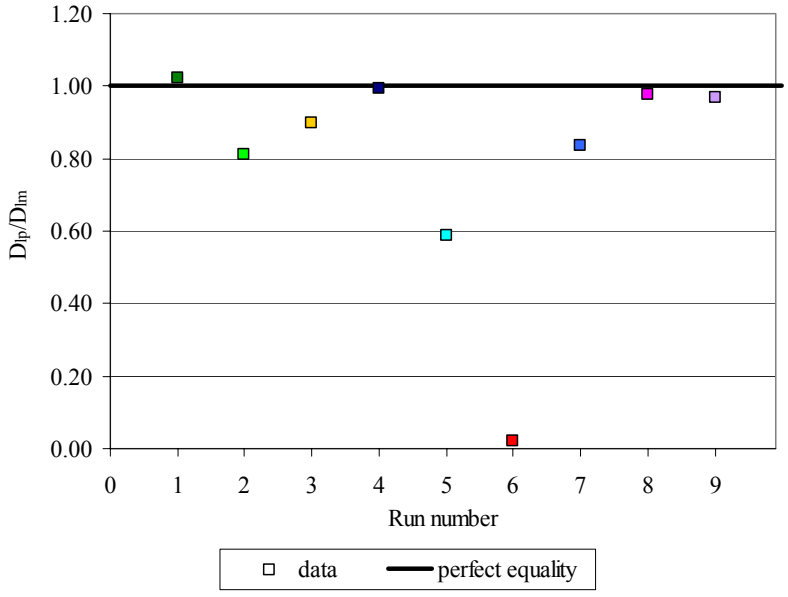

Figure 20 Comparison between predicted and measured geometric mean diameter in the sediment load for equation (75) with $\beta = 0.48$ in equation (73)

A better agreement between computed and measured grain size distributions of the sediment load can be obtained lowering the critical value of the Shields number from 0.05, as suggested by Ashida and Michiue, to 0.043, value that gives the best fit of the data. In Figure 21 and in Figure 22 measured sediment transport rates and bedload

geometric mean diameters are plotted against values computed with equations (73) and (75) for $\beta = 0.27$ and $\tau_{scg}^{*} = 0.043$ and it is evident that the proposed version of the Ashida and Michiue load relation gives a better fit of the laboratory data for the mixture represented in Figure 9 and the experiments described in the present paper.

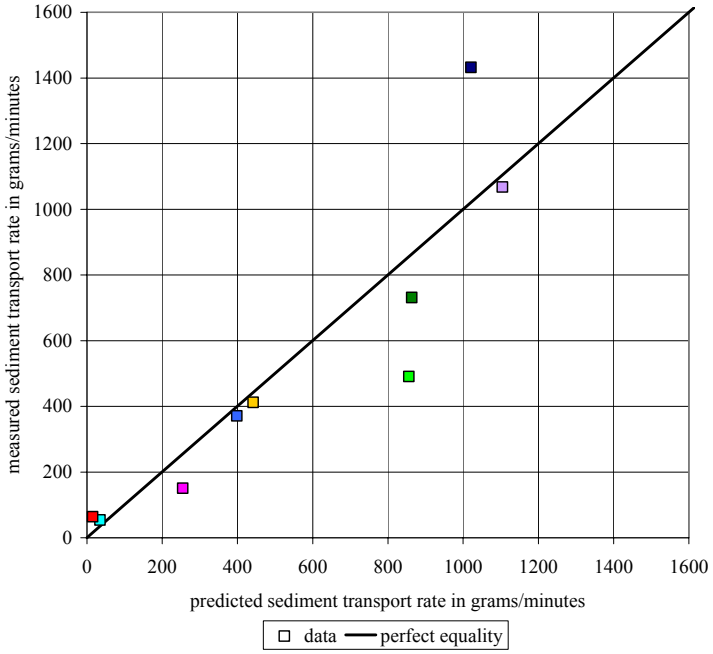

Figure 21

Comparison between predicted and measured sediment transport rates for equation (75) with $\tau_{scg}^{*} = 0.043$ and $\beta = 0.27$ in equation (73)

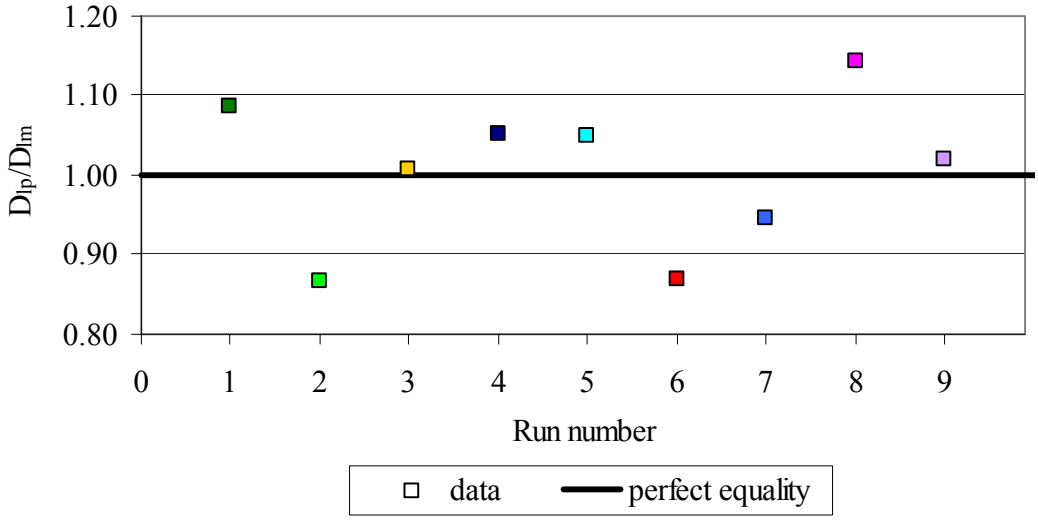

Figure 22

Comparison between predicted and measured geometric mean diameter in the sediment load for equation (75) with $\tau_{scg}^{*} = 0.043$ and $\beta = 0.27$ in equation (73).

In Figure 23 the bedload geometric mean diameters predicted with the relation of Ashida and Michiue with a critical value of the Shield parameter of 0.043 are plotted against measured values to show that even if a lower critical Shields number gives a

better fit of the data, the computed bedload is still significantly finer than the measured sediment transport.

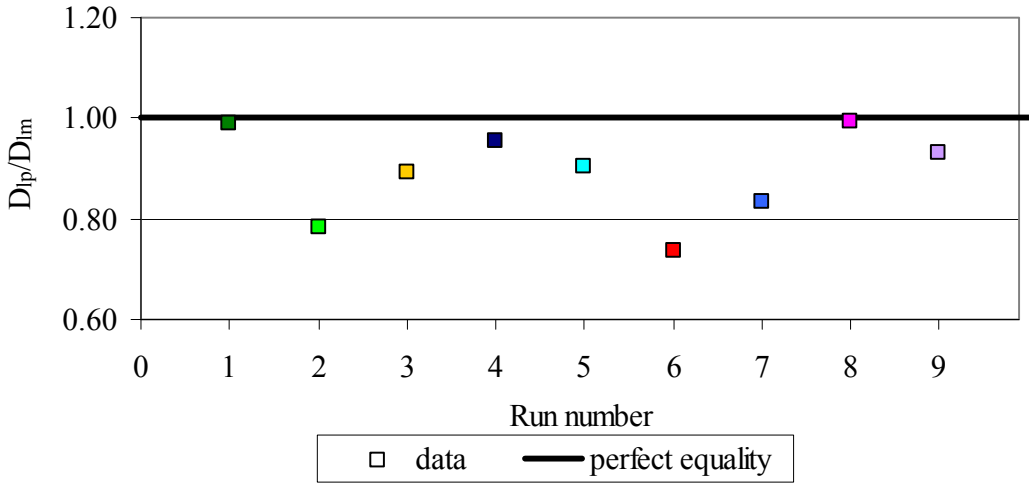

Figure 23 Comparison between predicted and measured geometric mean diameter in the sediment load for equation (12) with τ_{scg}^{*} = 0.043 and β = 0.24 in equation (73)

5.6 NUMERICAL SIMULATION OF LABORATORY EXPERIMENTS

To validate the procedure to store and access the stratigraphy of non cohesive deposits and the numerical model described in Chapter 3, numerical simulations of the experiments described in the present Chapter were performed. To run the numerical model several parameters have to be specified:

- α_r, the coefficient in the Manning – Strickler resistance relation (31) was equal to 8.1 (Parker, 1991 b);
- n_k, the coefficient to evaluate the roughness height as a linear function of the D_{s90}, was equal to 1.5;
- n_a, the parameter to evaluate the thickness of the surface layer as a linear function of the D_{s90}, was equal to 1 (Parker, 1991 a and b) because the surface layer was sampled to a depth equal to the hole created by removing the coarsest particle in the sampling area;
- λ_p, bed porosity, equal to 0.35;
- ρ, density of water, equal to 1000 kg/m^3;
- ρ_s, density of the sediment, equal to 2580 kg/m^3;
- α, parameter to evaluate the fraction of material in each grain size range at the active layer – substrate interface, equal to 0.2.

Considering that the load relation derived in the previous paragraph was based on these laboratory data, the same equation was used to verify the model. The spatial step length was equal to 10 cm and the temporal step length was equal to 2 seconds. The thickness of the grid to store and access the stratigraphy, L_s, was 1 cm equal to the layers in which core samples were divided.

To define the value of the parameter alpha the sensitivity of the model to this parameter has been verified. The channel slope averaged on the flume length, S, does not change significantly in the different runs, while the active layer becomes coarser as alpha decreases and, consequently, the bedload transport rate decreases. The better agreement between measured and predicted values of bedlaod transport rates, geometric mean diameters and D90 of the surface layer was obtained for alpha = 0.2, as shown in Table 5, Table 6 and Table 7.

Table 5: Comparison between predicted and measured values of sediment transport rates for different values of alpha.

	$G_{scomputed} \cdot 100/G_{smeasured}$					
Run	a=0.1	a=0.2	a=0.3	a = 0.4	a = 0.5	a=1
1	81	80	83	85	88	102
2	72	79	83	86	89	106
3	89	95	100	106	110	137
4	56	56	57	58	59	67
5	111	120	133	143	156	230
6	145	164	184	197	211	273
7	79	80	84	86	92	116
8	154	156	166	166	173	229
9	101	101	103	104	105	115

Table 6: Comparison between predicted and measured values of the geometric mean diameter of the active layer for different values of alpha.

	$D_{sgcomputed} \cdot 100/D_{sgmeasured}$					
Run	a=0.1	a=0.2	a=0.3	a = 0.4	a = 0.5	a=1
1	87	86	86	85	84	80
2	94	93	92	91	91	86
3	86	85	84	83	82	77
4	80	80	79	79	78	74
5	78	77	76	75	74	70
6	79	77	75	74	73	69
7	81	80	80	79	78	73
8	82	81	80	79	78	73
9	82	82	81	81	80	77

Table 7: Comparison between predicted and measured values of the D_{90} of the active layer for different values of alpha.

	$D_{s90computed} \cdot 100/D_{s90measured}$					
Run	a=0.1	a=0.2	a=0.3	a = 0.4	a = 0.5	a=1
1	98	98	97	97	96	93
2	100	100	99	99	98	95
3	98	97	96	96	95	92
4	95	95	94	94	94	91
5	94	94	93	93	92	89
6	95	94	93	92	91	87
7	96	96	95	94	93	91
8	97	97	96	95	95	91
9	95	95	95	95	94	91

In Figure 24 and in Figure 25 the good agreement between predicted and measured sediment transport rates and channel slopes at equilibrium is shown to state that the presented model can capture the global parameters of the flow, i.e. channel slope and bedload transport rates.

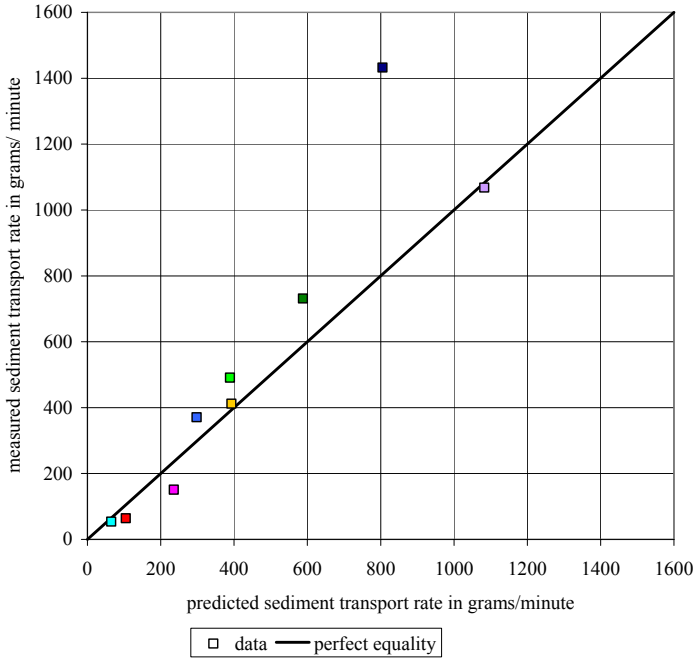

Figure 24 Comparison between predicted and measured sediment transport rates at equilibrium

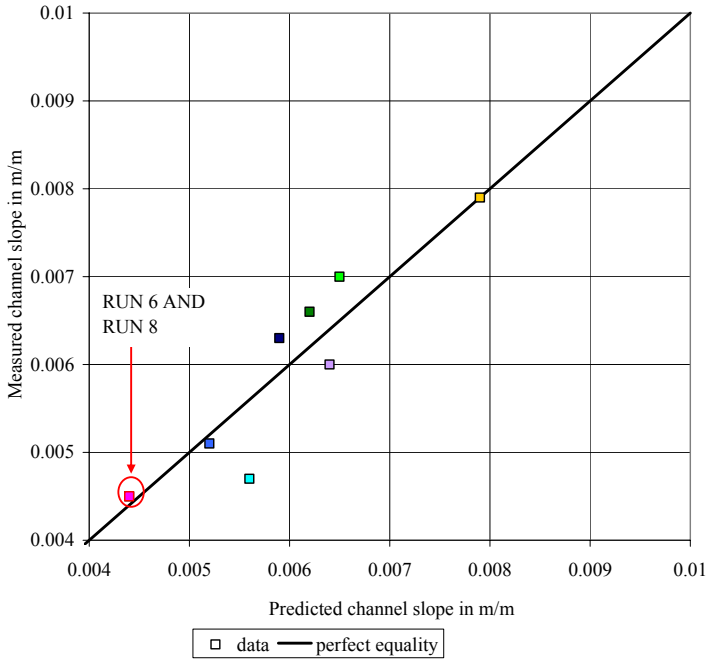

Figure 25 Comparison between predicted and measured channel slopes at equilibrium

In Table 8 predicted and measured geometric mean diameters of the bedload and of the bed surface are compared and the measured values are finer than those measured during the laboratory experiments. Their difference for the active layer is generally smaller than the 25% of the measured value while for the bedload it is smaller than the 40%.

Table 8: Comparison between predicted and measured geometric mean diameters at equilibrium for the load and the surface layer

		$(D_{gp}-D_{gm})/D_{gm}$				
Run	Load	2.5 m	4.3 m	6.5 m	8.5 m	10.5 m
1	-0.24	-0.14	-0.22	-0.13	-0.08	-0.11
2	-0.35	0.03	0.00	-0.07	-0.13	-0.12
3	-0.30	-0.23	-0.02	-0.15	-0.17	-0.13
4	-0.30	-0.26	-0.11	-0.11	-0.21	-0.22
5	-0.31	-0.13	-0.14	-0.23	-0.24	-0.31
6	-0.38	-0.24	-0.13	-0.20	-0.20	-0.25
7	-0.38	-0.17	-0.02	-0.21	-0.22	-0.20
8	-0.27	-0.20	0.17	-0.26	-0.09	-0.29
9	-0.30	-0.19	0.03	-0.15	-0.18	-0.17

This behavior can be explained considering that the code can not properly describe the beginning of the run when, as shown in Figure 26, a front migrates downstream and the reworking of the bed due to the procedure to sample the surface.

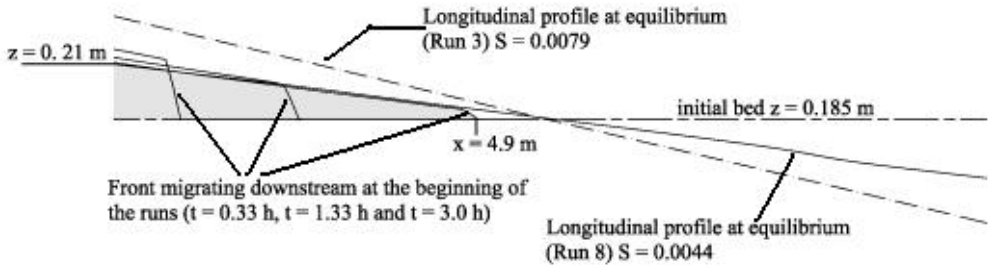

Figure 26 Longitudinal profiles. The grey area is the material deposited at the beginning of the run and its stratigraphy can not be properly computed with the presented numerical model.

When a front progrades the grain size distribution of the active layer is not governed by equation (42), because over a lee face coarser grains deposit in the lower part and finer grains deposit near the top (Bloom et al, 2006b). As the front migrates downstream, the coarse and deeper deposit becomes new substrate that consequently has a coarser grain size distribution than that computed with equation (42). If the substrate is coarser, the parameters f_{li} in equation (42) is bigger during degradation and the computed active layer is coarser.

Core samples were taken from the bed in ten different locations, as shown in Figure 13: every 50 cm in the first 3 meters of the flume, then every meter at x = 4 m and x = 5 m and finally every two meters at x = 7 m and x = 9 m, where x is a streamwise coordinate. Each sample was cut in layers 1 cm thick and the layers were dried in the oven and sieved. In Figure 27 the good agreement between predicted and measured grain sizes distribution in the substrate is shown for one of the deepest samples.

In Appendix 3 all the comparisons between predicted and measured grain size distributions in the deeper layer are recorded to prove the good agreement between measured and predicted values when the vertical sorting is not governed by front migration. In the upstream part of the flume, where deposition in the layers two and three centimeters below the bed surface is governed by front migration, the code predicts finer deposits than those measured at the end of the experiments.

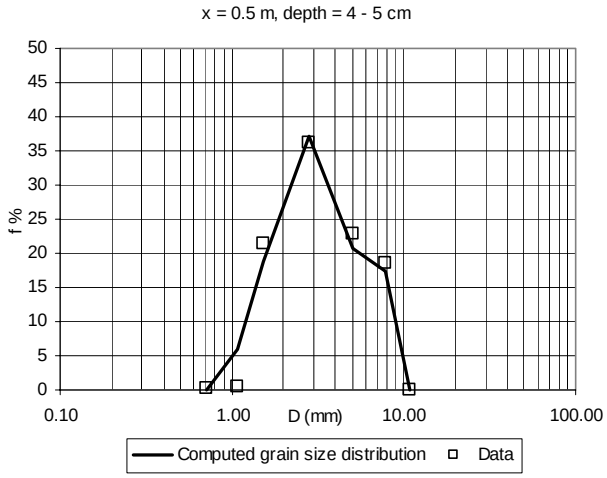

Figure 27 Comparison between computed and measured grain size distribution in the substrate 4 cm below the bed surface at x = 0.5 m.

Further downstream, as shown in Figure 28, the grain size distribution of deposits at the same depth is properly predicted because the grain sorting in the vertical direction can be modeled with equation (42). In Figure 29 the comparison between predicted and measure grain size distributions in the first centimeter of the bed is shown for the sample taken at x = 1.5 m and x = 9 m to confirm the hypothesis that the code predicts the grain size distribution of the deposits, if the grain sorting is not governed by a front migration.

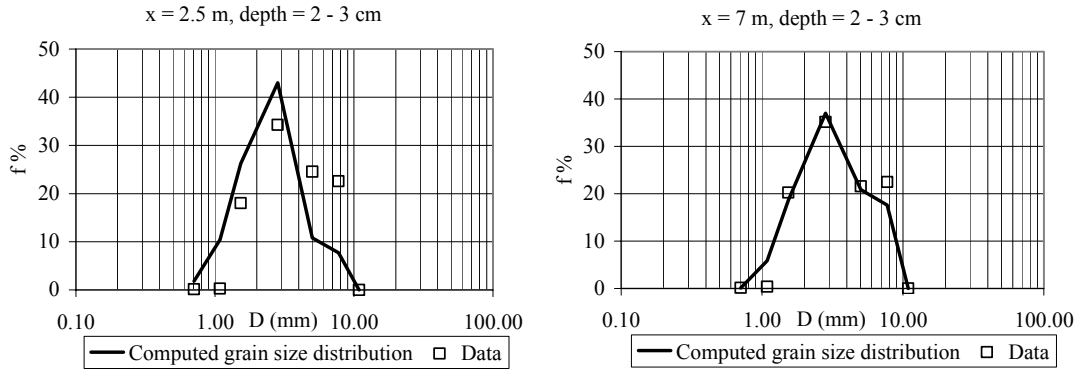

Figure 28 Comparison between computed and measured grain size distribution in the substrate 2 cm below the bed surface at x = 2.5 m and x = 7 m

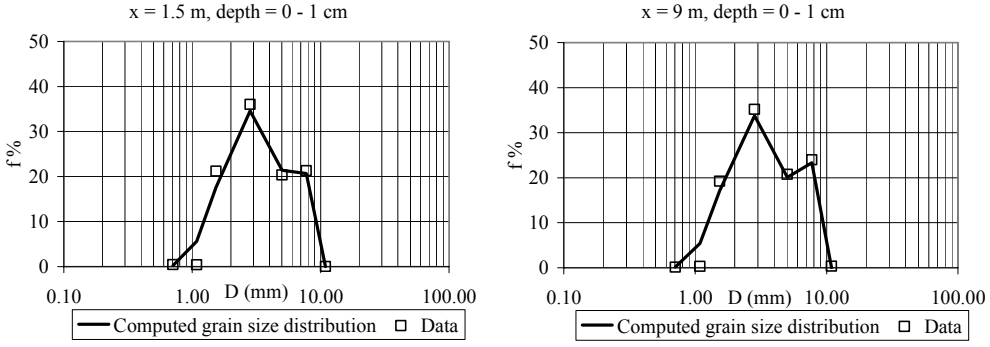

Figure 29 Comparison between computed and measured grain size distribution in the first centimeter of the bed surface at x = 1.5 m and x = 9 m

Considering that when a front migrates downstream the coarse material is transferred to the substrate because the coarse material of the topset collapses and deposits at the front toe, the procedure to store and access the stratigraphy of deposits presented in Chapter 3 was slightly modified to transfer to the substrate the material of the active layer only. Equation (49) was rewritten in the following form

$$f_i\big|_{j,t,N} = \frac{\left\{ f_i \cdot \left[\eta_{\text{int}} - (N-1) \cdot L_s \right] \right\}\big|_{j,t-\Delta t,N} + \left(\delta \cdot F_i \right)\big|_{j,t}}{\left[\eta_{\text{int}} - (N-1) \cdot L_s \right]_{j,t-\Delta t,N} + \delta\big|_{j,t}} \tag{76}$$

where F_i is the fraction of material in the i-th grain sizes range of the active layer.

This alternative version of the proposed procedure was tested against the laboratory data. The difference between this second set of numerical experiment and that previously described are:

- -the procedure to store the stratigraphy, i.e. equation (49) was substituted with equation (76);
- -the value of the parameter alpha, 0.3 instead of 0.2;
- -the value of the parameter to evaluate the roughness height n_k, 2.5 instead of 1.5. In the second set of experiments this parameter was calibrated to have the better agreement between predicted and measured values of the bedload transport rates. This calibration was necessary because in the numerical model the bed shear stress is computed with the closure relation (28) where the friction coefficient is evaluated with equation (31).

The validation of the new procedure against laboratory data shows that the coda can still reproduce the general characteristics of the flow – bedload transport rates and channel slope averaged on the flume length, as shown in Figure 30 and in Figure 31.

It is important to notice that the computed channel slope in this second set of numerical experiments is generally higher than that measured at the end of the laboratory experiments because of the high value of the friction slope in equation (30).

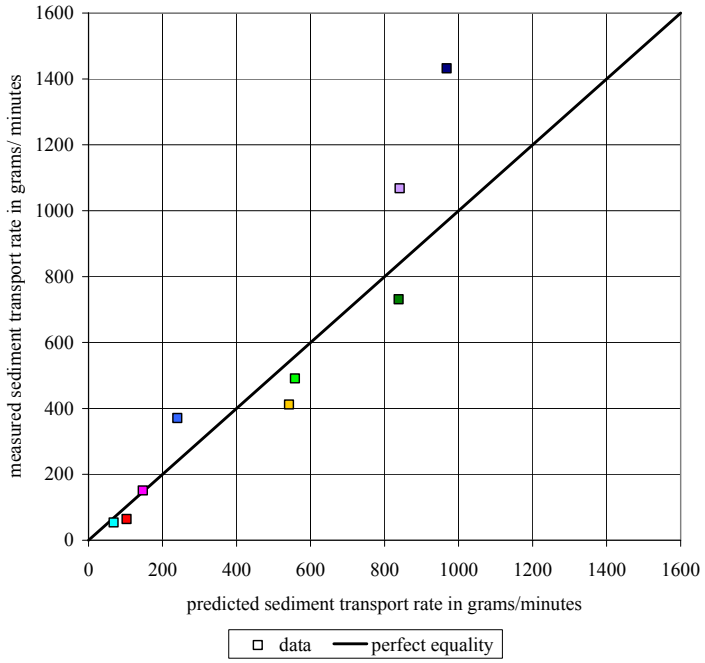

Figure 30 Comparison between predicted and measured sediment transport rates at equilibrium

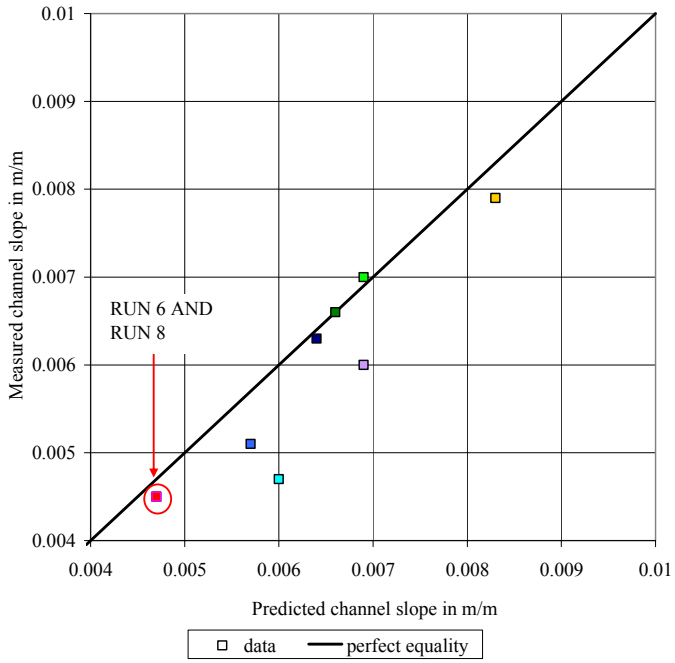

Figure 31 Comparison between predicted and measured channel slopes at equilibrium

In Table 9 the comparison between predicted and measured geometric mean diameters of the bedload and of the active layer is presented and the difference is generally smaller than the 20% of the measured value.

Table 9: Comparison between predicted and measured geometric mean diameters at equilibrium for the load and the surface layer

		$(D_{gp}-D_{gm})/D_{gm}$				
Run	Load	2.5 m	4.3 m	6.5 m	8.5 m	10.5 m
1	-0.04	-0.10	-0.17	-0.09	-0.05	-0.08
2	-0.18	0.05	0.00	-0.02	-0.08	-0.08
3	-0.12	-0.20	-0.02	-0.11	-0.13	-0.11
4	-0.06	-0.17	-0.11	-0.02	-0.13	-0.14
5	-0.16	-0.01	-0.14	-0.16	-0.17	-0.22
6	-0.21	-0.12	-0.13	-0.09	-0.09	-0.12
7	-0.14	0.01	-0.02	-0.05	-0.03	-0.05
8	0.01	-0.01	0.17	-0.08	0.09	-0.08
9	0.06	0.06	0.03	0.09	0.05	0.08

The better agreement between measured and predicted values with this new procedure confirms that the original version of the procedure predicts a finer grain size distribution of the active layer and of the bedload because the computed substrate was not coarse enough.

In Figure 32 and in Figure 33 the comparison between the measured and the computed grain size distribution of the deposits is shown for the same layers considered for the first set of numerical experiments.

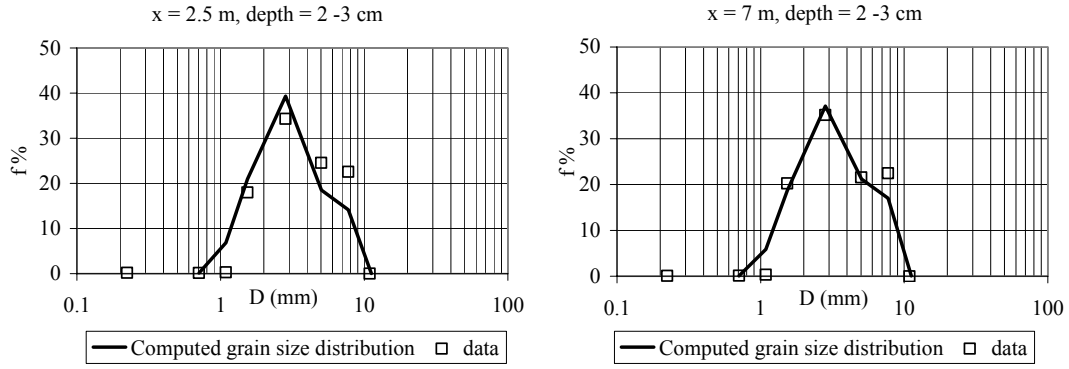

Figure 32 Comparison between computed and measured grain size distribution in the substrate 2 cm below the bed surface at x = 2.5 m and x = 7 m

It is evident that this new version of the procedure gives a better description of the grain size distribution of the deposits in the upstream part of the flume but for the whole flume length the first layer is systematically coarser than the measured samples. In Appendix 3 all the comparison between predicted and measured values are presented to show that the grain size distribution of the two upper layers is generally coarser than that measured while the grain size distribution of the deeper layers is properly predicted for the whole flume length.

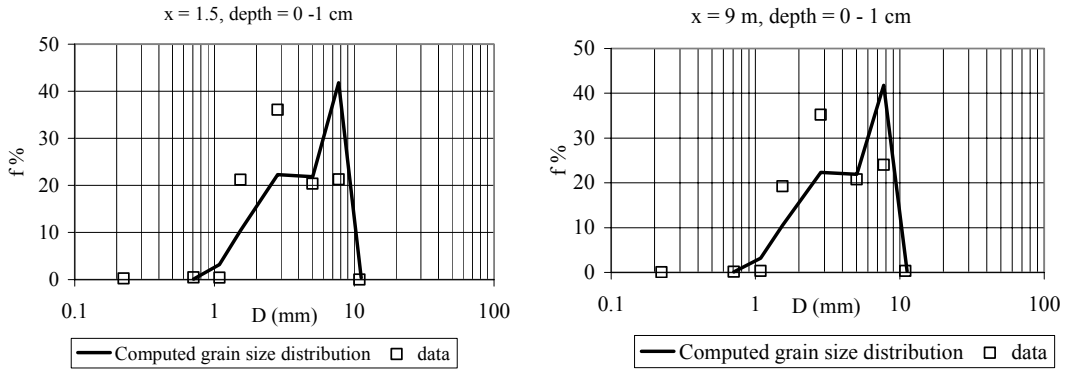

Figure 33 Comparison between computed and measured grain size distribution in the first centimetre of the bed surface at x = 1.5 m and x = 9 m

The systematic prediction of a coarser grain size distribution in the upper layers reveals that the second version of the procedure can properly describe the grain size distribution of deposits formed by front migration while the original procedure can capture the grain size distribution when the vertical sorting is governed by fluvial aggradation.

6 NUMERICAL EXPERIMENTS

In this paragraph two groups of numerical experiments are presented. The former group was performed for a further test of the original procedure to store and access the stratigraphy. The latter was run with the aim of comparing condition of mobile bed equilibrium in a sediment feed and in a sediment recirculating flume with uniform material and sediment mixtures. Considering that the initial condition was horizontal plane bed, the second version of the procedure to store and access the stratigraphy, summarized in equation (76) was implemented.

The numerical runs were performed in the same flume and with the same mixture used in the laboratory experiments.

6.1 FIRST GROUP OF NUMERICAL EXPERIMENTS

Five numerical experiments, described in Table 10, were performed to test of the novel procedure to store (Runs 10 and 12) and access (Runs 11, 13 and 14) the stratigraphy of deposits. The initial bed elevation averaged in the flume length is 18.5 cm and its initial slope is 0.004 to avoid deposition due to front migration. Runs 10 and 11 were performed in a sediment – recirculating flume and Runs 12 and 13 in a sediment – feed flume.

Table 10: Numerical experiments. Rec indicates a water – feed and sediment – recirculating flume and Feed a sediment - feed flume.

Run	Flume	Q (l/s)	ξ_d (cm)	G_s (grams/minutes)
10	Rec	20	19	642
11	Rec	35	24.8	374
12	Feed	20	19	642
13	Feed	35	24.8	374
14	Feed	35	19	374

Numerical Runs ended when the flow and the sediment transport reached equilibrium. To define this condition the tolerance in equation (56) had to be specified and his value was determined comparing the durations of Runs from 6 to 9 with numerical predictions. Runs from 1 to 5 were not considered because they were characterized by several problems with the diaphragm pump, therefore their durations can not properly represent the time for the flow and the sediment transport to reach equilibrium. The best fit of the data was obtained for a value of the tolerance ‘a’ of 0.05. The other parameters of the model, the spatial and temporal step lengths had the same values

reported in the previous paragraph. The load relation was that used for the numerical simulation of the laboratory experiments.

6.1.1 WATER – FEED AND SEDIMENT - RECIRCULATING FLUME RUNS

In a sediment – recirculating flume equilibrium depends on initial and boundary conditions because the amount of sediment in the system is constant (Parker et al., 1993). In Run 10 water discharge and water elevation at the end of the flume were the same of Run 3, presented in the previous Chapter. The bed surface at the beginning of Run 10 had the same grain size distribution of the substrate and not that at equilibrium at the end of Run 2 (see Chapter 5).

When the flow and the sediment transport reached equilibrium at the end of Run 10, the channel had the same slope that at the end of Run 3, 0.0079 m/m. The sediment transport rate was higher than that at the end of Run 3 (442 grams per minute against 393 grams per minute) and this can be ascribed to the different initial conditions. In Figure 34 the variation of the D_{50} in the substrate is represented.

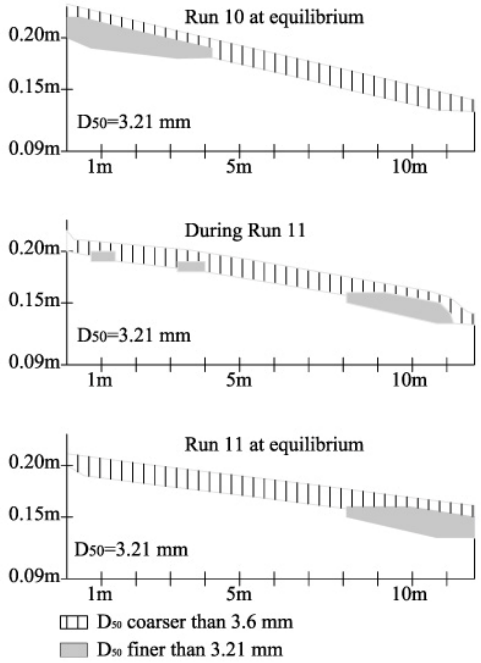

Figure 34 Variation of D_{50} in the vertical and in the streamwise direction for the numerical runs in a water feed and sediment recirculating flume

A lens of fine material is deposited at the upstream end of the flume at the beginning of the run when the flow eroded the downstream part of the flume and the recirculated sediment was deposited in the upstream part.

Water discharge and water elevation at the end of the flume for Run 11 were the same of Run 8 (see Chapter 5). The initial bed was that at the end of Run 10. Channel slope and sediment transport rate at equilibrium were very close to that at the end of Run 8 (0.0043 m/m against 0.0044 m/m and 217 grams per minute against the predicted 236 at the end of Run 8).

In Figure 34 the vertical and streamwise variation of D_{50} during and at the end of Run 11 is reported. The coarser surface layer and part of the fine lens in the upstream part of the flume were eroded and the material was deposited downstream.

6.1.2 SEDIMENT FEED FLUME RUNS

In a sediment – feed flume equilibrium is independent from the initial conditions; it depends on water discharge and sediment transport rates because the total amount of sediment in the system can vary (Parker et al., 1993). Run 12 was characterize by the same water discharge, gate elevation and sediment transport rate at equilibrium of Run 10. When the flow and the sediment transport reached equilibrium, the channel slope was steeper than at the end of Run 10 (0.0090 m/m against 0.0079 at the end of Run 10). In Figure 35 the variation of the D_{50} in the bed is represented.

The lens of finer material deposited at the upstream end of the flume is different than that deposited during Run 10 because in a sediment feed flume the sediment – feed rate and its grain size distribution are constant and coarser than that of the recirculating runs. The coarser feeded material deposited first and then the finer deposited on the coarser layer. As the slope increased the finer material was carried further downstream to build the other two fine lens. The active layer coarser than the substrate can also be observed.

The difference between Runs 13 and 14 was the gate elevation at the end of the flume, 24.8 cm in the former and 19 cm in the latter and consequently the bed elevation averaged on the flume length at the end of the runs. Water discharge and sediment feed rate were equal to that at equilibrium in Run 12 but their grain size distribution was that of the initial substrate, coarser that the sediment. transport rates at equilibrium in the recirculating runs When the flow and the sediment transport reached equilibrium, the channel slopes were slightly different (0.0052 m/m at the end of Run 13 and 0.0054 m/m at the end of Run 14) but always higher than the slope at the end of Run 11.

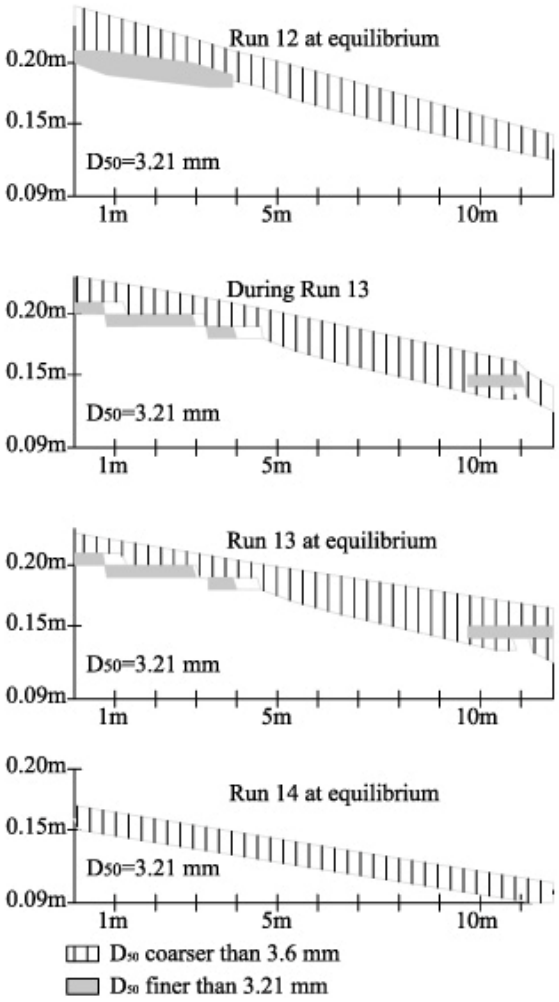

Figure 35 Variation of D_{50} in the vertical and in the streamwise direction for the numerical runs in a sediment feed flume.

During Run 13 the fine lens was eroded and deposited at the end of the flume on the coarser active layer of the initial bed. On the contrary, during Run 14, the water elevation at the end of the flume was low enough to erode the initial bed and at equilibrium only the division between the initial substrate and the active layer can be observed.

6.2 SEDIMENT FEED OR SEDIMENT RECIRCULATING FLUME?

In general, a water – feed flume can operate in two different modes: sediment – feed and sediment – recirculating. In a sediment – feed flume the water discharge is set by a supply pump, the upstream sediment transport rate is set by the sediment feeder and the downstream water elevation is set by the tail gate. In a sediment - recirculating flume water discharge is still set by a pump, downstream water elevation is set by the tail gate and the total amount of sediment in the system is a constant (if we assume

that the sediment stored in the recirculating line is negligible) (Parker 2003 and, 2004).

In the case of uniform grain size in a sediment - feed flume, the equilibrium bed profile depends on the water discharge and the sediment feed rate. In fact, the final state is independent of the water elevation set by the tail gate because the amount of sediment in the system can vary. In the case of a water – feed and sediment - recirculating flume the amount of sediment in the system is constant, and therefore the equilibrium bed profile depends on the tail gate elevation. This dependence is expressed in terms of a relation between the water depth and the channel slope at equilibrium (Parker, 2003). If initial conditions are the same, the final mobile-bed equilibrium is the same in both types of flumes.

When sediment is treated as a mixture of different grain sizes, mobile-bed equilibrium also depends on the feed sediment grain size distribution in a sediment – feed flume and on the grain size distribution of the initial bed in sediment – recirculating flume (Parker et al., 1993). Even when the initial conditions are the same, equilibrium differs between in the two types of flume because the stratigraphy of the deposit changes with the mode of feeding sediment. More specifically, in a sediment - feed flume the equilibrium bedload size distribution is equal to the sediment feed size distribution, whereas in a sediment – recirculating flume, the equilibrium bedload size distribution is a function of the process by which various grain sizes are stored in the bed during the approach to equilibrium.

In this paragraph numerical results are presented to compare equilibrium in

- a sediment – feed flume;
- a water – feed, sediment – recirculating flume.

Both the case of uniform material and the case of sediment mixtures are considered.

6.2.1 NUMERICAL EXPERIMENTS

Numerical experiments performed with the model are divided in two groups:

- experiments with uniform sediment to verify that the code predicts the same conditions of equilibrium for a sediment – feed and a sediment - recirculating flume, and to study how these conditions change for a variation of water discharge and gate elevation;
- experiments with sediment mixtures to compare equilibrium in the two type of flumes, to study how equilibrium changes with downstream gate elevation and

flow discharge and to discuss how the grain size distribution of the active layer and the vertical stratigraphy of the deposit varies with the mode of sediment delivery (feed or recirculating).

In all the experiments the laboratory flume and the sediment grain size distribution are those of physical experiments that were performed to test the model, see Chapter 5. The laboratory flume is 11.8 m long and 0.61 m wide with a plane bed that is initially set to be horizontal. The water elevation at the downstream end of the flume ξ_d is 29.3 cm and the water discharge is 40 l/s (Runs 15 and 16). When the flow and the sediment transport reach equilibrium, the downstream water elevation increases to 31.3 cm (Runs 17 and 18) and the water discharge decreases to 33 l/s (Runs 19 and 20).

The hypothesis of lower regime plane bed is verified considering that for coarse material (when the particle Reynolds number is much higher than 1) dunes do not form until the Shields parameter exceeds 0.0816 (Chabert et al., 1963).

Numerical experiments were run with a spatial step length of 20 cm and a maximum temporal step length of 10 seconds. If the maximum temporal interval causes numerical instability, the code computes a new temporal step length that satisfies a Courant condition for uniform material and very wide cross section.

Uniform sediment

The sediment considered in the following experiments has a geometric mean diameter of 3.39 mm and a D_{90} of 7.83mm.

In Table 11 experiments with uniform material are summarized. The sediment feed rates in Runs 16, 18 and 20 are equal to the bedload transport rate at equilibrium in the sediment – recirculating flume of Run 15.

Table 11: Initial and boundary conditions for the experiments with uniform material. Feed indicates a sediment – feed flume and Rec a sediment – recirculating flume. Q is the water discharge, ξ_d the downstream water elevation and G_s the transport rate.

Run	Flume	Q (l/s)	ξ_d (cm)	G_s (g/min)
15	Rec	40	29.3	2321
16	Feed	40	29.3	2321
17	Rec	40	31.3	407
18	Feed	40	31.3	2321
19	Rec	33	29.3	415
20	Feed	33	29.3	2321

In Table 12 results of the experiments are summarized. At the end of Runs 15 and 16 the condition of equilibrium is the same, but in a sediment recirculating flume the time for the flow and the sediment transport to reach equilibrium is longer than in a sediment - recirculating flume.

Table 12: Results of the numerical experiments with uniform sediment, where H is the water depth η_{av} is the average bed elevation above a datum, S is the average bed slope, τ_g* the Shields parameter, Fr is the Froude number and t_{eq} is the time for the flow and the sediment transport to reach equilibrium.

Run	H (cm)	η_{av} (cm)	S (m/m)	τ_g^*	Fr	t_{eq} (h)
15	0.079	23	0.0051	0.079	0.74	1.0
16	0.079	23	0.0051	0.079	0.74	6.1
17	0.061	23	0.0036	0.061	0.62	4.3
18	0.079	25	0.0051	0.079	0.74	7.3
19	0.062	23	0.0042	0.062	0.66	2.6
20	0.080	25	0.0060	0.080	0.78	7.5

This difference depends on the mode of sediment delivery in the two flumes: in a sediment feed flume the feed rate is constant while in a sediment – recirculating flume it varies in time because the sediment collected in the trap is recirculated. The variation of the sediment transport rate in space and time is shown in Figure 36 for a sediment – recirculating flume and in Figure 37 for a sediment – feed flume

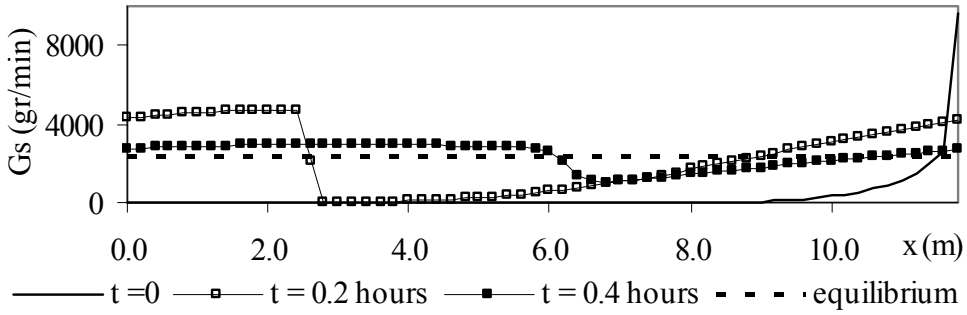

Figure 36 Variation of the sediment transport rate in space and time in a sediment – recirculating flume, i.e. Run 15.

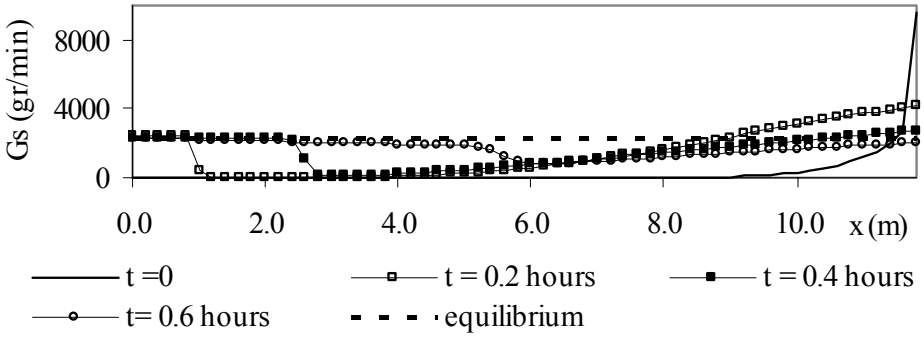

Figure 37 Variation of the sediment transport rate in space and time in a sediment – feed flume, i.e. Run 16

How the bed elevation changes in space and time in Runs 15, 17 and 19 and in Runs 16, 18, and 20 is shown in Figure 38 and Figure 39 respectively.

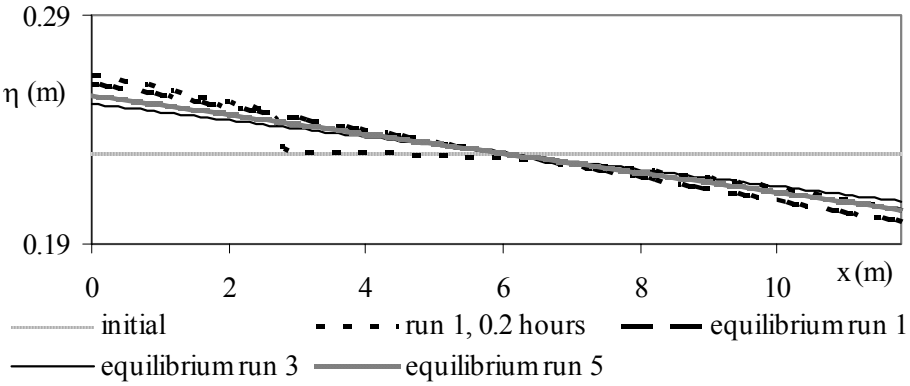

Figure 38 Longitudinal profiles in a water – feed and sediment –recirculating flume

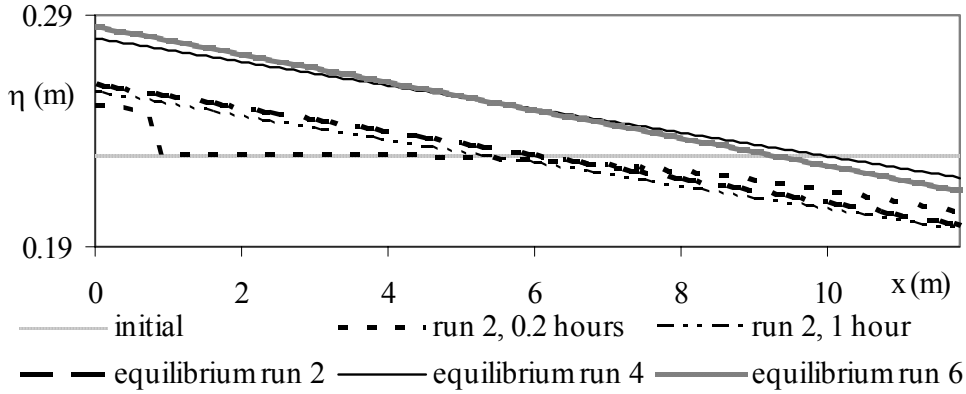

Figure 39 Longitudinal profiles in a sediment – feed flume

In a sediment – feed flume, where the feed rate is constant and smaller than the initial upstream transport rate of the sediment – recirculating flume, the amount of deposited material is smaller and so deposit progrades more slowly. The sediment transport rate increases again downstream because the flow is eroding the initial bed as it goes from an initially horizontal bed to one with a finite bed slope.

The initial condition for Runs 17 to 20 is the bed at equilibrium at the end of Runs 15 and 16. In Runs 17 and 18 and the water elevation at the downstream end of the flume was increased from 29.3 cm to 31.1 cm. In a water – feed and sediment – recirculating flume, where the total amount of sediment in the system is constant and equilibrium partially depends on initial conditions, the bed degrades upstream and aggrades downstream. The longitudinal profile rotates around a fixed point at the half-length of the flume, and consequently the bed slope and sediment transport rate decrease. On the contrary, in a sediment – feed flume, where equilibrium depends on

the discharge and the sediment feed rate, bed slope and sediment transport rate do not vary and the bed elevation averaged over the flume length increases from 23 cm to 25 cm.

In Runs 19 and 20 the discharge was decreased from 40 l/s to 33 l/s, but the gate elevation did not vary. In a sediment – recirculating flume the sediment transport rate and the bed slope drop. On the contrary, in a sediment – feed flume the bed aggrades and its slope increases because the discharge is smaller but the sediment – feed rate does not change.

Sediment mixtures

The initial bed and the sediment feed material of Runs 22, 24 and 26 have the grain size distribution shown in Figure 40. The Geometric mean diameter and D_{90} are the same as that of the uniform material of the previous set of experiments. In the same figure grain size distributions of bedload at equilibrium in Runs 21, 23 and 25 are shown.

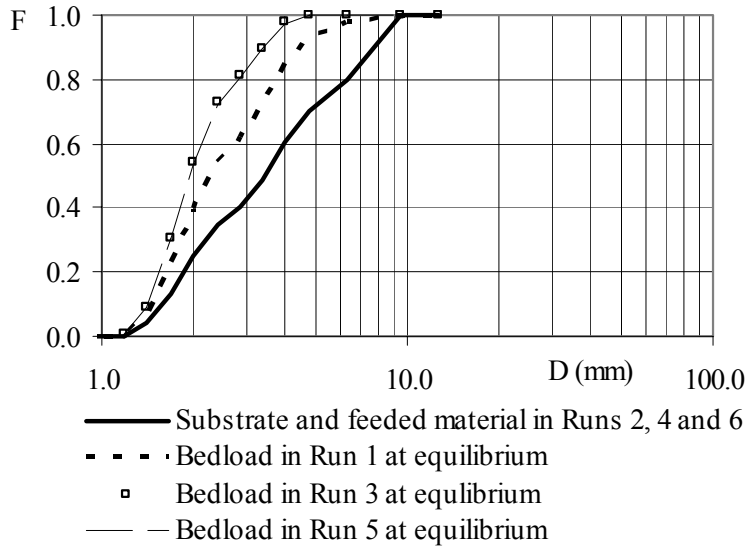

Figure 40 Grain size distributions of the substrate, the bedload and the sediment feed rate

The experiments with sediment mixtures are summarized inTable 13.

Results of the numerical experiments with sediment mixtures are summarized in Table 14 and Table 15.

Table 13: Initial and boundary condition for the experiments with sediment mixtures

Run	Flume	Q (l/s)	ξ_d (cm)	G_s (g/min)
21	Rec	40	29.3	1592
22	Feed	40	29.3	1592
23	Rec	40	31.3	195
24	Feed	40	31.3	1592
25	Rec	33	29.3	238
26	Feed	33	29.3	1592
27	Feed	40	29.3	1592
28	Feed	40	29.3	1592

Table 14: Results of the experiments with sediment mixtures. The Shields parameter has been computed with the geometric mean diameter of the active layer averaged on the flume length.

Run	H (cm)	η_{av} (cm)	S (m/m)	τ_g^*	Fr	t_{eq} (h)
21	9.3	23	0.0051	0.074	0.74	19.2
22	8.4	25.3	0.0074	0.069	0.86	17.2
23	10.4	23	0.0039	0.055	0.62	33.5
24	8.4	27.2	0.0075	0.069	0.86	12.3
25	8.8	23	0.0044	0.056	0.66	30.6
26	7.1	27.3	0.0087	0.069	0.91	12.5
27	9.3	23	0.0052	0.074	0.74	23.3
28	10.1	21.6	0.0039	0.078	0.65	37.5

Table 15: Characteristic diameters of the active layer (Ds) and of the bedload (Dl) at equilibrium averaged over the flume length

Run	D_{sg} (mm)	D_{s90} (mm)	D_{lg} (mm)	D_{l90} (mm)
21	3.72	8.16	2.46	4.47
22	5.22	8.99	3.39	7.83
23	3.93	8.24	2.04	3.33
24	5.22	8.99	3.39	7.83
25	3.83	8.21	2.05	3.4
26	5.22	8.99	3.39	7.83
27	3.75	8.24	2.46	4.47
28	2.9	7.73	2.04	3.33

In experiments with sediment mixtures the total bedload transport rate at equilibrium is smaller than in the experiments with uniform material. Consequently the time for the flow and sediment transport to reach equilibrium is longer.

In the numerical experiments the time to reach equilibrium in a sediment – feed flume is shorter than in a sediment – recirculating flume when the feeded material has the same grain size distribution of the substrate (Runs 22, 24 and 26). In Runs 27 and 28, the sediment feed has a grain size distribution finer than the initial bed and equal to the bedload at equilibrium in Runs 21 and 23, and the time for the flow and sediment to reach equilibrium is longer than in Run 21.

This result does not contradict the results of the experiments with uniform material, where the time for the flow and the sediment transport to reach equilibrium in a sediment – recirculating flume was smaller than in a sediment –feed flume (see Table 12). When sediment is considered as a mixture of different grain sizes, equilibrium depends not only on the water discharge and the sediment feed rate or the tail gate elevation, but also on the grain size distribution of the feed material in a sediment – feed flume and on the grain size distribution of the initial bed in a sediment – recirculating flume.

In Runs 21, 22 and 27 the grain size distribution of the initial bed is the same, but the feed material in Runs 22, 27 and 28 is different.

- In Run 22 the feed material is the same as the initial bed, and when the flow and the sediment transport reach equilibrium the bed slope is higher than in Run 21 and the average bed elevation increases. The geometric mean diameter and the D_{90} of the bedload and of the active layer are coarser than in Run 21.
- In Run 27 the feed material has the same grain size distribution as the bedload at equilibrium in Run 21, and at equilibrium the channel slope and the bed elevation averaged over the flume length are the same as Run 21. The geometric mean diameter and the D_{90} of the bedload and of the active layer are not significantly different from the same diameters at equilibrium for Run 21.
- In Run 28 the feed sediment has the same grain size distribution as the bedload at equilibrium in Run 23, which is finer than the sediment feed in Run 27. When the flow and the sediment transport reach equilibrium the channel slope and the bed elevation averaged over the flume length are smaller than at the end of Run 21. The channel slope at equilibrium is equal to the slope at the end of Run 23 but initial and boundary conditions are different: in Run 23 the initial bed is the bed at equilibrium at the end of Run 21, the gate elevation is higher than in Run 28 and the total bedload transport rate at equilibrium is much smaller than the sediment feed rate of Run 28. The difference in the sediment transport rate at equilibrium causes a higher shear stress in Run 28 and a finer grain size distribution of the active layer.

The initial condition for Runs 23 to 26 are the equilibrium conditions for Runs 21 and 22. Therefore the initial bed has a stratigraphy that varies in the streamwise direction. For Runs 23 and 24 the water elevation at the downstream end of the channel increases from 29.3 to 31.1 cm. In a sediment – recirculating flume this variation

causes erosion in the upstream half of the flume and deposition downstream, as in Run 23 with uniform material. The bed slope and the sediment transport rate decrease, the bedload becomes finer and the active layer becomes coarser because the bigger particles cannot be entrained into bedload. In a sediment – feed flume, the bed elevation averaged over the flume length is the only parameter that varies, and it increases from 25.3 cm to 27.2 cm.

In Runs 5 and 6 the water discharge decreases from 40 l/s to 33 l/s, as in Runs 25 and 26 with uniform material. In a sediment –recirculating flume the channel slope and the bedload transport rate decrease, the bedload becomes finer and the active layer becomes coarser. In a sediment – feed flume bed elevation averaged over the flume length and channel slope increase, but the grain size distributions of the active layer and the sediment load do not vary.

Grain size distribution of the active layer

The variation of the size D_{s90} is represented in Figure 41. At equilibrium in Runs 22, 24, 26 the active layer is coarser in the upstream part of the flume, while in Runs 21, 23, 25 and 26 D_{s90} is almost constant. In Run 28, where the sediment feed rate is much finer than the substrate, D_{s90} at equilibrium increases in the streamwise direction.

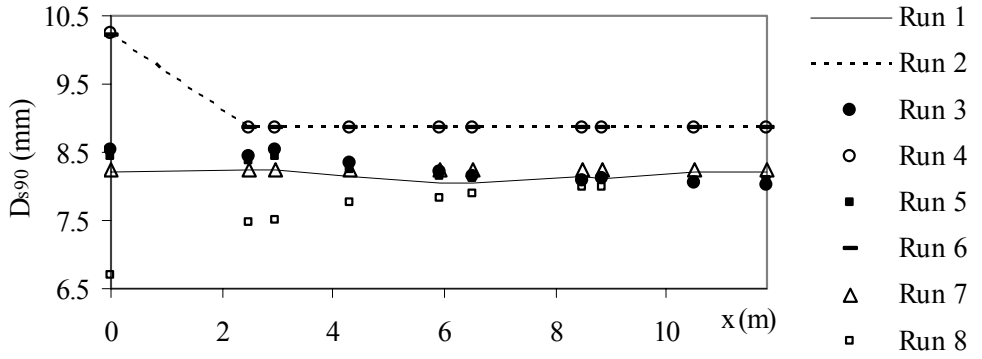

Figure 41 Downstream variation of the size D_{s90} at equilibrium

The variation of the active layer grain size distribution in Runs 22, 24, 26 and 28 depends on the definition of equilibrium. For the present code the flow and the sediment transport reach equilibrium when the total bedload transport rate is fairly constant for the flume length: if the transport rate is constant there is nor net erosion nor net deposition. The numerical condition to define equilibrium is that the coefficient of variation of the total bedload transport rate is smaller than 0.001.

To verify that the downstream variation of the active layer grain size distribution is a consequence of the definition of equilibrium, two more numerical tests have been performed; the results are described in Table 16. Initial and boundary conditions are the same of Run 22 but the runs continue for 70 and140 hours.

Table 16: Results of the two experiments that do not end when the flow and the sediment transport reach equilibrium.

Run	H (m)	S (m/m)	D_{sg} (mm)	D_{s90} (mm)
22 for 70 hours	8.4	0.0076	5.37	9.53
22 for 140 hours	8.4	0.0078	5.43	10.22

In Figure 42 the variation of the D_{s90} in space and time is presented. The active layer becomes coarser and the channel slope becomes steeper as the time passes.
After 70 hours the coarser front reaches the half-length of the flume, and after 140 hours the grain size distribution of the active layer does not vary in the streamwise direction.

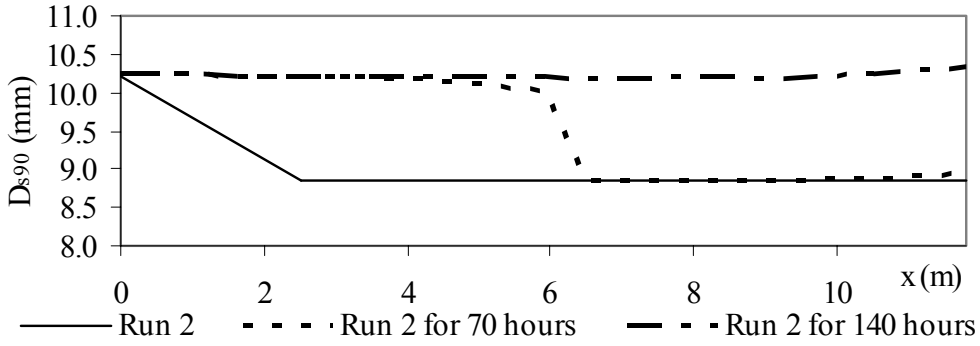

Figure 42 Variation in space and time of D_{s90}

Vertical stratigraphy

Deposits in a sediment - recirculating flume are generally not as thick as in a sediment – feed flume because the bed elevation averaged on the flume length is constant. In a sediment – feed flume the total amount of material in the system is not constant, and so it is easier to build a deposit with a grain size distribution that varies in the vertical and in the streamwise direction. The difference between the two type of flumes is shown in Figure 43 and Figure 44, where stratigraphy is plotted at equilibrium of Run 21 and 22.

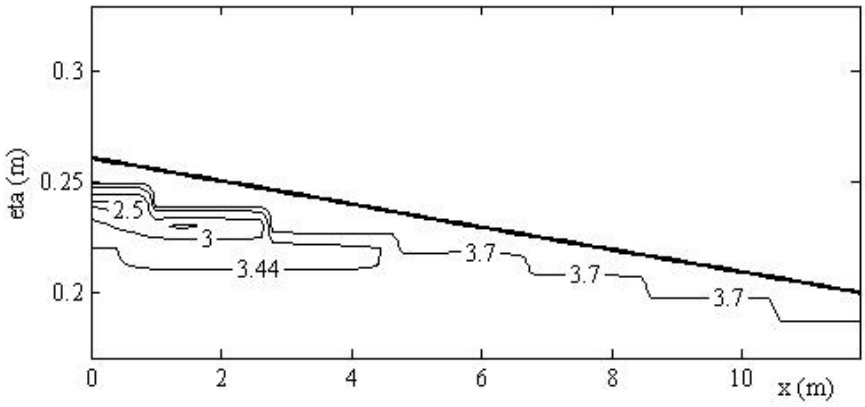

Figure 43 Variation in the vertical and in the streamwise direction of the size D_{50} at the end of Run 21

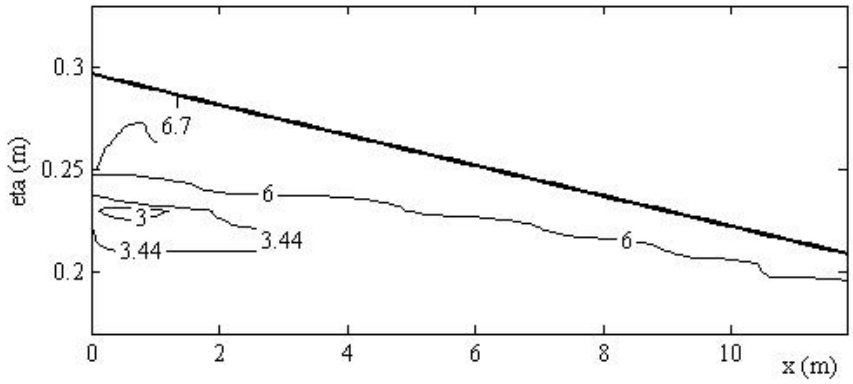

Figure 44 Variation in the vertical and in the streamwise direction of the size D_{50} at the end of Run 22

The original substrate is the same in the two runs but in Run 22 the deposit is much coarser that in Run 1, because the sediment feed is coarser than the bedload in Run 21. The larger particles are deposited and the finer fraction reaches the end of the flume and move out of the system. Moreover, in the model the version of the procedure to store the stratigraphy of deposits that considers front progradation is implemented and so the coarse active layer only is transferred to the substrate.

In Run 21 (Figure 43) a finer lens is deposited at the upstream end of the flume because at the beginning of the run the bed is horizontal and the finer particles are entrained into bedload in the downstream part of the flume. They reach the sediment trap and then they are deposited at the upstream end of the flume. In the same figure the variation in the downstream direction of the size D_{s50} is shown.

In Figure 45 the vertical stratigraphy at the end of Run 27, where the sediment feed has the same grain size distribution as the bedload at equilibrium in Run 21, is presented.

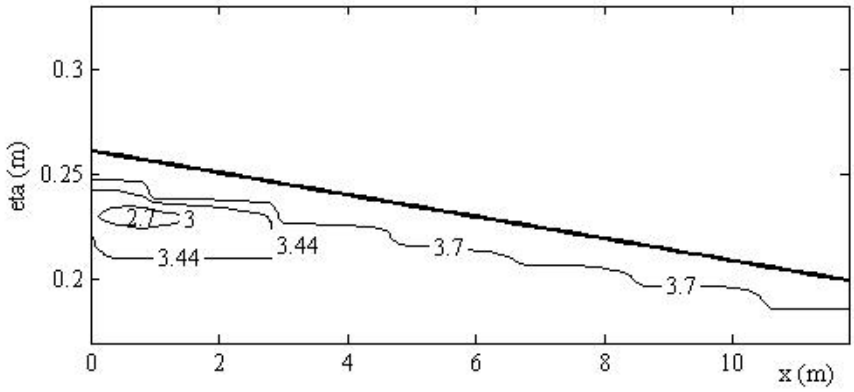

Figure 45 Variation in the vertical and in the streamwise direction of the size D_{50} at the end of Run 27

The deposits in Run 27 have a much finer grain size distribution than in Run 22, and the bed at equilibrium has the same characteristics as the bed at the end of Run 21. The difference between the deposits in Run 21 and 27 is the fine lens at the upstream end of the flume. The lens is not in the same place in the two runs because at the beginning of Run 27 all the feed material is deposited, the coarse fraction first and then the finer particles. Then the deposit progrades and coarser material is deposited on the fine lens and fine material is again deposited downstream, if it is not entrained into bedload.

In Run 24 the bed aggrades because the tail gate elevation increases, the water elevation increases in the streamwise direction and the flow deposits the coarser particles in the downstream part of the flume, where the water depth is higher and the shear stress is smaller. When the deposit reaches the upstream end of the flume, the flow deposits more material in the upstream part to so as to attain the initial slope, as shown in Figure 46.

At the downstream end of the flume there is a thin lens of finer material that has been deposited at the beginning of the run. when the sediment transport rate at the downstream end of the flume dropped and deposition started.

In Figure 47 the final stratigraphy of the bed is presented for Run 24.

In Run 26 aggradation began at the upstream end of the flume because the discharge decreases but the sediment feed rate remains constant. In Figure 48 and Figure 49 longitudinal profiles and the final stratigraphies are presented for this run.

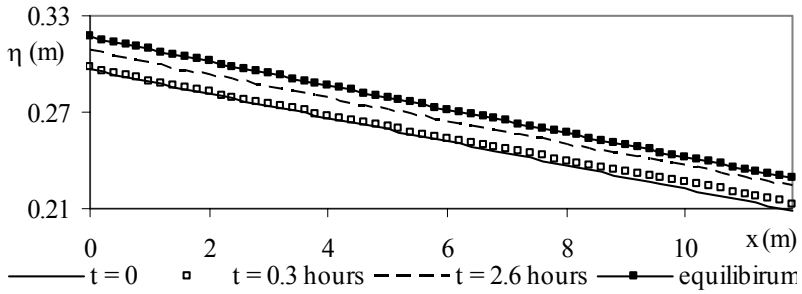

Figure 46 Longitudinal profiles in Run 24

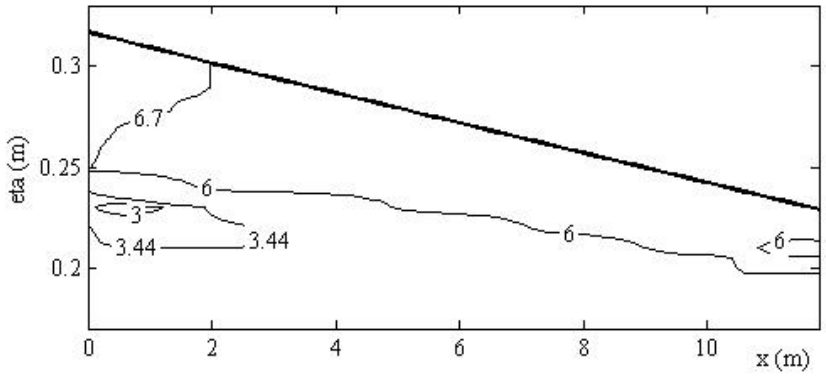

Figure 47 Variation in the vertical and in the streamwise direction of the D_{50} at the end of Run 24

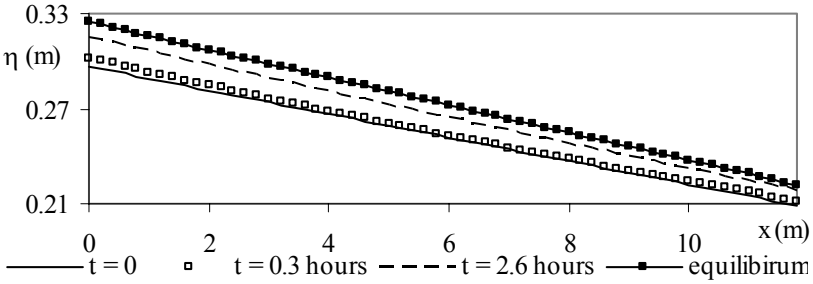

Figure 48 Longitudinal profiles in Run 26

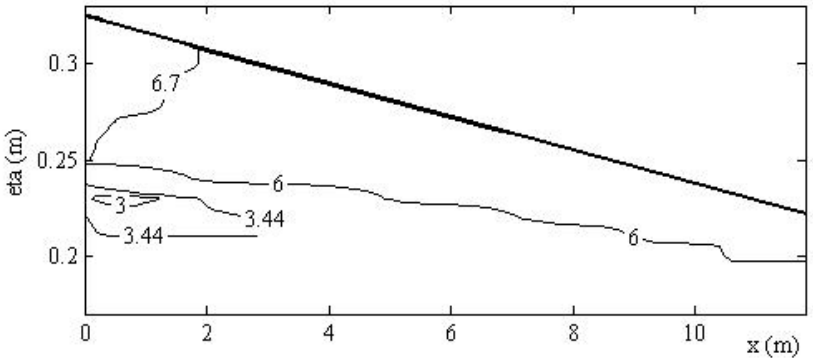

Figure 49 Variation in the vertical and in the streamwise direction of the D_{50} at the end of Run 26

When the flow and the sediment transport reach equilibrium, a variation in the downstream direction of the D_{s50} can be observed in Figure 47 and Figure 49.

It is important to notice that in the sediment feed runs, when the thickness of the deposited material is considerably higher than that of the active layer, the sharp division between active layer and substrate can not be observed because of the mode of transferring material to the deposits. This result can not be considered realistic because in sediment feed flume experiments the coarser active layer was always observed and because in river systems the substrate has a grain size distribution similar to the bedload input rate, that depends on the characteristic of the basin.

It is possible to conclude that the original version of the procedure to store and access the stratigraphy can reproduce the grain size distribution of deposits when the vertical sorting is not caused by a front migration. The modified version of the procedure gives a better agreement with laboratory data obtained in a water feed and sediment recirculating flume, where the total amount of material in the system is constant, but it gives unrealistically coarse deposits in a sediment feed flume.

7 APPLICATION TO THE TRINITY RIVER IN CALIFORNIA

In 1955 the Congress authorized the construction of the Trinity River Diversion of the Central Valley Project to divert water from the Trinity River Basin to the Sacramento River Basin and the Central Valley, for the development of important agricultural activities. The Trinity River Diversion consists of two dams: the Trinity Dam and the Lewiston Dam, approximately 13 km (8 miles) downstream of the Trinity Dam. The Trinity Dam is an earthfill structure 164 m (538 ft) high with a crest length of 747 m (2450 ft) that stores and regulates the flow for water supply, irrigation and production of electrical energy. The Lewiston dam is a earthfill structure smaller than the Trinity Dam (i.e. 28 m or 91 ft high with a crest length of 230 m or 754 ft) that regulates the releases into the Trinity River and the diversion to the Central Valley.

Construction works ended in 1963 and approximately the 90% of the water was diverted to the Central Valley. The released discharges raged between 4 and 8 m^3/s (150 – 250 cfs) for the next decade. This variation in flow regime caused several changes in the river reach downstream Lewiston Dam: it allowed riparian vegetation to grow, the mainstem could not migrate in the floodplain for the reduction of flood discharge and a significant coarsening of the surface layer was observed. Moreover, the flow in the mainstem was too low to transport the sediment supplied from the tributaries with a consequent formation of deltas at the confluences and the deposition of sand in the pools. The described variation of fluvial ecosystem caused a strong decrease of salmonid population.

In the second half of the 1970 the Californian Department of Fish and Games asked for an increase in flow release to partially restore the pre - dam fluvial ecosystem and to increase the salmonid population. In the 1990s a new increase of the release from Lewiston Dam was planned to restore the salmonid population of the Trinity River.

An increase of flow discharge is important but not sufficient to improve the fluvial ecosystem and to increase the salmonid population because the seasonal variability of the flow and many other parameters, such as water temperature, flow velocity, surface layer grain size distribution, river morphology, …, have to be considered. Therefore, since the 2000, an hydrograph is released from Lewiston Dam depending on the water year classification: extremely wet, wet, normal, dry and extremely dry.

The procedure to store and access the stratigraphy of non cohesive deposits presented in the previous Chapters was implemented in a numerical model to describe the effects of an hydrograph on a gravel bed river reach in terms of channel slope, bed shear stress and grain size distribution of the bed. This model was calibrated on the Trinity River for the pre - dam regime and for the post – dam period characterized by very low flows. The presented model is a useful tool to design river restoration activities based on the regulation of water discharge and sediment input rates.
In the following paragraphs a brief description of the Trinity River is presented to define the problem and to justify the input of the numerical runs. It is followed by the explanation o f the numerical model and the validation against field data.

7.1 SITE DESCRIPTION

The Trinity River is the largest tributary of the Klamath River in Northwest California. Before the construction of Trinity and Lewiston Dams it was densely populated by chinook and coho salmons and steelhead trout. Its mainstem originates from the Scott Mountains, Eddy Mountains, and Salmon-Trinity Alps of Northern California approximately 96 km (60 mile) upstream of Trinity Dam. The regulated mainstem, from Lewiston Dam to the confluence with the Klamath River, is approximately 180 km (112 miles) long and it received water and sediment from several tributaries. From the confluence with the Trinity River, the Klamath River flows for 70 km (43 miles) before discharging into the Pacific Ocean. The Trinity River watershed, excluding the South Fork, is 5271 km^2 (2036 mi^2) wide in a mountainous and scarcely populated area. Tributaries flows in V – shaped valleys and the elevation varies between more than 2740 m (9000ft) in the Trinity Alps and 90 m (300 ft) at the confluence with the Klamath River (Sediment source analysis for the mainstem of the Trinity River, 2001). A map of the Trinity River basin from its headwater to the studied reach is reported in Figure 50 and Figure 51.
Very few data are available to reconstruct the pre – dam Trinity River morphology because the area has been widely disturbed by human activities since the second half of the 1800 with the gold mining. Before the mining the Trinity River from Trinity Dam to the confluence with the North Fork was alluvial with a wide floodplain in reaches unconfined by valley walls. During the gold mining the fluvial environment was deeply modified because a lot of sediment was released in the mainstem and later most of the natural channels were dredged from one valley bank to the other.

Figure 50 Trinity River above Trinity Dam, from Sediment Source Analysis for the Mainstem Trinity River

Figure 51 Trinity River below Trinity Dam, from Sediment Source Analysis for the Mainstem Trinity River

The sediment input rate in the mainstem increased also for timber harvest that begun in the second half of the 1800 during the gold rush and continued for more than 100 years. Even if human activities caused the destruction of terraces, tailings were left everywhere in the valley and the sediment supply and the turbidity of the water increased, the population of salmons and trout in the river did not considerably decrease (Trinity River Flow Evaluation, 1999).

Historical pictures of the Trinity River below Lewiston dam show that the unregulated river was characterized by the alternation of low slope alluvial and bedrock controlled reaches, Figure 52.

Figure 52 Pre – dam Trinity River near Lewiston from Trinity River Flow Evaluation;

In alluvial reaches the channel migrated and avulsed across the valley floor over time; these reaches were characterized by alternate bars or by the mainstem wandering among the tailings and alluvial deposits shaping its cross section.

7.1.1 PRE – DAM HYDROLOGY

The climate of the Trinity River basin is characterized by precipitation in late fall, winter and spring, that are generally originated from storms coming from the Pacific Ocean. Temperature are generally colder in winter and warmer during the summer for the moderating effect of the ocean. Snow levels vary across the basin from one storm to the other; in general above the 2100 m (7000 ft) precipitation falls as snow while lower areas receive precipitation as rain. The boundary zone between rain and snow precipitation plays a very important role on run – off events: most large floods are due to warm rain falling on deep snow packs (Sediment source analysis for the mainstem of the Trinity River, 2001).

The pre – dam hydrology was characterized by a high flow variability: during rain – on –snow events the peak discharge at Lewiston (the area of the watershed is 1841

km^2 or 711 mi^2) could exceed the 1980 m^3/s (70000 cfs) while during the summer drought discharges of 3 m^3/s (100 cfs) were measured. The water year was generally characterized by a winter baseflow ranging between 14 and 85 m^3/s (500 and 3000 cfs) and some winter floods from November to March, a spring snowmelt runoff from March to July with its peak, generally smaller than the winter peak, between March and June and a summer baseflow ranging between 1 and 8.5 m^3/s (25 – 300 cfs).
This variability in flow discharges was responsible of the channel morphology for the development of an environment where the population of salmonid and trout could live: winter floods could mobilize all the material and cause channel migration over the valley floor, more frequent spring snowmelt peaks were responsible of smaller – scale benefits such as the control of the growth of riparian vegetation.

7.1.2 POST – DAM EVOLUTION OF THE MAINSTEM OF THE TRINITY RIVER

After the construction of the dams the seasonal variability of discharges was substituted with a constant discharge of 7 – 8 m^3/s (150 – 250 cfs). The consequences of such a sudden change in flow regime were noticeable not only on the river morphology but also on the vegetation and on the wildlife.
With the regulation of flow releases there were not winter floods, responsible for the formation and the migration of the alternate bars, anymore and the mainstem remained fix in the valley floor and the riparian vegetation grew in the river channel forming riparian berms on the banks, Figure 53.

Figure 53 Post dam Trinity River, from the Trinity River Flow Evaluation;

For the reduction of flow and sediment transport the sequence of riffles and pools, that represents the natural salmonid habitat, was substituted by a trapezoidal channel confined between riparian berms with a flat environment that is not appropriate for salmons. Moreover, flow discharges were not able to mobilize the coarser fraction of bed material and a significant coarsening of the bed surface was observed. The low flow in the mainstem can not carry downstream the sediment delivered from tributaries and so aggrading deltas formed, Figure 54.

Figure 54 Rush Creek delta

Coarser particles deposited at the confluences; part of the finer fraction was carried downstream in the mainstem and deposited in the deep pools over the coarser pre – dam bed.

The available data show that since the construction of the dams the natural spawning population of salmons dramatically reduced: the percent reduction of chinook salmon is the 68%, for coho salmons it is the 98% and for steelhead trout it is the 53%.

To restore the Trinity River below Lewiston Dam the regulated flow was increased and, as reported in Table 17, the annual released volume depends on the water year. To reproduce the seasonal variability of flow discharges five hydrographs, reported in Figure 55, were defined. They are characterized by a winter baseflow of 8.5 m^3/s (300 cfs) and the summer baseflow of 12.7 m^3/s (450 cfs) and the difference between the water years is on the spring peak discharge released for 5 days. According to filed

data, in wet years the peak snowmelt happens later in the spring than in dry years (Trinity River Flow Evaluation, 1999).

Table 17: Volumes of water annually released from Lewiston Dam since 2000

Water year	Released volume in thousands acre - feet	Released volume in millions of cubic meters
Extremely wet	140	173
Wet	815.2	1006
Normal	701	865
Dry	646.9	798
Critically dry	452.6	558

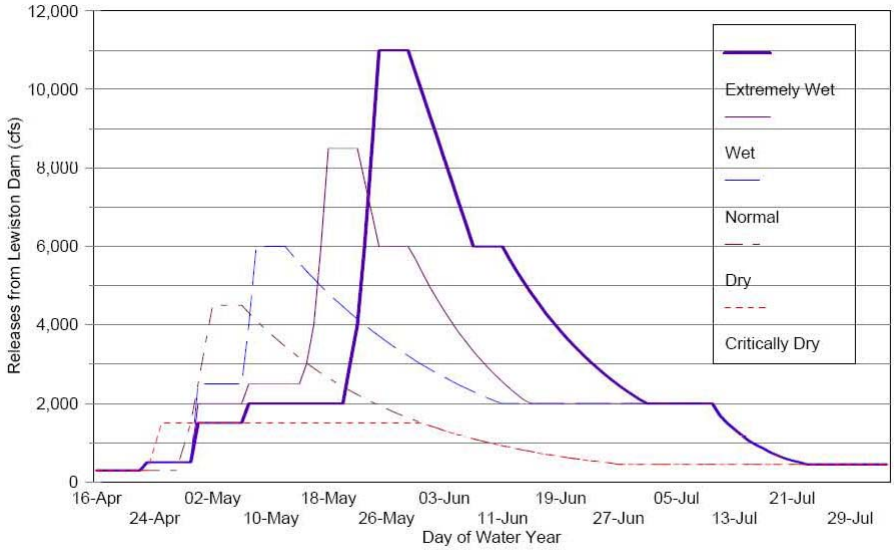

Figure 55 Hydrograph released from Lewiston Dam, from the Trinity River Flow Evaluation;

7.1.3 THE STUDIED REACH

The studied reach of the Trinity River goes from Lewiston Dam at river mile 112 to the confluence with Weaver Creek, at river mile 94. The reach is characterized by several small tributaries and can be divided in three parts:

- the upper part, from the new bridge at river mile 111, just below the confluence with Deadwood Creek, to the confluence with Rush Creek at river mile 108. Deadwood Creek drains a small basin of 23 km^2 (8.9 mi^2) and its bed material is made of coarse gravel. The tributaries of the reach are Hoadley Gulch, with a basin of 9 km^2 (3.8 mi^2), and Alder Gulch that carry a small amount of fine sediment in the mainstem. Rush Creek drains a 58.5 km^2 (22.6 mi^2) basin in the Trinity River hydraulic right. A sediment sampling station is located just upstream of the confluence with Hoadley Gulch. The confluence

with Rush Creek is characterized by a delta of coarse sediment that causes a backwater profile in the downstream part of the reach;

- the middle part, from river mile 108 to the confluence with Grass Valley Creek at river mile 104 – 105 A sediment sampling station is located approximately at river mile 105. Grass Valley Creek drain a 95.3 km^2 (36.8 mi^2) basin and, like most of the tributaries in hydraulic left, it transports fine sediment. This material is collected in four ponds located just upstream of the confluence. The ponds were built to prevent fine sediment input rates in the mainstem, because fine particles deposit in deep pools where salmons spawn;
- the lower reach, from the confluence with Grass Valley Creek to the confluence with Weaver Creek, at river mile 94. This reach is characterized by bedrock exposure and can not be properly modeled with the code presented in this paper because the numerical model applies to alluvial rivers only.

In the present Chapter, pre – dam numerical runs refer to the first two reaches of the Trinity River because the watershed from river mile 111 to river mile 104 does not increase significantly and input parameters can be considered constant. On the contrary, post – dam conditions, from 1963 to 2000, will be simulated on the upper part only because the increase of discharges at the confluence with Grass Valley Creek can not be neglected and an input hydrograph for the middle reach can not be defined because of the lack of data.

7.2 THE NUMERICAL MODEL

The numerical model to describe the evolution of a river reach for an imposed hydrograph and sediment input rate has the same structure of other one – dimensional models of river morphodynamic because it is based on the physical principles of mass and momentum conservation for water and of mass conservation for sediment (Wright et al., 2005). Considering that the model applies to gravel bed streams where the material is generally poorly sorted, sediment is modeled as a mixture of different sizes and a grain size based equation of conservation of mass for sediment was also implemented to describe the variation in space and time of the grain size distribution of the bed (Parker, 1991a).

Its main and innovative characteristics are that the annual variability of the water discharges is described with an hydrograph derived from the mean flow duration curve, the variability of the channel width with water discharge is considered and the

procedure to store and access the stratigraphy of deposits is implemented with an active layer formulation.

The load relation implemented in the numerical model is that of Wilcock and Crowe (2003), see Chapter 2, and the closure relation to evaluate the bed shear stress, and consequently the Shields parameter is

$$\tau = \rho g H S \qquad \tau^*_{sg} = \frac{H \cdot S}{R \cdot D_{sg}} \tag{77}$$

7.2.1 THE INPUT HYDROGRAPH

The annual variability of flow discharges can not be described in terms of a constant characteristic discharge and a flow intermittency because the model has been developed to predict the effect of a released hydrograph on the Trinity River and to design restoration projects based on seasonal variability of water discharges, sediment input rates and their grain size distributions. The input hydrograph, derived from the flow duration curve, has to be divided in a series of W constant water discharges of duration Δt_w, as shown in Figure 56 for the Trinity River at Lewiston.

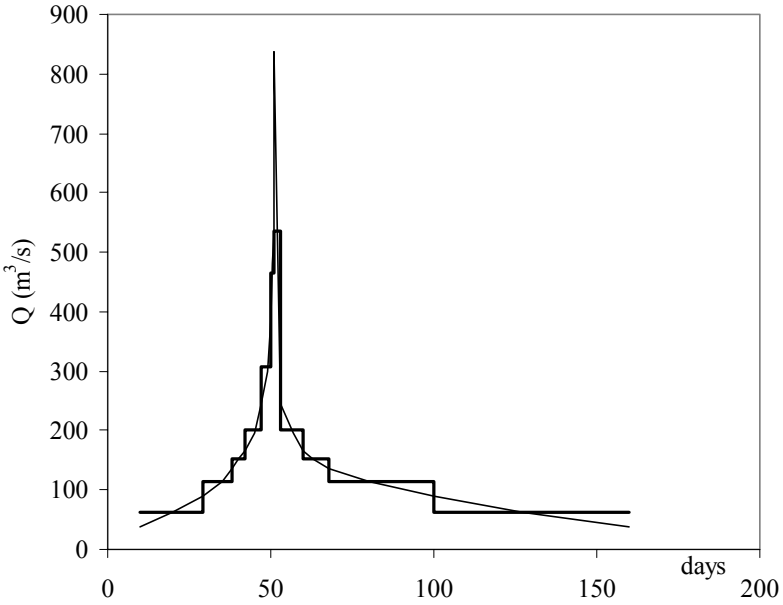

Figure 56 The thin line represents the hydrograph at Trinity River at Lewiston derived from the flow duration curve and the thick line represent its discretization for W = 11

The river is considered morphologically inactive when it is not in flood (Parker, 2004). To calculate the bed evolution during a flood a new time step for flood conditions, Δt_f, smaller than the time step Δt_w, has to be specified. The relation between Δt_w and Δt_f is

$$\Delta t_w = n_{step} \cdot \Delta t_f \tag{78}$$

where n_{step} represents the number of calculations done for each value of flow discharge. It is convenient to choose each flow duration Δt_w so that n_{step} is integer. In the numerical runs described in the following paragraphs Δt_f was equal to half a day and n_{step} varied between 0.2 and 66.

When water discharge is expressed as an input hydrograph, its evolution in the downstream direction should be considered. In a relatively short reach of a gravel bed stream without tributaries, the variation of the hydrograph can be reasonably neglected and it is assumed that the discharge is the same in each node.

To avoid numerical instability due to the variation of the water discharge with time, the normal flow assumption has been introduced. According to a Manning – Strickler formulation, the water depth in each node, H, is computed as:

$$H = \left(\frac{q_w^2 \cdot k_s^{1/3}}{\alpha_r^2 \cdot g \cdot S} \right) \tag{79}$$

where α_r is a coefficient in the Manning – Strickler resistance relation equal to 8.1 in the numerical runs (Parker, 1991b), g is the acceleration of gravity, S is the channel slope, q_w is the water discharge per unit width, that varies in time and k_s is the roughness height evaluated with equation (31) where n_k is equal to 2.

To compute the channel width with the flow discharge, the following equation was considered:

$$\begin{aligned} \frac{B}{B_{bf}} &= \left(\frac{Q}{Q_{bf}} \right)^n \quad \text{if} \quad Q \le Q_{bf} \\ B &= B_{bf} \quad \text{if} \quad Q > Q_{bf} \end{aligned} \tag{80}$$

where B is the channel width, B_{bf} is its bankfull value, Q is the flow discharge and Q_{bf} is the bankfull value. Pre – dam field data show that the bankfull width in the pre – dam condition in the Trinity River below Lewiston Dam varies between 75 and 85 m (250 – 280 ft) and in the pre – dam numerical simulations it is assumed to be 80 m. The definition of the pre – dam bankfull discharge is a delicate matter because it is difficult to define what is bankfull in a river, like the pre –dam Trinity River, where the cross section is not well incised in the bed and for higher flow the mainstem wandered in the valley. The analysis of the pre – dam data, recorded at the cableway and represented in Figure 57 shows that for discharges of 350 - 400 m^3/s (12000 -

14000 cfs) the relation between discharge and depth changes while the channel width can be considered constant and approximately equal to 80 m.

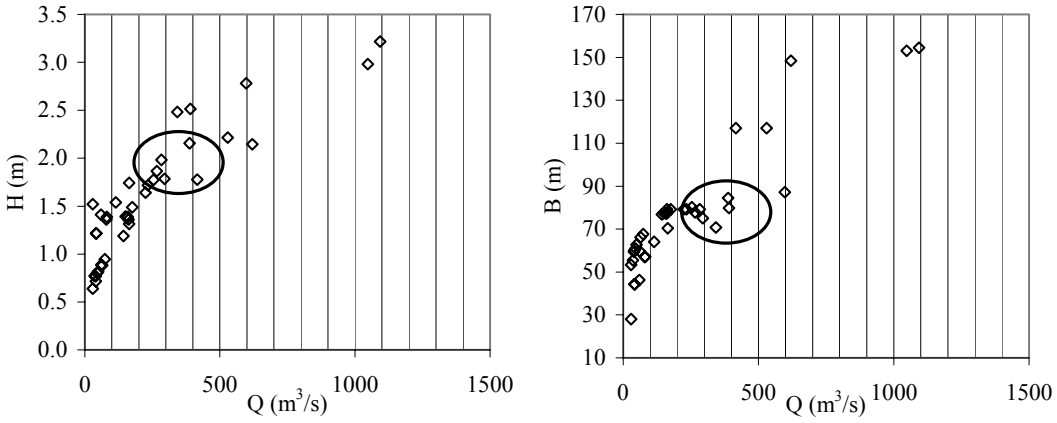

Figure 57 Pre – dam values of water discharge Q, water depth H and channel width recorded at the cableway

For higher discharges the water depth increases more slowly and a significant increase in channel width can be observed. In the pre – dam simulations a discharge of 370 m^3/s (13000 cfs) will be considered bankfull and the exponent 'n' in equation (80) is equal to 0.23.

7.2.2 INITIAL AND BOUNDARY CONDITIONS

The numerical problem is second order in x, streamwise coordinate, and first order in t, temporal coordinate, and so one initial and two boundary conditions are required for its solution (Parker, 2004).

The initial condition is expressed in terms of initial longitudinal profile and grain size distributions of the surface layer and of the substrate. The initial bed elevation is computed as a linear function of the initial channel slope, S_{fbl}, and downstream elevation, η_d:

$$\eta\big|_{t=0} = \eta_d\big|_{t=0} + \left(x - \frac{L}{2}\right) \cdot S\big|_{t=0} \tag{81}$$

where L is the reach length.

The upstream boundary condition is represented by the input hydrograph and the mean annual bedload input rate with its grain size distribution, that is assumed to be constant when the river is morphologically inactive.

The downstream boundary condition is expressed in terms of fixed bed elevation at the downstream node, that should be placed at a bedrock exposure, when this point is not available the downstream boundary condition can be placed (Parker, 2004)

-further downstream not to affect the computations for the time span of interest;
-in a confluence with a much larger river;
-where the water elevation is known.

7.3 PRE DAM CONDITIONS

The numerical model described in the previous paragraph was calibrated on the upper and middle part of the studied reach of the Trinity River, from river mile 111 to river mile 105 – 104. The reach length is approximately 10 km (6 -7 miles) and the input hydrograph represented in Figure 56 was derived from the data recorded at the Lewiston USGS station at river mile 111, where data were recorded since water year 1911. Numerical runs have been performed for a very long time to obtain a constant longitudinal profile that represents the pre – dam condition of mobile bed equilibrium. The computed channel slopes and the grain size distributions of the surface layer and of the substrate will be tested against field data to verify the model.
The pre – dam input hydrograph was derived from the flow duration curve computed with a 48 years long historical series of daily discharges from water year 1911 to water year 1959, when construction works started. In Figure 58 the historical series of daily discharges at Lewiston is represented to show the seasonal variability of the flow in the unregulated Trinity River and the thick horizontal line represents the bankfull discharge.

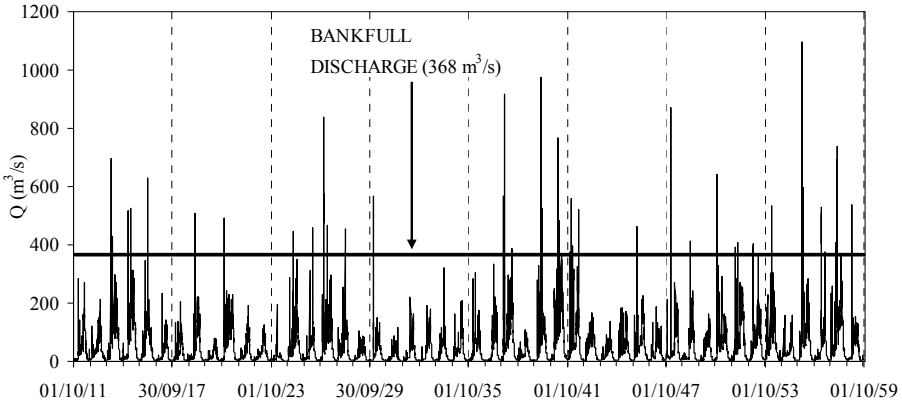

Figure 58 Historical series of daily discharges recorded at the USGS station at Lewiston from 1911 to 1959

The grain size distribution of the substrate is represented in Figure 59 and it is assumed that the substrate and the longitudinal profile did not change since the 1963 because the regulated flow was too low to erode the bed even if the sediment input rate was blocked by the dams.

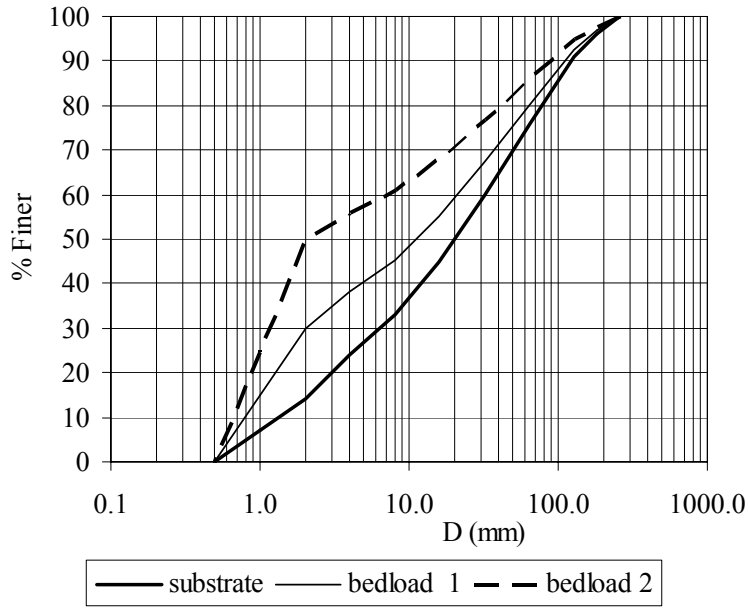

Figure 59 Grain size distributions of the substrate and of the bedload input rates in hypothesis 1 and 2

The initial bed does not have a coarser surface layer because the pre – dam grin size distribution of the bed surface is unknown. Considering that the pre – dam Trinity River was densely populated by salmons, characteristic diameters of the surface layer at equilibrium should be similar to the diameters that biologists consider typical in an healthy environment for these fishes.

The hardest parameter to evaluate is the mean annual bedload input rate and its grain size distribution. Sediment input rates have been estimated comparing the bathymetry of the deltas of Stuart Fork, Mule Creek and East Stuart Fork, with detailed maps that the Bureau of Reclamation prepared before the construction of the dams in 1957. Bathymetric measurements of the Stuart Fork delta were performed in 2001 (Sediment Source Analysis for the Mainstem Trinity River) while the other two deltas were surveyed in 2005 (Upper Trinity Sediment Source Analysis) and it is assumed that deposition started when the dam was closed in 1961. To convert the measured volume in a weight it was assumed that the bulk density of the material is 1.76 t/m^3 (110 lb/ft^3). In Table 18 results from the delta surveys are reported and a first estimate of the mean annual sediment yield for the three tributaries is presented.

The grain size distribution of the sediment yield is approximately characterized by the 10 – 30 % of clay, that is probably in suspension and it travels further in the lake, the 37 – 43 % is silt, that is mostly stored in the deltas and the rest is made of sand and gravel. In the Sediment Source

Table 18: Data from the delta survey

Delta	Net Fill (m^3)	Net Fill (tons)	WS Area (km^2)	years	Yield (tons/km^2/yr)
Stuart Fork	195764	348955	162	40	53.9
EF Stuart F	294602	525136	59	44	204.0
Mule Ck	128903	229773	16	44	320.2

Analysis reports the sediment yield from delta surveys is compared with results coming from the study of erosional processes and landslides in the watershed. The basin was divided in sub-basins and for each of them a mean annual sediment yield was estimates and the results varied between 56 and 211 tons/km^2/yr (160 – 600 English tons/mi^2/yr). Comparing the different procedures described in the reports, the mean annual sediment input rate in the reservoir was estimated to be 159406 tons/yr. The watershed area of the Trinity Lake is 1727 km^2 (667 mi^2) and so the sediment yield per unit area is 92 tons/km^2/yr (263 English tons/mi^2/yr).

Input parameter of the numerical model is the mean annual bedload input rate, therefore the fine fraction should be removed from the computed sediment yield because it is mainly transported further downstream in suspension and it is not involved in the processes of erosion, deposition and variation of the surface layer grain size distribution that are discussed in the present work.

To evaluate the mean annual bedload input rate three different hypothesis will be considered:

1) the fraction of material transported as bedload is equal to one third of the total sediment yield and the 30% of its grain size distribution is made of coarse sand (D = 0.5 – 2 mm): the annual yield is 30.5 tons/km^2/yr and the bedload input rate at Lewiston is 56706 t/yr with the same grain size distribution of the substrate. This hypothesis was introduced because one third of the surveyed deltas are made of coarse sediment;
2) the mean annual bedload input rate is the same of the previous scenario but the grain size distribution was obtained adding the 30% of sand to the gravel distribution of the substrate. The definition of a bedload input rate finer than the substrate can be justified because in gravel bed streams the sand is generally transported in suspension while the gravel involved in erosional and depositional events is carried as bedload (Parker, 1990). Moreover, the mobility of coarser particles increases as the sand fraction in the mixture

increases (Wilcock et al., 2003), therefore if the content of in the bedload input rate increases, the channel slope should decrease;

3) the bedload material is the 56% of the sediment yield because the 44% of material in the deltas is silt. The annual yield is 51.5 tons/km2/yr and the bedload input rate at Lewiston is 96277 tons/yr It is, then, assumed that half of this material is made of sand and half of gravel. The grain size distribution is computed adding the 50% of sand to the grain size distribution of the substrate.

In Figure 59 the two hypothetical grain size distributions of the bedload and the comparison with the substrate are represented.

The downstream boundary condition was placed very far from the downstream end of the modeled fluvial reach (the channel length is 20 km long while the reach to model is approximately 10 km) because a place with a fix and known bed elevation was not available.

7.3.1 NUMERICAL RUNS

Three hypothesis of bedload input rates is tested against field data and the results are compared in Table 19.

Table 19: Comparison between the three hypothesis on the bedload input rate with a = 0.5.

Hypothesis	S (m/m)	D_{sg} (mm)	$D_{gsubstrate}$ (mm)	$D_{30substrate}$ (mm)	$D_{50substrate}$ (mm)	$D_{70substrate}$ (mm)	$\sigma_{gsubstrate}$
1	0.0044	72	22	7.0	31	109	6.6
2	0.0036	67	17	3.5	26	119	8.2
3	0.0033	58	13	1.6	17	123	9.6
Pre-dam	**0.0024 0.0028**	**?**	**16**	**6.3**	**20**	**49**	**5.1**

The numerical runs were performed assuming that the material transferred to the substrate had a grain size distribution that is an average between the bedload and the surface layer: the value of α in equation (41) was 0.5.

The channel at equilibrium results always steeper than the Trinity River, whose slope varies between 0.0024 m/m (from field measurements in 2000) and 0.0028 m/m (pre – dam data).The hypothesis of degradation after the closure of the dams has to be rejected because in the last 50 years the flow was too low to erode the bed, therefore a pre – dam slope varying between 0.0024 m/m and 0.0028 m/m has to be considered

because the effect of the variation in flow regime was the transformation of a mobile pavement into a much coarser static armor. As the fraction of sand in the bedload input rate increases, the channel slope at equilibrium decreases, even if in hypothesis 3 the bedload input rate is much higher than in the other two conditions.

The geometric mean diameter of the surface layer decreases as the sand fraction in the bedload increases but the three results can not be tested against pre – dam data because of the lack of information. Considering that a healthy habitat for salmons is characterized by a surface geometric mean diameter of 60 – 70 mm and that the pre – dam Trinity River was densely populated by salmons, none of the three hypothesis can be rejected because predicted geometric mean diameters of the surface layer vary between 58 and 72 mm.

Grain size distributions of deposits averaged on the channel length and on the thickness of new deposits are presented in the last columns of Table 19 to compare the numerical and the real substrate of the Trinity River. The central parameters (geometric mean and median diameters) of the grain size distribution of the substrate are better predicted in hypothesis 2 and 3. On the other hand, the comparisons of geometric standard deviations, D_{30}, diameters of the substrate such that the 30% of material is finer, and distributions plotted in Figure 60 reveal that the sand fraction stored in the substrate considerably increases with the content of fine material in the bedload while characteristic diameters of the coarser fraction (i.e. D_{70} in Table 19) are always coarser than measured values but they increase with the sand fraction in the bedload input rate.

The comparison between predicted and measured grain size distribution of the substrate shows that the bedload input rate of hypothesis 1 gives a substrate more realistic than the feed rate of hypothesis 2 and 3, even if the central parameters of the grain size distribution of the substrate are coarser than the measured values. This result can be justified considering that the presented model does not consider the sand transported downstream that is not involved in depositional events but it reduces the mobility of coarser particles and consequently the channel slope.

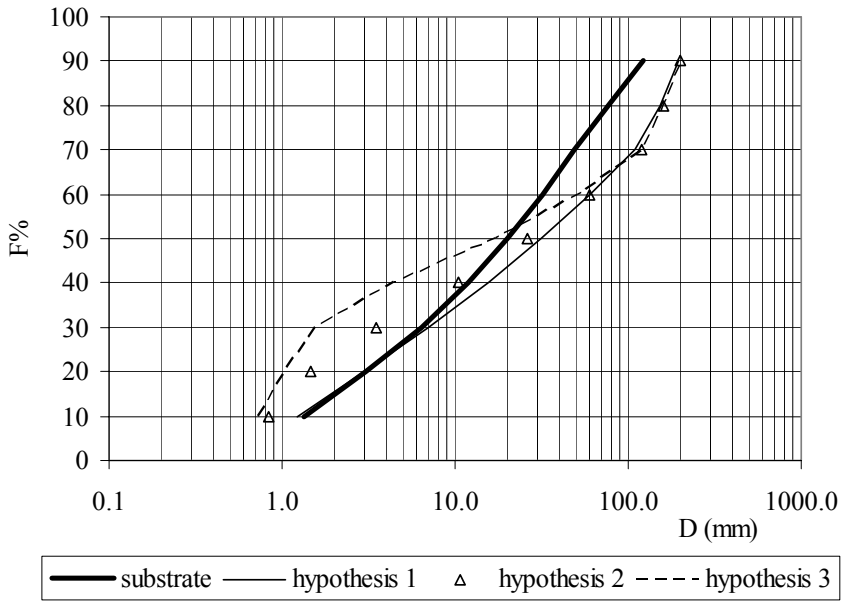

Figure 60 Average grain size distributions of the substrate for different values of the sand fraction in the bedload input rate;

To investigate the variability of the grain size distribution of the substrate with the parameter α that governs the mode of transferring material to the deposits with equation (41) four numerical runs were performed in hypothesis 1 for α equal to 0.2, 0.3, 0.4 and 0.7. Results are summarized in Table 20 and Figure 61. Channel slope and geometric mean diameter of the bed surface are almost constant with α, while the substrate becomes finer as α decreases, because more bedload material is transferred to the substrate. The best prediction of substrate material and of the central parameters of its grain size distribution (i.e. geometric mean and median diameters) was obtained for $\alpha = 0.4$.

Table 20: Comparison between numerical results for hypothesis 1 with different values of α.

α	S (m/m)	D_{sg} (mm)	$D_{gsubstrate}$ (mm)	$D_{30substrate}$ (mm)	$D_{50substrate}$ (mm)	$D_{70substrate}$ (mm)	$\sigma_{gsubstrate}$
0.2	0.0043	71	11	3.0	11	40	6.3
0.3	0.0043	71	14	3.7	15	56	6.6
0.4	0.0042	71	17	4.9	21	78	6.6
0.5	0.0044	72	22	7.0	31	109	6.6
0.7	0.0043	70	33	14.0	60	139	6.1
Pre-dam	**0.0024 0.0028**	**?**	**16**	**6.3**	**20**	**49**	**5.1**

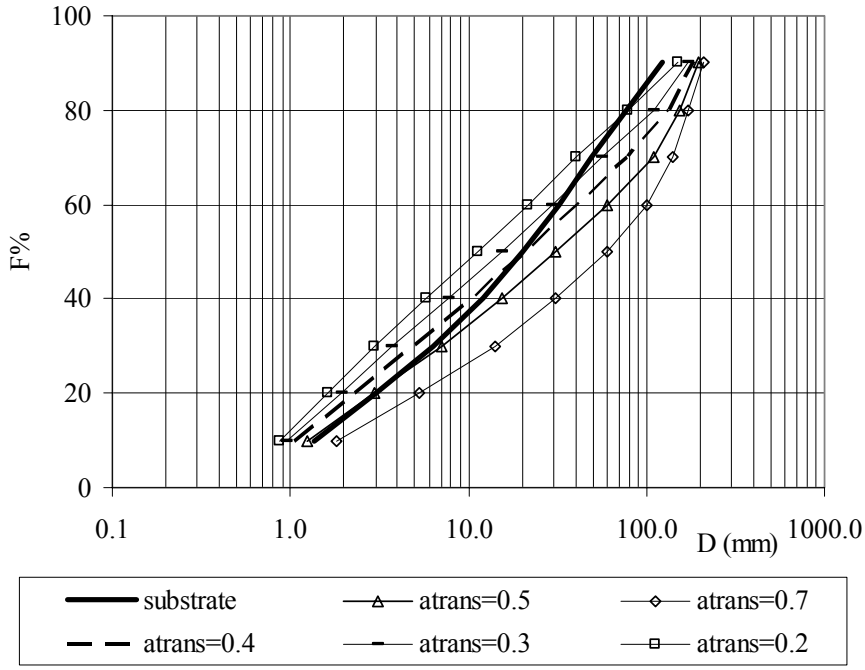

Figure 61 Average grain size distributions of the substrate for different values of α and for a sand fraction in the bedload input rate equal to 0.14;

The channel slope at equilibrium for hypothesis 1 and α equal to 0.4 is 0.0042 m/m while the measured channel slope varies between 0.0024 m/m and 0.0028 m/m. A last numerical run was performed to find the bedload input rate equilibrates the bed with a slope close to the measured value. For a bedload input rate of 10000 tons/yr the channel slope at equilibrium is approximately 0.0033 m/m and the geometric mean diameter is 83 mm, while it was 72 mm for a feed rate of 56706 tons/yr.

7.4 POST DAM CONDITIONS

The historical series of daily discharges recorded at Lewiston from the 1959 to the 2000 is reported in Figure 62 and the variation in flow regime after the closure of the dams is evident.

The bankfull discharge of 198 m^3/s (7000 cfs) was defined from field measurements and a bankfull width of approximately 40 m (130 ft) is assumed because, as shown in Figure 63, a riparian berm formed on a side of the channel and the cross section became trapezoidal. The exponent 'n' in equation (80) is still equal to 0.23 because it was derived for discharges smaller than 368 m^3/s (13000 cfs).

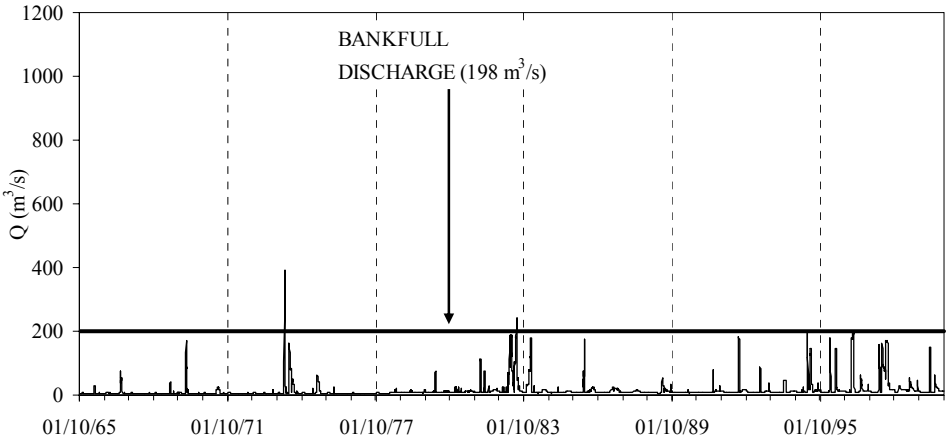

Figure 62 Daily discharges recorded at Lewiston from 1959 to 2000

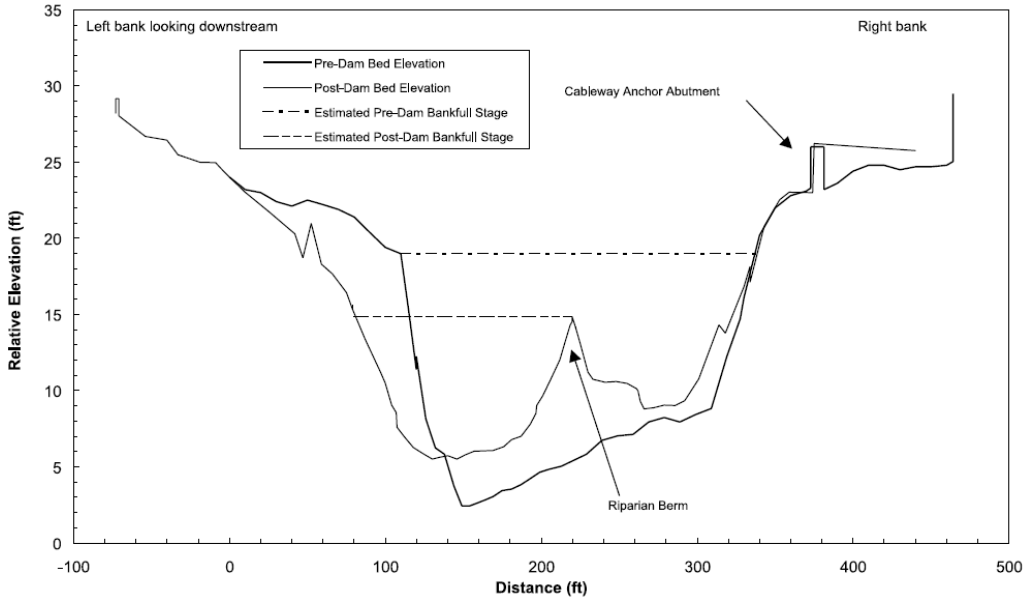

Figure 63 Evolution of the cross section at the USGS gaging station at Lewiston, from the Trinity River Flow Evaluation

The input hydrograph was derived from the flow duration curve for the Trinity River between the confluences with Deadwood Creek (river mile 111) and Rush Creek (river mile 108) and it is represented in Figure 64.

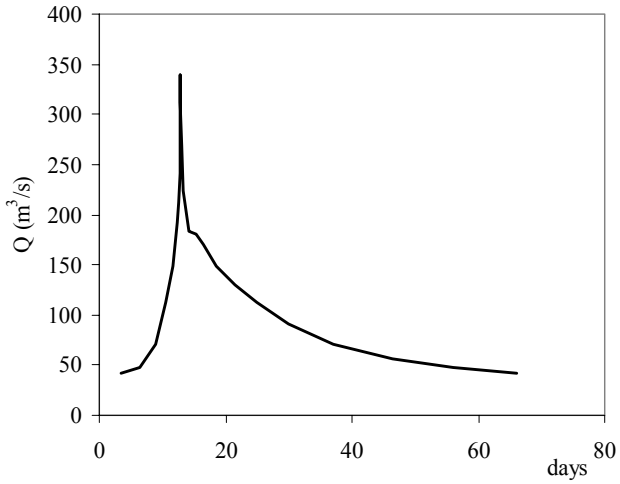

Figure 64 Mean annual input hydrograph for the post – dam simulations

The bedload input rate and its grain size distribution is equal to the bedload input rate estimated for Deadwood Creek in the Sediment Source Analysis for the mainstem Trinity River: the annual yield for this tributary was estimated to be 38 yons/km^2/yr and so the mean annual bedload input rate is 874 tons/yr, value close to the bedload transport rate measured for the water year 2004 (Water Year 2006 Winter Provisional Sediment Transport Data Report). The grain size distribution of the input bedload rate from Deadwood Creek was measured and it is represented in Figure 65.

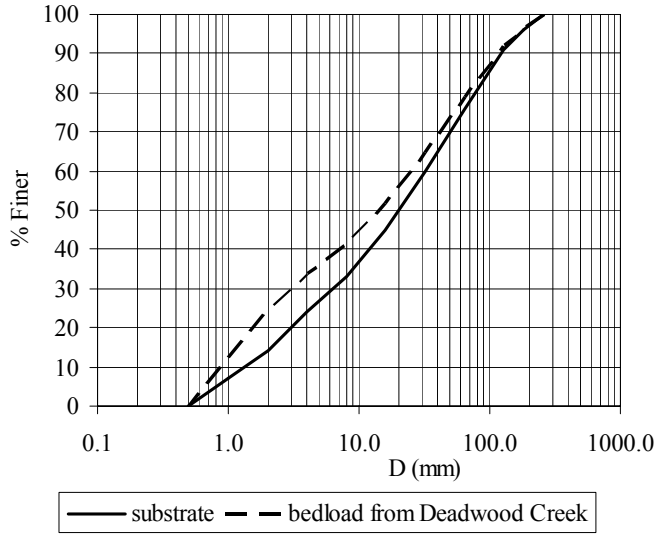

Figure 65 Grain size distributions of the bedload input rate from Deadwood Creek and the substrate of the mainstem Trinity River

7.4.1 NUMERICAL RESULTS

Four numerical runs were performed to simulate post – dam conditions, since 1963 to 1995, in the upper part of the studied reach of the Trinity River, from the new bridge

at river mile 111, just below the confluence with Deadwood Creek, to the confluence with Rush Creek at river mile 108. The channel length in the numerical simulation was assumed equal to 10 km because of the lack of a point with fix bed elevation to place the downstream boundary condition. The difference between these runs was the initial bed:

- Run 1: the channel slope is 0.0024, the substrate has the grain size distribution represented in Figure 59 and the surface layer has the same gravel distribution of the substrate but the fraction of sand is 0;
- Run 2: the channel slope is equal to 0.0028, the substrate and the surface have the same grain size distribution of Run 1;
- Run 3: the initial condition is the bed at the end of the pre – dam numerical simulation with a_{trans} equal to 0.4 and the bedload input rate of hypothesis 1;
- Run 4: the initial condition is the bed at the end of the pre – dam numerical run with a_{trans} equal to 0.4, the grain size distribution of the feeded material equal to the initial substrate and the bedload input rate of 10000 tons/yr.

During Runs 1 and 2, characterized by a finer initial surface layer, the bed slightly degrades and the final surface is characterized by a geometric mean diameter of 67 mm and 71 mm respectively, that are still representative of an healthy habitat for salmons and so they can not reproduce the post – dam Trinity River.

For runs 3 and 4 the initial bed surface is coarser and, after a 42 years numerical simulation of low flow, the bed does not degrade, even if the initial channel slope is higher than the measured value. A coarsening of the bed surface can be observed and the geometric mean diameter of the surface layer increases from 72 mm to 105 mm (Run 3) and from 82 mm to 99 mm (Run 4), values that are too coarse for salmons to spawn. In Figure 66 the comparison between the initial and the final surface layer in Run 3 is represented to show that the code predicts the coarsening of the bed surface for an imposed reduction in flow regime: the flow carries finer fractions downstream while coarser grains can not be mobilize and they form the typical static armor layer.

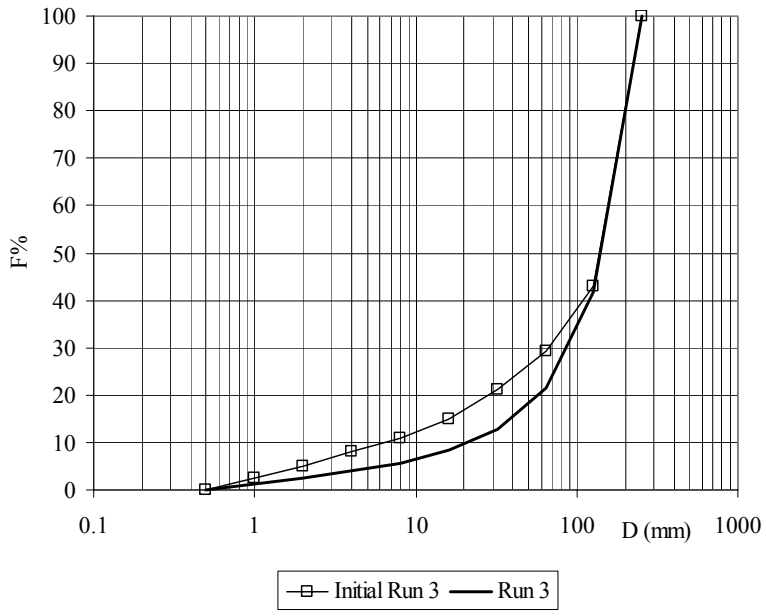

Figure 66 Comparison between the initial and the final surface layer in Run 3.

8 CONCLUSION

Characteristics of natural rivers depend on several parameters that are related to the climate and the morphology of the region and to the hydraulic processes in the fluvial network. The evaluation of these parameters is a complex matter because of their variability in space and time, therefore numerical models to describe natural river systems are based on several assumption and approximations that are generally very far from the reality. For example, load relations are derived in laboratory flumes with constant water discharge and channel width and they are then applied to natural rivers, where discharges and channel width continuously vary.

The concept of mobile bed equilibrium, first derived for irrigation canals and then extended to rivers, strongly helps to simplify the problem because in a river that reached a condition of equilibrium hydraulic parameters vary around a mean value that can be considered constant in time for practical problems and functional relations have been derived to describe how these mean values affect each other.

In rivers that reach a condition of equilibrium the evaluation of hydraulic parameters that depends on the regional environment - the effective water discharge, the mean annual sediment input rate and the grain sizes distribution of the transported sediment - is an extremely complex matter and only after specialized studies an order of magnitude can be hypothesized.

In the last decades numerical models to describe the evaluation of river systems for an imposed change in flow regime have been proposed. They are generally based on physical principles of mass and momentum conservation for water and mass conservation for sediment. When sediment is considered a mixture of different grain sizes sediment transport, erosion and deposition have to be modeled with a grain size based formulation and new approximations are introduced to describe theses phenomena.

The main assumption in numerical models for sediment mixture is the active layer approximation, first proposed by Hirano in 1961, that is necessary to model the continuous exchange of material between bed and bedload. Even if this process has a stochastic nature, the probability distribution functions to describe the interaction between bed and bedload have not yet been derived and so a deterministic simplification of the problem is introduced. The active layer is the upper part of the bed without vertical structure where particles have the same and finite probability to

be entrained into bedload. The substrate is the whole bed under the active layer whose particles can not be entrained into bedload and its grain size distribution can vary in the vertical and in the streamwise direction.

In the present thesis a procedure to store and access the stratigraphy of non cohesive deposits in active layer based models has been proposed. The procedure has been implemented

- in a numerical model to describe the bed evolution in a water –feed laboratory flume and it has then been tested against laboratory data;
- in a numerical model to describe the evolution of a gravel bed river under an imposed hydrograph, to test the procedure for larger temporal and spatial scales.

Laboratory experiments with poorly - sorted gravel have been performed in a water – feed and sediment – recirculating flume. During the experiments longitudinal profiles were periodically recorded and when the bed elevation was relatively constant in time it was assumed that the flow and the sediment transport reached equilibrium, the bedload transport rate was measured and the run ended. For different values of water discharge and water elevation at the downstream end of the flume, nine different conditions of equilibrium were reached and grain size distributions of the bedload and of the surface layer were measured. At the end of the experiments core samples were taken from the bed to measure the vertical stratigraphy of deposits. The sieve analysis revealed that the bedload had a grain size distribution similar to the initial mixture, except during two runs characterized by a finer load, and the bed surface was significantly coarser than the initial mixture in each run. The substrate is coarser than the initial mixture in its first layers but the analysis of deeper layers did not show the expected finer lens below the coarse surface. Experimental data are recorded in Appendix 1: Laboratory data.

A novel surface – based version of the Ashida and Michiue bedload relation has been derived to fit the data: the coefficient in the original relation was lowered from 17 to 4.6, the hiding function was modified to predict a higher mobility of coarse grains and the critical or “effective” value of the Shields number was lowered to 0.043. Comparisons between predicted and measured bedload transport rates and grain sizes distributions are reported in Appendix 2: Validation of the bedload relation.

The comparison between predicted and laboratory data, briefly presented in Chapter 5 and completely reported in Appendix 3: Validation of the procedure to store and

access the stratigraphy of non - cohesive deposits with laboratory data, shows that the proposed procedure properly predicts the grain size distribution of deposits governed by fluvial deposition. The main limitation of the model is that it can not represent the stratigraphy built when a front migrates downstream and so the substrate is not completely realistic.

A new version of the procedure has been proposed to describe vertical stratigraphy due to front migration and its validation, completely reported in Chapter 5, shows a good agreement between numerical and laboratory data even if the top layer of the deposits is systematically coarser than the sieved material. Moreover, numerical results in water – feed flumes, where the total amount if sediment in the system may vary and the bedload input rate is constant in time and in grain size distribution, reveal that the modified procedure tends to predict much coarser deposits than the feeded material. This result is definitely unrealistic because the substrate should have a grain size distribution similar to the bedload input rate, representative of the environmental parameters of the watershed. In the next months the procedure to predict vertical stratigraphy of deposits governed by front migration will be modified with the results of experimental studies on front migrations with poorly sorted sediment.

The proposed procedure was then implemented in a one dimensional numerical model to describe the evolution of a gravel bed rivers for an imposed hydrograph to describe the Trinity River below Lewiston Dam in California. The model considers a mixture of different grain sizes because in gravel bed rivers the sediment is poorly sorted and the approximation of uniform material is very far from the reality. Its innovative characteristics are a procedure to consider the variation of channel width with the discharge and the procedure to store and access the stratigraphy of deposits.

Input parameters are the hydrograph, the mean annual bedload input rate and the grain size distributions of substrate, surface layer and feed rate and they can not be easily defined. The hydrograph has to be derived from the flow duration curve. Bankfull values of discharge and width have to specified to consider the variation of channel width with the flow rate, but it is hard to define these parameters in gravel bed alluvial rivers with a strong variability in flow rates. Moreover, if the grain size distribution of the bed surface and of the substrate can be measured, the definition of

the bedload input rate is extremely difficult and an order of magnitude can only be specified after field campaigns.

Numerical runs were performed to reconstruct the pre – dam Trinity River for different bedload input rates and the results were tested comparing the grain size distributions of deposits with the measured distribution. Considering that the model is one – dimensional and it is based on several assumptions (the downstream variability of the hydrograph is neglected and the normal flow approximation is introduced, the bedload input rate is constant …), numerical results show that the code can reproduce the pre – dam Trinity River, even if numerical slopes are considerably higher than the measured value. This difference can be explained considering that in a fluvial system the sediment input rate is a mixture of particles that goes from clay to coarse gravel, while the input parameter of the model is the bedload input rate only and the sand transported downstream and not involved in depositional events can not be consider to reproduce the grain size distribution of the substrate even if it increases the mobility of coarse gravel.

Input parameters for the post – dam numerical simulations were easier to define and the results of the numerical runs reproduce the phenomenon observed on the Trinity River after the closure of the dams. During these runs, characterize by an initial bed steeper than the pre – dam Trinity River but with a similar grain size distribution of the bed, the coarsening of the surface layer was observed and the longitudinal profile did not change because the flow was too low to erode material from the bed even if the sediment input rate dramatically decreased because the material supplied from the watershed deposited in the reservoirs.

9 NOTATION

A_w Area of the wall region;

B Channel width;

B_{bf} Bankfull channel width;

C_f Friction coefficient;

C_{fb} Friction coefficient for the bed region;

C_{fw} Friction coefficient for the wall region;

D_{lm} Measured geometric mean diameter of the sediment load;

D_{lp} Predicted geometric mean diameter of the sediment load;

D_{sg} Geometric mean diameter of the surface layer;

D_{sm} Arithmetic mean diameter of the surface layer;

D_i Characteristic diameter of each grain size range;

D_{90} Diameter such that the 90% of sediment is finer;

f_i Fraction of substrate material in the i-th grain size range;

F_i Fraction of surface material in the i-th grain size range;

f_i' Fraction of bed material in the i-th grain size range;

f_{li} Fraction of material in the i-th grain size range at the active layer-substrate interface;

Fr Froude number;

f_w Darcy – Waisbach friction coefficient for the wall region;

g Acceleration of gravity;

G_s Bedload transport rate in grams per minute;

H Water depth;

k_s Roughness height;

L Flume length;

L_a Active layer thickness;

M Number of size ranges of the sediment mixture;

N Number of point on each vertical for the grid to build the stratigraphy;

n_a Parameter to compute the active layer thickness as a linear function of the D_{s90}. Generally varies between 1 and 2 in absence of bedforms;

n_k Parameter to compute the roughness height as a linear function of the D_{s90}. Generally varies between 1.5 and 3;

Nnode Number of nodes in the streamwise direction;

Q Water discharge;

Q_{bf} Bankfull water discharge;

p_i Fraction of bedload material in the i-th grain size range;

q_b Volumetric bedload transport rate per unit width;

q_{bT} Volumetric total bedload transport rate per unit width;

q_{bi} Volumetric total bedload transport rate per unit width in each grain size range;

q_b^* Einstein parameter defined as $q_b/[(RgD)^{0.5}D]$;

q_{bi}^* Einstein parameter defined for the i-th grain size range;

R Submerged specific gravity of the sediment defined as $[(\rho_s/\rho)-1]$;

R_H Hydraulic radius;

R_w Hydraulic radius for the wall region;

Re_w Reynolds number for the wall region;

S Bed slope;

t Time;

U Mean flow velocity;

u^* Shear velocity;

x streamwise coordinate;

W_i^* Grain size specific bedload transport rate;

z Coordinate in the vertical direction;

α Parameter governing grain size distribution transferred to substrate during bed aggradation;

α_r Coefficient in the Manning – Strikler resistance relation;

δ Variation of the active layer-substrate interface elevation above a datum in a time step, when the bed aggrades;

$\Delta\eta$ Variation of bed elevation in a time step;

γ_{qbT} Coefficient of variation of the bedload volume transport rate per unit width on the flume length;

η Bed elevation above a datum;

η_{int} Active layer-substrate interface elevation above a datum;

η_{av} Average bed elevation on the flume length;

λ_p Bed porosity;

μ_{qbT} Average bedload volume transport rate per unit width on the flume length;

χ_w Wetted perimeter for the wall region;

ν Kinematic viscosity of water;

ρ Density of water;

ρ_s Density of sediment;

σ_{qbT} Standard variation of the bedload volume transport rate per unit width on the flume length;

τ Shear stress

τ_b Shear stress in the bed region;

τ_b^* Shields parameter defined as $\tau_b/(\rho RgD)$;

τ_c^* Critical value of the Shields parameter;

τ_{bi}^* Shields parameter defined for each grain size;

τ_{ci}^* Critical value of the Shields parameter for each grain size;

τ_{scg}^* Effective critical value of the Shields parameter for the geometric mean size;

τ_{sg}^* Shields parameter as a function of the geometric mean size;

τ_w Shear stress in the wall region;

ξ_d Water elevation at the downstream end of the flume set by the tail gate.

10 REFERENCES

Bloom A., J. S. Ribberink and H. J. de Vriend, Vertical sorting in bed forms: flume experiments with a natural and a trimodal sediment mixture, Water Resources Research, vol. 39, n° 2, 2003;

Bloom A, G. Parker, J. S. Ribberink e H. J. de Vriend, Vertical sorting and the morphodynamics of bed – form dominated rivers: an equilibrium sorting model, Journal of Geophysical Research, vol. 11, 2006a;

Bloom A. and Kleinhans M. G., Modelling sorting over the lee face of individual bed forms, Proceedings of the International Conference on Fluvial Hydraulics River Flow 2006, Lisbon, Portugal, 6 – 8 September 2006b;

Cantelli A., C. Paola and G. Parker, Experiments on upstream-migrating erosional narrowing and widening of an incisional channel caused by dam removal, Water Resour. Res., Vol. 40, No. 3, March 2004;

Egiazaroff, I. V., Calculation of nonuniform sediment concentrations, Journal of Hydraulic Engineering, 91(4), 225-247, 1965;

Hoey T. B. e R. I. Ferguson, Numerical simulation of downstream fining by selective transport in gravel bed rivers: model development and illustration, Water Resources Research, 30, 2251 – 2260, 1994;

Kleinhans M. G. e L. C. Van Rijn, Stochastic prediction of sediment transport in sand – gravel bed rivers, Journal of Hydraulic Engineering, 128, 412 – 425, 2002;

Leopold L.B., M.G Wolman, River Channel Patterns: Braided, Meanderig and straight, Phisiogrphic and Hydraulic studies of Rivers (1957);

Leopold L.B., M.G Wolman e J.P Miller, Fluvial Processes in Geomorphology, W.H. Freeman and Company San Francisco and London (1964);

Marion A. e L. Francarollo, Experimental investigation on mobile armouring development, Water Resources Research, 33, 1447 – 1453, 1997;

Montuori C., Complementi di idraulica, Liguori editore, Napoli (1997);

Parker G., S. Dhamotharan e S. Stefan, Model experiments on mobile paved gravel bed streams, Water Resources Research, 18 (5), 1395 – 1408, 1982 (a);

Parker G. and P. C. Klingeman, On why gravel bed streams are paved, Water Resources Research, 18 (5), 1409 – 1423, 1982 (b);

Parker G., P. C. Klingeman e D. L. Mc Lean, Bedload and size distribution in paved gravel – bed streams, Journal of Hydraulic Division, ASCE, 108 (4), 544 – 571, 1982 (c);

Parker G., Surface – based bedload transport relation for gravel rivers, Journal of Hydraulic Research, 28 (4), 417 – 436, 1990;

Parker G., Selective sorting and abrasion of river gravel. I: theory, Journal of Hydraulic Engineering, 117 (2), 131 – 149, 1991 (a);

Parker G., Selective sorting and abrasion of river gravel. II: applications, Journal of Hydraulic Engineering, 117 (2), 150 – 171, 1991 (b);

Parker G. e P. R. Wilcock, Sediment feed and recirculating flumes: fundamental difference, Journal of Hydraulic Engineering, 119 (11), 1192 – 1204, 1993;

Parker G., C. Paola e S. Leclair, Probabilistic Exner sediment continuity equation for mixtures with no active layer, Journal of Hydraulic Engineering, November, 818 – 826, 2000;

Parker, G., Persistence of sediment lumps in approach to equilibrium in sediment-recirculating flumes. Proceedings, XXX International Association of Hydraulic Research Congress Thessaloniki, Greece, August 24-29 2003;

Parker, G. (2004) 1D Sediment Transport Morphodynamics with Applications to Rivers and Turbidity Currents, Copyrighted e-book downloadable at http://www.cee.uiuc.edu/people/parkerg /morphodynamics_e-book.htm;

Parker G., O. Sequeiros and River morphodynamic class of spring 2006, Large scale river morphodynamics: application to the Mississippi delta, Proceedings of the International Conference on Fluvial Hydraulics River Flow 2006, Lisbon, Portugal, 6 – 8 September 2006;

Seal R., C. Paola, G. Parker, J. B. Southard e P. R. Wilcock, Experiments on downstream fining of gravel: I. Narrow – channel runs, Journal of hydraulic Engineering, ASCE, 123 (10), 874 – 884, 1997;

Sediment Source Analysis for the Mainstem Trinity River, Trinity County, Ca, Prepared by Graham Matthews and Associates, October 2001;

Toro – Escobar C. M., G. Parker e C. Paola, Transfer function for the deposition of poorly sorted gravel in response to streambed aggradation, Journal of Hydraulic Research, 34 (1), 35 – 53, 1996;

Toro – Escobar C. M., C. Paola, G. Parker, P.R. Wilcock e J. B. Southard, Experiments on downstream fining of gravel. II: wide and sandy runs, Journal of Hydraulic Engineering 126 (3): 198 – 208, 2000;

Trinity River Flow Evaluation, final report, A report to the Secretary U. S. Department of the Interior Washington, D.C., June 1999;

Trush W. J., S. M. McBain and L. B. Leopold, Attributes of an alluvial river and their relation to water policy, Proceedings of the National Academy of Sciences, vol.97 no.22, 24 October 2000;

Upper Trinity River Sediment Source Analysis prepared by James Fitzgerald, Graham Matthews and Associates, February 2006.

Vanoni, V. A., ed. (1975). "Sedimentation Engineering." ASCE Manuals and Reports on Engineering Practice No. 54, ASCE, New York, 745 pp;

Viparelli C., Corsi d'acqua naturali e leggi che ne regolano il modellamento, Quaderno n° 4, Istituto di Idraulica e Costruzioni Idrauliche, Napoli 1972;

Viparelli E., O. Sequeiros, A. Cantelli and G. Parker, A numerical model to store and access the stratigraphy of non-cohesive sediment as an alluvial bed aggrades and degrades in a flume, 5th IAHR Symposium on River, Coastal and Estuarine Morphodynamics, 17 – 21 September 2007;

Wilcock P.R. e J. B. Southard, Bed load transport of mixed size sediment: fractional transport rates, bed forms and the development of a coarse bed surface layer, Water Resources Research, 25, 1629 – 1641, 1989;

Wilcock P. R., S. T. Kenworthy e J. C. Crowe, Experimental study of the transport of mixed sand and gravel, Water Resources Research, 37 (12), 3349 – 3358, 2001;

Wilcock P. R. e J. C .Crowe, Surface – based transport model for mixed – size sediment, Journal of Hydraulic Engineering 129 (2), 120 – 128, 2003;

Wright S. e G. Parker, Modeling downstream fining in sand – bed rivers. I: formulation, Journal of Hydraulic Research, 43 (6), 612 – 619, 2005 (a);

Wright S. e G. Parker, Modeling downstream fining in sand – bed rivers. II: application, Journal of Hydraulic Research, 43 (6), 620 – 630, 2005 (b);

Wong M., Does the bedload equation of Meyer – Peter and Muller fits its own data?, Proceedings, XXX Congress International Association of Hydraulic Research, Thessaloniki, J.F.K. Competition volume, 73 – 80, 2003;

Wong M., G. Parker, P. De Vries, T. M. Brown e S. J. Burges, Experiments on dispersion of tracer stones under low-regime plane bed equilibrium bedload transport, Water Resources Research 43 (3), 2007.

11 APPENDIX 1: LABORATORY DATA

List of symbols:

D	**Diameter that characterize the cumulative grain size distribution;**
Di	**Characteristic diameter of each grain size range;**
D_{lg}	**Geometric mean diameter of the bedload;**
D_{l50}	**Median diameter of the bedload;**
D_{l90}	**Diameter such that the 90% of sediment of the bedload is finer;**
D_{sg}	**Geometric mean diameter of the bed surface;**
D_{s50}	**Median diameter of the bed surface;**
D_{s90}	**Diameter such that the 90% of sediment of the bed surface is finer;**
f	**Fraction of bed material in each grain size range;**
F	**Fraction of surface material in each grain size range;**
G_s	**Sediment transport rate in grams per minute;**
H	**Water depth;**
p	**Fraction of bedload material in each grain size range;**
P	**Function denoting the mass fraction of a sample that is finer than size D;**
Q	**Water discharge;**
x	**Streamwise coordinate;**
ξ_d	**Water elevation at the downstream end of the flume;**
η	**Bed elevation above a datum;**
σ_{lg}	**Geometric standard deviation of the bedload;**
σ_{sg}	**Geometric standard deviation of the bed surface;**

EXPERIMENTAL CONDITIONS

RUN	Q (l/s)	ξ_d (cm)	G_s (g/min)
1	30	22	731
2	25	21	491
3	20	19	458
4	35	23	1432
5	20	21	54
6	30	24	64
7	30	23	371
8	35	24.8	151
9	35	22.5	1068

Initial mixture

D (mm)	P %	Di (mm)	fi %
0.01	0.00		
0.50	0.00	0.07	0.00
1.00	0.11	0.71	0.11
1.18	5.98	1.09	5.86
2.00	24.67	1.54	18.69
4.00	61.76	2.83	37.09
6.35	82.94	5.04	21.18
9.42	99.92	7.74	16.98
13.33	100.00	11.21	0.08

D_g	3.39	mm
σ_g	1.70	
D_{50}	3.44	mm
D_{90}	7.83	mm

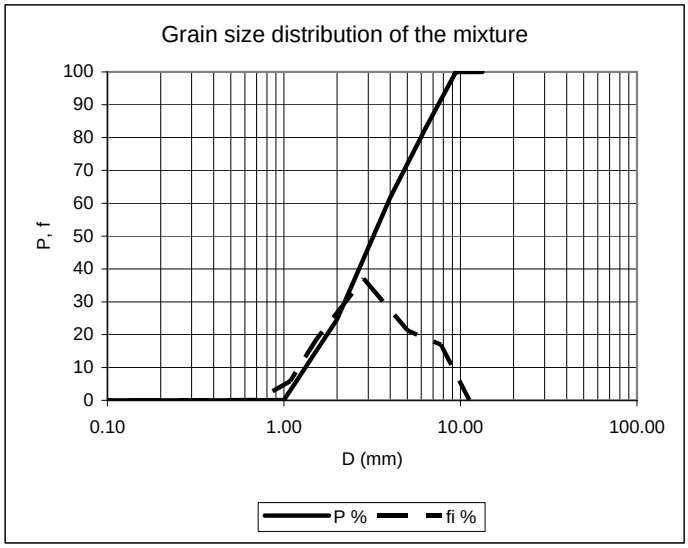

RUN 1

Water Discharge, Q	**30**	**l/s**
Downstream water elevation, ξ_d	**220**	**mm**
Sediment transport rate at equilibrium, G_s	**731**	**g/min**

Longitudinal profile at equilibrium

x (m)	η (mm)
2.5	205
2.9	201
3.3	202
3.7	202
4.1	197
4.3	196
4.5	196
4.9	194
5.3	188
5.7	188
6.1	182
6.5	180
6.9	178
7.3	175
7.7	172
8.1	169
8.5	169
8.9	166
9.3	161
9.7	160
10.1	158
10.5	153

Water surface at equilibrium

x (m)	H (mm)
2.5	284
4.3	274
6.5	258
8.5	244
10.5	229

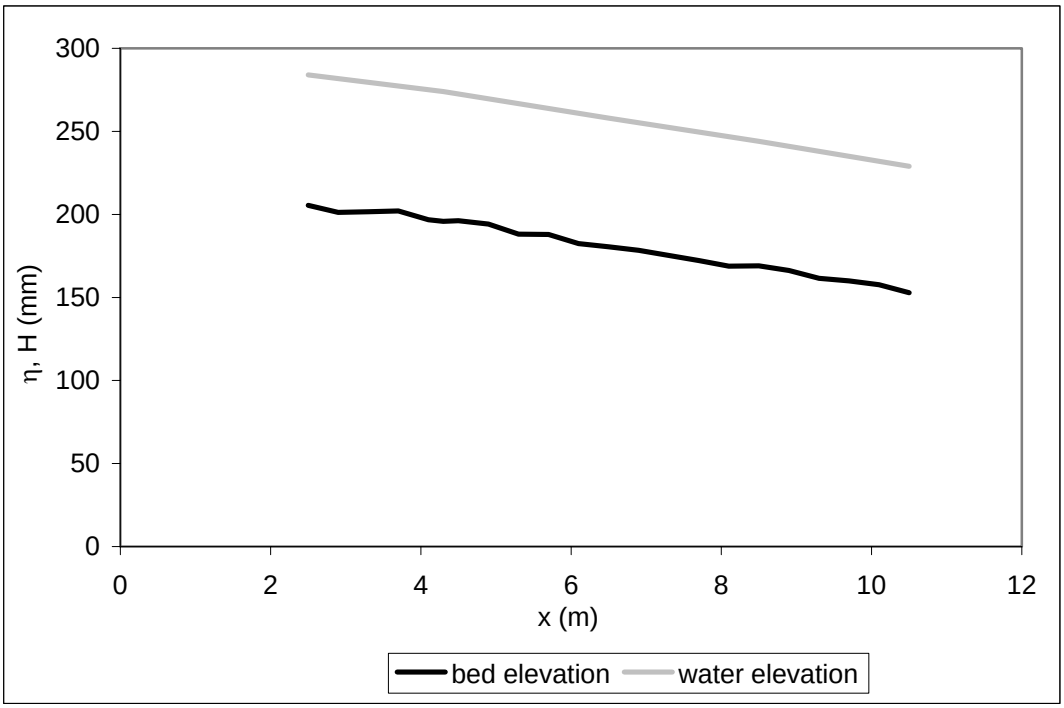

Water Discharge, Q	**30**	**l/s**
Downstream water elevation, ξ_d	**220**	**mm**
Sediment transport rate at equilibrium, G_s	**731**	**g/min**

Grain size distribution of the bedload at equilibrium

D (mm)	P %	Di (mm)	pi %
0.01	0.00		
0.50	0.03	0.07	0.03
1.00	0.09	0.71	0.06
1.18	0.25	1.09	0.17
2.00	23.56	1.54	23.31
4.00	59.95	2.83	36.39
6.30	83.31	5.02	23.36
9.50	100.00	7.74	16.69
12.50	100.00	10.90	0.00

D_{lg}	3.31	**mm**
σ_{lg}	1.75	
D_{l50}	3.31	**mm**
D_{l90}	7.43	**mm**

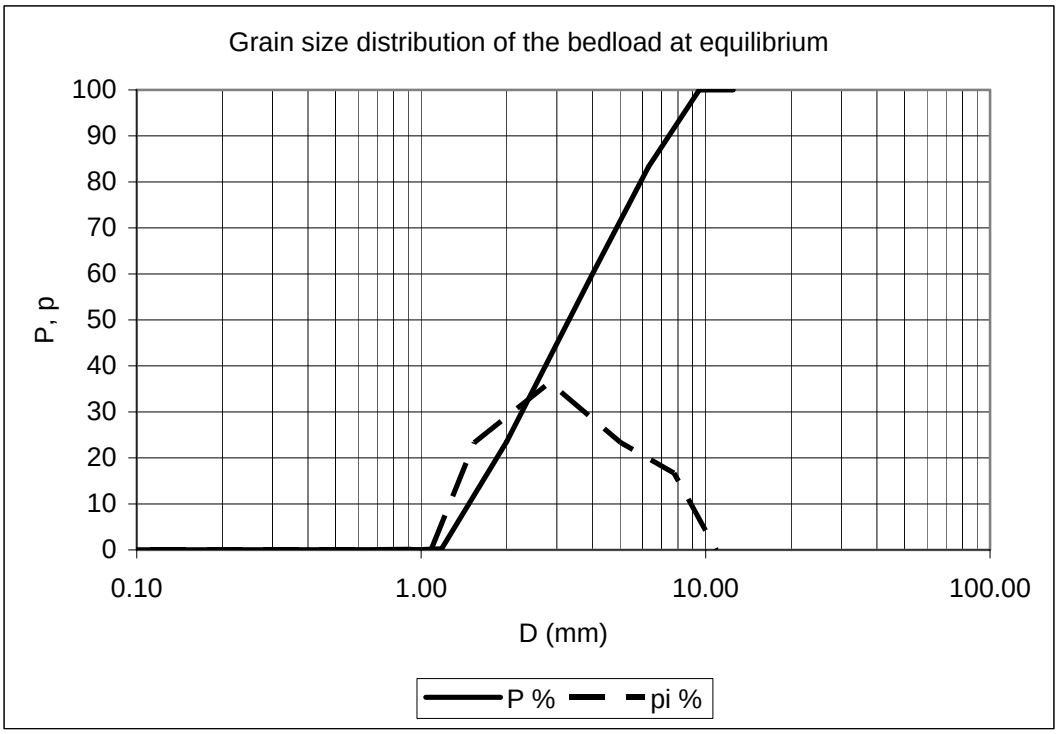

Water Discharge, Q	**30**	**l/s**
Downstream water elevation, ξ_d	**220**	**mm**
Sediment transport rate at equilibrium, G_s	**731**	**g/min**

Grain size distribution of the bed surface at x = 2.5 m

D (mm)	P %	Di (mm)	Fi %
0.01	0.00		
0.50	0.00	0.07	0.00
1.00	0.01	0.71	0.01
1.18	0.11	1.09	0.10
2.00	10.98	1.54	10.86
4.00	44.15	2.83	33.17
6.30	70.87	5.02	26.72
9.50	100.00	7.74	29.13
12.50	100.00	10.90	0.00

D_{sg}	4.13	**mm**
σ_{sg}	1.70	
D_{s50}	4.42	**mm**
D_{s90}	8.25	**mm**

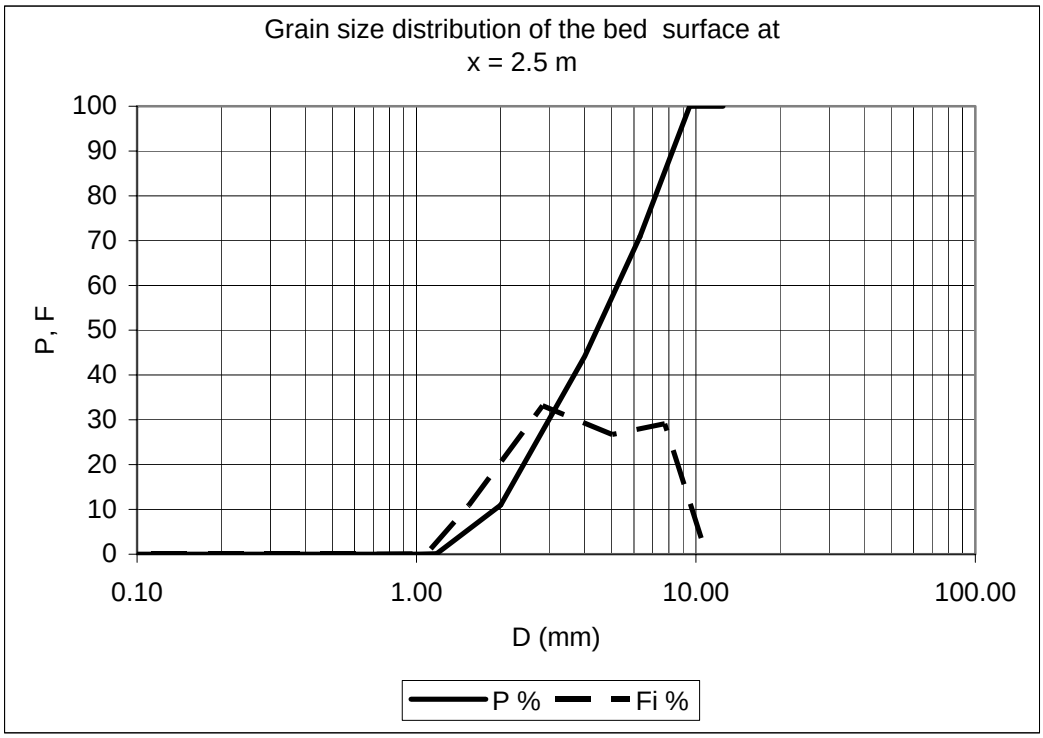

Water Discharge, Q	**30**	**l/s**
Downstream water elevation, ξ_d	**220**	**mm**
Sediment transport rate at equilibrium, G_s	**731**	**g/min**

Grain size distribution of the bed surface at x = 4.3 m

D (mm)	P %	Di (mm)	Fi %
0.01	0.00		
0.50	0.00	0.07	0.00
1.00	0.03	0.71	0.02
1.18	0.15	1.09	0.13
2.00	5.91	1.54	5.76
4.00	37.32	2.83	31.41
6.30	69.03	5.02	31.71
9.50	100.00	7.74	30.97
12.50	100.00	10.90	0.00

D_{sg}	4.47	**mm**
σ_{sg}	1.62	
D_{s50}	4.80	**mm**
D_{s90}	8.32	**mm**

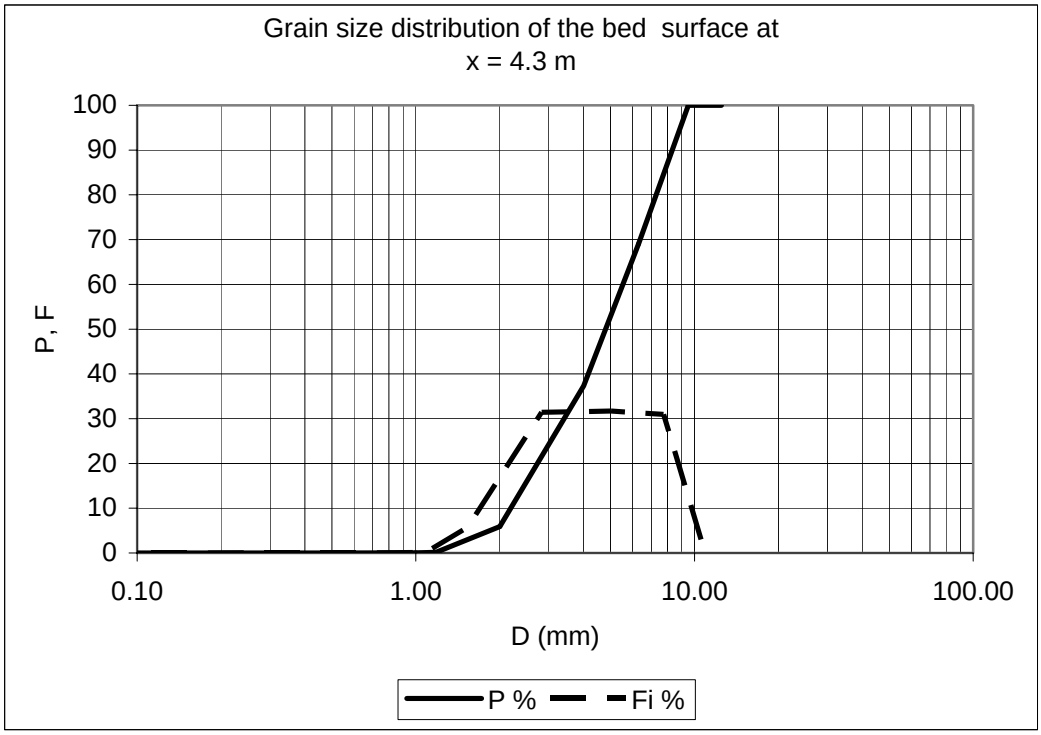

Water Discharge, Q	**30**	**l/s**
Downstream water elevation, ξ_d	**220**	**mm**
Sediment transport rate at equilibrium, G_s	**731**	**g/min**

Grain size distribution of the bed surface at x = 6.5 m

D (mm)	P %	Di (mm)	Fi %
0.01	0.00		
0.50	0.00	0.07	0.00
1.00	0.01	0.71	0.01
1.18	0.06	1.09	0.05
2.00	11.39	1.54	11.33
4.00	45.61	2.83	34.21
6.30	71.25	5.02	25.64
9.50	100.00	7.74	28.75
12.50	100.00	10.90	0.00

D_{sg}	4.08	**mm**
σ_{sg}	1.70	
D_{s50}	4.32	**mm**
D_{s90}	8.23	**mm**

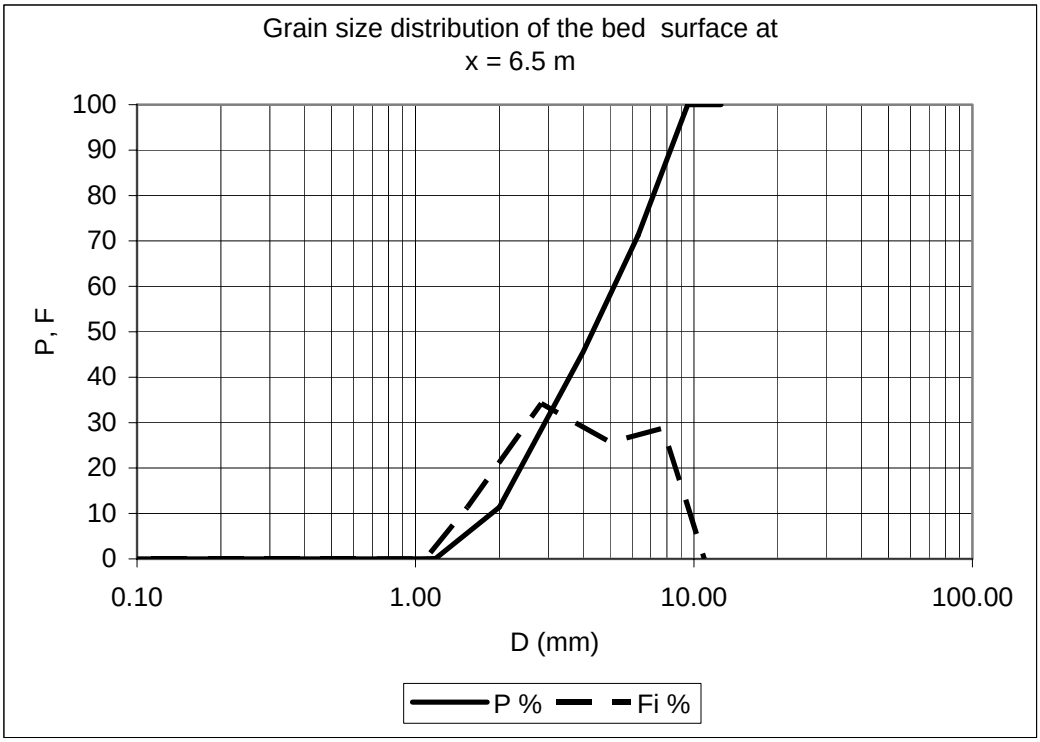

Water Discharge, Q	**30**	**l/s**
Downstream water elevation, ξ_d	**220**	**mm**
Sediment transport rate at equilibrium, G_s	**731**	**g/min**

Grain size distribution of the bed surface at x = 8.5 m

D (mm)	P %	Di (mm)	Fi %
0.01	0.00		
0.50	0.00	0.07	0.00
1.00	0.01	0.71	0.01
1.18	0.08	1.09	0.07
2.00	14.20	1.54	14.13
4.00	47.75	2.83	33.54
6.30	73.09	5.02	25.35
9.50	100.00	7.74	26.91
12.50	100.00	10.90	0.00

D_{sg}	3.93	**mm**
σ_{sg}	1.73	
D_{s50}	4.16	**mm**
D_{s90}	8.15	**mm**

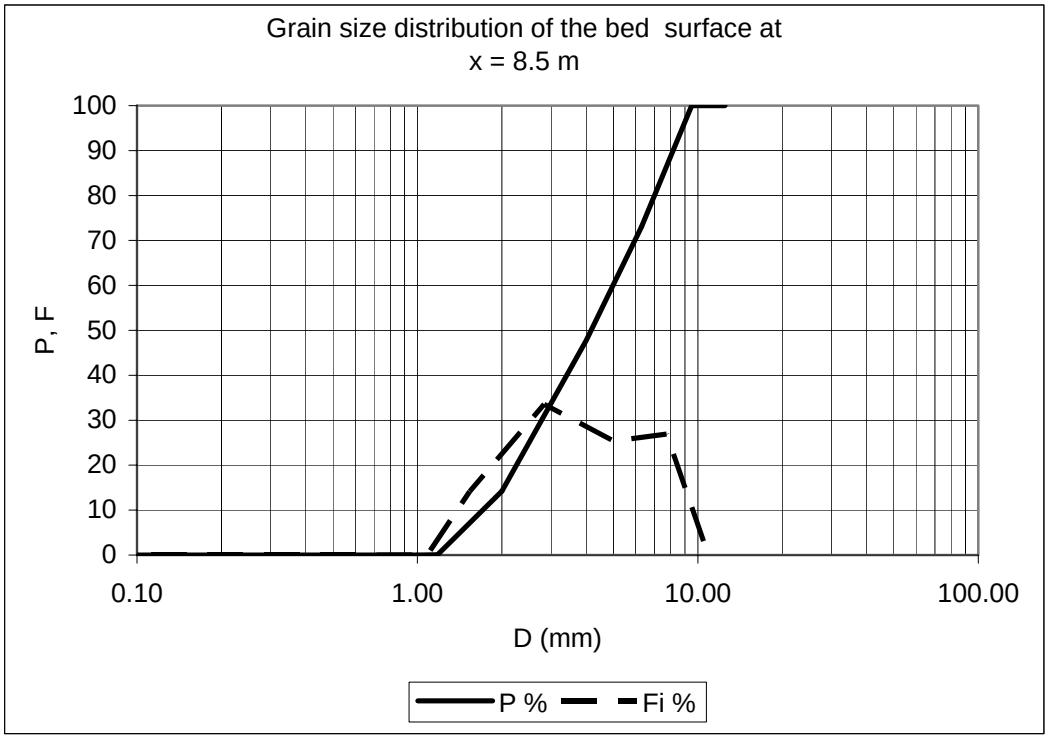

Water Discharge, Q	**30**	**l/s**
Downstream water elevation, ξ_d	**220**	**mm**
Sediment transport rate at equilibrium, G_s	**731**	**g/min**

Grain size distribution of the bed surface at x = 10.5 m

D (mm)	P %	Di (mm)	Fi %
0.01	0.00		
0.50	0.12	0.07	0.12
1.00	0.14	0.71	0.02
1.18	0.21	1.09	0.07
2.00	15.15	1.54	14.95
4.00	44.36	2.83	29.21
6.30	67.99	5.02	23.63
9.50	100.00	7.74	32.01
12.50	100.00	10.90	0.00

D_{sg}	4.06	**mm**
σ_{sg}	1.80	
D_{s50}	4.46	**mm**
D_{s90}	8.37	**mm**

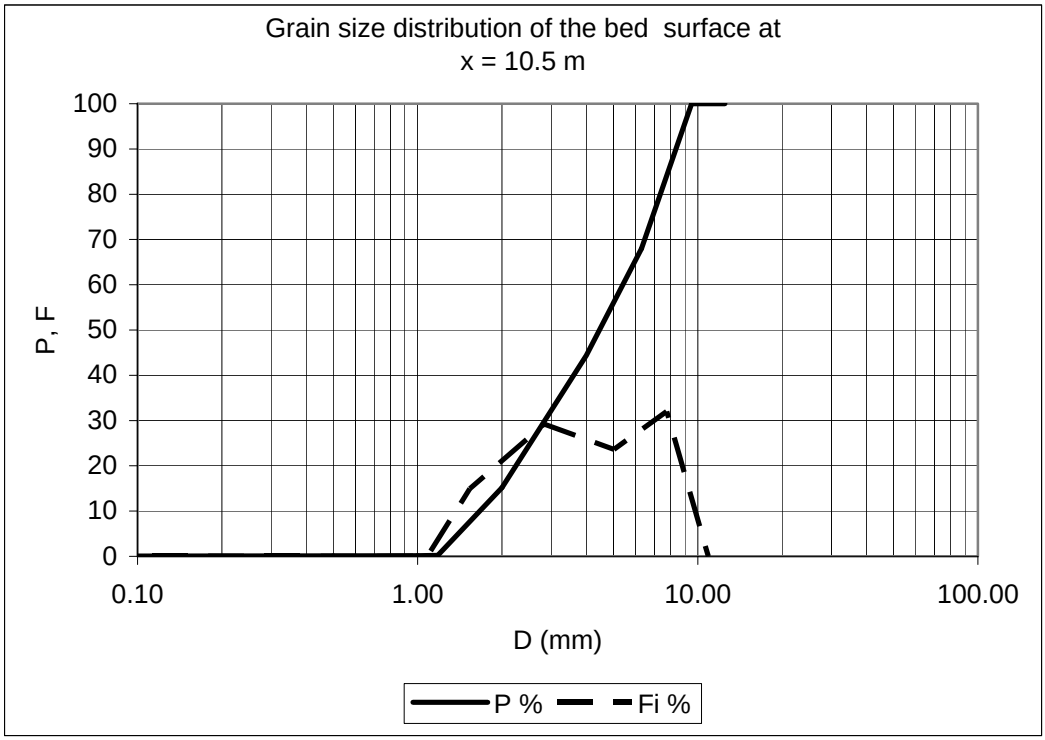

RUN 2

Water Discharge, Q	**25**	**l/s**
Downstream water elevation, ξ_d	**210**	**mm**
Sediment trasport rate at equilibrium, G_s	**491**	**g/min**

Longitudinal profile at equilibrium

x (m)	η (mm)
2.5	206
2.9	203
3.3	200
3.7	196
4.1	199
4.3	195
4.5	194
4.9	192
5.3	188
5.7	186
6.1	184
6.5	179
6.9	178
7.3	176
7.7	173
8.1	167
8.5	165
8.9	161
9.3	157
9.7	155
10.1	152
10.5	150

Water surface at equilibrium

x (m)	H (mm)
2.5	275
4.3	263
6.5	248
8.5	232
10.5	218

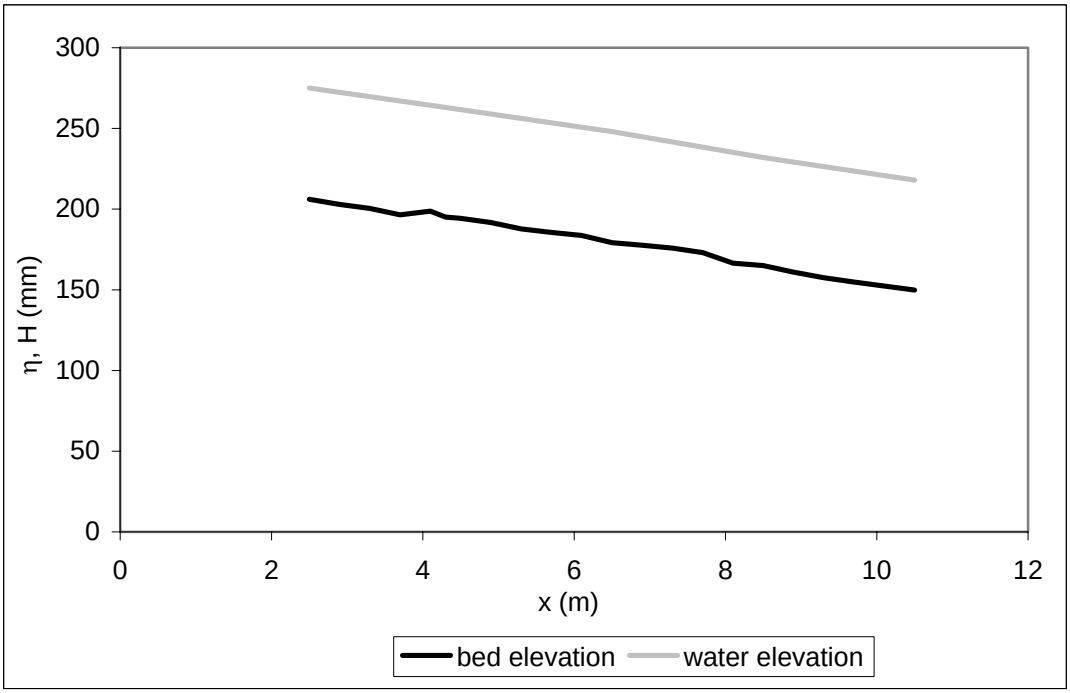

Water Discharge, Q	**25**	**l/s**
Downstream water elevation, ξ_d	**210**	**mm**
Sediment trasport rate at equilibrium, G_s	**491**	**g/min**

Grain size distribution of the bedload at equilibrium

D (mm)	P %	Di (mm)	pi %
0.01	0.00		
0.50	0.02	0.07	0.02
1.00	0.05	0.71	0.04
1.18	0.14	1.09	0.08
2.00	14.00	1.54	13.86
4.00	51.67	2.83	37.67
6.30	77.27	5.02	25.60
9.50	100.00	7.74	22.73
12.50	100.00	10.90	0.00

D_{lg}	3.78	**mm**
σ_{lg}	1.71	
D_{l50}	3.88	**mm**
D_{l90}	7.93	**mm**

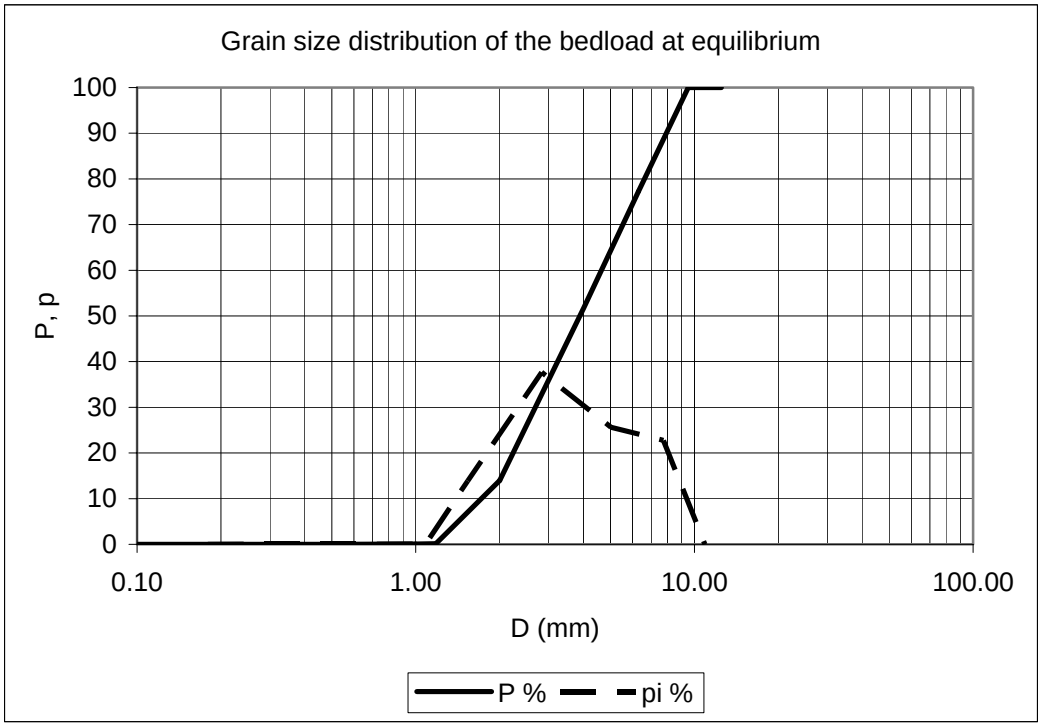

Water Discharge, Q	**25**	**l/s**
Downstream water elevation, ξ_d	**210**	**mm**
Sediment trasport rate at equilibrium, G_s	**491**	**g/min**

Grain size distribution of the bed surface at x = 2.5 m

D (mm)	P %	Di (mm)	Fi %
0.01	0.00		
0.50	0.01	0.07	0.01
1.00	0.05	0.71	0.04
1.18	0.16	1.09	0.11
2.00	17.34	1.54	17.18
4.00	56.32	2.83	38.97
6.30	79.85	5.02	23.54
9.50	100.00	7.74	20.15
12.50	100.00	10.90	0.00

D_{sg}	3.56	**mm**
σ_{sg}	1.72	
D_{s50}	3.57	**mm**
D_{s90}	7.75	**mm**

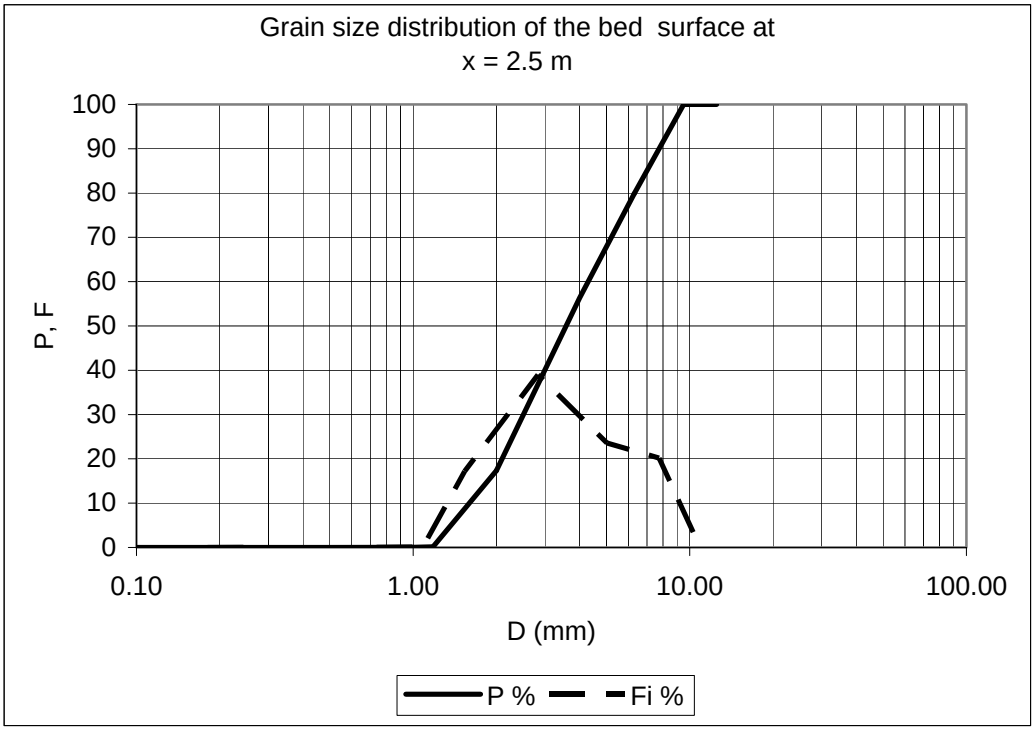

Water Discharge, Q	**25**	**l/s**
Downstream water elevation, ξ_d	**210**	**mm**
Sediment trasport rate at equilibrium, G_s	**491**	**g/min**

Grain size distribution of the bed surface at x = 4.3 m

D (mm)	P %	Di (mm)	Fi %
0.01	0.00		
0.50	0.01	0.07	0.01
1.00	0.11	0.71	0.11
1.18	0.41	1.09	0.29
2.00	20.01	1.54	19.61
4.00	51.25	2.83	31.23
6.30	71.92	5.02	20.67
9.50	100.00	7.74	28.08
12.50	100.00	10.90	0.00

D_{sg}	3.73	**mm**
σ_{sg}	1.81	
D_{s50}	3.89	**mm**
D_{s90}	8.21	**mm**

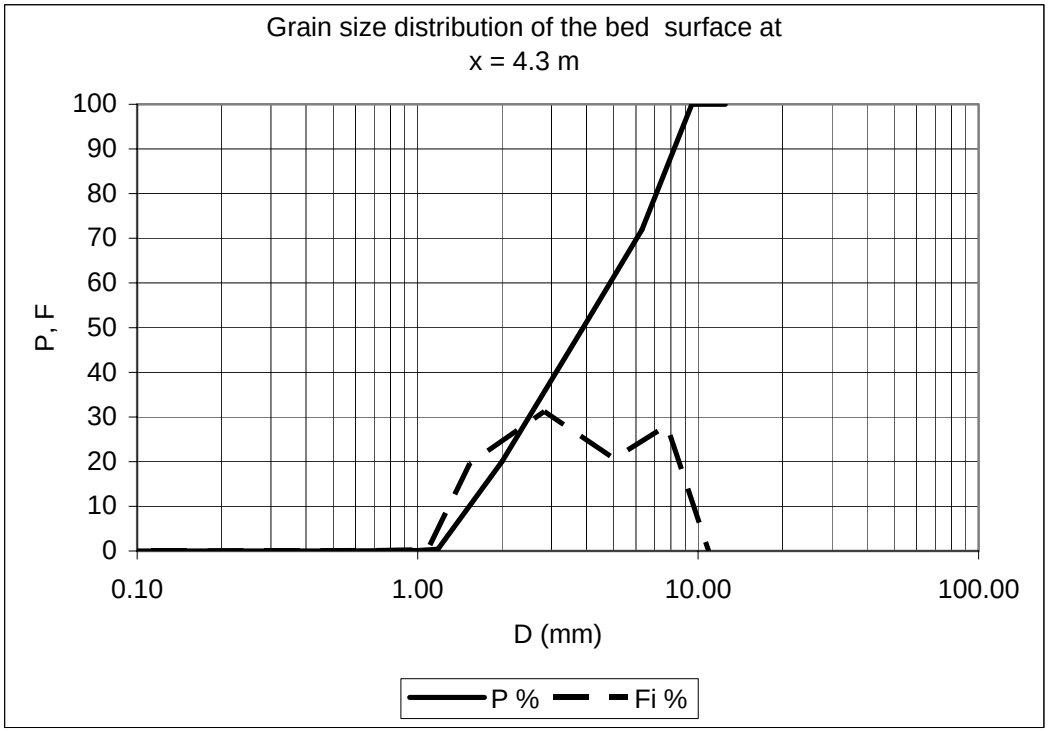

Water Discharge, Q	**25**	**l/s**
Downstream water elevation, ξ_d	**210**	**mm**
Sediment trasport rate at equilibrium, G_s	**491**	**g/min**

Grain size distribution of the bed surface at x = 6.5 m

D (mm)	P %	Di (mm)	Fi %
0.01	0.00		
0.50	0.01	0.07	0.01
1.00	0.07	0.71	0.06
1.18	0.36	1.09	0.30
2.00	19.92	1.54	19.56
4.00	48.35	2.83	28.43
6.30	71.94	5.02	23.59
9.50	99.79	7.74	27.85
12.50	100.00	10.90	0.21

D_{sg}	3.80	**mm**
σ_{sg}	1.81	
D_{s50}	4.13	**mm**
D_{s90}	8.22	**mm**

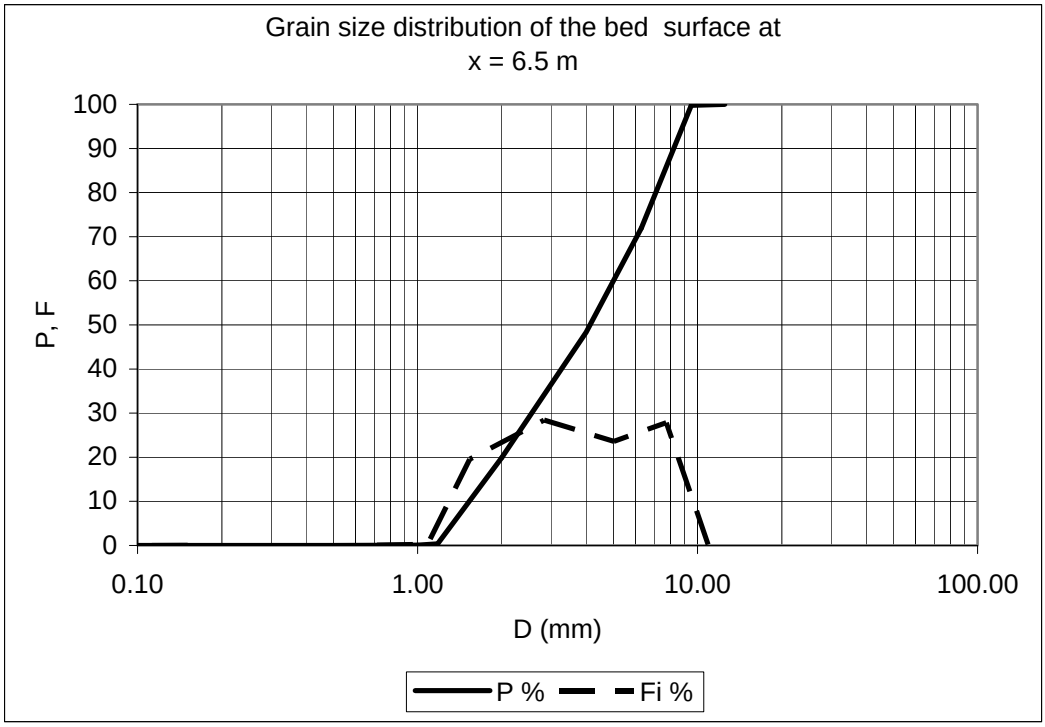

Water Discharge, Q	**25**	**l/s**
Downstream water elevation, ξ_d	**210**	**mm**
Sediment trasport rate at equilibrium, G_s	**491**	**g/min**

Grain size distribution of the bed surface at x = 8.5 m

D (mm)	P %	Di (mm)	Fi %
0.01	0.00		
0.50	0.00	0.07	0.00
1.00	0.03	0.71	0.03
1.18	0.17	1.09	0.13
2.00	14.10	1.54	13.93
4.00	45.74	2.83	31.64
6.30	68.88	5.02	23.15
9.50	100.00	7.74	31.12
12.50	100.00	10.90	0.00

D_{sg}	4.05	**mm**
σ_{sg}	1.75	
D_{s50}	4.35	**mm**
D_{s90}	8.32	**mm**

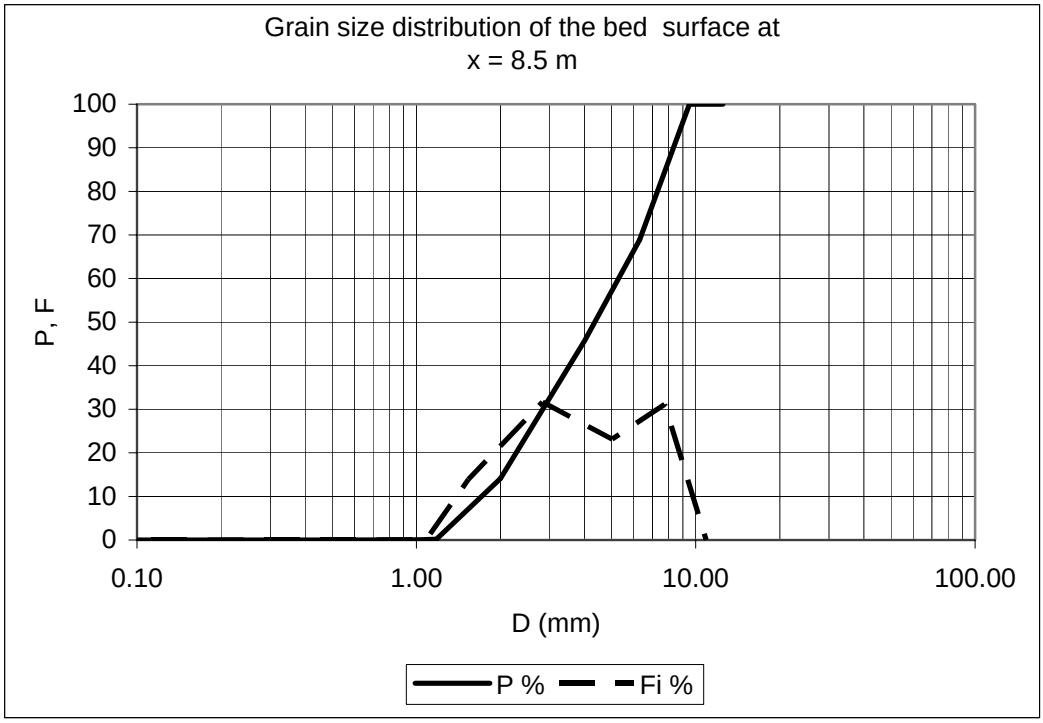

Water Discharge, Q	**25**	**l/s**
Downstream water elevation, ξ_d	**210**	**mm**
Sediment trasport rate at equilibrium, G_s	**491**	**g/min**

Grain size distribution of the bed surface at x = 10.5 m

D (mm)	P %	Di (mm)	Fi %
0.01	0.00		
0.50	0.01	0.07	0.01
1.00	0.05	0.71	0.04
1.18	0.29	1.09	0.24
2.00	15.65	1.54	15.35
4.00	44.58	2.83	28.93
6.30	67.56	5.02	22.98
9.50	100.00	7.74	32.44
12.50	100.00	10.90	0.00

D_{sg}	4.06	**mm**
σ_{sg}	1.78	
D_{s50}	4.45	**mm**
D_{s90}	8.37	**mm**

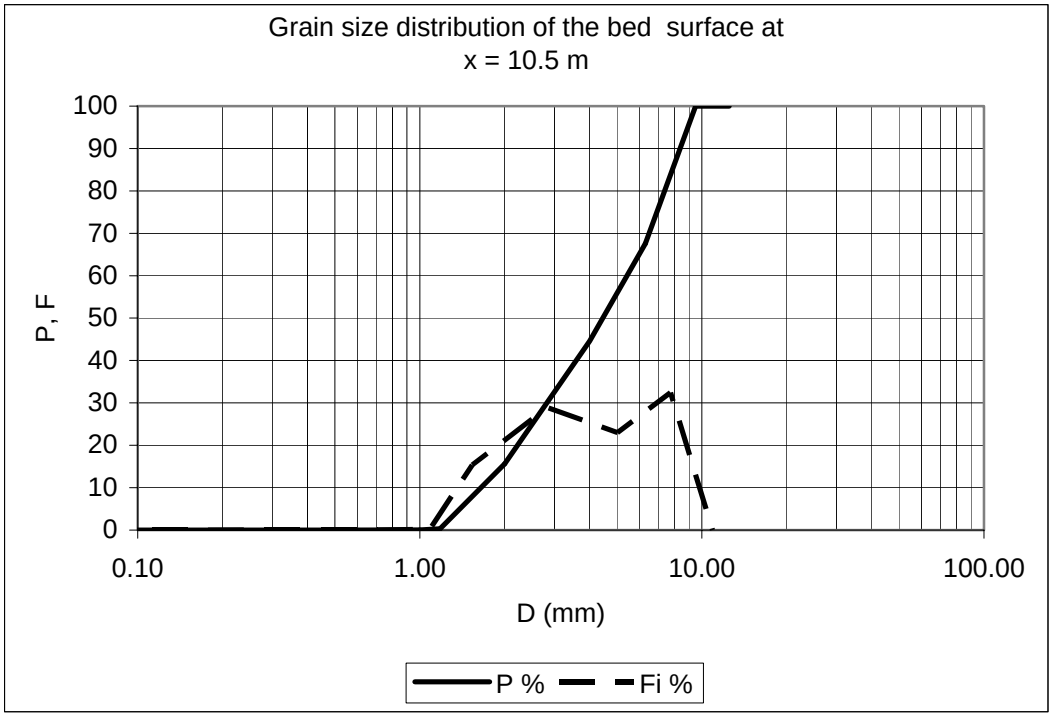

RUN 3

Water Discharge, Q	**20**	**l/s**
Downstream water elevation, ξ_d	**190**	**mm**
Sediment trasport rate at equilibrium, G_s	**458**	**g/min**

Longitudinal profile at equilibrium

x (m)	η (mm)
2.5	208
2.9	204
3.3	196
3.7	195
4.1	195
4.3	194
4.5	194
4.9	190
5.3	188
5.7	185
6.1	182
6.5	178
6.9	177
7.3	173
7.7	171
8.1	165
8.5	162
8.9	158
9.3	155
9.7	152
10.1	148
10.5	145

Water surface at equilibrium

x (m)	H (mm)
2.5	266
4.3	255
6.5	239
8.5	221
10.5	201

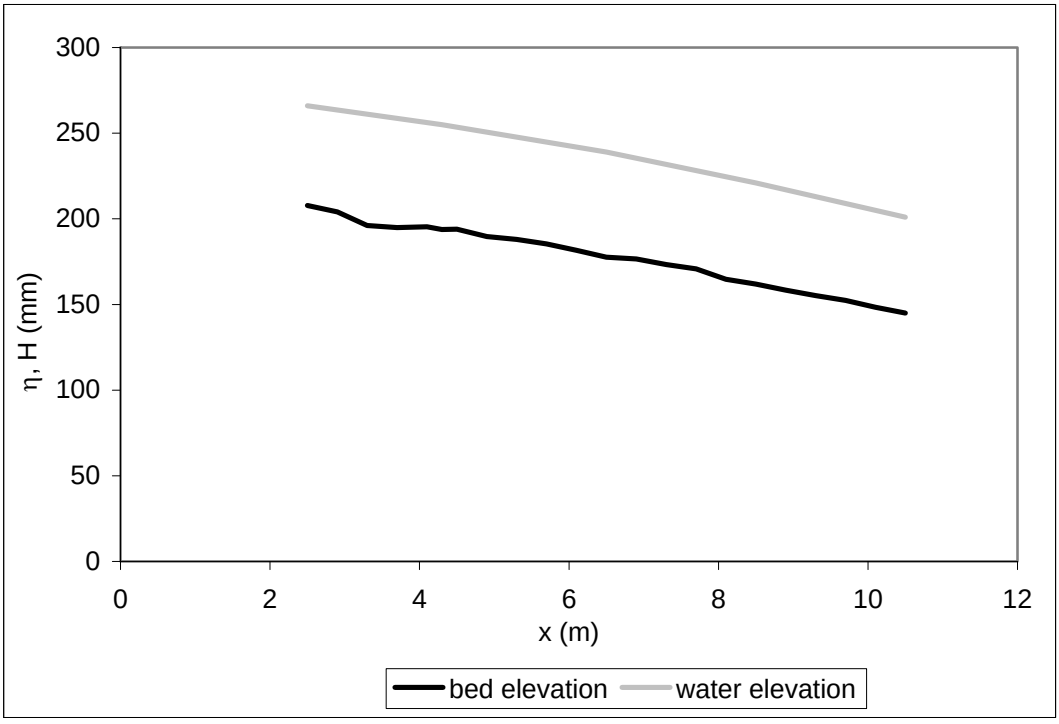

Water Discharge, Q	**20**	**l/s**
Downstream water elevation, ξ_d	**190**	**mm**
Sediment trasport rate at equilibrium, G_s	**458**	**g/min**

Grain size distribution of the bedload at equilibrium

D (mm)	P %	Di (mm)	pi %
0.01	0.00		
0.50	0.06	0.07	0.06
1.00	0.11	0.71	0.05
1.18	0.20	1.09	0.09
2.00	20.56	1.54	20.36
4.00	53.90	2.83	33.34
6.30	81.37	5.02	27.47
9.50	100.00	7.74	18.63
12.50	100.00	10.90	0.00

D_{lg}	3.51	**mm**
σ_{lg}	1.76	
D_{l50}	3.69	**mm**
D_{l90}	7.62	**mm**

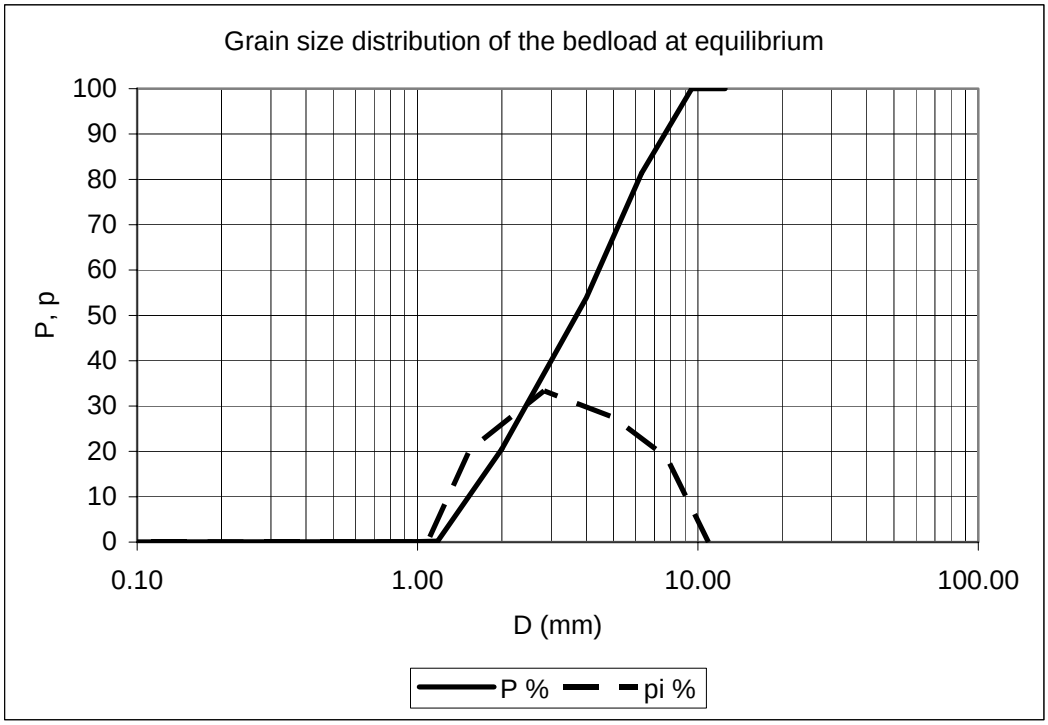

Water Discharge, Q	**20**	**l/s**
Downstream water elevation, ξ_d	**190**	**mm**
Sediment trasport rate at equilibrium, G_s	**458**	**g/min**

Grain size distribution of the bed surface at x = 2.5 m

D (mm)	P %	Di (mm)	Fi %
0.01	0.00		
0.50	0.00	0.07	0.00
1.00	0.00	0.71	0.00
1.18	0.01	1.09	0.01
2.00	4.24	1.54	4.23
4.00	31.83	2.83	27.59
6.30	65.06	5.02	33.22
9.50	100.00	7.74	34.94
12.50	100.00	10.90	0.00

D_{sg}	4.74	**mm**
σ_{sg}	1.59	
D_{s50}	5.13	**mm**
D_{s90}	8.45	**mm**

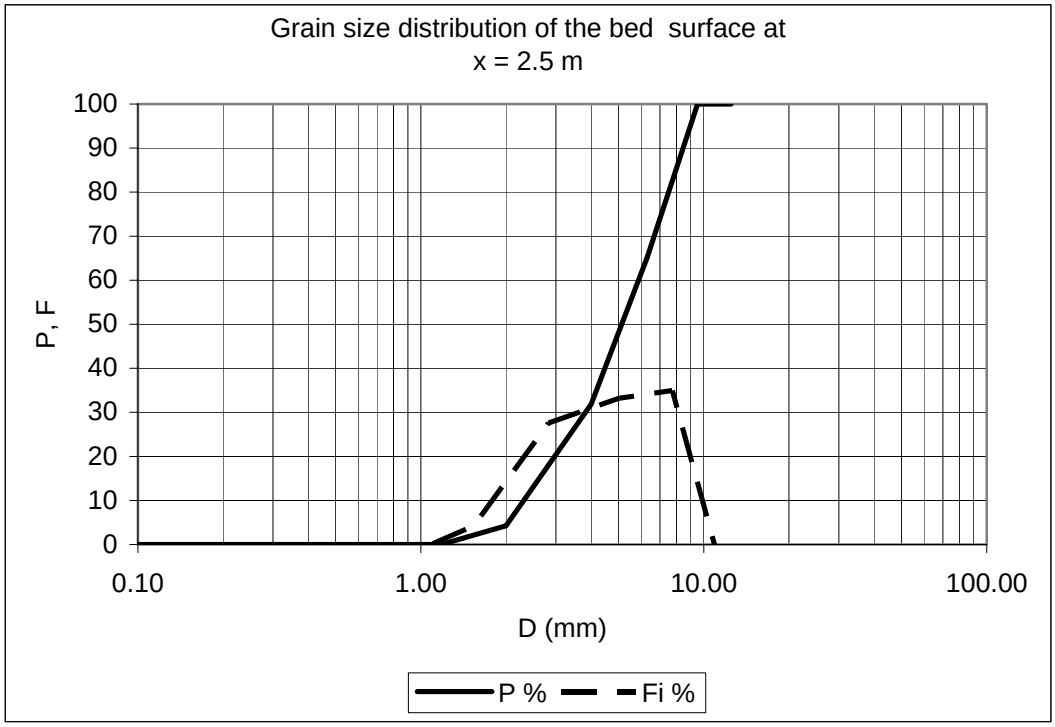

Water Discharge, Q	**20**	**l/s**
Downstream water elevation, ξ_d	**190**	**mm**
Sediment trasport rate at equilibrium, G_s	**458**	**g/min**

Grain size distribution of the bed surface at x = 4.3 m

D (mm)	P %	Di (mm)	Fi %
0.01	0.00		
0.50	0.01	0.07	0.01
1.00	0.03	0.71	0.02
1.18	0.15	1.09	0.12
2.00	16.05	1.54	15.90
4.00	49.15	2.83	33.11
6.30	71.84	5.02	22.68
9.50	100.00	7.74	28.16
12.50	100.00	10.90	0.00

D_{sg}	3.87	**mm**
σ_{sg}	1.76	
D_{s50}	4.07	**mm**
D_{s90}	8.21	**mm**

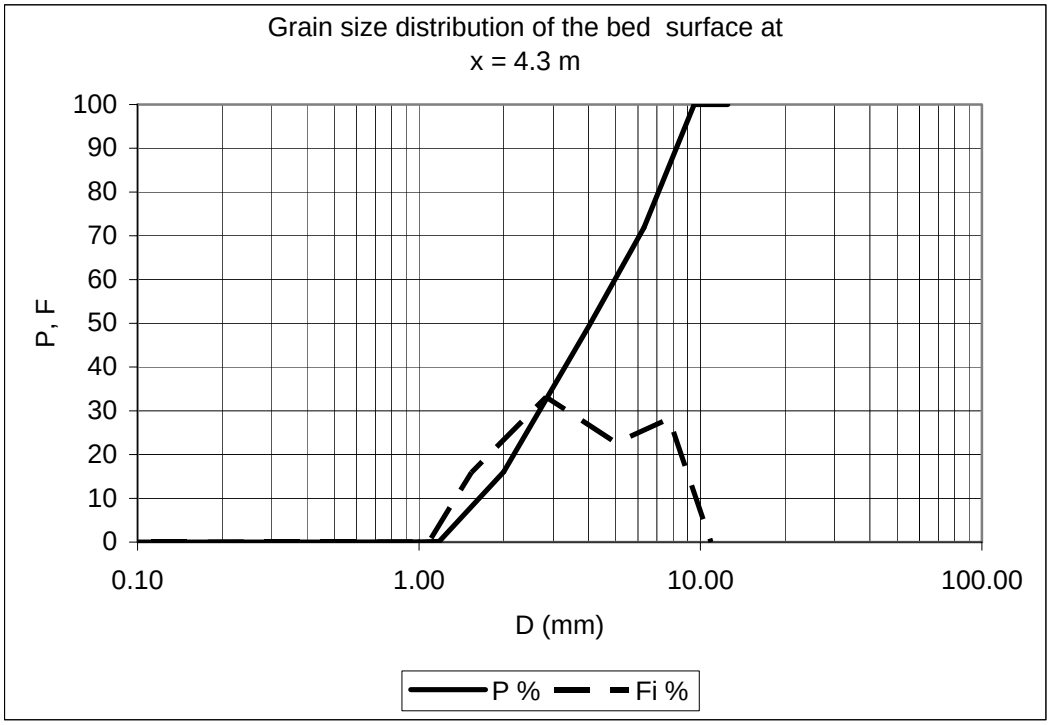

Water Discharge, Q	**20**	**l/s**
Downstream water elevation, ξ_d	**190**	**mm**
Sediment trasport rate at equilibrium, G_s	**458**	**g/min**

Grain size distribution of the bed surface at x = 6.5 m

D (mm)	P %	Di (mm)	Fi %
0.01	0.00		
0.50	0.00	0.07	0.00
1.00	0.02	0.71	0.02
1.18	0.22	1.09	0.20
2.00	13.51	1.54	13.28
4.00	40.19	2.83	26.69
6.30	67.02	5.02	26.82
9.50	100.00	7.74	32.98
12.50	100.00	10.90	0.00

D_{sg}	4.23	**mm**
σ_{sg}	1.75	
D_{s50}	4.72	**mm**
D_{s90}	8.39	**mm**

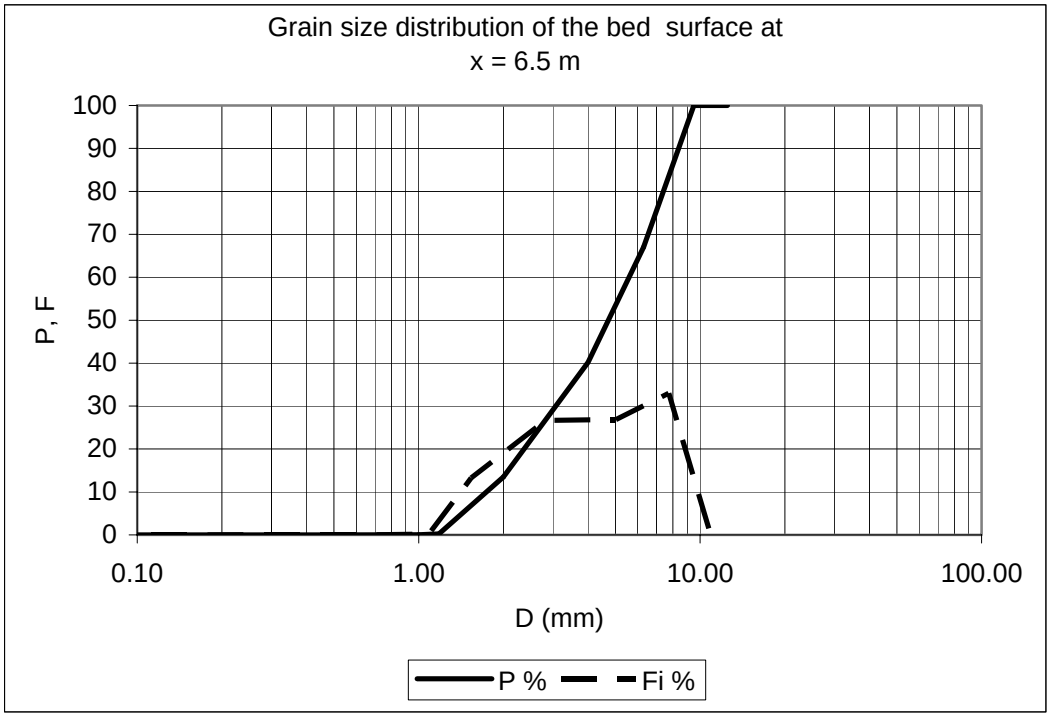

Water Discharge, Q	**20**	**l/s**
Downstream water elevation, ξ_d	**190**	**mm**
Sediment trasport rate at equilibrium, G_s	**458**	**g/min**

Grain size distribution of the bed surface at x = 8.5 m

D (mm)	P %	Di (mm)	Fi %
0.01	0.00		
0.50	0.00	0.07	0.00
1.00	0.01	0.71	0.01
1.18	0.12	1.09	0.11
2.00	13.68	1.54	13.56
4.00	38.87	2.83	25.19
6.30	63.86	5.02	24.99
9.50	100.00	7.74	36.14
12.50	100.00	10.90	0.00

D_{sg}	4.32	**mm**
σ_{sg}	1.76	
D_{s50}	4.90	**mm**
D_{s90}	8.48	**mm**

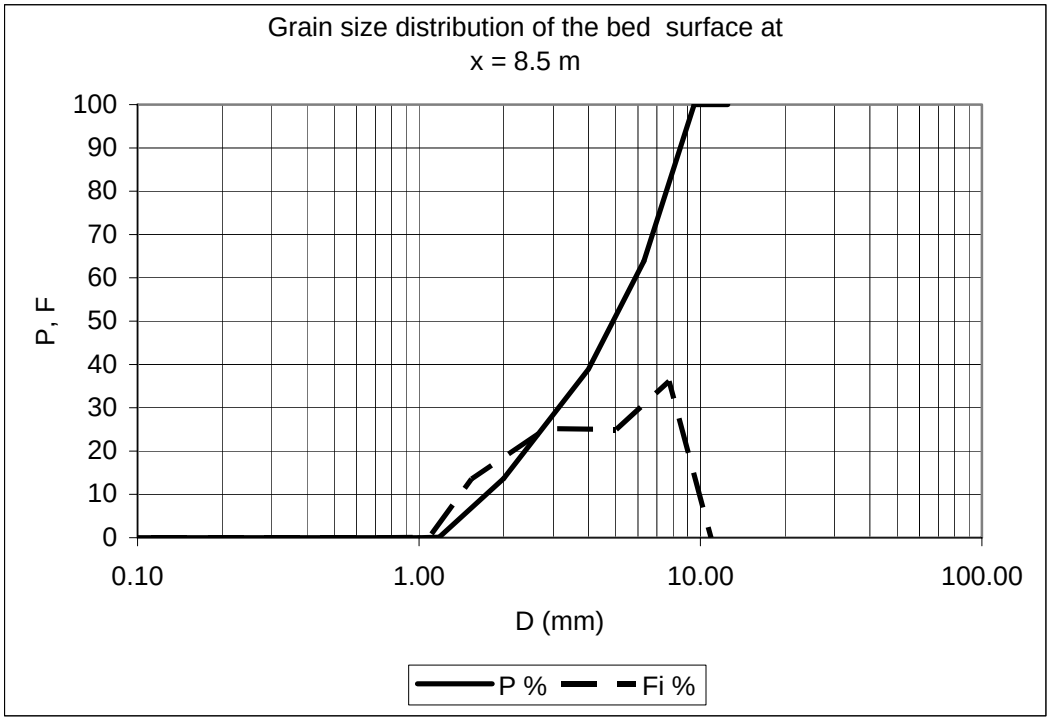

Grain size distribution of the bed surface at x = 10.5 m

D (mm)	P %	Di (mm)	Fi %
0.01	0.00		
0.50	0.00	0.07	0.00
1.00	0.00	0.71	0.00
1.18	0.03	1.09	0.02
2.00	9.25	1.54	9.22
4.00	43.74	2.83	34.50
6.30	69.37	5.02	25.62
9.50	100.00	7.74	30.63
12.50	100.00	10.90	0.00

D_{sg}	4.21	**mm**
σ_{sg}	1.68	
D_{s50}	4.47	**mm**
D_{s90}	8.31	**mm**

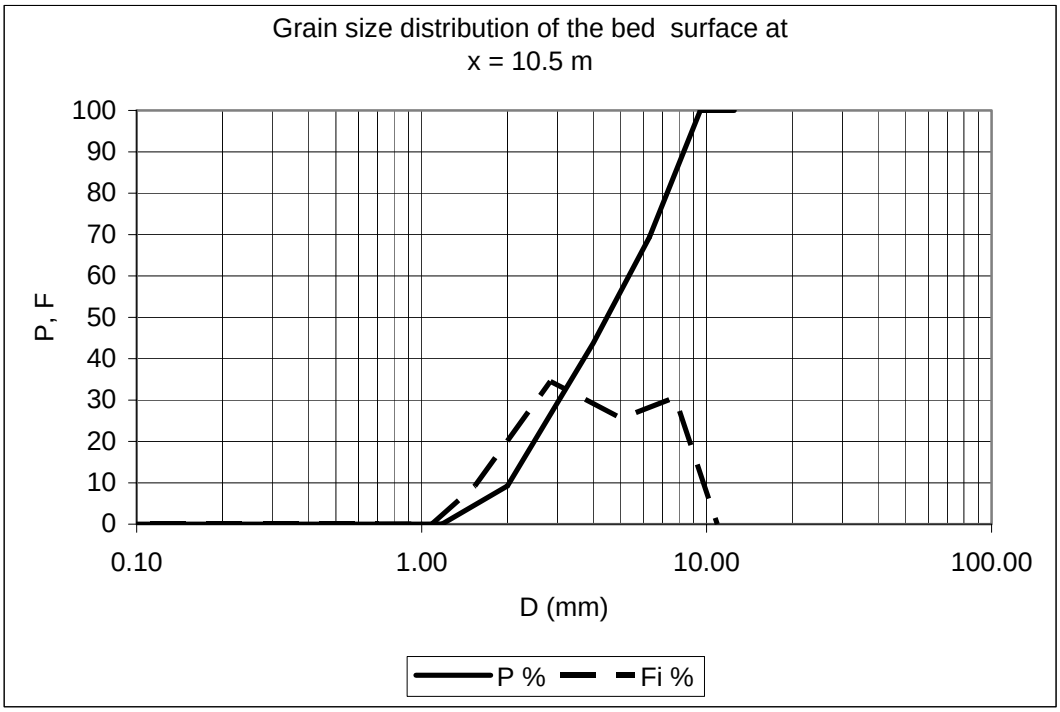

RUN 4

Water Discharge, Q	**35**	**l/s**
Downstream water elevation, ξ_d	**230**	**mm**
Sediment trasport rate at equilibrium, G_s	**1432**	**g/min**

Longitudinal profile at equilibrium

x (m)	η (mm)
2.5	205
2.9	202
3.3	200
3.7	200
4.1	198
4.3	198
4.5	193
4.9	192
5.3	187
5.7	183
6.1	181
6.5	180
6.9	178
7.3	176
7.7	173
8.1	171
8.5	167
8.9	163
9.3	164
9.7	159
10.1	156
10.5	155

Water surface at equilibrium

x (m)	H (mm)
2.5	291
4.3	278
6.5	264
8.5	252
10.5	239

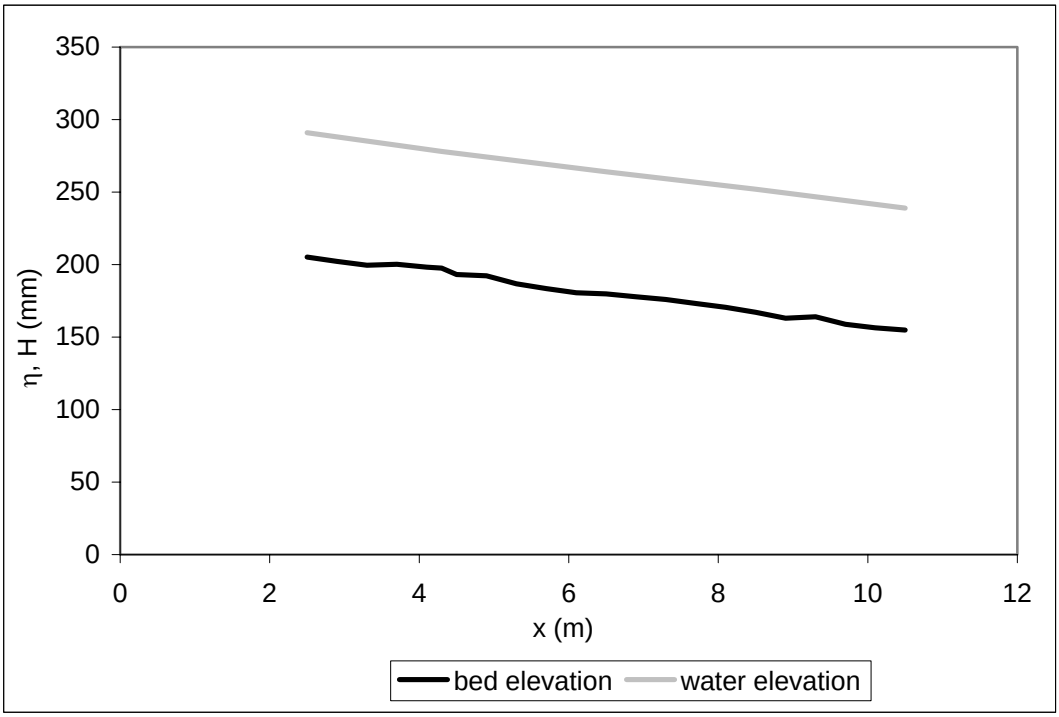

Water Discharge, Q	**35**	**l/s**
Downstream water elevation, ξ_d	**230**	**mm**
Sediment trasport rate at equilibrium, G_s	**1432**	**g/min**

Grain size distribution of the bedload at equilibrium

D (mm)	P %	Di (mm)	pi %
0.01	0.00		
0.50	0.04	0.07	0.04
1.00	0.08	0.71	0.03
1.18	0.13	1.09	0.06
2.00	12.92	1.54	12.79
4.00	54.20	2.83	41.28
6.30	79.90	5.02	25.69
9.50	100.00	7.74	20.10
12.50	100.00	10.90	0.00

D_{lg}	3.70	**mm**
σ_{lg}	1.68	
D_{l50}	3.73	**mm**
D_{l90}	7.74	**mm**

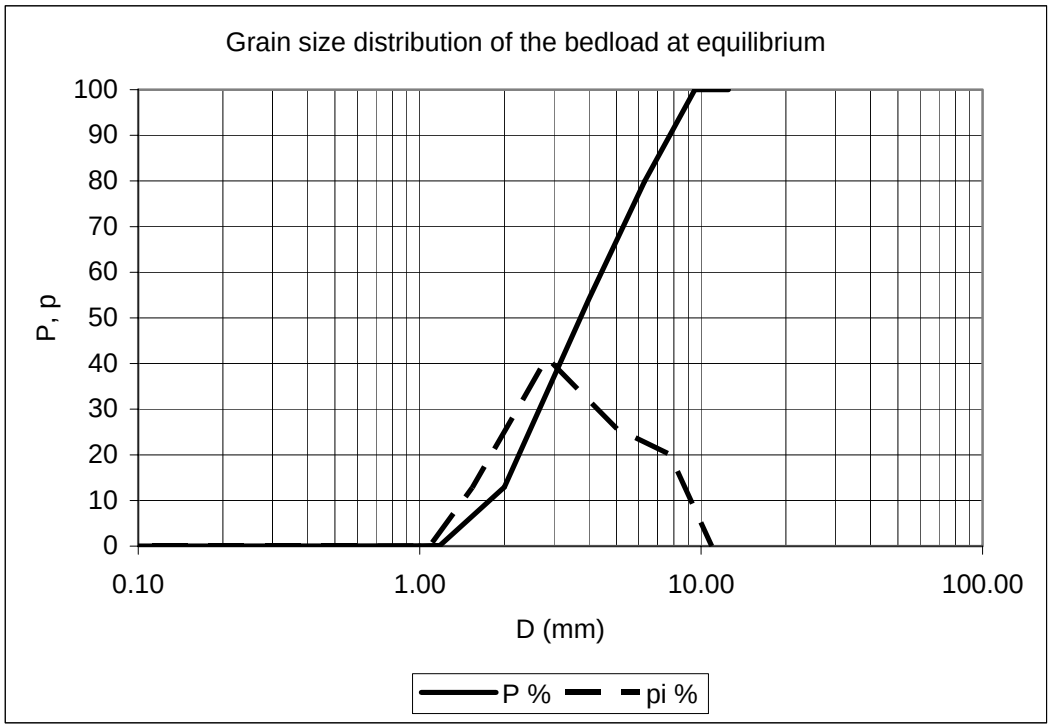

Water Discharge, Q	**35**	**l/s**
Downstream water elevation, ξ_d	**230**	**mm**
Sediment trasport rate at equilibrium, G_s	**1432**	**g/min**

Grain size distribution of the bed surface at x = 2.5 m

D (mm)	P %	Di (mm)	Fi %
0.01	0.00		
0.50	0.03	0.07	0.03
1.00	0.06	0.71	0.03
1.18	0.12	1.09	0.06
2.00	6.73	1.54	6.61
4.00	33.53	2.83	26.79
6.30	61.53	5.02	28.01
9.50	100.00	7.74	38.47
12.50	100.00	10.90	0.00

D_{sg}	4.69	**mm**
σ_{sg}	1.66	
D_{s50}	5.22	**mm**
D_{s90}	8.54	**mm**

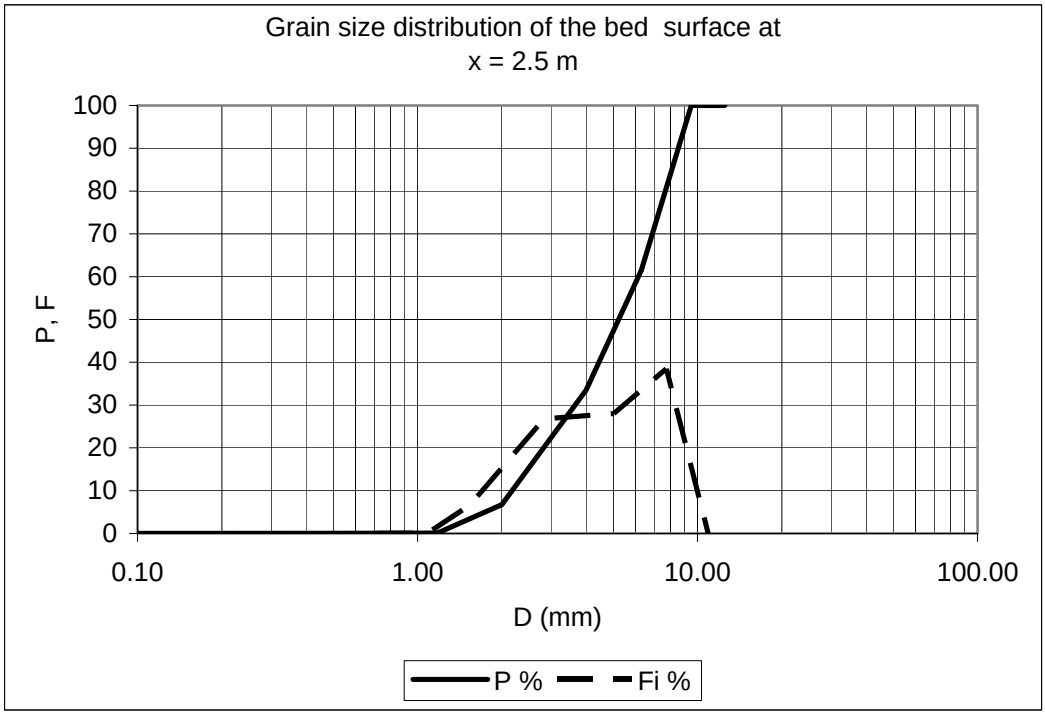

Water Discharge, Q	**35**	**l/s**
Downstream water elevation, ξ_d	**230**	**mm**
Sediment trasport rate at equilibrium, G_s	**1432**	**g/min**

Grain size distribution of the bed surface at x = 4.3 m

D (mm)	P %	Di (mm)	Fi %
0.01	0.00		
0.50	0.00	0.07	0.00
1.00	0.05	0.71	0.05
1.18	0.23	1.09	0.18
2.00	11.22	1.54	11.00
4.00	39.21	2.83	27.98
6.30	62.19	5.02	22.98
9.50	100.00	7.74	37.81
12.50	100.00	10.90	0.00

D_{sg}	4.40	**mm**
σ_{sg}	1.74	
D_{s50}	4.95	**mm**
D_{s90}	8.52	**mm**

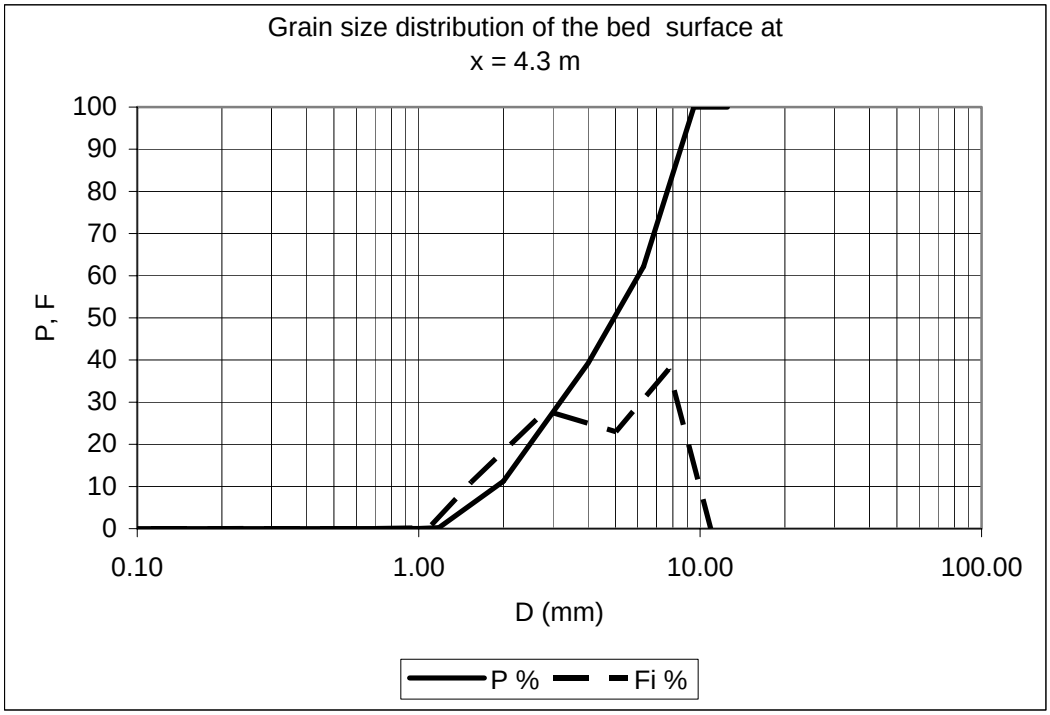

Water Discharge, Q	**35**	**l/s**
Downstream water elevation, ξ_d	**230**	**mm**
Sediment trasport rate at equilibrium, G_s	**1432**	**g/min**

Grain size distribution of the bed surface at x = 6.5 m

D (mm)	P %	Di (mm)	Fi %
0.01	0.00		
0.50	0.00	0.07	0.00
1.00	0.30	0.71	0.30
1.18	1.02	1.09	0.72
2.00	19.36	1.54	18.33
4.00	45.24	2.83	25.88
6.30	64.04	5.02	18.80
9.50	100.00	7.74	35.96
12.50	100.00	10.90	0.00

D_{sg}	4.00	**mm**
σ_{sg}	1.86	
D_{s50}	4.49	**mm**
D_{s90}	8.47	**mm**

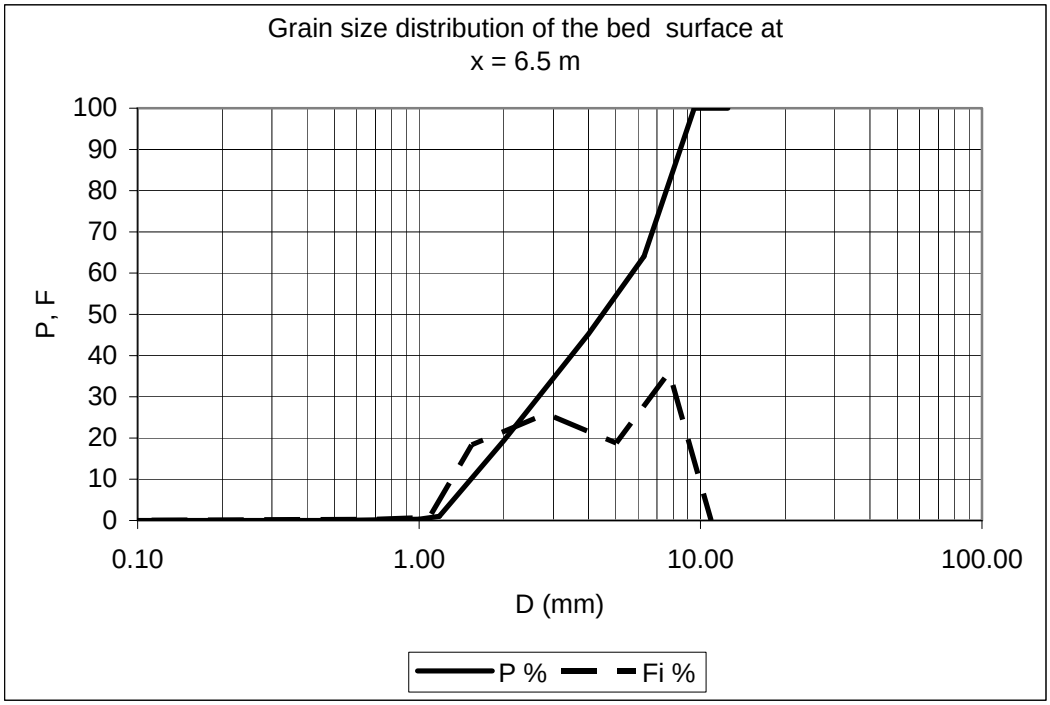

Water Discharge, Q	**35**	**l/s**
Downstream water elevation, ξ_d	**230**	**mm**
Sediment trasport rate at equilibrium, G_s	**1432**	**g/min**

Grain size distribution of the bed surface at x = 8.5 m

D (mm)	P %	Di (mm)	Fi %
0.01	0.00		
0.50	0.00	0.07	0.00
1.00	0.02	0.71	0.02
1.18	0.21	1.09	0.19
2.00	8.43	1.54	8.22
4.00	35.42	2.83	26.99
6.30	68.64	5.02	33.22
9.50	100.00	7.74	31.36
12.50	100.00	10.90	0.00

D_{sg}	4.45	**mm**
σ_{sg}	1.65	
D_{s50}	4.88	**mm**
D_{s90}	8.33	**mm**

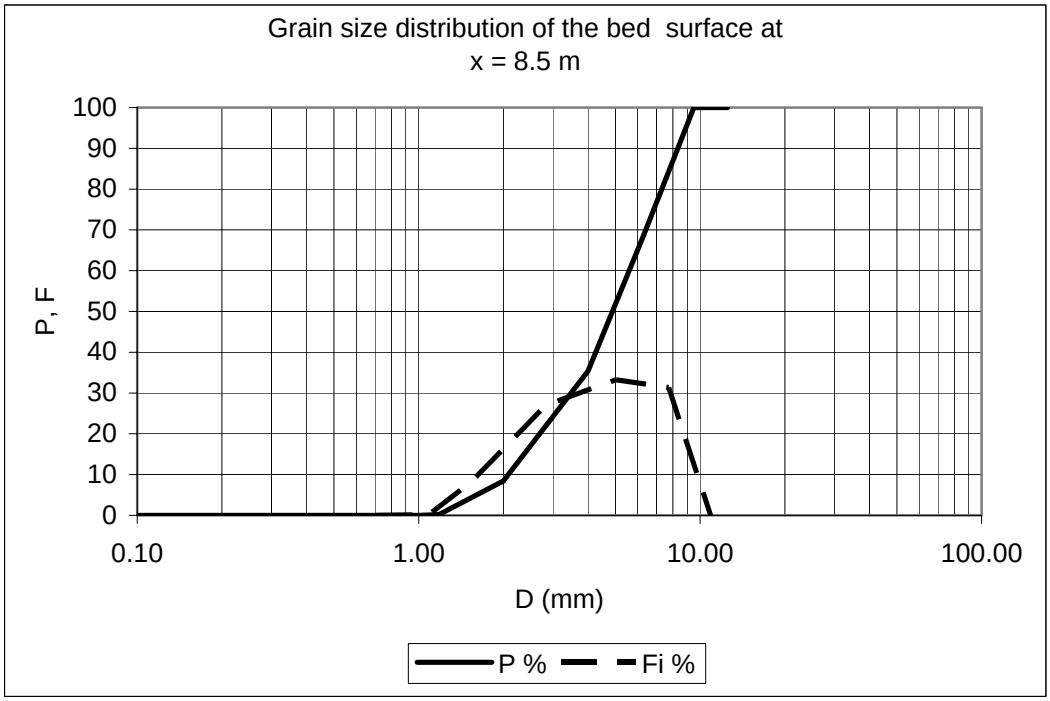

Water Discharge, Q	**35**	**l/s**
Downstream water elevation, ξ_d	**230**	**mm**
Sediment trasport rate at equilibrium, G_s	**1432**	**g/min**

Grain size distribution of the bed surface at x = 10.5 m

D (mm)	P %	Di (mm)	Fi %
0.01	0.00		
0.50	0.00	0.07	0.00
1.00	0.02	0.71	0.02
1.18	0.21	1.09	0.19
2.00	8.43	1.54	8.22
4.00	35.42	2.83	26.99
6.30	63.67	5.02	28.26
9.50	100.00	7.74	36.33
12.50	100.00	10.90	0.00

D_{sg}	4.55	**mm**
σ_{sg}	1.68	
D_{s50}	5.06	**mm**
D_{s90}	8.48	**mm**

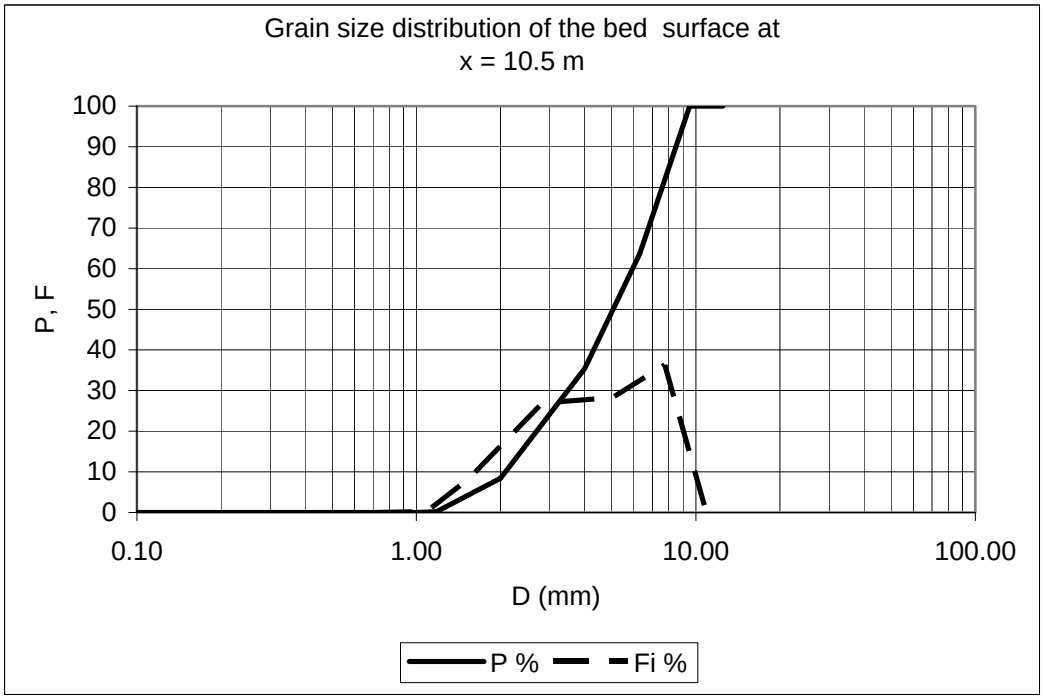

RUN 5

Water Discharge, Q	**20**	**l/s**
Downstream water elevation, ξ_d	**210**	**mm**
Sediment trasport rate at equilibrium, G_s	**54**	**g/min**

Longitudinal profile at equilibrium

x (m)	η (mm)
2.5	194
2.9	196
3.3	199
3.7	198
4.1	197
4.3	196
4.5	193
4.9	191
5.3	189
5.7	187
6.1	183
6.5	184
6.9	179
7.3	176
7.7	173
8.1	172
8.5	169
8.9	166
9.3	163
9.7	162
10.1	159
10.5	157

Water surface at equilibrium

x (m)	H (mm)
2.5	270
4.3	259
6.5	243
8.5	230
10.5	216

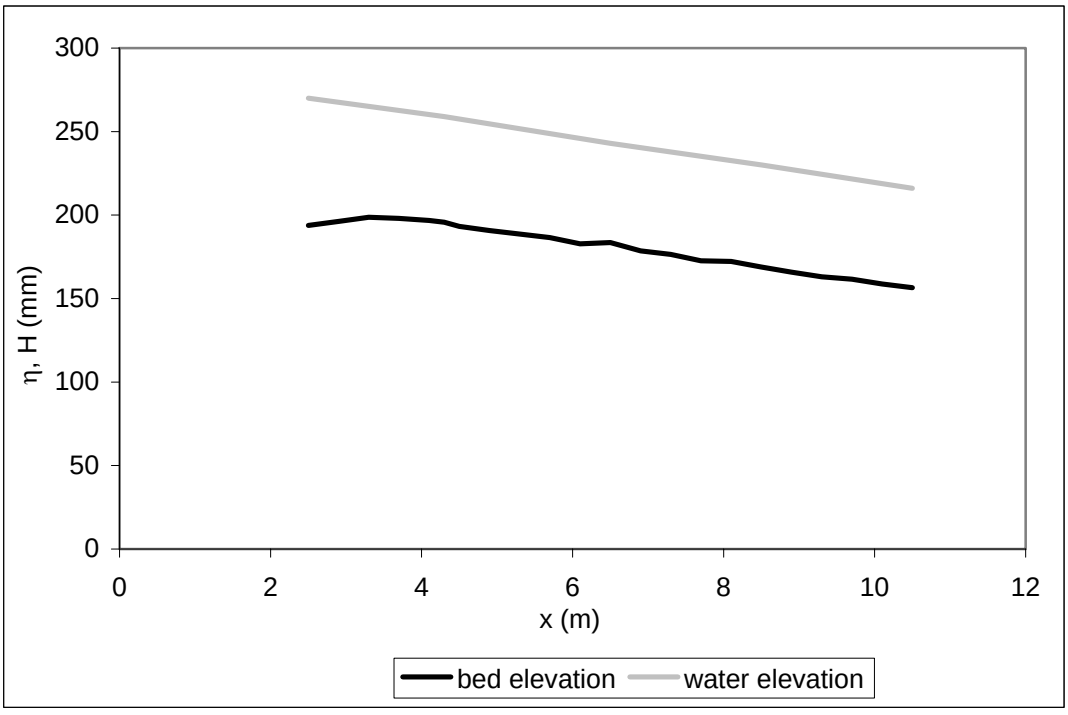

Water Discharge, Q	**20**	**l/s**
Downstream water elevation, ξ_d	**210**	**mm**
Sediment trasport rate at equilibrium, G_s	**54**	**g/min**

Grain size distribution of the bedload at equilibrium

D (mm)	P %	Di (mm)	pi %
0.01	0.00		
0.50	0.02	0.07	0.02
1.00	0.17	0.71	0.15
1.18	0.70	1.09	0.53
2.00	32.81	1.54	32.11
4.00	72.48	2.83	39.67
6.30	87.73	5.02	15.25
9.50	100.00	7.74	12.27
12.50	100.00	10.90	0.00

D_{lg}	2.85	**mm**
σ_{lg}	1.74	
D_{l50}	2.70	**mm**
D_{l90}	6.80	**mm**

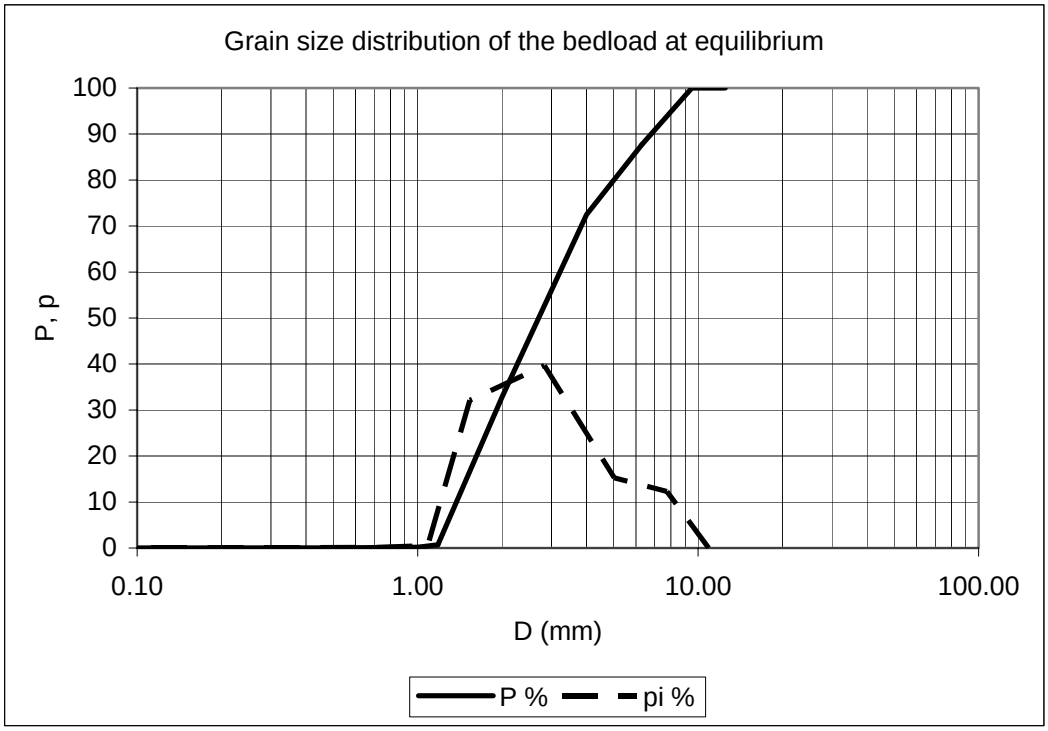

Water Discharge, Q	**20**	**l/s**
Downstream water elevation, ξ_d	**210**	**mm**
Sediment trasport rate at equilibrium, G_s	**54**	**g/min**

Grain size distribution of the bed surface at x = 2.5 m

D (mm)	P %	Di (mm)	Fi %
0.01	0.00		
0.50	0.02	0.07	0.02
1.00	0.41	0.71	0.39
1.18	0.66	1.09	0.25
2.00	14.80	1.54	14.14
4.00	44.27	2.83	29.47
6.30	65.29	5.02	21.02
9.50	100.00	7.74	34.71
12.50	100.00	10.90	0.00

D_{sg}	4.11	**mm**
σ_{sg}	1.80	
D_{s50}	4.53	**mm**
D_{s90}	8.44	**mm**

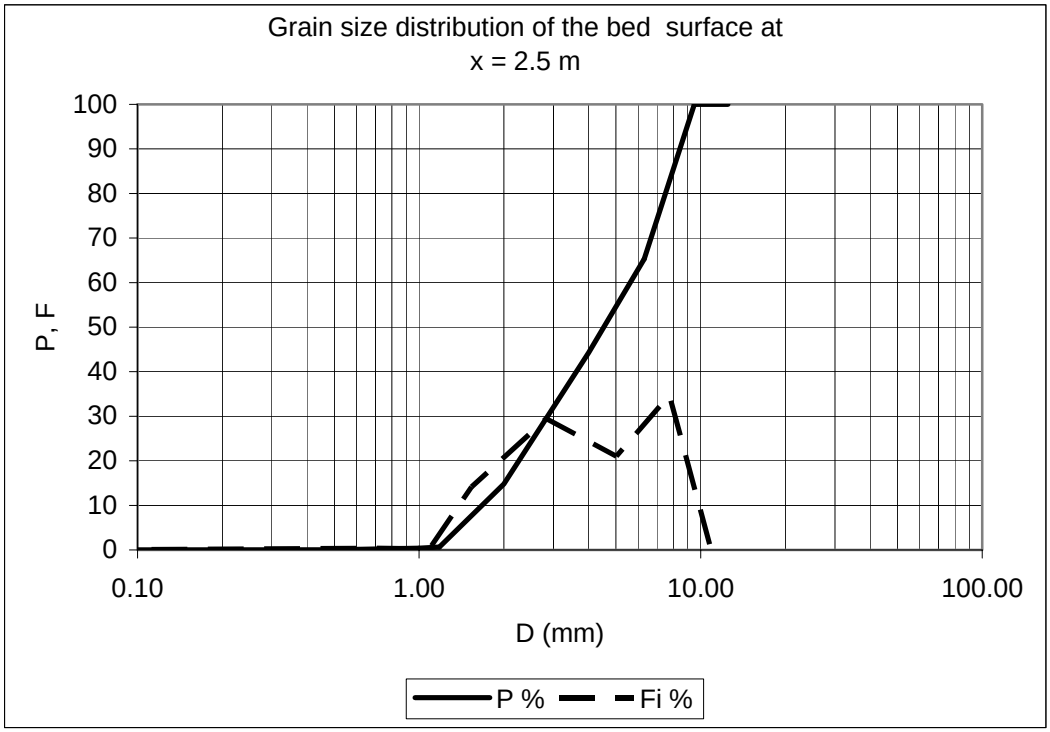

Water Discharge, Q	**20**	**l/s**
Downstream water elevation, ξ_d	**210**	**mm**
Sediment trasport rate at equilibrium, G_s	**54**	**g/min**

Grain size distribution of the bed surface at x = 4.3 m

D (mm)	P %	Di (mm)	Fi %
0.01	0.00		
0.50	0.01	0.07	0.01
1.00	0.07	0.71	0.06
1.18	0.20	1.09	0.13
2.00	7.99	1.54	7.78
4.00	33.54	2.83	25.56
6.30	60.18	5.02	26.63
9.50	99.78	7.74	39.60
12.50	100.00	10.90	0.22

D_{sg}	4.68	**mm**
σ_{sg}	1.68	
D_{s50}	5.30	**mm**
D_{s90}	8.58	**mm**

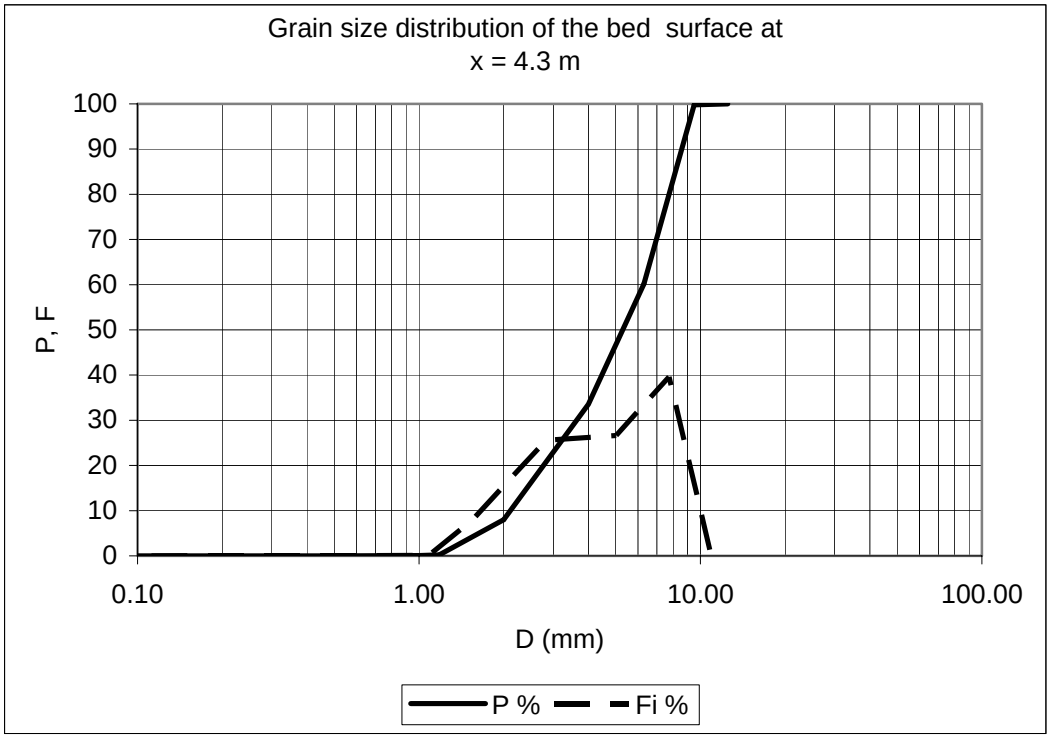

Water Discharge, Q	**20**	**l/s**
Downstream water elevation, ξ_d	**210**	**mm**
Sediment trasport rate at equilibrium, G_s	**54**	**g/min**

Grain size distribution of the bed surface at x = 6.5 m

D (mm)	P %	Di (mm)	Fi %
0.01	0.00		
0.50	0.01	0.07	0.01
1.00	0.02	0.71	0.01
1.18	0.12	1.09	0.10
2.00	8.24	1.54	8.12
4.00	32.06	2.83	23.82
6.30	57.65	5.02	25.60
9.50	100.00	7.74	42.35
12.50	100.00	10.90	0.00

D_{sg}	4.77	**mm**
σ_{sg}	1.69	
D_{s50}	5.50	**mm**
D_{s90}	8.62	**mm**

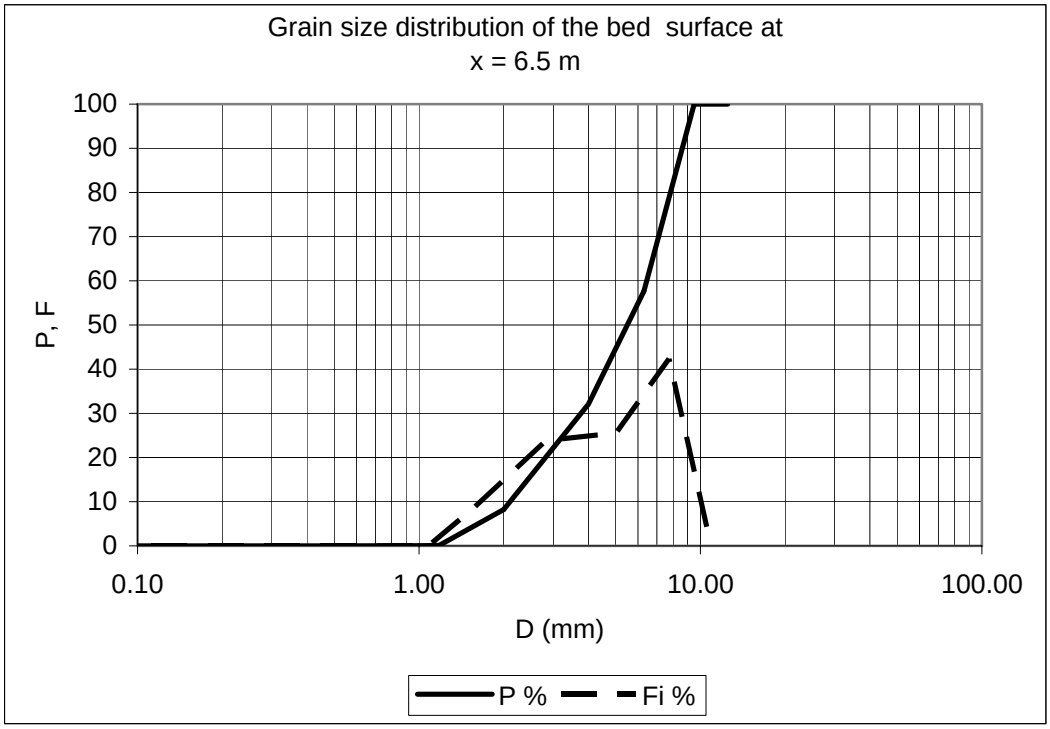

Water Discharge, Q	**20**	**l/s**
Downstream water elevation, ξ_d	**210**	**mm**
Sediment trasport rate at equilibrium, G_s	**54**	**g/min**

Grain size distribution of the bed surface at x = 8.5 m

D (mm)	P %	Di (mm)	Fi %
0.01	0.00		
0.50	0.01	0.07	0.01
1.00	0.02	0.71	0.01
1.18	0.10	1.09	0.08
2.00	9.10	1.54	9.00
4.00	30.96	2.83	21.86
6.30	56.78	5.02	25.83
9.50	100.00	7.74	43.22
12.50	100.00	10.90	0.00

D_{sg}	4.79	**mm**
σ_{sg}	1.70	
D_{s50}	5.59	**mm**
D_{s90}	8.64	**mm**

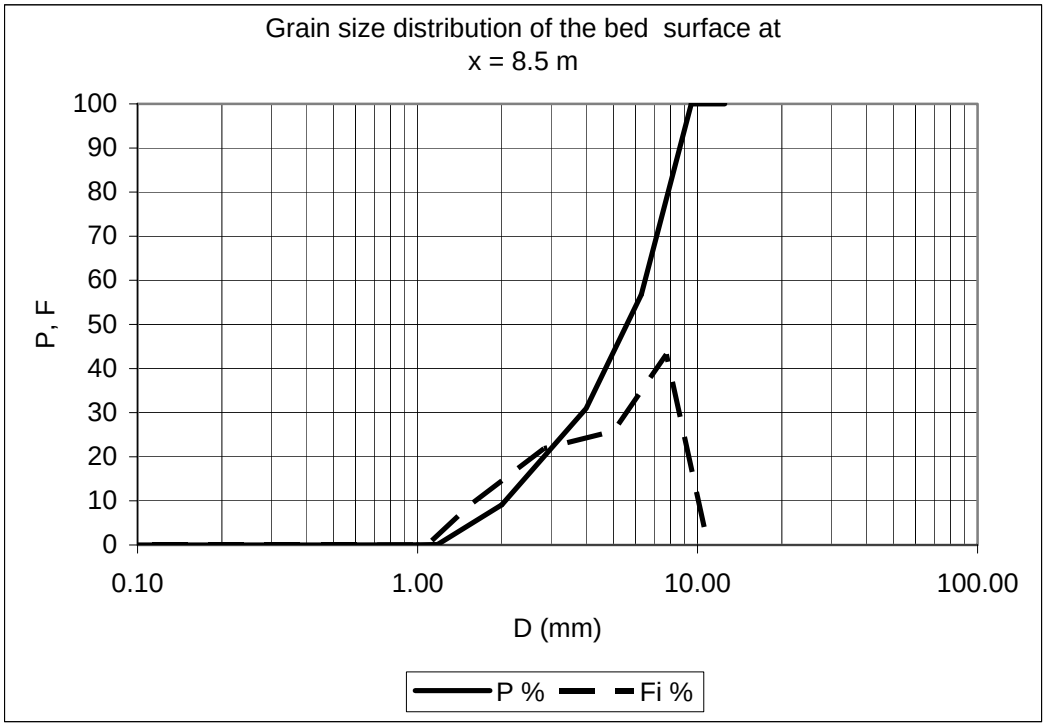

Water Discharge, Q	**20**	**l/s**
Downstream water elevation, ξ_d	**210**	**mm**
Sediment trasport rate at equilibrium, G_s	**54**	**g/min**

Grain size distribution of the bed surface at x = 10.5 m

D (mm)	P %	Di (mm)	Fi %
0.01	0.00		
0.50	0.02	0.07	0.02
1.00	0.02	0.71	0.00
1.18	0.03	1.09	0.02
2.00	5.29	1.54	5.26
4.00	26.82	2.83	21.52
6.30	53.88	5.02	27.06
9.50	100.00	7.74	46.12
12.50	100.00	10.90	0.00

D_{sg}	5.08	**mm**
σ_{sg}	1.62	
D_{s50}	5.90	**mm**
D_{s90}	8.69	**mm**

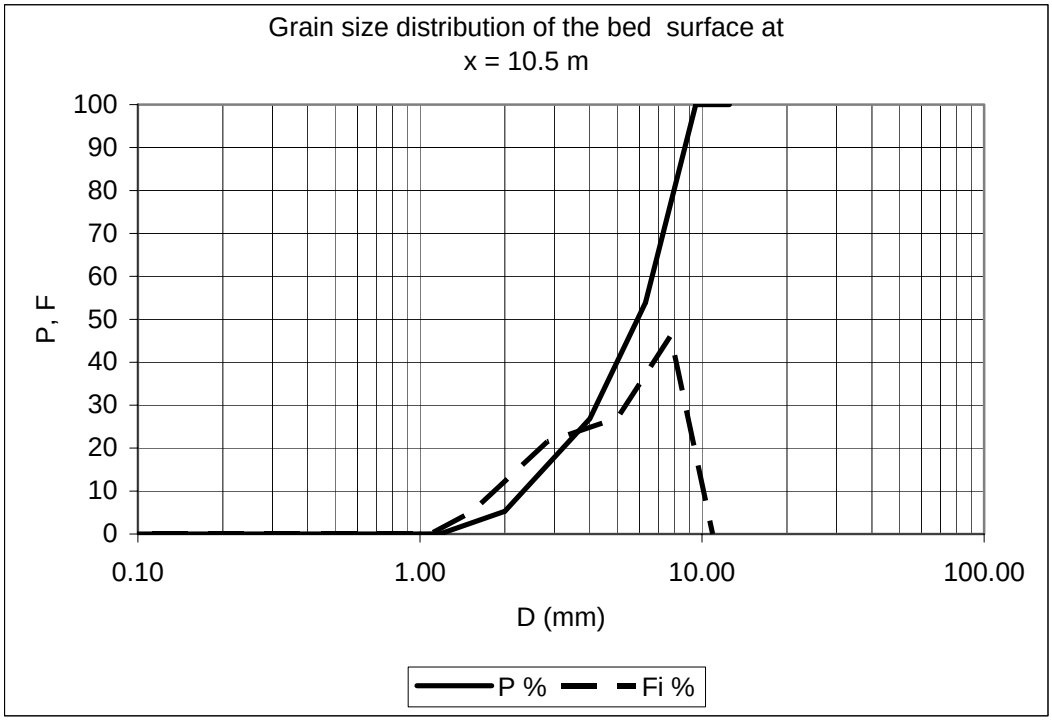

RUN 6

Water Discharge, Q	**30**	**l/s**
Downstream water elevation, ξ_d	**240**	**mm**
Sediment trasport rate at equilibrium, G_s	**64**	**gr/min**

Longitudinal profile at equilibrium

x (m)	η (mm)
2.5	201
2.9	200
3.3	199
3.7	196
4.1	194
4.3	193
4.5	191
4.9	190
5.3	186
5.7	183
6.1	183
6.5	181
6.9	180
7.3	177
7.7	176
8.1	175
8.5	173
8.9	172
9.3	169
9.7	167
10.1	165
10.5	164

Water surface at equilibrium

x (m)	H (mm)
2.5	283
4.3	276
6.5	265
8.5	255
10.5	245

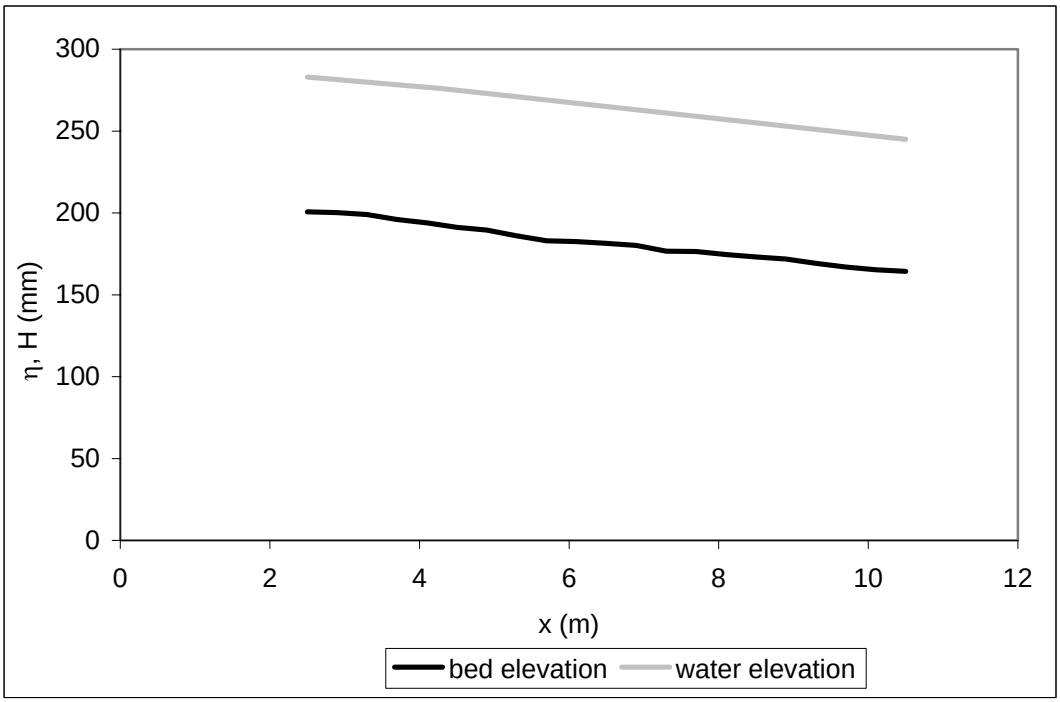

Water Discharge, Q	**30**	**l/s**
Downstream water elevation, ξ_d	**240**	**mm**
Sediment trasport rate at equilibrium, G_s	**64**	**gr/min**

Grain size distribution of the bedload at equilibrium

D (mm)	P %	Di (mm)	pi %
0.01	0.00		
0.50	0.02	0.07	0.02
1.00	0.10	0.71	0.08
1.18	0.20	1.09	0.10
2.00	22.08	1.54	21.88
4.00	60.60	2.83	38.52
6.30	80.59	5.02	19.99
9.50	100.00	7.74	19.41
12.50	100.00	10.90	0.00

D_{lg}	3.36	**mm**
σ_{lg}	1.76	
D_{l50}	3.30	**mm**
D_{l90}	7.69	**mm**

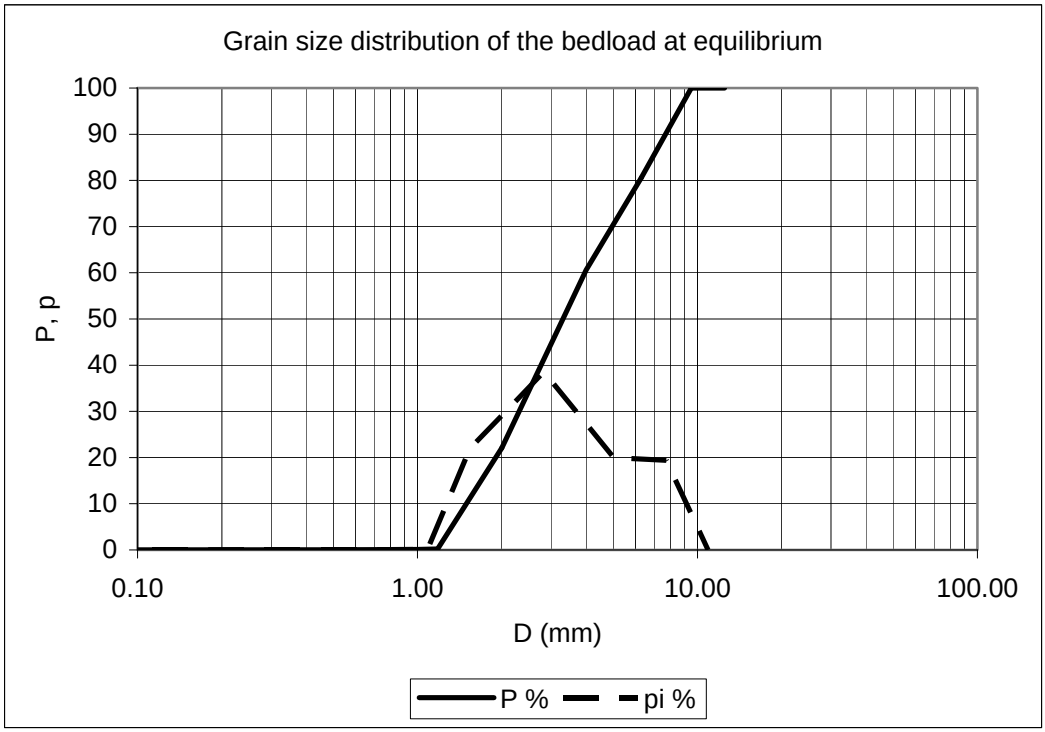

Water Discharge, Q	**30**	**l/s**
Downstream water elevation, ξ_d	**240**	**mm**
Sediment trasport rate at equilibrium, G_s	**64**	**gr/min**

Grain size distribution of the bed surface at x = 2.5 m

D (mm)	P %	Di (mm)	Fi %
0.01	0.00		
0.50	0.01	0.07	0.01
1.00	0.07	0.71	0.06
1.18	0.23	1.09	0.16
2.00	6.03	1.54	5.80
4.00	30.74	2.83	24.72
6.30	57.54	5.02	26.79
9.50	100.00	7.74	42.46
12.50	100.00	10.90	0.00

D_{sg}	4.89	**mm**
σ_{sg}	1.65	
D_{s50}	5.54	**mm**
D_{s90}	8.62	**mm**

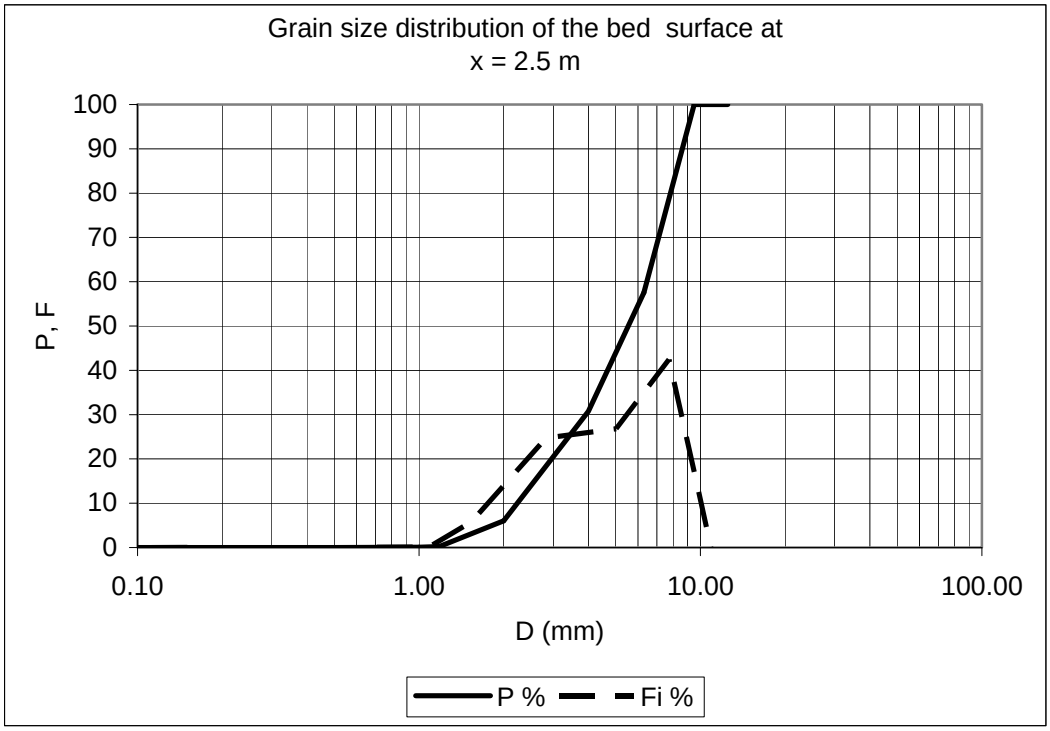

Water Discharge, Q	**30**	**l/s**
Downstream water elevation, ξ_d	**240**	**mm**
Sediment trasport rate at equilibrium, G_s	**64**	**gr/min**

Grain size distribution of the bed surface at x = 4.3 m

D (mm)	P %	Di (mm)	Fi %
0.01	0.00		
0.50	0.01	0.07	0.01
1.00	0.10	0.71	0.09
1.18	0.30	1.09	0.20
2.00	7.64	1.54	7.34
4.00	29.34	2.83	21.69
6.30	57.38	5.02	28.05
9.50	100.00	7.74	42.62
12.50	100.00	10.90	0.00

D_{sg}	4.86	**mm**
σ_{sg}	1.67	
D_{s50}	5.59	**mm**
D_{s90}	8.63	**mm**

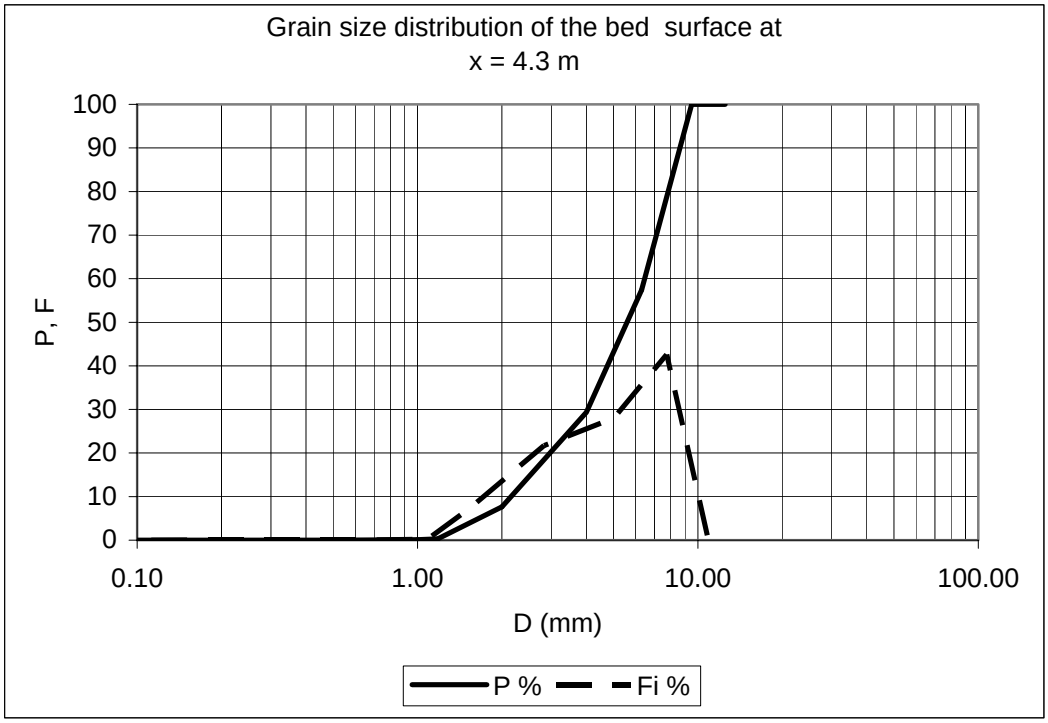

Water Discharge, Q	**30**	**l/s**
Downstream water elevation, ξ_d	**240**	**mm**
Sediment trasport rate at equilibrium, G_s	**64**	**gr/min**

Grain size distribution of the bed surface at x = 6.5 m

D (mm)	P %	Di (mm)	Fi %
0.01	0.00		
0.50	0.01	0.07	0.01
1.00	0.06	0.71	0.05
1.18	0.27	1.09	0.21
2.00	10.89	1.54	10.63
4.00	34.65	2.83	23.76
6.30	57.65	5.02	23.00
9.50	100.00	7.74	42.35
12.50	100.00	10.90	0.00

D_{sg}	4.62	**mm**
σ_{sg}	1.74	
D_{s50}	5.42	**mm**
D_{s90}	8.62	**mm**

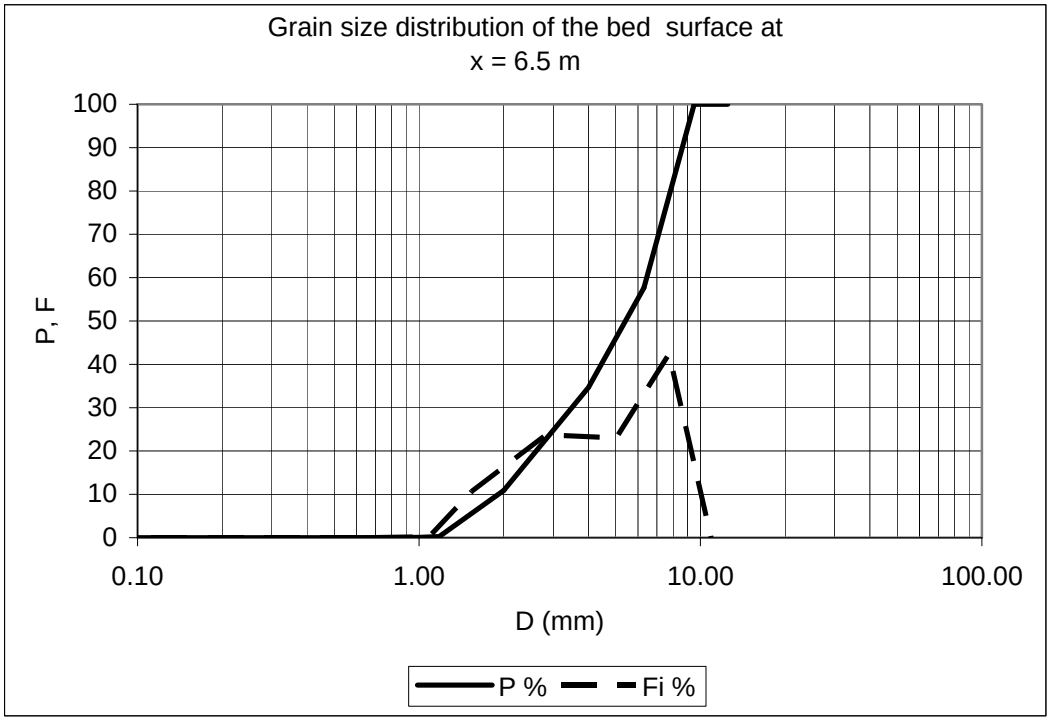

Water Discharge, Q	**30**	**l/s**
Downstream water elevation, ξ_d	**240**	**mm**
Sediment trasport rate at equilibrium, G_s	**64**	**gr/min**

Grain size distribution of the bed surface at x = 8.5 m

D (mm)	P %	Di (mm)	Fi %
0.01	0.00		
0.50	0.01	0.07	0.01
1.00	0.02	0.71	0.01
1.18	0.15	1.09	0.13
2.00	11.34	1.54	11.18
4.00	34.25	2.83	22.91
6.30	58.54	5.02	24.29
9.50	100.00	7.74	41.46
12.50	100.00	10.90	0.00

D_{sg}	4.60	**mm**
σ_{sg}	1.74	
D_{s50}	5.37	**mm**
D_{s90}	8.60	**mm**

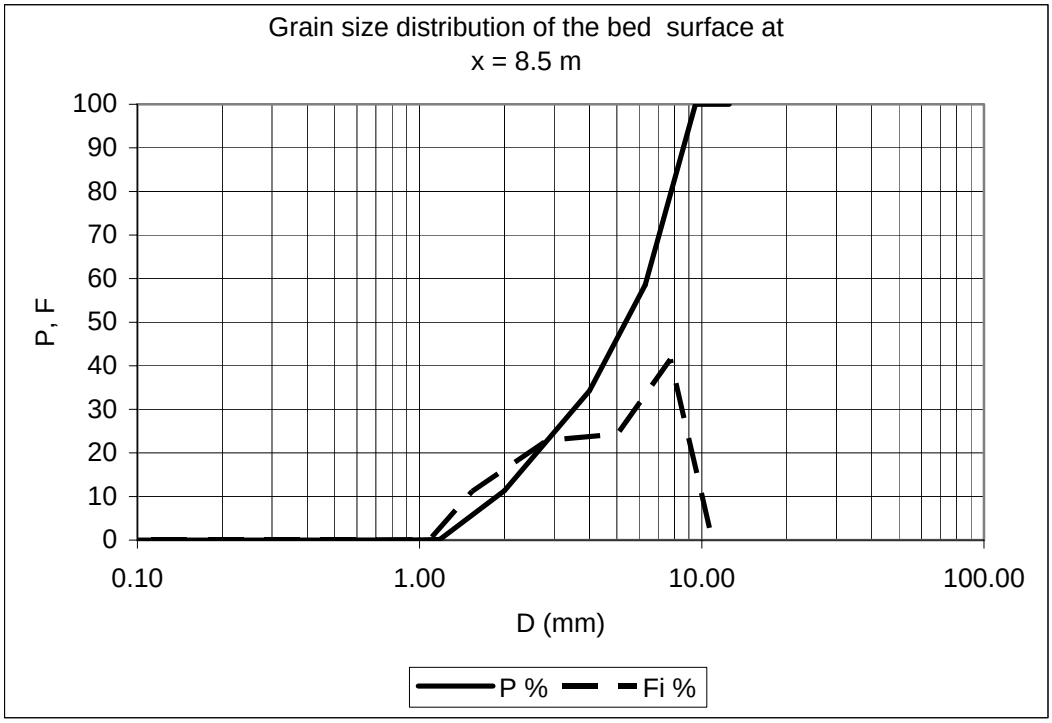

Water Discharge, Q	**30**	**l/s**
Downstream water elevation, ξ_d	**240**	**mm**
Sediment trasport rate at equilibrium, G_s	**64**	**gr/min**

Grain size distribution of the bed surface at x = 10.5 m

D (mm)	P %	Di (mm)	Fi %
0.01	0.00		
0.50	0.00	0.07	0.00
1.00	0.00	0.71	0.00
1.18	0.05	1.09	0.05
2.00	6.71	1.54	6.66
4.00	33.45	2.83	26.75
6.30	61.94	5.02	28.48
9.50	100.00	7.74	38.06
12.50	100.00	10.90	0.00

D_{sg}	4.69	**mm**
σ_{sg}	1.65	
D_{s50}	5.21	**mm**
D_{s90}	8.53	**mm**

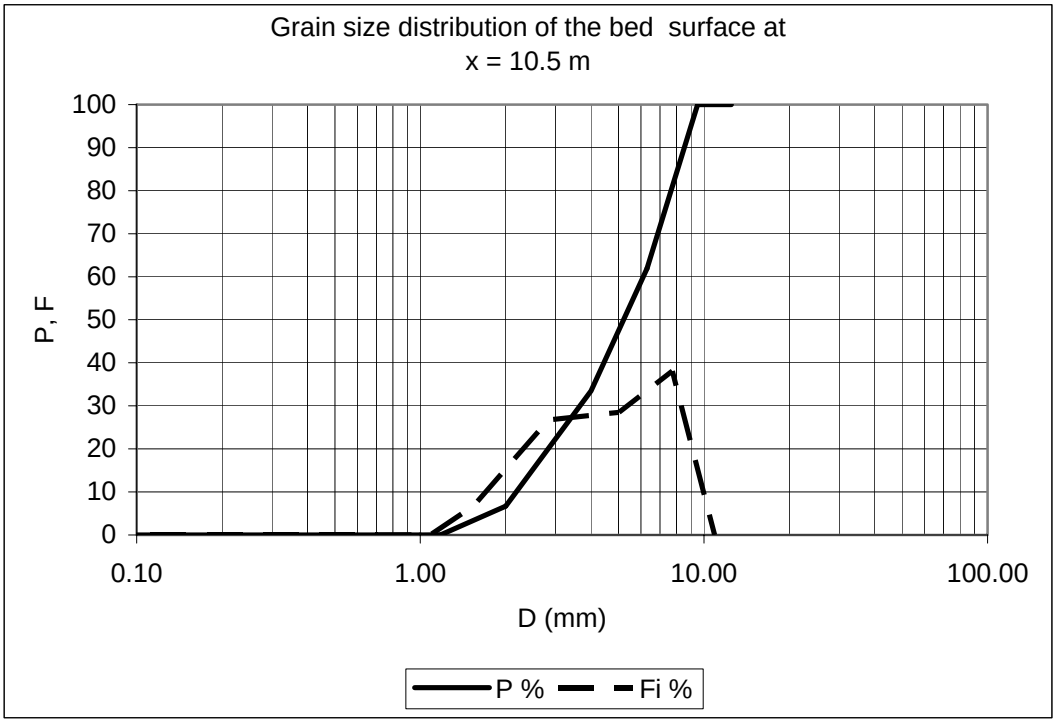

RUN 7

Water Discharge, Q	**30**	**l/s**
Downstream water elevation, ξ_d	**230**	**mm**
Sediment trasport rate at equilibrium, G_s	**371**	**gr/min**

Longitudinal profile at equilibrium

x (m)	η (mm)
2.5	198
2.9	202
3.3	199
3.7	198
4.1	196
4.3	195
4.5	192
4.9	190
5.3	187
5.7	185
6.1	182
6.5	180
6.9	179
7.3	175
7.7	173
8.1	172
8.5	171
8.9	170
9.3	168
9.7	165
10.1	160
10.5	158

Water surface at equilibrium

x (m)	H (mm)
2.5	283
4.3	273
6.5	260
8.5	250
10.5	239

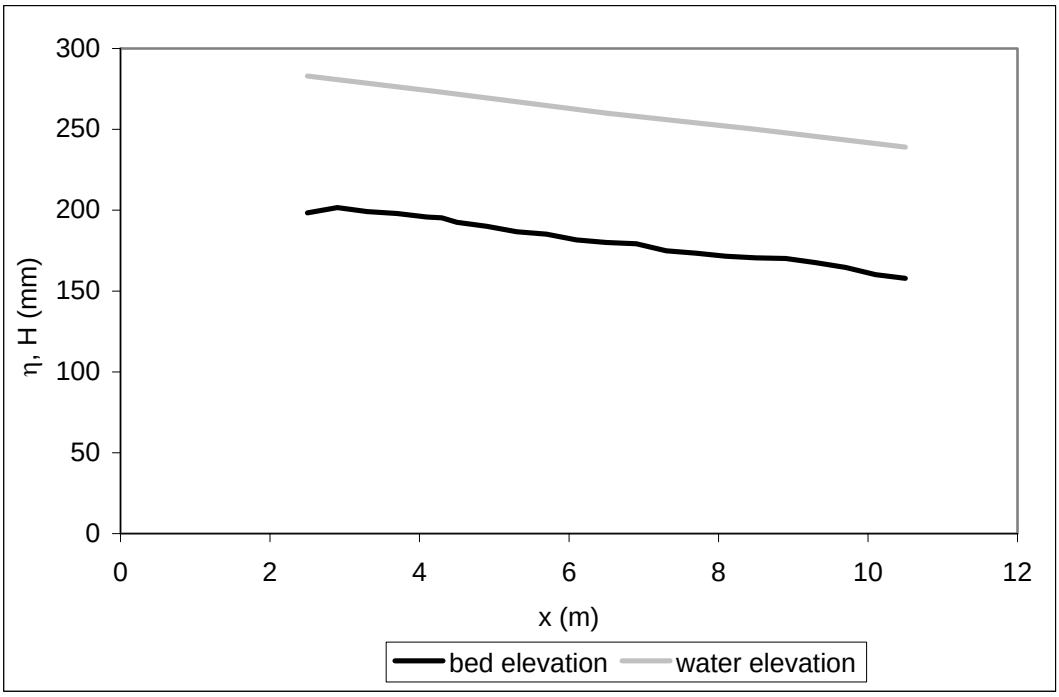

Water Discharge, Q	**30**	**l/s**
Downstream water elevation, ξ_d	**230**	**mm**
Sediment trasport rate at equilibrium, G_s	**371**	**gr/min**

Grain size distribution of the bedload at equilibrium

D (mm)	P %	Di (mm)	pi %
0.01	0.00		
0.50	0.02	0.07	0.02
1.00	0.03	0.71	0.01
1.18	0.09	1.09	0.06
2.00	9.41	1.54	9.32
4.00	50.29	2.83	40.88
6.30	78.77	5.02	28.48
9.50	100.00	7.74	21.23
12.50	100.00	10.90	0.00

D_{lg}	3.89	**mm**
σ_{lg}	1.64	
D_{l50}	3.98	**mm**
D_{l90}	7.83	**mm**

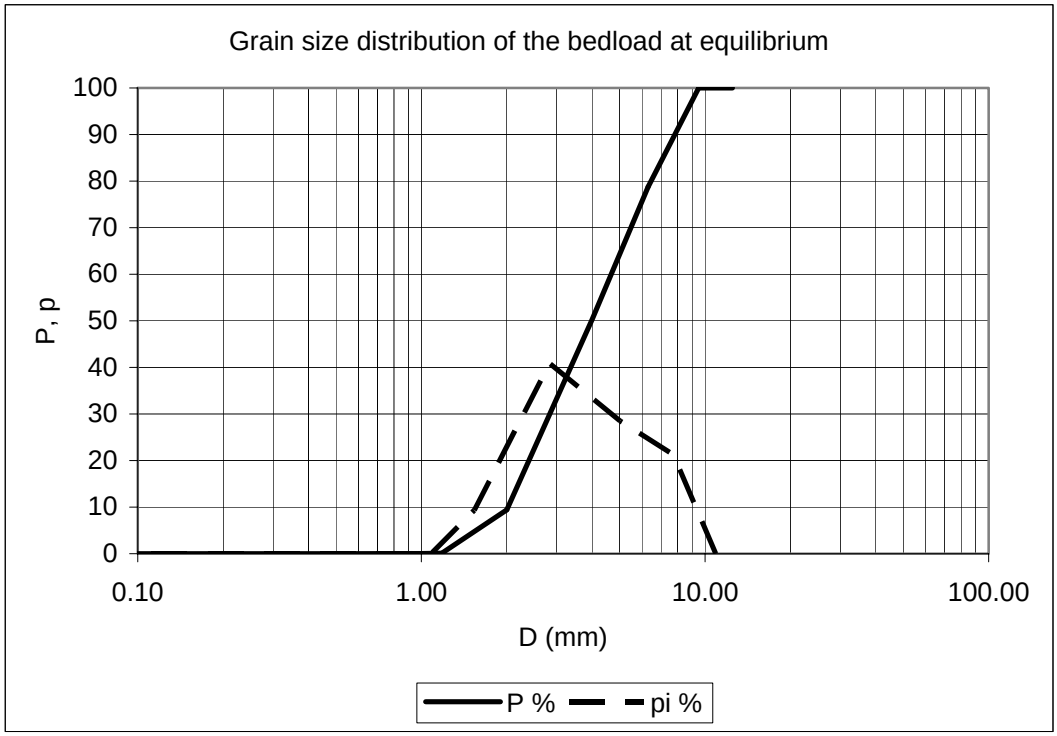

Water Discharge, Q	**30**	**l/s**
Downstream water elevation, ξ_d	**230**	**mm**
Sediment trasport rate at equilibrium, G_s	**371**	**gr/min**

Grain size distribution of the bed surface at x = 2.5 m

D (mm)	P %	Di (mm)	Fi %
0.01	0.00		
0.50	0.01	0.07	0.01
1.00	0.03	0.71	0.02
1.18	0.09	1.09	0.06
2.00	9.86	1.54	9.77
4.00	39.75	2.83	29.88
6.30	67.58	5.02	27.84
9.50	100.00	7.74	32.42
12.50	100.00	10.90	0.00

D_{sg}	4.33	**mm**
σ_{sg}	1.69	
D_{s50}	4.73	**mm**
D_{s90}	8.37	**mm**

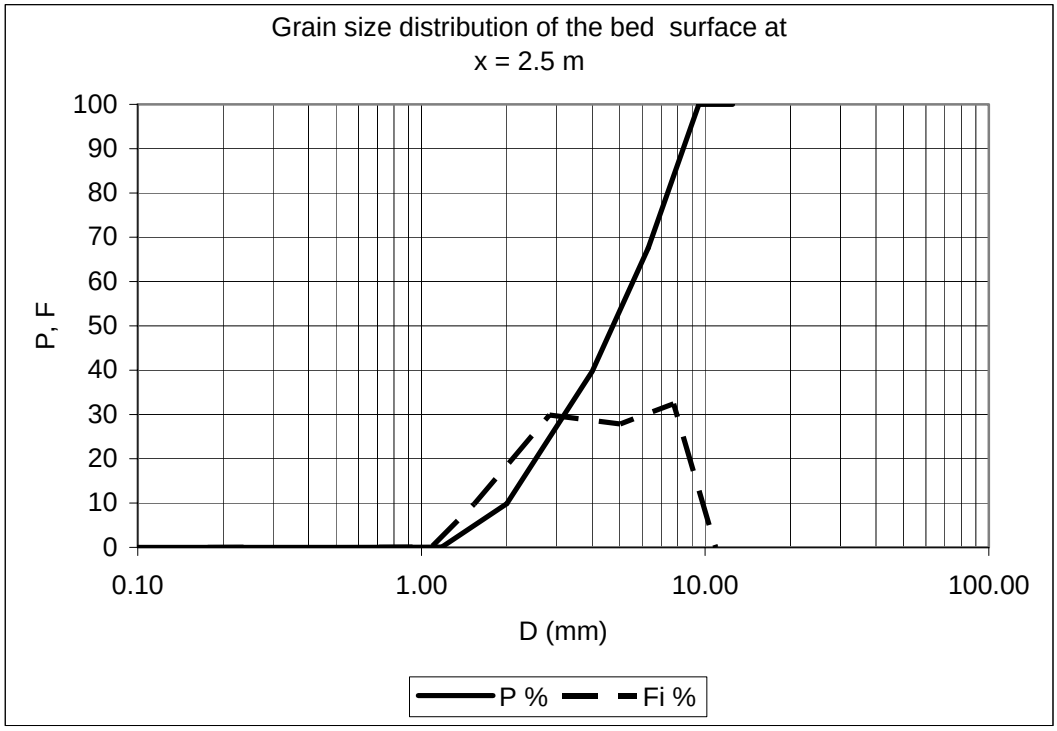

Water Discharge, Q	**30**	**l/s**
Downstream water elevation, ξ_d	**230**	**mm**
Sediment trasport rate at equilibrium, G_s	**371**	**gr/min**

Grain size distribution of the bed surface at x = 4.3 m

D (mm)	P %	Di (mm)	Fi %
0.01	0.00		
0.50	0.01	0.07	0.01
1.00	0.02	0.71	0.01
1.18	0.05	1.09	0.03
2.00	6.80	1.54	6.75
4.00	39.10	2.83	32.30
6.30	66.27	5.02	27.16
9.50	100.00	7.74	33.73
12.50	100.00	10.90	0.00

D_{sg}	4.45	**mm**
σ_{sg}	1.65	
D_{s50}	4.80	**mm**
D_{s90}	8.41	**mm**

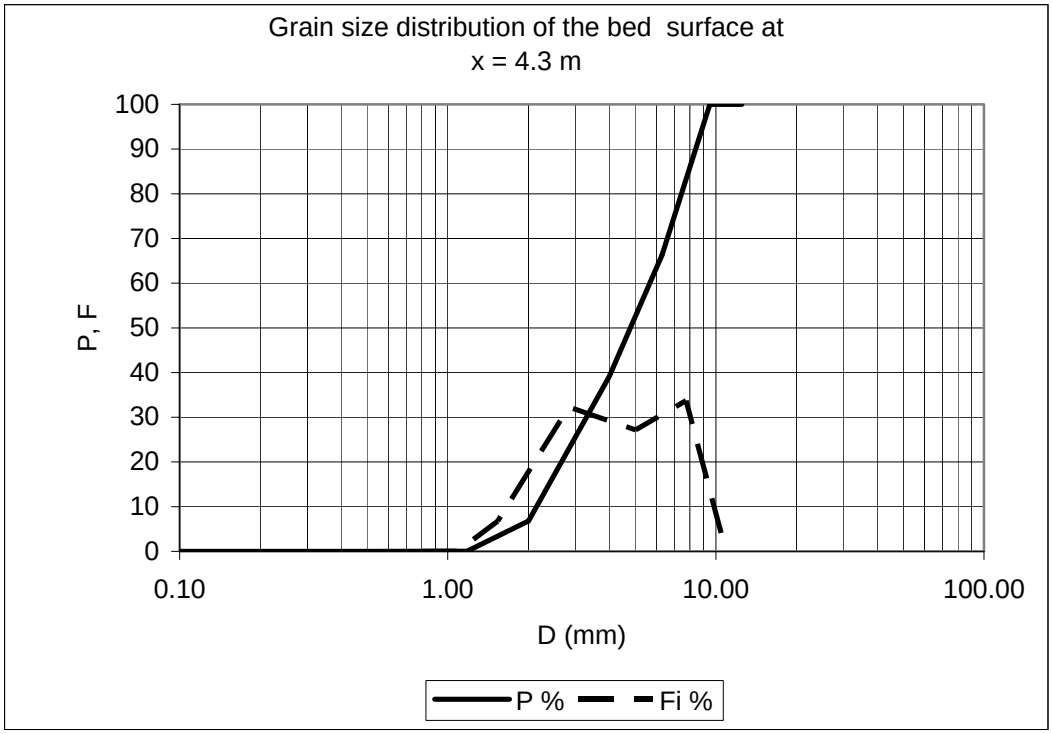

Water Discharge, Q	**30**	**l/s**
Downstream water elevation, ξ_d	**230**	**mm**
Sediment trasport rate at equilibrium, G_s	**371**	**gr/min**

Grain size distribution of the bed surface at x = 6.5 m

D (mm)	P %	Di (mm)	Fi %
0.01	0.00		
0.50	0.02	0.07	0.02
1.00	0.05	0.71	0.02
1.18	0.16	1.09	0.12
2.00	10.51	1.54	10.34
4.00	35.33	2.83	24.82
6.30	61.57	5.02	26.24
9.50	100.00	7.74	38.43
12.50	100.00	10.90	0.00

D_{sg}	4.53	**mm**
σ_{sg}	1.72	
D_{s50}	5.16	**mm**
D_{s90}	8.54	**mm**

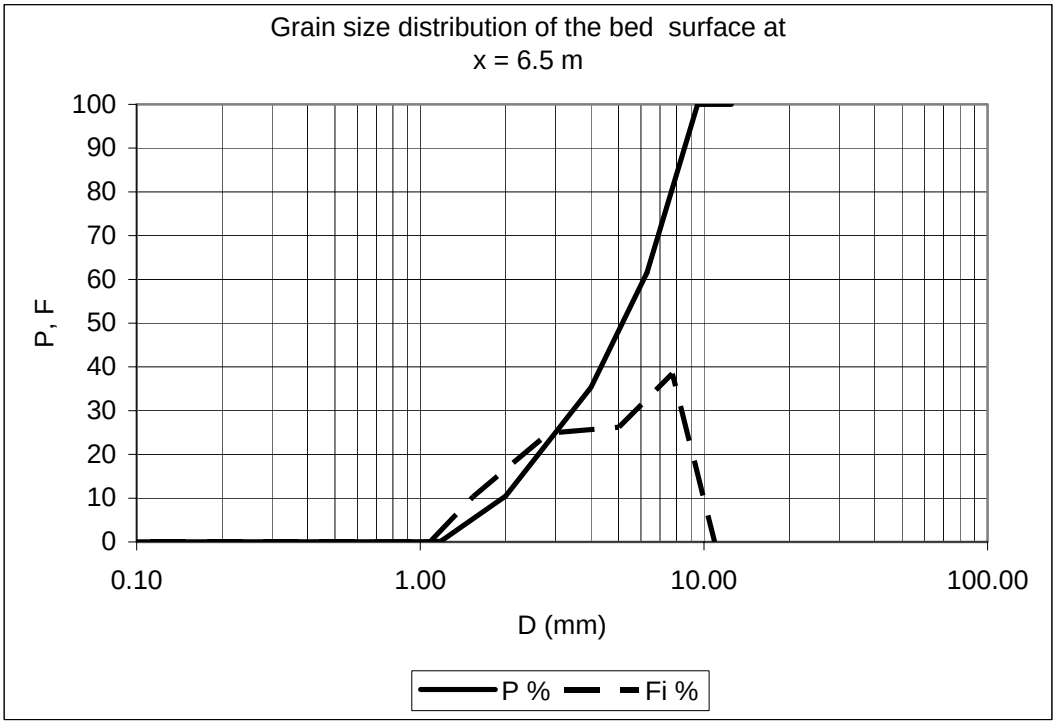

Water Discharge, Q	**30**	**l/s**
Downstream water elevation, ξ_d	**230**	**mm**
Sediment trasport rate at equilibrium, G_s	**371**	**gr/min**

Grain size distribution of the bed surface at x = 8.5 m

D (mm)	P %	Di (mm)	Fi %
0.01	0.00		
0.50	0.01	0.07	0.01
1.00	0.02	0.71	0.01
1.18	0.09	1.09	0.06
2.00	8.15	1.54	8.06
4.00	38.77	2.83	30.62
6.30	65.29	5.02	26.53
9.50	100.00	7.74	34.71
12.50	100.00	10.90	0.00

D_{sg}	4.44	**mm**
σ_{sg}	1.68	
D_{s50}	4.85	**mm**
D_{s90}	8.44	**mm**

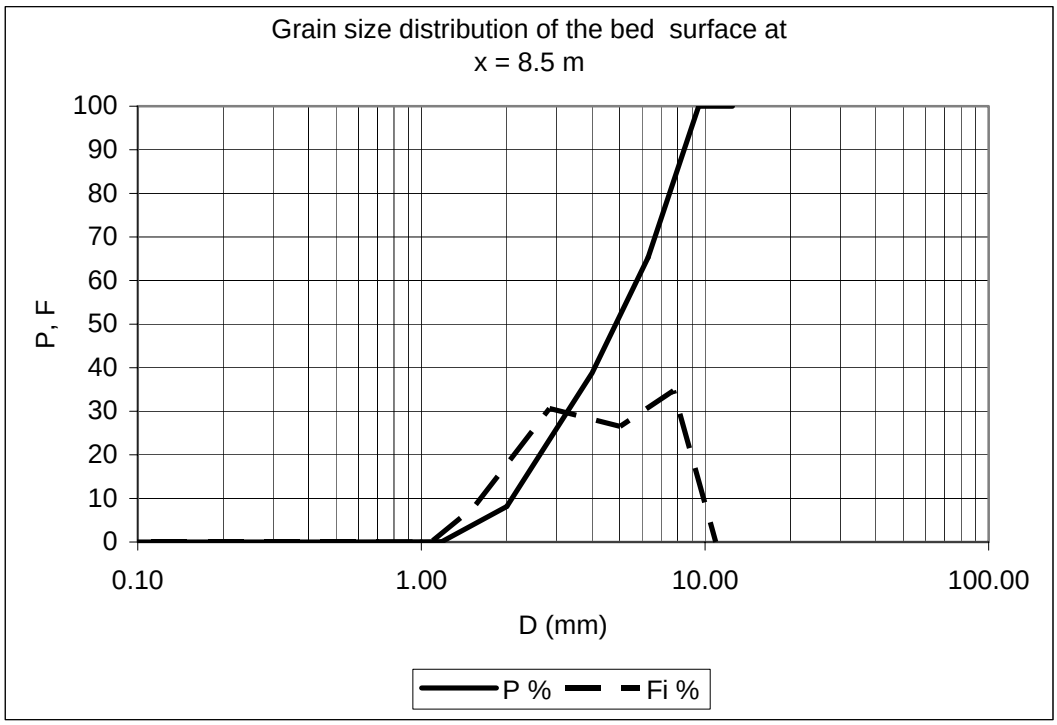

Water Discharge, Q	**30**	**l/s**
Downstream water elevation, ξ_d	**230**	**mm**
Sediment trasport rate at equilibrium, G_s	**371**	**gr/min**

Grain size distribution of the bed surface at x = 10.5 m

D (mm)	P %	Di (mm)	Fi %
0.01	0.00		
0.50	0.01	0.07	0.01
1.00	0.03	0.71	0.01
1.18	0.17	1.09	0.14
2.00	11.50	1.54	11.34
4.00	36.26	2.83	24.75
6.30	62.43	5.02	26.17
9.50	100.00	7.74	37.57
12.50	100.00	10.90	0.00

D_{sg}	4.47	**mm**
σ_{sg}	1.73	
D_{s50}	5.08	**mm**
D_{s90}	8.52	**mm**

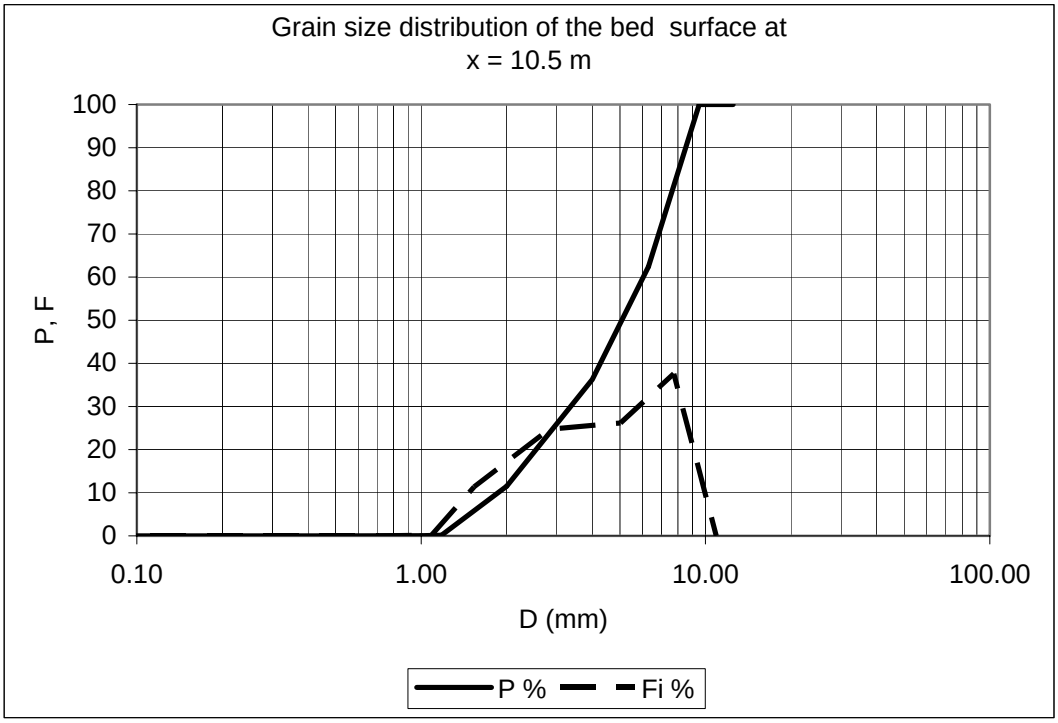

RUN 8

Water Discharge, Q	**35**	**l/s**
Downstream water elevation, ξ_d	**248**	**mm**
Sediment trasport rate at equilibrium, G_s	**151**	**gr/min**

Longitudinal profile at equilibrium

x (m)	η (mm)
2.5	201
2.9	200
3.3	199
3.7	199
4.1	196
4.3	197
4.5	196
4.9	192
5.3	189
5.7	187
6.1	186
6.5	184
6.9	184
7.3	182
7.7	179
8.1	176
8.5	173
8.9	171
9.3	171
9.7	168
10.1	166
10.5	165

Water surface at equilibrium

x (m)	H (mm)
2.5	293
4.3	283
6.5	271
8.5	263
10.5	252

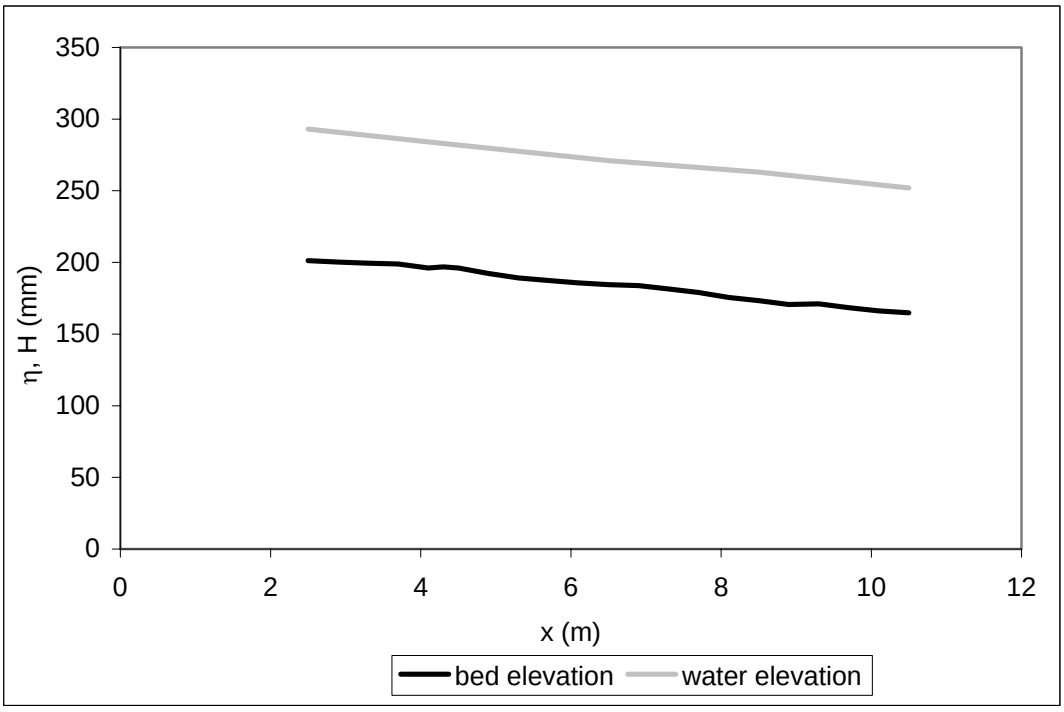

Water Discharge, Q	**35**	**l/s**
Downstream water elevation, ξ_d	**248**	**mm**
Sediment trasport rate at equilibrium, G_s	**151**	**gr/min**

Grain size distribution of the bedload at equilibrium

D (mm)	P %	Di (mm)	pi %
0.01	0.00		
0.50	0.03	0.07	0.03
1.00	0.10	0.71	0.07
1.18	0.40	1.09	0.30
2.00	35.18	1.54	34.78
4.00	66.31	2.83	31.13
6.30	81.85	5.02	15.54
9.50	100.00	7.74	18.15
12.50	100.00	10.90	0.00

D_{lg}	2.99	**mm**
σ_{lg}	1.84	
D_{l50}	2.78	**mm**
D_{l90}	7.58	**mm**

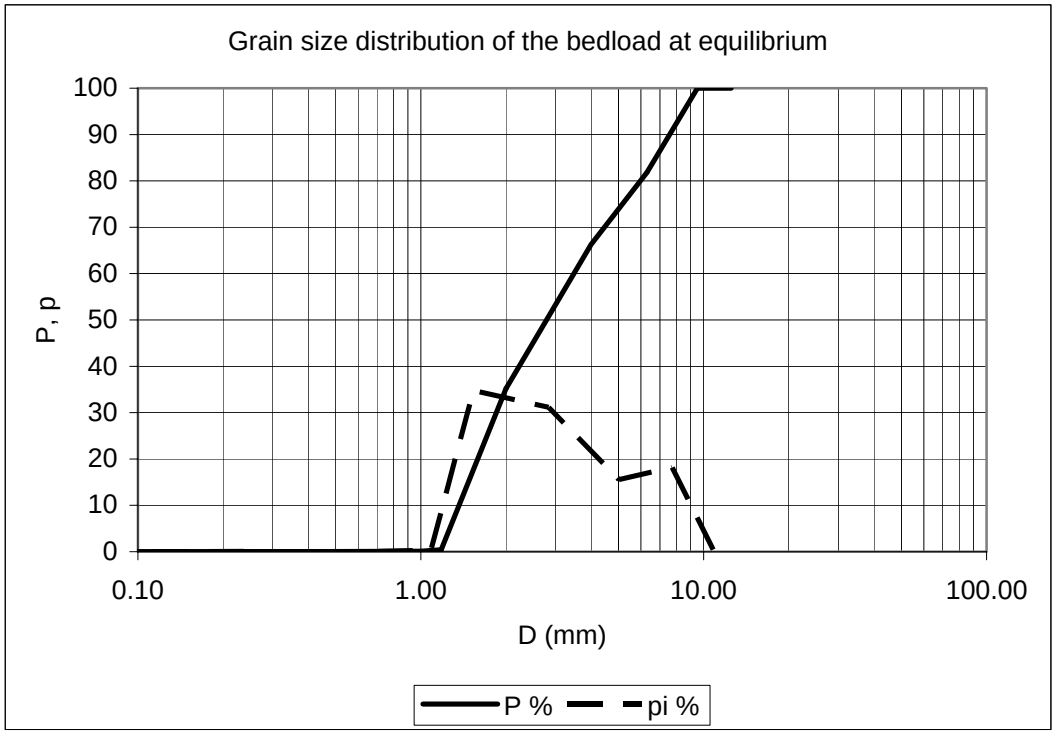

Water Discharge, Q	**35**	**l/s**
Downstream water elevation, ξ_d	**248**	**mm**
Sediment trasport rate at equilibrium, G_s	**151**	**gr/min**

Grain size distribution of the bed surface at x = 2.5 m

D (mm)	P %	Di (mm)	Fi %
0.01	0.00		
0.50	0.01	0.07	0.01
1.00	0.04	0.71	0.02
1.18	0.11	1.09	0.07
2.00	8.08	1.54	7.97
4.00	37.14	2.83	29.05
6.30	67.31	5.02	30.18
9.50	100.00	7.74	32.69
12.50	100.00	10.90	0.00

D_{sg}	4.44	**mm**
σ_{sg}	1.66	
D_{s50}	4.85	**mm**
D_{s90}	8.38	**mm**

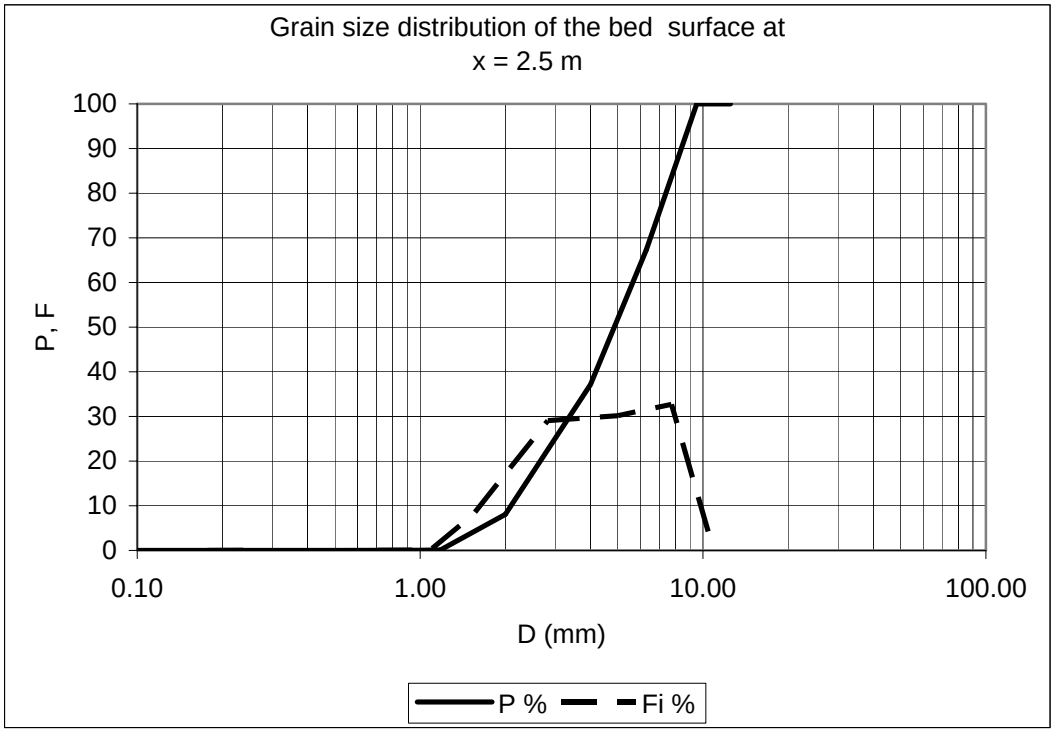

Water Discharge, Q	**35**	**l/s**
Downstream water elevation, ξ_d	**248**	**mm**
Sediment trasport rate at equilibrium, G_s	**151**	**gr/min**

Grain size distribution of the bed surface at x = 4.3 m

D (mm)	P %	Di (mm)	Fi %
0.01	0.00		
0.50	0.02	0.07	0.02
1.00	0.04	0.71	0.02
1.18	0.14	1.09	0.10
2.00	15.98	1.54	15.85
4.00	50.49	2.83	34.50
6.30	73.97	5.02	23.48
9.50	100.00	7.74	26.03
12.50	100.00	10.90	0.00

D_{sg}	3.81	**mm**
σ_{sg}	1.75	
D_{s50}	3.96	**mm**
D_{s90}	8.11	**mm**

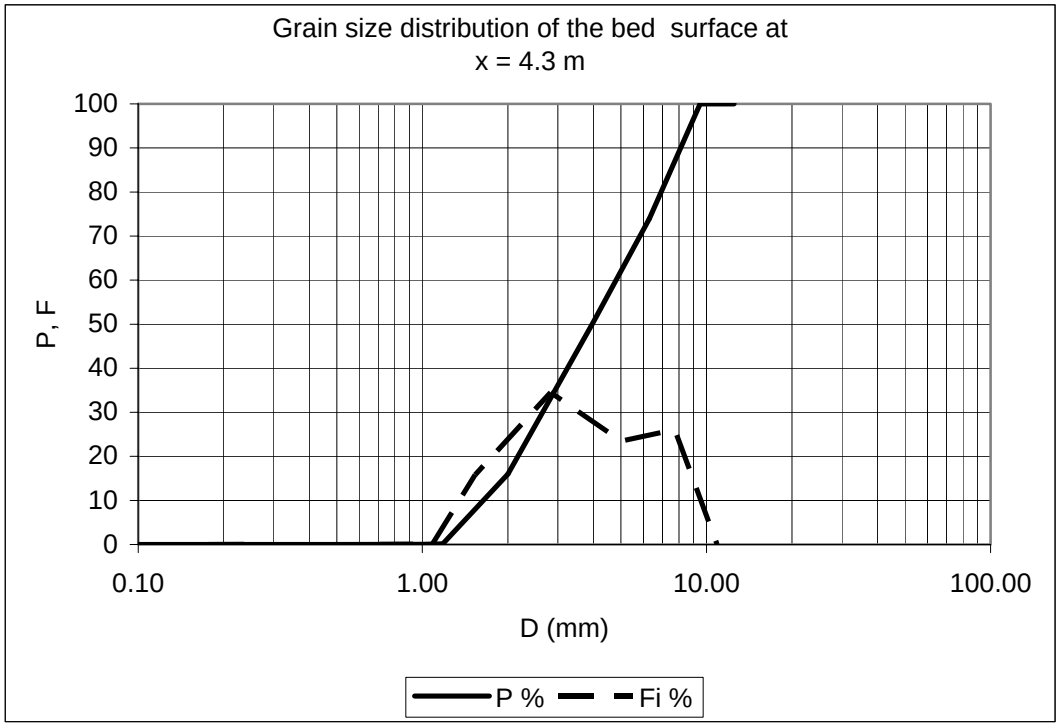

Water Discharge, Q	**35**	**l/s**
Downstream water elevation, ξ_d	**248**	**mm**
Sediment trasport rate at equilibrium, G_s	**151**	**gr/min**

Grain size distribution of the bed surface at x = 6.5 m

D (mm)	P %	Di (mm)	Fi %
0.01	0.00		
0.50	0.01	0.07	0.01
1.00	0.02	0.71	0.01
1.18	0.13	1.09	0.10
2.00	9.71	1.54	9.58
4.00	37.37	2.83	27.66
6.30	62.54	5.02	25.17
9.50	100.00	7.74	37.46
12.50	100.00	10.90	0.00

D_{sg}	4.49	**mm**
σ_{sg}	1.71	
D_{s50}	5.02	**mm**
D_{s90}	8.51	**mm**

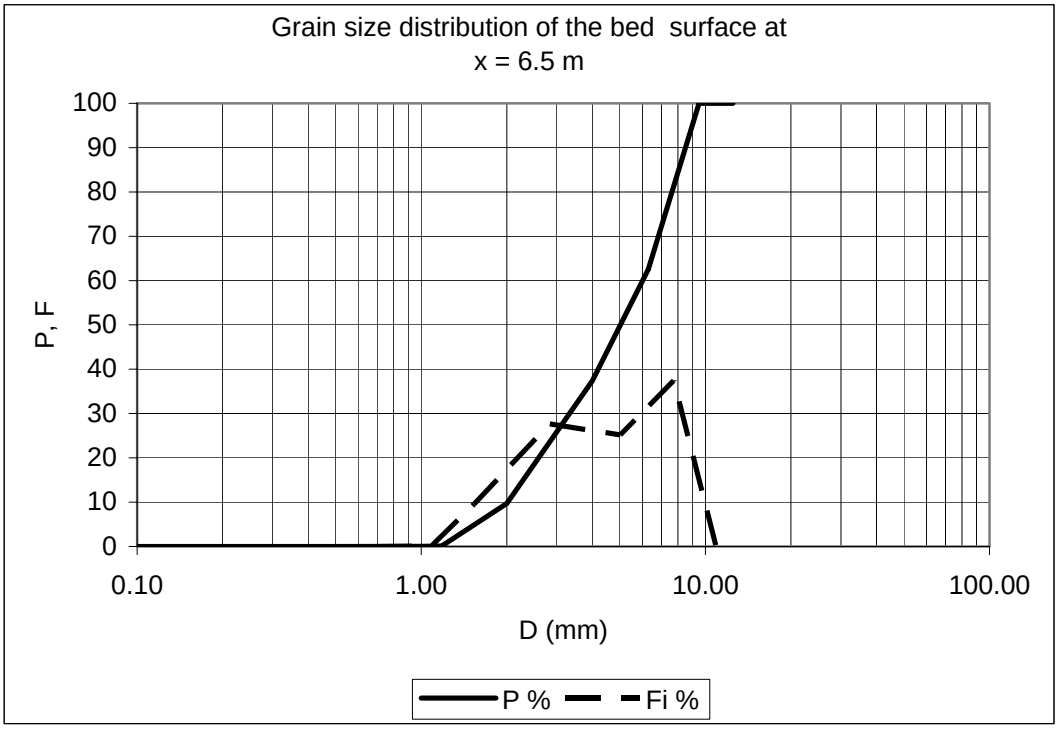

Water Discharge, Q	**35**	**l/s**
Downstream water elevation, ξ_d	**248**	**mm**
Sediment trasport rate at equilibrium, G_s	**151**	**gr/min**

Grain size distribution of the bed surface at x = 8.5 m

D (mm)	P %	Di (mm)	Fi %
0.01	0.00		
0.50	0.02	0.07	0.02
1.00	0.06	0.71	0.04
1.18	0.22	1.09	0.16
2.00	13.12	1.54	12.90
4.00	44.58	2.83	31.46
6.30	68.86	5.02	24.28
9.50	100.00	7.74	31.14
12.50	100.00	10.90	0.00

D_{sg}	4.10	**mm**
σ_{sg}	1.75	
D_{s50}	4.43	**mm**
D_{s90}	8.33	**mm**

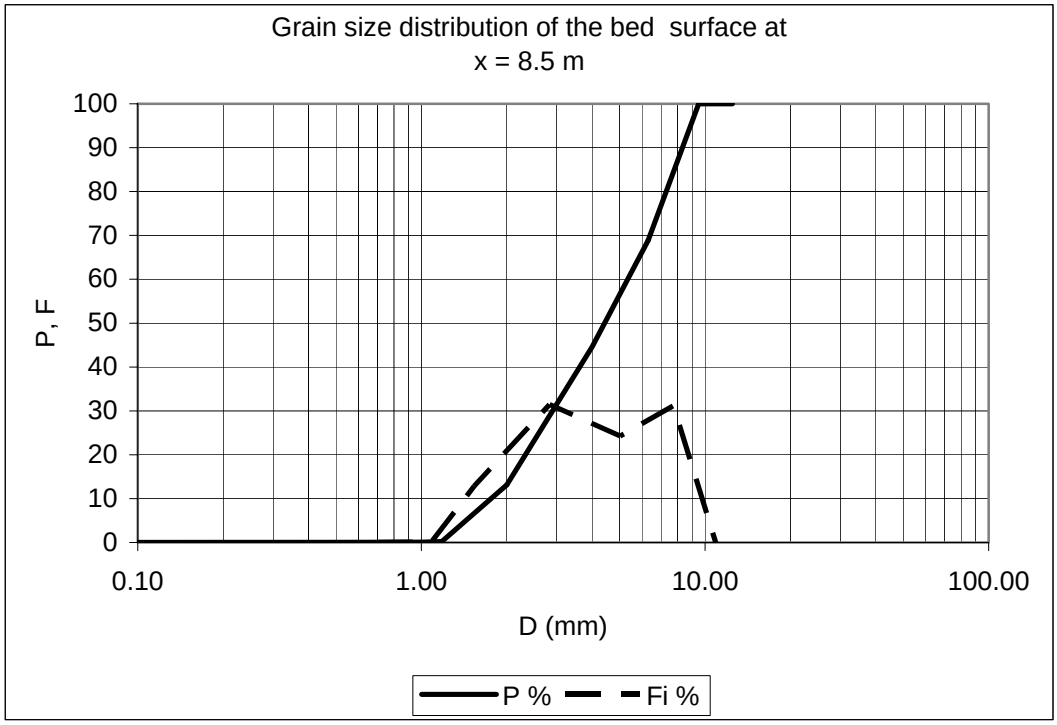

Water Discharge, Q	**35**	**l/s**
Downstream water elevation, ξ_d	**248**	**mm**
Sediment trasport rate at equilibrium, G_s	**151**	**gr/min**

Grain size distribution of the bed surface at x = 10.5 m

D (mm)	P %	Di (mm)	Fi %
0.01	0.00		
0.50	0.01	0.07	0.01
1.00	0.02	0.71	0.01
1.18	0.08	1.09	0.06
2.00	6.13	1.54	6.05
4.00	30.64	2.83	24.51
6.30	58.39	5.02	27.75
9.50	100.00	7.74	41.61
12.50	100.00	10.90	0.00

D_{sg}	4.85	**mm**
σ_{sg}	1.64	
D_{s50}	5.49	**mm**
D_{s90}	8.61	**mm**

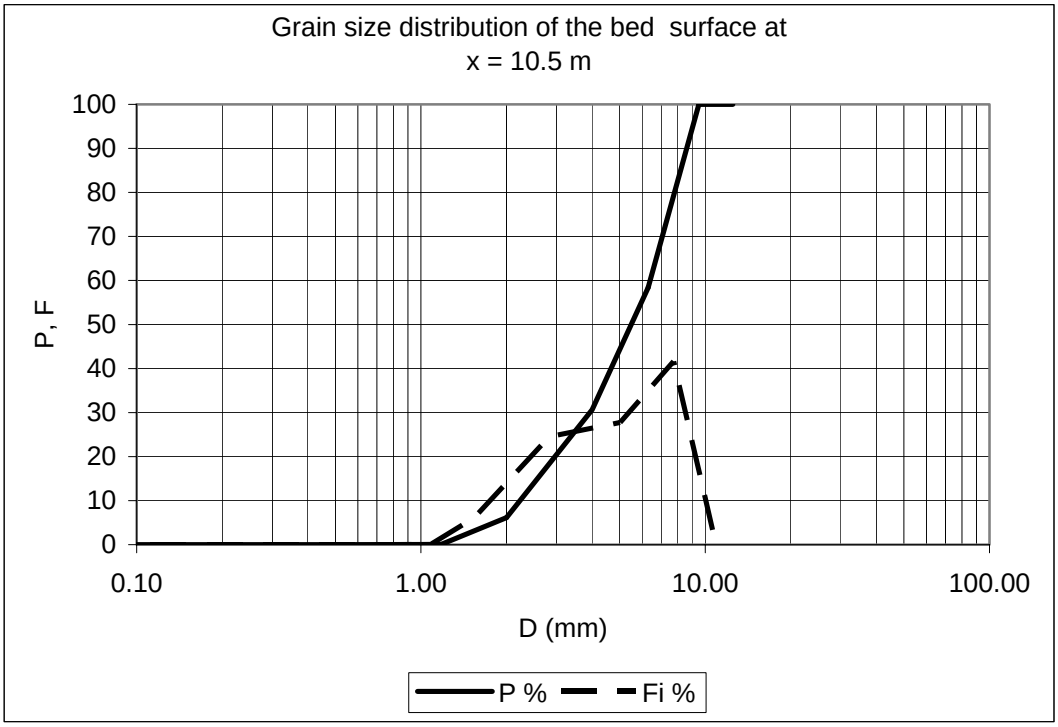

RUN 9

Water Discharge, Q	**35**	**l/s**
Downstream water elevation, ξ_d	**225**	**mm**
Sediment trasport rate at equilibrium, G_s	**1068**	**gr/min**

Longitudinal profile at equilibrium

x (m)	η (mm)
2.5	201
2.9	201
3.3	199
3.7	198
4.1	196
4.3	196
4.5	194
4.9	191
5.3	188
5.7	186
6.1	183
6.5	180
6.9	181
7.3	176
7.7	172
8.1	168
8.5	166
8.9	165
9.3	160
9.7	158
10.1	158
10.5	153

Water surface at equilibrium

x (m)	H (mm)
2.5	292
4.3	278
6.5	261
8.5	249
10.5	237

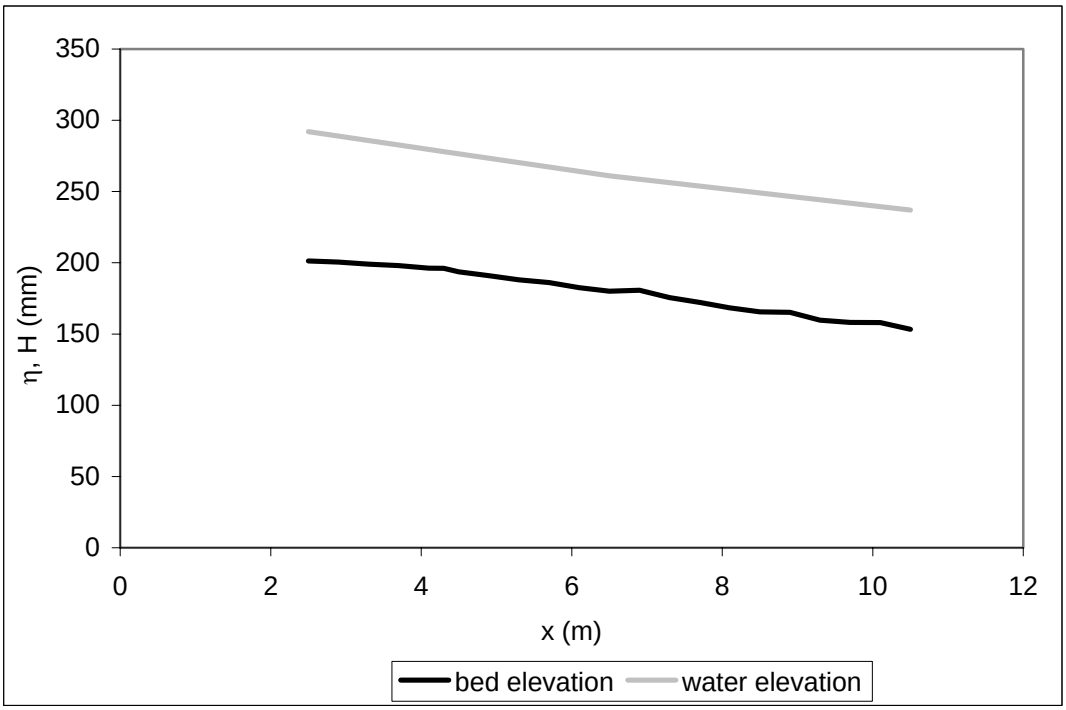

Water Discharge, Q	**35**	**l/s**
Downstream water elevation, ξ_d	**225**	**mm**
Sediment trasport rate at equilibrium, G_s	**1068**	**gr/min**

Grain size distribution of the bedload at equilibrium

D (mm)	P %	Di (mm)	pi %
0.01	0.00		
0.50	0.05	0.07	0.05
1.00	0.11	0.71	0.06
1.18	0.28	1.09	0.18
2.00	17.17	1.54	16.89
4.00	53.49	2.83	36.32
6.30	77.22	5.02	23.73
9.50	100.00	7.74	22.78
12.50	100.00	10.90	0.00

D_{lg}	3.66	**mm**
σ_{lg}	1.75	
D_{l50}	3.74	**mm**
D_{l90}	7.93	**mm**

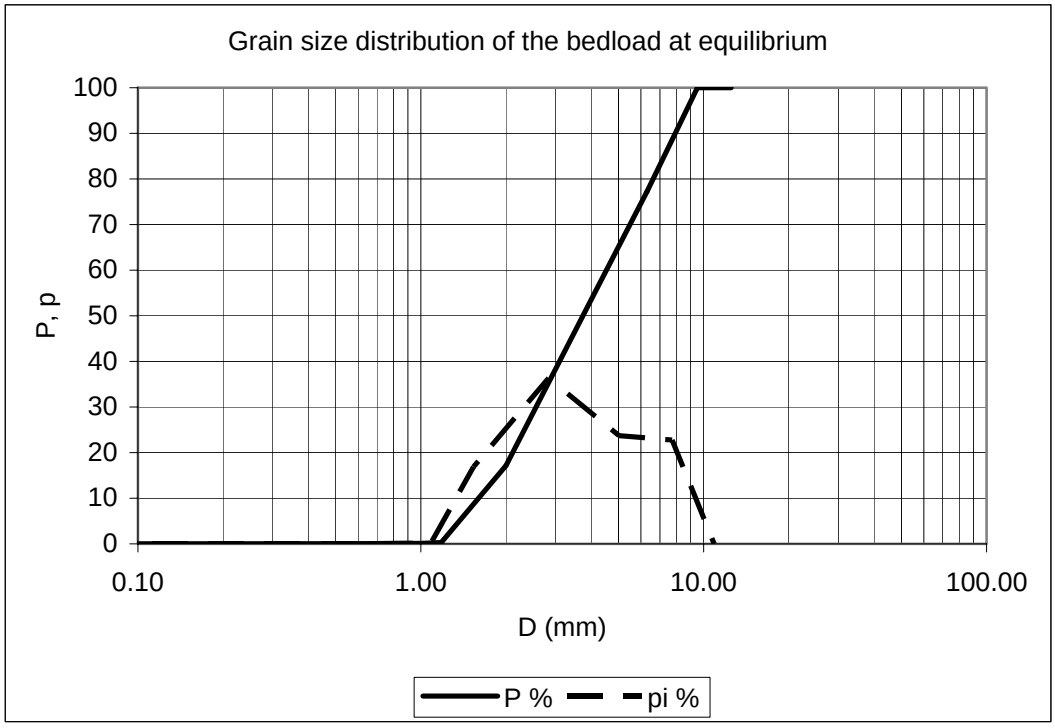

Water Discharge, Q	**35**	**l/s**
Downstream water elevation, ξ_d	**225**	**mm**
Sediment trasport rate at equilibrium, G_s	**1068**	**gr/min**

Grain size distribution of the bed surface at x = 2.5 m

D (mm)	P %	Di (mm)	Fi %
0.01	0.00		
0.50	0.01	0.07	0.01
1.00	0.08	0.71	0.07
1.18	0.33	1.09	0.25
2.00	13.72	1.54	13.40
4.00	40.97	2.83	27.25
6.30	67.67	5.02	26.70
9.50	100.00	7.74	32.33
12.50	100.00	10.90	0.00

D_{sg}	4.19	**mm**
σ_{sg}	1.75	
D_{s50}	4.66	**mm**
D_{s90}	8.37	**mm**

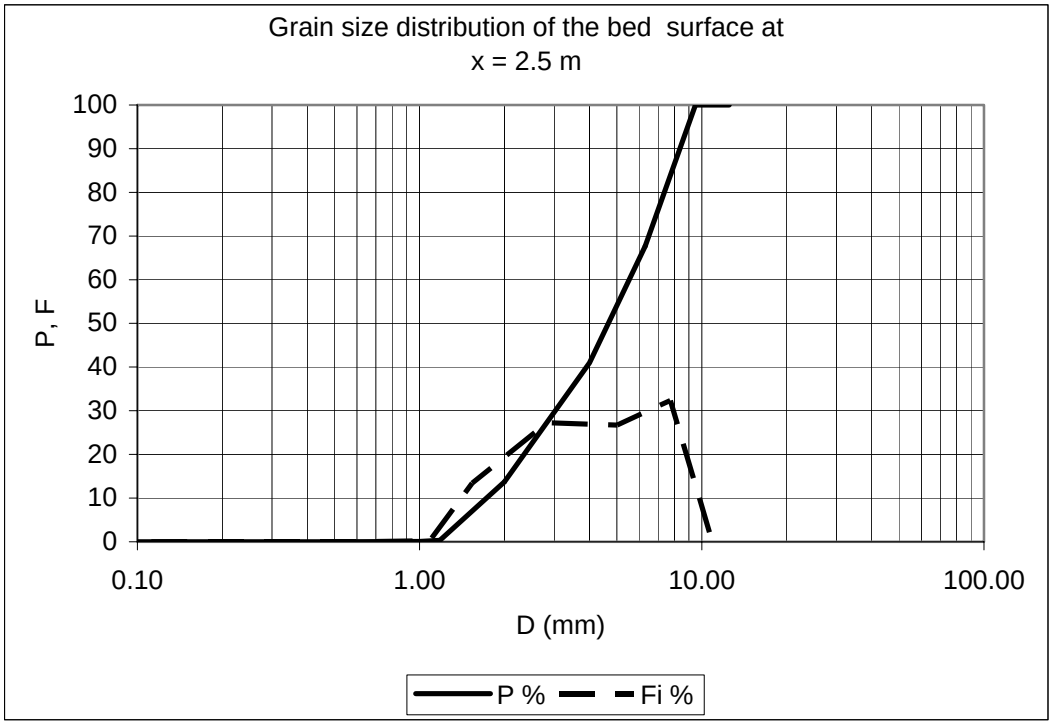

Water Discharge, Q	**35**	**l/s**
Downstream water elevation, ξ_d	**225**	**mm**
Sediment trasport rate at equilibrium, G_s	**1068**	**gr/min**

Grain size distribution of the bed surface at x = 4.3 m

D (mm)	P %	Di (mm)	Fi %
0.01	0.00		
0.50	0.00	0.07	0.00
1.00	0.02	0.71	0.01
1.18	0.13	1.09	0.12
2.00	10.11	1.54	9.98
4.00	40.42	2.83	30.31
6.30	66.15	5.02	25.73
9.50	100.00	7.74	33.85
12.50	100.00	10.90	0.00

D_{sg}	4.33	**mm**
σ_{sg}	1.70	
D_{s50}	4.74	**mm**
D_{s90}	8.41	**mm**

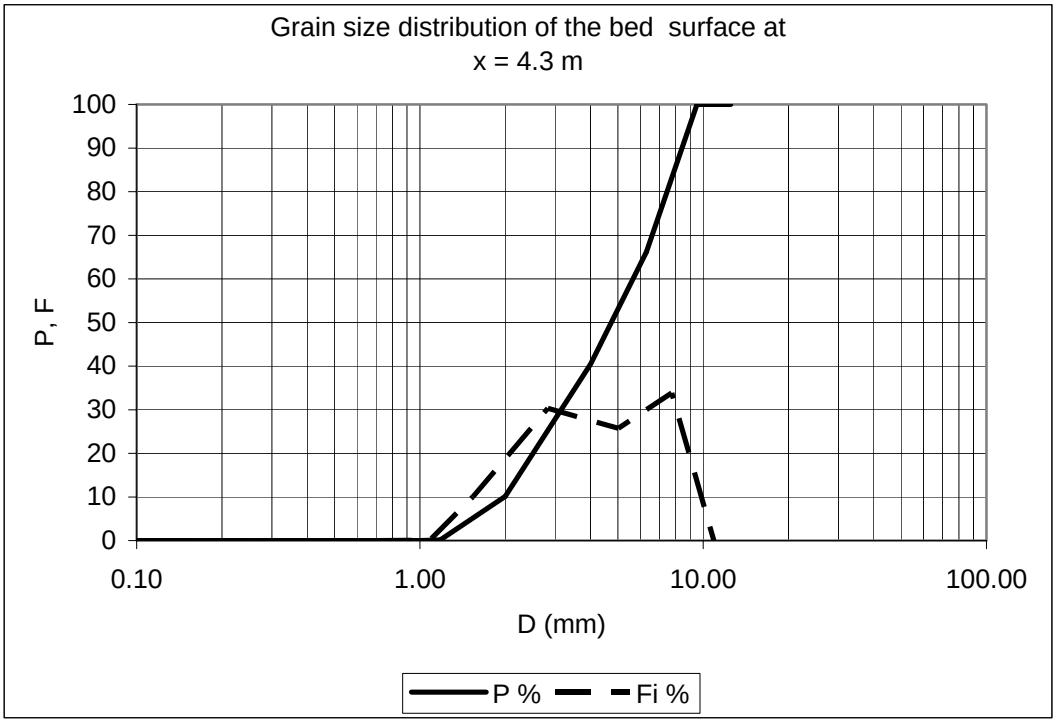

Water Discharge, Q	**35**	**l/s**
Downstream water elevation, ξ_d	**225**	**mm**
Sediment trasport rate at equilibrium, G_s	**1068**	**gr/min**

Grain size distribution of the bed surface at x = 6.5 m

D (mm)	P %	Di (mm)	Fi %
0.01	0.00		
0.50	0.01	0.07	0.01
1.00	0.02	0.71	0.01
1.18	0.11	1.09	0.10
2.00	12.26	1.54	12.15
4.00	44.60	2.83	32.33
6.30	70.59	5.02	26.00
9.50	100.00	7.74	29.41
12.50	100.00	10.90	0.00

D_{sg}	4.09	**mm**
σ_{sg}	1.72	
D_{s50}	4.40	**mm**
D_{s90}	8.27	**mm**

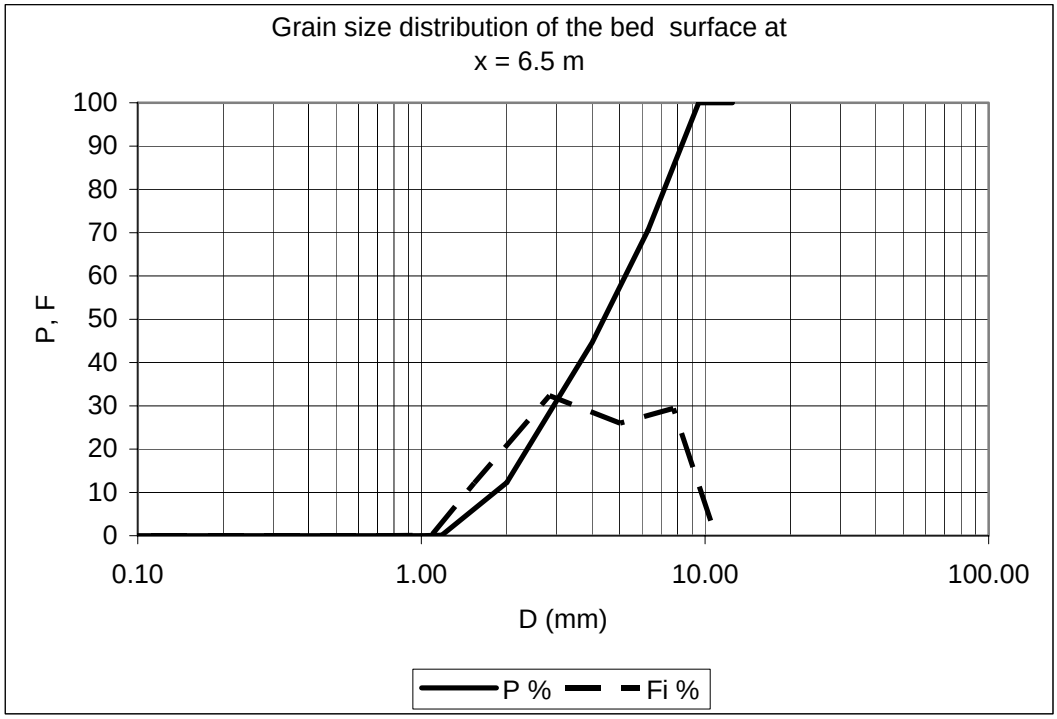

Water Discharge, Q	**35**	**l/s**
Downstream water elevation, ξ_d	**225**	**mm**
Sediment trasport rate at equilibrium, G_s	**1068**	**gr/min**

Grain size distribution of the bed surface at x = 8.5 m

D (mm)	P %	Di (mm)	Fi %
0.01	0.00		
0.50	0.01	0.07	0.01
1.00	0.03	0.71	0.02
1.18	0.25	1.09	0.22
2.00	13.31	1.54	13.07
4.00	39.18	2.83	25.86
6.30	63.95	5.02	24.77
9.50	100.00	7.74	36.05
12.50	100.00	10.90	0.00

D_{sg}	4.31	**mm**
σ_{sg}	1.76	
D_{s50}	4.88	**mm**
D_{s90}	8.48	**mm**

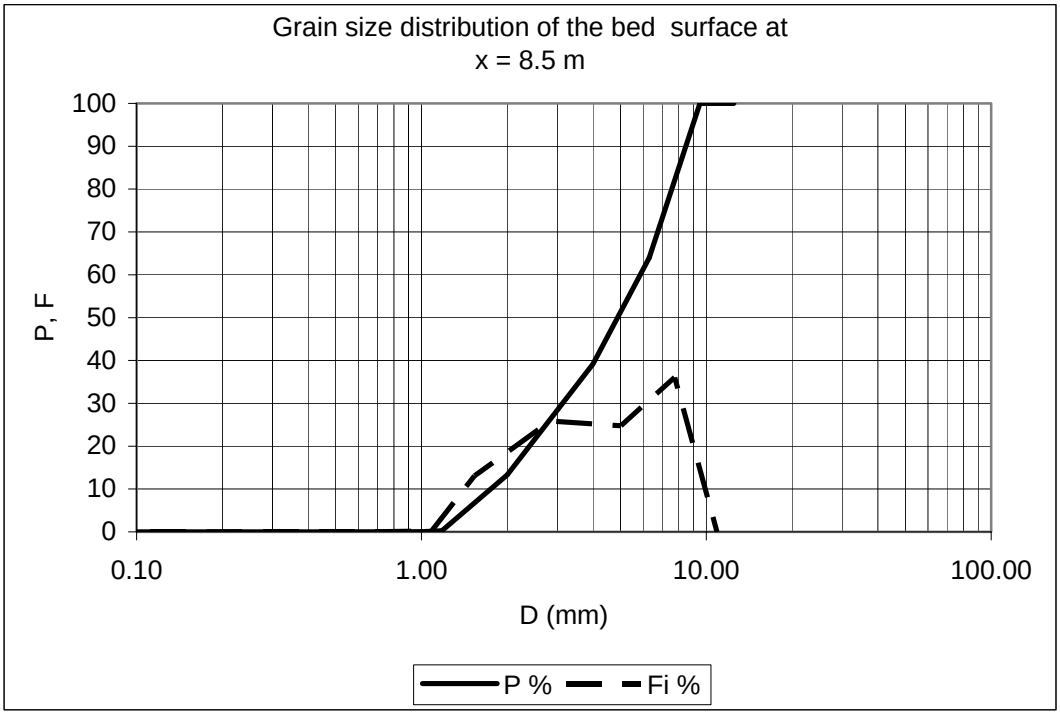

Water Discharge, Q	**35**	**l/s**
Downstream water elevation, ξ_d	**225**	**mm**
Sediment trasport rate at equilibrium, G_s	**1068**	**gr/min**

Grain size distribution of the bed surface at x = 10.5 m

D (mm)	P %	Di (mm)	Fi %
0.01	0.00		
0.50	0.00	0.07	0.00
1.00	0.02	0.71	0.02
1.18	0.16	1.09	0.13
2.00	9.08	1.54	8.92
4.00	43.45	2.83	34.37
6.30	71.12	5.02	27.67
9.50	100.00	7.74	28.88
12.50	100.00	10.90	0.00

D_{sg}	4.19	**mm**
σ_{sg}	1.67	
D_{s50}	4.45	**mm**
D_{s90}	8.24	**mm**

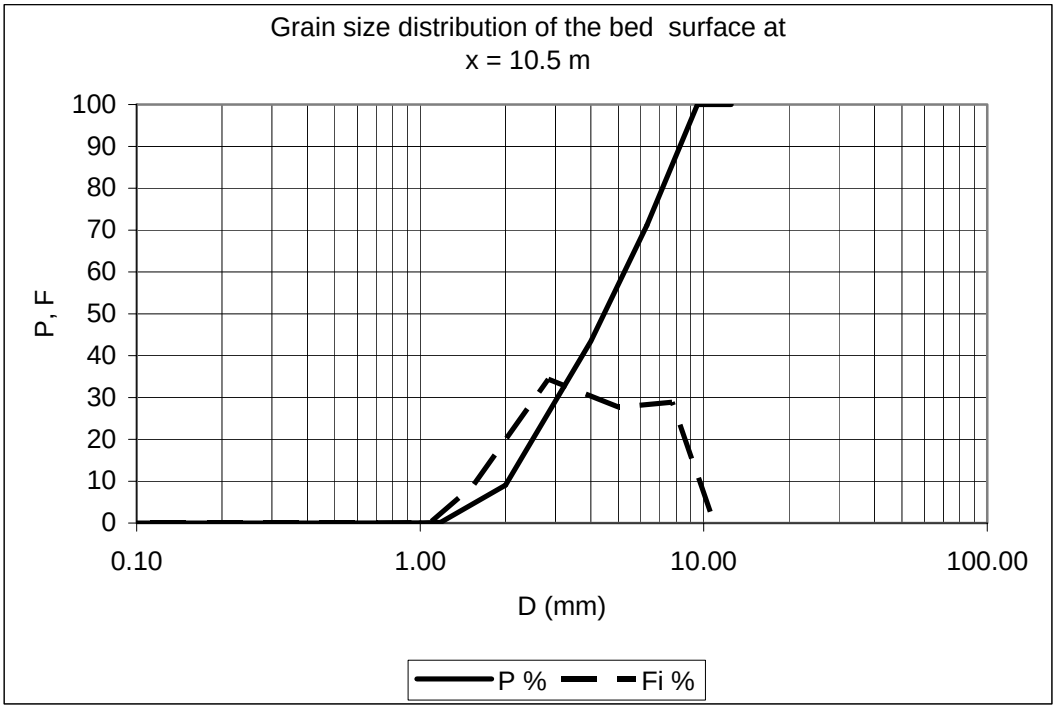

SUBSTRATE

x = 0.5 m

P %

D (mm)	0 -1 cm	1 - 2 cm	2 - 3 cm	3 - 4 cm	4 - 5 cm	5 - 7 cm
0.01	0.00	0.00	0.00	0.00	0.00	0.00
0.50	0.11	0.36	0.31	0.39	0.28	0.24
1.00	0.54	0.75	0.67	0.71	0.52	0.42
1.18	1.04	1.18	1.03	1.10	0.95	0.78
2.00	23.23	23.48	21.97	23.99	22.42	22.60
4.00	54.28	57.32	55.27	59.77	58.58	57.31
6.30	75.94	77.49	76.55	81.91	81.35	78.15
9.50	100.00	100.00	100.00	100.00	100.00	100.00
12.50	100.00	100.00	100.00	100.00	100.00	100.00

f %

Di (mm)	0 -1 cm	1 - 2 cm	2 - 3 cm	3 - 4 cm	4 - 5 cm	5 - 7 cm
0.07	0.11	0.36	0.31	0.39	0.28	0.24
0.71	0.44	0.40	0.35	0.32	0.24	0.18
1.09	0.50	0.42	0.37	0.38	0.43	0.36
1.54	22.20	22.30	20.93	22.89	21.47	21.82
2.83	31.05	33.85	33.30	35.78	36.16	34.72
5.02	21.66	20.17	21.28	22.14	22.77	20.84
7.74	24.06	22.51	23.45	18.09	18.65	21.85
10.90	0.00	0.00	0.00	0.00	0.00	0.00

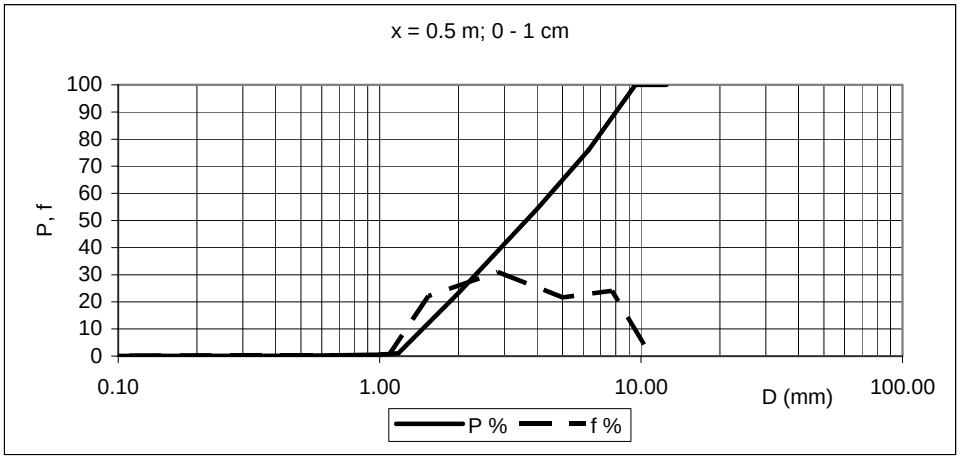

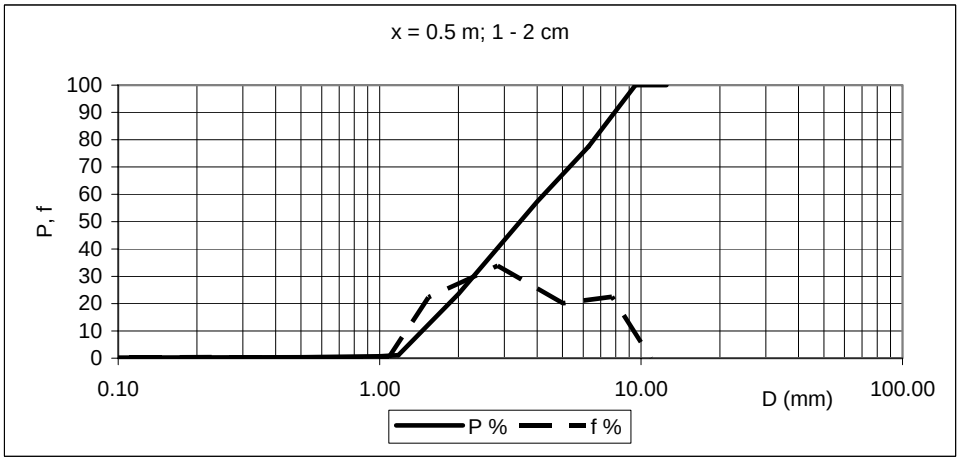

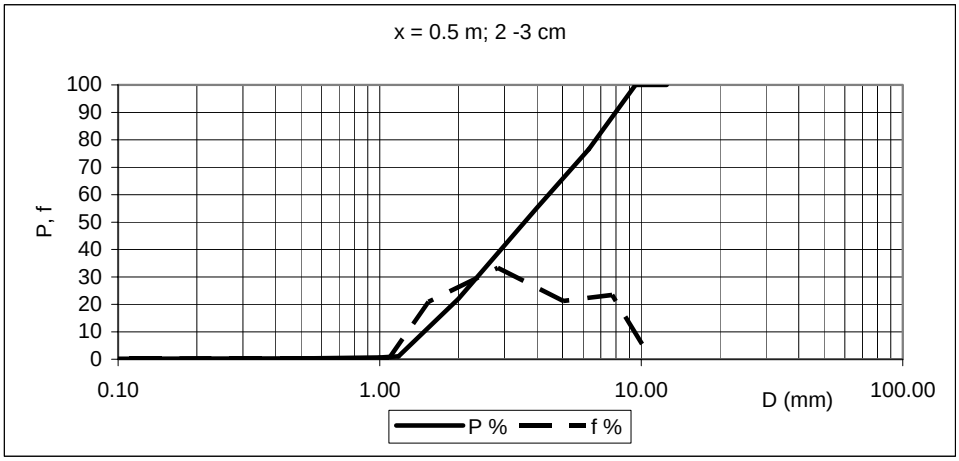
x = 0.5 m; 2 -3 cm
P, f
100
90
80
70
60
50
40
30
20
10
0
0.10
1.00
10.00
100.00
D (mm)
P %
f %

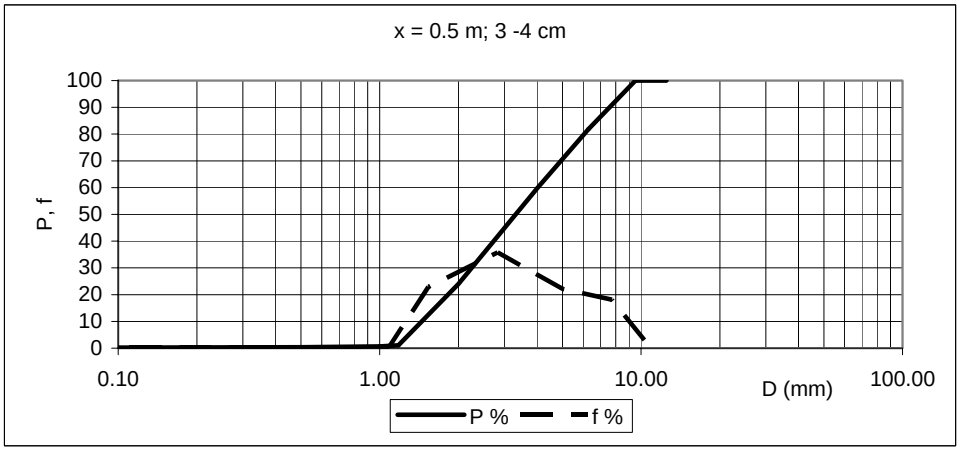
x = 0.5 m; 3 -4 cm
P, f
100
90
80
70
60
50
40
30
20
10
0
0.10
1.00
10.00
100.00
D (mm)
P %
f %

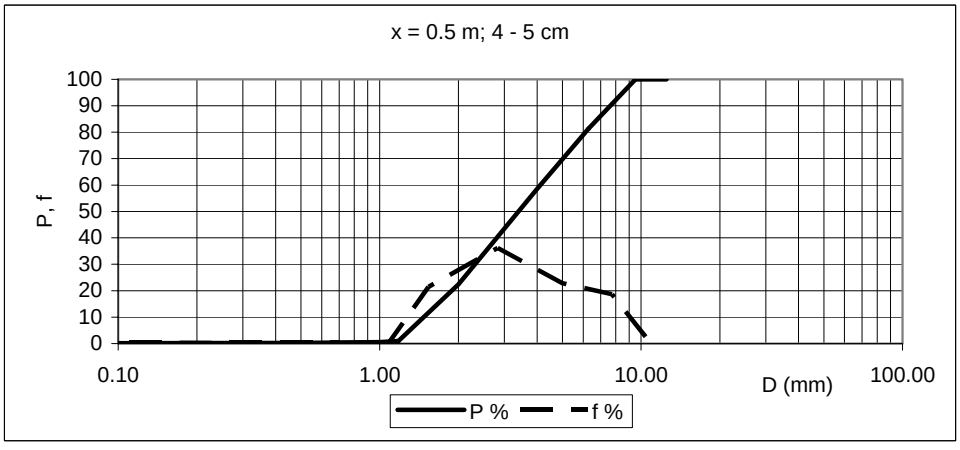
x = 0.5 m; 4 - 5 cm
P, f
100
90
80
70
60
50
40
30
20
10
0
0.10
1.00
10.00
100.00
D (mm)
P %
f %

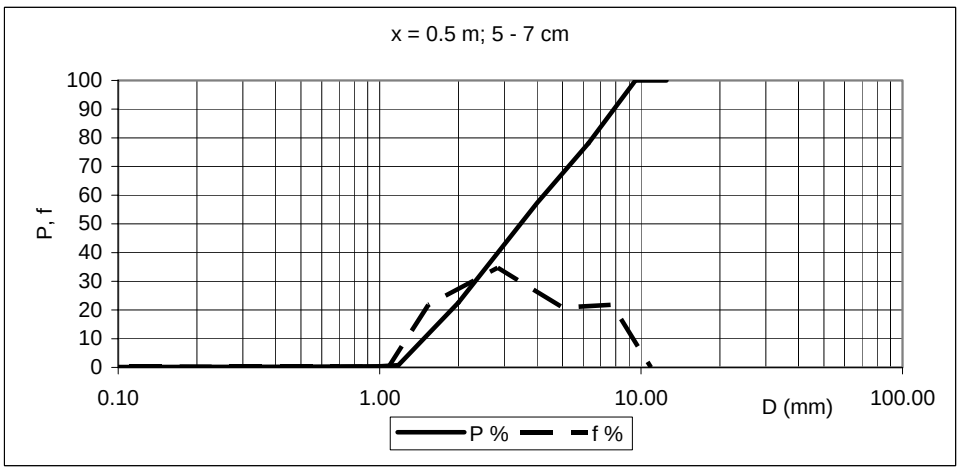
x = 0.5 m; 5 - 7 cm
P, f
100
90
80
70
60
50
40
30
20
10
0
0.10
1.00
10.00
100.00
D (mm)
P %
f %

x = 1.0 m

P %

D (mm)	0 -1 cm	1 - 2 cm	2 - 3 cm	3 - 4 cm	4 - 5 cm	5 - 6 cm	6 - 7 cm
0.01	0.00	0.00	0.00	0.00	0.00	0.00	0.00
0.5	0.24	0.48	0.56	0.50	0.40	0.32	0.25
1	0.69	0.88	0.93	0.77	0.57	0.47	0.39
1.18	1.06	1.19	1.31	1.16	0.95	0.82	0.74
2	17.92	16.50	22.26	23.93	22.45	22.21	22.40
4	48.88	43.44	55.43	57.97	57.29	58.13	58.85
6.3	72.81	76.92	75.90	78.56	78.07	79.93	81.03
9.5	100.00	100.00	100.00	100.00	100.00	100.00	100.00
12.5	100.00	100.00	100.00	100.00	100.00	100.00	100.00

f %

Di (mm)	0 -1 cm	1 - 2 cm	2 - 3 cm	3 - 4 cm	4 - 5 cm	5 - 6 cm	6 - 7 cm
0.07	0.24	0.48	0.56	0.50	0.40	0.32	0.25
0.71	0.45	0.40	0.37	0.27	0.18	0.15	0.14
1.09	0.37	0.31	0.38	0.39	0.38	0.35	0.35
1.54	16.87	15.31	20.95	22.77	21.50	21.39	21.66
2.83	30.96	26.94	33.17	34.04	34.84	35.93	36.45
5.02	23.93	33.48	20.47	20.60	20.78	21.79	22.18
7.74	27.19	23.08	24.10	21.44	21.93	20.07	18.97
10.90	0.00	0.00	0.00	0.00	0.00	0.00	0.00

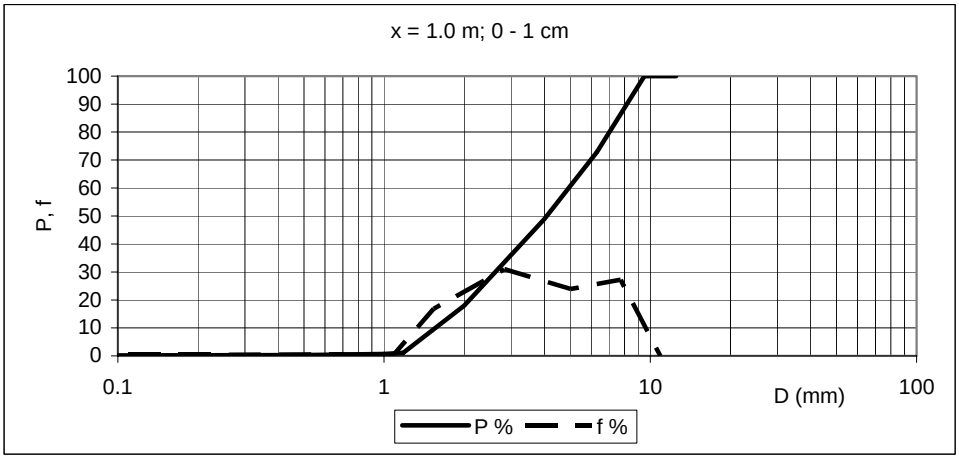

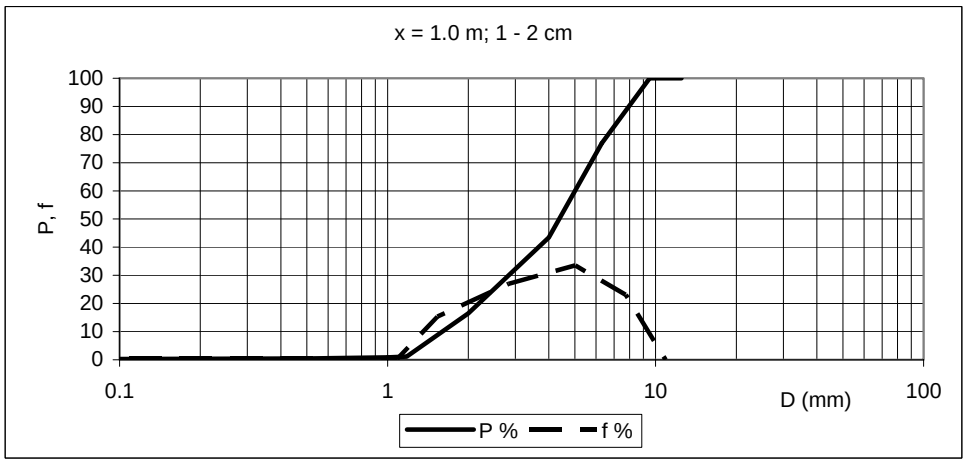

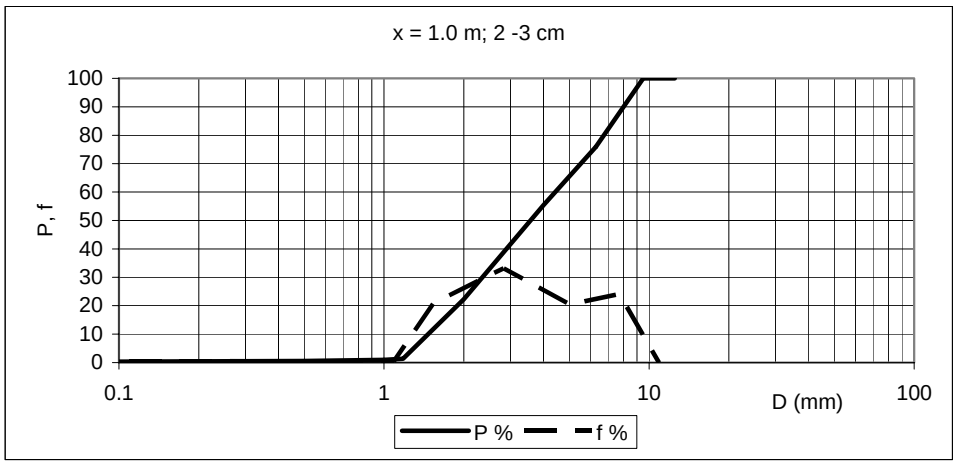
x = 1.0 m; 2 -3 cm
P, f
100
90
80
70
60
50
40
30
20
10
0
0.1
1
10
100
D (mm)
P %
f %

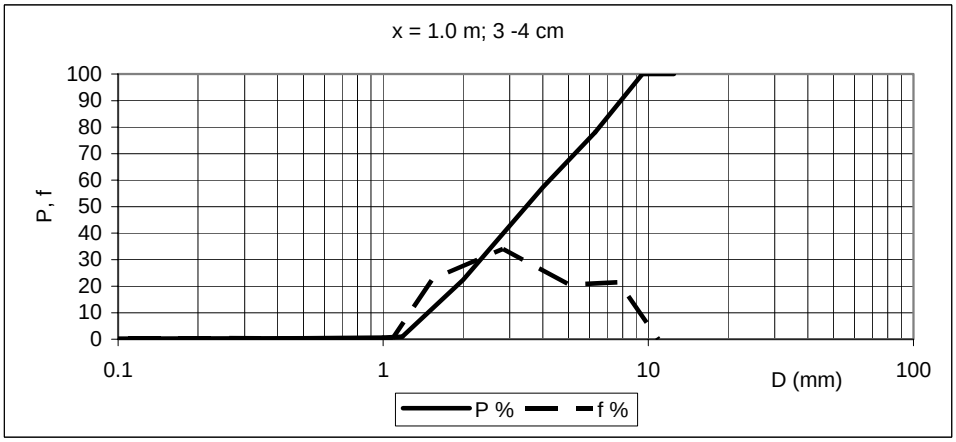
x = 1.0 m; 3 -4 cm
P, f
100
90
80
70
60
50
40
30
20
10
0
0.1
1
10
100
D (mm)
P %
f %

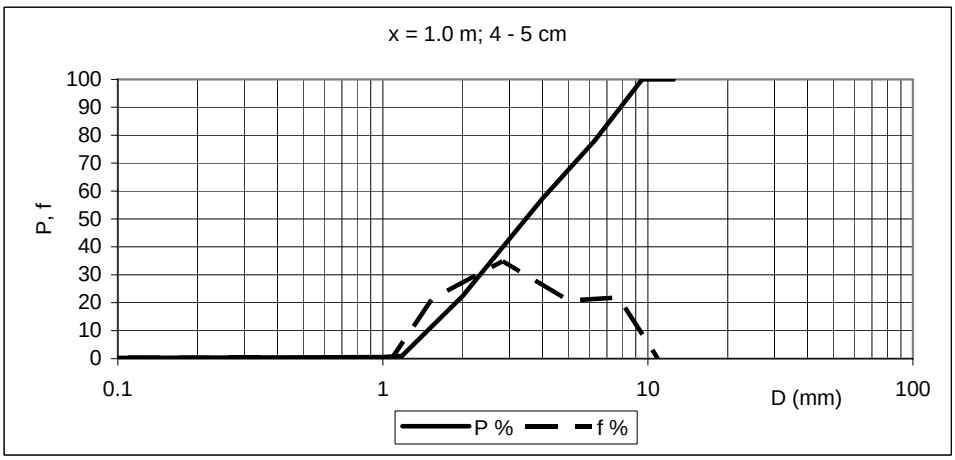
x = 1.0 m; 4 - 5 cm
P, f
100
90
80
70
60
50
40
30
20
10
0
0.1
1
10
100
D (mm)
P %
f %

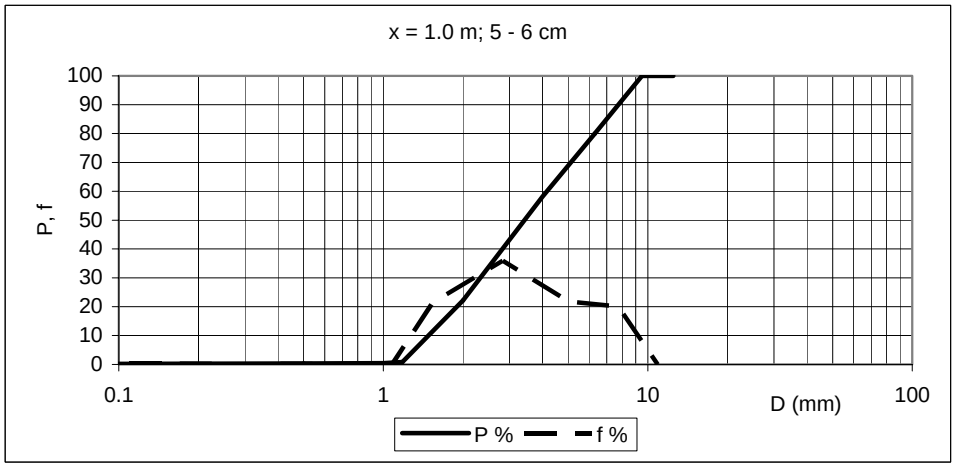
x = 1.0 m; 5 - 6 cm
P, f
100
90
80
70
60
50
40
30
20
10
0
0.1
1
10
100
D (mm)
P %
f %

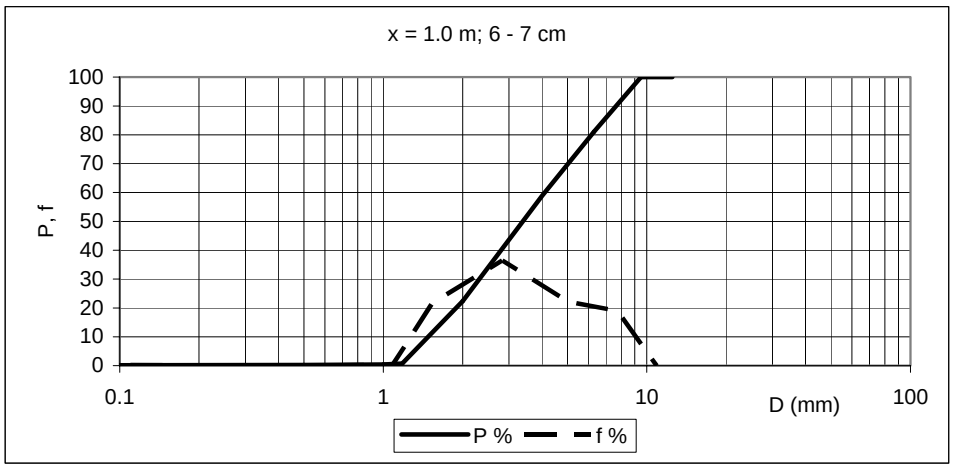
x = 1.0 m; 6 - 7 cm
P, f
100
90
80
70
60
50
40
30
20
10
0
0.1
1
10
100
D (mm)
P %
f %

x = 1.5 m

P %

D (mm)	0 -1 cm	1 - 2 cm	2 - 3 cm	3 - 4 cm	4 - 5 cm	5 - 6 cm	6 - 7 cm
0.1	0.00	0.00	0.00	0.00	0.00	0.00	0.00
0.5	0.24	0.46	0.13	0.30	0.25	0.22	0.20
1	0.67	0.76	0.51	0.47	0.41	0.37	0.33
1.18	1.08	1.11	0.89	0.83	0.79	0.73	0.65
2	22.28	20.99	21.79	22.82	22.80	22.51	22.34
4	58.33	56.39	56.22	56.79	58.61	58.71	59.59
6.3	78.69	79.16	77.81	78.54	81.00	80.31	80.60
9.5	100.00	100.00	100.00	100.00	100.00	100.00	99.70
12.5	100.00	100.00	100.00	100.00	100.00	100.00	100.00

f %

Di (mm)	0 -1 cm	1 - 2 cm	2 - 3 cm	3 - 4 cm	4 - 5 cm	5 - 6 cm	6 - 7 cm
0.22	0.24	0.46	0.13	0.30	0.25	0.22	0.20
0.71	0.44	0.30	0.38	0.17	0.16	0.15	0.14
1.09	0.41	0.36	0.39	0.36	0.38	0.36	0.31
1.54	21.20	19.88	20.89	21.98	22.02	21.78	21.69
2.83	36.05	35.39	34.43	33.97	35.81	36.19	37.25
5.02	20.36	22.77	21.59	21.75	22.39	21.60	21.01
7.74	21.31	20.84	22.19	21.46	19.00	19.69	19.09
10.90	0.00	0.00	0.00	0.00	0.00	0.00	0.30

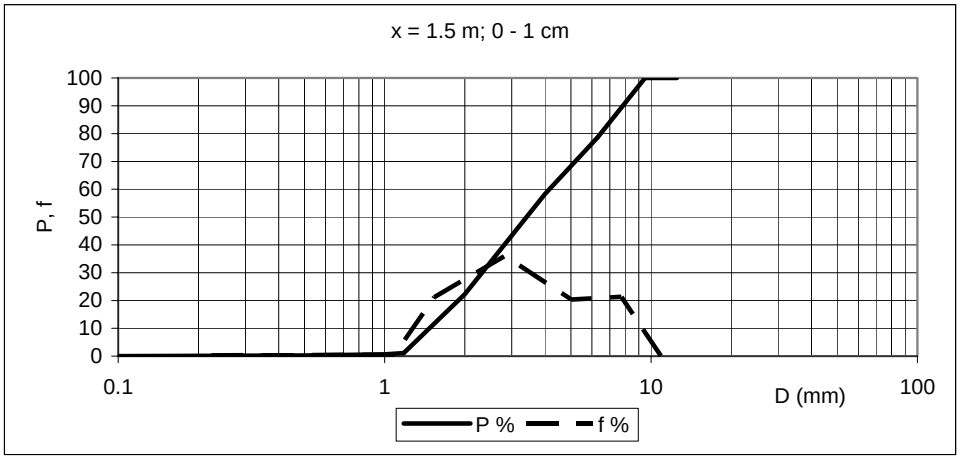

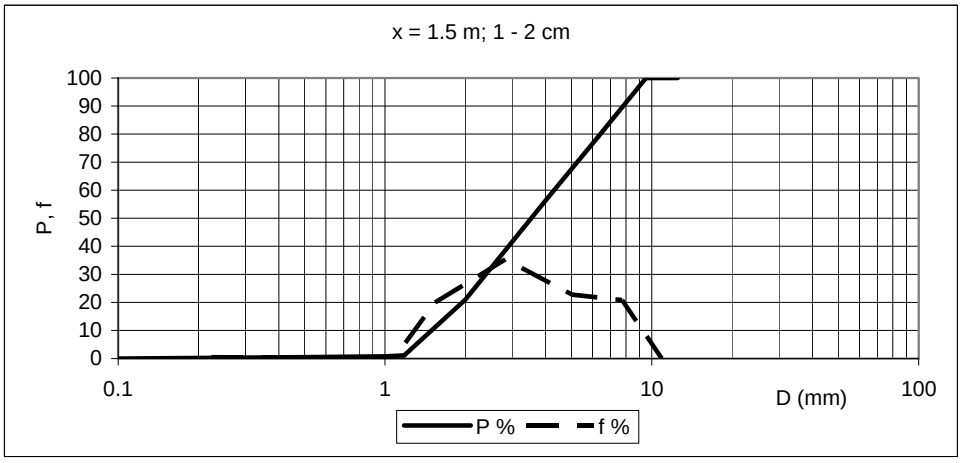

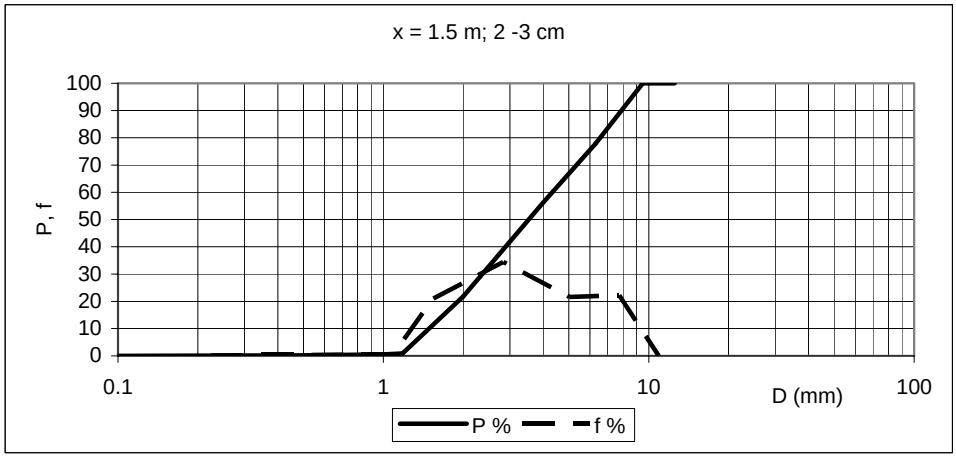
x = 1.5 m; 2 -3 cm
P, f
100
90
80
70
60
50
40
30
20
10
0
0.1
1
10
100
D (mm)
P %
f %

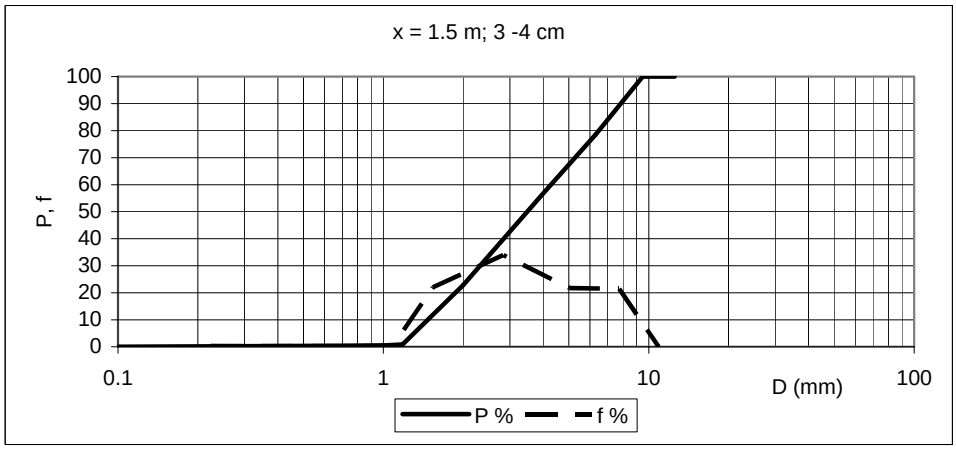
x = 1.5 m; 3 -4 cm
P, f
100
90
80
70
60
50
40
30
20
10
0
0.1
1
10
100
D (mm)
P %
f %

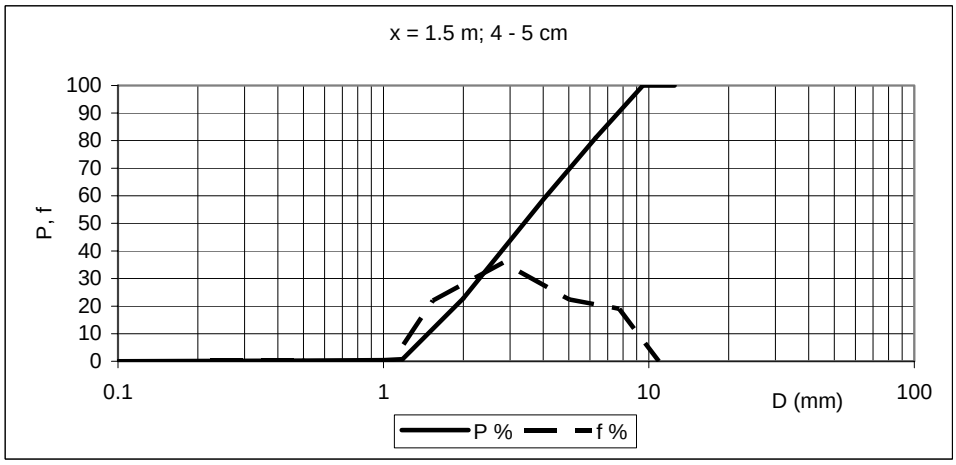
x = 1.5 m; 4 - 5 cm
P, f
100
90
80
70
60
50
40
30
20
10
0
0.1
1
10
100
D (mm)
P %
f %

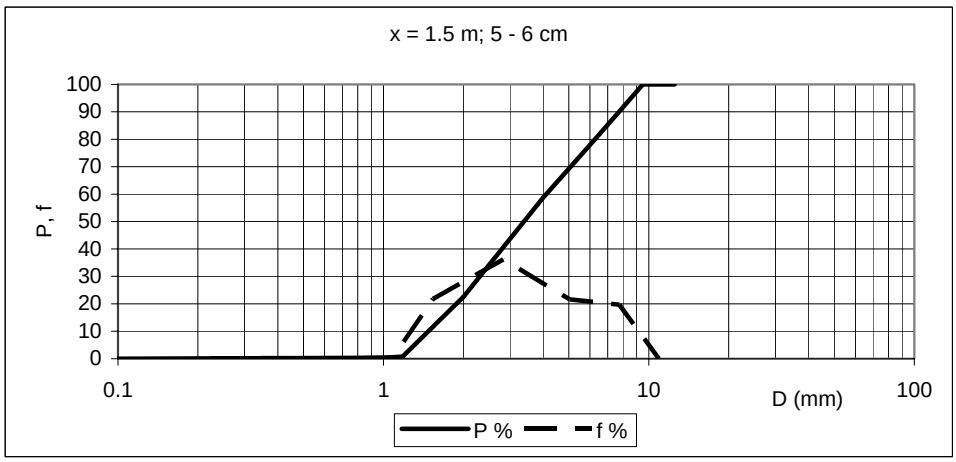
x = 1.5 m; 5 - 6 cm
P, f
100
90
80
70
60
50
40
30
20
10
0
0.1
1
10
100
D (mm)
P %
f %

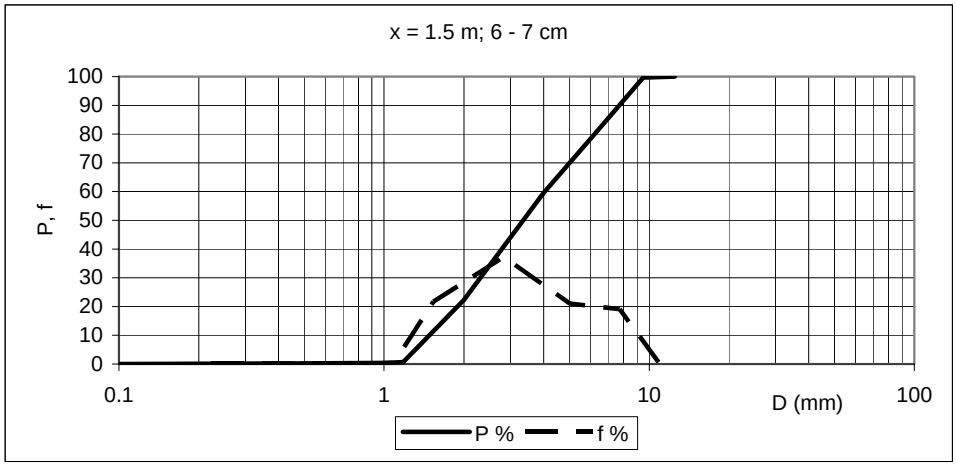
x = 1.5 m; 6 - 7 cm
100
90
80
70
60
50
40
30
20
10
0
P, f
0.1
1
10
100
D (mm)
P %
f %

x = 2.0 m

P %

D (mm)	0 -1 cm	1 - 2 cm	2 - 3 cm	3 - 4 cm	4 - 5 cm	5 - 6 cm	6 - 7 cm
0.1	0.00	0.00	0.00	0.00	0.00	0.00	0.00
0.5	0.24	0.33	0.30	0.22	0.22	0.19	0.14
1	0.59	0.55	0.46	0.34	0.35	0.30	0.26
1.18	0.81	0.81	0.78	0.63	0.64	0.64	0.60
2	18.14	17.85	19.69	19.78	21.62	21.83	21.16
4	51.26	52.17	54.13	52.34	57.01	55.60	54.19
6.3	74.27	76.26	77.05	77.56	78.39	78.00	77.41
9.5	99.87	100.00	100.00	99.89	99.82	99.63	99.89
12.5	100.00	100.00	100.00	100.00	100.00	100.00	100.00

f %

Di (mm)	0 -1 cm	1 - 2 cm	2 - 3 cm	3 - 4 cm	4 - 5 cm	5 - 6 cm	6 - 7 cm
0.22	0.24	0.33	0.30	0.22	0.22	0.19	0.14
0.71	0.35	0.22	0.16	0.11	0.13	0.11	0.11
1.09	0.22	0.26	0.32	0.29	0.29	0.34	0.34
1.54	17.34	17.05	18.91	19.15	20.98	21.19	20.56
2.83	33.12	34.31	34.44	32.56	35.39	33.78	33.04
5.02	23.00	24.10	22.92	25.22	21.38	22.39	23.22
7.74	25.61	23.74	22.95	22.33	21.43	21.63	22.48
10.90	0.13	0.00	0.00	0.11	0.18	0.37	0.11

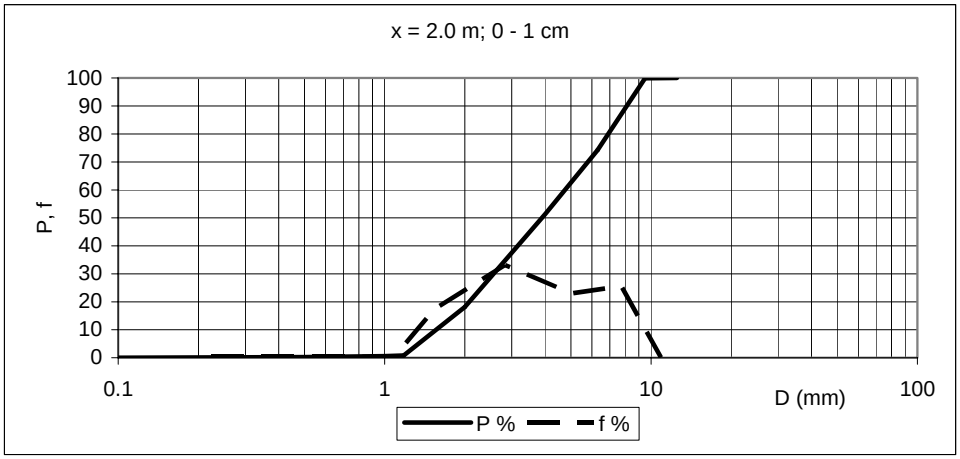

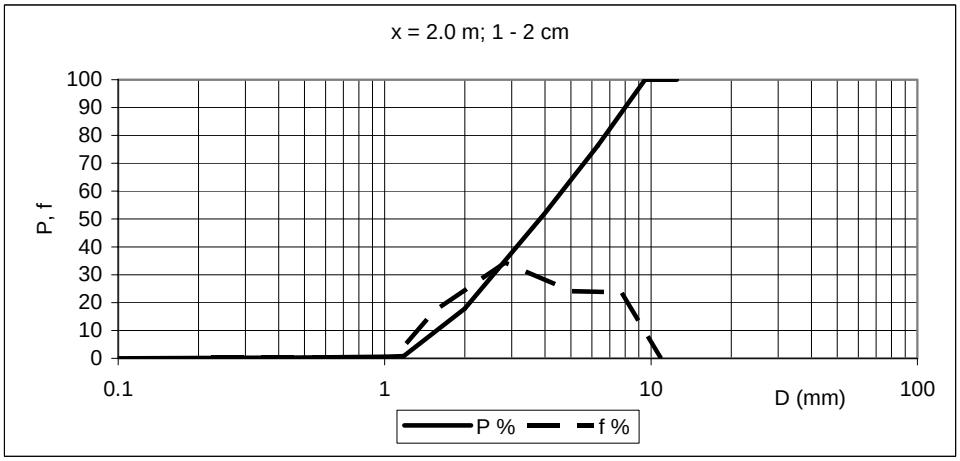

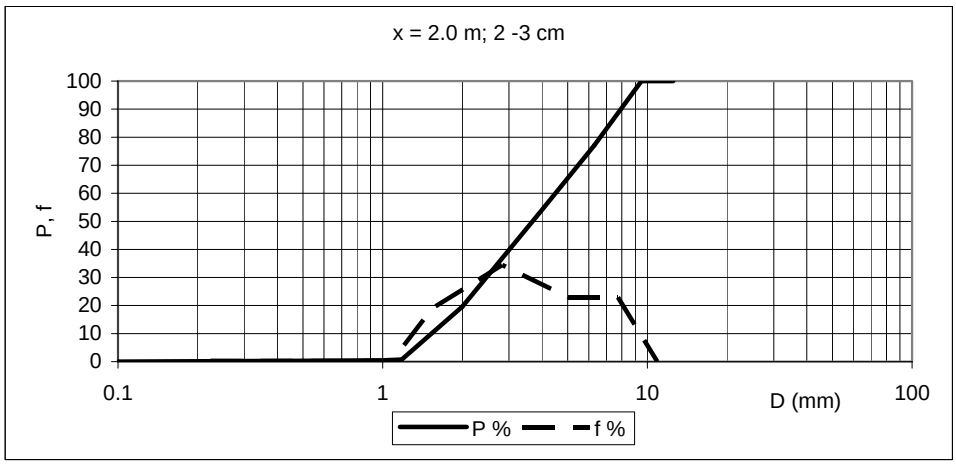
x = 2.0 m; 2 -3 cm
P, f
100
90
80
70
60
50
40
30
20
10
0
0.1
1
10
100
D (mm)
P %
f %

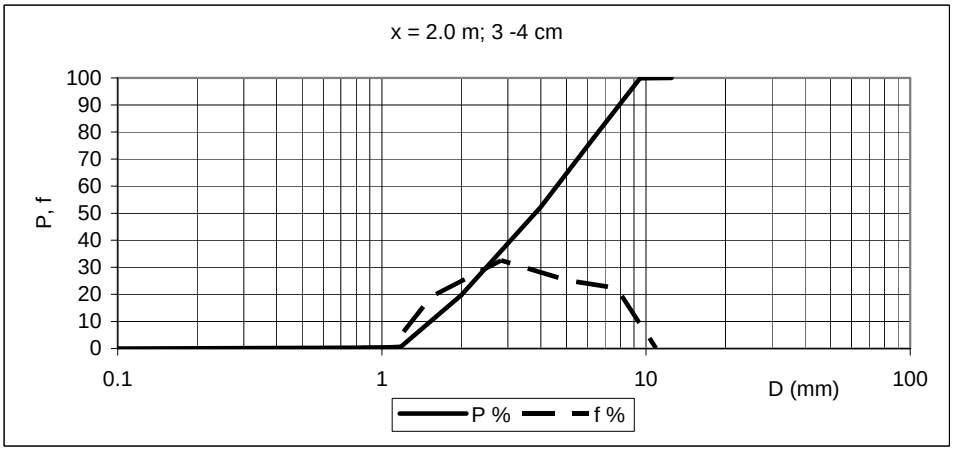
x = 2.0 m; 3 -4 cm
P, f
100
90
80
70
60
50
40
30
20
10
0
0.1
1
10
100
D (mm)
P %
f %

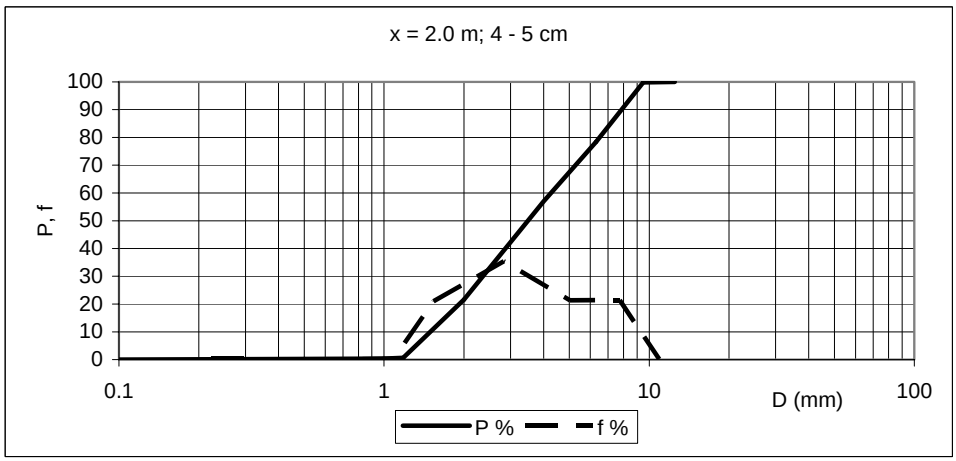
x = 2.0 m; 4 - 5 cm
P, f
100
90
80
70
60
50
40
30
20
10
0
0.1
1
10
100
D (mm)
P %
f %

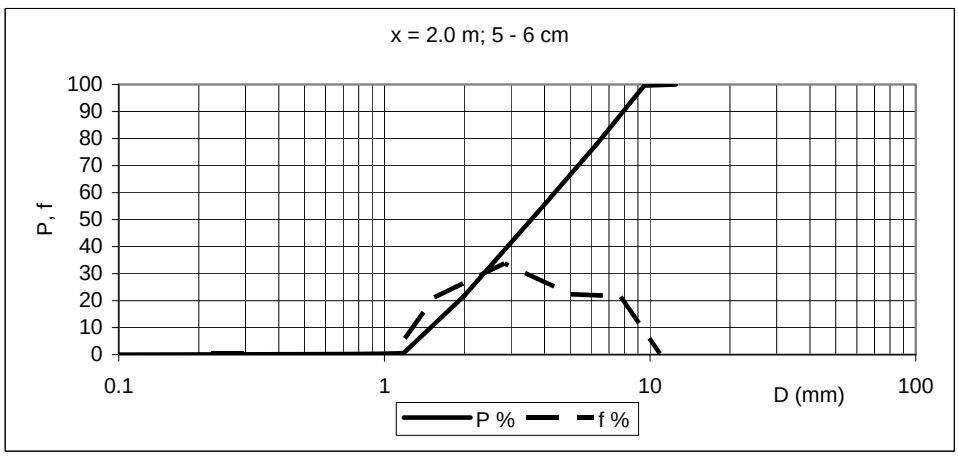
x = 2.0 m; 5 - 6 cm
P, f
100
90
80
70
60
50
40
30
20
10
0
0.1
1
10
100
D (mm)
P %
f %

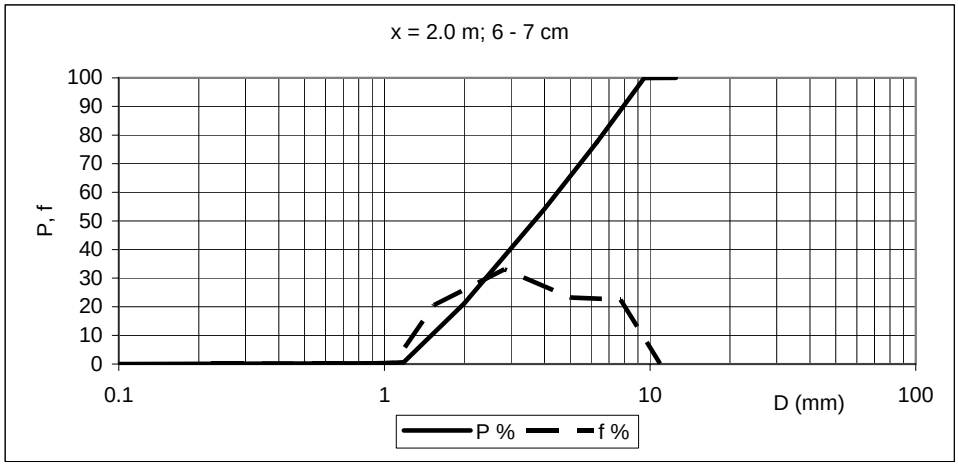
x = 2.0 m; 6 - 7 cm
P, f
100
90
80
70
60
50
40
30
20
10
0
0.1
1
10
100
D (mm)
P %
f %

x = 2.5 m

P %

D (mm)	0 -1 cm	1 - 2 cm	2 - 3 cm	3 - 4 cm	4 - 5 cm	5 - 6 cm	6 - 7 cm
0.1	0.00	0.00	0.00	0.00	0.00	0.00	0.00
0.5	0.19	0.22	0.17	0.16	0.16	0.16	0.15
1	0.49	0.42	0.32	0.27	0.26	0.28	0.26
1.18	0.80	0.70	0.60	0.54	0.57	0.58	0.58
2	18.20	19.03	18.59	18.07	20.75	21.01	22.38
4	53.00	53.31	52.88	52.37	55.50	55.70	57.32
6.3	75.94	76.41	77.43	74.82	79.11	80.02	78.92
9.5	100.00	99.82	100.00	100.00	100.00	99.82	100.00
12.5	100.00	100.00	100.00	100.00	100.00	100.00	100.00

f %

Di (mm)	0 -1 cm	1 - 2 cm	2 - 3 cm	3 - 4 cm	4 - 5 cm	5 - 6 cm	6 - 7 cm
0.22	0.19	0.22	0.17	0.16	0.16	0.16	0.15
0.71	0.30	0.21	0.15	0.12	0.11	0.12	0.11
1.09	0.31	0.27	0.28	0.26	0.30	0.30	0.33
1.54	17.40	18.34	17.99	17.54	20.19	20.42	21.80
2.83	34.81	34.28	34.29	34.29	34.75	34.69	34.94
5.02	22.94	23.10	24.55	22.46	23.61	24.32	21.59
7.74	24.06	23.41	22.57	25.18	20.89	19.81	21.08
10.90	0.00	0.18	0.00	0.00	0.00	0.18	0.00

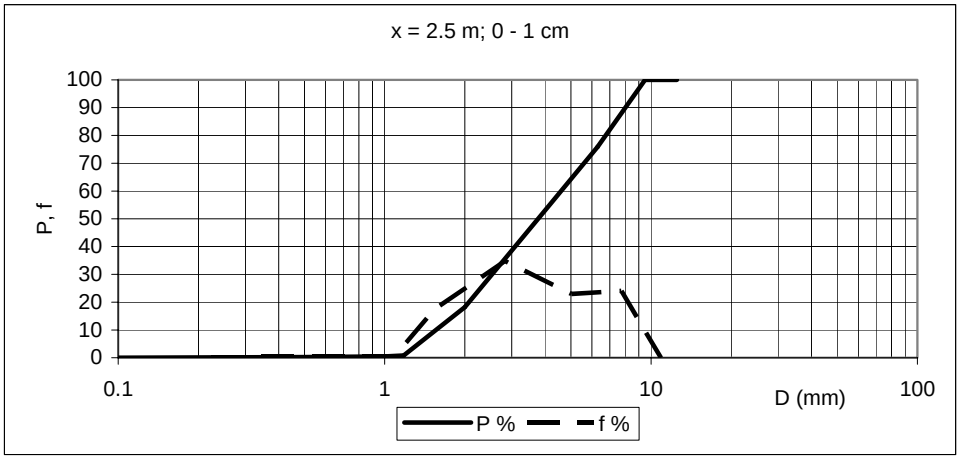

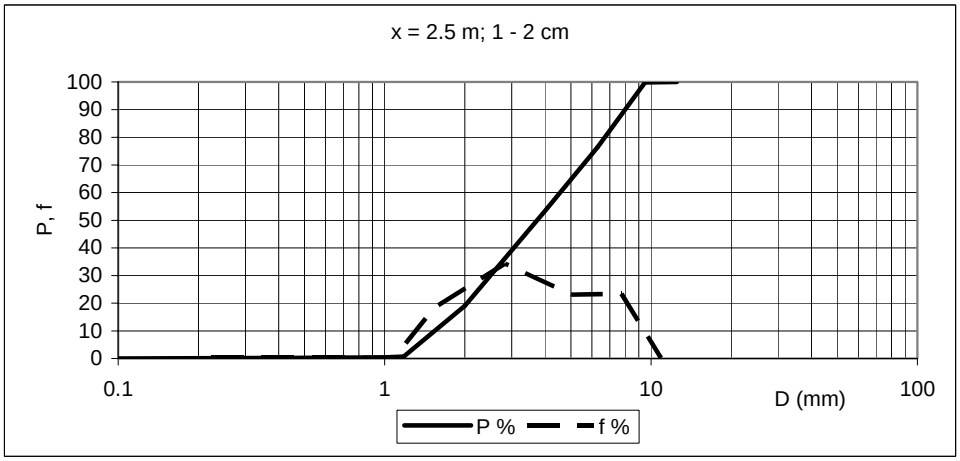

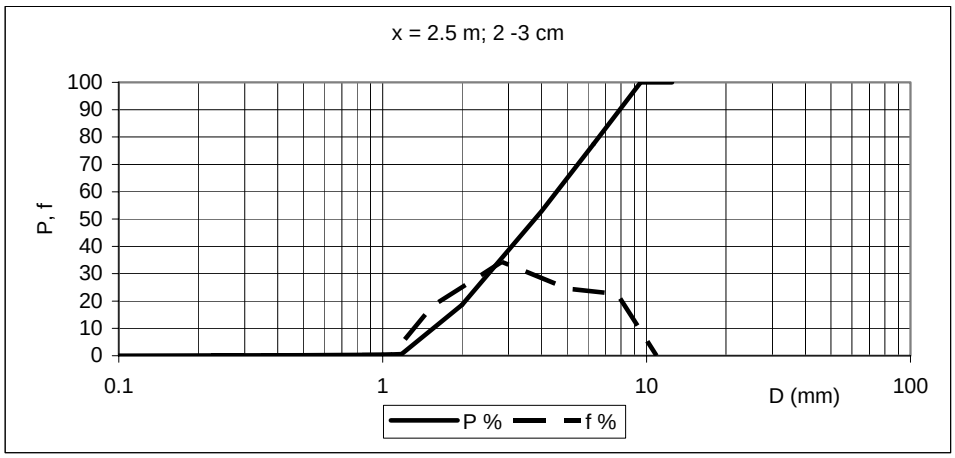
x = 2.5 m; 2 -3 cm
P, f
100
90
80
70
60
50
40
30
20
10
0
0.1
1
10
100
D (mm)
P %
f %

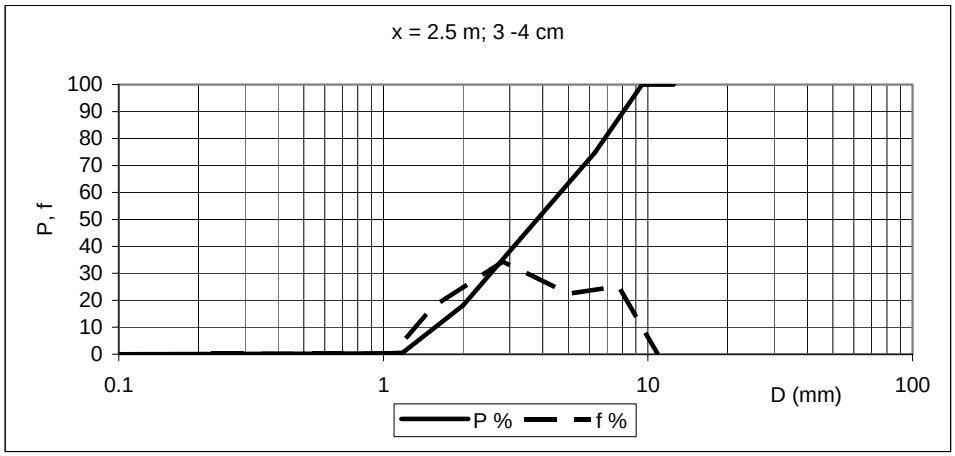
x = 2.5 m; 3 -4 cm
P, f
100
90
80
70
60
50
40
30
20
10
0
0.1
1
10
100
D (mm)
P %
f %

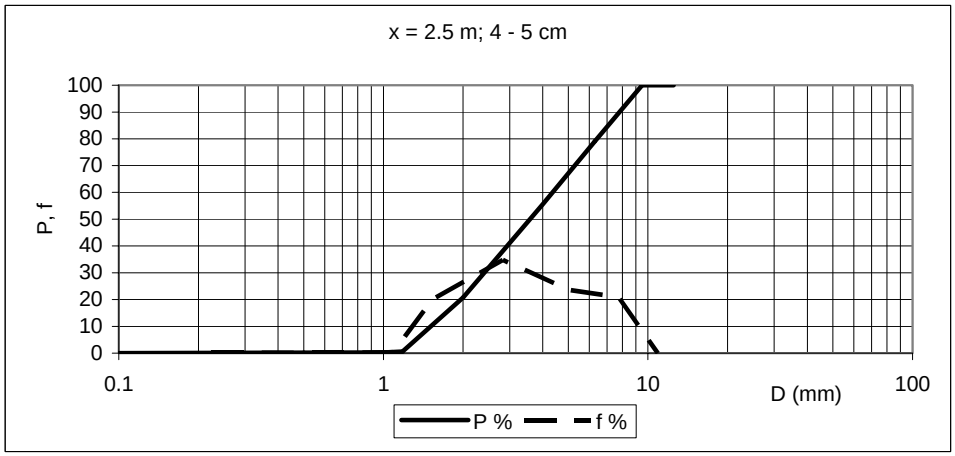
x = 2.5 m; 4 - 5 cm
P, f
100
90
80
70
60
50
40
30
20
10
0
0.1
1
10
100
D (mm)
P %
f %

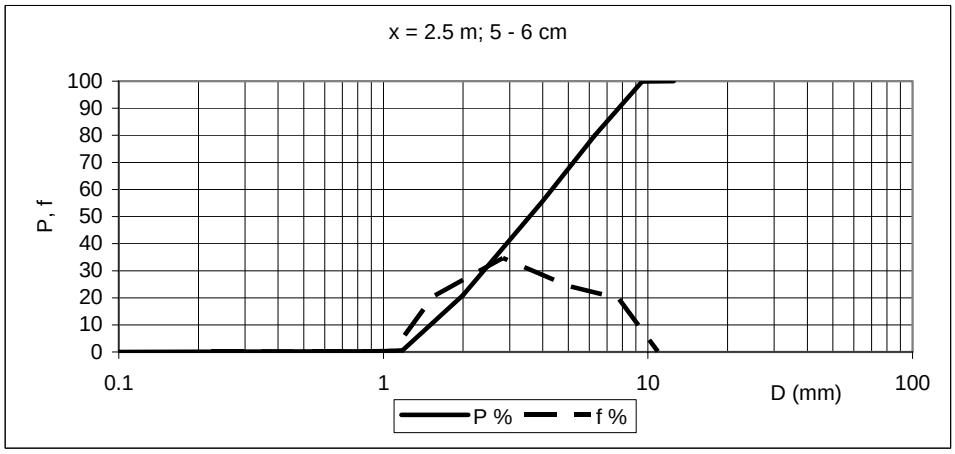
x = 2.5 m; 5 - 6 cm
P, f
100
90
80
70
60
50
40
30
20
10
0
0.1
1
10
100
D (mm)
P %
f %

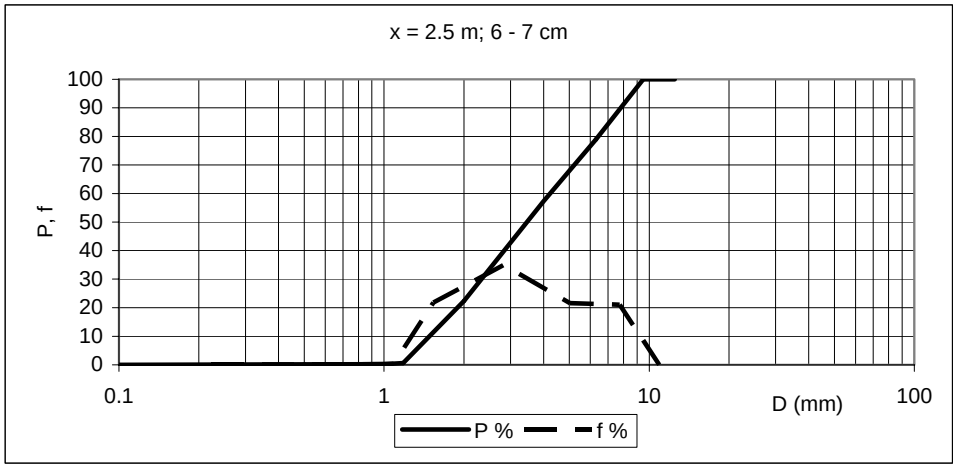
x = 2.5 m; 6 - 7 cm
100
90
80
70
60
50
40
30
20
10
0
P, f
0.1
1
10
100
D (mm)
P %
f %

x = 3.0 m

P %

D (mm)	0 -1 cm	1 - 2 cm	2 - 3 cm	3 - 4 cm	4 - 5 cm
0.1	0.00	0.00	0.00	0.00	0.00
0.5	0.13	0.18	0.13	0.12	0.16
1	0.36	0.34	0.26	0.34	0.26
1.18	0.70	0.69	0.59	0.54	0.58
2	20.02	20.94	21.05	19.84	20.76
4	54.10	55.33	56.02	52.59	55.82
6.3	77.57	77.64	78.47	74.45	78.74
9.5	100.00	100.00	100.00	99.81	100.00
12.5	100.00	100.00	100.00	100.00	100.00

f %

Di (mm)	0 -1 cm	1 - 2 cm	2 - 3 cm	3 - 4 cm	4 - 5 cm
0.22	0.13	0.18	0.13	0.12	0.16
0.71	0.24	0.17	0.13	0.23	0.10
1.09	0.34	0.34	0.33	0.20	0.32
1.54	19.32	20.25	20.46	19.30	20.18
2.83	34.08	34.39	34.97	32.75	35.07
5.02	23.46	22.30	22.45	21.86	22.92
7.74	22.43	22.36	21.53	25.36	21.26
10.90	0.00	0.00	0.00	0.19	0.00

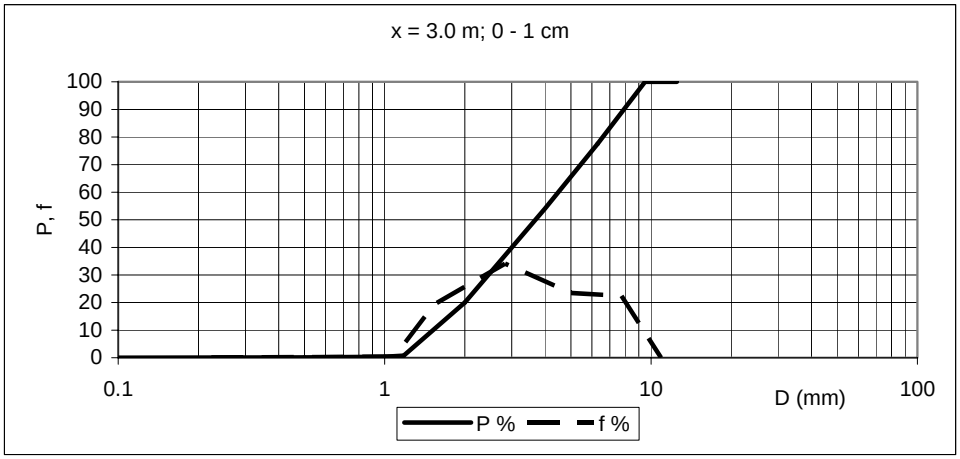

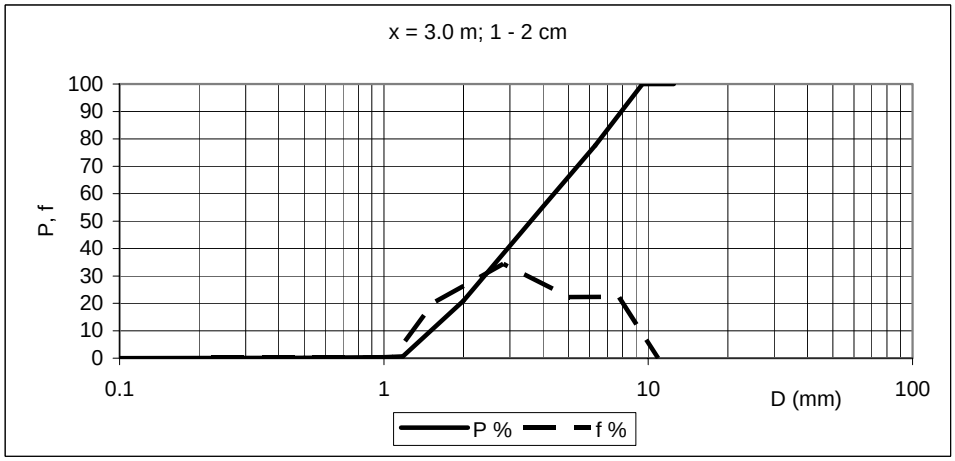

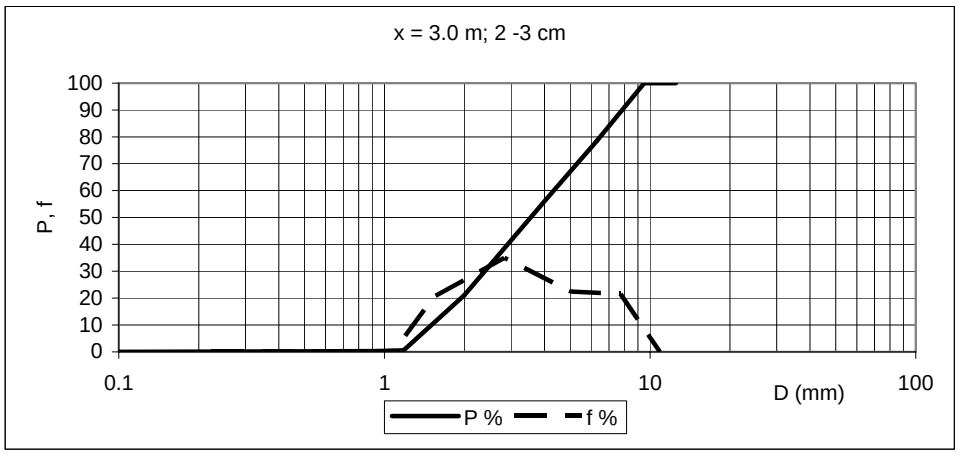
x = 3.0 m; 2 -3 cm
P, f
100
90
80
70
60
50
40
30
20
10
0
0.1
1
10
100
D (mm)
P %
f %

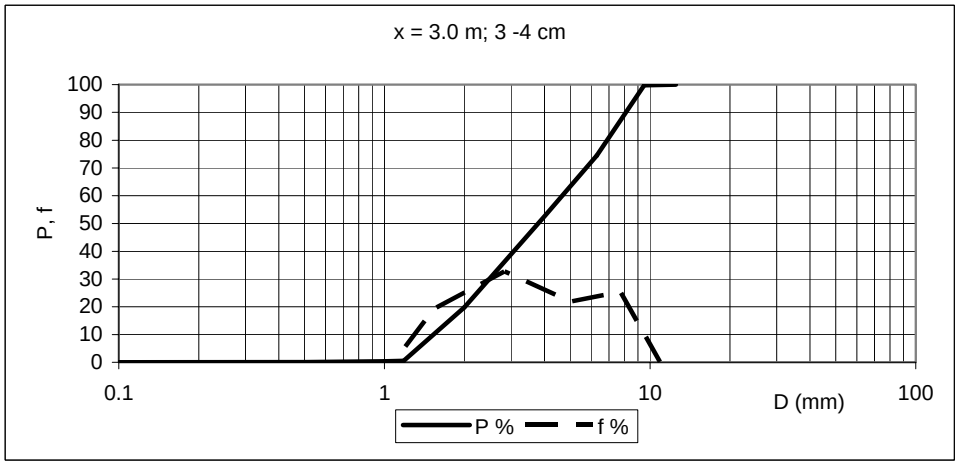
x = 3.0 m; 3 -4 cm
P, f
100
90
80
70
60
50
40
30
20
10
0
0.1
1
10
100
D (mm)
P %
f %

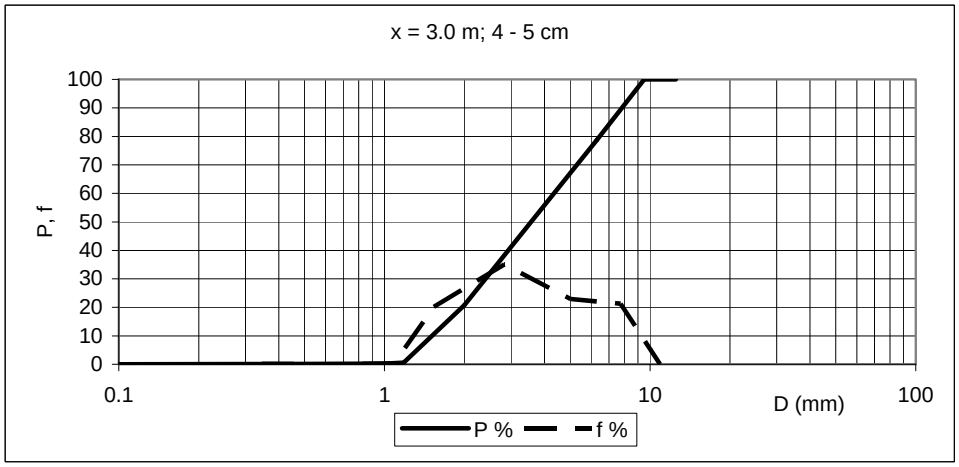
x = 3.0 m; 4 - 5 cm
P, f
100
90
80
70
60
50
40
30
20
10
0
0.1
1
10
100
D (mm)
P %
f %

x = 4.0 m

P %

D (mm)	0 -1 cm	1 - 2 cm	2 - 3 cm	3 - 4 cm	4 - 5 cm
0.1	0.00	0.00	0.00	0.00	0.00
0.5	0.10	0.12	0.12	0.11	0.10
1	0.31	0.25	0.23	0.23	0.22
1.18	0.71	0.61	0.62	0.67	0.63
2	23.56	22.32	24.72	27.53	24.96
4	56.30	58.71	60.33	63.69	59.48
6.3	76.07	81.63	82.34	85.63	79.95
9.5	100.00	100.00	100.00	100.00	100.00
12.5	100.00	100.00	100.00	100.00	100.00

f %

Di (mm)	0 -1 cm	1 - 2 cm	2 - 3 cm	3 - 4 cm	4 - 5 cm
0.22	0.10	0.12	0.12	0.11	0.10
0.71	0.21	0.13	0.11	0.12	0.12
1.09	0.39	0.36	0.39	0.45	0.42
1.54	22.86	21.71	24.10	26.85	24.33
2.83	32.73	36.39	35.61	36.17	34.52
5.02	19.77	22.92	22.01	21.94	20.47
7.74	23.93	18.37	17.66	14.37	20.05
10.90	0.00	0.00	0.00	0.00	0.00

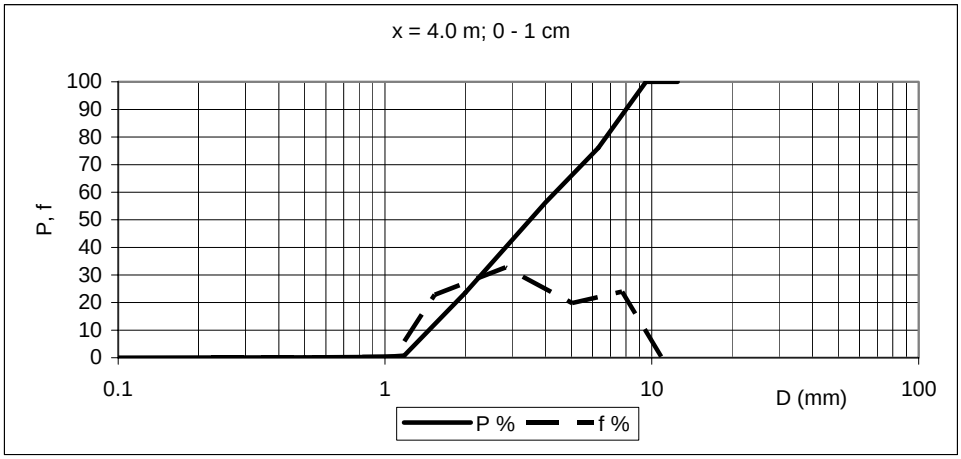

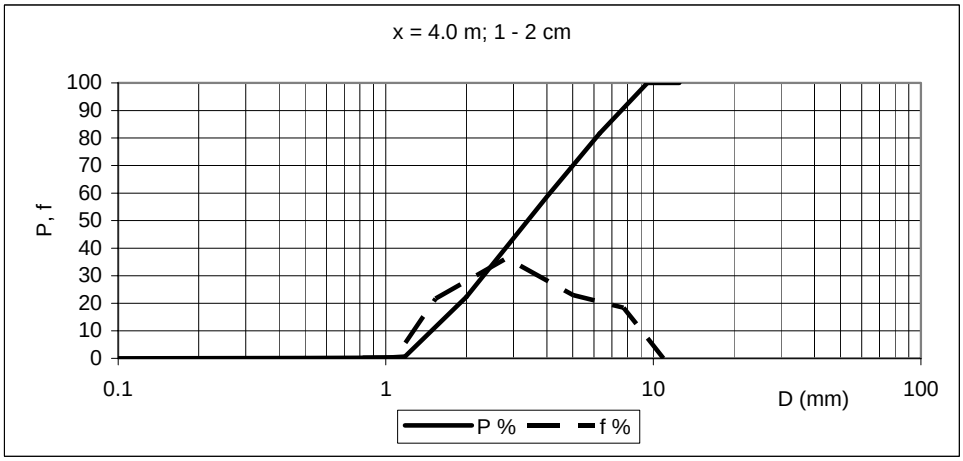

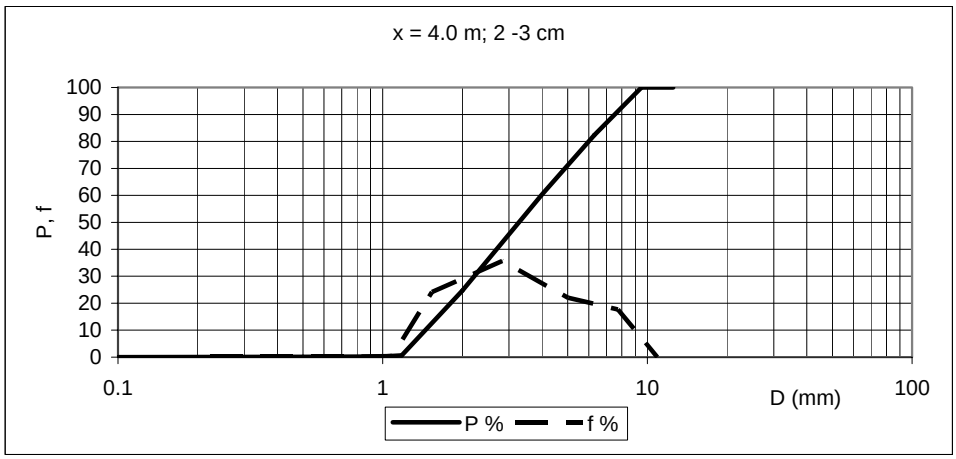
x = 4.0 m; 2 -3 cm
P, f
100
90
80
70
60
50
40
30
20
10
0
0.1
1
10
100
D (mm)
P %
f %

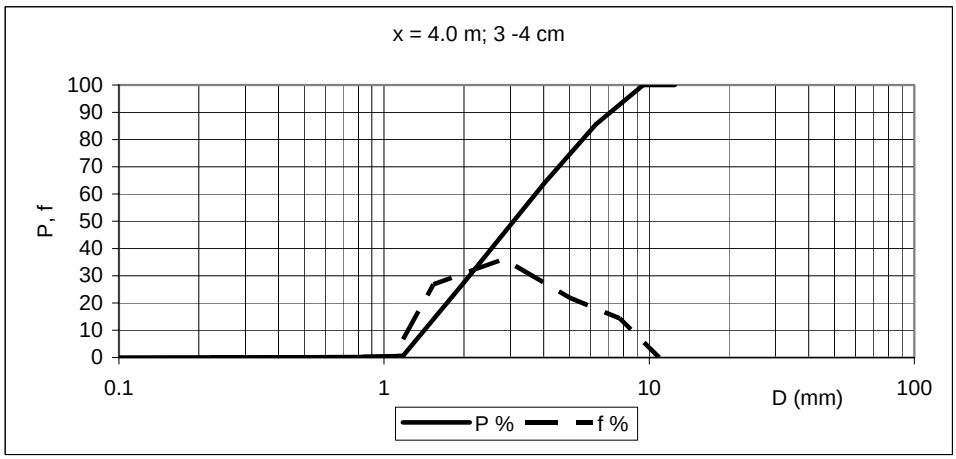
x = 4.0 m; 3 -4 cm
P, f
100
90
80
70
60
50
40
30
20
10
0
0.1
1
10
100
D (mm)
P %
f %

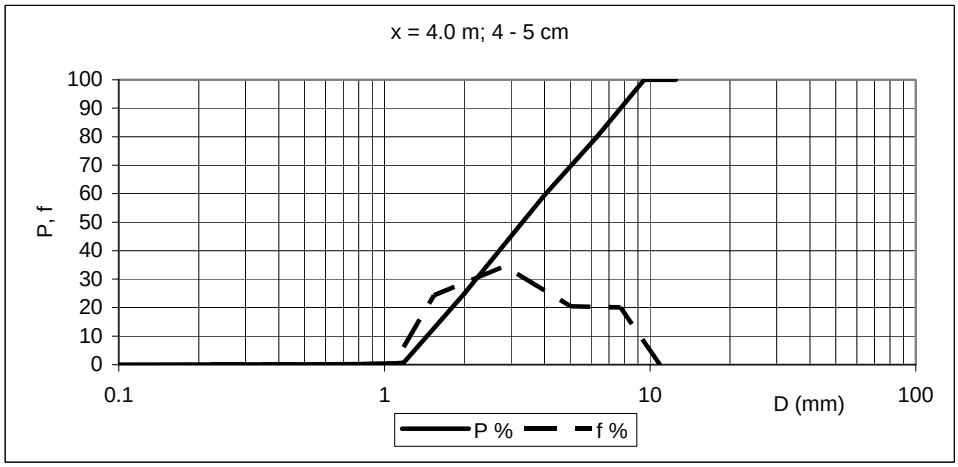
x = 4.0 m; 4 - 5 cm
P, f
100
90
80
70
60
50
40
30
20
10
0
0.1
1
10
100
D (mm)
P %
f %

x = 5.0 m

P %

D (mm)	0 -1 cm	1 - 2 cm	2 - 3 cm	3 - 4 cm	4 - 5 cm
0.1	0.00	0.00	0.00	0.00	0.00
0.5	0.06	0.09	0.10	0.14	0.10
1	0.22	0.21	0.22	0.25	0.20
1.18	0.54	0.53	0.53	0.63	0.54
2	18.48	17.57	19.60	21.49	21.57
4	47.47	48.46	52.92	54.11	56.88
6.3	71.44	73.46	76.49	77.05	79.09
9.5	100.00	100.00	100.00	100.00	100.00
12.5	100.00	100.00	100.00	100.00	100.00

f %

Di (mm)	0 -1 cm	1 - 2 cm	2 - 3 cm	3 - 4 cm	4 - 5 cm
0.22	0.06	0.09	0.10	0.14	0.10
0.71	0.16	0.13	0.12	0.11	0.10
1.09	0.32	0.32	0.31	0.38	0.34
1.54	17.95	17.03	19.07	20.86	21.03
2.83	28.98	30.89	33.32	32.62	35.31
5.02	23.97	25.00	23.58	22.94	22.21
7.74	28.56	26.54	23.51	22.95	20.91
10.90	0.00	0.00	0.00	0.00	0.00

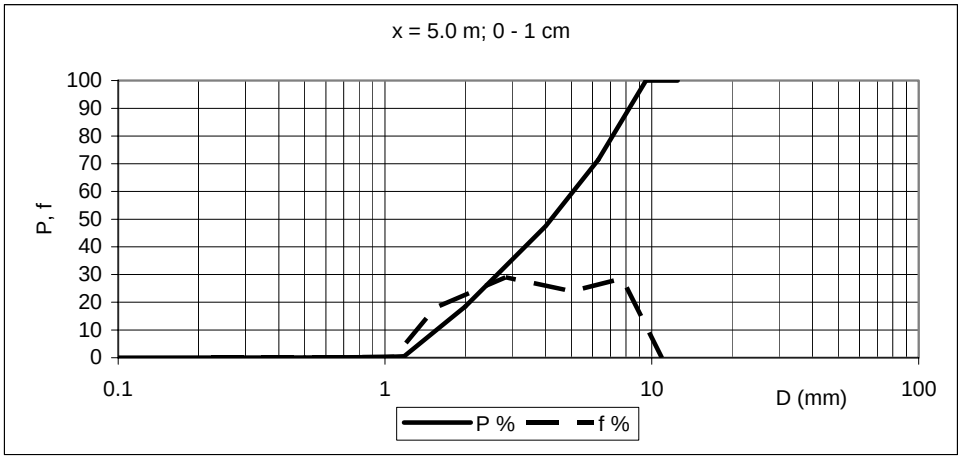

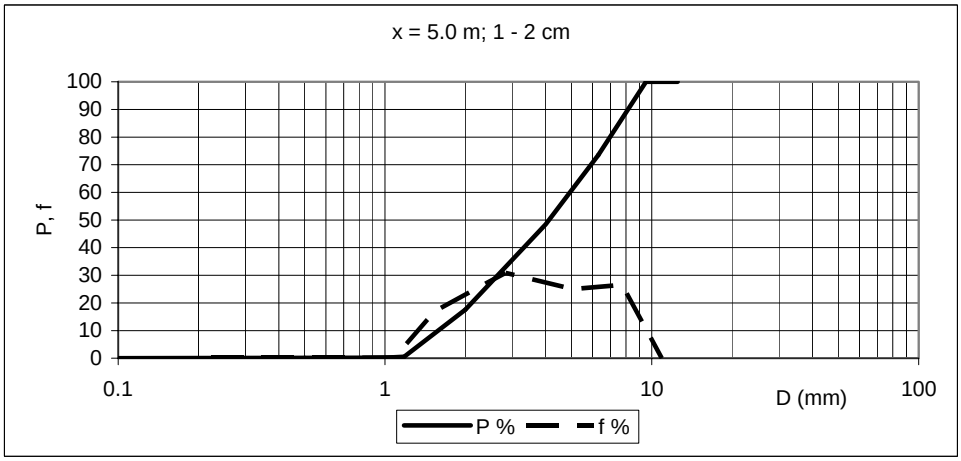

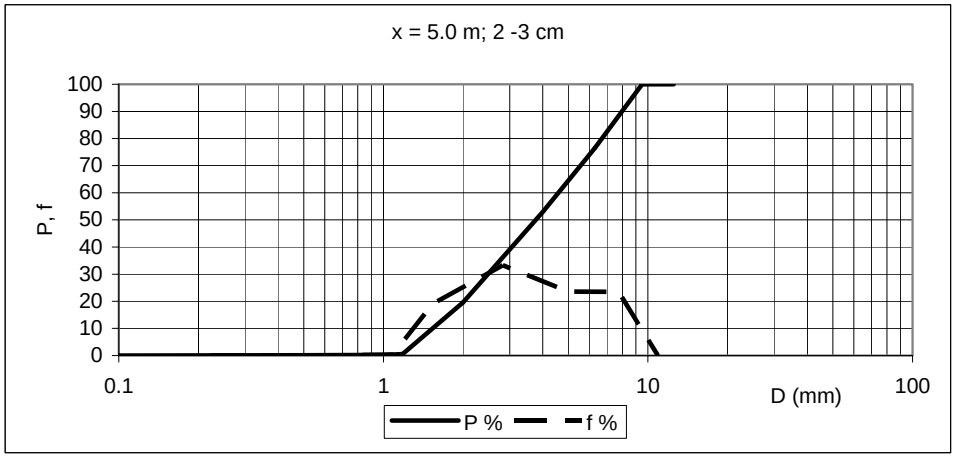
x = 5.0 m; 2 -3 cm
P, f
100
90
80
70
60
50
40
30
20
10
0
0.1
1
10
100
D (mm)
P %
f %

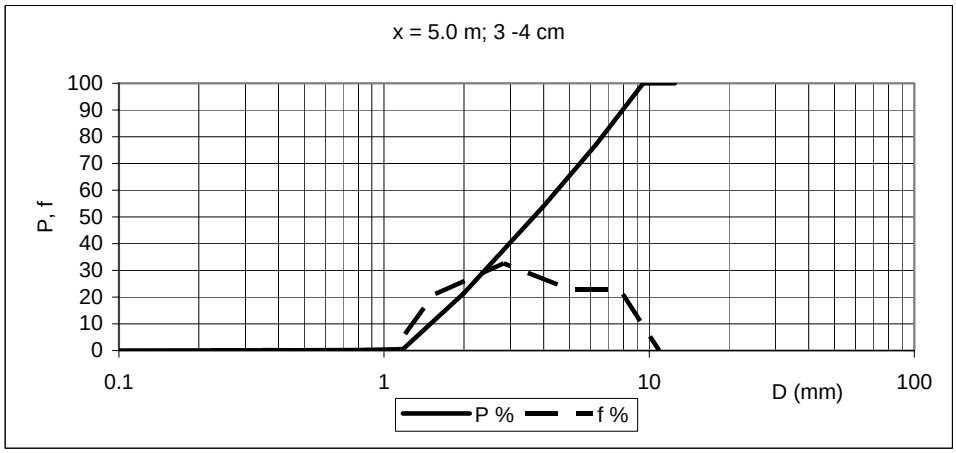
x = 5.0 m; 3 -4 cm
P, f
100
90
80
70
60
50
40
30
20
10
0
0.1
1
10
100
D (mm)
P %
f %

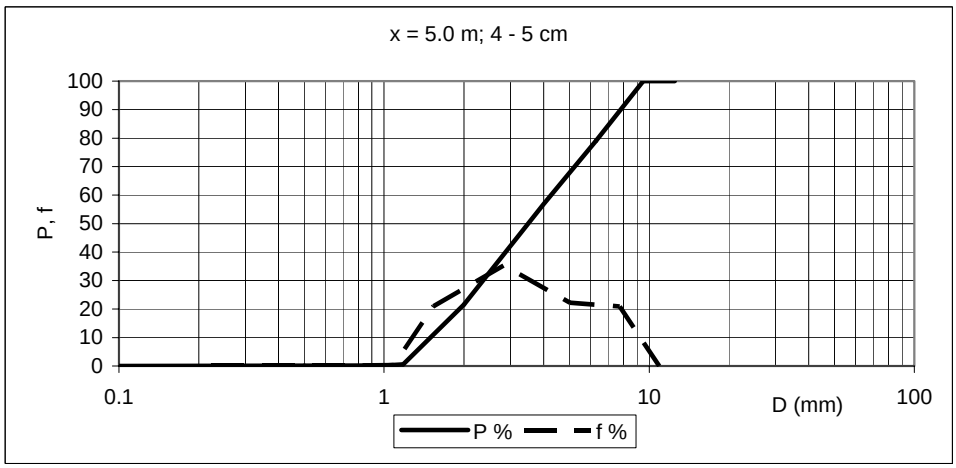
x = 5.0 m; 4 - 5 cm
P, f
100
90
80
70
60
50
40
30
20
10
0
0.1
1
10
100
D (mm)
P %
f %

x = 7.0 m

P %

D (mm)	0 -1 cm	1 - 2 cm	2 - 3 cm	3 - 4 cm	4 - 5 cm
0.1	0.00	0.00	0.00	0.00	0.00
0.5	0.09	0.10	0.10	0.09	0.09
1	0.30	0.24	0.22	0.20	0.20
1.18	0.72	0.60	0.57	0.54	0.55
2	21.66	20.52	20.82	21.12	22.18
4	54.05	54.30	55.99	56.58	56.90
6.3	75.58	76.55	77.53	79.88	78.18
9.5	100.00	100.00	100.00	99.79	99.81
12.5	100.00	100.00	100.00	100.00	100.00

f %

Di (mm)	0 -1 cm	1 - 2 cm	2 - 3 cm	3 - 4 cm	4 - 5 cm
0.22	0.09	0.10	0.10	0.09	0.09
0.71	0.21	0.14	0.12	0.11	0.10
1.09	0.42	0.36	0.35	0.34	0.36
1.54	20.94	19.92	20.25	20.58	21.63
2.83	32.40	33.77	35.16	35.46	34.72
5.02	21.53	22.25	21.54	23.30	21.28
7.74	24.42	23.45	22.47	19.91	21.63
10.90	0.00	0.00	0.00	0.21	0.19

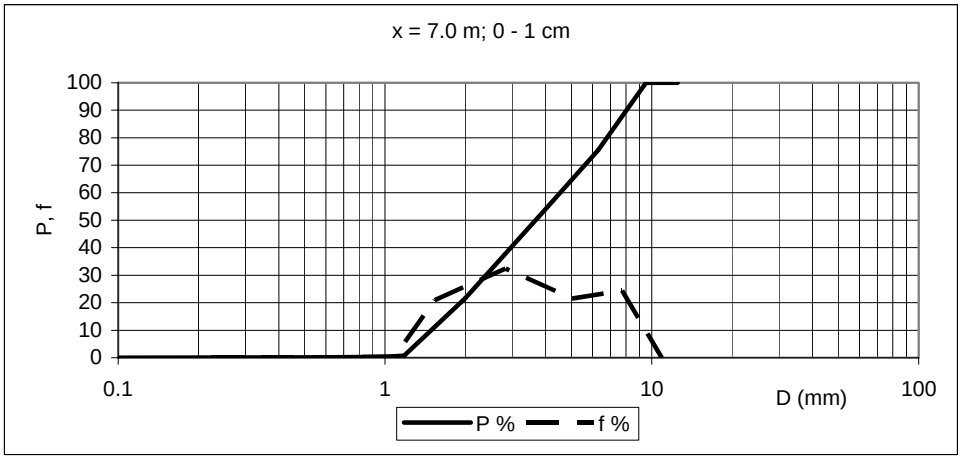

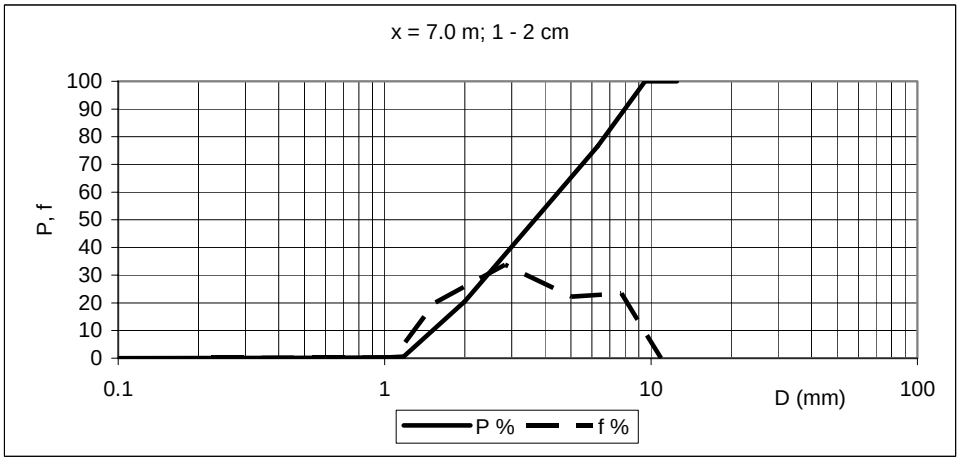

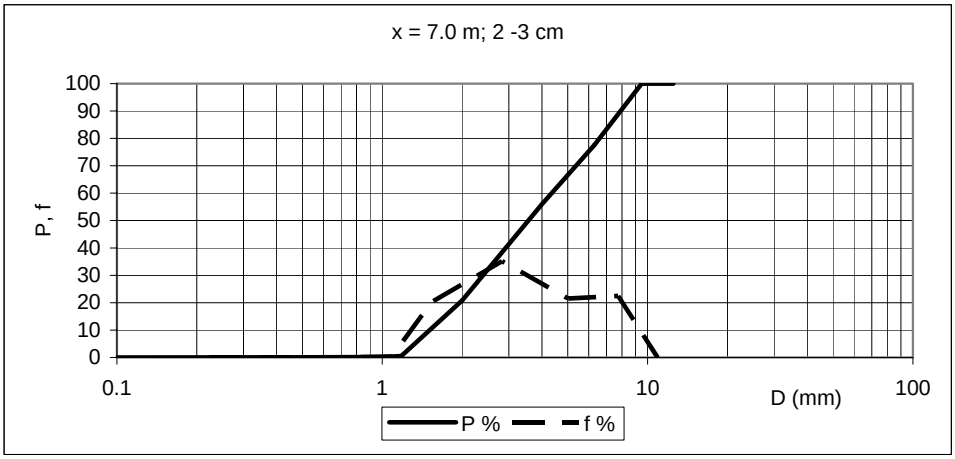
x = 7.0 m; 2 -3 cm
P, f
100
90
80
70
60
50
40
30
20
10
0
0.1
1
10
100
D (mm)
P %
f %

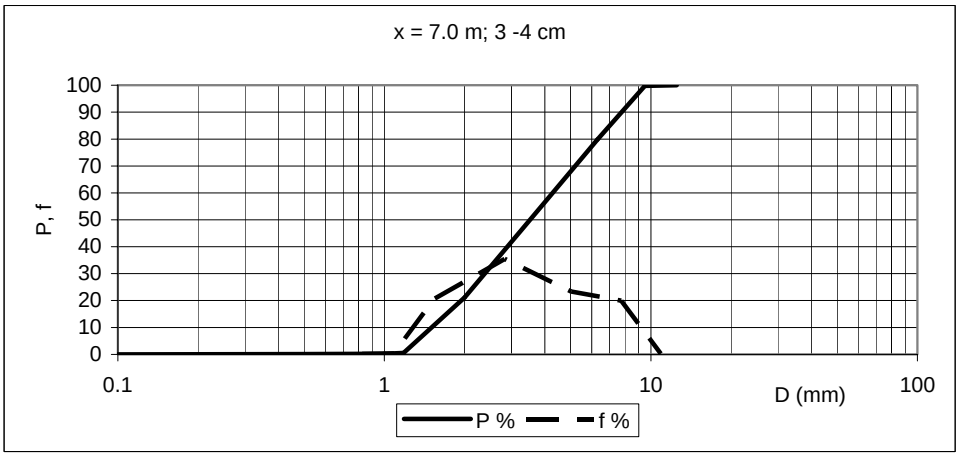
x = 7.0 m; 3 -4 cm
P, f
100
90
80
70
60
50
40
30
20
10
0
0.1
1
10
100
D (mm)
P %
f %

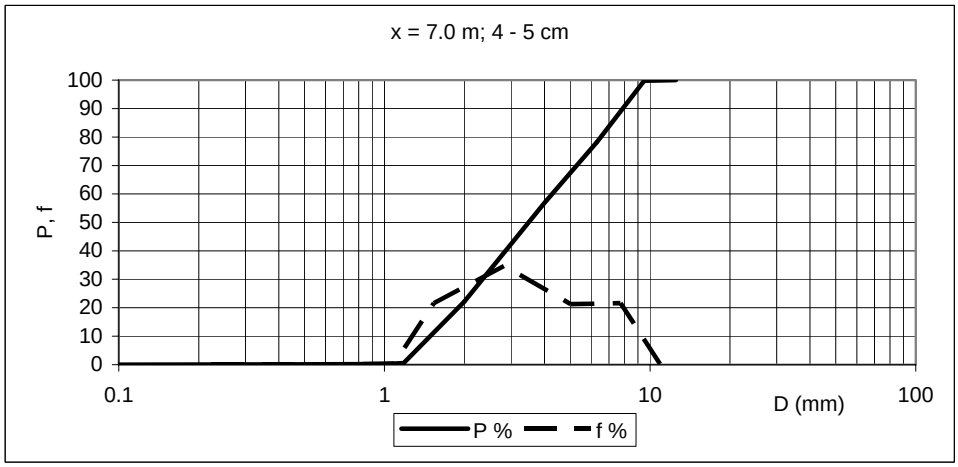
x = 7.0 m; 4 - 5 cm
P, f
100
90
80
70
60
50
40
30
20
10
0
0.1
1
10
100
D (mm)
P %
f %

x = 9.0 m

P %

D (mm)	0 -1 cm	1 - 2 cm	2 - 3 cm	3 - 4 cm	4 - 5 cm
0.1	0.00	0.00	0.00	0.00	0.00
0.5	0.03	0.07	0.07	0.07	0.06
1	0.17	0.22	0.18	0.17	0.14
1.18	0.49	0.57	0.51	0.46	0.45
2	19.71	21.70	20.58	21.24	20.16
4	54.90	57.11	55.25	58.46	55.81
6.3	75.66	78.82	78.09	81.80	78.22
9.5	99.67	100.00	100.00	100.00	100.00
12.5	100.00	100.00	100.00	100.00	100.00

f %

Di (mm)	0 -1 cm	1 - 2 cm	2 - 3 cm	3 - 4 cm	4 - 5 cm
0.22	0.03	0.07	0.07	0.07	0.06
0.71	0.14	0.15	0.11	0.09	0.08
1.09	0.32	0.35	0.33	0.30	0.30
1.54	19.22	21.13	20.06	20.78	19.71
2.83	35.19	35.41	34.67	37.22	35.65
5.02	20.77	21.72	22.84	23.34	22.41
7.74	24.00	21.18	21.91	18.20	21.78
10.90	0.33	0.00	0.00	0.00	0.00

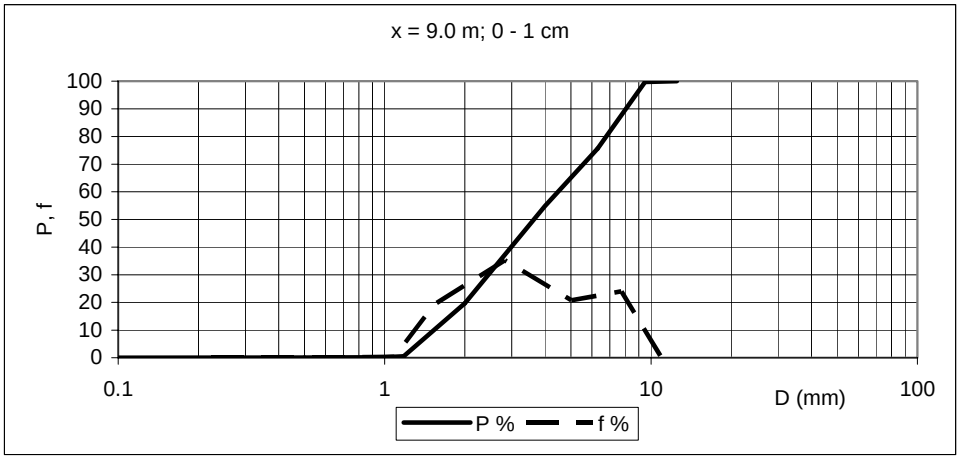

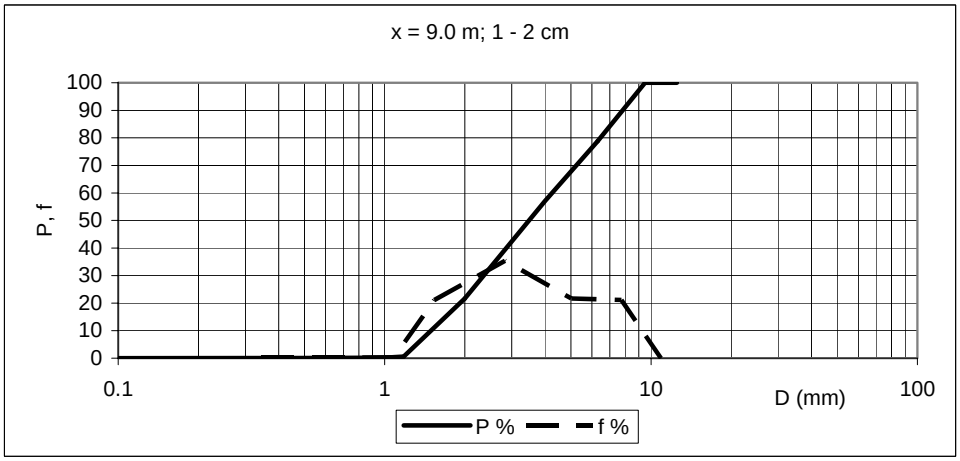

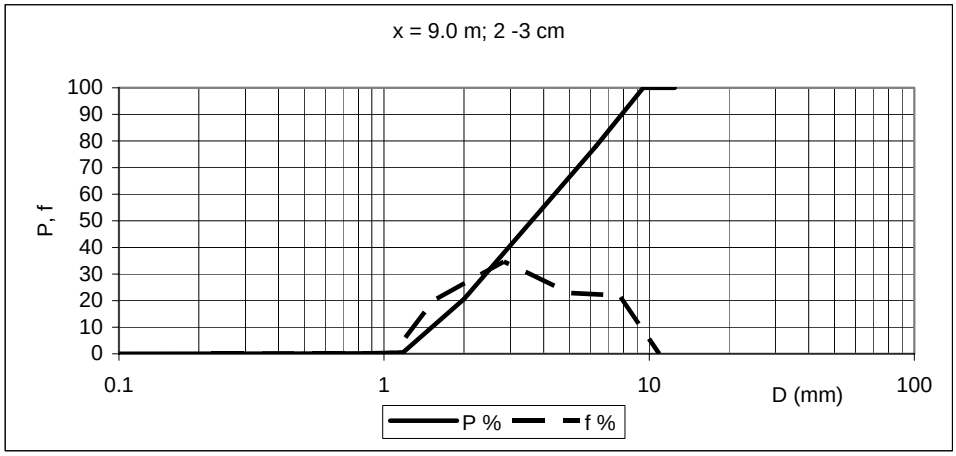
x = 9.0 m; 2 -3 cm
P, f
100
90
80
70
60
50
40
30
20
10
0
0.1
1
10
100
D (mm)
P %
f %

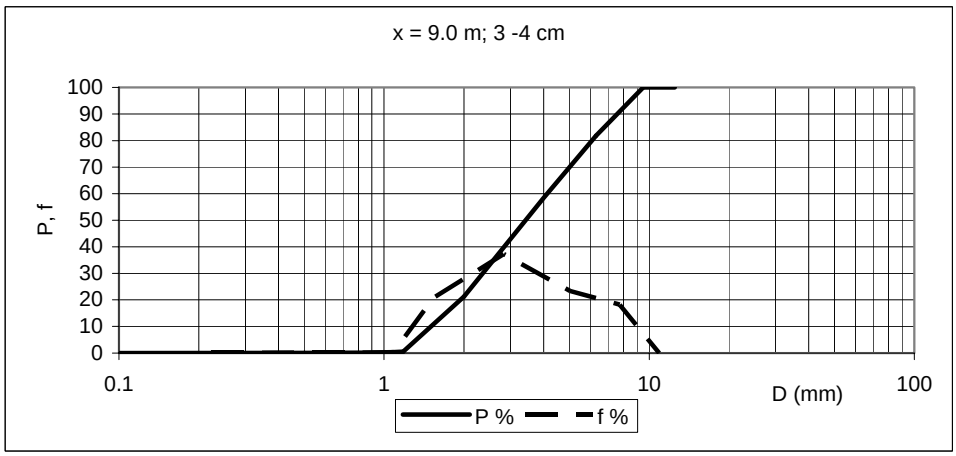
x = 9.0 m; 3 -4 cm
P, f
100
90
80
70
60
50
40
30
20
10
0
0.1
1
10
100
D (mm)
P %
f %

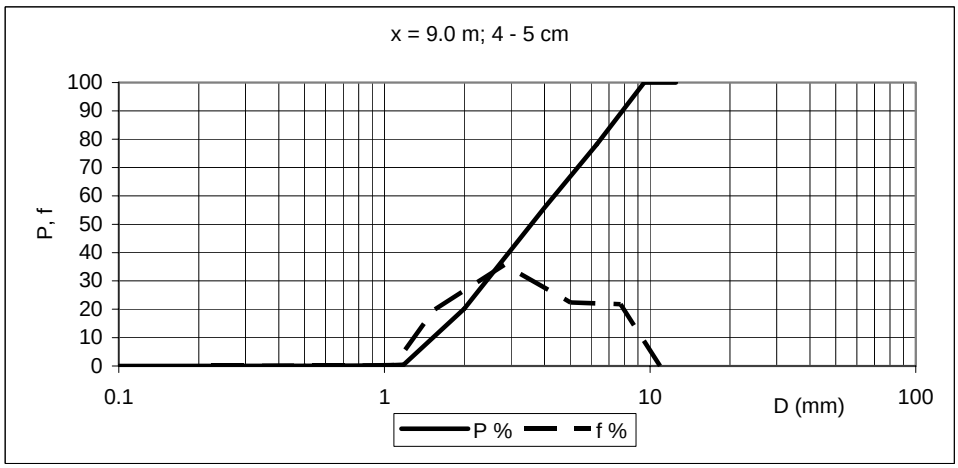
x = 9.0 m; 4 - 5 cm
P, f
100
90
80
70
60
50
40
30
20
10
0
0.1
1
10
100
D (mm)
P %
f %

12 APPENDIX 2: VALIDATION OF THE BEDLOAD RELATION

List of symbols:

D_i	Characteristic diameter of each grain size range
D_{lg}	Geometric mean diameter of the bedload
D_{l50}	Median diameter of the bedload
D_{l90}	Diameter such that the 90% of sediment of the bedload is finer;
F_i	Fraction of surface material in that range;
g	Acceleration of gravity;
G_s	Sediment transport rate in grams per minute
p	Fraction of bedload material in each grain size range
P	Function denoting the mass fraction of a sample that is finer than size D;
Q	Water discharge
q_{bi}^*	Einstein parameter for each grain size range;
q_{bi}	Bedload volume transport rate per unit width in the i-th grain size range;
q_{bT}	Total volume bedload per unit width;
R	Submerged specific gravity of sediment;
β	Coefficient in the bedload relation;
ρ	Desity of the sediment;
σ_{lg}	Geometric standars deviation of the bedload
τ_{bi}^*	Shields number for each grain size range;
τ_b	Shear stress on the bed;
τ_{ci}^*	Effective value of the Shields parameter for each grain size range;
τ_{scg}^*	Reference value for the effective Shields parameter
ξ_d	Water elevation at the downstream end of the flume

BEDLOAD DATA

RUN	Q (l/s)	G_s (g/min)	D_{lg} (mm)	σ_{lg} (mm)	D_{l50} (mm)	D_{l90} (mm)
1	30	731	3.31	1.75	3.31	7.43
2	25	491	3.78	1.71	3.88	7.93
3	20	458	3.51	1.76	3.69	7.62
4	35	1432	3.70	1.68	3.73	7.74
5	20	54	2.85	1.74	2.70	6.79
6	30	64	3.36	1.76	3.3	7.69
7	30	371	3.89	1.64	3.98	7.83
8	35	151	2.99	1.84	2.78	7.58
9	35	1068	3.66	1.75	3.74	7.93

RUN 1

Grain size distribution of the bedload at equilibrium

D (mm)	P %	Di (mm)	pi %
0.01	0.00		
0.50	0.03	0.07	0.03
1.00	0.09	0.71	0.06
1.18	0.25	1.09	0.17
2.00	23.56	1.54	23.31
4.00	59.95	2.83	36.39
6.30	83.31	5.02	23.36
9.50	100.00	7.74	16.69
12.50	100.00	10.90	0.00

RUN 2

Grain size distribution of the bedload at equilibrium

D (mm)	P %	Di (mm)	pi %
0.01	0.00		
0.50	0.02	0.07	0.02
1.00	0.05	0.71	0.04
1.18	0.14	1.09	0.08
2.00	14.00	1.54	13.86
4.00	51.67	2.83	37.67
6.30	77.27	5.02	25.60
9.50	100.00	7.74	22.73
12.50	100.00	10.90	0.00

RUN 3

Grain size distribution of the bedload at equilibrium

D (mm)	P %	Di (mm)	pi %
0.01	0.00		
0.50	0.06	0.07	0.06
1.00	0.11	0.71	0.05
1.18	0.20	1.09	0.09
2.00	20.56	1.54	20.36
4.00	53.90	2.83	33.34
6.30	81.37	5.02	27.47
9.50	100.00	7.74	18.63
12.50	100.00	10.90	0.00

RUN 4

Grain size distribution of the bedload at equilibrium

D (mm)	P %	Di (mm)	pi %
0.01	0.00		
0.50	0.04	0.07	0.04
1.00	0.08	0.71	0.03
1.18	0.13	1.09	0.06
2.00	12.92	1.54	12.79
4.00	54.20	2.83	41.28
6.30	79.90	5.02	25.69
9.50	100.00	7.74	20.10
12.50	100.00	10.90	0.00

RUN 5

Grain size distribution of the bedload

D (mm)	P %	Di (mm)	pi %
0.01	0.00		
0.50	0.02	0.07	0.02
1.00	0.17	0.71	0.15
1.18	0.70	1.09	0.53
2.00	32.81	1.54	32.11
4.00	72.48	2.83	39.67
6.30	87.73	5.02	15.25
9.50	100.00	7.74	12.27
12.50	100.00	10.90	0.00

RUN 6

Grain size distribution of the

D (mm)	P %	Di (mm)	pi %
0.01	0.00		
0.50	0.02	0.07	0.02
1.00	0.10	0.71	0.08
1.18	0.20	1.09	0.10
2.00	22.08	1.54	21.88
4.00	60.60	2.83	38.52
6.30	80.59	5.02	19.99
9.50	100.00	7.74	19.41
12.50	100.00	10.90	0.00

RUN 7

Grain size distribution of the

D (mm)	P %	Di (mm)	pi %
0.01	0.00		
0.50	0.02	0.07	0.02
1.00	0.03	0.71	0.01
1.18	0.09	1.09	0.06
2.00	9.41	1.54	9.32
4.00	50.29	2.83	40.88
6.30	78.77	5.02	28.48
9.50	100.00	7.74	21.23
12.50	100.00	10.90	0.00

RUN 8

Grain size distribution of the

D (mm)	P %	Di (mm)	pi %
0.01	0.00		
0.50	0.03	0.07	0.03
1.00	0.10	0.71	0.07
1.18	0.40	1.09	0.30
2.00	35.18	1.54	34.78
4.00	66.31	2.83	31.13
6.30	81.85	5.02	15.54
9.50	100.00	7.74	18.15
12.50	100.00	10.90	0.00

RUN 9

Grain size distribution of the bedload

D (mm)	P %	Di (mm)	pi %
0.01	0.00		
0.50	0.05	0.07	0.05
1.00	0.11	0.71	0.06
1.18	0.28	1.09	0.18
2.00	17.17	1.54	16.89
4.00	53.49	2.83	36.32
6.30	77.22	5.02	23.73
9.50	100.00	7.74	22.78
12.50	100.00	10.90	0.00

PROPOSED RELATION

RUN	Q (l/s)	G_s (g/min)	D_{lg} (mm)	σ_{lg} (mm)	D_{l50} (mm)	D_{l90} (mm)
1	30	852	3.58	1.68	3.62	7.50
2	25	846	3.25	1.73	3.20	7.30
3	20	433	3.50	1.67	3.56	7.27
4	35	1006	3.87	1.72	4.13	7.99
5	20	33	2.93	1.54	3.00	5.40
6	30	14	2.83	1.52	2.87	5.27
7	30	390	3.64	1.66	3.75	7.44
8	35	248	3.38	1.64	3.41	6.70
9	35	1090	3.71	1.7	3.83	7.80

β	0.27	τ_{sgc}^*	0.043

RUN 1

Grain size distribution of the bedload at equilibrium

D (mm)	P %	Di (mm)	pi %
0.01	0.00		
0.50	0.03	0.07	0.03
1.00	0.05	0.71	0.02
1.18	0.17	1.09	0.11
2.00	15.07	1.54	14.91
4.00	55.88	2.83	40.80
6.30	82.59	5.02	26.71
9.50	100.00	7.74	17.41
12.50	100.00	10.90	0.00

RUN 2

Grain size distribution of the bedload at equilibrium

D (mm)	P %	Di (mm)	pi %
0.01	0.00		
0.50	0.01	0.07	0.01
1.00	0.09	0.71	0.08
1.18	0.37	1.09	0.29
2.00	22.69	1.54	22.32
4.00	62.86	2.83	40.16
6.30	84.43	5.02	21.58
9.50	99.99	7.74	15.56
12.50	100.00	10.90	0.01

RUN 3

Grain size distribution of the bedload at equilibrium

D (mm)	P %	Di (mm)	pi %
0.01	0.00		
0.50	0.01	0.07	0.01
1.00	0.02	0.71	0.02
1.18	0.16	1.09	0.14
2.00	16.36	1.54	16.20
4.00	56.82	2.83	40.46
6.30	84.63	5.02	27.81
9.50	100.00	7.74	15.37
12.50	100.00	10.90	0.00

RUN 4

Grain size distribution of the bedload at equilibrium

D (mm)	P %	Di (mm)	pi %
0.01	0.00		
0.50	0.01	0.07	0.01
1.00	0.12	0.71	0.11
1.18	0.48	1.09	0.36
2.00	14.11	1.54	13.63
4.00	48.00	2.83	33.89
6.30	76.22	5.02	28.22
9.50	100.00	7.74	23.78
12.50	100.00	10.90	0.00

RUN 5

Grain size distribution of the bedload

D (mm)	P %	Di (mm)	pi %
0.01	0.00		
0.50	0.05	0.07	0.05
1.00	0.30	0.71	0.25
1.18	0.59	1.09	0.29
2.00	21.23	1.54	20.63
4.00	70.42	2.83	49.19
6.30	100.00	5.02	29.58
9.50	100.00	7.74	0.00
12.50	100.00	10.90	0.00

RUN 6

Grain size distribution of the

D (mm)	P %	Di (mm)	pi %
0.01	0.00		
0.50	0.02	0.07	0.02
1.00	0.17	0.71	0.15
1.18	0.62	1.09	0.45
2.00	22.89	1.54	22.27
4.00	74.65	2.83	51.76
6.30	100.00	5.02	25.35
9.50	100.00	7.74	0.00
12.50	100.00	10.90	0.00

RUN 7

Grain size distribution of the

D (mm)	P %	Di (mm)	pi %
0.01	0.00		
0.50	0.02	0.07	0.02
1.00	0.05	0.71	0.03
1.18	0.17	1.09	0.12
2.00	13.80	1.54	13.63
4.00	53.66	2.83	39.86
6.30	83.16	5.02	29.51
9.50	100.00	7.74	16.84
12.50	100.00	10.90	0.00

RUN 8

Grain size distribution of the

D (mm)	P %	Di (mm)	pi %
0.01	0.00		
0.50	0.03	0.07	0.03
1.00	0.06	0.71	0.04
1.18	0.22	1.09	0.16
2.00	16.62	1.54	16.39
4.00	59.98	2.83	43.36
6.30	88.22	5.02	28.25
9.50	100.00	7.74	11.78
12.50	100.00	10.90	0.00

RUN 9

Grain size distribution of the bedload

D (mm)	P %	Di (mm)	pi %
0.01	0.00		
0.50	0.01	0.07	0.01
1.00	0.04	0.71	0.04
1.18	0.26	1.09	0.21
2.00	14.99	1.54	14.74
4.00	52.28	2.83	37.29
6.30	79.21	5.02	26.93
9.50	100.00	7.74	20.79
12.50	100.00	10.90	0.00

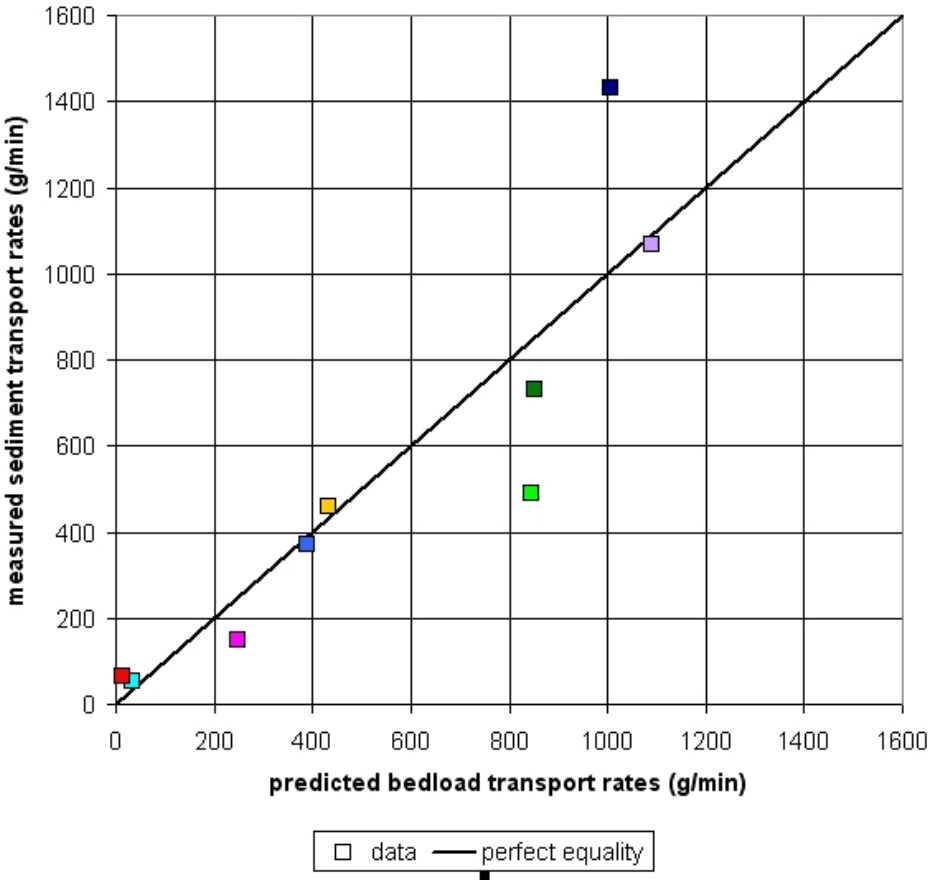
measured sediment transport rates (g/min)
predicted bedload transport rates (g/min)
0
200
400
600
800
1000
1200
1400
1600
data
perfect equality

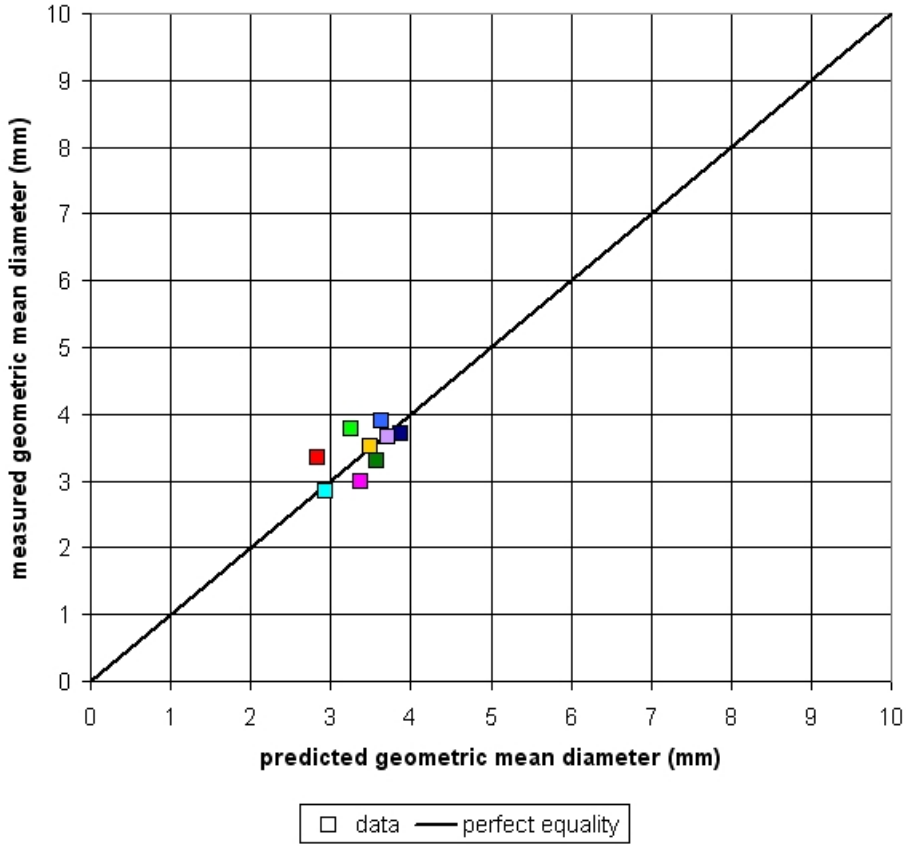
measured geometric mean diameter (mm)
predicted geometric mean diameter (mm)
0
1
2
3
4
5
6
7
8
9
10
data
perfect equality

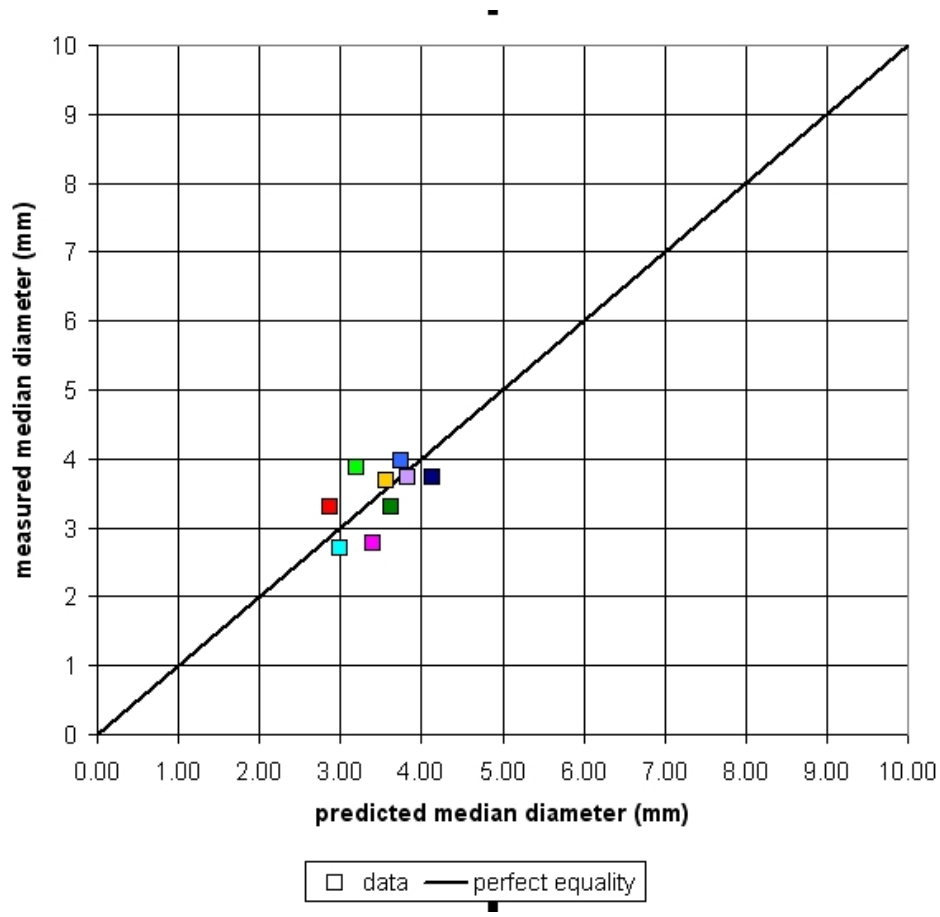
measured median diameter (mm)
predicted median diameter (mm)
0
1
2
3
4
5
6
7
8
9
10
0.00
1.00
2.00
3.00
4.00
5.00
6.00
7.00
8.00
9.00
10.00
data
perfect equality

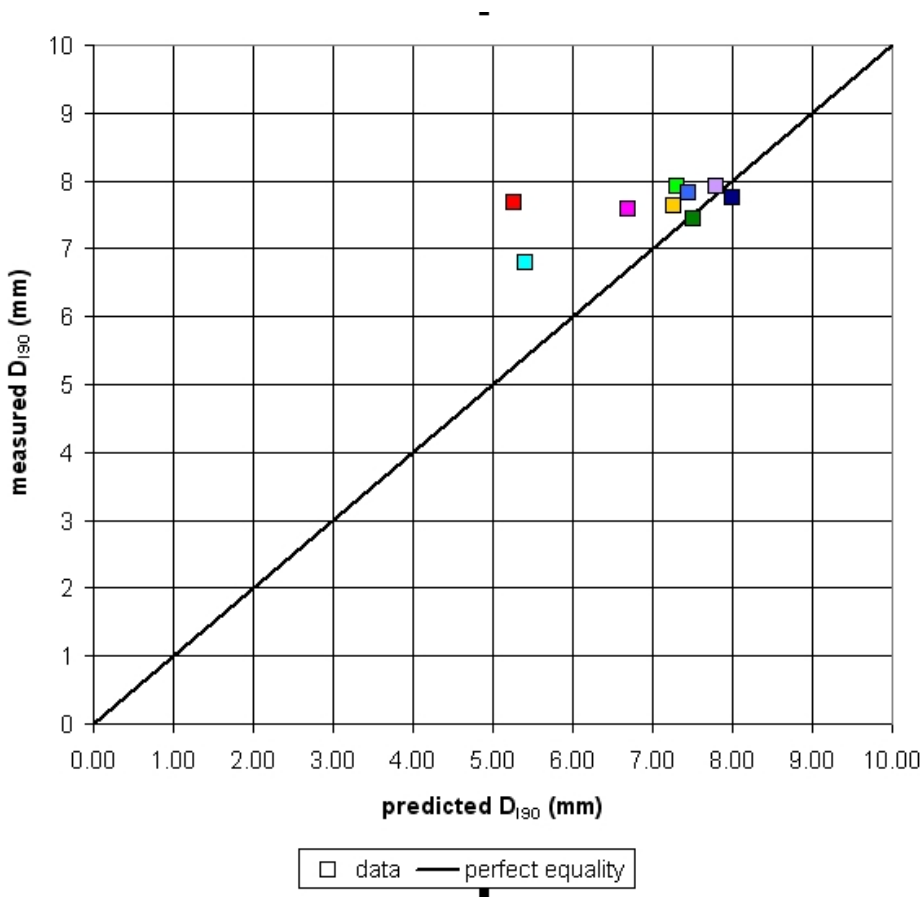
measured D90 (mm)
predicted D90 (mm)
0
1
2
3
4
5
6
7
8
9
10
0.00
1.00
2.00
3.00
4.00
5.00
6.00
7.00
8.00
9.00
10.00
data
perfect equality

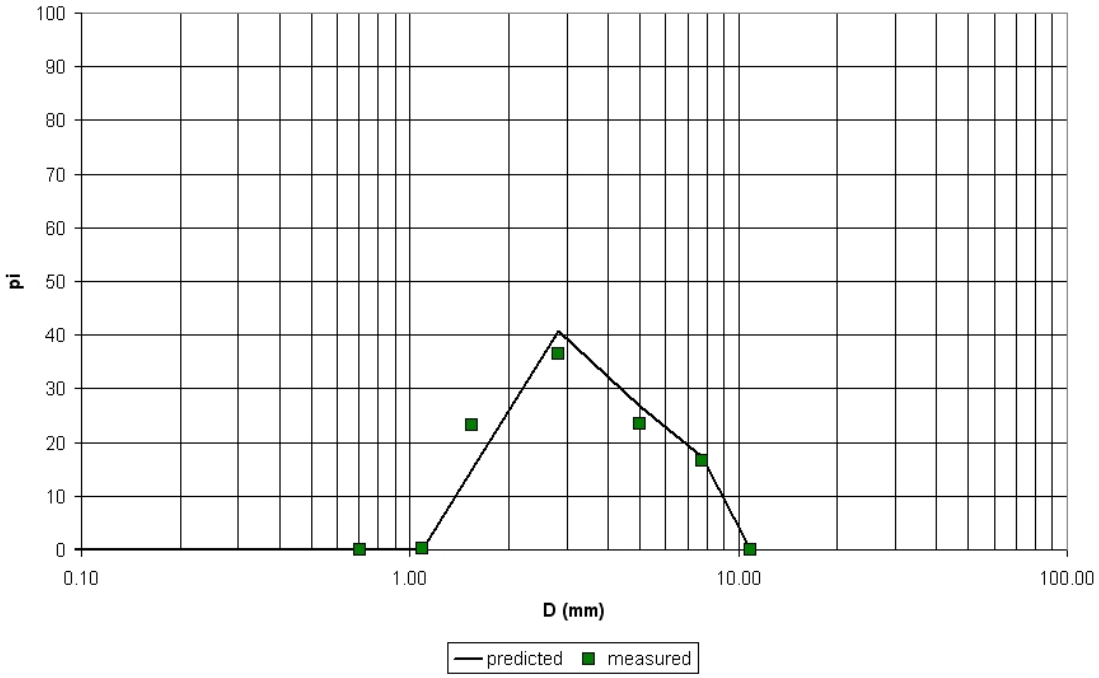
100
90
80
70
60
50
40
30
20
10
0
pi
0.10
1.00
10.00
100.00
D (mm)
predicted
measured

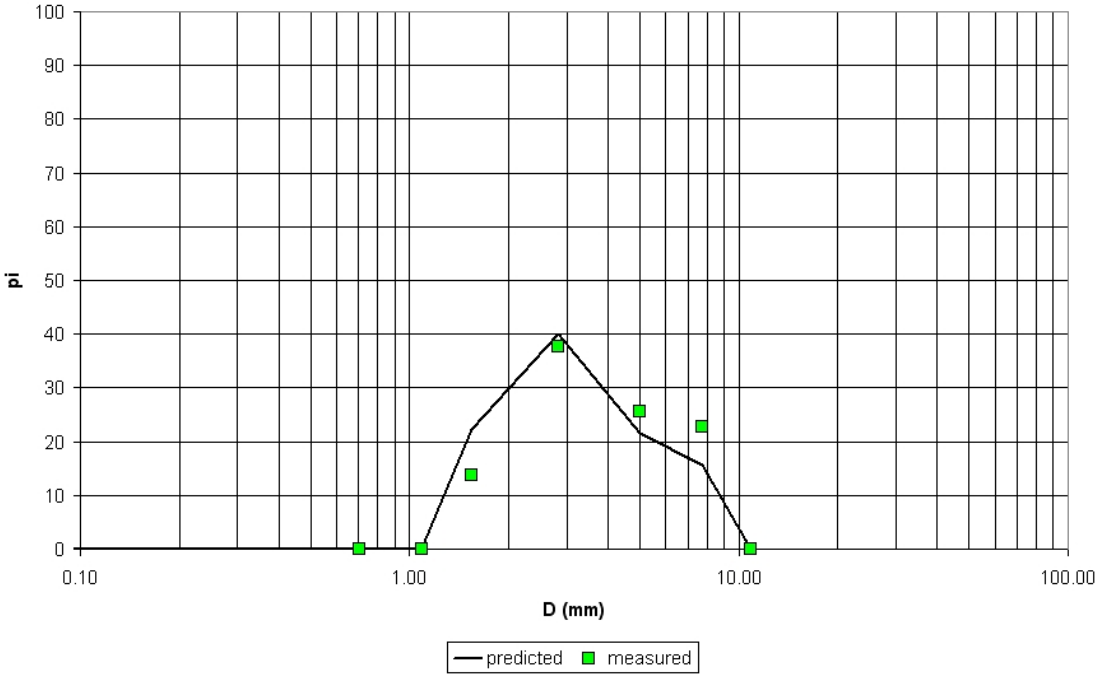
100
90
80
70
60
50
40
30
20
10
0
pi
0.10
1.00
10.00
100.00
D (mm)
predicted
measured

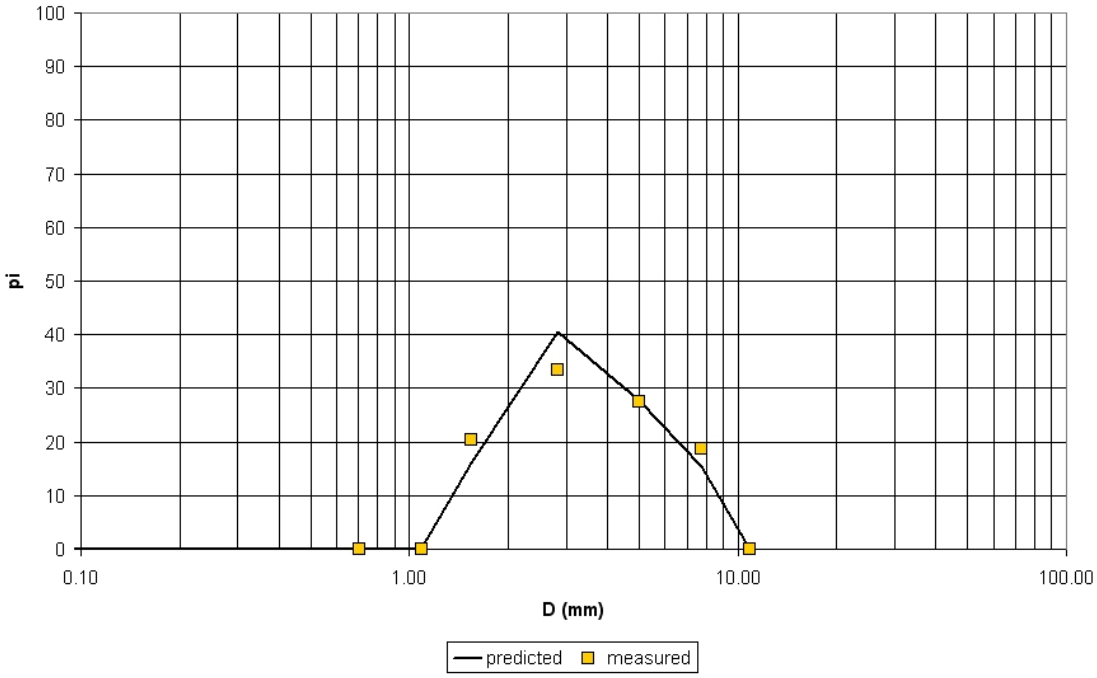
100
90
80
70
60
50
40
30
20
10
0
pi
0.10
1.00
10.00
100.00
D (mm)
predicted
measured

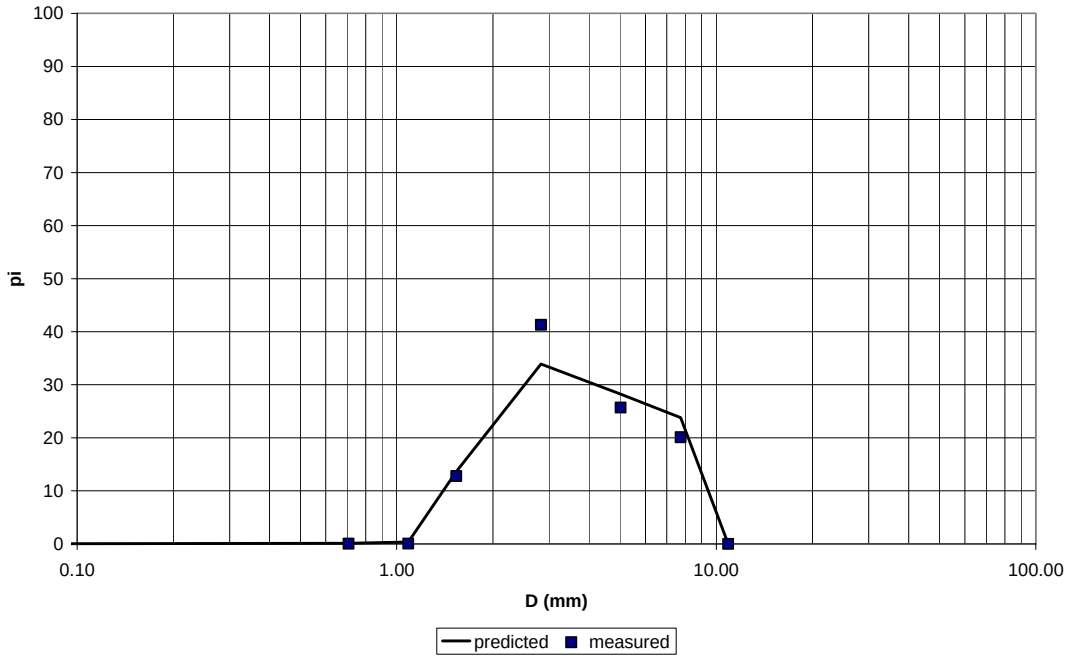
100
90
80
70
60
50
40
30
20
10
0
pi
0.10
1.00
10.00
100.00
D (mm)
predicted
measured

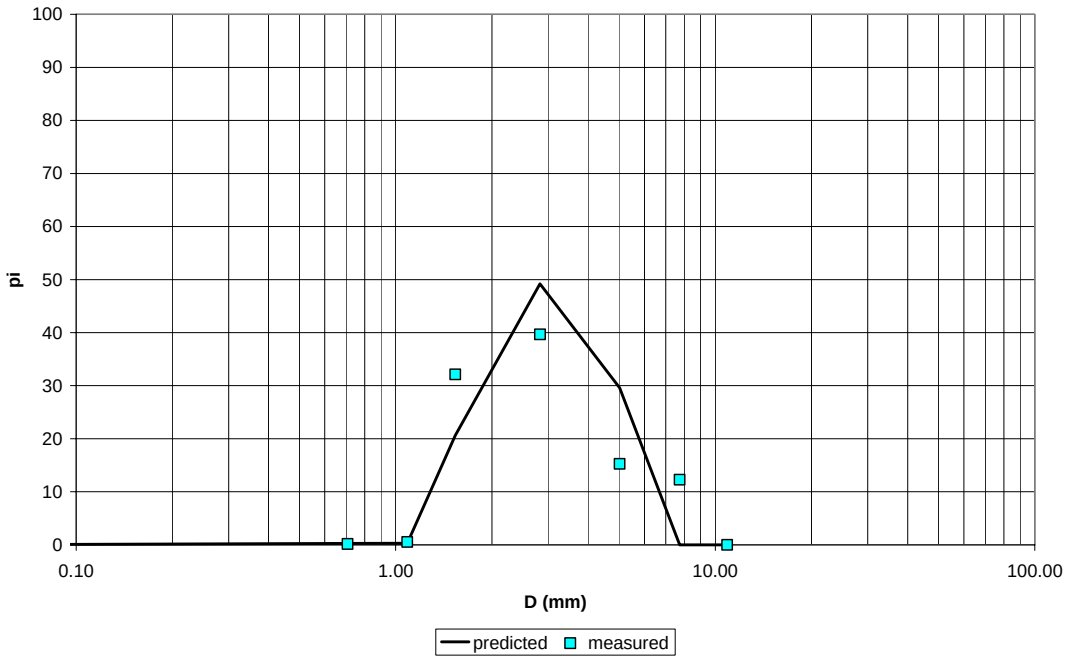
100
90
80
70
60
50
40
30
20
10
0
pi
0.10
1.00
10.00
100.00
D (mm)
predicted
measured

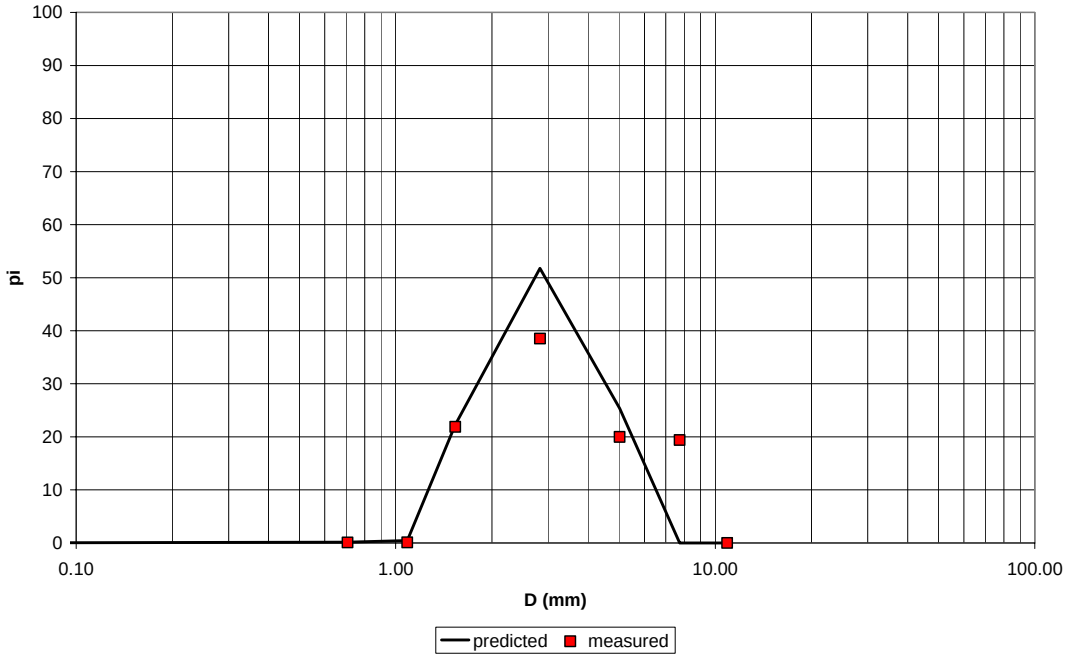
100
90
80
70
60
50
40
30
20
10
0
pi
0.10
1.00
10.00
100.00
D (mm)
predicted
measured

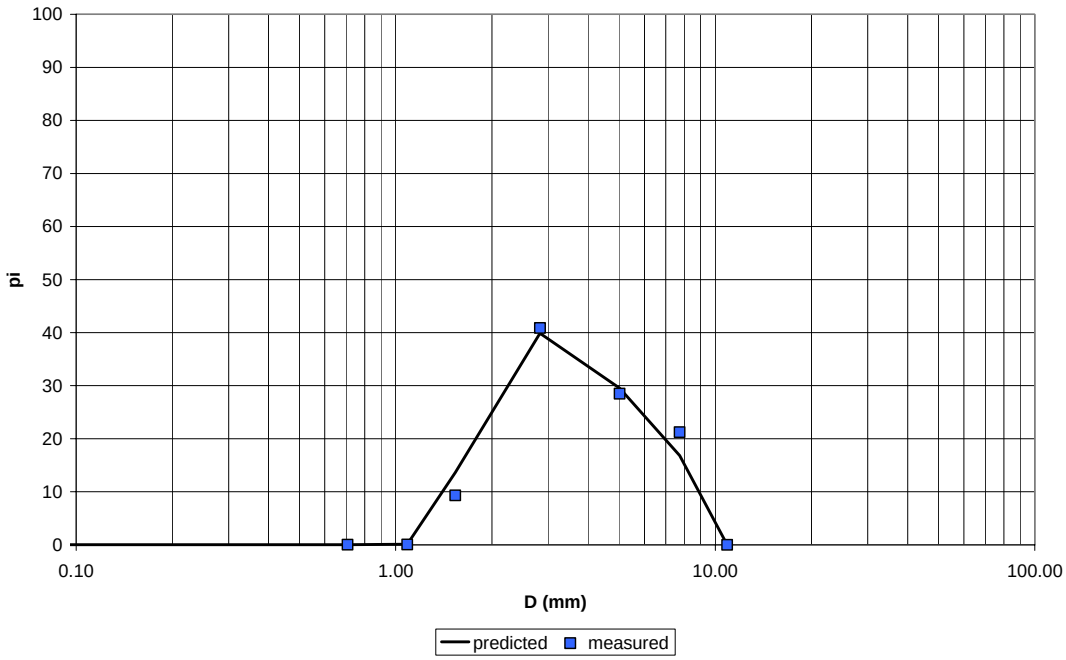
100
90
80
70
60
50
40
30
20
10
0
pi
0.10
1.00
10.00
100.00
D (mm)
predicted
measured

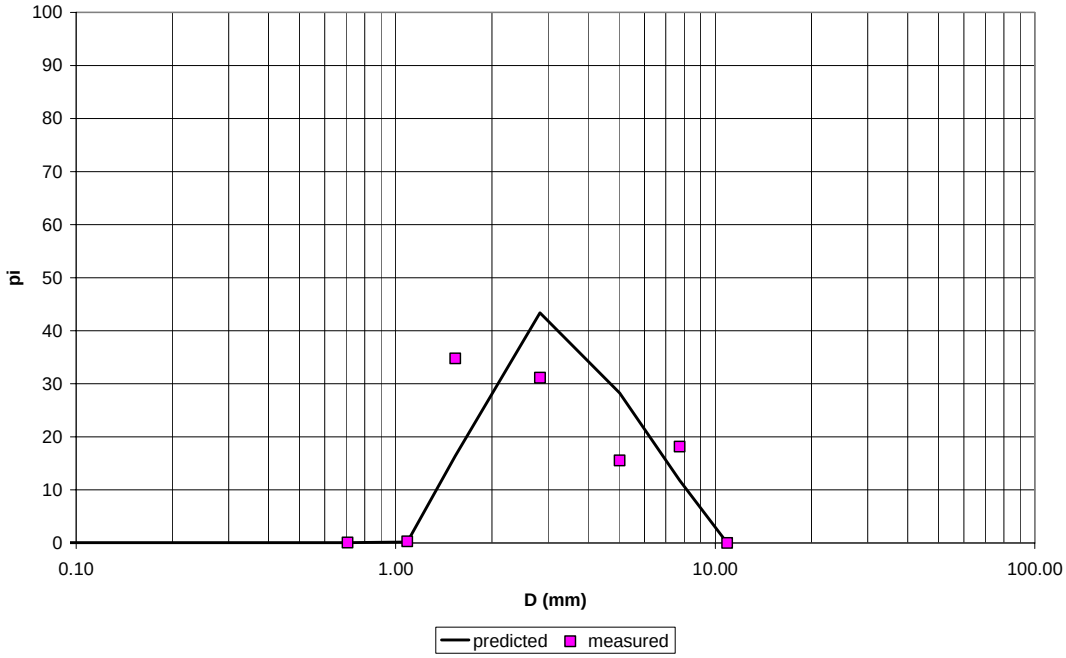
100
90
80
70
60
50
40
30
20
10
0
pi
0.10
1.00
10.00
100.00
D (mm)
predicted
measured

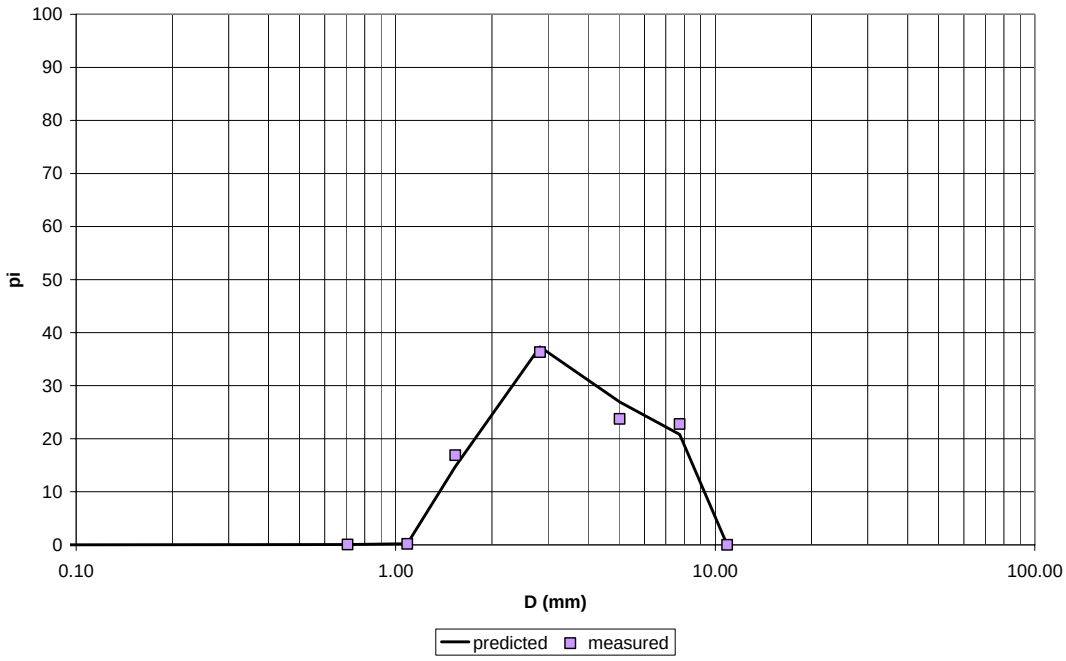
100
90
80
70
60
50
40
30
20
10
0
pi
0.10
1.00
10.00
100.00
D (mm)
predicted
measured

PRELIMINARY VERSIONS OF THE BEDLOAD RELATION

RUN	Q (l/s)	G_s (g/min)	D_{lg} (mm)	σ_{lg} (mm)	D_{l50} (mm)	D_{l90} (mm)
1	30	882	3.00	1.61	2.97	5.93
2	25	901	2.71	1.62	2.63	5.60
3	20	403	2.73	1.53	2.73	5.18
4	35	1039	3.24	1.68	3.22	6.81
5	20	26	2.21	1.38	2.27	3.57
6	30	10	2.15	1.37	2.15	3.53
7	30	349	2.80	1.52	2.81	5.21
8	35	220	2.58	1.47	2.61	4.55
9	35	1160	3.16	1.65	3.11	6.49

Hiding/exposure function of Ashida and Michiue

β	0.4	τ_{sgc}^*	0.05

RUN 1

Grain size distribution of the bedload at equilibrium

D (mm)	P %	Di (mm)	pi %
0.01	0.00		
0.50	0.00	0.07	0.00
1.00	7.15	0.71	7.15
1.18	28.51	1.09	21.36
2.00	78.41	1.54	49.90
4.00	99.77	2.83	21.36
6.30	99.93	5.02	0.16
9.50	99.95	7.74	0.03
12.50	100.00	10.90	0.05

RUN 2

Grain size distribution of the bedload at equilibrium

D (mm)	P %	Di (mm)	pi %
0.01	0.00		
0.50	0.00	0.07	0.00
1.00	5.72	0.71	5.72
1.18	22.26	1.09	16.54
2.00	68.27	1.54	46.01
4.00	99.49	2.83	31.23
6.30	99.88	5.02	0.39
9.50	99.99	7.74	0.10
12.50	100.00	10.90	0.01

RUN 3

Grain size distribution of the bedload at equilibrium

D (mm)	P %	Di (mm)	pi %
0.01	0.00		
0.50	0.00	0.07	0.00
1.00	1.89	0.71	1.89
1.18	20.64	1.09	18.76
2.00	73.93	1.54	53.28
4.00	99.76	2.83	25.83
6.30	99.97	5.02	0.21
9.50	99.99	7.74	0.02
12.50	100.00	10.90	0.01

RUN 4

Grain size distribution of the bedload at equilibrium

D (mm)	P %	Di (mm)	pi %
0.01	0.00		
0.50	0.00	0.07	0.00
1.00	12.33	0.71	12.33
1.18	36.42	1.09	24.08
2.00	79.82	1.54	43.41
4.00	99.33	2.83	19.51
6.30	99.83	5.02	0.50
9.50	99.99	7.74	0.15
12.50	100.00	10.90	0.01

RUN 5

Grain size distribution of the bedload

D (mm)	P %	Di (mm)	pi %
0.01	0.00		
0.50	0.00	0.07	0.00
1.00	0.00	0.71	0.00
1.18	0.00	1.09	0.00
2.00	60.98	1.54	60.98
4.00	99.04	2.83	38.06
6.30	99.54	5.02	0.50
9.50	99.94	7.74	0.40
12.50	100.00	10.90	0.06

RUN 6

Grain size distribution of the

D (mm)	P %	Di (mm)	pi %
0.01	0.00		
0.50	0.00	0.07	0.00
1.00	0.00	0.71	0.00
1.18	0.00	1.09	0.00
2.00	55.62	1.54	55.62
4.00	98.97	2.83	43.34
6.30	99.75	5.02	0.78
9.50	99.97	7.74	0.23
12.50	100.00	10.90	0.03

RUN 7

Grain size distribution of the

D (mm)	P %	Di (mm)	pi %
0.01	0.00		
0.50	0.00	0.07	0.00
1.00	1.70	0.71	1.70
1.18	21.57	1.09	19.87
2.00	77.22	1.54	55.65
4.00	99.73	2.83	22.51
6.30	99.93	5.02	0.20
9.50	99.97	7.74	0.04
12.50	100.00	10.90	0.03

RUN 8

Grain size distribution of the

D (mm)	P %	Di (mm)	pi %
0.01	0.00		
0.50	0.00	0.07	0.00
1.00	0.00	0.71	0.00
1.18	13.92	1.09	13.92
2.00	72.27	1.54	58.35
4.00	99.65	2.83	27.38
6.30	99.90	5.02	0.26
9.50	99.96	7.74	0.06
12.50	100.00	10.90	0.04

RUN 9

Grain size distribution of the bedload

D (mm)	P %	Di (mm)	pi %
0.01	0.00		
0.50	0.00	0.07	0.00
1.00	10.78	0.71	10.78
1.18	33.51	1.09	22.73
2.00	79.12	1.54	45.61
4.00	99.65	2.83	20.54
6.30	99.94	5.02	0.29
9.50	99.99	7.74	0.05
12.50	100.00	10.90	0.01

RUN	Q (l/s)	G_s (g/min)	D_{lg} (mm)	σ_{lg} (mm)	D_{l50} (mm)	D_{l90} (mm)
1	30	871	3.28	1.67	3.24	6.89
2	25	863	2.96	1.69	2.88	6.53
3	20	476	3.13	1.64	3.09	6.28
4	35	1018	3.54	1.72	3.59	7.62
5	20	71	2.57	1.48	2.60	4.54
6	30	44	2.48	1.43	2.52	3.95
7	30	435	3.24	1.64	3.21	6.50
8	35	300	2.98	1.60	2.95	5.81
9	35	1095	3.41	1.70	3.40	7.37

Hiding/exposure function of Ashida and Michiue

β	0.24	τ_{sgc}^*	0.043

RUN 1

Grain size distribution of the bedload at equilibrium

D (mm)	P %	Di (mm)	pi %
0.01	0.00		
0.50	0.00	0.07	0.00
1.00	12.81	0.71	12.81
1.18	36.31	1.09	23.50
2.00	81.42	1.54	45.11
4.00	99.80	2.83	18.38
6.30	99.94	5.02	0.14
9.50	99.96	7.74	0.02
12.50	100.00	10.90	0.04

RUN 2

Grain size distribution of the bedload at equilibrium

D (mm)	P %	Di (mm)	pi %
0.01	0.00		
0.50	0.00	0.07	0.00
1.00	10.95	0.71	10.94
1.18	29.75	1.09	18.80
2.00	72.32	1.54	42.57
4.00	99.56	2.83	27.24
6.30	99.90	5.02	0.34
9.50	99.99	7.74	0.09
12.50	100.00	10.90	0.01

RUN 3

Grain size distribution of the bedload at equilibrium

D (mm)	P %	Di (mm)	pi %
0.01	0.00		
0.50	0.00	0.07	0.00
1.00	9.80	0.71	9.80
1.18	32.84	1.09	23.03
2.00	78.99	1.54	46.15
4.00	99.81	2.83	20.82
6.30	99.97	5.02	0.17
9.50	99.99	7.74	0.02
12.50	100.00	10.90	0.01

RUN 4

Grain size distribution of the bedload at equilibrium

D (mm)	P %	Di (mm)	pi %
0.01	0.00		
0.50	0.00	0.07	0.00
1.00	18.67	0.71	18.67
1.18	43.92	1.09	25.26
2.00	82.64	1.54	38.72
4.00	99.43	2.83	16.78
6.30	99.86	5.02	0.43
9.50	99.99	7.74	0.13
12.50	100.00	10.90	0.01

RUN 5

Grain size distribution of the bedload

D (mm)	P %	Di (mm)	pi %
0.01	0.00		
0.50	0.00	0.07	0.00
1.00	0.00	0.71	0.00
1.18	13.86	1.09	13.86
2.00	72.14	1.54	58.28
4.00	99.32	2.83	27.18
6.30	99.67	5.02	0.36
9.50	99.95	7.74	0.28
12.50	100.00	10.90	0.05

RUN 6

Grain size distribution of the

D (mm)	P %	Di (mm)	pi %
0.01	0.00		
0.50	0.00	0.07	0.00
1.00	0.00	0.71	0.00
1.18	8.89	1.09	8.89
2.00	70.52	1.54	61.63
4.00	99.31	2.83	28.79
6.30	99.83	5.02	0.52
9.50	99.98	7.74	0.15
12.50	100.00	10.90	0.02

RUN 7

Grain size distribution of the

D (mm)	P %	Di (mm)	pi %
0.01	0.00		
0.50	0.00	0.07	0.00
1.00	10.83	0.71	10.83
1.18	35.08	1.09	24.25
2.00	82.05	1.54	46.97
4.00	99.79	2.83	17.74
6.30	99.94	5.02	0.16
9.50	99.97	7.74	0.03
12.50	100.00	10.90	0.03

RUN 8

Grain size distribution of the

D (mm)	P %	Di (mm)	pi %
0.01	0.00		
0.50	0.00	0.07	0.00
1.00	6.20	0.71	6.20
1.18	27.75	1.09	21.55
2.00	78.21	1.54	50.47
4.00	99.72	2.83	21.51
6.30	99.92	5.02	0.20
9.50	99.97	7.74	0.04
12.50	100.00	10.90	0.03

RUN 9

Grain size distribution of the bedload

D (mm)	P %	Di (mm)	pi %
0.01	0.00		
0.50	0.00	0.07	0.00
1.00	16.15	0.71	16.15
1.18	40.30	1.09	24.15
2.00	81.75	1.54	41.45
4.00	99.69	2.83	17.94
6.30	99.95	5.02	0.25
9.50	99.99	7.74	0.04
12.50	100.00	10.90	0.01

RUN	Q (l/s)	G_s (g/min)	D_{lg} (mm)	σ_{lg} (mm)	D_{l50} (mm)	D_{l90} (mm)
1	30	861	3.38	1.65	3.39	6.87
2	25	881	3.06	1.68	3.00	6.55
3	20	332	3.15	1.60	3.17	5.96
4	35	1036	3.67	1.70	3.86	7.64
5	20	0.27	1.67	1.70	1.67	3.09
6	30	0.00	0.07	1.00	0.07	0.34
7	30	275	3.25	1.59	3.30	5.98
8	35	138	2.92	1.53	2.96	5.37
9	35	1173	3.54	1.68	3.60	7.42

Proposed hiding/exposure function

β	**0.48**	τ_{sgc}^*	**0.05**

RUN 1

Grain size distribution of the bedload at equilibrium

D (mm)	P %	Di (mm)	pi %
0.01	0.00		
0.50	0.00	0.07	0.00
1.00	12.65	0.71	12.65
1.18	39.47	1.09	26.82
2.00	83.52	1.54	44.05
4.00	99.81	2.83	16.29
6.30	99.94	5.02	0.12
9.50	99.96	7.74	0.02
12.50	100.00	10.90	0.04

RUN 2

Grain size distribution of the bedload at equilibrium

D (mm)	P %	Di (mm)	pi %
0.01	0.00		
0.50	0.00	0.07	0.00
1.00	11.05	0.71	11.04
1.18	32.12	1.09	21.08
2.00	75.31	1.54	43.19
4.00	99.59	2.83	24.28
6.30	99.90	5.02	0.31
9.50	99.99	7.74	0.09
12.50	100.00	10.90	0.01

RUN 3

Grain size distribution of the bedload at equilibrium

D (mm)	P %	Di (mm)	pi %
0.01	0.00		
0.50	0.00	0.07	0.00
1.00	6.63	0.71	6.63
1.18	34.57	1.09	27.94
2.00	80.83	1.54	46.25
4.00	99.81	2.83	18.99
6.30	99.97	5.02	0.16
9.50	99.99	7.74	0.02
12.50	100.00	10.90	0.01

RUN 4

Grain size distribution of the bedload at equilibrium

D (mm)	P %	Di (mm)	pi %
0.01	0.00		
0.50	0.00	0.07	0.00
1.00	18.89	0.71	18.89
1.18	48.13	1.09	29.23
2.00	84.62	1.54	36.50
4.00	99.47	2.83	14.85
6.30	99.86	5.02	0.39
9.50	99.99	7.74	0.12
12.50	100.00	10.90	0.01

RUN 5

Grain size distribution of the bedload

D (mm)	P %	Di (mm)	pi %
0.01	0.00		
0.50	0.00	0.07	0.00
1.00	0.00	0.71	0.00
1.18	0.00	1.09	0.00
2.00	26.91	1.54	26.91
4.00	94.34	2.83	67.43
6.30	95.95	5.02	1.61
9.50	98.18	7.74	2.22
12.50	100.00	10.90	1.82

RUN 6

Grain size distribution of the

D (mm)	P %	Di (mm)	pi %
0.01	0.00		
0.50	0.00	0.07	0.00
1.00	0.00	0.71	0.00
1.18	0.00	1.09	0.00
2.00	0.00	1.54	0.00
4.00	0.00	2.83	0.00
6.30	0.00	5.02	0.00
9.50	0.00	7.74	0.00
12.50	100.00	10.90	100.00

RUN 7

Grain size distribution of the

D (mm)	P %	Di (mm)	pi %
0.01	0.00		
0.50	0.00	0.07	0.00
1.00	6.47	0.71	6.47
1.18	37.12	1.09	30.66
2.00	83.48	1.54	46.35
4.00	99.79	2.83	16.31
6.30	99.93	5.02	0.15
9.50	99.97	7.74	0.03
12.50	100.00	10.90	0.03

RUN 8

Grain size distribution of the

D (mm)	P %	Di (mm)	pi %
0.01	0.00		
0.50	0.00	0.07	0.00
1.00	0.47	0.71	0.47
1.18	27.64	1.09	27.18
2.00	79.28	1.54	51.63
4.00	99.70	2.83	20.42
6.30	99.91	5.02	0.20
9.50	99.95	7.74	0.05
12.50	100.00	10.90	0.05

RUN 9

Grain size distribution of the bedload

D (mm)	P %	Di (mm)	pi %
0.01	0.00		
0.50	0.00	0.07	0.00
1.00	16.62	0.71	16.62
1.18	43.99	1.09	27.37
2.00	83.82	1.54	39.82
4.00	99.72	2.83	15.90
6.30	99.95	5.02	0.23
9.50	99.99	7.74	0.04
12.50	100.00	10.90	0.01

13 APPENDIX 3: VALIDATION OF THE PROCEDURE TO STORE AND ACCESS THE STRATIGRAPHY OF NON - COHESIVE DEPOSITS WITH LABORATORY DATA

VALIDATION OF THE ORIGINAL PROCEDURE

Longitudinal profile

RUN 1								RUN 2								RUN 3				
Computed			Data					Computed			Data					Computed			Data	
x (m)	η (m)	η (mm)	x (m)	η (mm)				x (m)	η (m)	η (mm)	x (m)	η (mm)				x (m)	η (m)	η (mm)	x (m)	η (mm)
0.000	0.221	221	2.5	205				0.000	0.224	224	2.5	206				0.000	0.232	232	2.5	208
0.100	0.221	221	2.9	201				0.100	0.223	223	2.9	203				0.100	0.231	231	2.9	204
0.200	0.220	220	3.3	202				0.200	0.222	222	3.3	200				0.200	0.230	230	3.3	196
0.300	0.220	220	3.7	202				0.300	0.222	222	3.7	196				0.300	0.229	229	3.7	195
0.400	0.219	219	4.1	197				0.400	0.221	221	4.1	199				0.400	0.229	229	4.1	195
0.500	0.218	218	4.3	196				0.500	0.220	220	4.3	195				0.500	0.228	228	4.3	194
0.600	0.218	218	4.5	196				0.600	0.220	220	4.5	194				0.600	0.227	227	4.5	194
0.700	0.217	217	4.9	194				0.700	0.219	219	4.9	192				0.700	0.226	226	4.9	190
0.800	0.216	216	5.3	188				0.800	0.218	218	5.3	188				0.800	0.225	225	5.3	188
0.900	0.216	216	5.7	188				0.900	0.218	218	5.7	186				0.900	0.225	225	5.7	185
1.000	0.215	215	6.1	182				1.000	0.217	217	6.1	184				1.000	0.224	224	6.1	182
1.100	0.215	215	6.5	180				1.100	0.216	216	6.5	179				1.100	0.223	223	6.5	178
1.200	0.214	214	6.9	178				1.200	0.216	216	6.9	178				1.200	0.222	222	6.9	177
1.300	0.213	213	7.3	175				1.300	0.215	215	7.3	176				1.300	0.221	221	7.3	173
1.400	0.213	213	7.7	172				1.400	0.214	214	7.7	173				1.400	0.221	221	7.7	171
1.500	0.212	212	8.1	169				1.500	0.214	214	8.1	167				1.500	0.220	220	8.1	165
1.600	0.211	211	8.5	169				1.600	0.213	213	8.5	165				1.600	0.219	219	8.5	162
1.700	0.211	211	8.9	166				1.700	0.212	212	8.9	161				1.700	0.218	218	8.9	158
1.800	0.210	210	9.3	161				1.800	0.212	212	9.3	157				1.800	0.217	217	9.3	155
1.900	0.210	210	9.7	160				1.900	0.211	211	9.7	155				1.900	0.217	217	9.7	152
2.000	0.209	209	10.1	158				2.000	0.210	210	10.1	152				2.000	0.216	216	10.1	148
2.100	0.208	208	10.5	153				2.100	0.210	210	10.5	150				2.100	0.215	215	10.5	145
2.200	0.208	208						2.200	0.209	209						2.200	0.214	214		
2.300	0.207	207						2.300	0.208	208						2.300	0.213	213		
2.400	0.206	206						2.400	0.208	208						2.400	0.213	213		
2.500	0.206	206						2.500	0.207	207						2.500	0.212	212		
2.600	0.205	205						2.600	0.206	206						2.600	0.211	211		
2.700	0.205	205						2.700	0.206	206						2.700	0.210	210		
2.800	0.204	204						2.800	0.205	205						2.800	0.210	210		
2.900	0.203	203						2.900	0.204	204						2.900	0.209	209		
3.000	0.203	203						3.000	0.204	204						3.000	0.208	208		
3.100	0.202	202						3.100	0.203	203						3.100	0.207	207		
3.200	0.202	202						3.200	0.202	202						3.200	0.206	206		
3.300	0.201	201						3.300	0.202	202						3.300	0.206	206		
3.400	0.200	200						3.400	0.201	201						3.400	0.205	205		
3.500	0.200	200						3.500	0.200	200						3.500	0.204	204		
3.600	0.199	199						3.600	0.200	200						3.600	0.203	203		
3.700	0.198	198						3.700	0.199	199						3.700	0.202	202		
3.800	0.198	198						3.800	0.198	198						3.800	0.202	202		
3.900	0.197	197						3.900	0.198	198						3.900	0.201	201		
4.000	0.197	197						4.000	0.197	197						4.000	0.200	200		
4.100	0.196	196						4.100	0.196	196						4.100	0.199	199		
4.200	0.195	195						4.200	0.196	196						4.200	0.198	198		
4.300	0.195	195						4.300	0.195	195						4.300	0.198	198		
4.400	0.194	194						4.400	0.194	194						4.400	0.197	197		
4.500	0.194	194						4.500	0.194	194						4.500	0.196	196		
4.600	0.193	193						4.600	0.193	193						4.600	0.195	195		
4.700	0.192	192						4.700	0.192	192						4.700	0.194	194		
4.800	0.192	192						4.800	0.192	192						4.800	0.194	194		
4.900	0.191	191						4.900	0.191	191						4.900	0.193	193		
5.000	0.191	191						5.000	0.190	190						5.000	0.192	192		
5.100	0.190	190						5.100	0.190	190						5.100	0.191	191		
5.200	0.189	189						5.200	0.189	189						5.200	0.190	190		
5.300	0.189	189						5.300	0.188	188						5.300	0.190	190		
5.400	0.188	188						5.400	0.188	188						5.400	0.189	189		
5.500	0.188	188						5.500	0.187	187						5.500	0.188	188		
5.600	0.187	187						5.600	0.187	187						5.600	0.187	187		
5.700	0.186	186						5.700	0.186	186						5.700	0.186	186		
5.800	0.186	186						5.800	0.185	185						5.800	0.186	186		
5.900	0.185	185						5.900	0.185	185						5.900	0.185	185		
6.000	0.185	185						6.000	0.184	184						6.000	0.184	184		
6.100	0.184	184						6.100	0.183	183						6.100	0.183	183		
6.200	0.183	183						6.200	0.183	183						6.200	0.182	182		
6.300	0.183	183						6.300	0.182	182						6.300	0.182	182		
6.400	0.182	182						6.400	0.181	181						6.400	0.181	181		
6.500	0.181	181						6.500	0.181	181						6.500	0.180	180		
6.600	0.181	181						6.600	0.180	180						6.600	0.179	179		
6.700	0.180	180						6.700	0.179	179						6.700	0.178	178		
6.800	0.180	180						6.800	0.179	179						6.800	0.178	178		
6.900	0.179	179						6.900	0.178	178						6.900	0.177	177		
7.000	0.178	178						7.000	0.178	178						7.000	0.176	176		
7.100	0.178	178						7.100	0.177	177						7.100	0.175	175		
7.200	0.177	177						7.200	0.176	176						7.200	0.175	175		
7.300	0.177	177						7.300	0.176	176						7.300	0.174	174		
7.400	0.176	176						7.400	0.175	175						7.400	0.173	173		
7.500	0.175	175						7.500	0.174	174						7.500	0.172	172		
7.600	0.175	175						7.600	0.174	174						7.600	0.171	171		
7.700	0.174	174						7.700	0.173	173						7.700	0.171	171		
7.800	0.173	173						7.800	0.173	173						7.800	0.170	170		
7.900	0.173	173						7.900	0.172	172						7.900	0.169	169		
8.000	0.172	172						8.000	0.171	171						8.000	0.168	168		
8.100	0.172	172						8.100	0.171	171						8.100	0.168	168		
8.200	0.171	171						8.200	0.170	170						8.200	0.167	167		
8.300	0.170	170						8.300	0.169	169						8.300	0.166	166		
8.400	0.170	170						8.400	0.169	169						8.400	0.165	165		
8.500	0.169	169						8.500	0.168	168						8.500	0.164	164		
8.600	0.168	168						8.600	0.168	168						8.600	0.164	164		
8.700	0.168	168						8.700	0.167	167						8.700	0.163	163		
8.800	0.167	167						8.800	0.166	166						8.800	0.162	162		
8.900	0.167	167						8.900	0.166	166						8.900	0.161	161		
9.000	0.166	166						9.000	0.165	165						9.000	0.161	161		
9.100	0.165	165						9.100	0.164	164						9.100	0.160	160		
9.200	0.165	165						9.200	0.164	164						9.200	0.159	159		
9.300	0.164	164						9.300	0.163	163						9.300	0.158	158		
9.400	0.163	163						9.400	0.162	162						9.400	0.157	157		
9.500	0.163	163						9.500	0.162	162						9.500	0.157	157		
9.600	0.162	162						9.600	0.161	161						9.600	0.156	156		
9.700	0.161	161						9.700	0.161	161						9.700	0.155	155		
9.800	0.161	161						9.800	0.160	160						9.800	0.154	154		
9.900	0.160	160						9.900	0.159	159						9.900	0.153	153		
10.000	0.160	160						10.000	0.159	159						10.000	0.153	153		
10.100	0.159	159						10.100	0.158	158						10.100	0.152	152		
10.200	0.158	158						10.200	0.157	157						10.200	0.151	151		
10.300	0.158	158						10.300	0.157	157						10.300	0.150	150		
10.400	0.157	157						10.400	0.156	156						10.400	0.149	149		
10.500	0.156	156						10.500	0.155	155						10.500	0.149	149		
10.600	0.156	156						10.600	0.155	155						10.600	0.148	148		
10.700	0.155	155						10.700	0.154	154						10.700	0.147	147		
10.800	0.154	154						10.800	0.153	153						10.800	0.146	146		
10.900	0.154	154						10.900	0.153	153						10.900	0.145	145		
11.000	0.153	153						11.000	0.152	152						11.000	0.145	145		
11.100	0.153	153						11.100	0.152	152						11.100	0.144	144		
11.200	0.152	152						11.200	0.151	151						11.200	0.143	143		
11.300	0.151	151						11.300	0.150	150						11.300	0.142	142		
11.400	0.151	151						11.400	0.150	150						11.400	0.141	141		
11.500	0.150	150						11.500	0.149	149						11.500	0.141	141		
11.600	0.149	149						11.600	0.148	148						11.600	0.140	140		
11.700	0.149	149						11.700	0.148	148						11.700	0.139	139		
11.800	0.148	148						11.800	0.147	147						11.800	0.138	138		

RUN 4								RUN 5								RUN 6				
Computed			Data					Computed			Data					Computed			Data	
x (m)	η (m)	η (mm)	x (m)	η (mm)				x (m)	η (m)	η (mm)	x (m)	η (mm)				x (m)	η (m)	η (mm)	x (m)	η (mm)
0.000	0.220	220	2.5	205				0.000	0.218	218	2.5	194				0.000	0.211	211	2.5	201
0.100	0.219	219	2.9	202				0.100	0.217	217	2.9	196				0.100	0.210	210	2.9	200
0.200	0.219	219	3.3	200				0.200	0.217	217	3.3	199				0.200	0.210	210	3.3	199
0.300	0.218	218	3.7	200				0.300	0.216	216	3.7	198				0.300	0.210	210	3.7	196
0.400	0.217	217	4.1	198				0.400	0.216	216	4.1	197				0.400	0.209	209	4.1	194
0.500	0.217	217	4.3	198				0.500	0.215	215	4.3	196				0.500	0.209	209	4.3	193
0.600	0.216	216	4.5	193				0.600	0.215	215	4.5	193				0.600	0.209	209	4.5	191
0.700	0.216	216	4.9	192				0.700	0.214	214	4.9	191				0.700	0.208	208	4.9	190
0.800	0.215	215	5.3	187				0.800	0.214	214	5.3	189				0.800	0.208	208	5.3	186
0.900	0.214	214	5.7	183				0.900	0.213	213	5.7	187				0.900	0.208	208	5.7	183
1.000	0.214	214	6.1	181				1.000	0.212	212	6.1	183				1.000	0.207	207	6.1	183
1.100	0.213	213	6.5	180				1.100	0.212	212	6.5	184				1.100	0.207	207	6.5	181
1.200	0.213	213	6.9	178				1.200	0.211	211	6.9	179				1.200	0.206	206	6.9	180
1.300	0.212	212	7.3	176				1.300	0.211	211	7.3	176				1.300	0.206	206	7.3	177
1.400	0.212	212	7.7	173				1.400	0.210	210	7.7	173				1.400	0.206	206	7.7	176
1.500	0.211	211	8.1	171				1.500	0.210	210	8.1	172				1.500	0.205	205	8.1	175
1.600	0.210	210	8.5	167				1.600	0.209	209	8.5	169				1.600	0.204	204	8.5	173
1.700	0.210	210	8.9	163				1.700	0.209	209	8.9	166				1.700	0.204	204	8.9	172
1.800	0.209	209	9.3	164				1.800	0.208	208	9.3	163				1.800	0.203	203	9.3	169
1.900	0.209	209	9.7	159				1.900	0.207	207	9.7	162				1.900	0.203	203	9.7	167
2.000	0.208	208	10.1	156				2.000	0.207	207	10.1	159				2.000	0.203	203	10.1	165
2.100	0.208	208	10.5	155				2.100	0.206	206	10.5	157				2.100	0.202	202	10.5	164
2.200	0.207	207						2.200	0.206	206						2.200	0.202	202		
2.300	0.206	206						2.300	0.205	205						2.300	0.201	201		
2.400	0.206	206						2.400	0.205	205						2.400	0.201	201		
2.500	0.205	205						2.500	0.204	204						2.500	0.200	200		
2.600	0.205	205						2.600	0.204	204						2.600	0.200	200		
2.700	0.204	204						2.700	0.203	203						2.700	0.200	200		
2.800	0.203	203						2.800	0.202	202						2.800	0.199	199		
2.900	0.203	203						2.900	0.202	202						2.900	0.199	199		
3.000	0.202	202						3.000	0.201	201						3.000	0.198	198		
3.100	0.202	202						3.100	0.201	201						3.100	0.198	198		
3.200	0.201	201						3.200	0.200	200						3.200	0.197	197		
3.300	0.201	201						3.300	0.200	200						3.300	0.197	197		
3.400	0.200	200						3.400	0.199	199						3.400	0.197	197		
3.500	0.199	199						3.500	0.199	199						3.500	0.196	196		
3.600	0.199	199						3.600	0.198	198						3.600	0.196	196		
3.700	0.198	198						3.700	0.197	197						3.700	0.195	195		
3.800	0.198	198						3.800	0.197	197						3.800	0.195	195		
3.900	0.197	197						3.900	0.196	196						3.900	0.194	194		
4.000	0.196	196						4.000	0.196	196						4.000	0.194	194		
4.100	0.196	196						4.100	0.195	195						4.100	0.193	193		
4.200	0.195	195						4.200	0.195	195						4.200	0.193	193		
4.300	0.195	195						4.300	0.194	194						4.300	0.193	193		
4.400	0.194	194						4.400	0.194	194						4.400	0.192	192		
4.500	0.194	194						4.500	0.193	193						4.500	0.192	192		
4.600	0.193	193						4.600	0.192	192						4.600	0.191	191		
4.700	0.192	192						4.700	0.192	192						4.700	0.191	191		
4.800	0.192	192						4.800	0.191	191						4.800	0.190	190		
4.900	0.191	191						4.900	0.191	191						4.900	0.190	190		
5.000	0.191	191						5.000	0.190	190						5.000	0.189	189		
5.100	0.190	190						5.100	0.190	190						5.100	0.189	189		
5.200	0.189	189						5.200	0.189	189						5.200	0.188	188		
5.300	0.189	189						5.300	0.189	189						5.300	0.188	188		
5.400	0.188	188						5.400	0.188	188						5.400	0.187	187		
5.500	0.188	188						5.500	0.187	187						5.500	0.187	187		
5.600	0.187	187						5.600	0.187	187						5.600	0.186	186		
5.700	0.186	186						5.700	0.186	186						5.700	0.186	186		
5.800	0.186	186						5.800	0.186	186						5.800	0.185	185		
5.900	0.185	185						5.900	0.185	185						5.900	0.185	185		
6.000	0.185	185						6.000	0.185	185						6.000	0.184	184		
6.100	0.184	184						6.100	0.184	184						6.100	0.184	184		
6.200	0.183	183						6.200	0.183	183						6.200	0.183	183		
6.300	0.183	183						6.300	0.183	183						6.300	0.183	183		
6.400	0.182	182						6.400	0.182	182						6.400	0.182	182		
6.500	0.182	182						6.500	0.182	182						6.500	0.182	182		
6.600	0.181	181						6.600	0.181	181						6.600	0.181	181		
6.700	0.180	180						6.700	0.181	181						6.700	0.181	181		
6.800	0.180	180						6.800	0.180	180						6.800	0.180	180		
6.900	0.179	179						6.900	0.180	180						6.900	0.180	180		
7.000	0.179	179						7.000	0.179	179						7.000	0.180	180		
7.100	0.178	178						7.100	0.178	178						7.100	0.179	179		
7.200	0.177	177						7.200	0.178	178						7.200	0.179	179		
7.300	0.177	177						7.300	0.177	177						7.300	0.178	178		
7.400	0.176	176						7.400	0.177	177						7.400	0.178	178		
7.500	0.176	176						7.500	0.176	176						7.500	0.177	177		
7.600	0.175	175						7.600	0.175	175						7.600	0.177	177		
7.700	0.174	174						7.700	0.175	175						7.700	0.177	177		
7.800	0.174	174						7.800	0.174	174						7.800	0.176	176		
7.900	0.173	173						7.900	0.174	174						7.900	0.176	176		
8.000	0.172	172						8.000	0.173	173						8.000	0.175	175		
8.100	0.172	172						8.100	0.173	173						8.100	0.175	175		
8.200	0.171	171						8.200	0.172	172						8.200	0.174	174		
8.300	0.171	171						8.300	0.171	171						8.300	0.174	174		
8.400	0.170	170						8.400	0.171	171						8.400	0.174	174		
8.500	0.169	169						8.500	0.170	170						8.500	0.173	173		
8.600	0.169	169						8.600	0.170	170						8.600	0.173	173		
8.700	0.168	168						8.700	0.169	169						8.700	0.172	172		
8.800	0.168	168						8.800	0.168	168						8.800	0.172	172		
8.900	0.167	167						8.900	0.168	168						8.900	0.171	171		
9.000	0.166	166						9.000	0.167	167						9.000	0.171	171		
9.100	0.166	166						9.100	0.167	167						9.100	0.170	170		
9.200	0.165	165						9.200	0.166	166						9.200	0.170	170		
9.300	0.165	165						9.300	0.166	166						9.300	0.170	170		
9.400	0.164	164						9.400	0.165	165						9.400	0.169	169		
9.500	0.163	163						9.500	0.164	164						9.500	0.169	169		
9.600	0.163	163						9.600	0.164	164						9.600	0.168	168		
9.700	0.162	162						9.700	0.163	163						9.700	0.168	168		
9.800	0.162	162						9.800	0.163	163						9.800	0.167	167		
9.900	0.161	161						9.900	0.162	162						9.900	0.167	167		
10.000	0.160	160						10.000	0.162	162						10.000	0.166	166		
10.100	0.160	160						10.100	0.161	161						10.100	0.166	166		
10.200	0.159	159						10.200	0.160	160						10.200	0.165	165		
10.300	0.159	159						10.300	0.160	160						10.300	0.165	165		
10.400	0.158	158						10.400	0.159	159						10.400	0.164	164		
10.500	0.157	157						10.500	0.159	159						10.500	0.164	164		
10.600	0.157	157						10.600	0.158	158						10.600	0.164	164		
10.700	0.156	156						10.700	0.158	158						10.700	0.163	163		
10.800	0.156	156						10.800	0.157	157						10.800	0.163	163		
10.900	0.155	155						10.900	0.157	157						10.900	0.162	162		
11.000	0.154	154						11.000	0.156	156						11.000	0.162	162		
11.100	0.154	154						11.100	0.156	156						11.100	0.161	161		
11.200	0.153	153						11.200	0.155	155						11.200	0.161	161		
11.300	0.153	153						11.300	0.154	154						11.300	0.161	161		
11.400	0.152	152						11.400	0.154	154						11.400	0.160	160		
11.500	0.151	151						11.500	0.153	153						11.500	0.160	160		
11.600	0.151	151						11.600	0.153	153						11.600	0.159	159		
11.700	0.150	150						11.700	0.152	152						11.700	0.159	159		
11.800	0.150	150						11.800	0.152	152						11.800	0.159	159		

RUN 7								RUN 8								RUN 9				
Computed			Data					Computed			Data					Computed			Data	
x (m)	η (m)	η (mm)	x (m)	η (mm)				x (m)	η (m)	η (mm)	x (m)	η (mm)				x (m)	η (m)	η (mm)	x (m)	η (mm)
0.000	0.216	216	2.5	198				0.000	0.210	210	2.5	201				0.000	0.223	223	2.5	201
0.100	0.216	216	2.9	202				0.100	0.210	210	2.9	200				0.100	0.222	222	2.9	201
0.200	0.215	215	3.3	199				0.200	0.209	209	3.3	199				0.200	0.221	221	3.3	199
0.300	0.215	215	3.7	198				0.300	0.209	209	3.7	199				0.300	0.221	221	3.7	198
0.400	0.214	214	4.1	196				0.400	0.208	208	4.1	196				0.400	0.220	220	4.1	196
0.500	0.213	213	4.3	195				0.500	0.208	208	4.3	197				0.500	0.220	220	4.3	196
0.600	0.213	213	4.5	192				0.600	0.208	208	4.5	196				0.600	0.219	219	4.5	194
0.700	0.212	212	4.9	190				0.700	0.207	207	4.9	192				0.700	0.218	218	4.9	191
0.800	0.212	212	5.3	187				0.800	0.207	207	5.3	189				0.800	0.218	218	5.3	188
0.900	0.211	211	5.7	185				0.900	0.206	206	5.7	187				0.900	0.217	217	5.7	186
1.000	0.211	211	6.1	182				1.000	0.206	206	6.1	186				1.000	0.216	216	6.1	183
1.100	0.210	210	6.5	180				1.100	0.206	206	6.5	184				1.100	0.216	216	6.5	180
1.200	0.210	210	6.9	179				1.200	0.205	205	6.9	184				1.200	0.215	215	6.9	181
1.300	0.209	209	7.3	175				1.300	0.205	205	7.3	182				1.300	0.214	214	7.3	176
1.400	0.209	209	7.7	173				1.400	0.204	204	7.7	179				1.400	0.214	214	7.7	172
1.500	0.208	208	8.1	172				1.500	0.204	204	8.1	176				1.500	0.213	213	8.1	168
1.600	0.208	208	8.5	171				1.600	0.204	204	8.5	173				1.600	0.213	213	8.5	166
1.700	0.207	207	8.9	170				1.700	0.203	203	8.9	171				1.700	0.212	212	8.9	165
1.800	0.207	207	9.3	168				1.800	0.203	203	9.3	171				1.800	0.211	211	9.3	160
1.900	0.206	206	9.7	165				1.900	0.202	202	9.7	168				1.900	0.211	211	9.7	158
2.000	0.206	206	10.1	160				2.000	0.202	202	10.1	166				2.000	0.210	210	10.1	158
2.100	0.205	205	10.5	158				2.100	0.202	202	10.5	165				2.100	0.209	209	10.5	153
2.200	0.205	205						2.200	0.201	201						2.200	0.209	209		
2.300	0.204	204						2.300	0.201	201						2.300	0.208	208		
2.400	0.204	204						2.400	0.200	200						2.400	0.207	207		
2.500	0.203	203						2.500	0.200	200						2.500	0.207	207		
2.600	0.202	202						2.600	0.200	200						2.600	0.206	206		
2.700	0.202	202						2.700	0.199	199						2.700	0.206	206		
2.800	0.201	201						2.800	0.199	199						2.800	0.205	205		
2.900	0.201	201						2.900	0.198	198						2.900	0.204	204		
3.000	0.200	200						3.000	0.198	198						3.000	0.204	204		
3.100	0.200	200						3.100	0.197	197						3.100	0.203	203		
3.200	0.199	199						3.200	0.197	197						3.200	0.202	202		
3.300	0.199	199						3.300	0.196	196						3.300	0.202	202		
3.400	0.198	198						3.400	0.196	196						3.400	0.201	201		
3.500	0.198	198						3.500	0.196	196						3.500	0.200	200		
3.600	0.197	197						3.600	0.195	195						3.600	0.200	200		
3.700	0.197	197						3.700	0.195	195						3.700	0.199	199		
3.800	0.196	196						3.800	0.194	194						3.800	0.199	199		
3.900	0.196	196						3.900	0.194	194						3.900	0.198	198		
4.000	0.195	195						4.000	0.193	193						4.000	0.197	197		
4.100	0.195	195						4.100	0.193	193						4.100	0.197	197		
4.200	0.194	194						4.200	0.193	193						4.200	0.196	196		
4.300	0.194	194						4.300	0.192	192						4.300	0.195	195		
4.400	0.193	193						4.400	0.192	192						4.400	0.195	195		
4.500	0.192	192						4.500	0.191	191						4.500	0.194	194		
4.600	0.192	192						4.600	0.191	191						4.600	0.193	193		
4.700	0.191	191						4.700	0.190	190						4.700	0.193	193		
4.800	0.191	191						4.800	0.190	190						4.800	0.192	192		
4.900	0.190	190						4.900	0.190	190						4.900	0.192	192		
5.000	0.190	190						5.000	0.189	189						5.000	0.191	191		
5.100	0.189	189						5.100	0.189	189						5.100	0.190	190		
5.200	0.189	189						5.200	0.188	188						5.200	0.190	190		
5.300	0.188	188						5.300	0.188	188						5.300	0.189	189		
5.400	0.188	188						5.400	0.187	187						5.400	0.188	188		
5.500	0.187	187						5.500	0.187	187						5.500	0.188	188		
5.600	0.187	187						5.600	0.187	187						5.600	0.187	187		
5.700	0.186	186						5.700	0.186	186						5.700	0.186	186		
5.800	0.185	185						5.800	0.186	186						5.800	0.186	186		
5.900	0.185	185						5.900	0.185	185						5.900	0.185	185		
6.000	0.184	184						6.000	0.185	185						6.000	0.185	185		
6.100	0.184	184						6.100	0.185	185						6.100	0.184	184		
6.200	0.183	183						6.200	0.184	184						6.200	0.183	183		
6.300	0.183	183						6.300	0.184	184						6.300	0.183	183		
6.400	0.182	182						6.400	0.183	183						6.400	0.182	182		
6.500	0.182	182						6.500	0.183	183						6.500	0.181	181		
6.600	0.181	181						6.600	0.182	182						6.600	0.181	181		
6.700	0.181	181						6.700	0.182	182						6.700	0.180	180		
6.800	0.180	180						6.800	0.182	182						6.800	0.179	179		
6.900	0.179	179						6.900	0.181	181						6.900	0.179	179		
7.000	0.179	179						7.000	0.181	181						7.000	0.178	178		
7.100	0.178	178						7.100	0.180	180						7.100	0.177	177		
7.200	0.178	178						7.200	0.180	180						7.200	0.177	177		
7.300	0.177	177						7.300	0.179	179						7.300	0.176	176		
7.400	0.177	177						7.400	0.179	179						7.400	0.175	175		
7.500	0.176	176						7.500	0.179	179						7.500	0.175	175		
7.600	0.175	175						7.600	0.178	178						7.600	0.174	174		
7.700	0.175	175						7.700	0.178	178						7.700	0.173	173		
7.800	0.174	174						7.800	0.177	177						7.800	0.173	173		
7.900	0.174	174						7.900	0.177	177						7.900	0.172	172		
8.000	0.173	173						8.000	0.176	176						8.000	0.172	172		
8.100	0.173	173						8.100	0.176	176						8.100	0.171	171		
8.200	0.172	172						8.200	0.176	176						8.200	0.170	170		
8.300	0.172	172						8.300	0.175	175						8.300	0.170	170		
8.400	0.171	171						8.400	0.175	175						8.400	0.169	169		
8.500	0.171	171						8.500	0.174	174						8.500	0.168	168		
8.600	0.170	170						8.600	0.174	174						8.600	0.168	168		
8.700	0.170	170						8.700	0.173	173						8.700	0.167	167		
8.800	0.169	169						8.800	0.173	173						8.800	0.166	166		
8.900	0.169	169						8.900	0.172	172						8.900	0.166	166		
9.000	0.168	168						9.000	0.172	172						9.000	0.165	165		
9.100	0.168	168						9.100	0.171	171						9.100	0.164	164		
9.200	0.167	167						9.200	0.171	171						9.200	0.164	164		
9.300	0.167	167						9.300	0.170	170						9.300	0.163	163		
9.400	0.166	166						9.400	0.169	169						9.400	0.162	162		
9.500	0.166	166						9.500	0.169	169						9.500	0.162	162		
9.600	0.165	165						9.600	0.168	168						9.600	0.161	161		
9.700	0.165	165						9.700	0.168	168						9.700	0.160	160		
9.800	0.164	164						9.800	0.167	167						9.800	0.160	160		
9.900	0.164	164						9.900	0.166	166						9.900	0.159	159		
10.000	0.163	163						10.000	0.166	166						10.000	0.158	158		
10.100	0.163	163						10.100	0.165	165						10.100	0.158	158		
10.200	0.162	162						10.200	0.165	165						10.200	0.157	157		
10.300	0.162	162						10.300	0.165	165						10.300	0.156	156		
10.400	0.161	161						10.400	0.164	164						10.400	0.156	156		
10.500	0.161	161						10.500	0.164	164						10.500	0.155	155		
10.600	0.160	160						10.600	0.163	163						10.600	0.154	154		
10.700	0.160	160						10.700	0.163	163						10.700	0.154	154		
10.800	0.159	159						10.800	0.163	163						10.800	0.153	153		
10.900	0.159	159						10.900	0.162	162						10.900	0.153	153		
11.000	0.158	158						11.000	0.162	162						11.000	0.152	152		
11.100	0.158	158						11.100	0.161	161						11.100	0.151	151		
11.200	0.157	157						11.200	0.161	161						11.200	0.151	151		
11.300	0.157	157						11.300	0.161	161						11.300	0.150	150		
11.400	0.156	156						11.400	0.160	160						11.400	0.149	149		
11.500	0.156	156						11.500	0.160	160						11.500	0.149	149		
11.600	0.155	155						11.600	0.159	159						11.600	0.148	148		
11.700	0.155	155						11.700	0.159	159						11.700	0.147	147		
11.800	0.154	154						11.800	0.159	159						11.800	0.147	147		

RUN 1

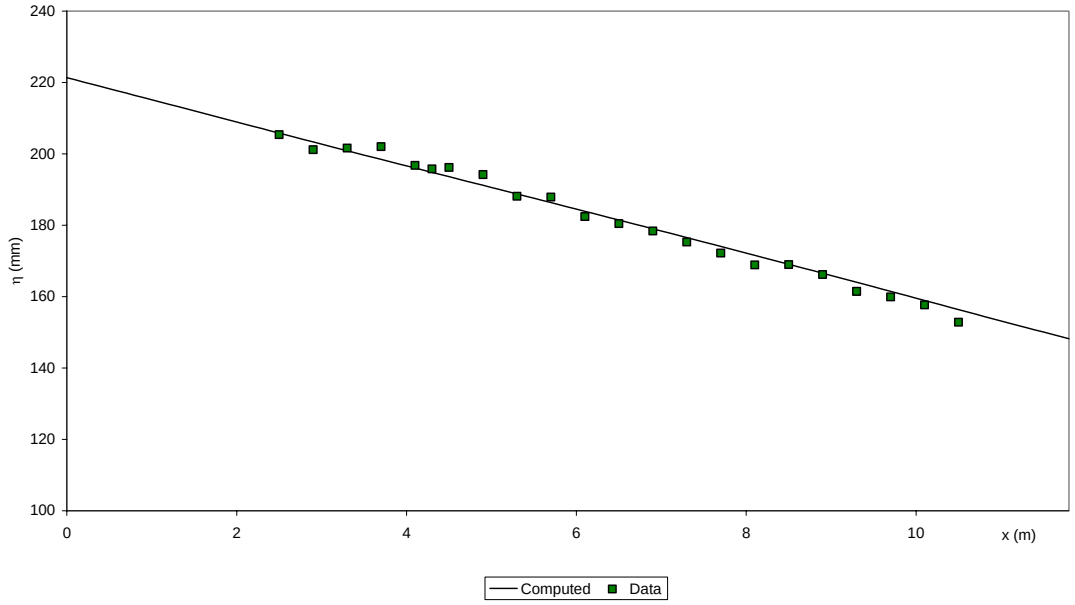
240
220
200
180
160
140
120
100
η (mm)
0
2
4
6
8
10
x (m)
Computed
Data

RUN 2

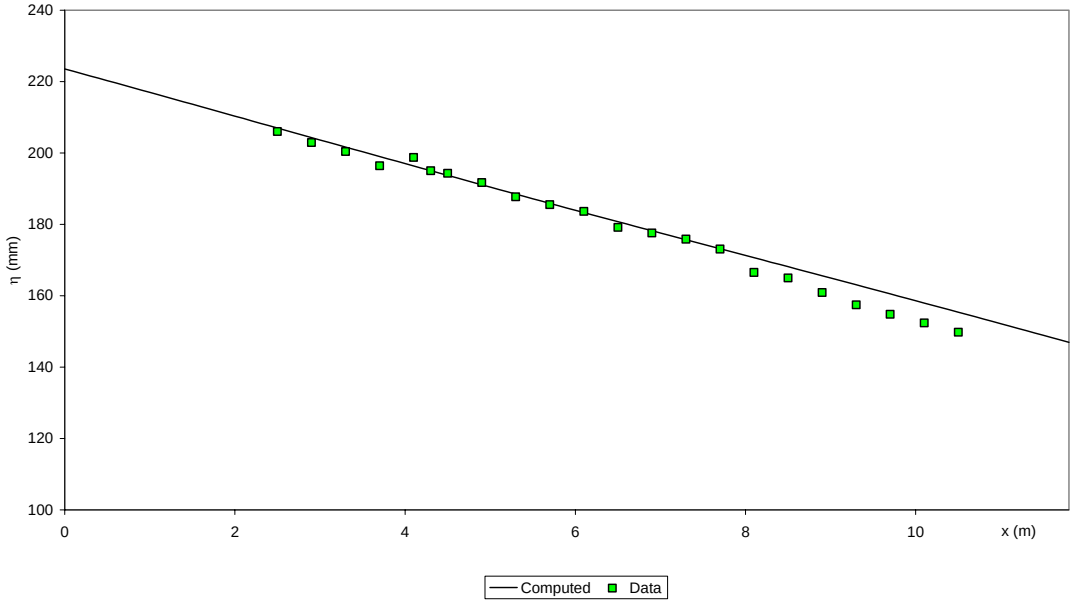
240
220
200
180
160
140
120
100
η (mm)
0
2
4
6
8
10
x (m)
Computed
Data

RUN 3

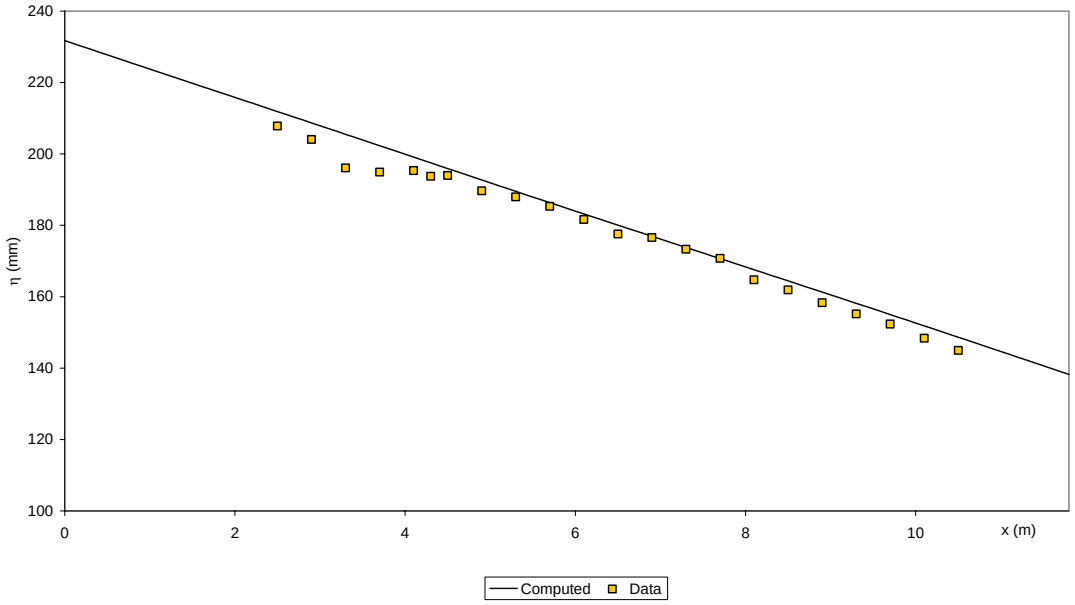
240
220
200
180
160
140
120
100
η (mm)
0
2
4
6
8
10
x (m)
Computed
Data

RUN 4

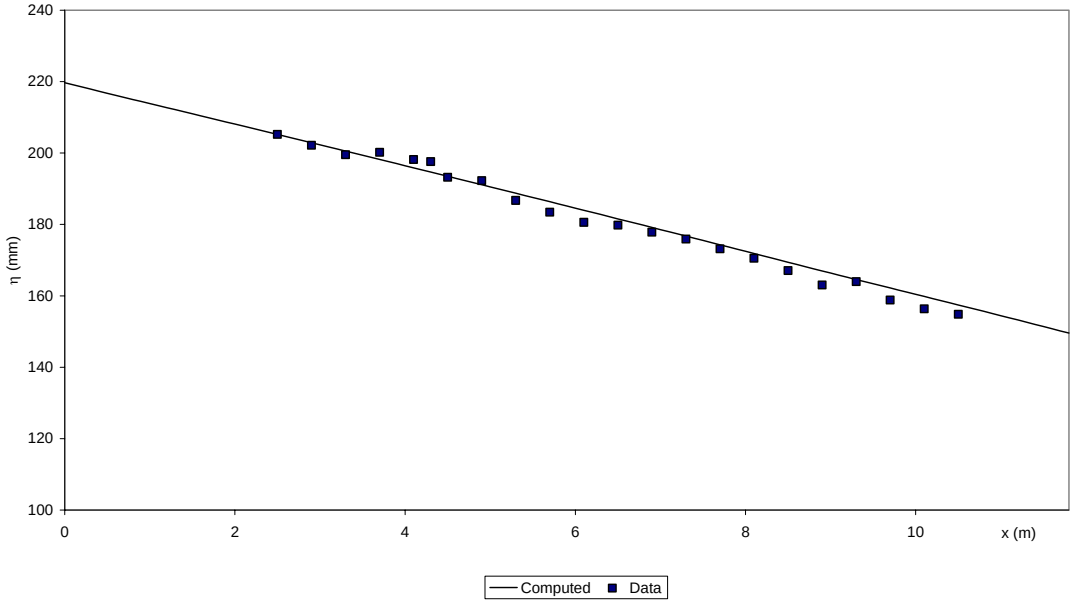
240
220
200
180
160
140
120
100
η (mm)
0
2
4
6
8
10
x (m)
Computed
Data

RUN 5

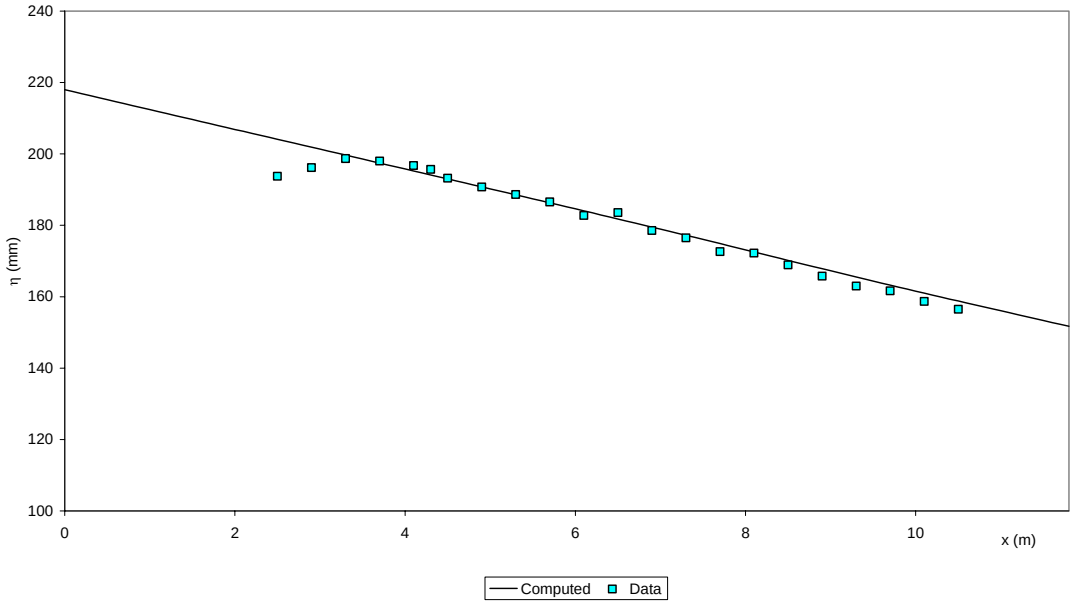
240
220
200
180
160
140
120
100
η (mm)
0
2
4
6
8
10
x (m)
Computed
Data

RUN 6

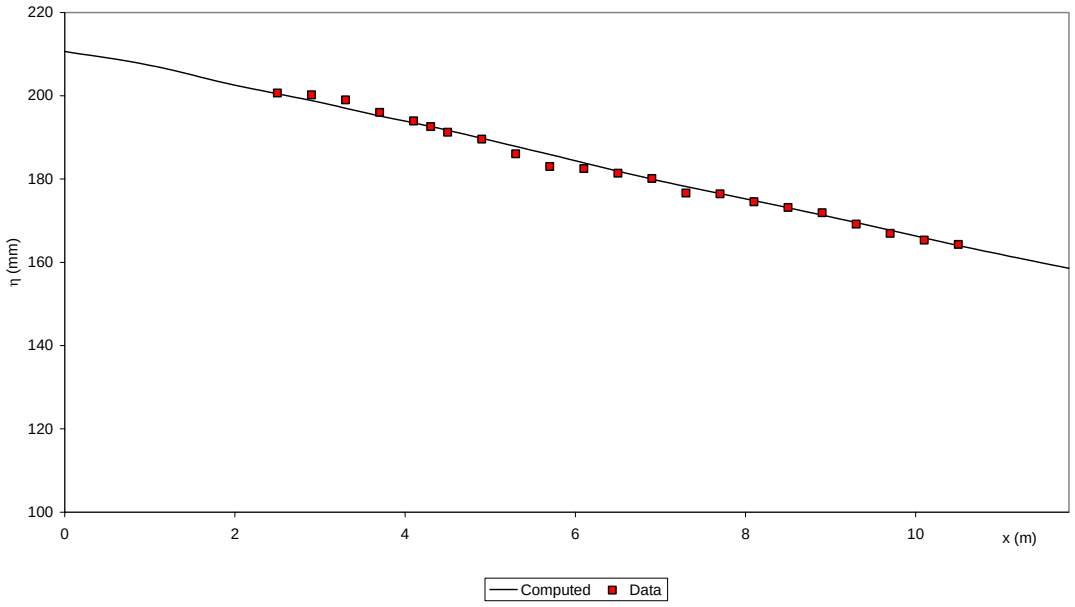
220
200
180
160
140
120
100
η (mm)
0
2
4
6
8
10
x (m)
Computed
Data

RUN 7

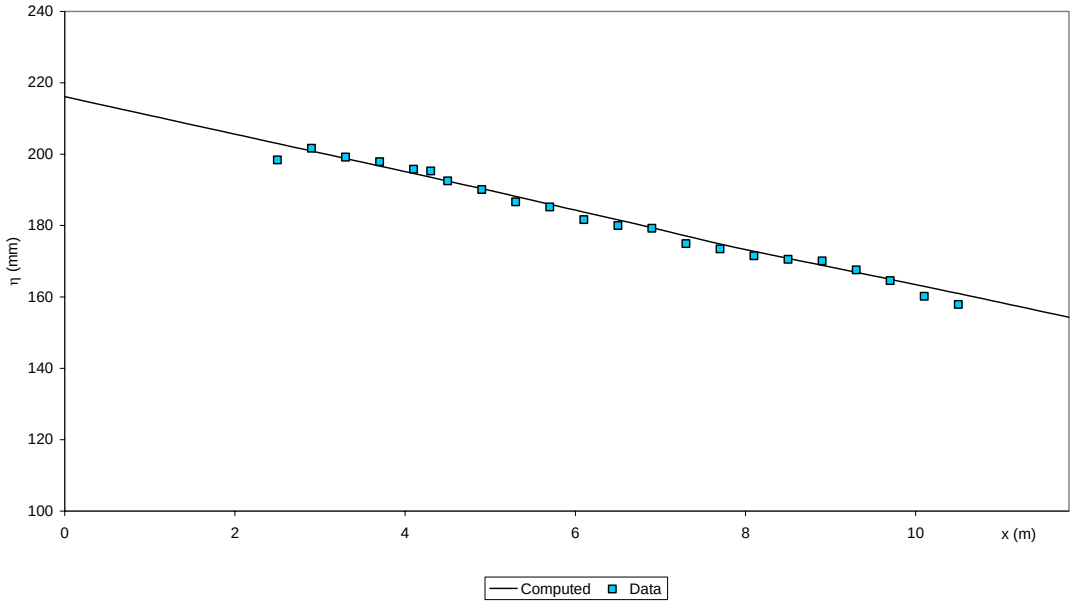
240
220
200
180
160
140
120
100
η (mm)
0
2
4
6
8
10
x (m)
Computed
Data

RUN 8

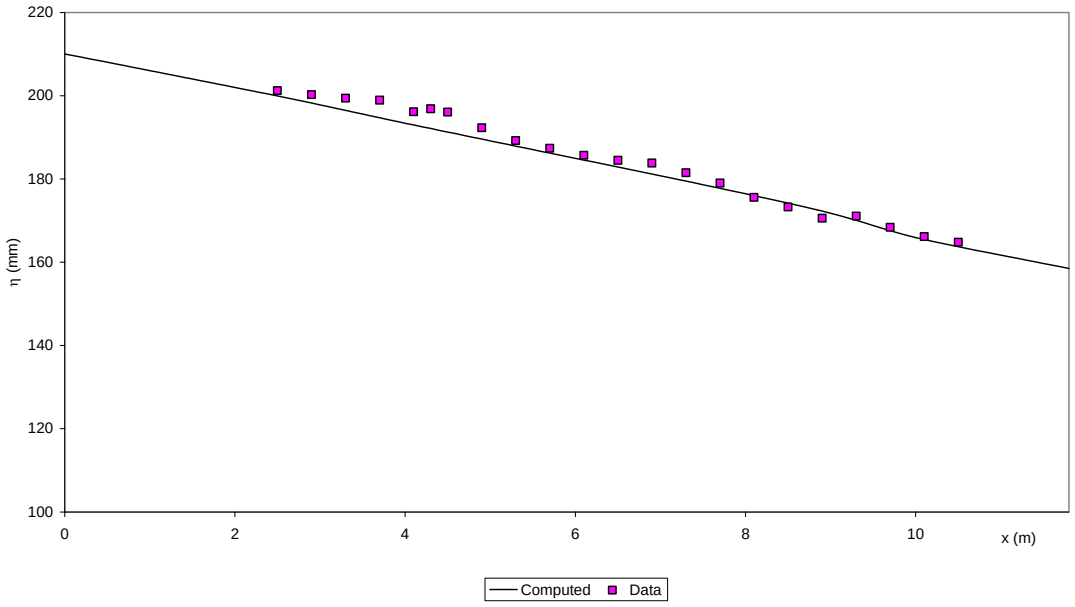
220
200
180
160
140
120
100
η (mm)
0
2
4
6
8
10
x (m)
Computed
Data

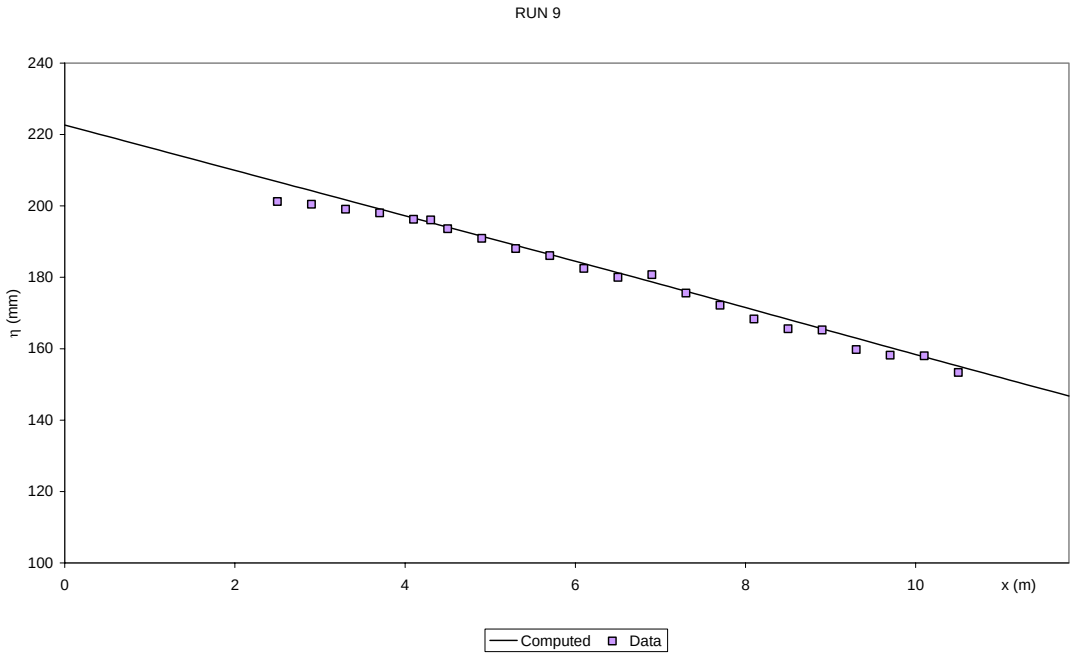
RUN 9
240
220
200
180
160
140
120
100
η (mm)
0
2
4
6
8
10
x (m)
Computed
Data

Water surface elevation

RUN 1								RUN 2								RUN 3				
Computed			Data					Computed			Data					Computed			Data	
x (m)	H (m)	H (mm)	x (m)	H (mm)				x (m)	H (m)	H (mm)	x (m)	H (mm)				x (m)	H (m)	H (mm)	x (m)	H (mm)
0.000	0.293	293	2.5	284				0.000	0.287	287	2.5	275				0.000	0.284	284	2.5	266
0.100	0.293	293	4.3	274				0.100	0.286	286	4.3	263				0.100	0.283	283	4.3	255
0.200	0.292	292	6.5	258				0.200	0.285	285	6.5	248				0.200	0.282	282	6.5	239
0.300	0.291	291	8.5	244				0.300	0.285	285	8.5	232				0.300	0.281	281	8.5	221
0.400	0.291	291	10.5	229				0.400	0.284	284	10.5	218				0.400	0.280	280	10.5	201
0.500	0.290	290						0.500	0.283	283						0.500	0.280	280		
0.600	0.289	289						0.600	0.283	283						0.600	0.279	279		
0.700	0.289	289						0.700	0.282	282						0.700	0.278	278		
0.800	0.288	288						0.800	0.281	281						0.800	0.277	277		
0.900	0.288	288						0.900	0.281	281						0.900	0.276	276		
1.000	0.287	287						1.000	0.280	280						1.000	0.276	276		
1.100	0.286	286						1.100	0.279	279						1.100	0.275	275		
1.200	0.286	286						1.200	0.279	279						1.200	0.274	274		
1.300	0.285	285						1.300	0.278	278						1.300	0.273	273		
1.400	0.284	284						1.400	0.277	277						1.400	0.272	272		
1.500	0.284	284						1.500	0.277	277						1.500	0.272	272		
1.600	0.283	283						1.600	0.276	276						1.600	0.271	271		
1.700	0.283	283						1.700	0.275	275						1.700	0.270	270		
1.800	0.282	282						1.800	0.275	275						1.800	0.269	269		
1.900	0.281	281						1.900	0.274	274						1.900	0.269	269		
2.000	0.281	281						2.000	0.273	273						2.000	0.268	268		
2.100	0.280	280						2.100	0.273	273						2.100	0.267	267		
2.200	0.280	280						2.200	0.272	272						2.200	0.266	266		
2.300	0.279	279						2.300	0.271	271						2.300	0.265	265		
2.400	0.278	278						2.400	0.271	271						2.400	0.265	265		
2.500	0.278	278						2.500	0.270	270						2.500	0.264	264		
2.600	0.277	277						2.600	0.269	269						2.600	0.263	263		
2.700	0.277	277						2.700	0.269	269						2.700	0.262	262		
2.800	0.276	276						2.800	0.268	268						2.800	0.261	261		
2.900	0.276	276						2.900	0.267	267						2.900	0.260	260		
3.000	0.275	275						3.000	0.267	267						3.000	0.260	260		
3.100	0.274	274						3.100	0.266	266						3.100	0.259	259		
3.200	0.274	274						3.200	0.265	265						3.200	0.258	258		
3.300	0.273	273						3.300	0.265	265						3.300	0.257	257		
3.400	0.273	273						3.400	0.264	264						3.400	0.256	256		
3.500	0.272	272						3.500	0.263	263						3.500	0.256	256		
3.600	0.271	271						3.600	0.263	263						3.600	0.255	255		
3.700	0.271	271						3.700	0.262	262						3.700	0.254	254		
3.800	0.270	270						3.800	0.261	261						3.800	0.253	253		
3.900	0.270	270						3.900	0.261	261						3.900	0.252	252		
4.000	0.269	269						4.000	0.260	260						4.000	0.252	252		
4.100	0.268	268						4.100	0.259	259						4.100	0.251	251		
4.200	0.268	268						4.200	0.259	259						4.200	0.250	250		
4.300	0.267	267						4.300	0.258	258						4.300	0.249	249		
4.400	0.266	266						4.400	0.258	258						4.400	0.248	248		
4.500	0.266	266						4.500	0.257	257						4.500	0.248	248		
4.600	0.265	265						4.600	0.256	256						4.600	0.247	247		
4.700	0.265	265						4.700	0.256	256						4.700	0.246	246		
4.800	0.264	264						4.800	0.255	255						4.800	0.245	245		
4.900	0.263	263						4.900	0.254	254						4.900	0.245	245		
5.000	0.263	263						5.000	0.254	254						5.000	0.244	244		
5.100	0.262	262						5.100	0.253	253						5.100	0.243	243		
5.200	0.262	262						5.200	0.253	253						5.200	0.242	242		
5.300	0.261	261						5.300	0.252	252						5.300	0.241	241		
5.400	0.260	260						5.400	0.251	251						5.400	0.241	241		
5.500	0.260	260						5.500	0.251	251						5.500	0.240	240		
5.600	0.259	259						5.600	0.250	250						5.600	0.239	239		
5.700	0.258	258						5.700	0.249	249						5.700	0.238	238		
5.800	0.258	258						5.800	0.249	249						5.800	0.238	238		
5.900	0.257	257						5.900	0.248	248						5.900	0.237	237		
6.000	0.257	257						6.000	0.248	248						6.000	0.236	236		
6.100	0.256	256						6.100	0.247	247						6.100	0.235	235		
6.200	0.255	255						6.200	0.246	246						6.200	0.235	235		
6.300	0.255	255						6.300	0.246	246						6.300	0.234	234		
6.400	0.254	254						6.400	0.245	245						6.400	0.233	233		
6.500	0.253	253						6.500	0.245	245						6.500	0.232	232		
6.600	0.253	253						6.600	0.244	244						6.600	0.231	231		
6.700	0.252	252						6.700	0.243	243						6.700	0.231	231		
6.800	0.251	251						6.800	0.243	243						6.800	0.230	230		
6.900	0.251	251						6.900	0.242	242						6.900	0.229	229		
7.000	0.250	250						7.000	0.241	241						7.000	0.228	228		
7.100	0.250	250						7.100	0.241	241						7.100	0.228	228		
7.200	0.249	249						7.200	0.240	240						7.200	0.227	227		
7.300	0.248	248						7.300	0.239	239						7.300	0.226	226		
7.400	0.248	248						7.400	0.239	239						7.400	0.225	225		
7.500	0.247	247						7.500	0.238	238						7.500	0.224	224		
7.600	0.246	246						7.600	0.238	238						7.600	0.224	224		
7.700	0.246	246						7.700	0.237	237						7.700	0.223	223		
7.800	0.245	245						7.800	0.236	236						7.800	0.222	222		
7.900	0.244	244						7.900	0.236	236						7.900	0.221	221		
8.000	0.244	244						8.000	0.235	235						8.000	0.220	220		
8.100	0.243	243						8.100	0.234	234						8.100	0.220	220		
8.200	0.243	243						8.200	0.234	234						8.200	0.219	219		
8.300	0.242	242						8.300	0.233	233						8.300	0.218	218		
8.400	0.241	241						8.400	0.232	232						8.400	0.217	217		
8.500	0.241	241						8.500	0.232	232						8.500	0.217	217		
8.600	0.240	240						8.600	0.231	231						8.600	0.216	216		
8.700	0.239	239						8.700	0.230	230						8.700	0.215	215		
8.800	0.239	239						8.800	0.230	230						8.800	0.214	214		
8.900	0.238	238						8.900	0.229	229						8.900	0.213	213		
9.000	0.237	237						9.000	0.229	229						9.000	0.213	213		
9.100	0.237	237						9.100	0.228	228						9.100	0.212	212		
9.200	0.236	236						9.200	0.227	227						9.200	0.211	211		
9.300	0.235	235						9.300	0.227	227						9.300	0.210	210		
9.400	0.235	235						9.400	0.226	226						9.400	0.209	209		
9.500	0.234	234						9.500	0.225	225						9.500	0.209	209		
9.600	0.234	234						9.600	0.225	225						9.600	0.208	208		
9.700	0.233	233						9.700	0.224	224						9.700	0.207	207		
9.800	0.232	232						9.800	0.223	223						9.800	0.206	206		
9.900	0.232	232						9.900	0.223	223						9.900	0.205	205		
10.000	0.231	231						10.000	0.222	222						10.000	0.205	205		
10.100	0.230	230						10.100	0.221	221						10.100	0.204	204		
10.200	0.230	230						10.200	0.221	221						10.200	0.203	203		
10.300	0.229	229						10.300	0.220	220						10.300	0.202	202		
10.400	0.229	229						10.400	0.219	219						10.400	0.201	201		
10.500	0.228	228						10.500	0.219	219						10.500	0.200	200		
10.600	0.227	227						10.600	0.218	218						10.600	0.200	200		
10.700	0.227	227						10.700	0.217	217						10.700	0.199	199		
10.800	0.226	226						10.800	0.217	217						10.800	0.198	198		
10.900	0.226	226						10.900	0.216	216						10.900	0.197	197		
11.000	0.225	225						11.000	0.215	215						11.000	0.196	196		
11.100	0.224	224						11.100	0.215	215						11.100	0.196	196		
11.200	0.224	224						11.200	0.214	214						11.200	0.195	195		
11.300	0.223	223						11.300	0.213	213						11.300	0.194	194		
11.400	0.222	222						11.400	0.213	213						11.400	0.193	193		
11.500	0.222	222						11.500	0.212	212						11.500	0.192	192		
11.600	0.221	221						11.600	0.211	211						11.600	0.192	192		
11.700	0.221	221						11.700	0.211	211						11.700	0.191	191		
11.800	0.220	220						11.800	0.210	210						11.800	0.190	190		

RUN 4								RUN 5								RUN 6				
Computed			Data					Computed			Data					Computed			Data	
x (m)	H (m)	H (mm)	x (m)	H (mm)				x (m)	H (m)	H (mm)	x (m)	H (mm)				x (m)	H (m)	H (mm)	x (m)	H (mm)
0.000	0.300	300	2.5	291				0.000	0.276	276	2.5	270				0.000	0.292	292	2.5	283
0.100	0.300	300	4.3	278				0.100	0.275	275	4.3	259				0.100	0.291	291	4.3	276
0.200	0.299	299	6.5	264				0.200	0.275	275	6.5	243				0.200	0.291	291	6.5	265
0.300	0.299	299	8.5	252				0.300	0.274	274	8.5	230				0.300	0.290	290	8.5	255
0.400	0.298	298	10.5	239				0.400	0.274	274	10.5	216				0.400	0.290	290	10.5	245
0.500	0.297	297						0.500	0.273	273						0.500	0.289	289		
0.600	0.297	297						0.600	0.273	273						0.600	0.289	289		
0.700	0.296	296						0.700	0.272	272						0.700	0.288	288		
0.800	0.296	296						0.800	0.271	271						0.800	0.288	288		
0.900	0.295	295						0.900	0.271	271						0.900	0.287	287		
1.000	0.294	294						1.000	0.270	270						1.000	0.287	287		
1.100	0.294	294						1.100	0.270	270						1.100	0.286	286		
1.200	0.293	293						1.200	0.269	269						1.200	0.286	286		
1.300	0.293	293						1.300	0.269	269						1.300	0.285	285		
1.400	0.292	292						1.400	0.268	268						1.400	0.285	285		
1.500	0.292	292						1.500	0.268	268						1.500	0.284	284		
1.600	0.291	291						1.600	0.267	267						1.600	0.284	284		
1.700	0.290	290						1.700	0.266	266						1.700	0.284	284		
1.800	0.290	290						1.800	0.266	266						1.800	0.283	283		
1.900	0.289	289						1.900	0.265	265						1.900	0.283	283		
2.000	0.289	289						2.000	0.265	265						2.000	0.282	282		
2.100	0.288	288						2.100	0.264	264						2.100	0.282	282		
2.200	0.287	287						2.200	0.264	264						2.200	0.281	281		
2.300	0.287	287						2.300	0.263	263						2.300	0.281	281		
2.400	0.286	286						2.400	0.263	263						2.400	0.280	280		
2.500	0.286	286						2.500	0.262	262						2.500	0.280	280		
2.600	0.285	285						2.600	0.261	261						2.600	0.279	279		
2.700	0.284	284						2.700	0.261	261						2.700	0.279	279		
2.800	0.284	284						2.800	0.260	260						2.800	0.278	278		
2.900	0.283	283						2.900	0.260	260						2.900	0.278	278		
3.000	0.283	283						3.000	0.259	259						3.000	0.277	277		
3.100	0.282	282						3.100	0.259	259						3.100	0.277	277		
3.200	0.281	281						3.200	0.258	258						3.200	0.277	277		
3.300	0.281	281						3.300	0.257	257						3.300	0.276	276		
3.400	0.280	280						3.400	0.257	257						3.400	0.276	276		
3.500	0.280	280						3.500	0.256	256						3.500	0.275	275		
3.600	0.279	279						3.600	0.256	256						3.600	0.275	275		
3.700	0.278	278						3.700	0.255	255						3.700	0.274	274		
3.800	0.278	278						3.800	0.255	255						3.800	0.274	274		
3.900	0.277	277						3.900	0.254	254						3.900	0.273	273		
4.000	0.277	277						4.000	0.254	254						4.000	0.273	273		
4.100	0.276	276						4.100	0.253	253						4.100	0.272	272		
4.200	0.275	275						4.200	0.252	252						4.200	0.272	272		
4.300	0.275	275						4.300	0.252	252						4.300	0.271	271		
4.400	0.274	274						4.400	0.251	251						4.400	0.271	271		
4.500	0.273	273						4.500	0.251	251						4.500	0.270	270		
4.600	0.273	273						4.600	0.250	250						4.600	0.270	270		
4.700	0.272	272						4.700	0.250	250						4.700	0.269	269		
4.800	0.272	272						4.800	0.249	249						4.800	0.269	269		
4.900	0.271	271						4.900	0.248	248						4.900	0.269	269		
5.000	0.270	270						5.000	0.248	248						5.000	0.268	268		
5.100	0.270	270						5.100	0.247	247						5.100	0.268	268		
5.200	0.269	269						5.200	0.247	247						5.200	0.267	267		
5.300	0.269	269						5.300	0.246	246						5.300	0.267	267		
5.400	0.268	268						5.400	0.246	246						5.400	0.266	266		
5.500	0.267	267						5.500	0.245	245						5.500	0.266	266		
5.600	0.267	267						5.600	0.244	244						5.600	0.266	266		
5.700	0.266	266						5.700	0.244	244						5.700	0.265	265		
5.800	0.266	266						5.800	0.243	243						5.800	0.265	265		
5.900	0.265	265						5.900	0.243	243						5.900	0.264	264		
6.000	0.264	264						6.000	0.242	242						6.000	0.264	264		
6.100	0.264	264						6.100	0.241	241						6.100	0.264	264		
6.200	0.263	263						6.200	0.241	241						6.200	0.263	263		
6.300	0.262	262						6.300	0.240	240						6.300	0.263	263		
6.400	0.262	262						6.400	0.240	240						6.400	0.262	262		
6.500	0.261	261						6.500	0.239	239						6.500	0.262	262		
6.600	0.261	261						6.600	0.239	239						6.600	0.262	262		
6.700	0.260	260						6.700	0.238	238						6.700	0.261	261		
6.800	0.259	259						6.800	0.237	237						6.800	0.261	261		
6.900	0.259	259						6.900	0.237	237						6.900	0.260	260		
7.000	0.258	258						7.000	0.236	236						7.000	0.260	260		
7.100	0.258	258						7.100	0.236	236						7.100	0.260	260		
7.200	0.257	257						7.200	0.235	235						7.200	0.259	259		
7.300	0.256	256						7.300	0.234	234						7.300	0.259	259		
7.400	0.256	256						7.400	0.234	234						7.400	0.258	258		
7.500	0.255	255						7.500	0.233	233						7.500	0.258	258		
7.600	0.255	255						7.600	0.233	233						7.600	0.257	257		
7.700	0.254	254						7.700	0.232	232						7.700	0.257	257		
7.800	0.253	253						7.800	0.232	232						7.800	0.257	257		
7.900	0.253	253						7.900	0.231	231						7.900	0.256	256		
8.000	0.252	252						8.000	0.230	230						8.000	0.256	256		
8.100	0.252	252						8.100	0.230	230						8.100	0.255	255		
8.200	0.251	251						8.200	0.229	229						8.200	0.255	255		
8.300	0.250	250						8.300	0.229	229						8.300	0.254	254		
8.400	0.250	250						8.400	0.228	228						8.400	0.254	254		
8.500	0.249	249						8.500	0.228	228						8.500	0.253	253		
8.600	0.249	249						8.600	0.227	227						8.600	0.253	253		
8.700	0.248	248						8.700	0.227	227						8.700	0.253	253		
8.800	0.247	247						8.800	0.226	226						8.800	0.252	252		
8.900	0.247	247						8.900	0.225	225						8.900	0.252	252		
9.000	0.246	246						9.000	0.225	225						9.000	0.251	251		
9.100	0.246	246						9.100	0.224	224						9.100	0.251	251		
9.200	0.245	245						9.200	0.224	224						9.200	0.250	250		
9.300	0.245	245						9.300	0.223	223						9.300	0.250	250		
9.400	0.244	244						9.400	0.223	223						9.400	0.250	250		
9.500	0.243	243						9.500	0.222	222						9.500	0.249	249		
9.600	0.243	243						9.600	0.222	222						9.600	0.249	249		
9.700	0.242	242						9.700	0.221	221						9.700	0.248	248		
9.800	0.242	242						9.800	0.221	221						9.800	0.248	248		
9.900	0.241	241						9.900	0.220	220						9.900	0.248	248		
10.000	0.240	240						10.000	0.220	220						10.000	0.247	247		
10.100	0.240	240						10.100	0.219	219						10.100	0.247	247		
10.200	0.239	239						10.200	0.219	219						10.200	0.246	246		
10.300	0.239	239						10.300	0.218	218						10.300	0.246	246		
10.400	0.238	238						10.400	0.218	218						10.400	0.246	246		
10.500	0.237	237						10.500	0.217	217						10.500	0.245	245		
10.600	0.237	237						10.600	0.216	216						10.600	0.245	245		
10.700	0.236	236						10.700	0.216	216						10.700	0.244	244		
10.800	0.236	236						10.800	0.215	215						10.800	0.244	244		
10.900	0.235	235						10.900	0.215	215						10.900	0.244	244		
11.000	0.234	234						11.000	0.214	214						11.000	0.243	243		
11.100	0.234	234						11.100	0.214	214						11.100	0.243	243		
11.200	0.233	233						11.200	0.213	213						11.200	0.242	242		
11.300	0.233	233						11.300	0.213	213						11.300	0.242	242		
11.400	0.232	232						11.400	0.212	212						11.400	0.242	242		
11.500	0.232	232						11.500	0.212	212						11.500	0.241	241		
11.600	0.231	231						11.600	0.211	211						11.600	0.241	241		
11.700	0.231	231						11.700	0.211	211						11.700	0.240	240		
11.800	0.230	230						11.800	0.210	210						11.800	0.240	240		

RUN 7								RUN 8								RUN 9				
Computed			Data					Computed			Data					Computed			Data	
x (m)	H (m)	H (mm)	x (m)	H (mm)				x (m)	H (m)	H (mm)	x (m)	H (mm)				x (m)	H (m)	H (mm)	x (m)	H (mm)
0.000	0.292	292	2.5	283				0.000	0.299	299	2.5	293				0.000	0.301	301	2.5	292
0.100	0.291	291	4.3	273				0.100	0.299	299	4.3	283				0.100	0.300	300	4.3	278
0.200	0.291	291	6.5	260				0.200	0.299	299	6.5	271				0.200	0.300	300	6.5	261
0.300	0.290	290	8.5	250				0.300	0.298	298	8.5	263				0.300	0.299	299	8.5	249
0.400	0.290	290	10.5	239				0.400	0.298	298	10.5	252				0.400	0.298	298	10.5	237
0.500	0.289	289						0.500	0.297	297						0.500	0.298	298		
0.600	0.289	289						0.600	0.297	297						0.600	0.297	297		
0.700	0.288	288						0.700	0.296	296						0.700	0.296	296		
0.800	0.288	288						0.800	0.296	296						0.800	0.296	296		
0.900	0.287	287						0.900	0.296	296						0.900	0.295	295		
1.000	0.287	287						1.000	0.295	295						1.000	0.295	295		
1.100	0.286	286						1.100	0.295	295						1.100	0.294	294		
1.200	0.285	285						1.200	0.294	294						1.200	0.293	293		
1.300	0.285	285						1.300	0.294	294						1.300	0.293	293		
1.400	0.284	284						1.400	0.293	293						1.400	0.292	292		
1.500	0.284	284						1.500	0.293	293						1.500	0.291	291		
1.600	0.283	283						1.600	0.292	292						1.600	0.291	291		
1.700	0.283	283						1.700	0.292	292						1.700	0.290	290		
1.800	0.282	282						1.800	0.292	292						1.800	0.289	289		
1.900	0.282	282						1.900	0.291	291						1.900	0.289	289		
2.000	0.281	281						2.000	0.291	291						2.000	0.288	288		
2.100	0.281	281						2.100	0.290	290						2.100	0.288	288		
2.200	0.280	280						2.200	0.290	290						2.200	0.287	287		
2.300	0.280	280						2.300	0.289	289						2.300	0.286	286		
2.400	0.279	279						2.400	0.289	289						2.400	0.286	286		
2.500	0.278	278						2.500	0.288	288						2.500	0.285	285		
2.600	0.278	278						2.600	0.288	288						2.600	0.284	284		
2.700	0.277	277						2.700	0.287	287						2.700	0.284	284		
2.800	0.277	277						2.800	0.287	287						2.800	0.283	283		
2.900	0.276	276						2.900	0.287	287						2.900	0.282	282		
3.000	0.276	276						3.000	0.286	286						3.000	0.282	282		
3.100	0.275	275						3.100	0.286	286						3.100	0.281	281		
3.200	0.275	275						3.200	0.285	285						3.200	0.281	281		
3.300	0.274	274						3.300	0.285	285						3.300	0.280	280		
3.400	0.274	274						3.400	0.284	284						3.400	0.279	279		
3.500	0.273	273						3.500	0.284	284						3.500	0.279	279		
3.600	0.273	273						3.600	0.284	284						3.600	0.278	278		
3.700	0.272	272						3.700	0.283	283						3.700	0.277	277		
3.800	0.271	271						3.800	0.283	283						3.800	0.277	277		
3.900	0.271	271						3.900	0.282	282						3.900	0.276	276		
4.000	0.270	270						4.000	0.282	282						4.000	0.275	275		
4.100	0.270	270						4.100	0.281	281						4.100	0.275	275		
4.200	0.269	269						4.200	0.281	281						4.200	0.274	274		
4.300	0.269	269						4.300	0.281	281						4.300	0.273	273		
4.400	0.268	268						4.400	0.280	280						4.400	0.273	273		
4.500	0.268	268						4.500	0.280	280						4.500	0.272	272		
4.600	0.267	267						4.600	0.279	279						4.600	0.272	272		
4.700	0.266	266						4.700	0.279	279						4.700	0.271	271		
4.800	0.266	266						4.800	0.278	278						4.800	0.270	270		
4.900	0.265	265						4.900	0.278	278						4.900	0.270	270		
5.000	0.265	265						5.000	0.277	277						5.000	0.269	269		
5.100	0.264	264						5.100	0.277	277						5.100	0.268	268		
5.200	0.264	264						5.200	0.276	276						5.200	0.268	268		
5.300	0.263	263						5.300	0.276	276						5.300	0.267	267		
5.400	0.263	263						5.400	0.276	276						5.400	0.266	266		
5.500	0.262	262						5.500	0.275	275						5.500	0.266	266		
5.600	0.262	262						5.600	0.275	275						5.600	0.265	265		
5.700	0.261	261						5.700	0.274	274						5.700	0.264	264		
5.800	0.261	261						5.800	0.274	274						5.800	0.264	264		
5.900	0.260	260						5.900	0.273	273						5.900	0.263	263		
6.000	0.259	259						6.000	0.273	273						6.000	0.262	262		
6.100	0.259	259						6.100	0.272	272						6.100	0.262	262		
6.200	0.258	258						6.200	0.272	272						6.200	0.261	261		
6.300	0.258	258						6.300	0.271	271						6.300	0.260	260		
6.400	0.257	257						6.400	0.271	271						6.400	0.260	260		
6.500	0.257	257						6.500	0.270	270						6.500	0.259	259		
6.600	0.256	256						6.600	0.270	270						6.600	0.258	258		
6.700	0.256	256						6.700	0.269	269						6.700	0.258	258		
6.800	0.255	255						6.800	0.269	269						6.800	0.257	257		
6.900	0.255	255						6.900	0.268	268						6.900	0.256	256		
7.000	0.254	254						7.000	0.268	268						7.000	0.256	256		
7.100	0.254	254						7.100	0.267	267						7.100	0.255	255		
7.200	0.254	254						7.200	0.267	267						7.200	0.254	254		
7.300	0.253	253						7.300	0.267	267						7.300	0.254	254		
7.400	0.253	253						7.400	0.266	266						7.400	0.253	253		
7.500	0.252	252						7.500	0.266	266						7.500	0.252	252		
7.600	0.252	252						7.600	0.265	265						7.600	0.252	252		
7.700	0.251	251						7.700	0.265	265						7.700	0.251	251		
7.800	0.251	251						7.800	0.264	264						7.800	0.250	250		
7.900	0.251	251						7.900	0.264	264						7.900	0.250	250		
8.000	0.250	250						8.000	0.263	263						8.000	0.249	249		
8.100	0.250	250						8.100	0.263	263						8.100	0.248	248		
8.200	0.249	249						8.200	0.262	262						8.200	0.248	248		
8.300	0.249	249						8.300	0.262	262						8.300	0.247	247		
8.400	0.248	248						8.400	0.261	261						8.400	0.247	247		
8.500	0.248	248						8.500	0.261	261						8.500	0.246	246		
8.600	0.247	247						8.600	0.260	260						8.600	0.245	245		
8.700	0.247	247						8.700	0.260	260						8.700	0.245	245		
8.800	0.246	246						8.800	0.259	259						8.800	0.244	244		
8.900	0.245	245						8.900	0.259	259						8.900	0.243	243		
9.000	0.245	245						9.000	0.258	258						9.000	0.243	243		
9.100	0.244	244						9.100	0.258	258						9.100	0.242	242		
9.200	0.244	244						9.200	0.258	258						9.200	0.241	241		
9.300	0.243	243						9.300	0.257	257						9.300	0.241	241		
9.400	0.243	243						9.400	0.257	257						9.400	0.240	240		
9.500	0.242	242						9.500	0.257	257						9.500	0.239	239		
9.600	0.242	242						9.600	0.257	257						9.600	0.239	239		
9.700	0.241	241						9.700	0.256	256						9.700	0.238	238		
9.800	0.241	241						9.800	0.256	256						9.800	0.238	238		
9.900	0.240	240						9.900	0.256	256						9.900	0.237	237		
10.000	0.240	240						10.000	0.255	255						10.000	0.236	236		
10.100	0.239	239						10.100	0.255	255						10.100	0.236	236		
10.200	0.239	239						10.200	0.255	255						10.200	0.235	235		
10.300	0.238	238						10.300	0.254	254						10.300	0.234	234		
10.400	0.238	238						10.400	0.254	254						10.400	0.234	234		
10.500	0.237	237						10.500	0.253	253						10.500	0.233	233		
10.600	0.236	236						10.600	0.253	253						10.600	0.233	233		
10.700	0.236	236						10.700	0.253	253						10.700	0.232	232		
10.800	0.235	235						10.800	0.252	252						10.800	0.231	231		
10.900	0.235	235						10.900	0.252	252						10.900	0.231	231		
11.000	0.234	234						11.000	0.251	251						11.000	0.230	230		
11.100	0.234	234						11.100	0.251	251						11.100	0.229	229		
11.200	0.233	233						11.200	0.251	251						11.200	0.229	229		
11.300	0.233	233						11.300	0.250	250						11.300	0.228	228		
11.400	0.232	232						11.400	0.250	250						11.400	0.228	228		
11.500	0.232	232						11.500	0.249	249						11.500	0.227	227		
11.600	0.231	231						11.600	0.249	249						11.600	0.226	226		
11.700	0.231	231						11.700	0.248	248						11.700	0.226	226		
11.800	0.230	230						11.800	0.248	248						11.800	0.225	225		

RUN 1

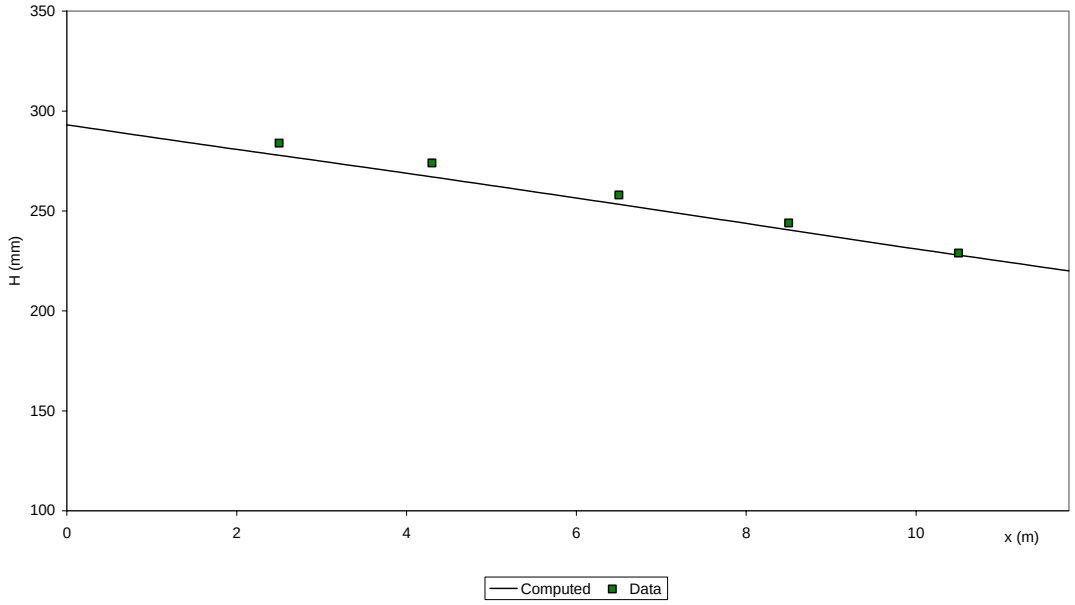
350
300
250
200
150
100
H (mm)
0
2
4
6
8
10
x (m)
Computed
Data

RUN 2

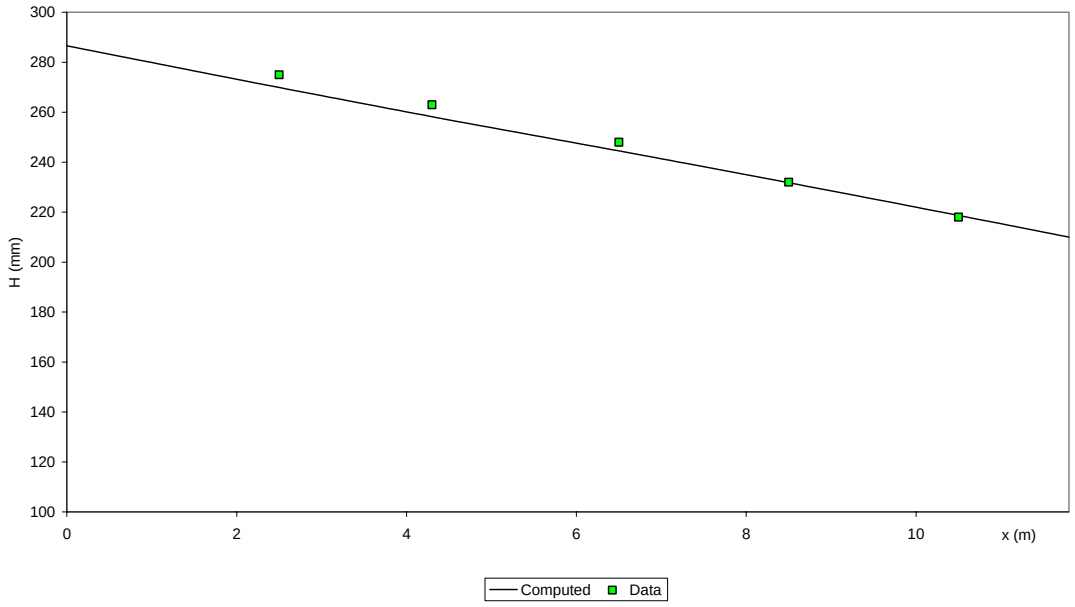
300
280
260
240
220
200
180
160
140
120
100
H (mm)
0
2
4
6
8
10
x (m)
Computed
Data

RUN 3

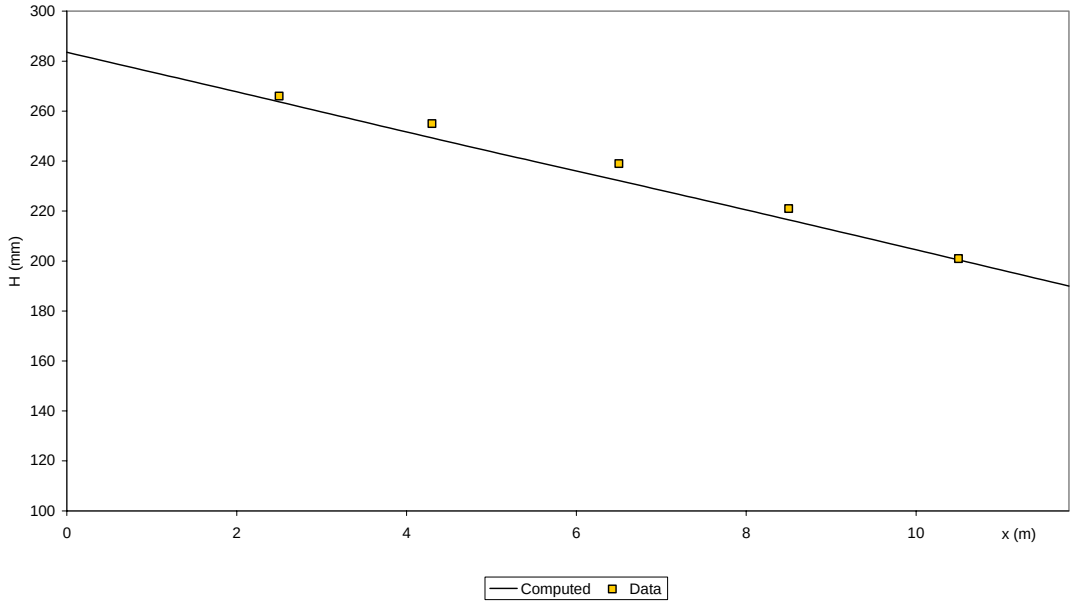
300
280
260
240
220
200
180
160
140
120
100
H (mm)
0
2
4
6
8
10
x (m)
Computed
Data

RUN 4

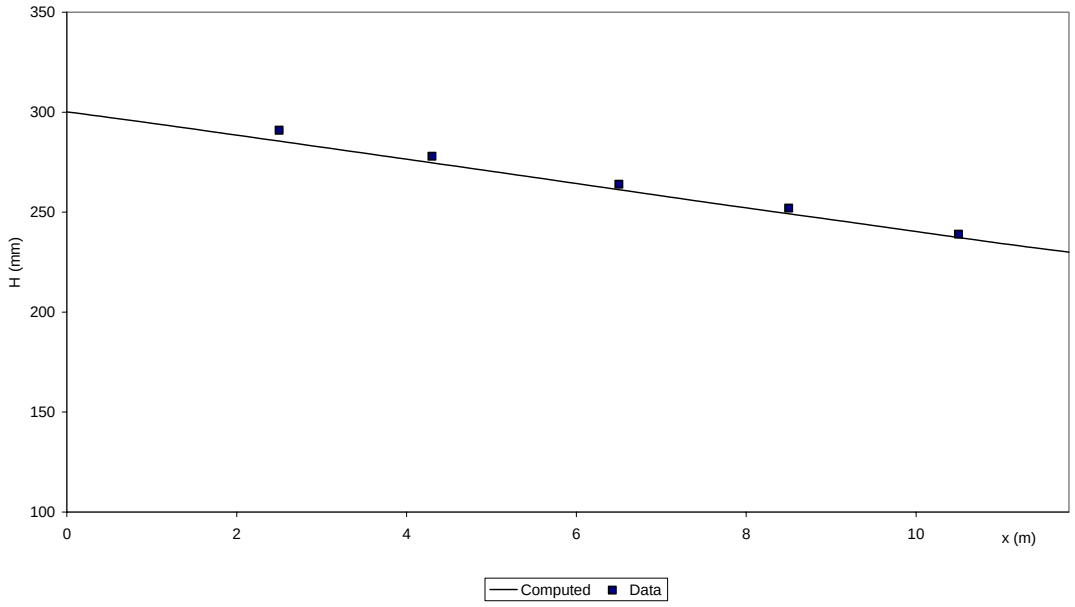
350
300
250
200
150
100
H (mm)
0
2
4
6
8
10
x (m)
Computed
Data

RUN 5

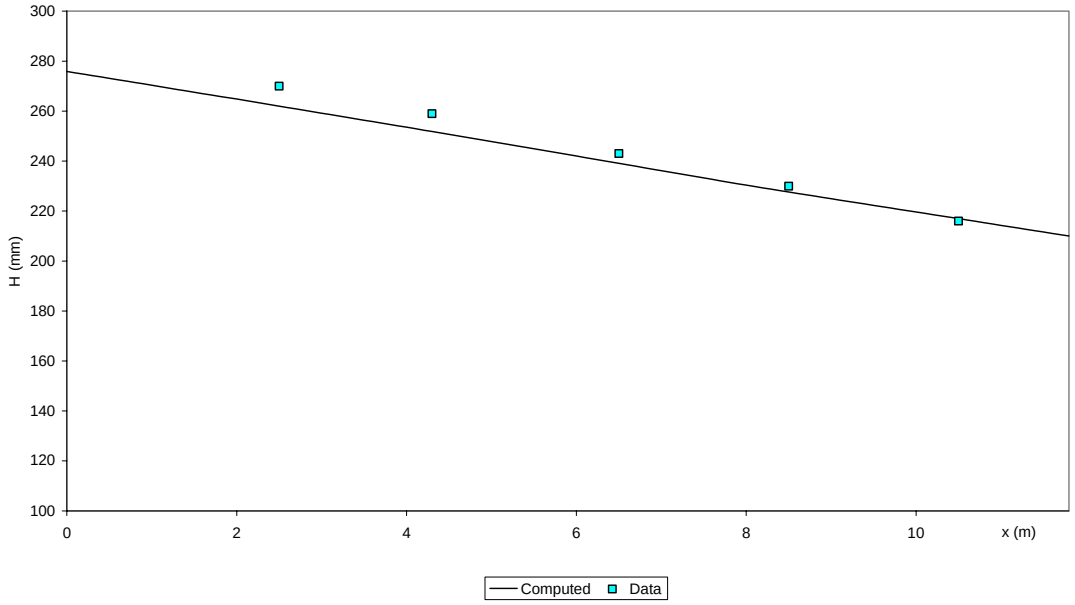
300
280
260
240
220
200
180
160
140
120
100
H (mm)
0
2
4
6
8
10
x (m)
Computed
Data

RUN 6

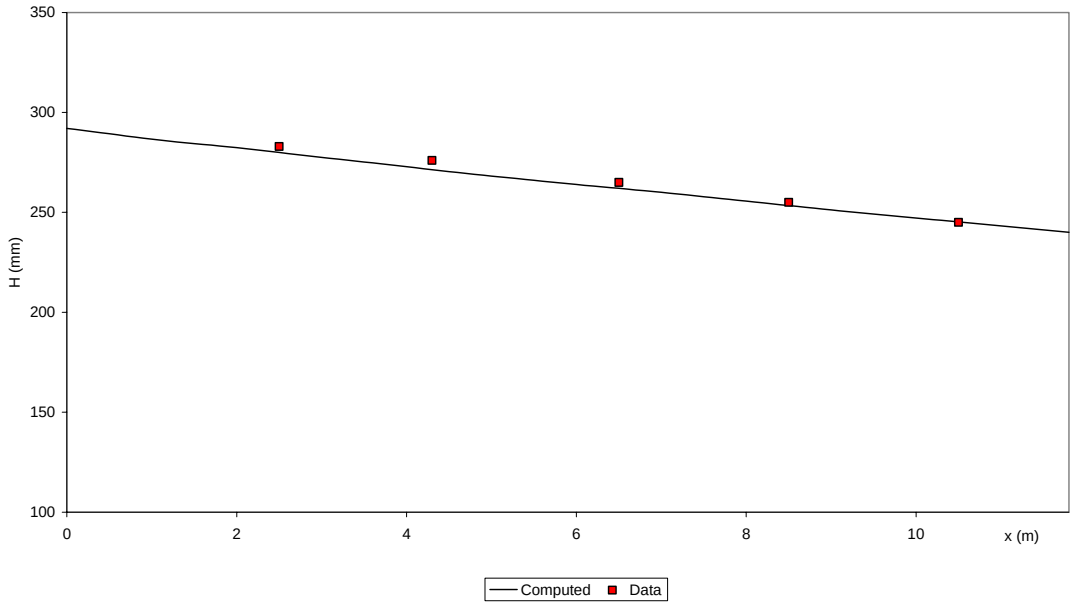
350
300
250
200
150
100
H (mm)
0
2
4
6
8
10
x (m)
Computed
Data

RUN 7

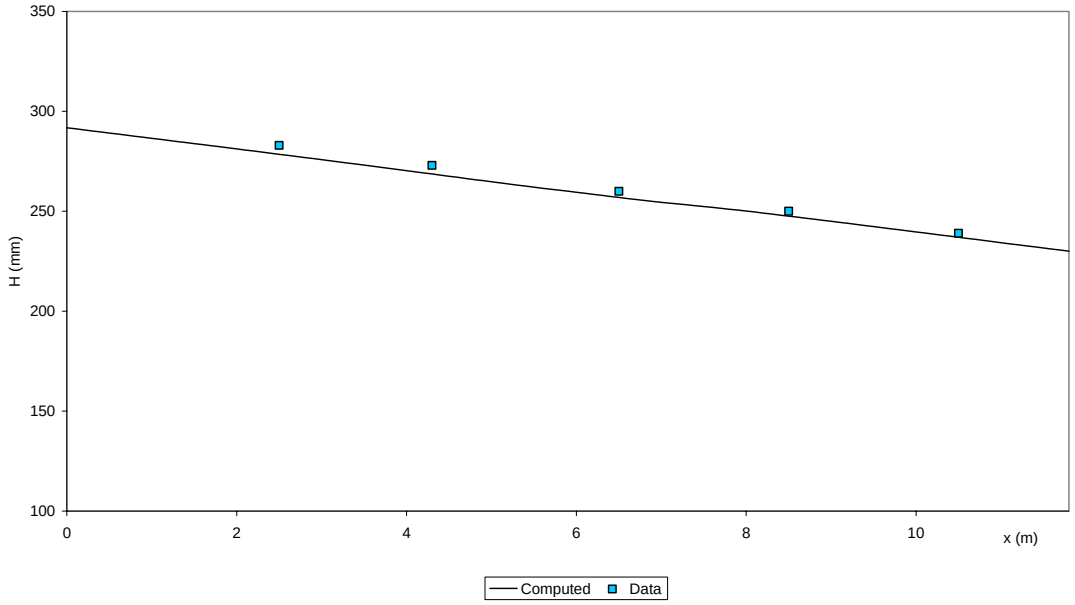
350
300
250
200
150
100
H (mm)
0
2
4
6
8
10
x (m)
Computed
Data

RUN 8

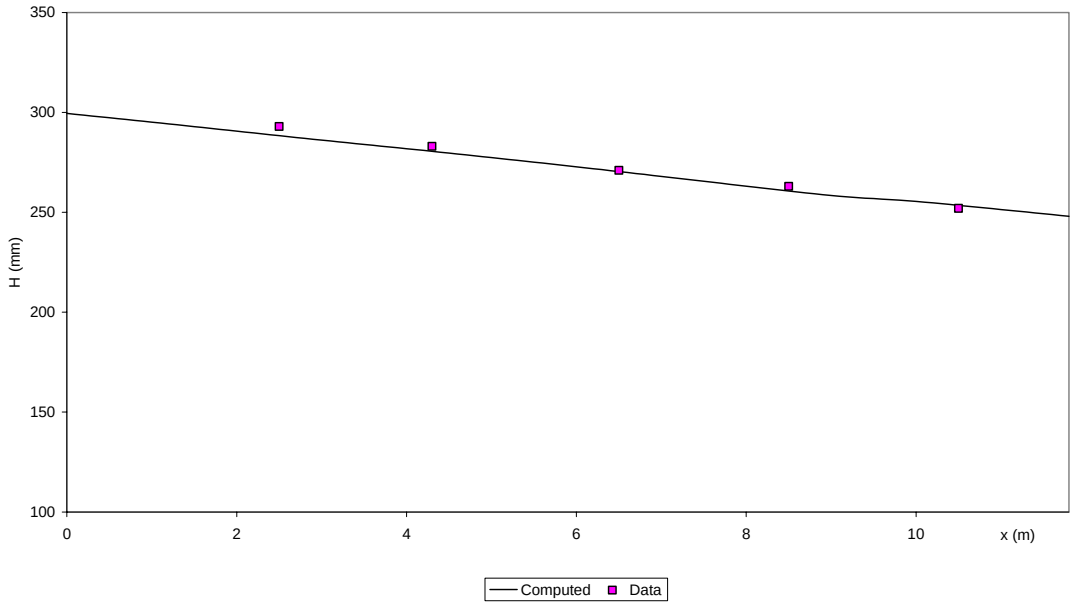
350
300
250
200
150
100
H (mm)
0
2
4
6
8
10
x (m)
Computed
Data

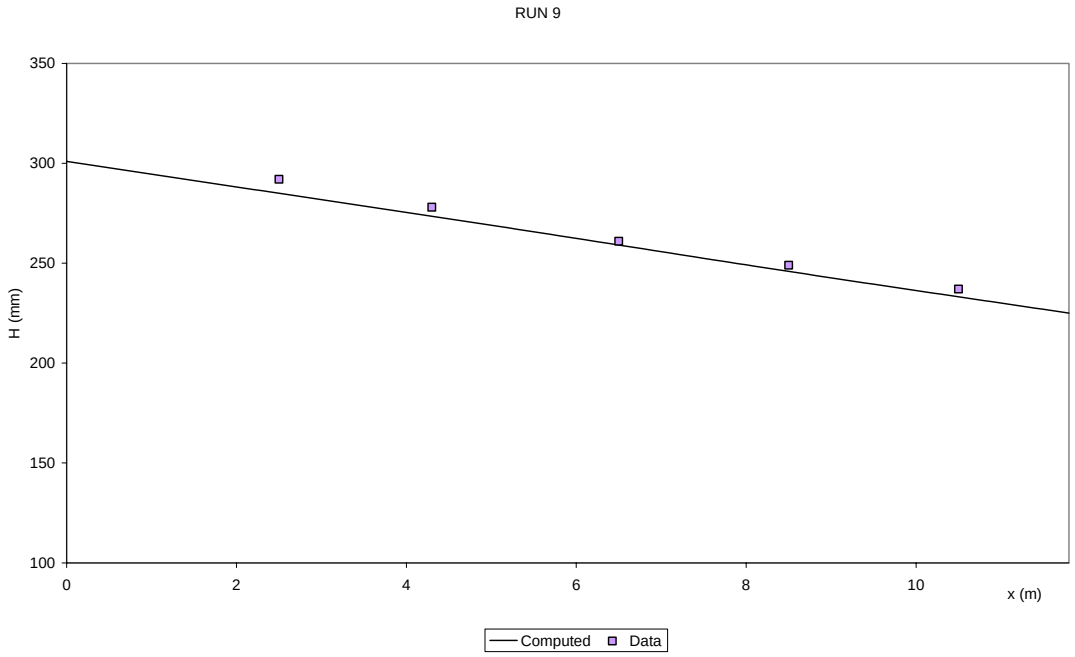
RUN 9
350
300
250
200
150
100
H (mm)
0
2
4
6
8
10
x (m)
Computed
Data

Bedload

RUN	G_s predicted (g/min)	G_s measured (g/min)
1	588	731
2	389	491
3	393	458
4	805	1432
5	65	54
6	105	64
7	298	371
8	236	151
9	1083	1068

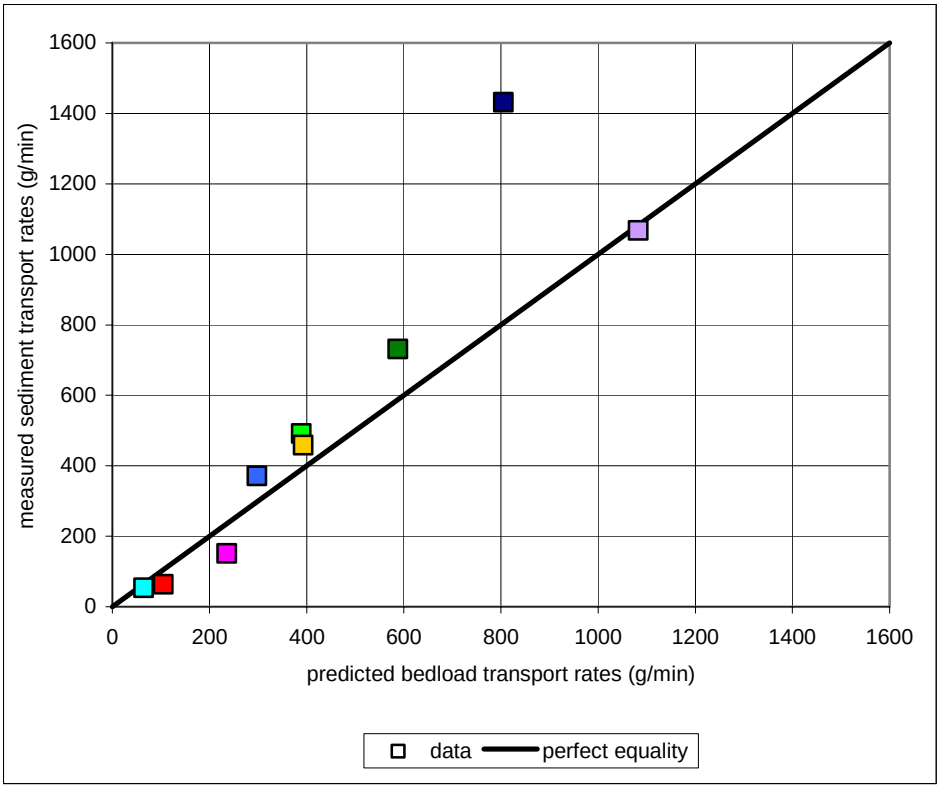

RUN 1

Computed		Data	
Di (mm)	**pi %**	**Di (mm)**	**pi %**
0.071	0.000	0.071	0.029
0.707	0.223	0.707	0.058
1.086	6.735	1.086	0.168
1.536	21.114	1.536	23.307
2.828	41.031	2.828	36.390
5.040	19.687	5.020	23.360
7.735	11.204	7.736	16.690
11.208	0.006	10.897	0.000

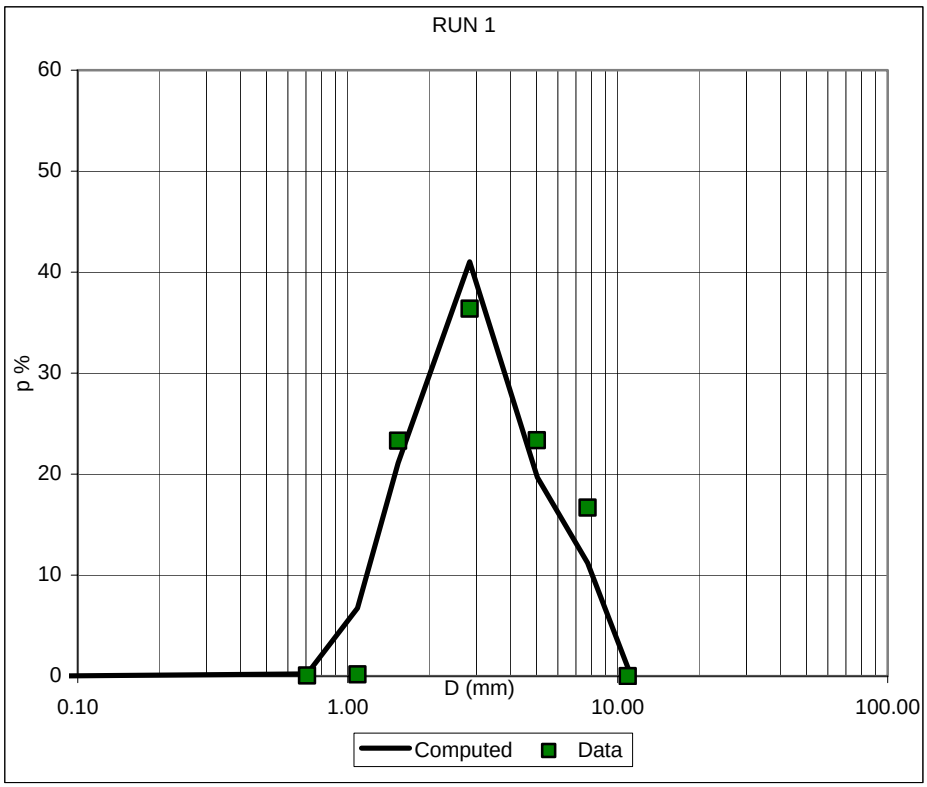

RUN 2

Computed		Data	
Di (mm)	**pi %**	**Di (mm)**	**pi %**
0.071	0.000	0.071	0.017
0.707	0.233	0.707	0.038
1.086	7.072	1.086	0.083
1.536	22.126	1.536	13.860
2.828	42.820	2.828	37.668
5.040	18.453	5.020	25.600
7.735	9.293	7.736	22.735
11.208	0.003	10.897	0.000

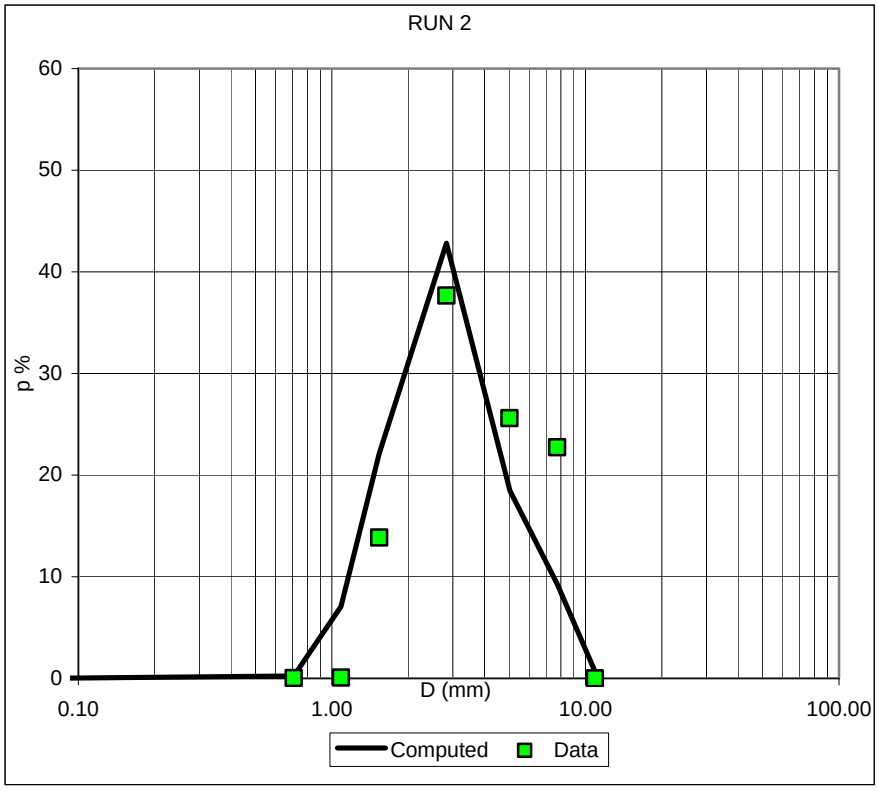

RUN 3

Computed		Data	
Di (mm)	**pi %**	**Di (mm)**	**pi %**
0.071	0.000	0.071	0.061
0.707	0.211	0.707	0.051
1.086	6.926	1.086	0.085
1.536	21.741	1.536	20.363
2.828	42.255	2.828	33.343
5.040	18.963	5.020	27.470
7.735	9.900	7.736	18.627
11.208	0.004	10.897	0.000

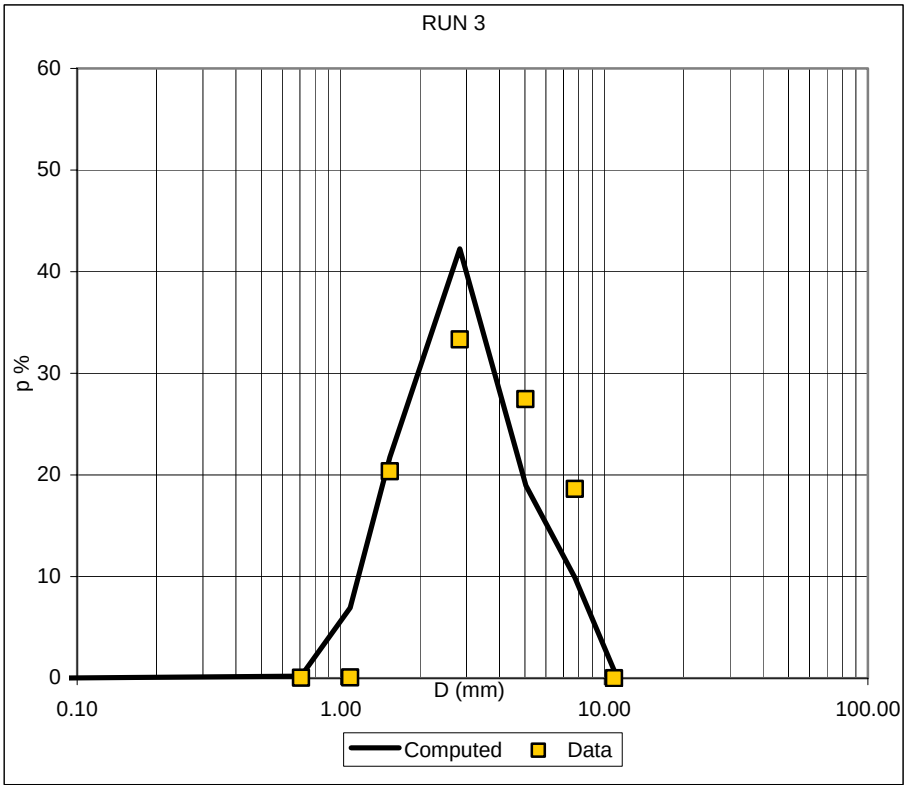

RUN 4

Computed		Data	
Di (mm)	**pi %**	**Di (mm)**	**pi %**
0.071	0.000	0.071	0.042
0.707	0.210	0.707	0.034
1.086	6.606	1.086	0.059
1.536	20.754	1.536	12.787
2.828	40.443	2.828	41.284
5.040	19.512	5.020	25.693
7.735	12.468	7.736	20.102
11.208	0.008	10.897	0.000

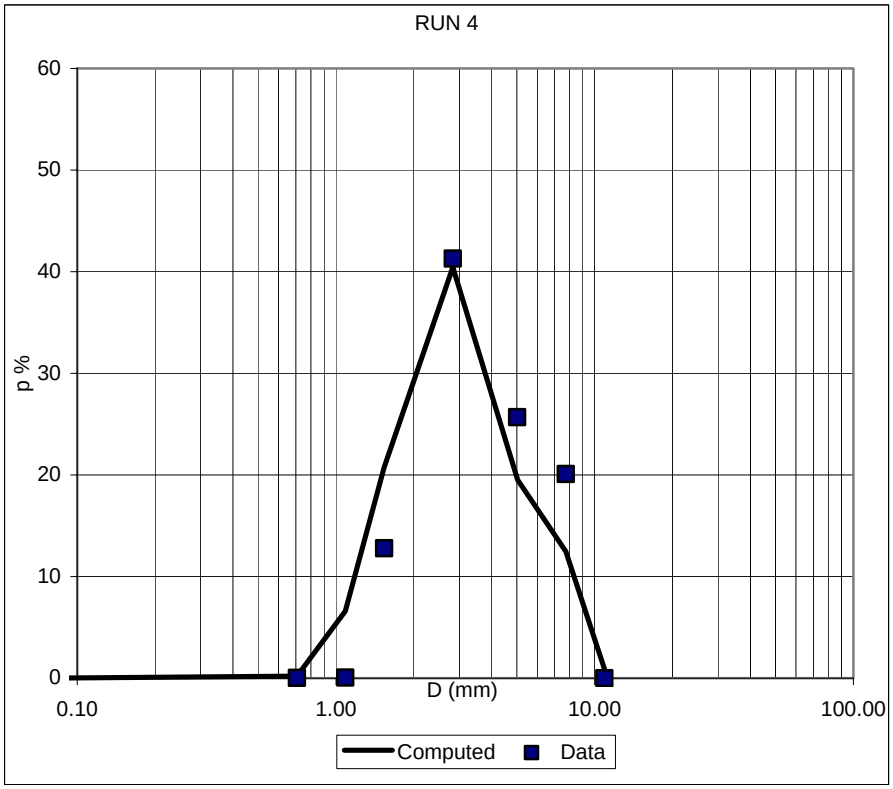

RUN 5

Computed		Data	
Di (mm)	pi %	Di (mm)	pi %
0.071	0.000	0.071	0.018
0.707	0.303	0.707	0.154
1.086	9.162	1.086	0.526
1.536	28.013	1.536	32.110
2.828	51.795	2.828	39.674
5.040	10.727	5.020	15.250
7.735	0.000	7.736	12.267
11.208	0.000	10.897	0.000

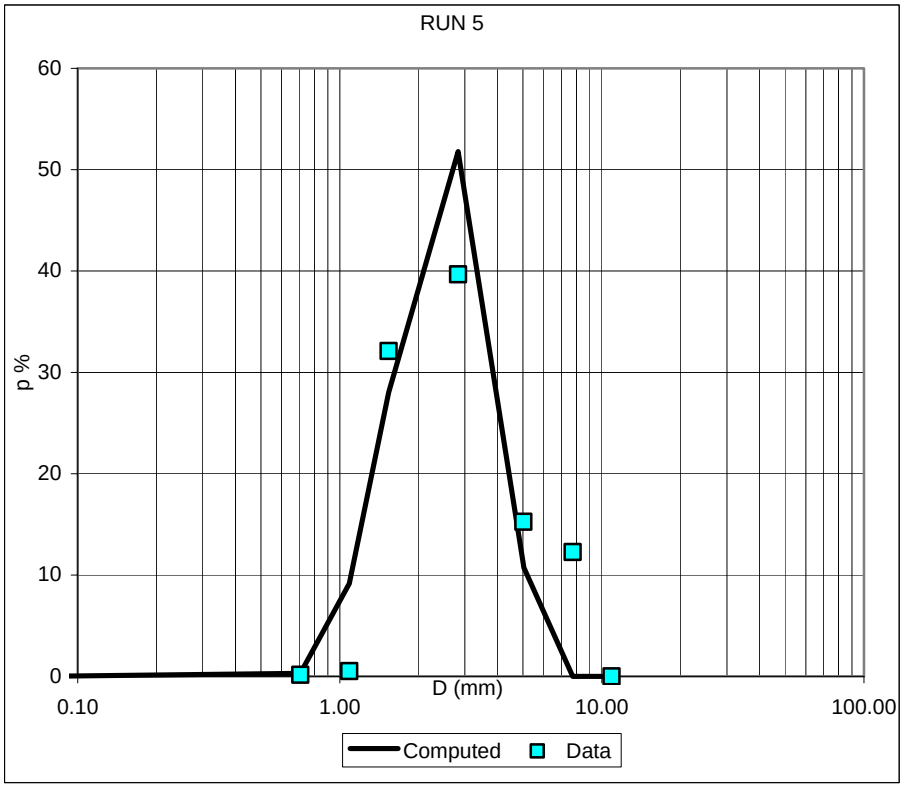

RUN 6

Computed		Data	
Di (mm)	pi %	Di (mm)	pi %
0.071	0.000	0.071	0.019
0.707	0.336	0.707	0.079
1.086	8.553	1.086	0.098
1.536	26.186	1.536	21.883
2.828	49.065	2.828	38.525
5.040	14.954	5.020	19.991
7.735	0.905	7.736	19.406
11.208	0.000	10.897	0.000

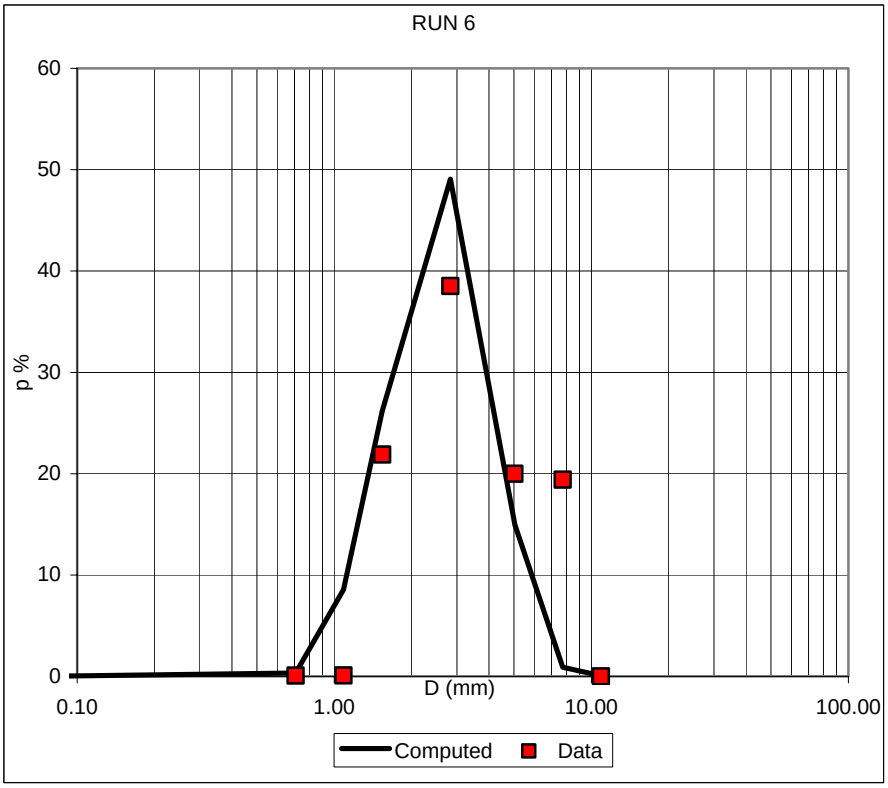

RUN 7

Computed		Data	
Di (mm)	**pi %**	**Di (mm)**	**pi %**
0.071	0.000	0.071	0.017
0.707	0.274	0.707	0.011
1.086	7.450	1.086	0.060
1.536	23.195	1.536	9.324
2.828	44.411	2.828	40.876
5.040	17.067	5.020	28.478
7.735	7.602	7.736	21.234
11.208	0.001	10.897	0.000

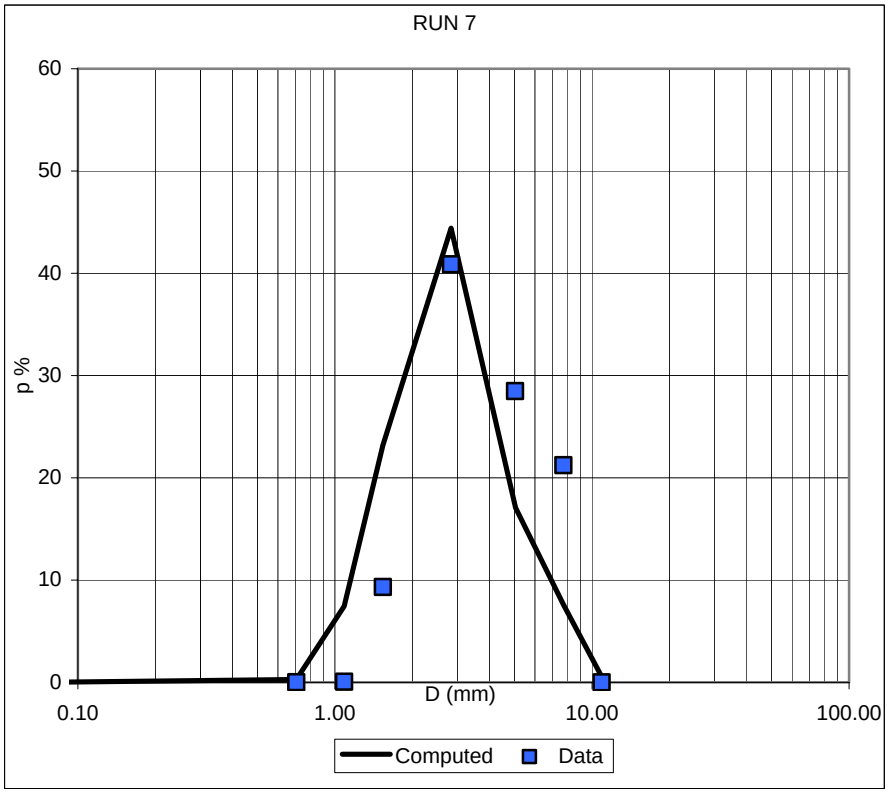

RUN 8

Computed		Data	
Di (mm)	pi %	Di (mm)	pi %
0.071	0.000	0.071	0.030
0.707	0.331	0.707	0.072
1.086	7.848	1.086	0.299
1.536	24.169	1.536	34.776
2.828	45.521	2.828	31.132
5.040	16.468	5.020	15.545
7.735	5.662	7.736	18.146
11.208	0.000	10.897	0.000

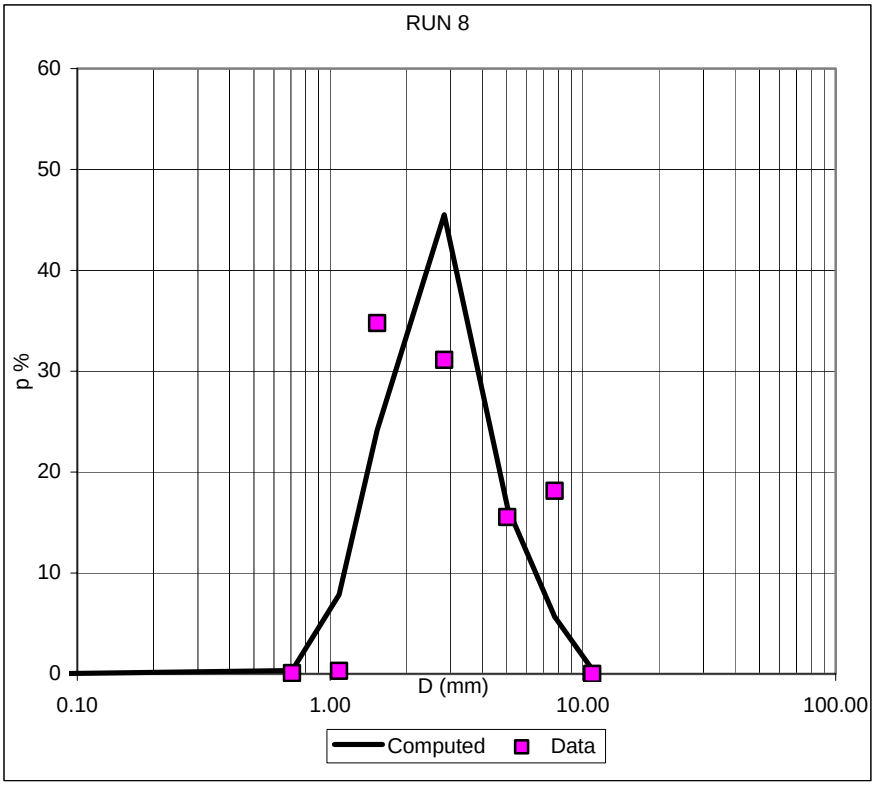

RUN 9

Computed		Data	
Di (mm)	pi %	Di (mm)	pi %
0.071	0.000	0.071	0.050
0.707	0.263	0.707	0.056
1.086	6.717	1.086	0.179
1.536	20.883	1.536	16.889
2.828	40.203	2.828	36.319
5.040	18.885	5.020	23.731
7.735	13.039	7.736	22.776
11.208	0.010	10.897	0.000

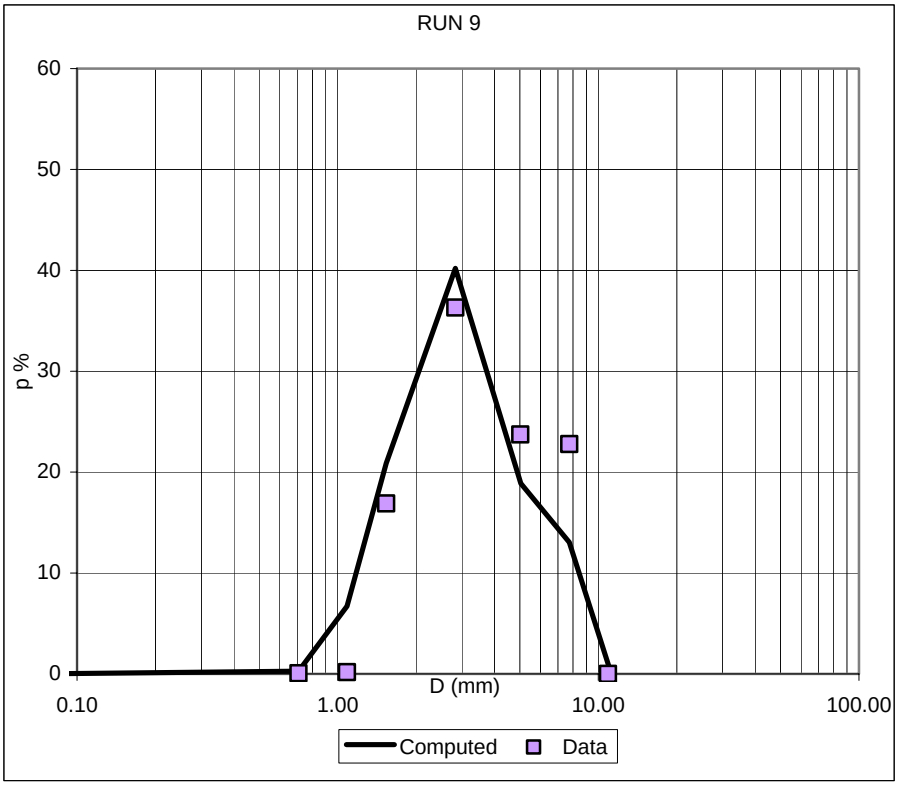

Bed surface

RUN 1

Section 1, x = 2.5 m

Computed		Data	
Di (mm)	Fi %	Di (mm)	Fi %
0.071	0.000	0.071	0.000
0.707	0.160	0.707	0.010
1.086	4.917	1.086	0.103
1.536	15.732	1.536	10.864
2.828	31.733	2.828	33.169
5.020	23.988	5.020	26.721
7.736	23.443	7.736	29.134
10.897	0.026	10.897	0.000

Section 2, x = 4.3 m

Computed		Data	
Di (mm)	Fi %	Di (mm)	Fi %
0.071	0.000	0.071	0.002
0.707	0.166	0.707	0.024
1.086	5.081	1.086	0.126
1.536	16.277	1.536	5.756
2.828	32.878	2.828	31.410
5.020	21.968	5.020	31.706
7.736	23.597	7.736	30.974
10.897	0.034	10.897	0.000

Section 3, x = 6.5 m

Computed		Data	
Di (mm)	Fi %	Di (mm)	Fi %
0.071	0.000	0.071	0.000
0.707	0.163	0.707	0.010
1.086	5.056	1.086	0.052
1.536	16.182	1.536	11.333
2.828	32.619	2.828	34.214
5.020	20.741	5.020	25.639
7.736	25.200	7.736	28.752
10.897	0.038	10.897	0.000

Section 4, x = 8.5 m

Computed		Data	
Di (mm)	Fi %	Di (mm)	Fi %
0.071	0.000	0.071	0.000
0.707	0.159	0.707	0.010
1.086	4.945	1.086	0.068
1.536	15.810	1.536	14.125
2.828	31.835	2.828	33.544
5.020	19.691	5.020	25.347
7.736	27.525	7.736	26.906
10.897	0.035	10.897	0.000

Section 5, x = 10.5 m

Computed		Data	
Di (mm)	Fi %	Di (mm)	Fi %
0.071	0.000	0.071	0.119
0.707	0.157	0.707	0.017
1.086	4.890	1.086	0.071
1.536	15.621	1.536	14.947
2.828	31.411	2.828	29.207
5.020	21.285	5.020	23.629
7.736	26.610	7.736	32.010
10.897	0.026	10.897	0.000

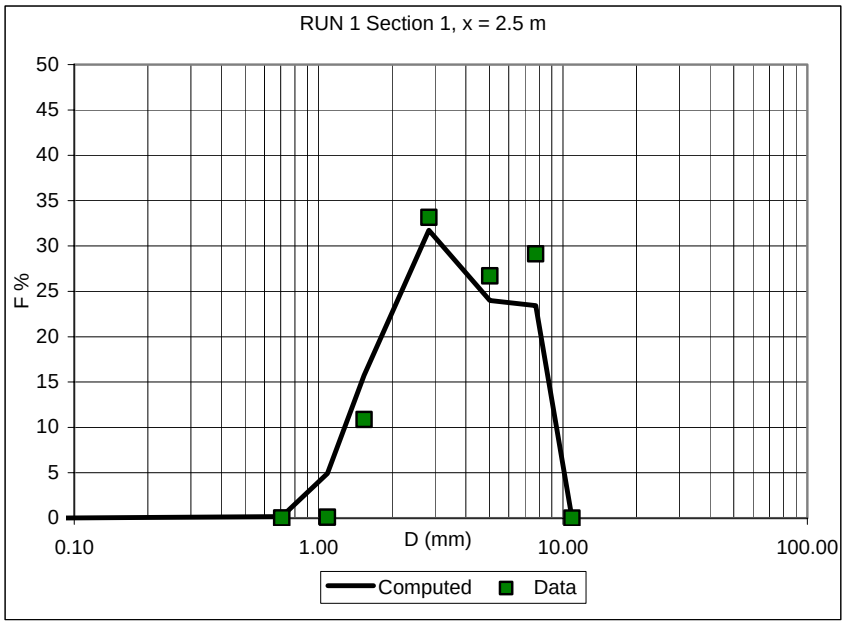
RUN 1 Section 1, x = 2.5 m
50
45
40
35
30
25
20
15
10
5
0
F %
0.10
1.00
10.00
100.00
D (mm)
Computed
Data

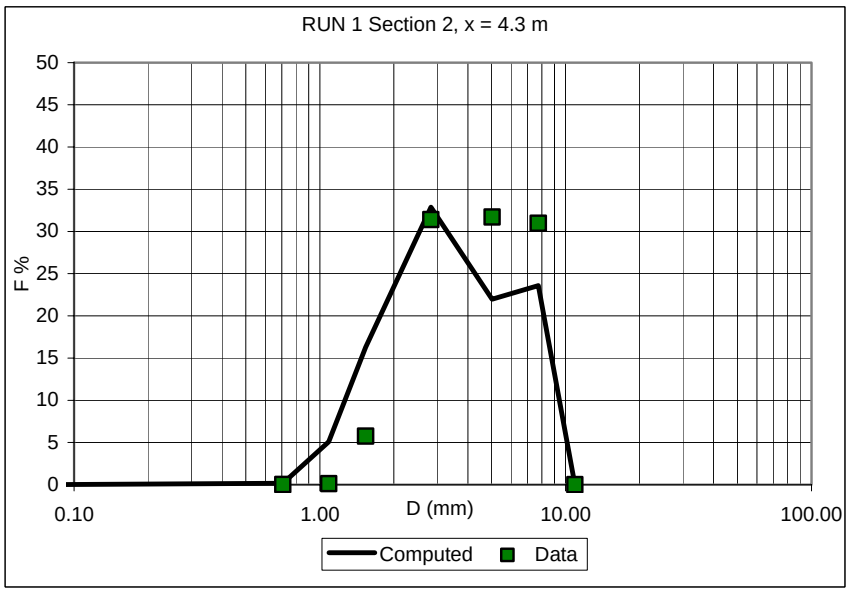
RUN 1 Section 2, x = 4.3 m
50
45
40
35
30
25
20
15
10
5
0
F %
0.10
1.00
10.00
100.00
D (mm)
Computed
Data

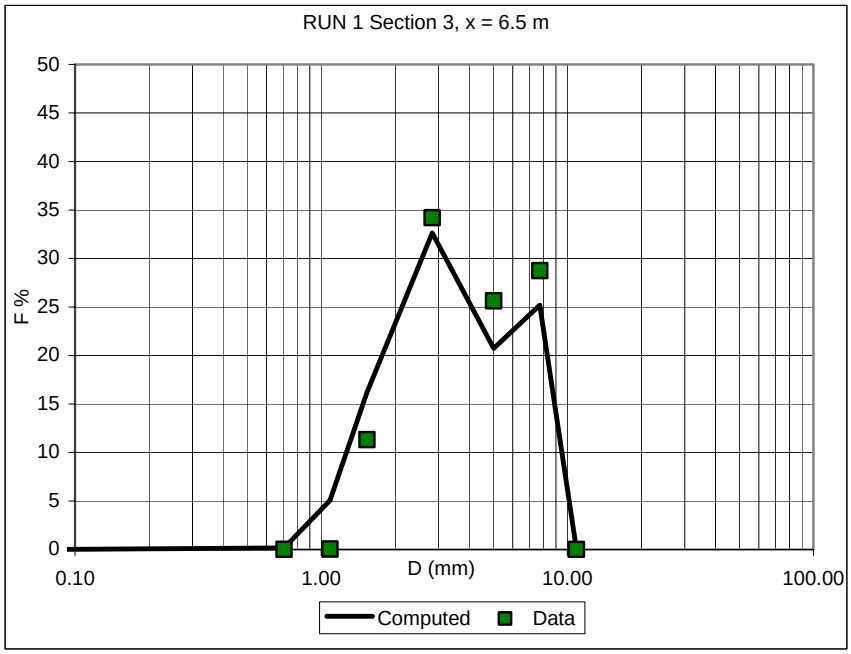
RUN 1 Section 3, x = 6.5 m
50
45
40
35
30
25
20
15
10
5
0
F %
0.10
1.00
10.00
100.00
D (mm)
Computed
Data

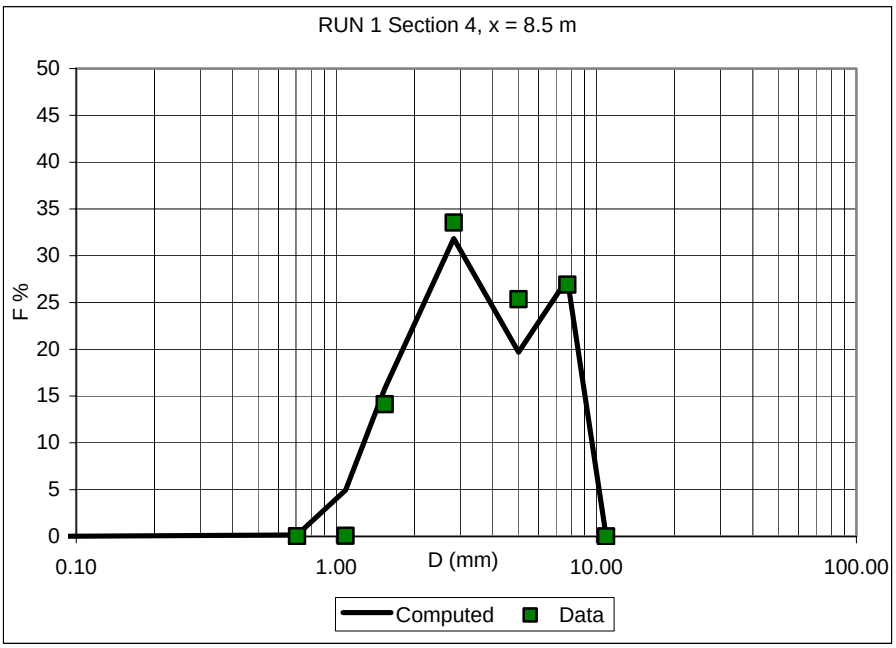
RUN 1 Section 4, x = 8.5 m
50
45
40
35
30
25
20
15
10
5
0
F %
0.10
1.00
10.00
100.00
D (mm)
Computed
Data

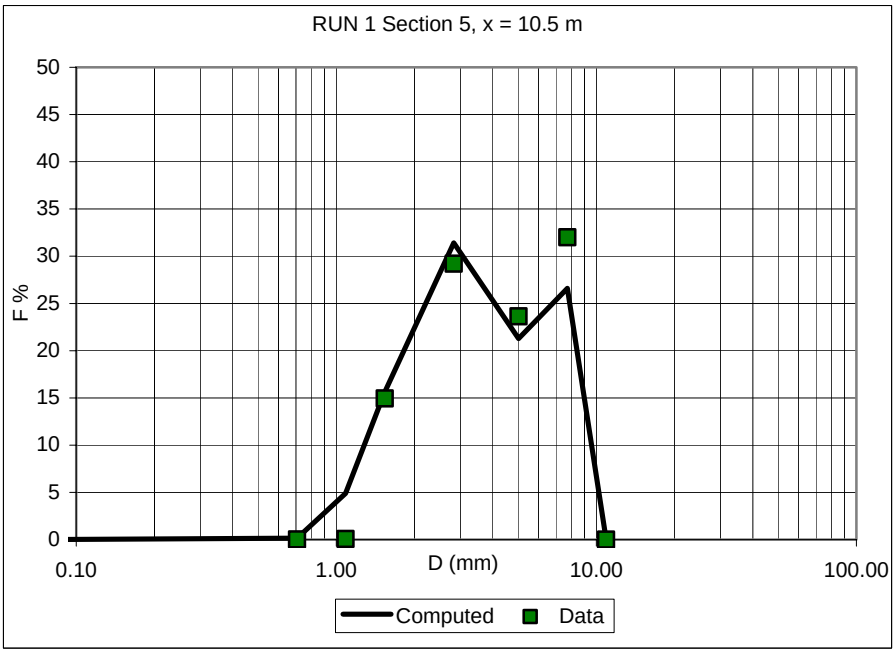
RUN 1 Section 5, x = 10.5 m
50
45
40
35
30
25
20
15
10
5
0
F %
0.10
1.00
10.00
100.00
D (mm)
Computed
Data

RUN 2

Section 1, x = 2.5 m

Computed		Data	
Di (mm)	**Fi %**	**Di (mm)**	**Fi %**
0.071	0.000	0.071	0.008
0.707	0.153	0.707	0.041
1.086	4.779	1.086	0.112
1.536	15.300	1.536	17.182
2.828	30.776	2.828	38.974
5.020	21.634	5.020	23.537
7.736	27.332	7.736	20.147
10.897	0.026	10.897	0.000

Section 2, x = 4.3 m

Computed		Data	
Di (mm)	**Fi %**	**Di (mm)**	**Fi %**
0.071	0.000	0.071	0.005
0.707	0.152	0.707	0.110
1.086	4.753	1.086	0.293
1.536	15.213	1.536	19.606
2.828	30.597	2.828	31.234
5.020	24.583	5.020	20.668
7.736	24.679	7.736	28.084
10.897	0.023	10.897	0.000

Section 3, x = 6.5 m

Computed		Data	
Di (mm)	**Fi %**	**Di (mm)**	**Fi %**
0.071	0.000	0.071	0.009
0.707	0.159	0.707	0.059
1.086	4.974	1.086	0.297
1.536	15.960	1.536	19.556
2.828	32.343	2.828	28.426
5.020	22.486	5.020	23.594
7.736	24.048	7.736	27.845
10.897	0.029	10.897	0.214

Section 4, x = 8.5 m

Computed		Data	
Di (mm)	**Fi %**	**Di (mm)**	**Fi %**
0.071	0.000	0.071	0.003
0.707	0.161	0.707	0.031
1.086	5.033	1.086	0.135
1.536	16.119	1.536	13.928
2.828	32.597	2.828	31.640
5.020	21.670	5.020	23.145
7.736	24.383	7.736	31.117
10.897	0.036	10.897	0.000

Section 5, x = 10.5 m

Computed		Data	
Di (mm)	**Fi %**	**Di (mm)**	**Fi %**
0.071	0.000	0.071	0.007
0.707	0.160	0.707	0.045
1.086	4.993	1.086	0.239
1.536	15.982	1.536	15.355
2.828	32.285	2.828	28.934
5.020	20.995	5.020	22.976
7.736	25.549	7.736	32.443
10.897	0.038	10.897	0.000

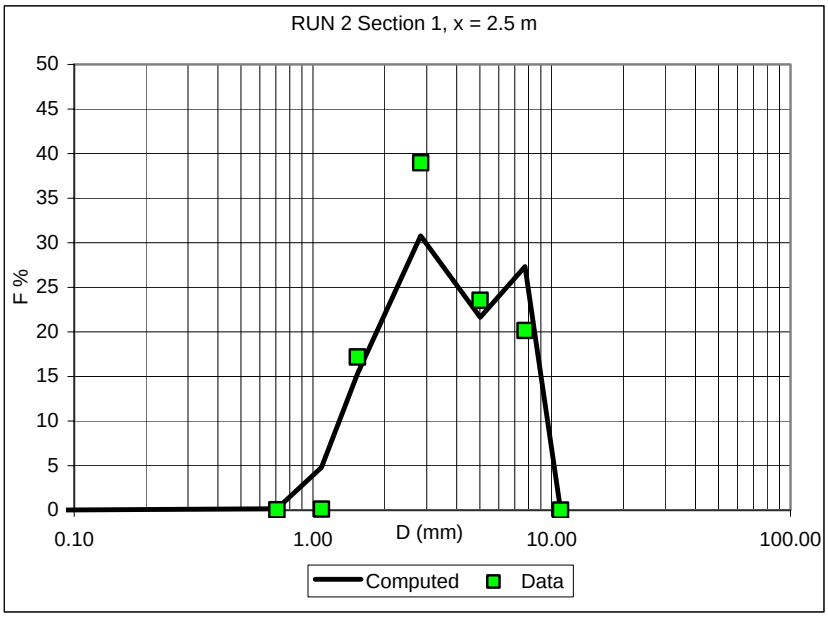
RUN 2 Section 1, x = 2.5 m
50
45
40
35
30
25
20
15
10
5
0
F %
0.10
1.00
10.00
100.00
D (mm)
Computed
Data

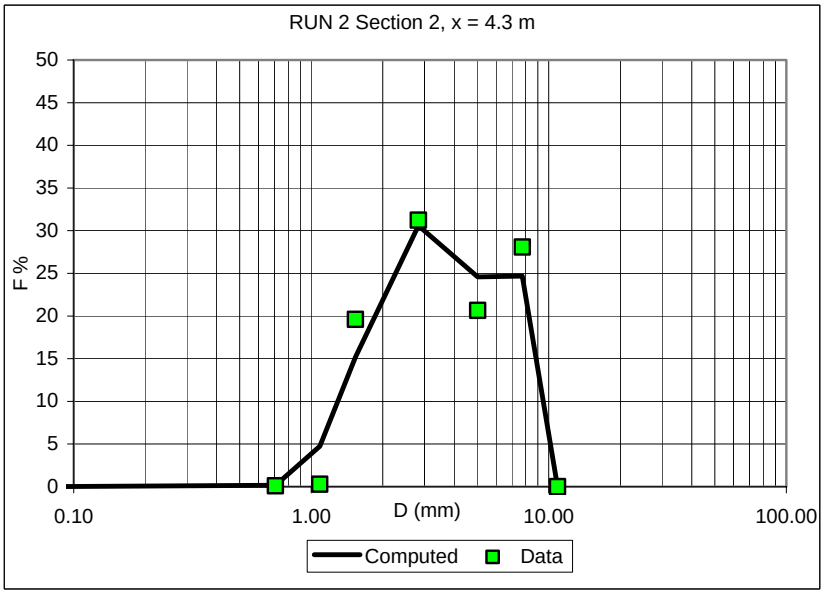
RUN 2 Section 2, x = 4.3 m
50
45
40
35
30
25
20
15
10
5
0
F %
0.10
1.00
10.00
100.00
D (mm)
Computed
Data

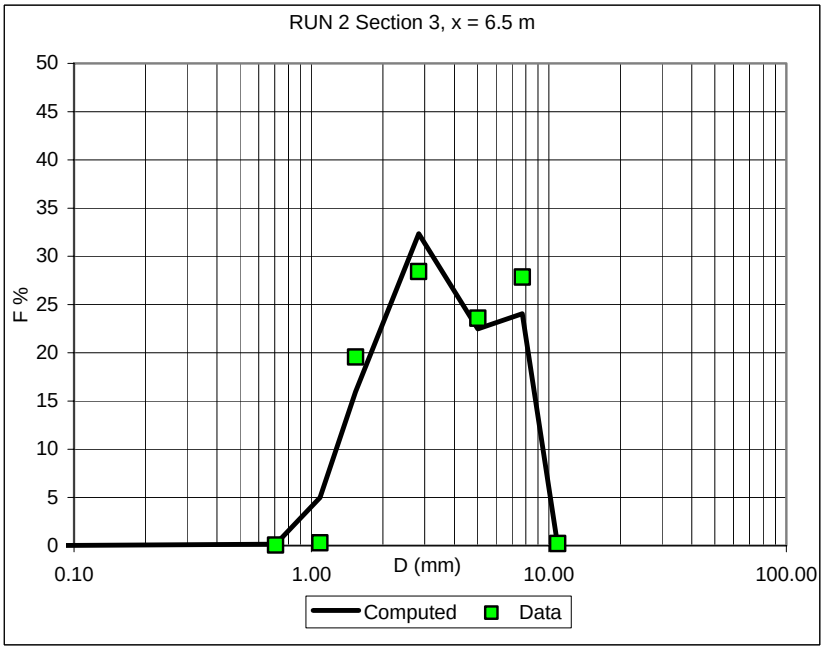
RUN 2 Section 3, x = 6.5 m
50
45
40
35
30
25
20
15
10
5
0
F %
0.10
1.00
10.00
100.00
D (mm)
Computed
Data

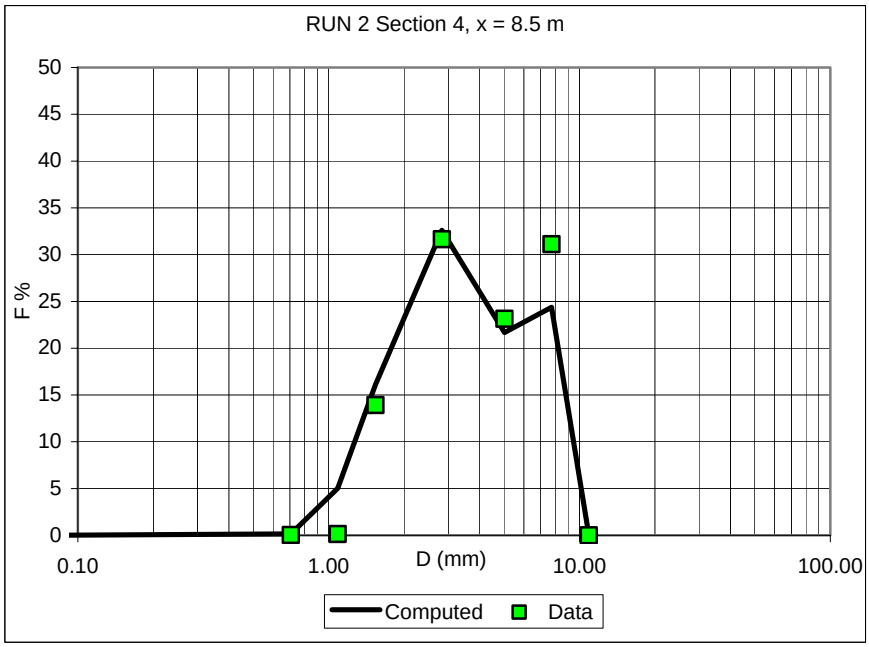
RUN 2 Section 4, x = 8.5 m
50
45
40
35
30
25
20
15
10
5
0
F %
0.10
1.00
10.00
100.00
D (mm)
Computed
Data

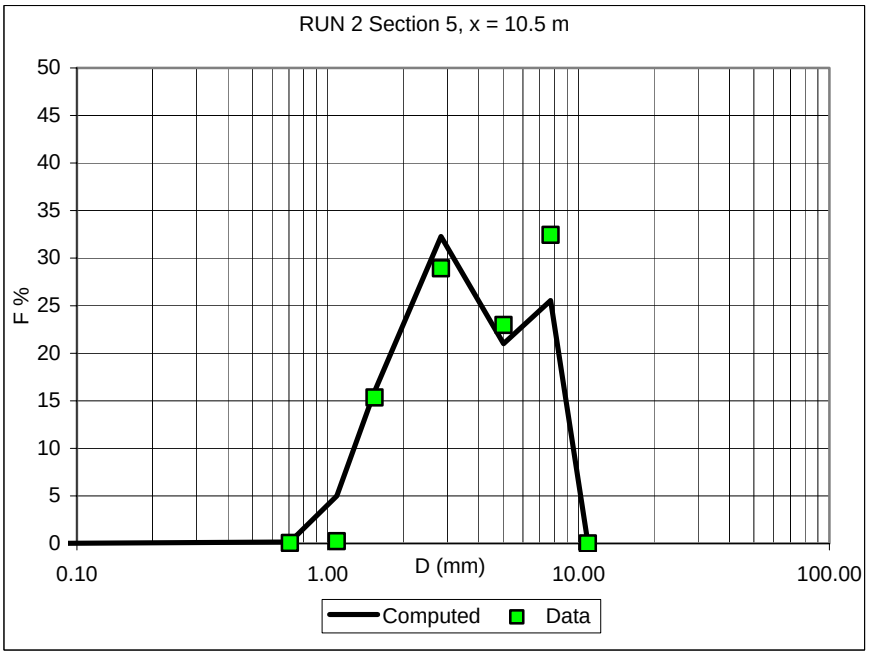
RUN 2 Section 5, x = 10.5 m
50
45
40
35
30
25
20
15
10
5
0
F %
0.10
1.00
10.00
100.00
D (mm)
Computed
Data

RUN 3

Section 1, x = 2.5 m

Computed		Data	
Di (mm)	Fi %	Di (mm)	Fi %
0.071	0.000	0.071	0.002
0.707	0.139	0.707	0.002
1.086	4.743	1.086	0.007
1.536	15.242	1.536	4.230
2.828	30.784	2.828	27.594
5.020	23.605	5.020	33.223
7.736	25.448	7.736	34.943
10.897	0.039	10.897	0.000

Section 2, x = 4.3 m

Computed		Data	
Di (mm)	Fi %	Di (mm)	Fi %
0.071	0.000	0.071	0.008
0.707	0.137	0.707	0.020
1.086	4.623	1.086	0.120
1.536	14.859	1.536	15.901
2.828	29.973	2.828	33.106
5.020	24.701	5.020	22.683
7.736	25.670	7.736	28.162
10.897	0.036	10.897	0.000

Section 3, x = 6.5 m

Computed		Data	
Di (mm)	Fi %	Di (mm)	Fi %
0.071	0.000	0.071	0.003
0.707	0.144	0.707	0.021
1.086	4.816	1.086	0.198
1.536	15.494	1.536	13.284
2.828	31.487	2.828	26.686
5.020	22.380	5.020	26.825
7.736	25.650	7.736	32.983
10.897	0.029	10.897	0.000

Section 4, x = 8.5 m

Computed		Data	
Di (mm)	Fi %	Di (mm)	Fi %
0.071	0.000	0.071	0.003
0.707	0.146	0.707	0.009
1.086	4.882	1.086	0.108
1.536	15.687	1.536	13.564
2.828	31.878	2.828	25.187
5.020	21.129	5.020	24.989
7.736	26.254	7.736	36.141
10.897	0.024	10.897	0.000

Section 5, x = 10.5 m

Computed		Data	
Di (mm)	Fi %	Di (mm)	Fi %
0.071	0.000	0.071	0.003
0.707	0.142	0.707	0.000
1.086	4.831	1.086	0.023
1.536	15.516	1.536	9.223
2.828	31.520	2.828	34.495
5.020	20.109	5.020	25.622
7.736	27.852	7.736	30.634
10.897	0.029	10.897	0.000

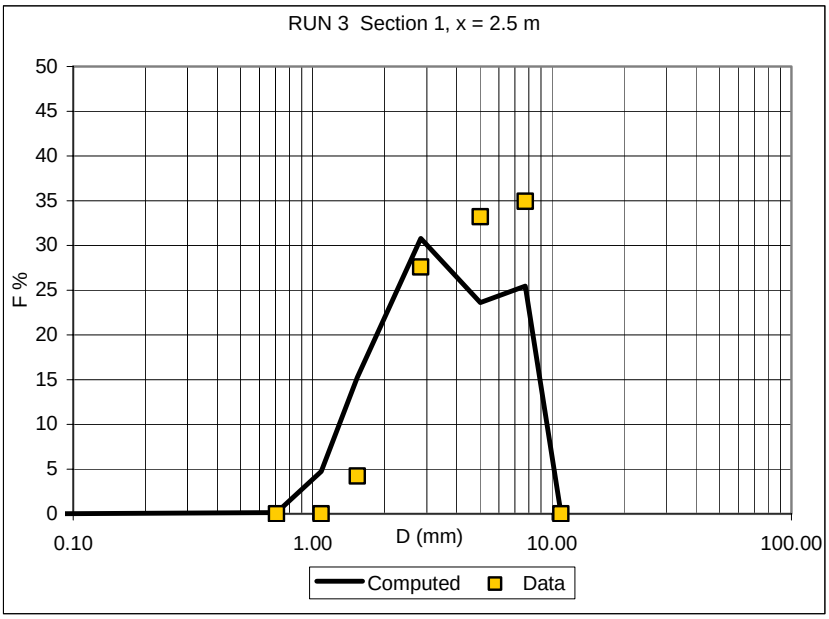
RUN 3 Section 1, x = 2.5 m
F %
D (mm)
0.10
1.00
10.00
100.00
Computed
Data

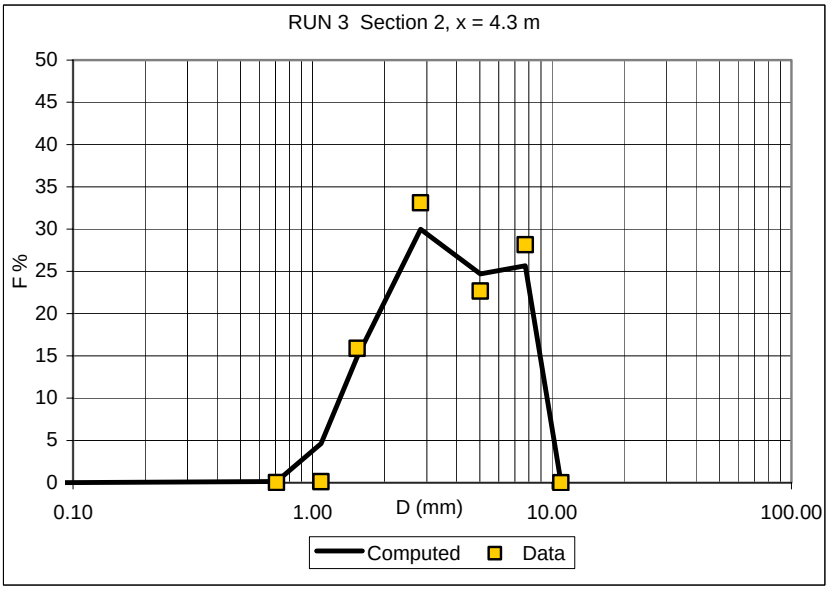
RUN 3 Section 2, x = 4.3 m
F %
D (mm)
0.10
1.00
10.00
100.00
Computed
Data

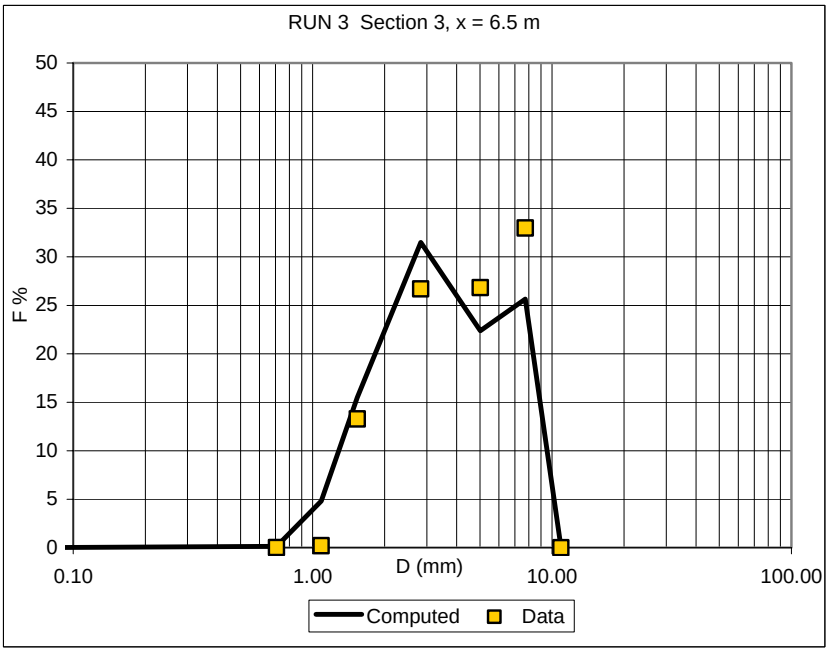
RUN 3 Section 3, x = 6.5 m
F %
D (mm)
0.10
1.00
10.00
100.00
Computed
Data

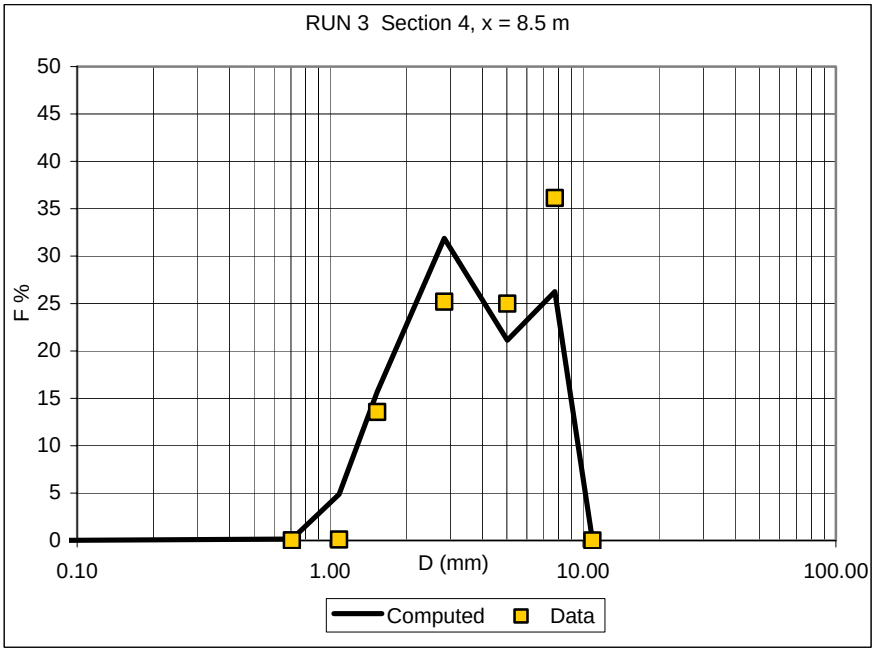
RUN 3 Section 4, x = 8.5 m
50
45
40
35
30
25
20
15
10
5
0
F %
0.10
1.00
10.00
100.00
D (mm)
Computed
Data

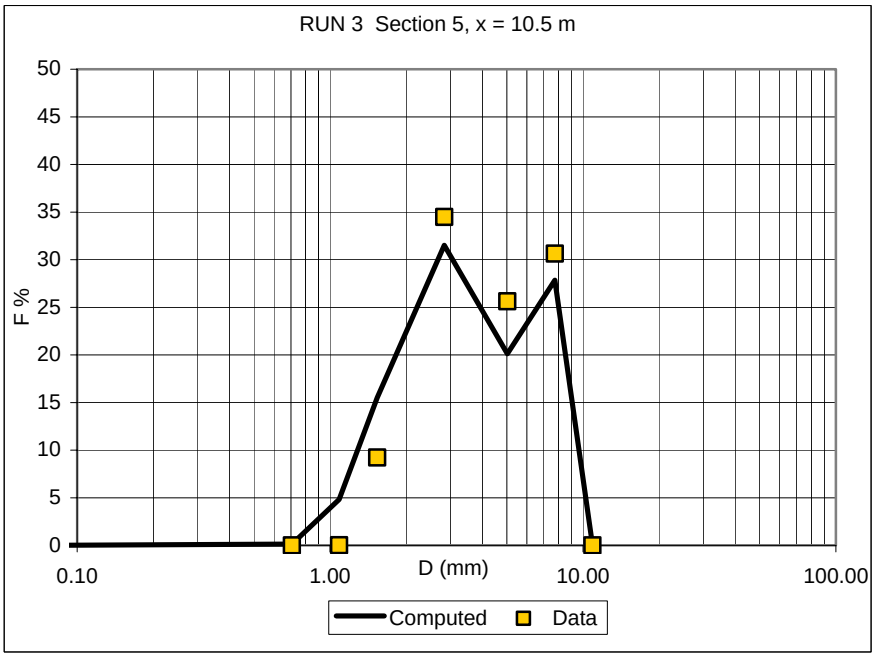
RUN 3 Section 5, x = 10.5 m
50
45
40
35
30
25
20
15
10
5
0
F %
0.10
1.00
10.00
100.00
D (mm)
Computed
Data

RUN 4

Section 1, x = 2.5 m

Computed		Data	
Di (mm)	Fi %	Di (mm)	Fi %
0.071	0.000	0.071	0.031
0.707	0.160	0.707	0.026
1.086	5.142	1.086	0.061
1.536	16.477	1.536	6.614
2.828	33.439	2.828	26.794
5.020	21.064	5.020	28.009
7.736	23.685	7.736	38.466
10.897	0.033	10.897	0.000

Section 2, x = 4.3 m

Computed		Data	
Di (mm)	Fi %	Di (mm)	Fi %
0.071	0.000	0.071	0.000
0.707	0.158	0.707	0.053
1.086	5.123	1.086	0.175
1.536	16.444	1.536	10.997
2.828	33.233	2.828	27.984
5.020	20.058	5.020	22.984
7.736	24.951	7.736	37.807
10.897	0.033	10.897	0.000

Section 3, x = 6.5 m

Computed		Data	
Di (mm)	Fi %	Di (mm)	Fi %
0.071	0.000	0.071	0.000
0.707	0.156	0.707	0.302
1.086	5.056	1.086	0.721
1.536	16.212	1.536	18.333
2.828	32.600	2.828	25.882
5.020	18.952	5.020	18.803
7.736	26.996	7.736	35.959
10.897	0.028	10.897	0.000

Section 4, x = 8.5 m

Computed		Data	
Di (mm)	Fi %	Di (mm)	Fi %
0.071	0.000	0.071	0.003
0.707	0.156	0.707	0.015
1.086	5.026	1.086	0.195
1.536	16.066	1.536	8.215
2.828	32.070	2.828	26.989
5.020	20.938	5.020	33.225
7.736	25.712	7.736	31.359
10.897	0.030	10.897	0.000

Section 5, x = 10.5 m

Computed		Data	
Di (mm)	Fi %	Di (mm)	Fi %
0.071	0.000	0.071	0.003
0.707	0.155	0.707	0.015
1.086	4.947	1.086	0.195
1.536	15.734	1.536	8.215
2.828	31.142	2.828	26.989
5.020	25.203	5.020	28.258
7.736	22.789	7.736	36.325
10.897	0.029	10.897	0.000

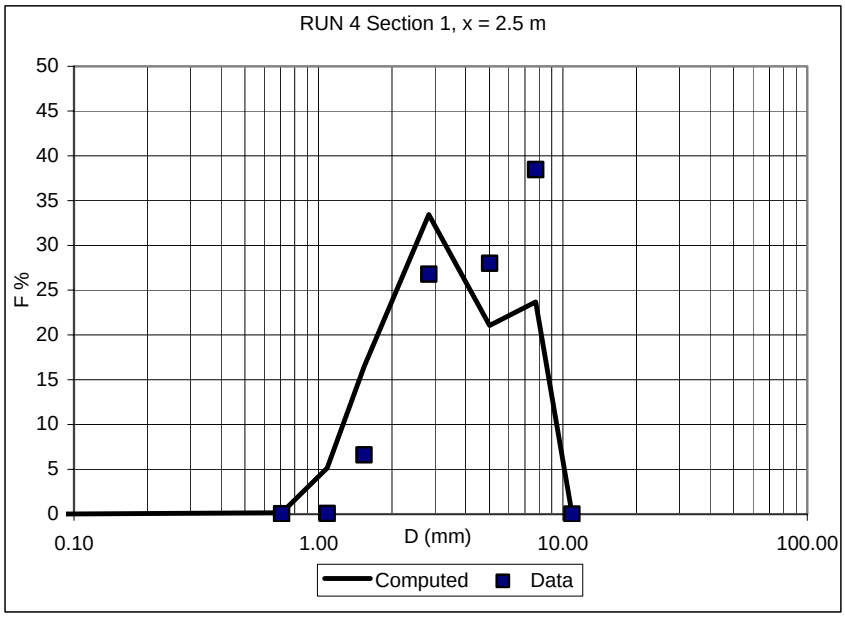
RUN 4 Section 1, x = 2.5 m
F %
D (mm)
0.10
1.00
10.00
100.00
Computed
Data

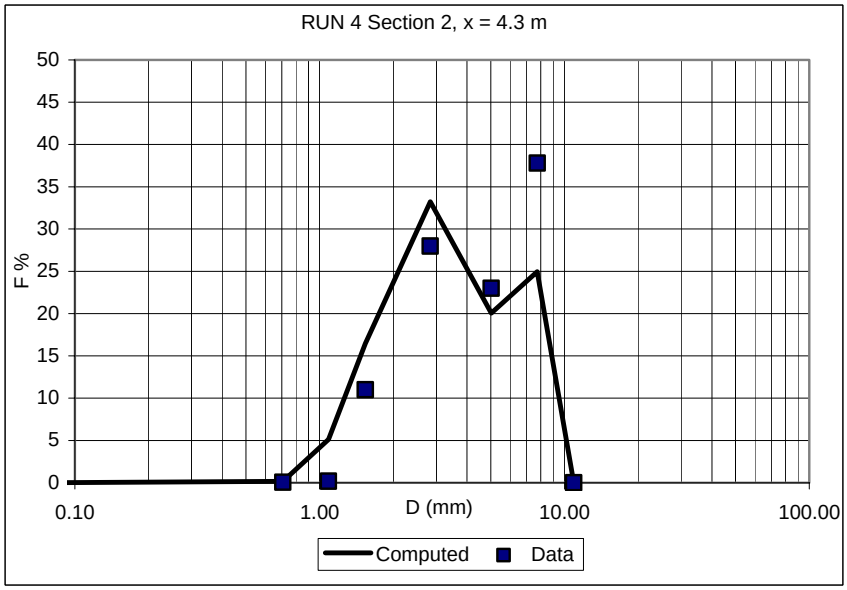
RUN 4 Section 2, x = 4.3 m
F %
D (mm)
0.10
1.00
10.00
100.00
Computed
Data

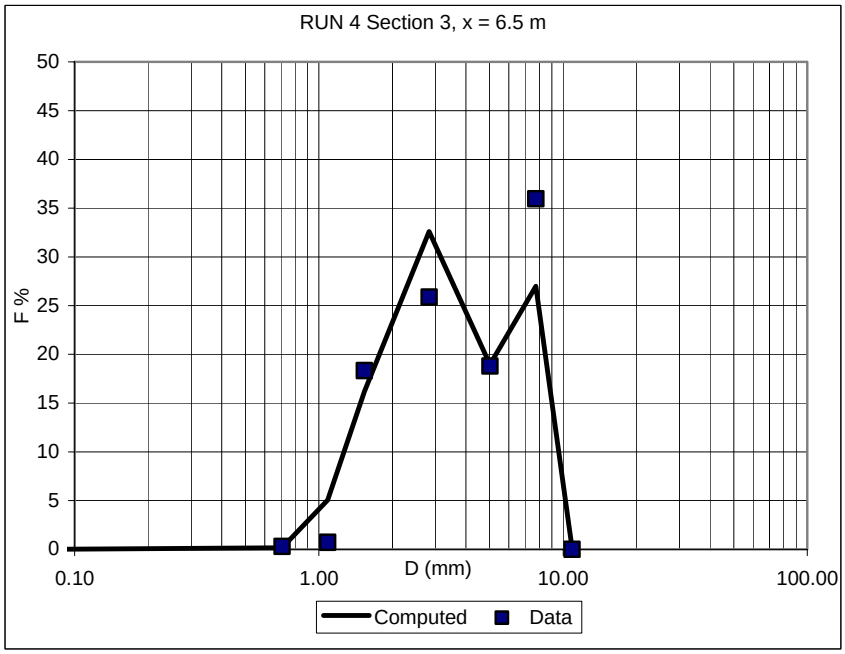
RUN 4 Section 3, x = 6.5 m
F %
D (mm)
0.10
1.00
10.00
100.00
Computed
Data

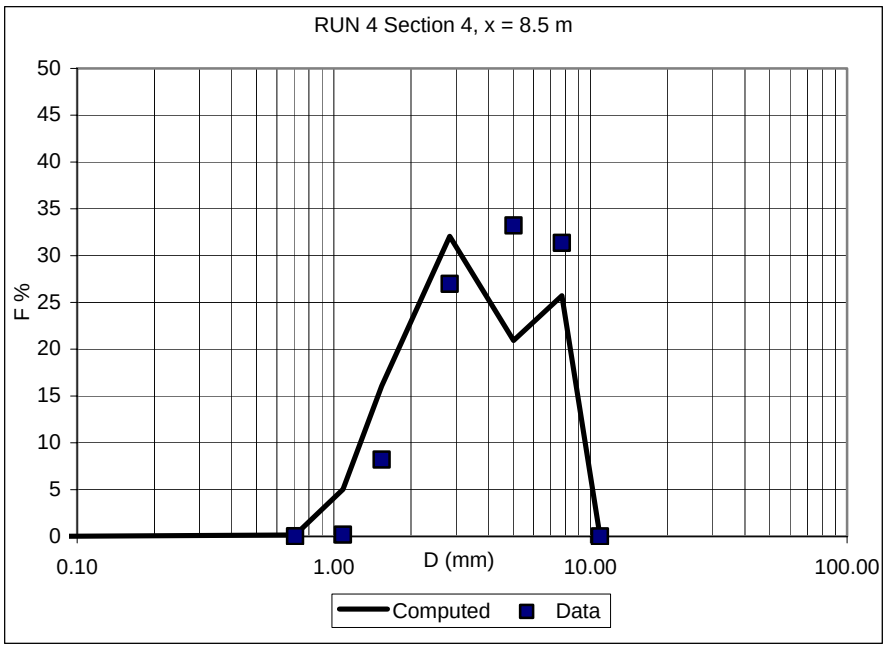
RUN 4 Section 4, x = 8.5 m
50
45
40
35
30
25
20
15
10
5
0
F %
0.10
1.00
10.00
100.00
D (mm)
Computed
Data

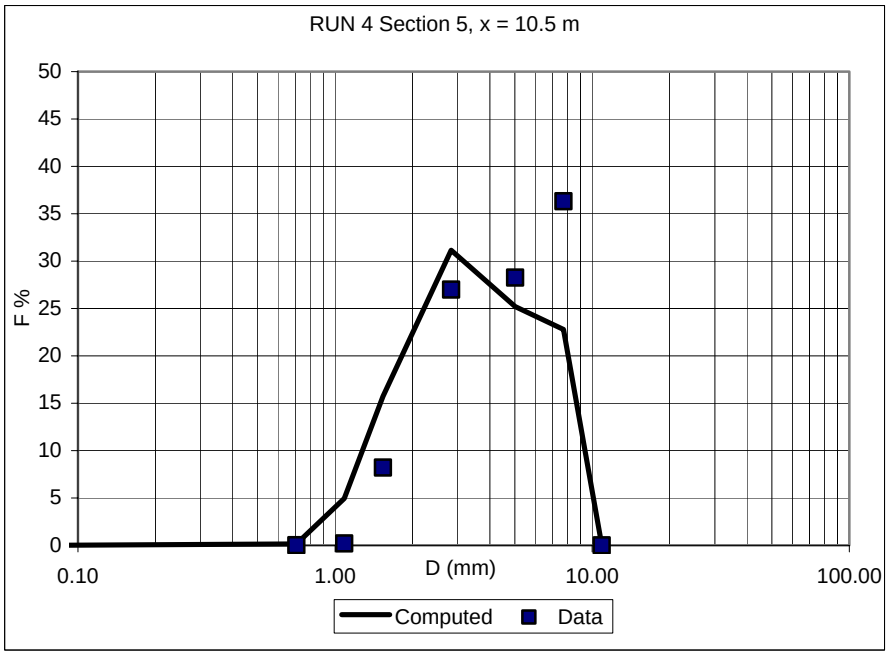
RUN 4 Section 5, x = 10.5 m
50
45
40
35
30
25
20
15
10
5
0
F %
0.10
1.00
10.00
100.00
D (mm)
Computed
Data

RUN 5

Section 1, x = 2.5 m

Computed		Data	
Di (mm)	**Fi %**	**Di (mm)**	**Fi %**
0.071	0.000	0.071	0.025
0.707	0.154	0.707	0.388
1.086	4.905	1.086	0.248
1.536	15.765	1.536	14.140
2.828	32.121	2.828	29.471
5.020	20.938	5.020	21.019
7.736	26.083	7.736	34.710
10.897	0.035	10.897	0.000

Section 2, x = 4.3 m

Computed		Data	
Di (mm)	**Fi %**	**Di (mm)**	**Fi %**
0.071	0.000	0.071	0.012
0.707	0.154	0.707	0.056
1.086	4.850	1.086	0.133
1.536	15.562	1.536	7.785
2.828	31.611	2.828	25.559
5.020	21.642	5.020	26.634
7.736	26.147	7.736	39.597
10.897	0.034	10.897	0.225

Section 3, x = 6.5 m

Computed		Data	
Di (mm)	**Fi %**	**Di (mm)**	**Fi %**
0.071	0.000	0.071	0.008
0.707	0.148	0.707	0.011
1.086	4.730	1.086	0.099
1.536	15.178	1.536	8.117
2.828	30.639	2.828	23.823
5.020	21.872	5.020	25.596
7.736	27.405	7.736	42.345
10.897	0.028	10.897	0.000

Section 4, x = 8.5 m

Computed		Data	
Di (mm)	**Fi %**	**Di (mm)**	**Fi %**
0.071	0.000	0.071	0.013
0.707	0.147	0.707	0.007
1.086	4.730	1.086	0.085
1.536	15.172	1.536	8.995
2.828	30.502	2.828	21.859
5.020	23.498	5.020	25.825
7.736	25.921	7.736	43.216
10.897	0.030	10.897	0.000

Section 5, x = 10.5 m

Computed		Data	
Di (mm)	**Fi %**	**Di (mm)**	**Fi %**
0.071	0.000	0.071	0.016
0.707	0.153	0.707	0.000
1.086	4.968	1.086	0.016
1.536	15.977	1.536	5.263
2.828	32.393	2.828	21.522
5.020	24.351	5.020	27.059
7.736	22.129	7.736	46.123
10.897	0.028	10.897	0.000

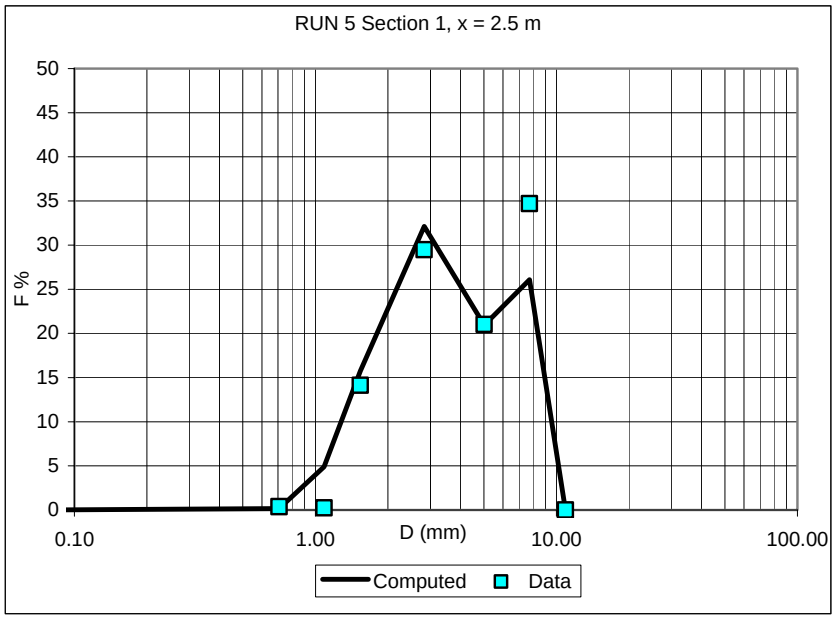
RUN 5 Section 1, x = 2.5 m
50
45
40
35
30
25
20
15
10
5
0
F %
0.10
1.00
10.00
100.00
D (mm)
Computed
Data

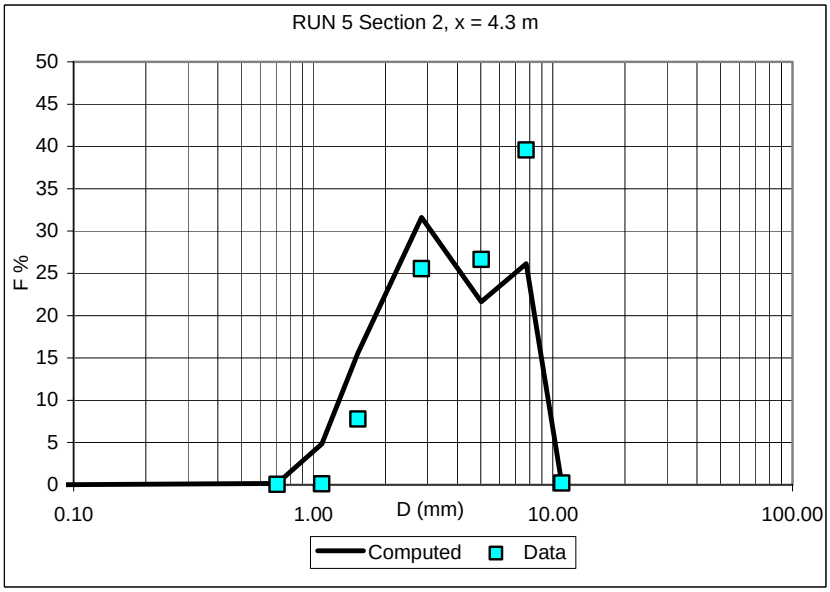
RUN 5 Section 2, x = 4.3 m
50
45
40
35
30
25
20
15
10
5
0
F %
0.10
1.00
10.00
100.00
D (mm)
Computed
Data

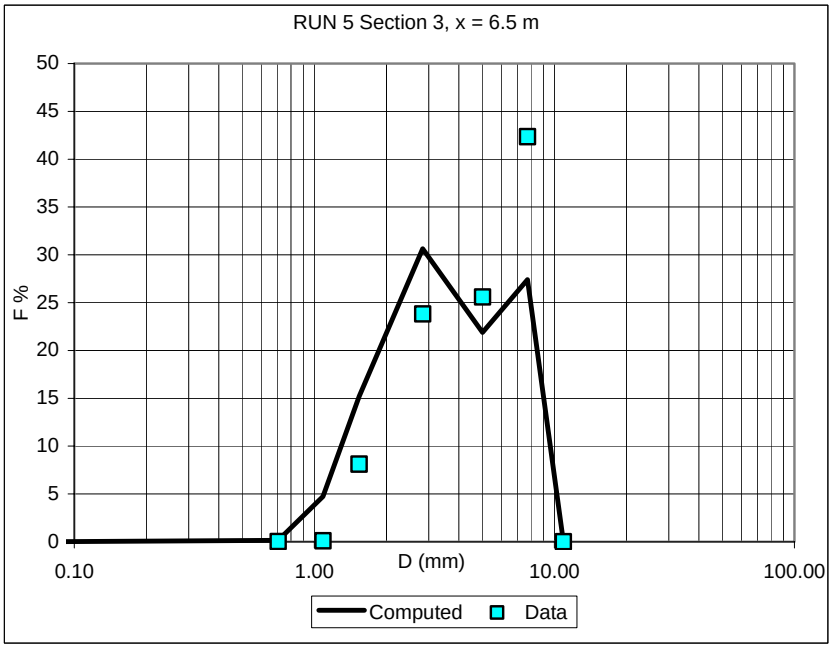
RUN 5 Section 3, x = 6.5 m
50
45
40
35
30
25
20
15
10
5
0
F %
0.10
1.00
10.00
100.00
D (mm)
Computed
Data

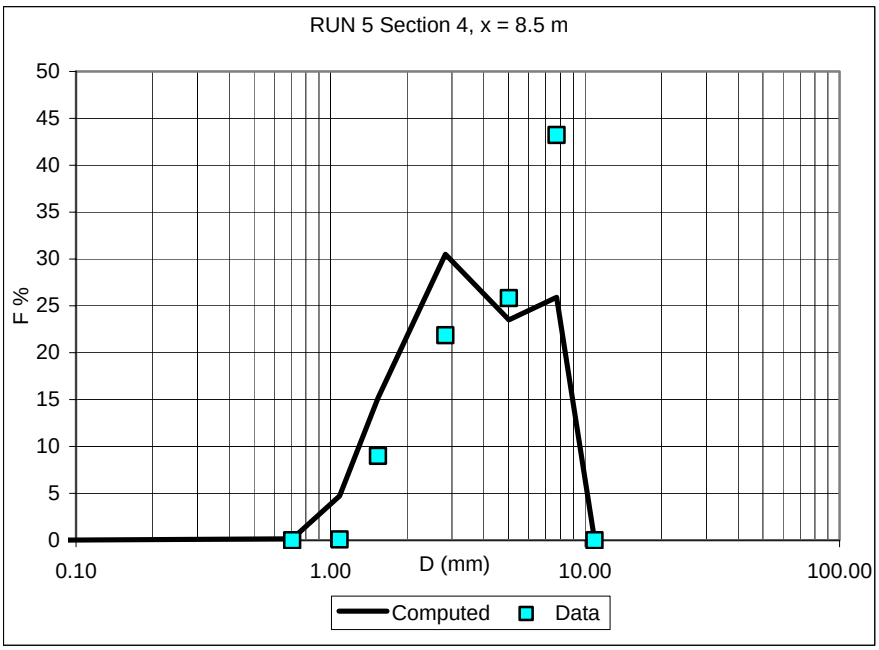
RUN 5 Section 4, x = 8.5 m
50
45
40
35
30
25
20
15
10
5
0
F %
0.10
1.00
10.00
100.00
D (mm)
Computed
Data

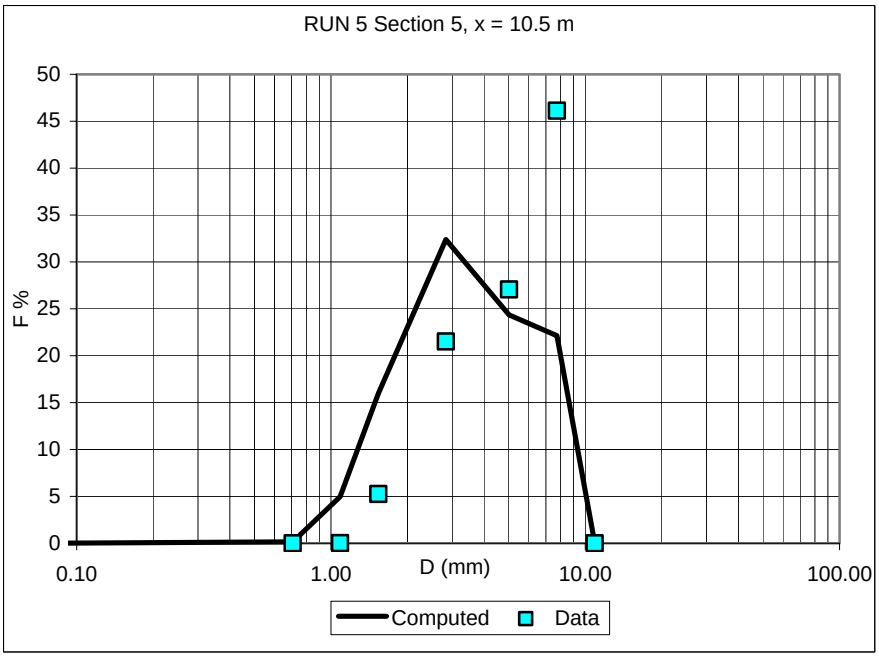
RUN 5 Section 5, x = 10.5 m
50
45
40
35
30
25
20
15
10
5
0
F %
0.10
1.00
10.00
100.00
D (mm)
Computed
Data

RUN 6

Section 1, x = 2.5 m

Computed		Data	
Di (mm)	**Fi %**	**Di (mm)**	**Fi %**
0.071	0.000	0.071	0.005
0.707	0.159	0.707	0.060
1.086	4.735	1.086	0.161
1.536	15.072	1.536	5.802
2.828	30.234	2.828	24.717
5.020	22.074	5.020	26.793
7.736	27.688	7.736	42.463
10.897	0.038	10.897	0.000

Section 2, x = 4.3 m

Computed		Data	
Di (mm)	**Fi %**	**Di (mm)**	**Fi %**
0.071	0.000	0.071	0.008
0.707	0.140	0.707	0.091
1.086	4.400	1.086	0.204
1.536	14.098	1.536	7.342
2.828	28.873	2.828	21.693
5.020	24.372	5.020	28.047
7.736	28.081	7.736	42.615
10.897	0.036	10.897	0.000

Section 3, x = 6.5 m

Computed		Data	
Di (mm)	**Fi %**	**Di (mm)**	**Fi %**
0.071	0.000	0.071	0.005
0.707	0.159	0.707	0.053
1.086	4.540	1.086	0.207
1.536	14.934	1.536	10.627
2.828	30.830	2.828	23.756
5.020	21.295	5.020	22.998
7.736	28.212	7.736	42.353
10.897	0.030	10.897	0.000

Section 4, x = 8.5 m

Computed		Data	
Di (mm)	**Fi %**	**Di (mm)**	**Fi %**
0.071	0.000	0.071	0.008
0.707	0.247	0.707	0.013
1.086	4.873	1.086	0.132
1.536	15.286	1.536	11.183
2.828	30.262	2.828	22.910
5.020	20.265	5.020	24.293
7.736	29.040	7.736	41.461
10.897	0.028	10.897	0.000

Section 5, x = 10.5 m

Computed		Data	
Di (mm)	**Fi %**	**Di (mm)**	**Fi %**
0.071	0.000	0.071	0.000
0.707	0.205	0.707	0.000
1.086	5.072	1.086	0.047
1.536	16.032	1.536	6.661
2.828	31.982	2.828	26.746
5.020	24.179	5.020	28.481
7.736	22.506	7.736	38.065
10.897	0.025	10.897	0.000

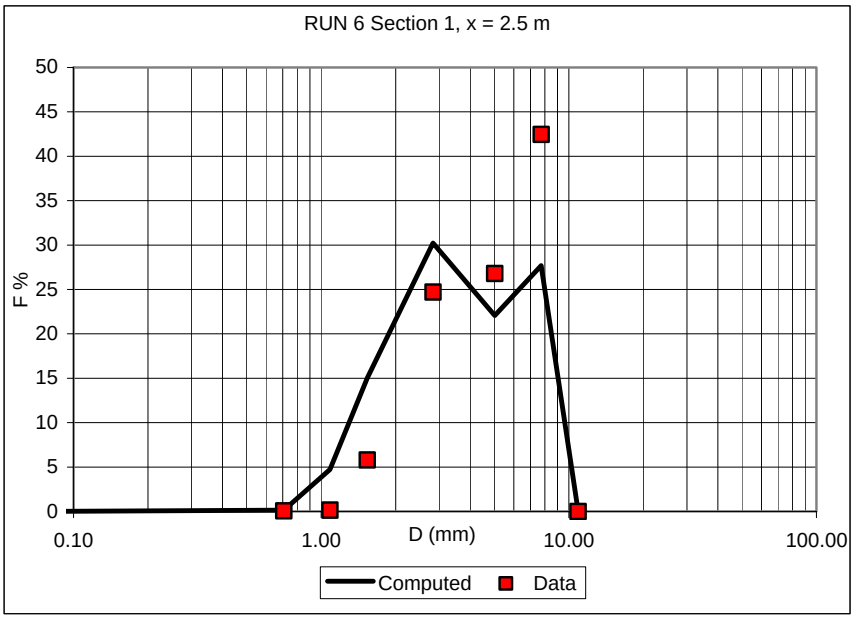
RUN 6 Section 1, x = 2.5 m
50
45
40
35
30
25
20
15
10
5
0
F %
0.10
1.00
10.00
100.00
D (mm)
Computed
Data

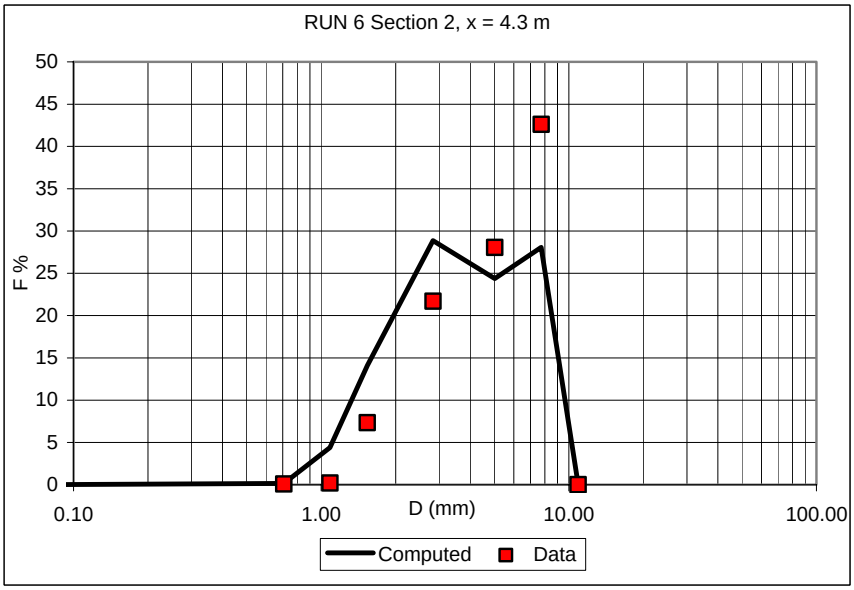
RUN 6 Section 2, x = 4.3 m
50
45
40
35
30
25
20
15
10
5
0
F %
0.10
1.00
10.00
100.00
D (mm)
Computed
Data

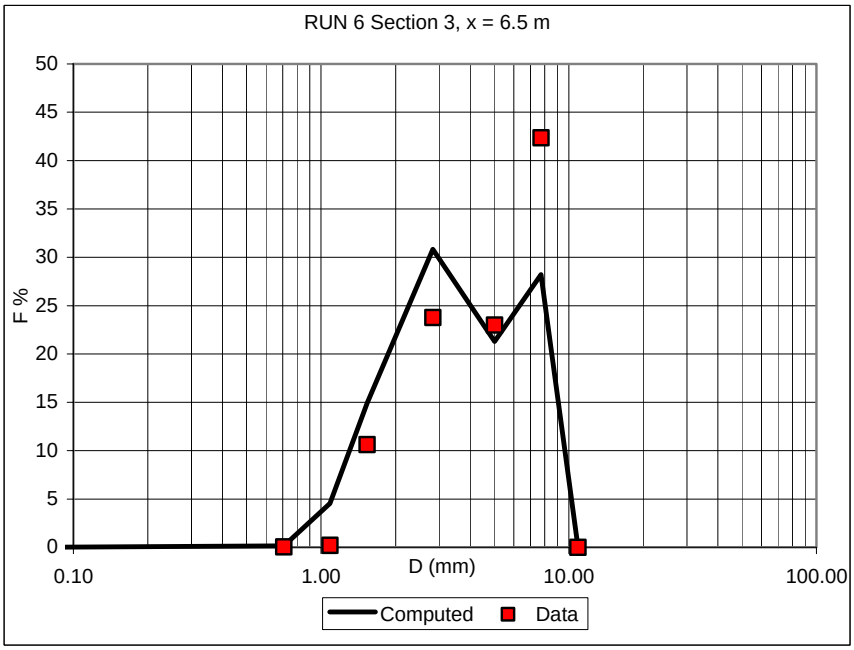
RUN 6 Section 3, x = 6.5 m
50
45
40
35
30
25
20
15
10
5
0
F %
0.10
1.00
10.00
100.00
D (mm)
Computed
Data

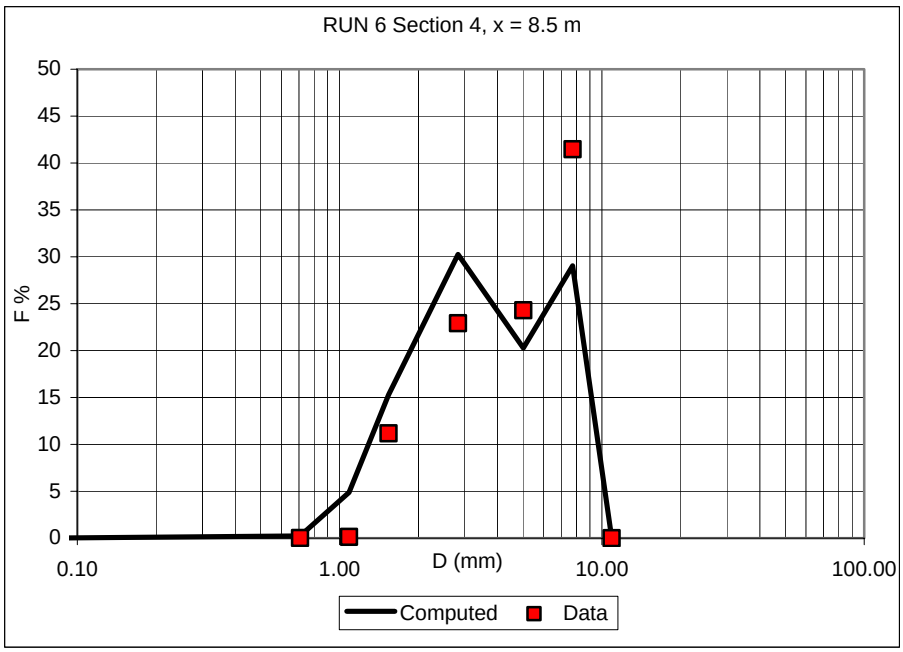
RUN 6 Section 4, x = 8.5 m
50
45
40
35
30
25
20
15
10
5
0
F %
0.10
1.00
10.00
100.00
D (mm)
Computed
Data

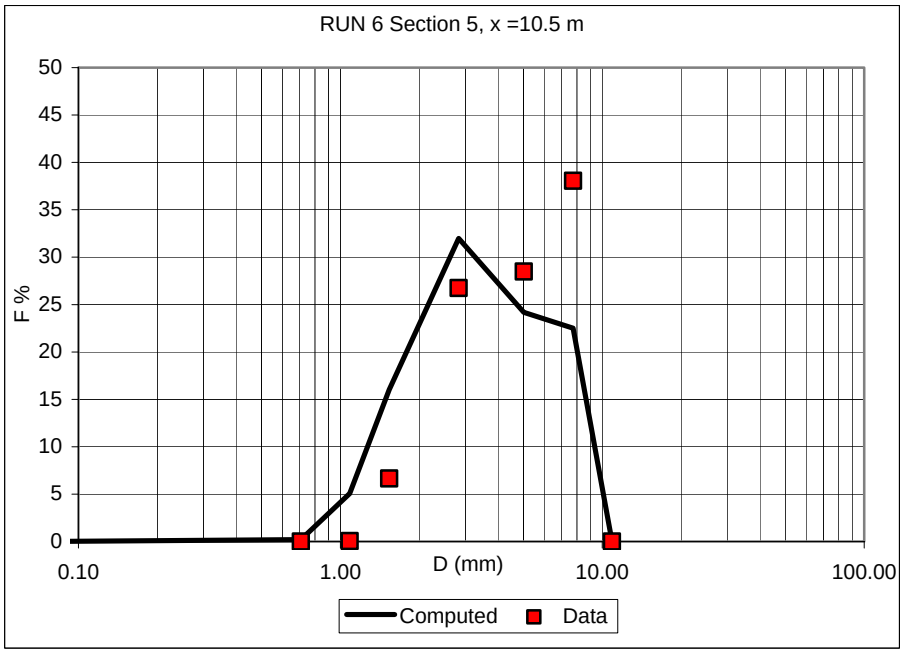
RUN 6 Section 5, x =10.5 m
50
45
40
35
30
25
20
15
10
5
0
F %
0.10
1.00
10.00
100.00
D (mm)
Computed
Data

RUN 7

Section 1, x = 2.5 m

Computed		Data	
Di (mm)	**Fi %**	**Di (mm)**	**Fi %**
0.071	0.000	0.071	0.010
0.707	0.171	0.707	0.020
1.086	5.002	1.086	0.057
1.536	16.008	1.536	9.775
2.828	31.829	2.828	29.884
5.020	19.341	5.020	27.837
7.736	27.615	7.736	32.417
10.897	0.033	10.897	0.000

Section 2, x = 4.3 m

Computed		Data	
Di (mm)	**Fi %**	**Di (mm)**	**Fi %**
0.071	0.000	0.071	0.011
0.707	0.172	0.707	0.011
1.086	4.880	1.086	0.027
1.536	15.510	1.536	6.750
2.828	30.511	2.828	32.305
5.020	20.991	5.020	27.163
7.736	27.900	7.736	33.732
10.897	0.036	10.897	0.000

Section 3, x = 6.5 m

Computed		Data	
Di (mm)	**Fi %**	**Di (mm)**	**Fi %**
0.071	0.000	0.071	0.021
0.707	0.180	0.707	0.025
1.086	4.818	1.086	0.118
1.536	15.189	1.536	10.344
2.828	29.728	2.828	24.818
5.020	27.952	5.020	26.242
7.736	22.099	7.736	38.433
10.897	0.034	10.897	0.000

Section 4, x = 8.5 m

Computed		Data	
Di (mm)	**Fi %**	**Di (mm)**	**Fi %**
0.071	0.000	0.071	0.013
0.707	0.195	0.707	0.011
1.086	5.088	1.086	0.063
1.536	16.230	1.536	8.064
2.828	33.410	2.828	30.618
5.020	21.884	5.020	26.525
7.736	23.161	7.736	34.706
10.897	0.031	10.897	0.000

Section 5, x = 10.5 m

Computed		Data	
Di (mm)	**Fi %**	**Di (mm)**	**Fi %**
0.071	0.000	0.071	0.012
0.707	0.179	0.707	0.015
1.086	4.997	1.086	0.139
1.536	16.056	1.536	11.336
2.828	32.733	2.828	24.754
5.020	19.618	5.020	26.170
7.736	26.390	7.736	37.573
10.897	0.028	10.897	0.000

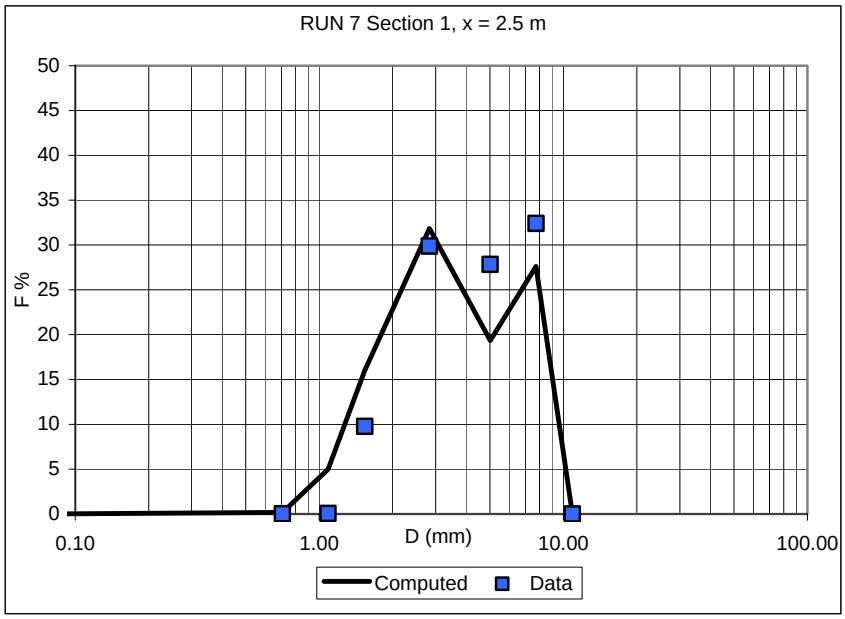
RUN 7 Section 1, x = 2.5 m
F %
D (mm)
0.10
1.00
10.00
100.00
Computed
Data

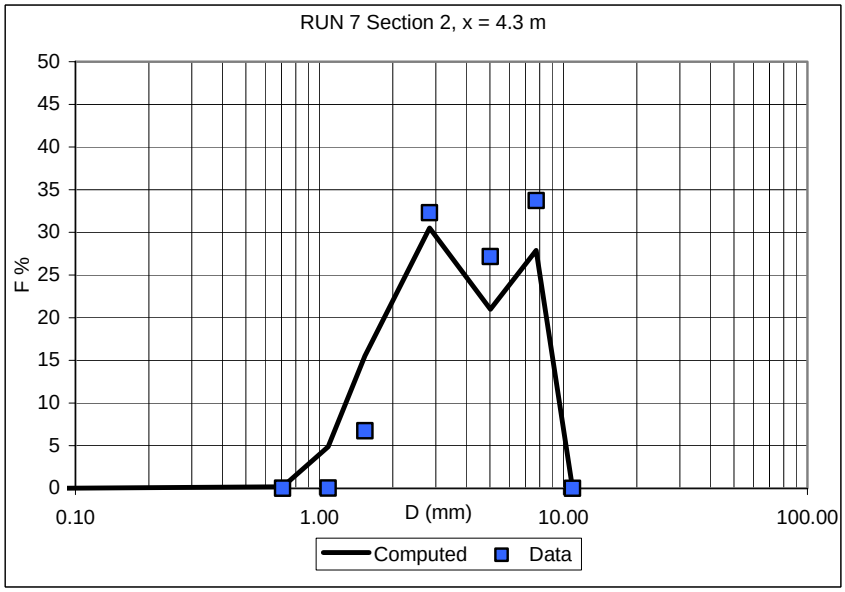
RUN 7 Section 2, x = 4.3 m
F %
D (mm)
0.10
1.00
10.00
100.00
Computed
Data

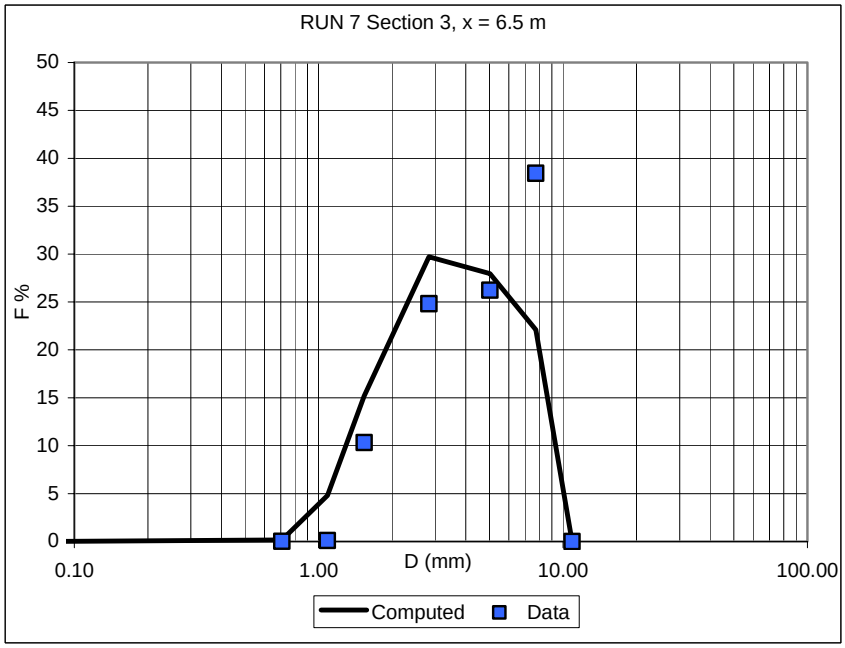
RUN 7 Section 3, x = 6.5 m
F %
D (mm)
0.10
1.00
10.00
100.00
Computed
Data

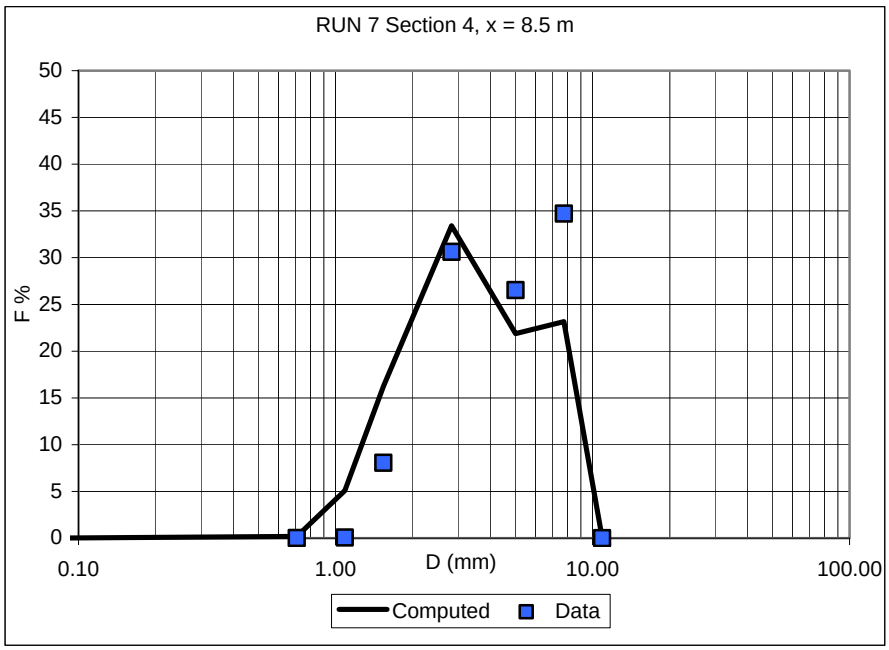
RUN 7 Section 4, x = 8.5 m
50
45
40
35
30
25
20
15
10
5
0
F %
0.10
1.00
10.00
100.00
D (mm)
Computed
Data

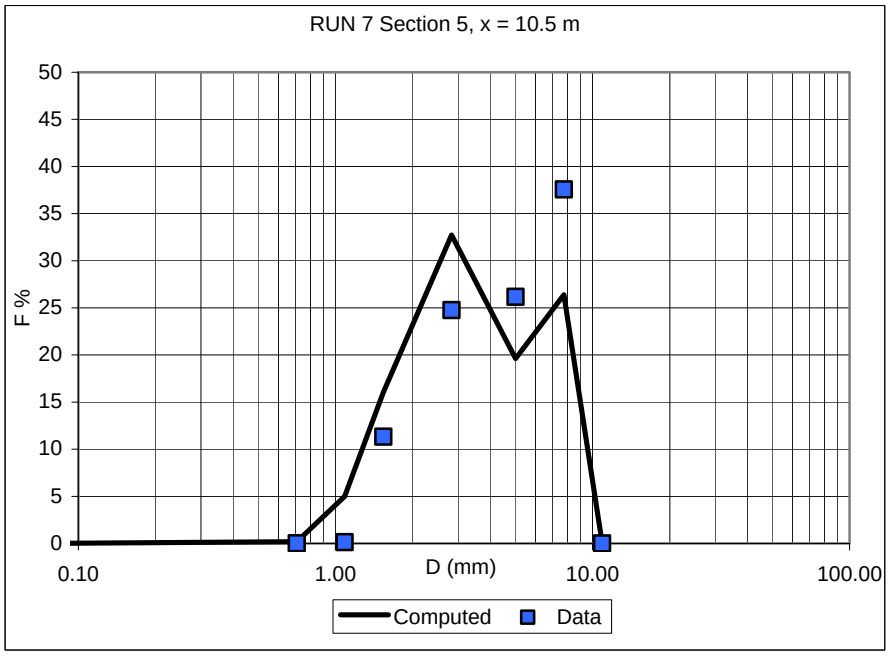
RUN 7 Section 5, x = 10.5 m
50
45
40
35
30
25
20
15
10
5
0
F %
0.10
1.00
10.00
100.00
D (mm)
Computed
Data

RUN 8

Section 1, x = 2.5 m

Computed		Data	
Di (mm)	**Fi %**	**Di (mm)**	**Fi %**
0.071	0.000	0.071	0.012
0.707	0.234	0.707	0.025
1.086	5.195	1.086	0.075
1.536	16.354	1.536	7.970
2.828	32.129	2.828	29.055
5.020	18.952	5.020	30.176
7.736	27.101	7.736	32.687
10.897	0.034	10.897	0.000

Section 2, x = 4.3 m

Computed		Data	
Di (mm)	**Fi %**	**Di (mm)**	**Fi %**
0.071	0.000	0.071	0.018
0.707	0.235	0.707	0.023
1.086	5.241	1.086	0.097
1.536	16.428	1.536	15.847
2.828	32.266	2.828	34.504
5.020	20.265	5.020	23.478
7.736	25.529	7.736	26.033
10.897	0.037	10.897	0.000

Section 3, x = 6.5 m

Computed		Data	
Di (mm)	**Fi %**	**Di (mm)**	**Fi %**
0.071	0.000	0.071	0.012
0.707	0.208	0.707	0.012
1.086	5.047	1.086	0.102
1.536	15.850	1.536	9.584
2.828	31.191	2.828	27.658
5.020	21.008	5.020	25.172
7.736	26.660	7.736	37.460
10.897	0.036	10.897	0.000

Section 4, x = 8.5 m

Computed		Data	
Di (mm)	**Fi %**	**Di (mm)**	**Fi %**
0.071	0.000	0.071	0.021
0.707	0.178	0.707	0.041
1.086	4.692	1.086	0.162
1.536	14.806	1.536	12.896
2.828	29.152	2.828	31.460
5.020	22.832	5.020	24.278
7.736	28.310	7.736	31.142
10.897	0.030	10.897	0.000

Section 5, x = 10.5 m

Computed		Data	
Di (mm)	**Fi %**	**Di (mm)**	**Fi %**
0.071	0.000	0.071	0.013
0.707	0.186	0.707	0.006
1.086	5.072	1.086	0.058
1.536	16.409	1.536	6.050
2.828	33.813	2.828	24.509
5.020	21.860	5.020	27.752
7.736	22.633	7.736	41.611
10.897	0.026	10.897	0.000

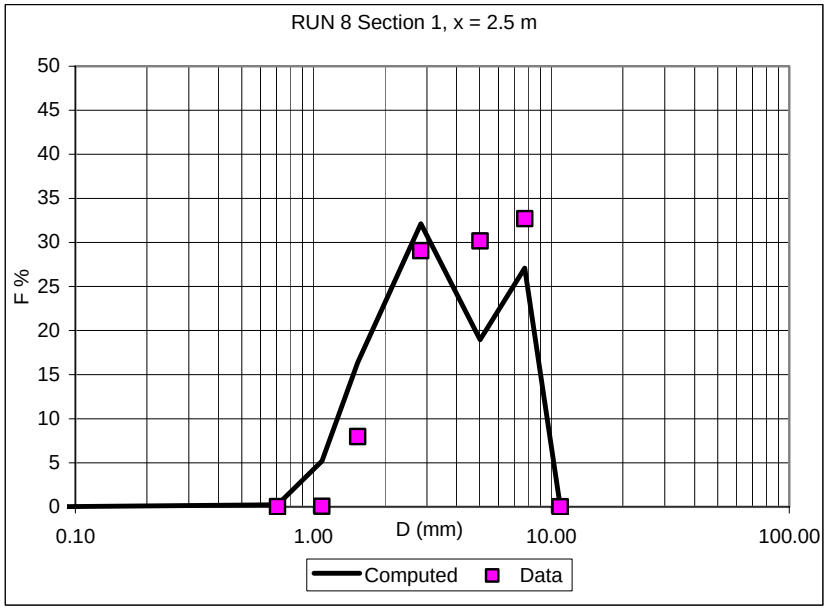
RUN 8 Section 1, x = 2.5 m
50
45
40
35
30
25
20
15
10
5
0
F %
0.10
1.00
10.00
100.00
D (mm)
Computed
Data

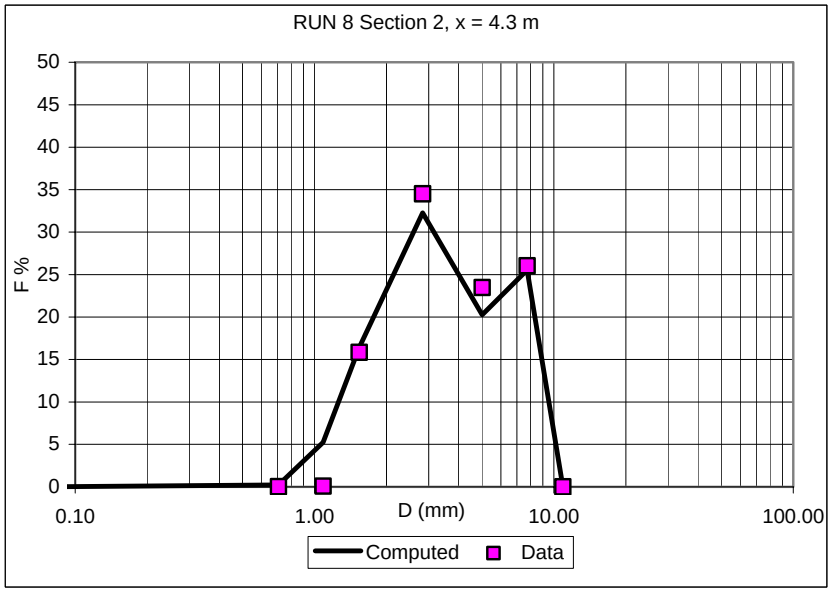
RUN 8 Section 2, x = 4.3 m
50
45
40
35
30
25
20
15
10
5
0
F %
0.10
1.00
10.00
100.00
D (mm)
Computed
Data

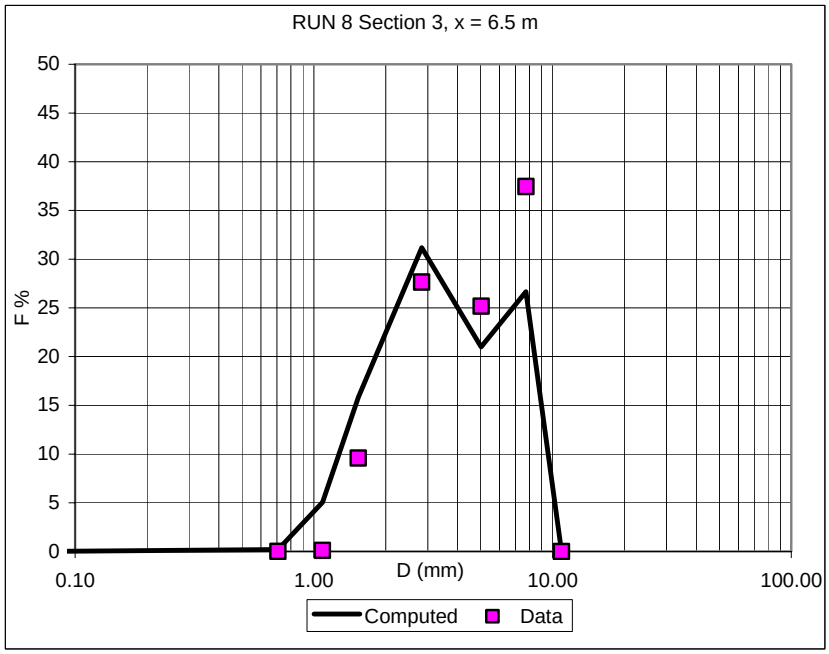
RUN 8 Section 3, x = 6.5 m
50
45
40
35
30
25
20
15
10
5
0
F %
0.10
1.00
10.00
100.00
D (mm)
Computed
Data

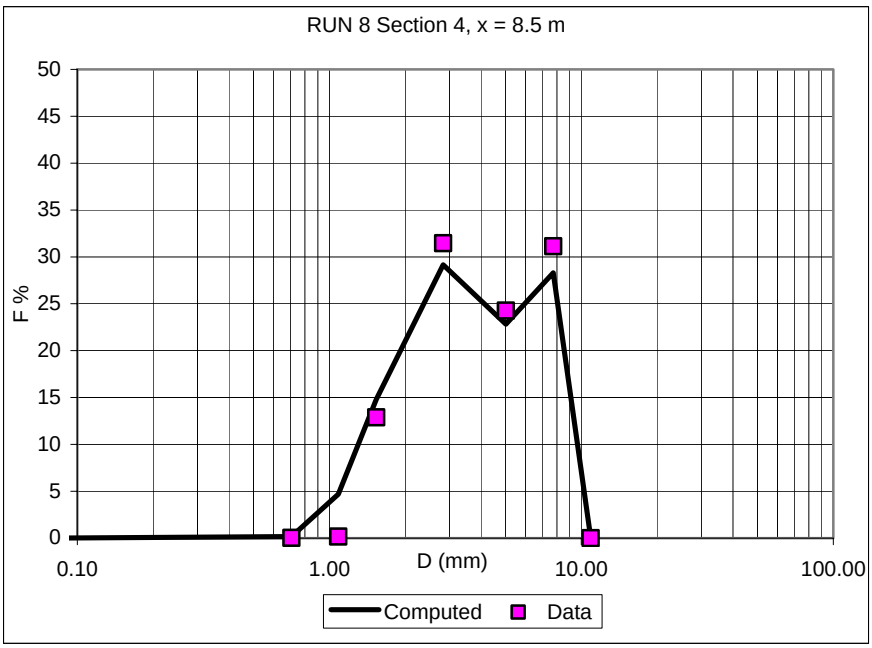
RUN 8 Section 4, x = 8.5 m
50
45
40
35
30
25
20
15
10
5
0
F %
0.10
1.00
10.00
100.00
D (mm)
Computed
Data

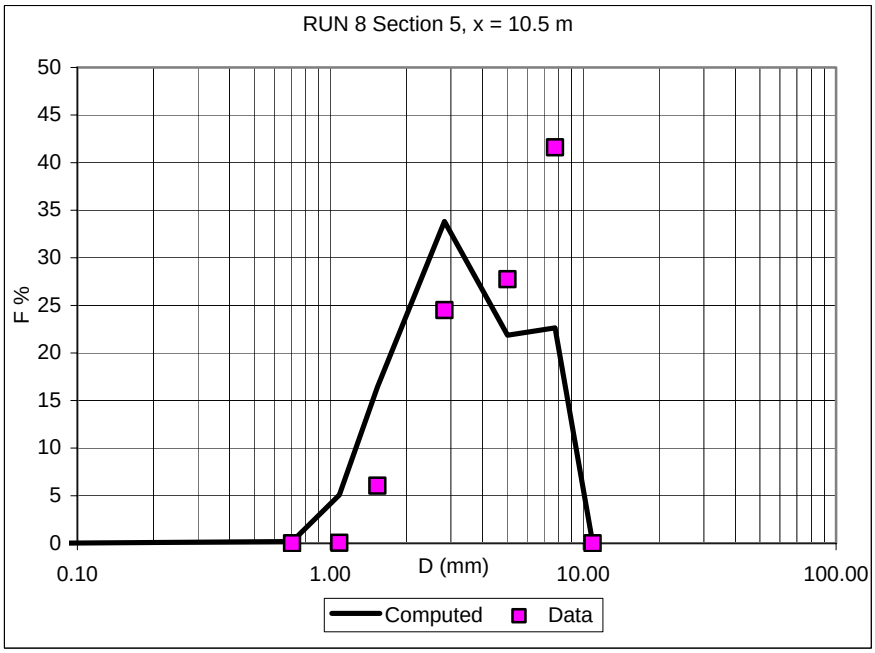
RUN 8 Section 5, x = 10.5 m
50
45
40
35
30
25
20
15
10
5
0
F %
0.10
1.00
10.00
100.00
D (mm)
Computed
Data

RUN 9

Section 1, x = 2.5 m

Computed		Data	
Di (mm)	Fi %	Di (mm)	Fi %
0.071	0.000	0.071	0.007
0.707	0.210	0.707	0.073
1.086	5.417	1.086	0.248
1.536	17.050	1.536	13.395
2.828	33.617	2.828	27.246
5.020	22.068	5.020	26.696
7.736	21.616	7.736	32.334
10.897	0.023	10.897	0.000

Section 2, x = 4.3 m

Computed		Data	
Di (mm)	Fi %	Di (mm)	Fi %
0.071	0.000	0.071	0.003
0.707	0.206	0.707	0.014
1.086	5.444	1.086	0.117
1.536	17.150	1.536	9.979
2.828	33.956	2.828	30.310
5.020	21.504	5.020	25.730
7.736	21.712	7.736	33.847
10.897	0.027	10.897	0.000

Section 3, x = 6.5 m

Computed		Data	
Di (mm)	Fi %	Di (mm)	Fi %
0.071	0.000	0.071	0.006
0.707	0.199	0.707	0.009
1.086	5.328	1.086	0.098
1.536	16.822	1.536	12.150
2.828	33.419	2.828	32.334
5.020	20.275	5.020	25.998
7.736	23.922	7.736	29.405
10.897	0.034	10.897	0.000

Section 4, x = 8.5 m

Computed		Data	
Di (mm)	Fi %	Di (mm)	Fi %
0.071	0.000	0.071	0.008
0.707	0.195	0.707	0.023
1.086	5.194	1.086	0.218
1.536	16.437	1.536	13.066
2.828	32.603	2.828	25.865
5.020	19.825	5.020	24.774
7.736	25.712	7.736	36.047
10.897	0.034	10.897	0.000

Section 5, x = 10.5 m

Computed		Data	
Di (mm)	Fi %	Di (mm)	Fi %
0.071	0.000	0.071	0.004
0.707	0.204	0.707	0.017
1.086	5.273	1.086	0.134
1.536	16.668	1.536	8.921
2.828	32.913	2.828	34.373
5.020	21.314	5.020	27.669
7.736	23.599	7.736	28.882
10.897	0.028	10.897	0.000

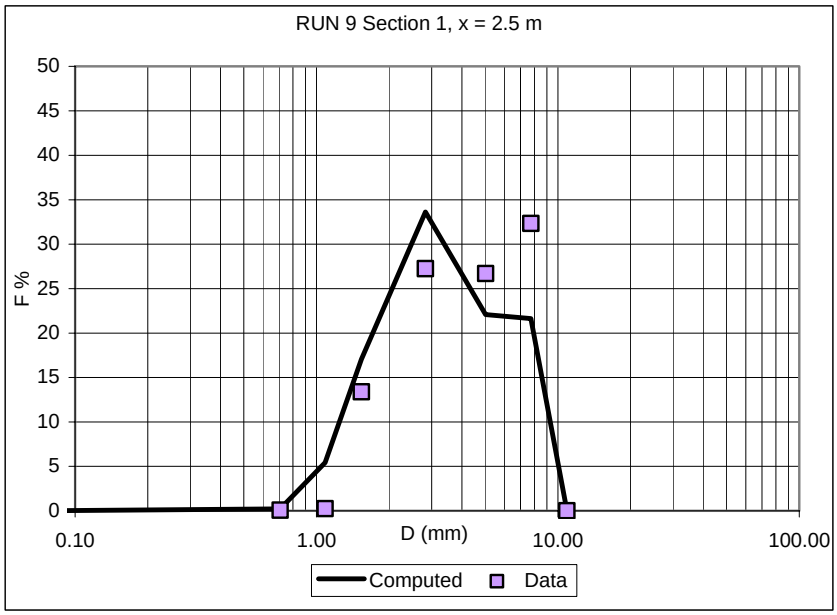
RUN 9 Section 1, x = 2.5 m
F %
D (mm)
0.10
1.00
10.00
100.00
Computed
Data

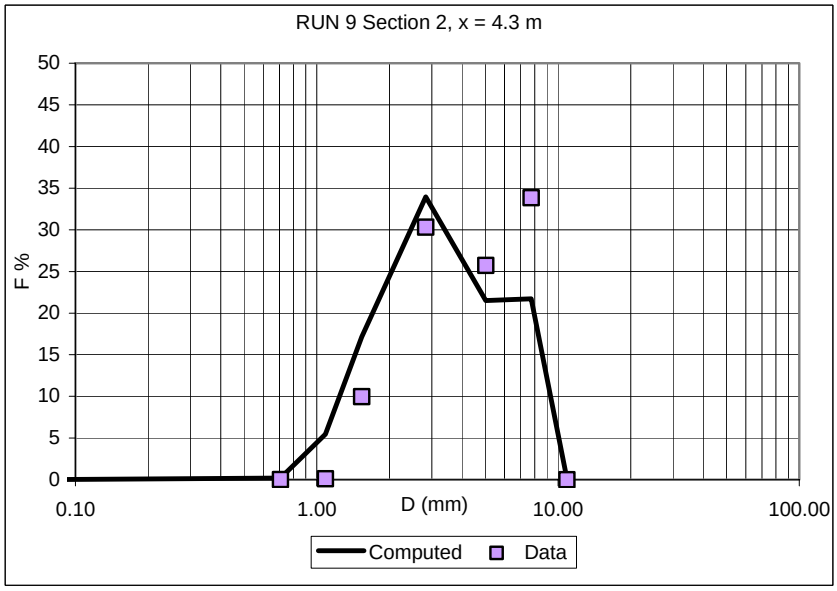
RUN 9 Section 2, x = 4.3 m
F %
D (mm)
0.10
1.00
10.00
100.00
Computed
Data

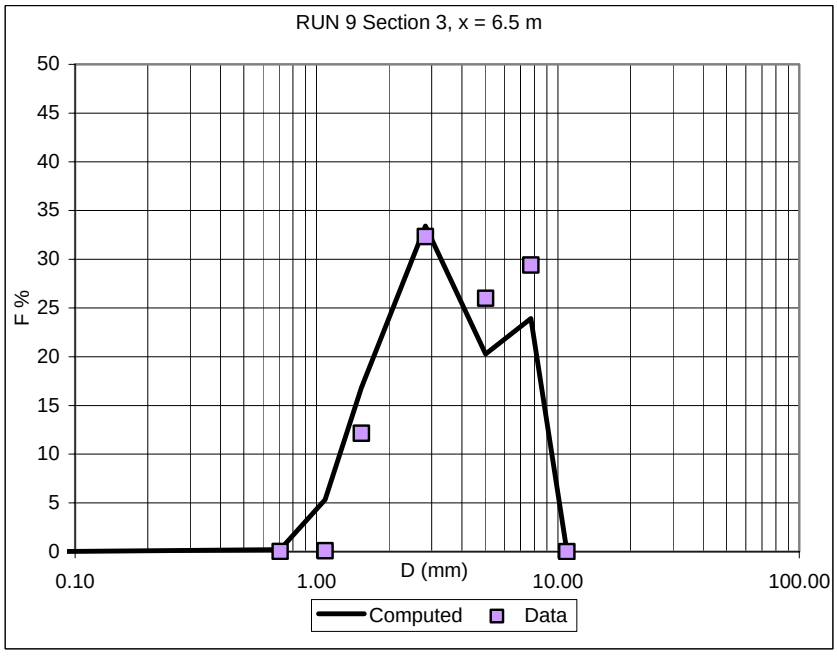
RUN 9 Section 3, x = 6.5 m
F %
D (mm)
0.10
1.00
10.00
100.00
Computed
Data

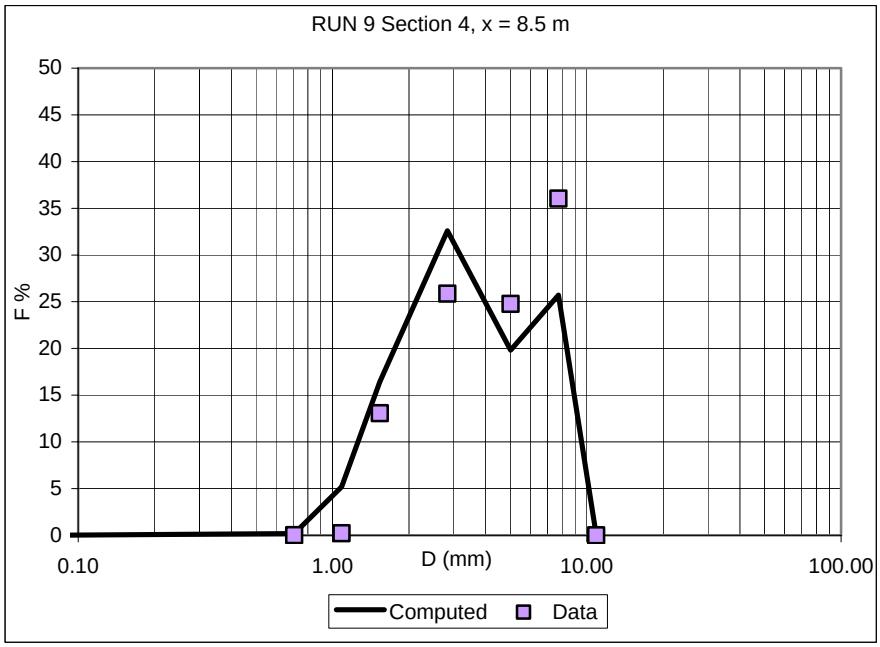
RUN 9 Section 4, x = 8.5 m
50
45
40
35
30
25
20
15
10
5
0
F %
0.10
1.00
10.00
100.00
D (mm)
Computed
Data

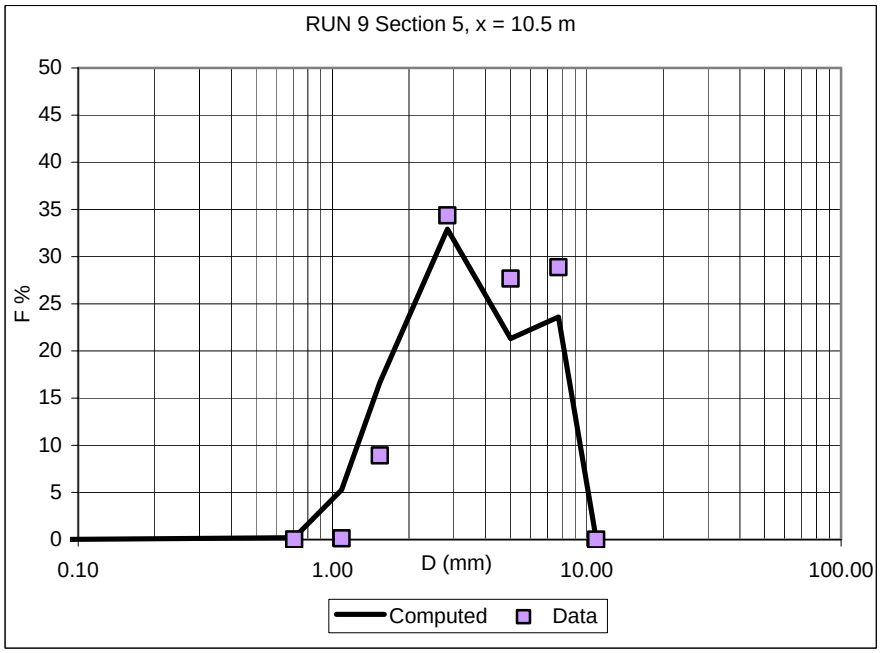
RUN 9 Section 5, x = 10.5 m
50
45
40
35
30
25
20
15
10
5
0
F %
0.10
1.00
10.00
100.00
D (mm)
Computed
Data

Substrate

x = 0.5 m								
First layer 0 -1 cm					Second layer 1 - 2 cm			
Computed		Data			Computed		Data	
Di (mm)	fi %	Di (mm)	fi %		Di (mm)	fi %	Di (mm)	fi %
0.707	0.219	0.071	0.107		0.707	0.364	0.071	0.356
1.086	5.594	0.707	0.437		1.086	6.746	0.707	0.396
1.536	17.605	1.086	0.496		1.536	21.047	1.086	0.424
2.828	34.566	1.536	22.195		2.828	40.651	1.536	22.301
5.020	21.261	2.828	31.045		5.020	18.082	2.828	33.847
7.736	20.734	5.020	21.661		7.736	13.100	5.020	20.169
10.897	0.021	7.736	24.059		10.897	0.010	7.736	22.508
		10.897	0.000				10.897	0.000
Third layer 2 - 3 cm					Fourth layer 3 - 4 cm			
Computed		Data			Computed		Data	
Di (mm)	fi %	Di (mm)	fi %		Di (mm)	fi %	Di (mm)	fi %
0.707	1.544	0.071	0.312		0.707	3.660	0.071	0.389
1.086	8.801	0.707	0.353		1.086	8.203	0.707	0.324
1.536	25.502	1.086	0.368		1.536	21.545	1.086	0.384
2.828	45.220	1.536	20.935		2.828	35.739	1.536	22.894
5.020	12.762	2.828	33.300		5.020	16.795	2.828	35.782
7.736	6.166	5.020	21.279		7.736	14.046	5.020	22.139
10.897	0.005	7.736	23.451		10.897	0.014	7.736	18.088
		10.897	0.000				10.897	0.000
Fifth layer 4 - 5 cm					Sixth layer 5 - 7 cm			
Computed		Data			Computed		Data	
Di (mm)	fi %	Di (mm)	fi %		Di (mm)	fi %	Di (mm)	fi %
0.707	0.114	0.071	0.280		0.707	0.114	0.071	0.238
1.086	5.863	0.707	0.241		1.086	5.863	0.707	0.177
1.536	18.691	1.086	0.429		1.536	18.691	1.086	0.362
2.828	37.088	1.536	21.467		2.828	37.088	1.536	21.819
5.020	20.817	2.828	36.161		5.020	20.817	2.828	34.716
7.736	17.410	5.020	22.768		7.736	17.410	5.020	20.836
10.897	0.017	7.736	18.654		10.897	0.017	7.736	21.851
		10.897	0.000				10.897	0.000

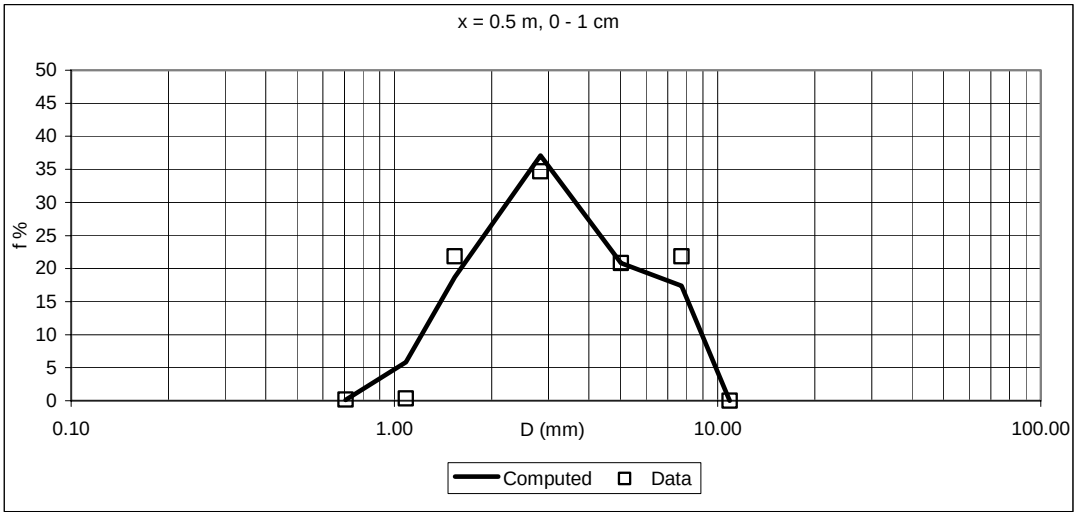
x = 0.5 m, 0 - 1 cm
f %
50
45
40
35
30
25
20
15
10
5
0
0.10
1.00
D (mm)
10.00
100.00
Computed
Data

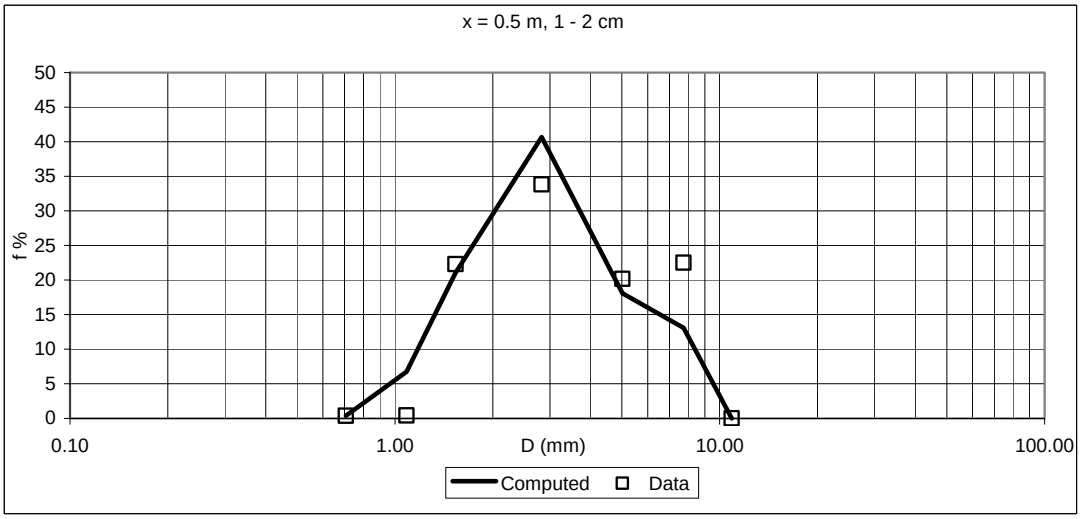
x = 0.5 m, 1 - 2 cm
f %
50
45
40
35
30
25
20
15
10
5
0
0.10
1.00
D (mm)
10.00
100.00
Computed
Data

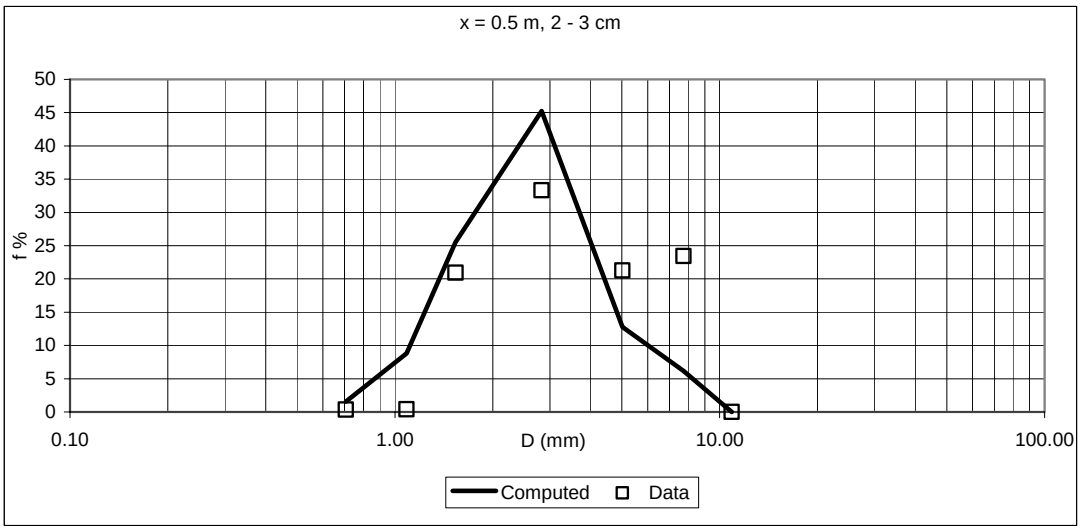
x = 0.5 m, 2 - 3 cm
f %
50
45
40
35
30
25
20
15
10
5
0
0.10
1.00
D (mm)
10.00
100.00
Computed
Data

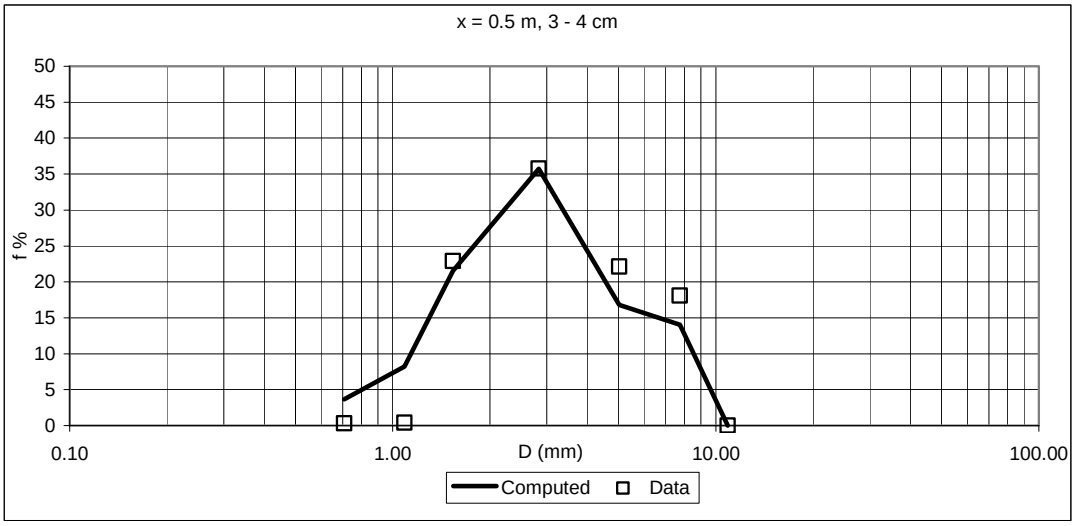
x = 0.5 m, 3 - 4 cm
f %
D (mm)
0.10
1.00
10.00
100.00
Computed
Data

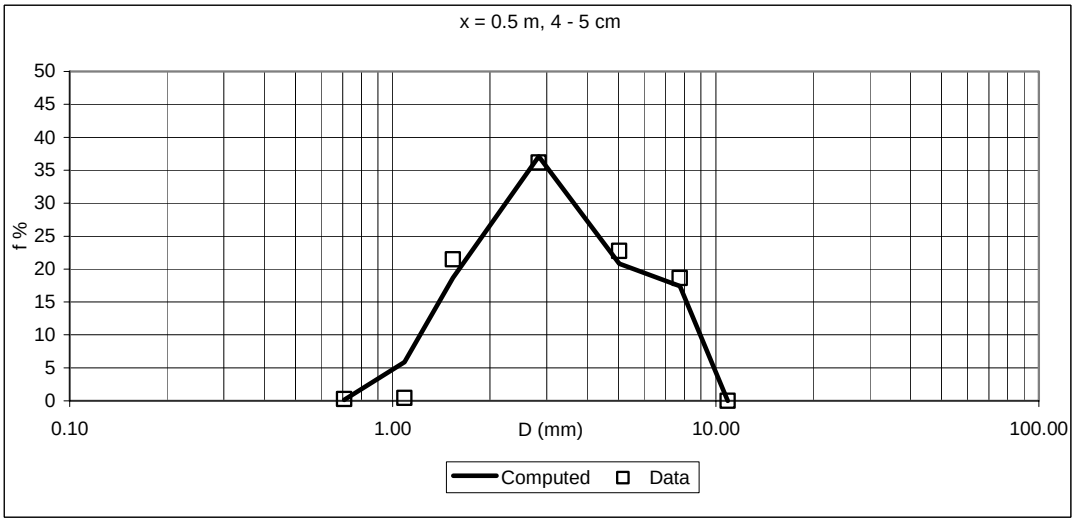
x = 0.5 m, 4 - 5 cm
f %
D (mm)
0.10
1.00
10.00
100.00
Computed
Data

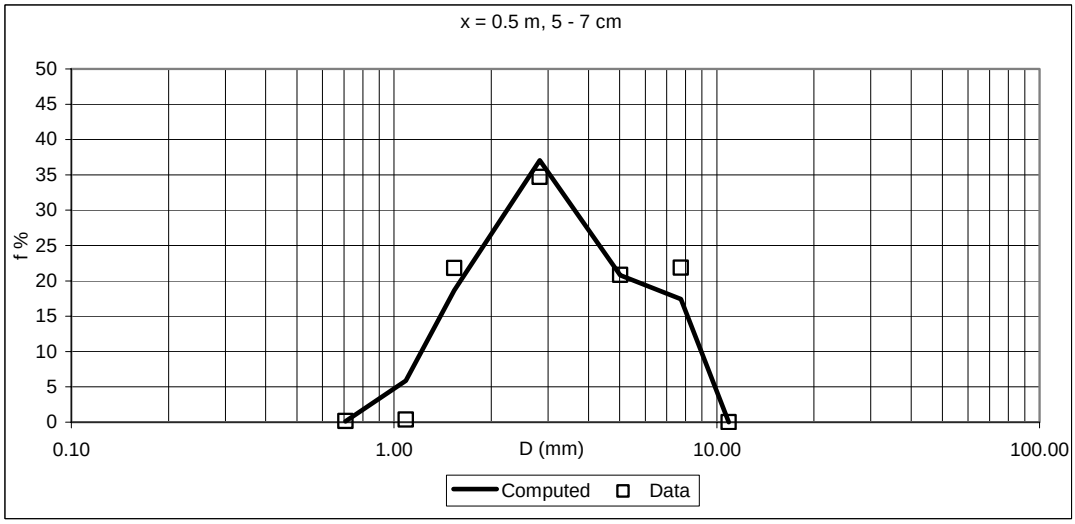
x = 0.5 m, 5 - 7 cm
f %
D (mm)
0.10
1.00
10.00
100.00
Computed
Data

x = 1 m								
First layer 0 -1 cm					Second layer 1 - 2 cm			
Computed		Data			Computed		Data	
Di (mm)	fi %	Di (mm)	fi %		Di (mm)	fi %	Di (mm)	fi %
0.707	0.219	0.071	0.238		0.707	0.351	0.071	0.481
1.086	5.590	0.707	0.449		1.086	6.889	0.707	0.398
1.536	17.598	1.086	0.369		1.536	21.336	1.086	0.312
2.828	34.579	1.536	16.866		2.828	40.938	1.536	15.306
5.020	21.332	2.828	30.960		5.020	18.014	2.828	26.940
7.736	20.660	5.020	23.926		7.736	12.461	5.020	33.484
10.897	0.021	7.736	27.192		10.897	0.010	7.736	23.079
		10.897	0.000				10.897	0.000
Third layer 2 - 3 cm					Fourth layer 3 - 4 cm			
Computed		Data			Computed		Data	
Di (mm)	fi %	Di (mm)	fi %		Di (mm)	fi %	Di (mm)	fi %
0.707	1.596	0.071	0.565		0.707	2.225	0.071	0.498
1.086	8.593	0.707	0.368		1.086	8.496	0.707	0.270
1.536	23.779	1.086	0.381		1.536	22.149	1.086	0.392
2.828	41.850	1.536	20.947		2.828	37.616	1.536	22.769
5.020	15.215	2.828	33.167		5.020	16.065	2.828	34.036
7.736	8.960	5.020	20.473		7.736	13.435	5.020	20.596
10.897	0.007	7.736	24.099		10.897	0.013	7.736	21.438
		10.897	0.000				10.897	0.000
Fifth layer 4 - 5 cm					Sixth layer 5 - 6 cm			
Computed		Data			Computed		Data	
Di (mm)	fi %	Di (mm)	fi %		Di (mm)	fi %	Di (mm)	fi %
0.707	0.114	0.071	0.399		0.707	0.114	0.071	0.315
1.086	5.863	0.707	0.176		1.086	5.863	0.707	0.155
1.536	18.691	1.086	0.379		1.536	18.691	1.086	0.350
2.828	37.088	1.536	21.495		2.828	37.088	1.536	21.389
5.020	20.817	2.828	34.838		5.020	20.817	2.828	35.925
7.736	17.410	5.020	20.785		7.736	17.410	5.020	21.792
10.897	0.017	7.736	21.928		10.897	0.017	7.736	20.074
		10.897	0.000				10.897	0.000
Seventh layer 6 - 7 cm								
Computed		Data						
Di (mm)	fi %	Di (mm)	fi %					
0.707	0.114	0.071	0.254					
1.086	5.863	0.707	0.138					
1.536	18.691	1.086	0.348					
2.828	37.088	1.536	21.660					
5.020	20.817	2.828	36.446					
7.736	17.410	5.020	22.181					
10.897	0.017	7.736	18.973					
		10.897	0.000					

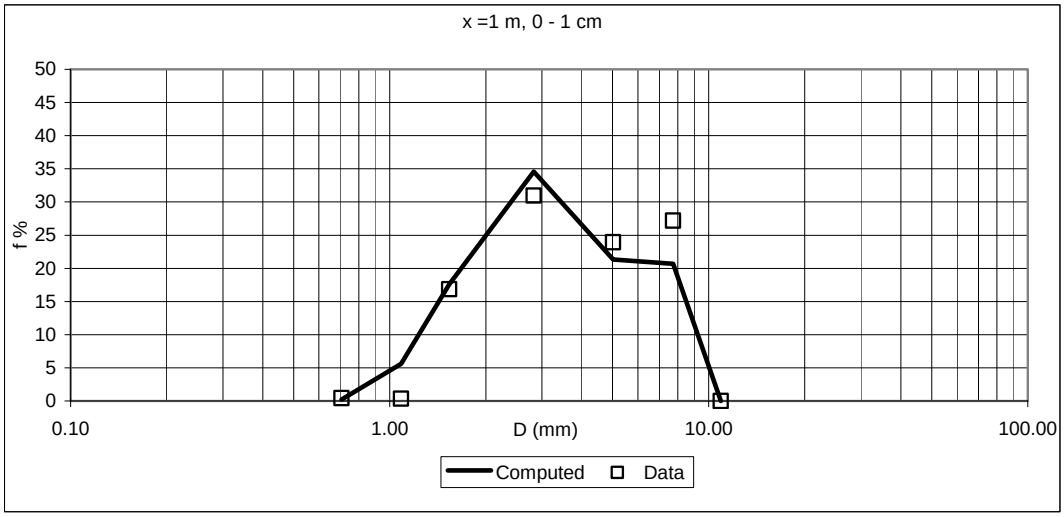
x =1 m, 0 - 1 cm
f %
50
45
40
35
30
25
20
15
10
5
0
0.10
1.00
D (mm)
10.00
100.00
Computed
Data

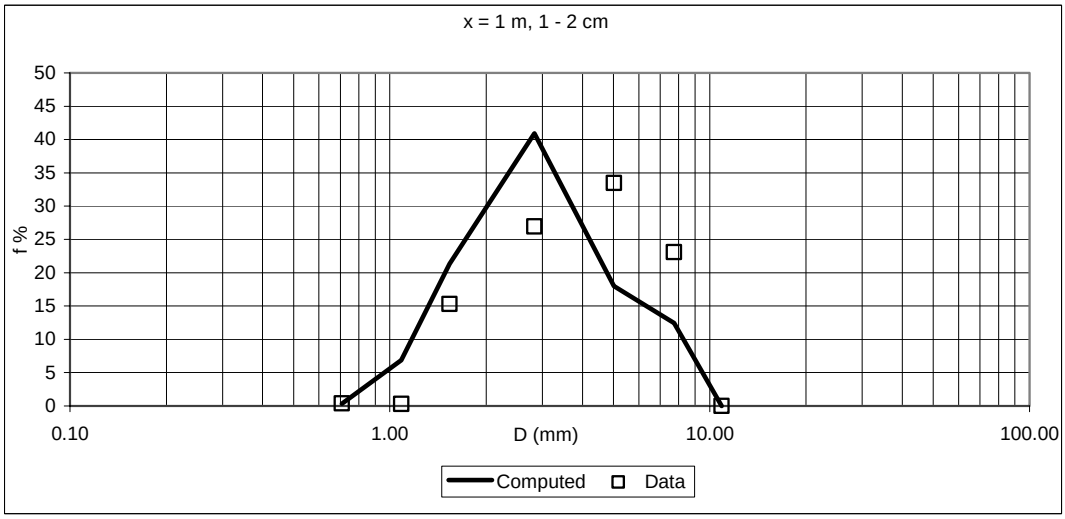
x = 1 m, 1 - 2 cm
f %
50
45
40
35
30
25
20
15
10
5
0
0.10
1.00
D (mm)
10.00
100.00
Computed
Data

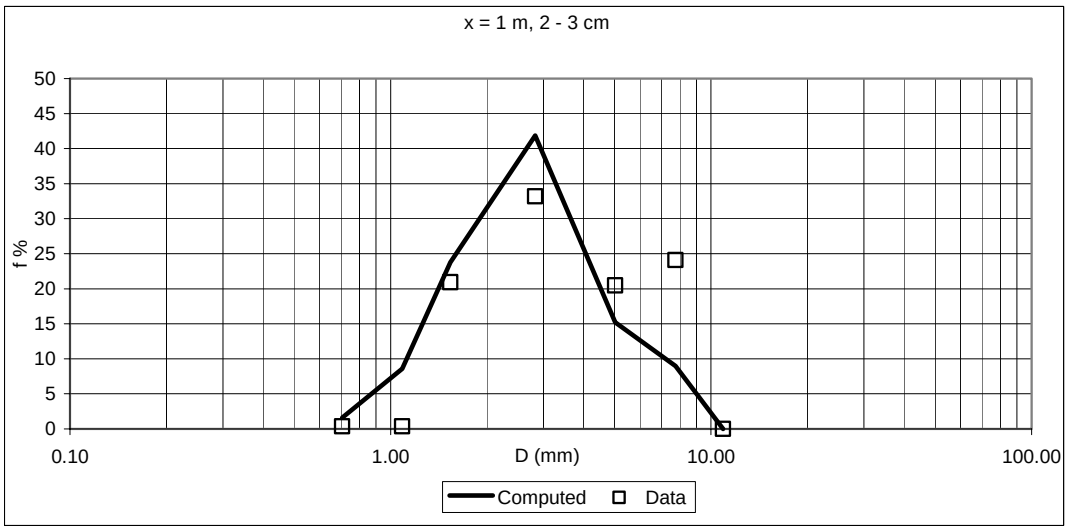
x = 1 m, 2 - 3 cm
f %
50
45
40
35
30
25
20
15
10
5
0
0.10
1.00
D (mm)
10.00
100.00
Computed
Data

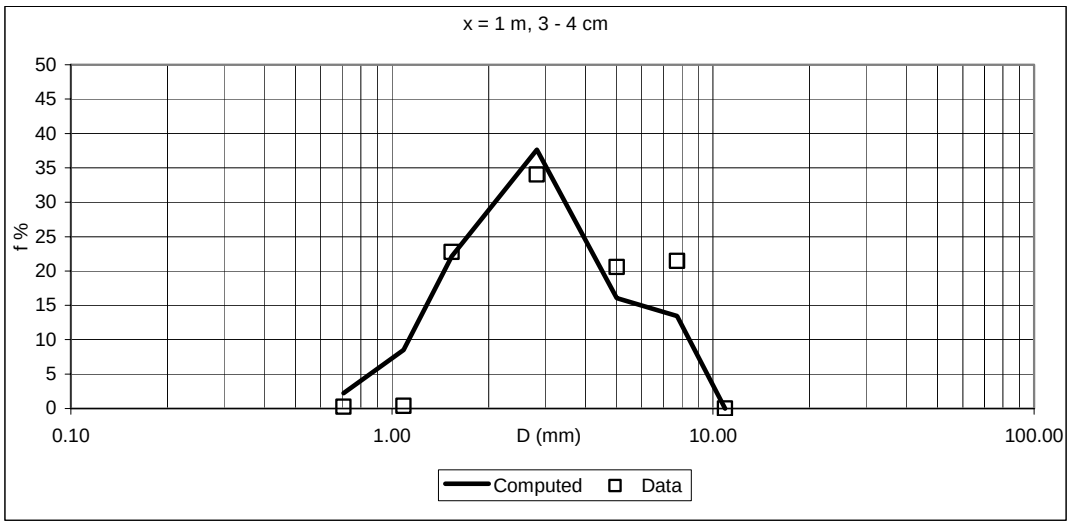
x = 1 m, 3 - 4 cm
f %
50
45
40
35
30
25
20
15
10
5
0
0.10
1.00
D (mm)
10.00
100.00
Computed
Data

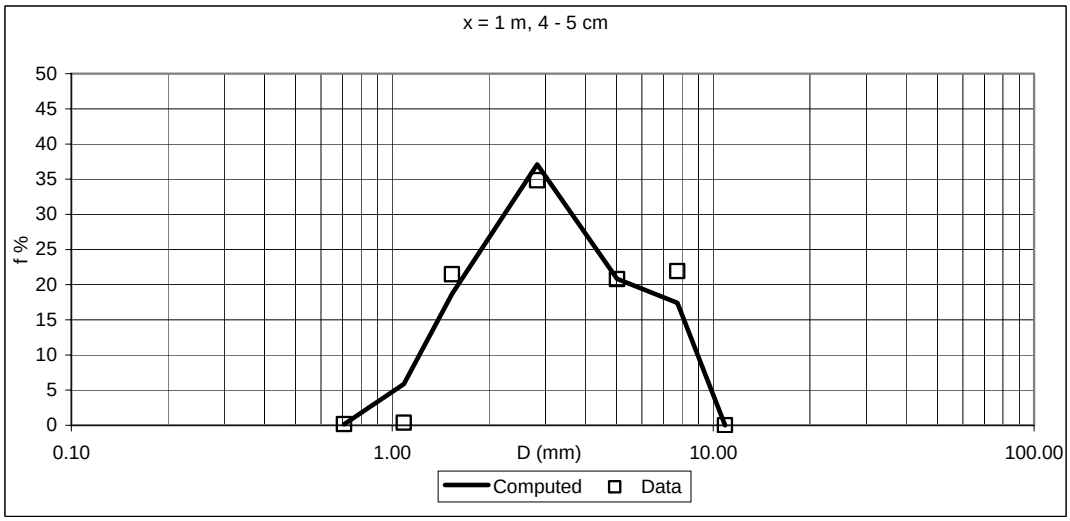
x = 1 m, 4 - 5 cm
f %
50
45
40
35
30
25
20
15
10
5
0
0.10
1.00
D (mm)
10.00
100.00
Computed
Data

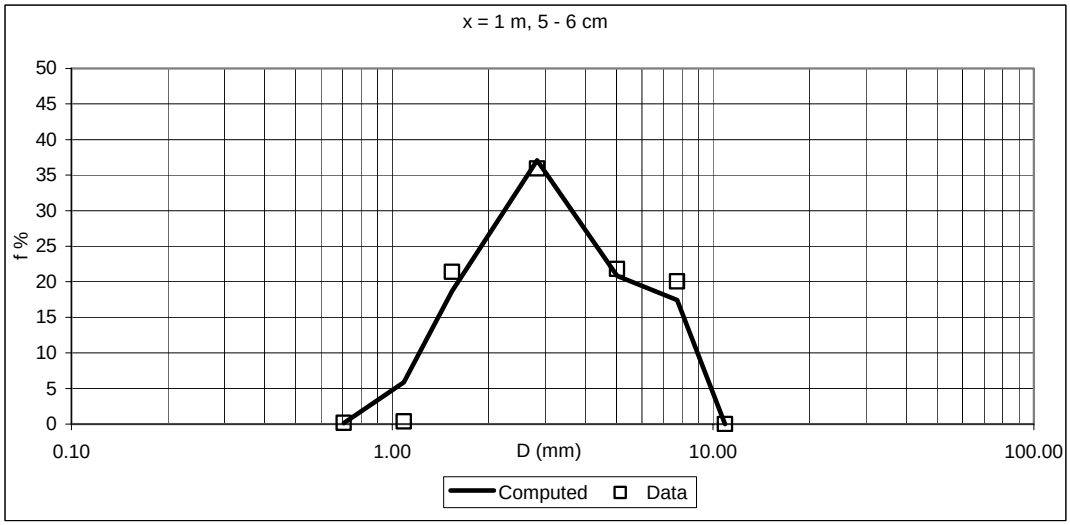
x = 1 m, 5 - 6 cm
f %
50
45
40
35
30
25
20
15
10
5
0
0.10
1.00
D (mm)
10.00
100.00
Computed
Data

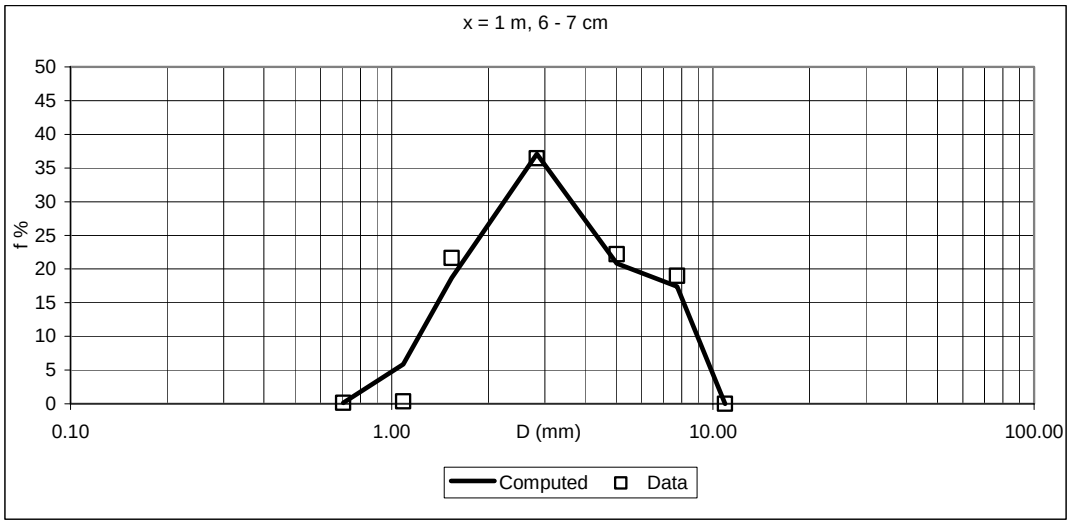
x = 1 m, 6 - 7 cm
50
45
40
35
30
25
20
15
10
5
0
f %
0.10
1.00
D (mm)
10.00
100.00
Computed
Data

x = 1.5 m								
First layer 0 -1 cm					Second layer 1 - 2 cm			
Computed		Data			Computed		Data	
Di (mm)	fi %	Di (mm)	fi %		Di (mm)	fi %	Di (mm)	fi %
0.707	0.218	0.071	0.235		0.707	0.290	0.071	0.461
1.086	5.591	0.707	0.438		1.086	6.789	0.707	0.296
1.536	17.590	1.086	0.406		1.536	21.130	1.086	0.355
2.828	34.571	1.536	21.199		2.828	40.705	1.536	19.881
5.020	21.374	2.828	36.052		5.020	18.668	2.828	35.393
7.736	20.635	5.020	20.363		7.736	12.408	5.020	22.770
10.897	0.021	7.736	21.307		10.897	0.010	7.736	20.843
		10.897	0.000				10.897	0.000
Third layer 2 - 3 cm					Fourth layer 3 - 4 cm			
Computed		Data			Computed		Data	
Di (mm)	fi %	Di (mm)	fi %		Di (mm)	fi %	Di (mm)	fi %
0.707	2.325	0.071	0.132		0.707	1.104	0.071	0.302
1.086	9.999	0.707	0.375		1.086	7.603	0.707	0.173
1.536	25.018	1.086	0.386		1.536	21.166	1.086	0.360
2.828	40.991	1.536	20.893		2.828	38.232	1.536	21.983
5.020	12.639	2.828	34.429		5.020	17.381	2.828	33.968
7.736	9.020	5.020	21.591		7.736	14.501	5.020	21.754
10.897	0.008	7.736	22.193		10.897	0.014	7.736	21.459
		10.897	0.000				10.897	0.000
Fifth layer 4 - 5 cm					Sixth layer 5 - 6 cm			
Computed		Data			Computed		Data	
Di (mm)	fi %	Di (mm)	fi %		Di (mm)	fi %	Di (mm)	fi %
0.707	0.114	0.071	0.247		0.707	0.114	0.071	0.224
1.086	5.863	0.707	0.165		1.086	5.863	0.707	0.145
1.536	18.691	1.086	0.376		1.536	18.691	1.086	0.360
2.828	37.088	1.536	22.015		2.828	37.088	1.536	21.784
5.020	20.817	2.828	35.809		5.020	20.817	2.828	36.193
7.736	17.410	5.020	22.385		7.736	17.410	5.020	21.601
10.897	0.017	7.736	19.002		10.897	0.017	7.736	19.694
		10.897	0.000				10.897	0.000
Seventh layer 6 - 7 cm								
Computed		Data						
Di (mm)	fi %	Di (mm)	fi %					
0.707	0.114	0.071	0.196					
1.086	5.863087	0.707	0.139					
1.536	18.69056	1.086	0.313					
2.828	37.08786	1.536	21.693					
5.020	20.81719	2.828	37.254					
7.736	17.40982	5.020	21.010					
10.897	0.017136	7.736	19.094					
		10.897	0.301					

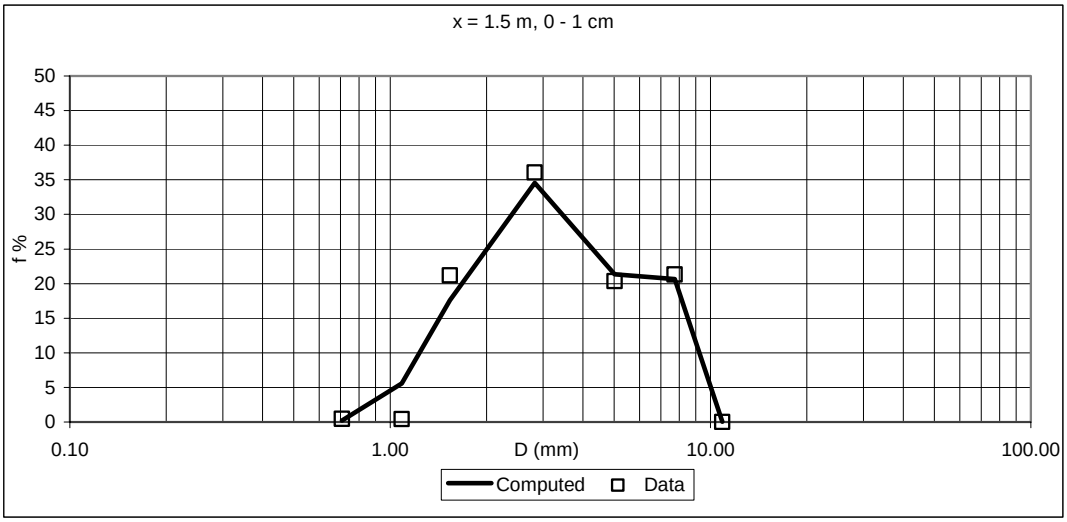
x = 1.5 m, 0 - 1 cm
f %
50
45
40
35
30
25
20
15
10
5
0
0.10
1.00
D (mm)
10.00
100.00
Computed
Data

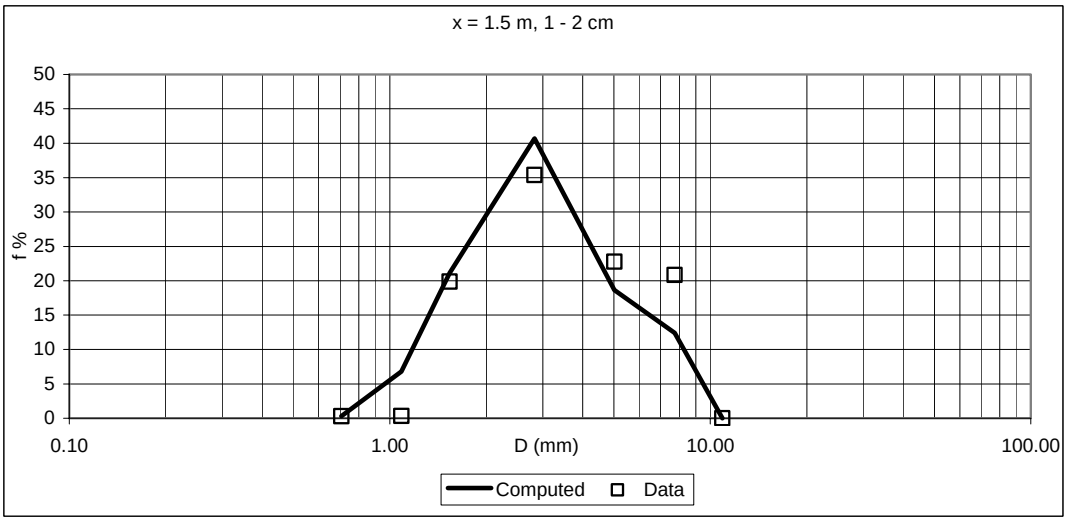
x = 1.5 m, 1 - 2 cm
f %
50
45
40
35
30
25
20
15
10
5
0
0.10
1.00
D (mm)
10.00
100.00
Computed
Data

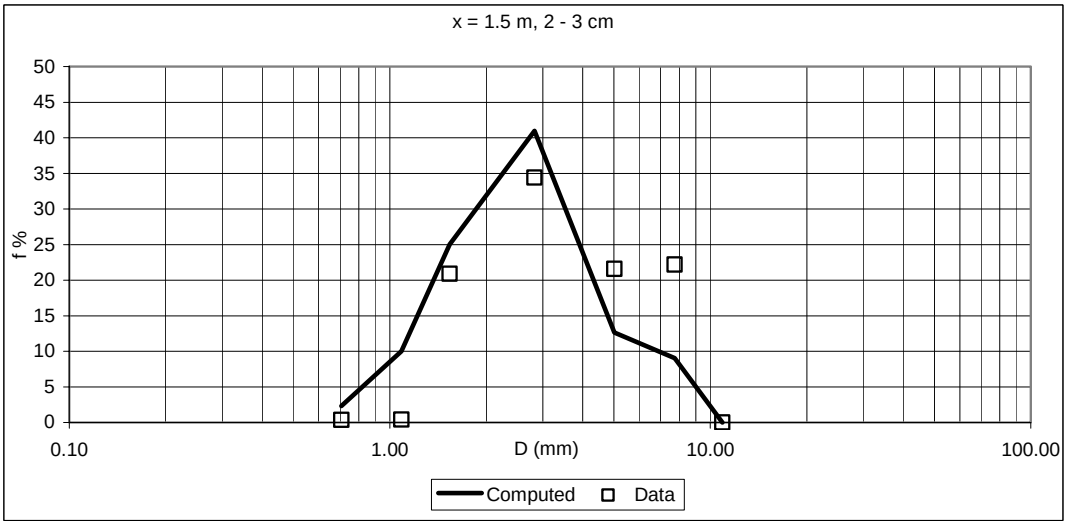
x = 1.5 m, 2 - 3 cm
f %
50
45
40
35
30
25
20
15
10
5
0
0.10
1.00
D (mm)
10.00
100.00
Computed
Data

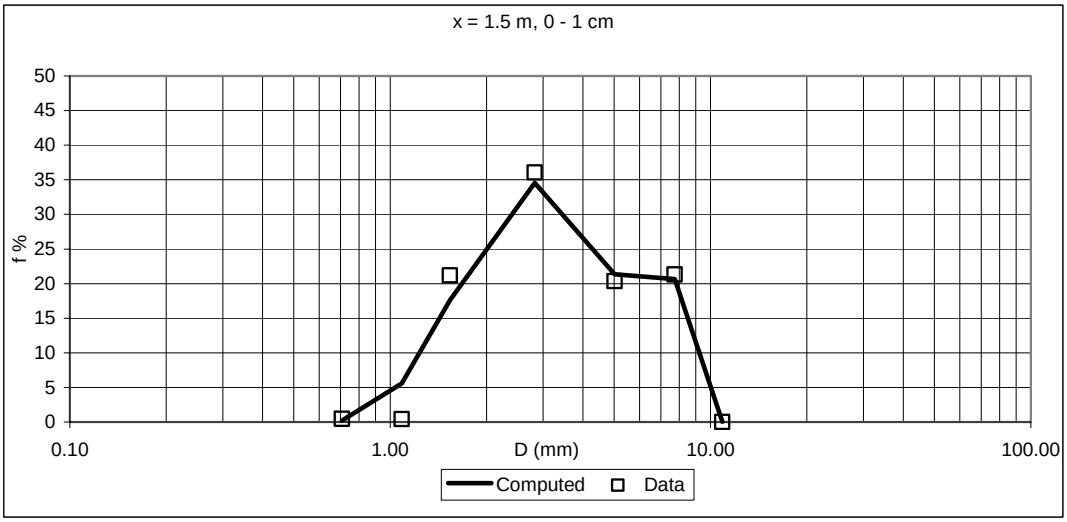
x = 1.5 m, 0 - 1 cm
f %
50
45
40
35
30
25
20
15
10
5
0
0.10
1.00
D (mm)
10.00
100.00
Computed
Data

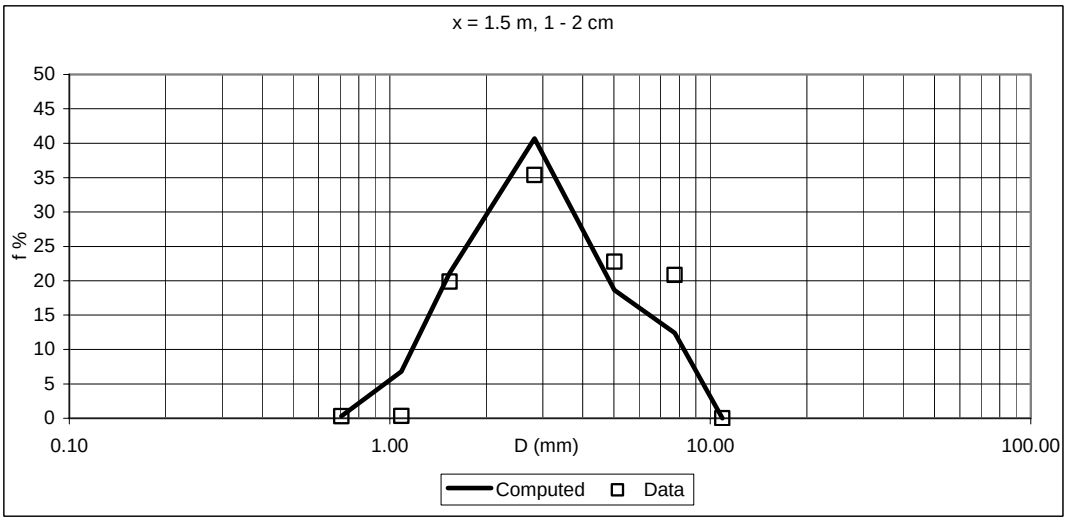
x = 1.5 m, 1 - 2 cm
f %
50
45
40
35
30
25
20
15
10
5
0
0.10
1.00
D (mm)
10.00
100.00
Computed
Data

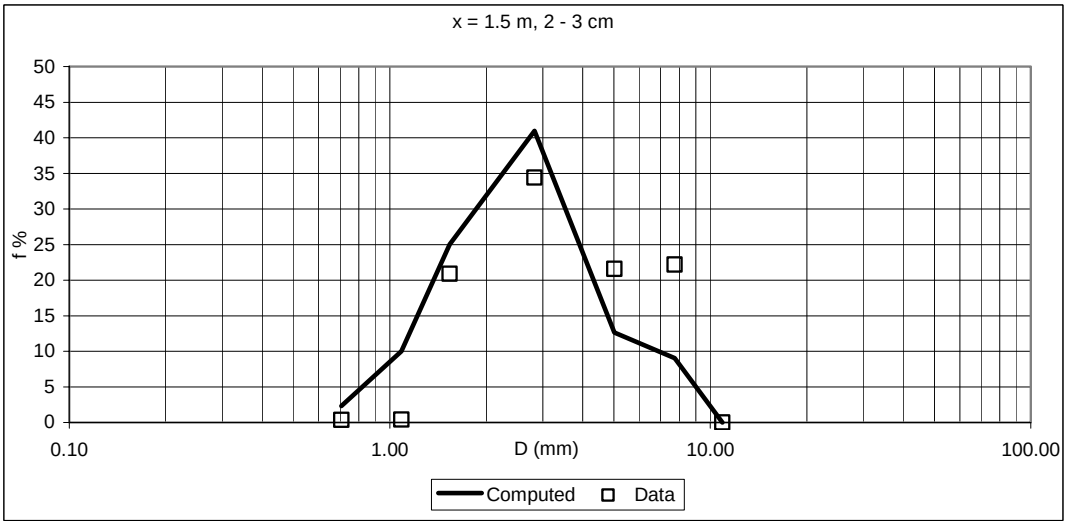
x = 1.5 m, 2 - 3 cm
f %
50
45
40
35
30
25
20
15
10
5
0
0.10
1.00
D (mm)
10.00
100.00
Computed
Data

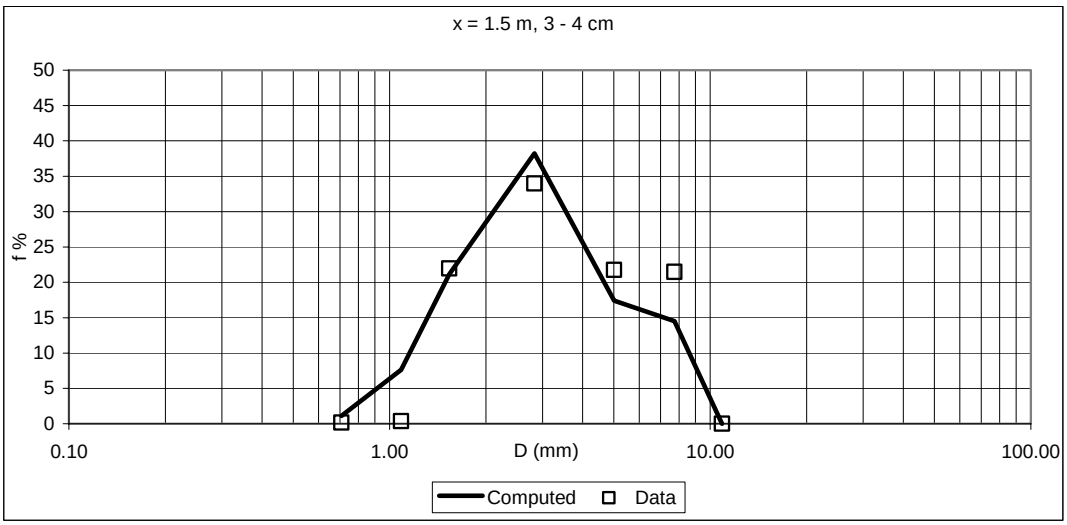
x = 1.5 m, 3 - 4 cm
f %
50
45
40
35
30
25
20
15
10
5
0
0.10
1.00
D (mm)
10.00
100.00
Computed
Data

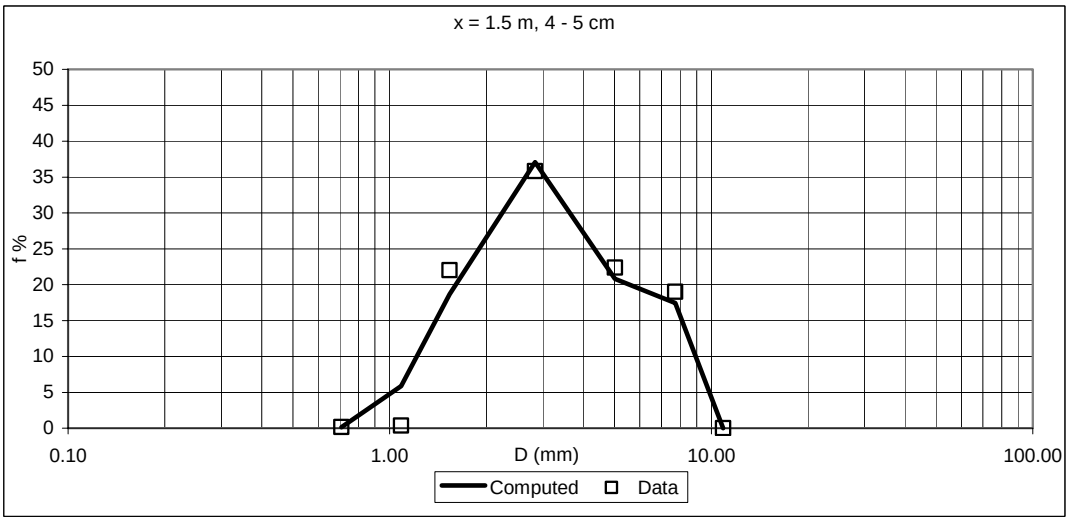
x = 1.5 m, 4 - 5 cm
f %
50
45
40
35
30
25
20
15
10
5
0
0.10
1.00
D (mm)
10.00
100.00
Computed
Data

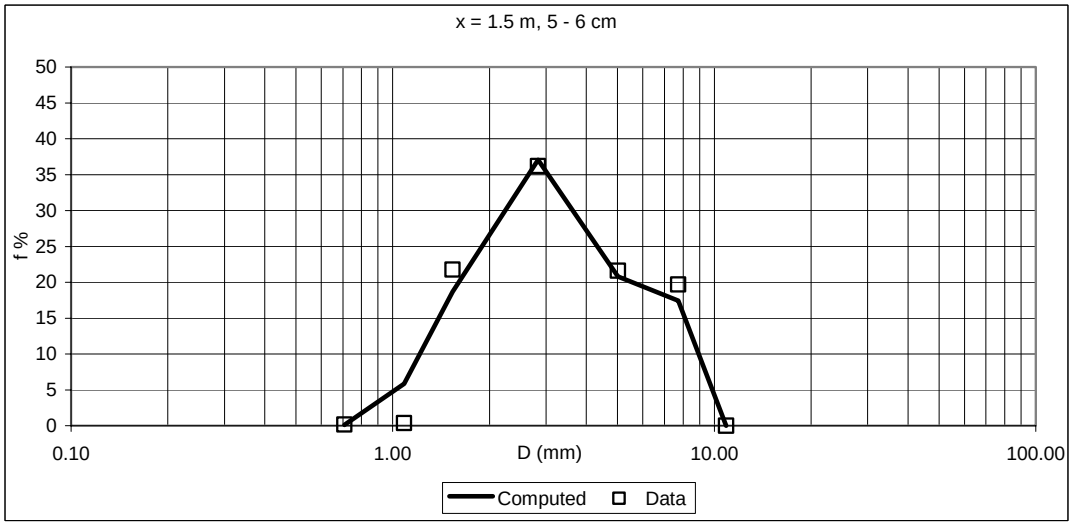
x = 1.5 m, 5 - 6 cm
f %
50
45
40
35
30
25
20
15
10
5
0
0.10
1.00
D (mm)
10.00
100.00
Computed
Data

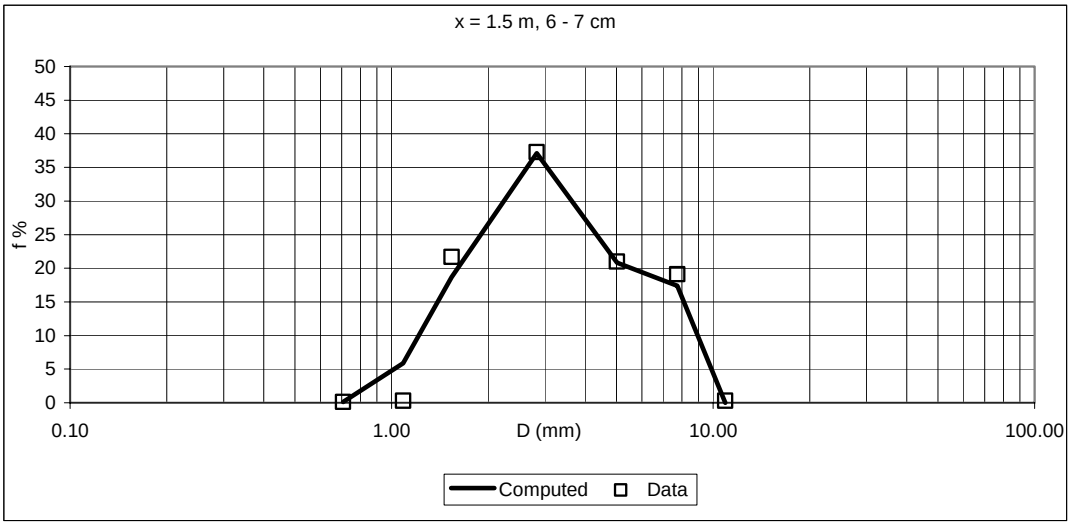
x = 1.5 m, 6 - 7 cm
50
45
40
35
30
25
20
15
10
5
0
f %
0.10
1.00
D (mm)
10.00
100.00
Computed
Data

x = 2 m								
First layer 0 -1 cm					Second layer 1 - 2 cm			
Computed		Data			Computed		Data	
Di (mm)	fi %	Di (mm)	fi %		Di (mm)	fi %	Di (mm)	fi %
0.707	0.218	0.071	0.236		0.707	0.283	0.071	0.328
1.086	5.622	0.707	0.350		1.086	6.686	0.707	0.220
1.536	17.665	1.086	0.222		1.536	20.864	1.086	0.262
2.828	34.688	1.536	17.337		2.828	40.282	1.536	17.046
5.020	21.406	2.828	33.119		5.020	18.615	2.828	34.314
7.736	20.381	5.020	23.003		7.736	13.258	5.020	24.096
10.897	0.021	7.736	25.607		10.897	0.011	7.736	23.735
		10.897	0.127				10.897	0.000
Third layer 2 - 3 cm					Fourth layer 3 - 4 cm			
Computed		Data			Computed		Data	
Di (mm)	fi %	Di (mm)	fi %		Di (mm)	fi %	Di (mm)	fi %
0.707	3.848	0.071	0.296		0.707	0.114	0.071	0.225
1.086	12.009	0.707	0.164		1.086	5.863	0.707	0.114
1.536	28.318	1.086	0.320		1.536	18.691	1.086	0.292
2.828	43.130	1.536	18.907		2.828	37.088	1.536	19.149
5.020	7.274	2.828	34.444		5.020	20.817	2.828	32.565
7.736	5.417	5.020	22.923		7.736	17.410	5.020	25.217
10.897	0.005	7.736	22.946		10.897	0.017	7.736	22.325
		10.897	0.000				10.897	0.114
Fifth layer 4 - 5 cm					Sixth layer 5 - 6 cm			
Computed		Data			Computed		Data	
Di (mm)	fi %	Di (mm)	fi %		Di (mm)	fi %	Di (mm)	fi %
0.707	0.114	0.071	0.219		0.707	0.114	0.071	0.185
1.086	5.863	0.707	0.127		1.086	5.863	0.707	0.114
1.536	18.691	1.086	0.291		1.536	18.691	1.086	0.338
2.828	37.088	1.536	20.983		2.828	37.088	1.536	21.188
5.020	20.817	2.828	35.390		5.020	20.817	2.828	33.778
7.736	17.410	5.020	21.384		7.736	17.410	5.020	22.394
10.897	0.017	7.736	21.428		10.897	0.017	7.736	21.629
		10.897	0.178				10.897	0.374
Seventh layer 6 - 7 cm								
Computed		Data						
Di (mm)	fi %	Di (mm)	fi %					
0.707	0.114	0.071	0.144					
1.086	5.863087	0.707	0.112999					
1.536	18.69056	1.086	0.340465					
2.828	37.08786	1.536	20.56001					
5.020	20.81719	2.828	33.03543					
7.736	17.40982	5.020	23.21916					
10.897	0.017136	7.736	22.47806					
		10.897	0.110064					

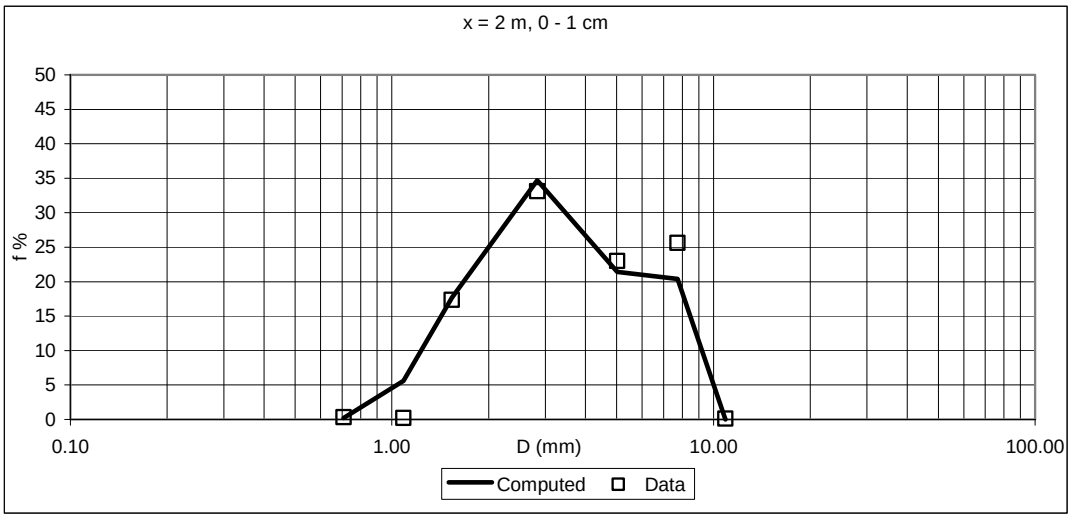
x = 2 m, 0 - 1 cm
f %
50
45
40
35
30
25
20
15
10
5
0
0.10
1.00
D (mm)
10.00
100.00
Computed
Data

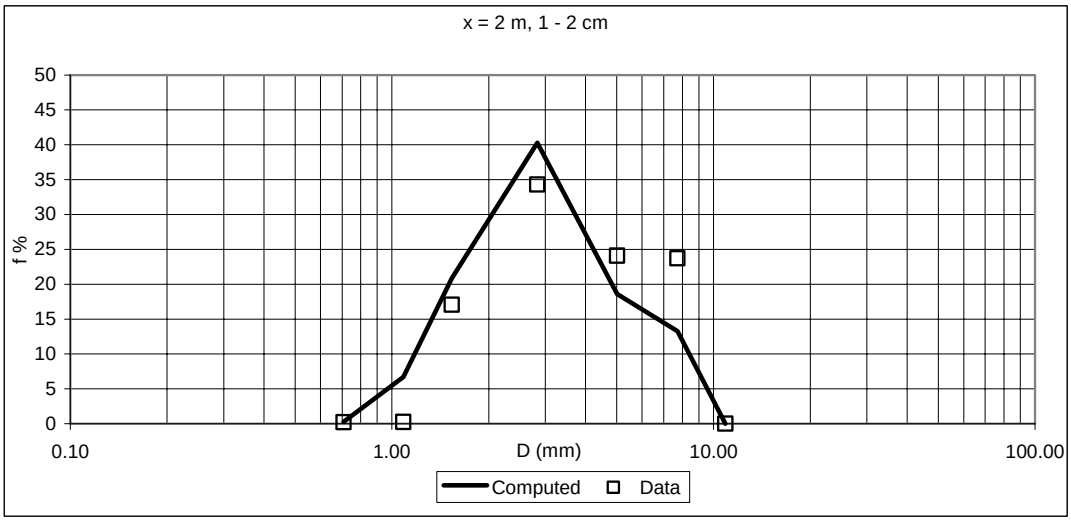
x = 2 m, 1 - 2 cm
f %
50
45
40
35
30
25
20
15
10
5
0
0.10
1.00
D (mm)
10.00
100.00
Computed
Data

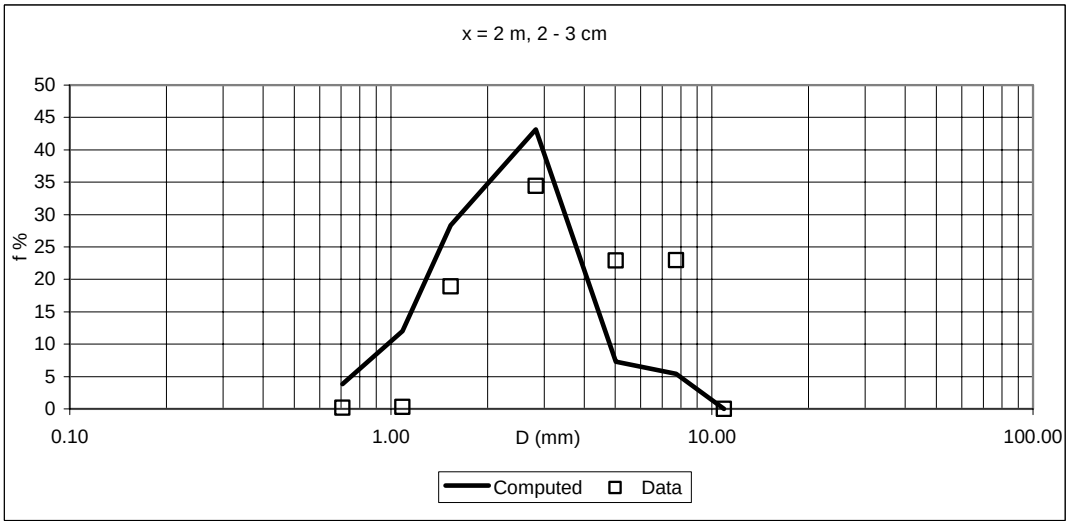
x = 2 m, 2 - 3 cm
f %
50
45
40
35
30
25
20
15
10
5
0
0.10
1.00
D (mm)
10.00
100.00
Computed
Data

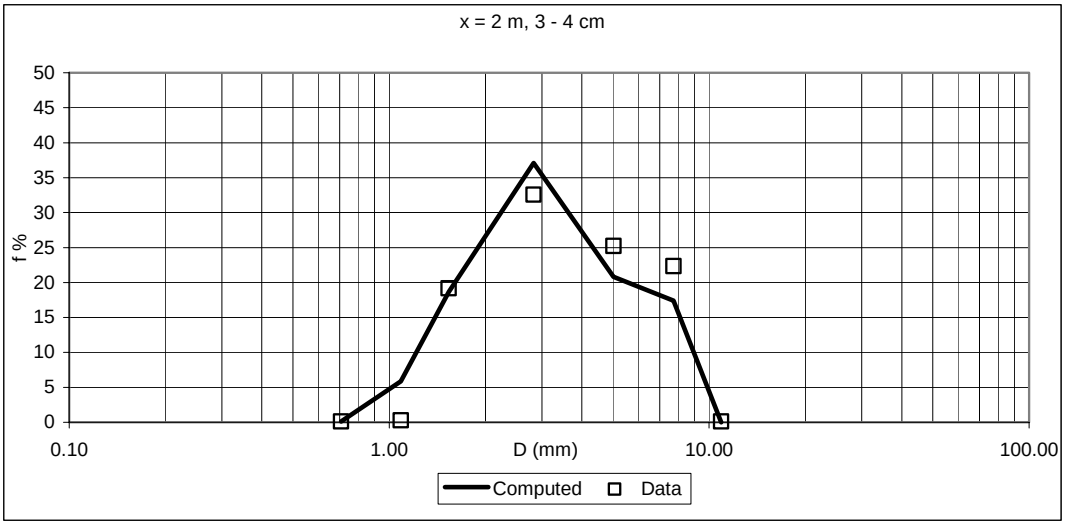
x = 2 m, 3 - 4 cm
f %
50
45
40
35
30
25
20
15
10
5
0
0.10
1.00
D (mm)
10.00
100.00
Computed
Data

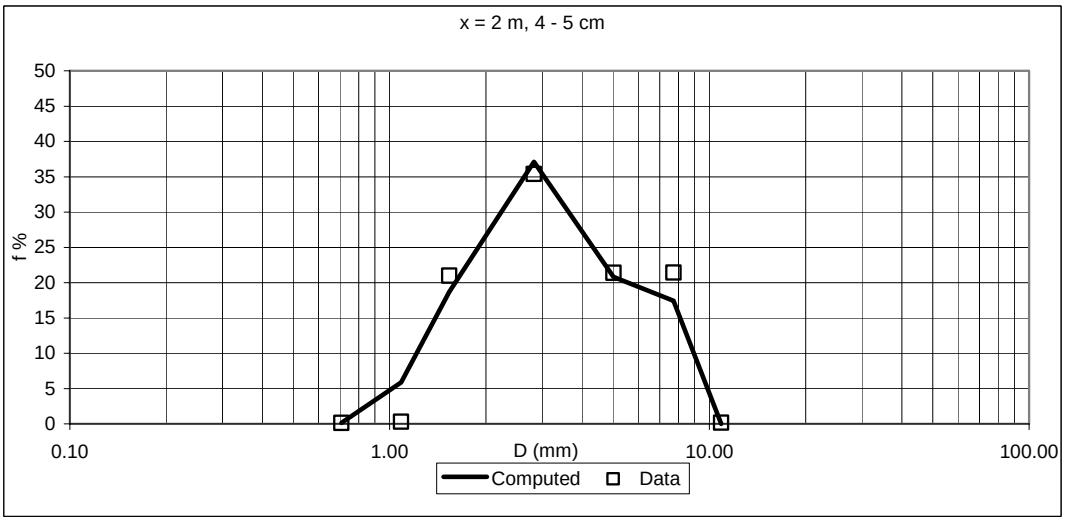
x = 2 m, 4 - 5 cm
f %
50
45
40
35
30
25
20
15
10
5
0
0.10
1.00
D (mm)
10.00
100.00
Computed
Data

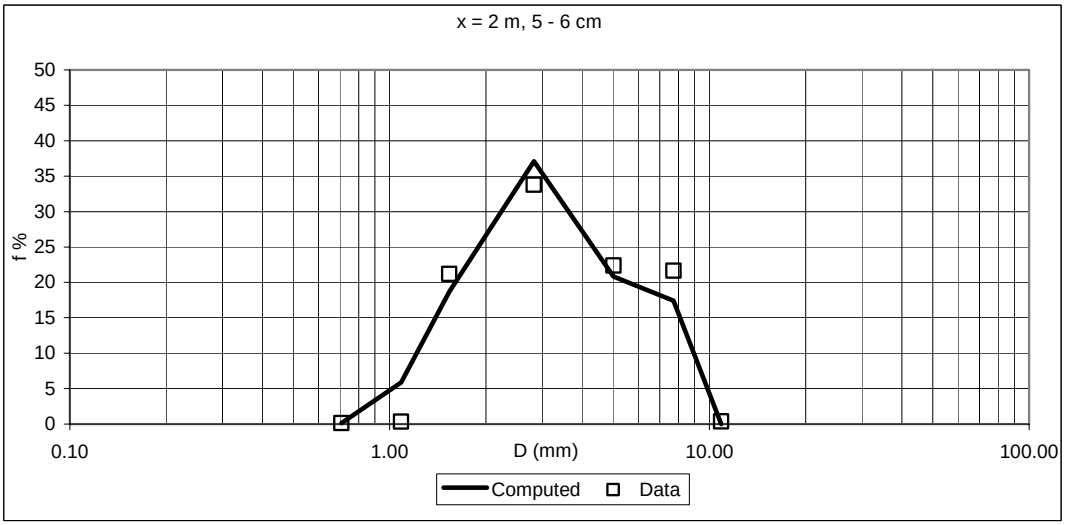
x = 2 m, 5 - 6 cm
f %
50
45
40
35
30
25
20
15
10
5
0
0.10
1.00
D (mm)
10.00
100.00
Computed
Data

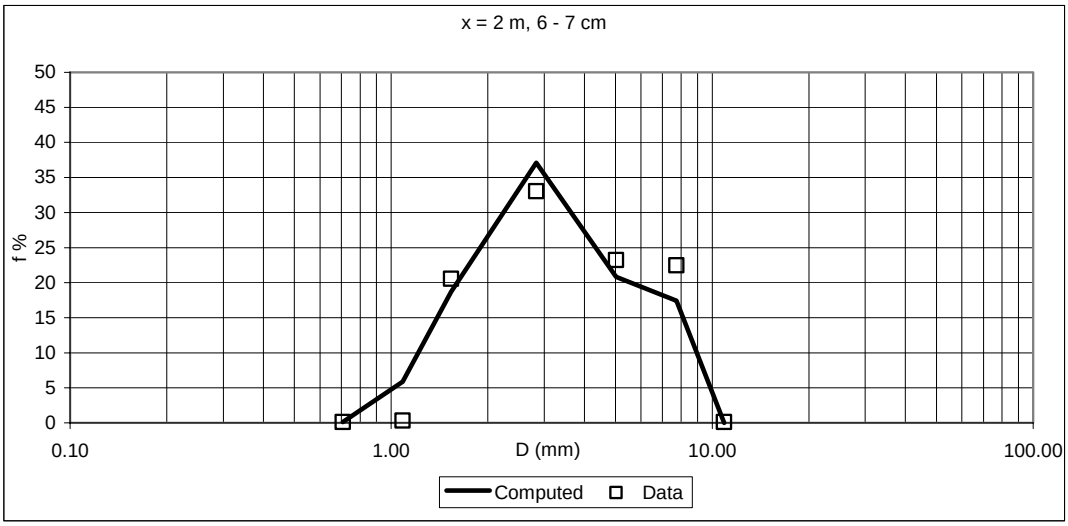
x = 2 m, 6 - 7 cm
50
45
40
35
30
25
20
15
10
5
0
f %
0.10
1.00
D (mm)
10.00
100.00
Computed
Data

x = 2.5 m								
First layer 0 -1 cm					Second layer 1 - 2 cm			
Computed		Data			Computed		Data	
Di (mm)	fi %	Di (mm)	fi %		Di (mm)	fi %	Di (mm)	fi %
0.707	0.222	0.071	0.185		0.707	0.830	0.071	0.216
1.086	5.656	0.707	0.300		1.086	8.455	0.707	0.208
1.536	17.771	1.086	0.313		1.536	23.472	1.086	0.272
2.828	34.886	1.536	17.398		2.828	41.633	1.536	18.336
5.020	21.291	2.828	34.805		5.020	14.520	2.828	34.280
7.736	20.155	5.020	22.940		7.736	11.080	5.020	23.101
10.897	0.021	7.736	24.059		10.897	0.010	7.736	23.410
		10.897	0.000				10.897	0.176
Third layer 2 - 3 cm					Fourth layer 3 - 4 cm			
Computed		Data			Computed		Data	
Di (mm)	fi %	Di (mm)	fi %		Di (mm)	fi %	Di (mm)	fi %
0.707	1.819	0.071	0.170		0.707	0.975	0.071	0.158
1.086	10.378	0.707	0.152		1.086	5.839	0.707	0.116
1.536	26.259	1.086	0.279		1.536	18.524	1.086	0.260
2.828	43.022	1.536	17.992		2.828	36.758	1.536	17.539
5.020	10.813	2.828	34.286		5.020	20.632	2.828	34.293
7.736	7.701	5.020	24.555		7.736	17.255	5.020	22.456
10.897	0.007	7.736	22.566		10.897	0.017	7.736	25.178
		10.897	0.000				10.897	0.000
Fifth layer 4 - 5 cm					Sixth layer 5 - 6 cm			
Computed		Data			Computed		Data	
Di (mm)	fi %	Di (mm)	fi %		Di (mm)	fi %	Di (mm)	fi %
0.707	0.114	0.071	0.156		0.707	0.114	0.071	0.162
1.086	5.863	0.707	0.105		1.086	5.863	0.707	0.116
1.536	18.691	1.086	0.303		1.536	18.691	1.086	0.303
2.828	37.088	1.536	20.186		2.828	37.088	1.536	20.425
5.020	20.817	2.828	34.748		5.020	20.817	2.828	34.694
7.736	17.410	5.020	23.611		7.736	17.410	5.020	24.315
10.897	0.017	7.736	20.890		10.897	0.017	7.736	19.805
		10.897	0.000				10.897	0.180
Seventh layer 6 - 7 cm								
Computed		Data						
Di (mm)	fi %	Di (mm)	fi %					
0.707	0.114	0.071	0.146					
1.086	5.863087	0.707	0.110					
1.536	18.69056	1.086	0.327					
2.828	37.08786	1.536	21.796					
5.020	20.81719	2.828	34.944					
7.736	17.40982	5.020	21.594					
10.897	0.017136	7.736	21.082					
		10.897	0.000					

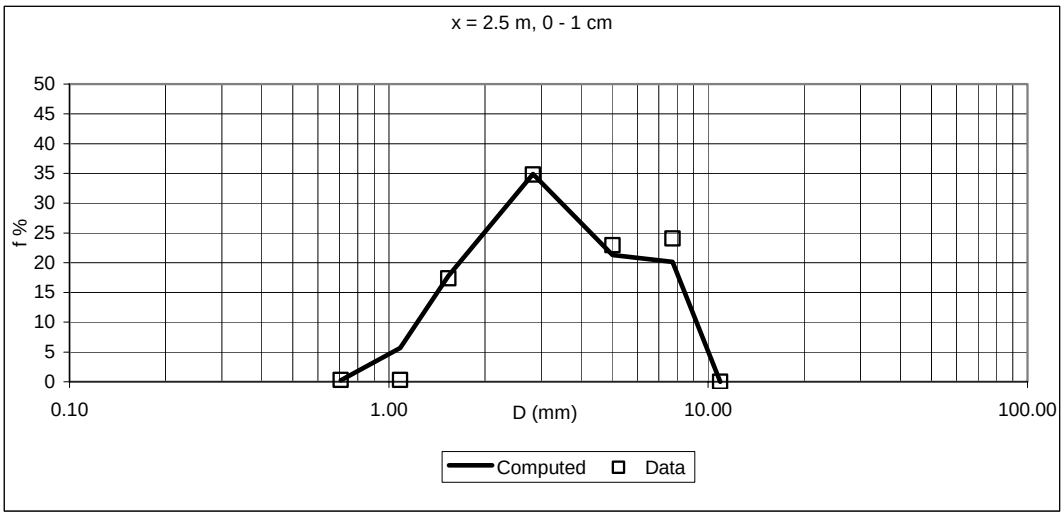
x = 2.5 m, 0 - 1 cm
f %
50
45
40
35
30
25
20
15
10
5
0
0.10
1.00
D (mm)
10.00
100.00
Computed
Data

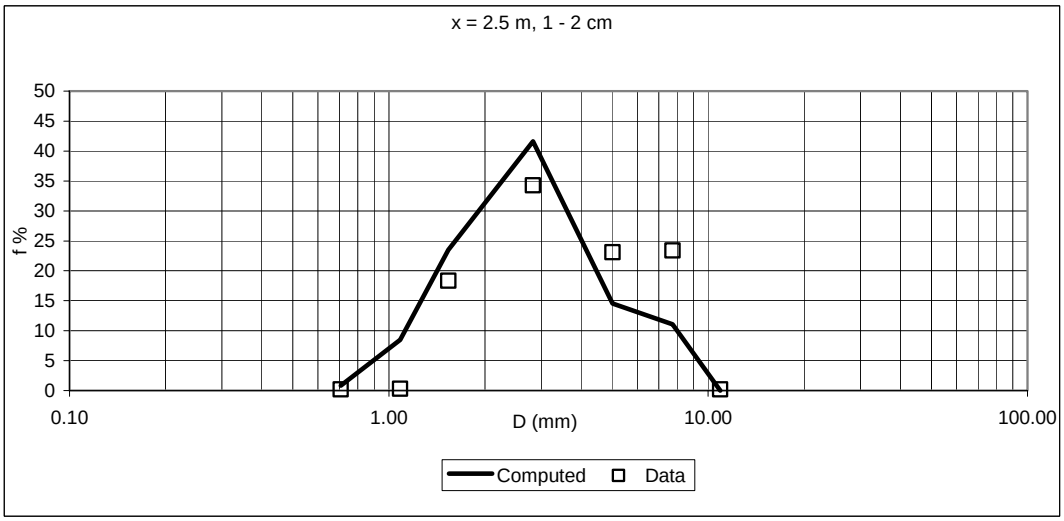
x = 2.5 m, 1 - 2 cm
f %
50
45
40
35
30
25
20
15
10
5
0
0.10
1.00
D (mm)
10.00
100.00
Computed
Data

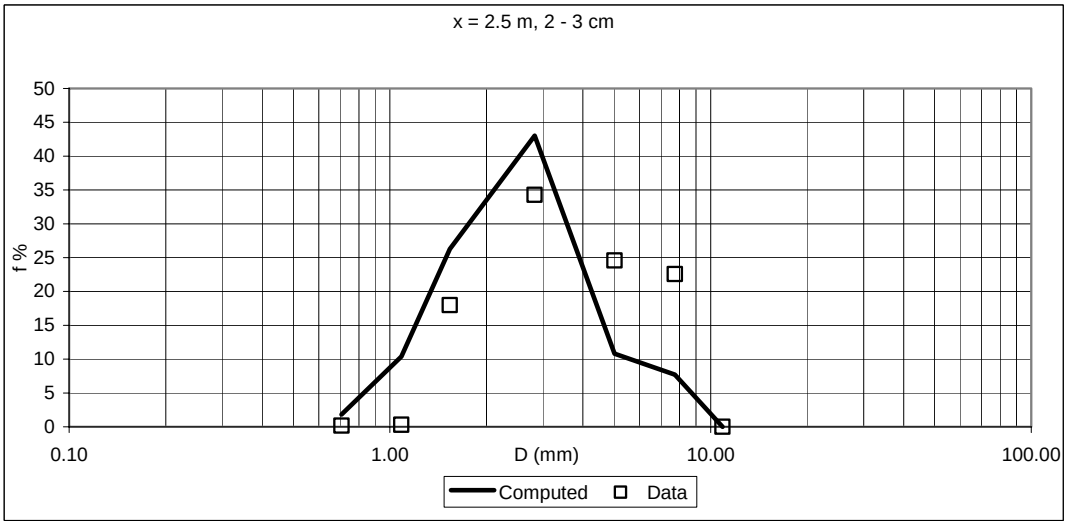
x = 2.5 m, 2 - 3 cm
f %
50
45
40
35
30
25
20
15
10
5
0
0.10
1.00
D (mm)
10.00
100.00
Computed
Data

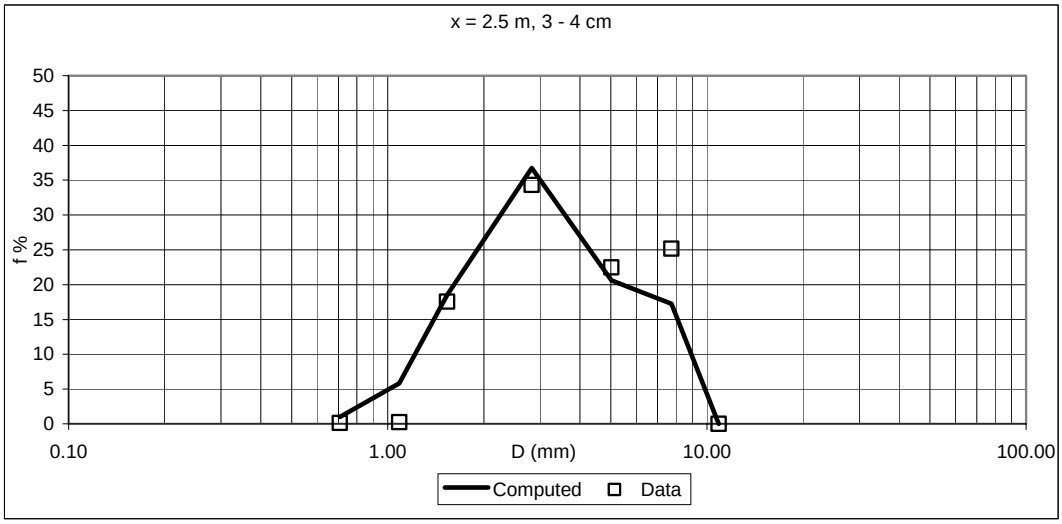
x = 2.5 m, 3 - 4 cm
f %
D (mm)
0.10
1.00
10.00
100.00
Computed
Data

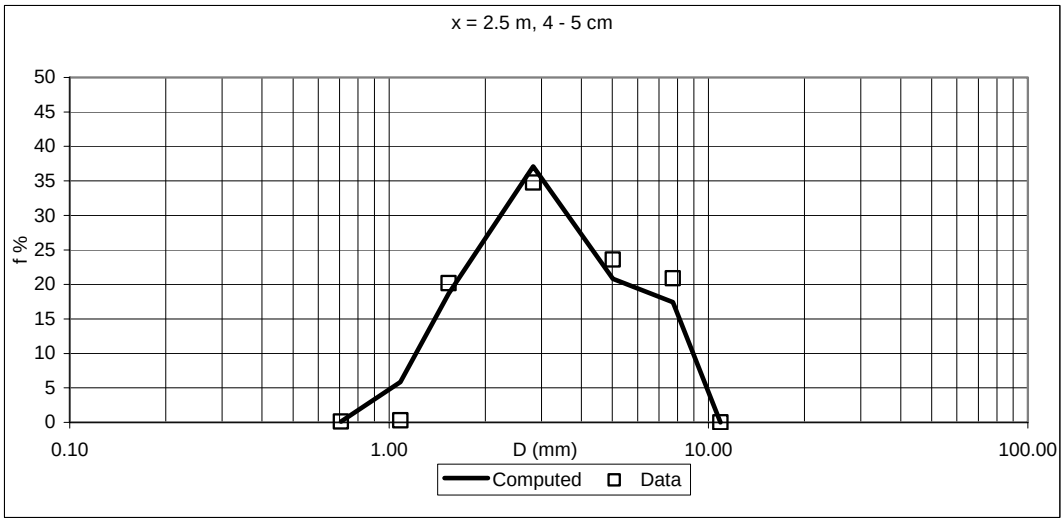
x = 2.5 m, 4 - 5 cm
f %
D (mm)
0.10
1.00
10.00
100.00
Computed
Data

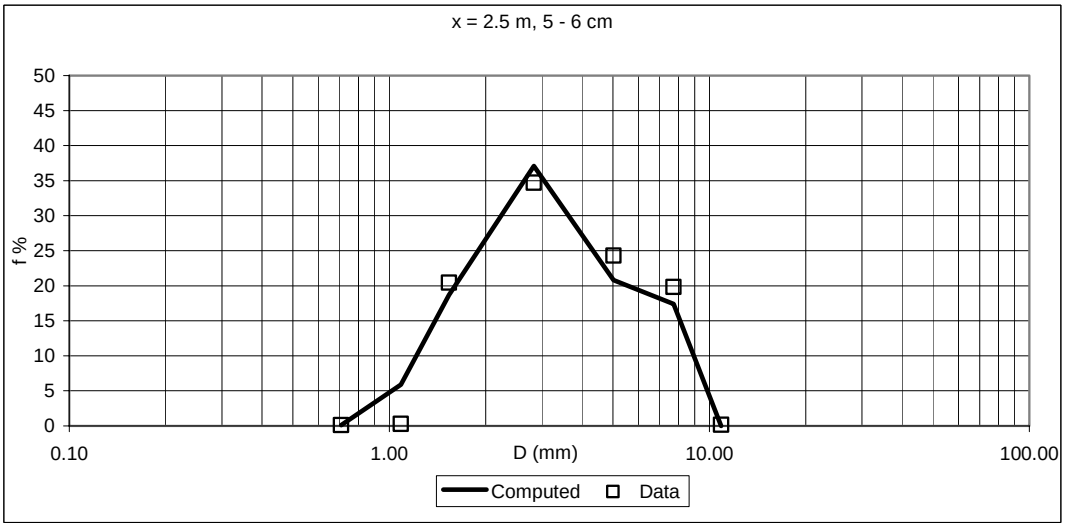
x = 2.5 m, 5 - 6 cm
f %
D (mm)
0.10
1.00
10.00
100.00
Computed
Data

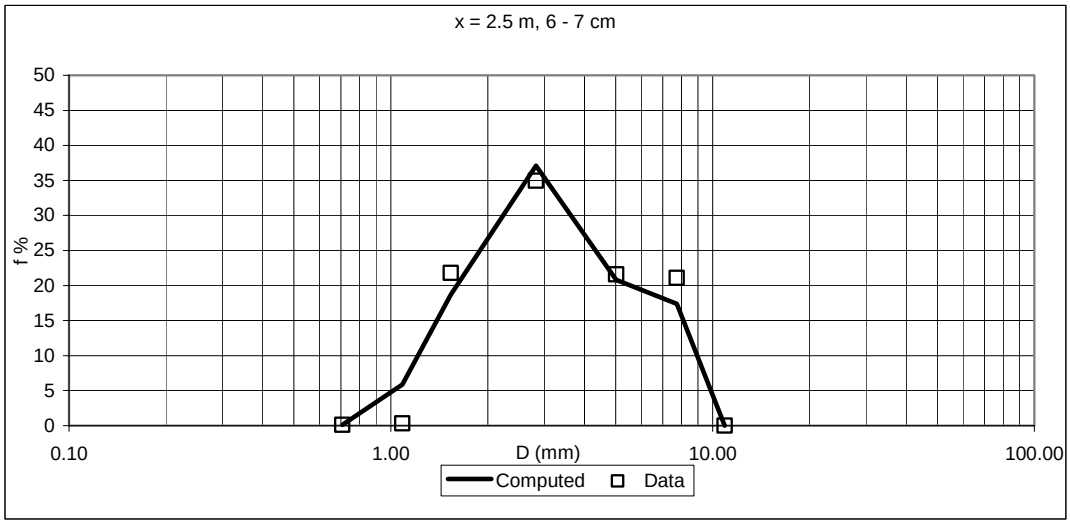
x = 2.5 m, 6 - 7 cm
50
45
40
35
30
25
20
15
10
5
0
f %
0.10
1.00
D (mm)
10.00
100.00
Computed
Data

x = 3 m								
First layer 0 -1 cm					Second layer 1 - 2 cm			
Computed		Data			Computed		Data	
Di (mm)	fi %	Di (mm)	fi %		Di (mm)	fi %	Di (mm)	fi %
0.707	0.221	0.071	0.129		0.707	0.505	0.071	0.176
1.086	5.640	0.707	0.235		1.086	7.782	0.707	0.166
1.536	17.719	1.086	0.337		1.536	23.359	1.086	0.344
2.828	34.809	1.536	19.320		2.828	43.466	1.536	20.253
5.020	21.185	2.828	34.082		5.020	15.426	2.828	34.391
7.736	20.405	5.020	23.464		7.736	9.453	5.020	22.305
10.897	0.021	7.736	22.432		10.897	0.008	7.736	22.364
		10.897	0.000				10.897	0.000
Third layer 2 - 3 cm					Fourth layer 3 - 4 cm			
Computed		Data			Computed		Data	
Di (mm)	fi %	Di (mm)	fi %		Di (mm)	fi %	Di (mm)	fi %
0.707	1.796	0.071	0.135		0.707	0.958	0.071	0.117
1.086	8.639	0.707	0.126		1.086	6.882	0.707	0.227
1.536	22.581	1.086	0.330		1.536	19.550	1.086	0.199
2.828	39.239	1.536	20.458		2.828	36.456	1.536	19.296
5.020	16.292	2.828	34.969		5.020	19.680	2.828	32.747
7.736	11.442	5.020	22.451		7.736	16.458	5.020	21.864
10.897	0.011	7.736	21.532		10.897	0.016	7.736	25.358
		10.897	0.000				10.897	0.191
Fifth layer 4 - 5 cm								
Computed		Data						
Di (mm)	fi %	Di (mm)	fi %					
0.707	0.114	0.071	0.157					
1.086	5.863	0.707	0.100					
1.536	18.691	1.086	0.322					
2.828	37.088	1.536	20.177					
5.020	20.817	2.828	35.067					
7.736	17.410	5.020	22.919					
10.897	0.017	7.736	21.257					
		10.897	0.000					

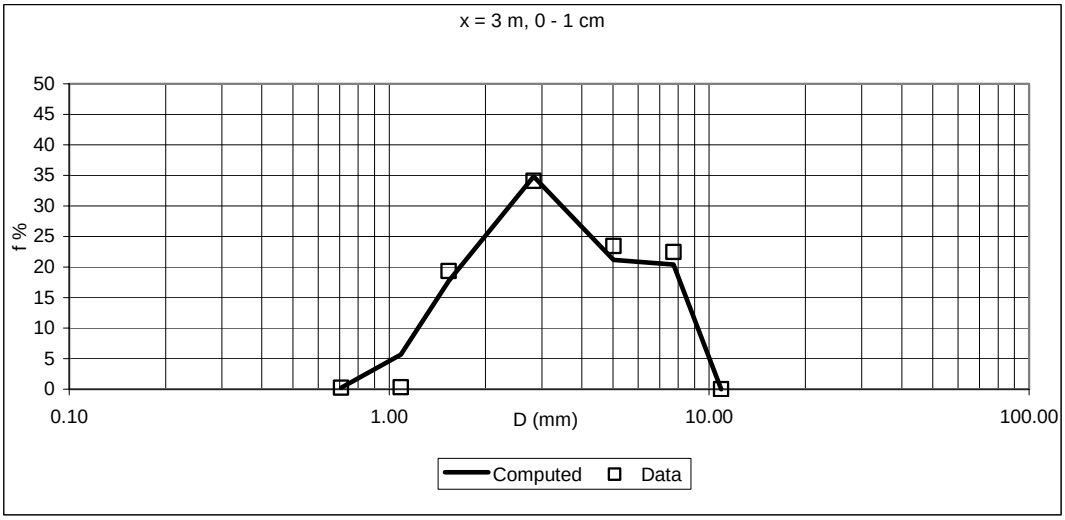
x = 3 m, 0 - 1 cm
f %
50
45
40
35
30
25
20
15
10
5
0
0.10
1.00
D (mm)
10.00
100.00
Computed
Data

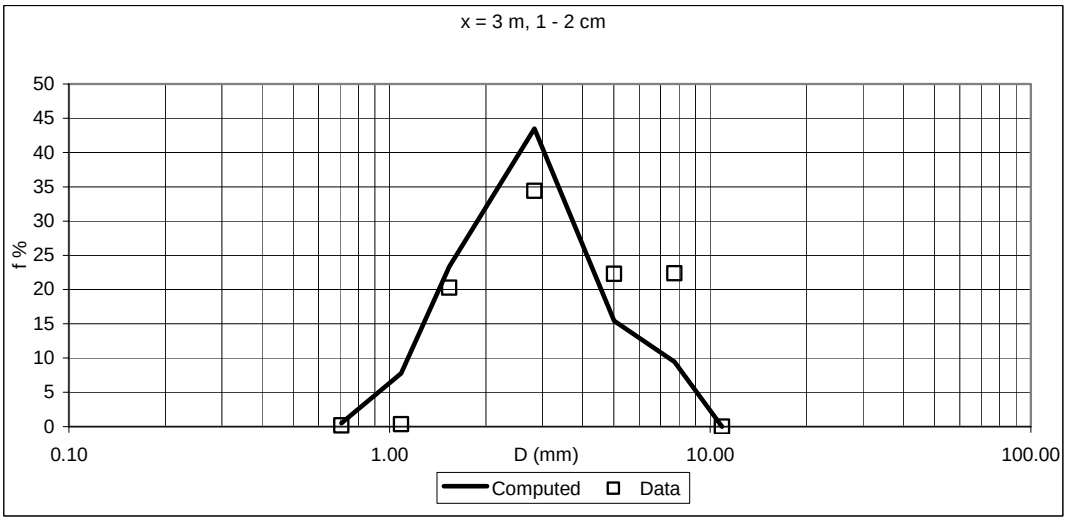
x = 3 m, 1 - 2 cm
f %
50
45
40
35
30
25
20
15
10
5
0
0.10
1.00
D (mm)
10.00
100.00
Computed
Data

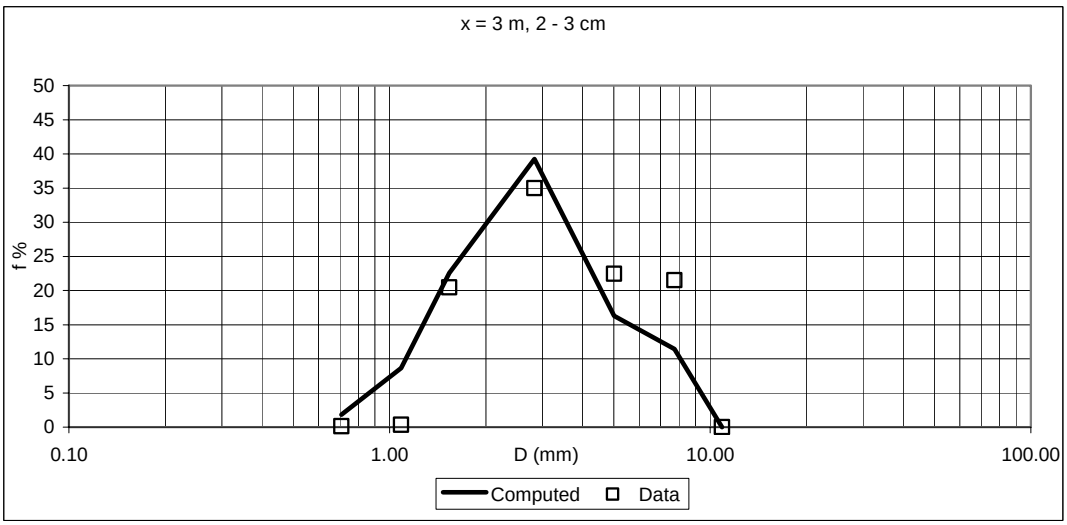
x = 3 m, 2 - 3 cm
f %
50
45
40
35
30
25
20
15
10
5
0
0.10
1.00
D (mm)
10.00
100.00
Computed
Data

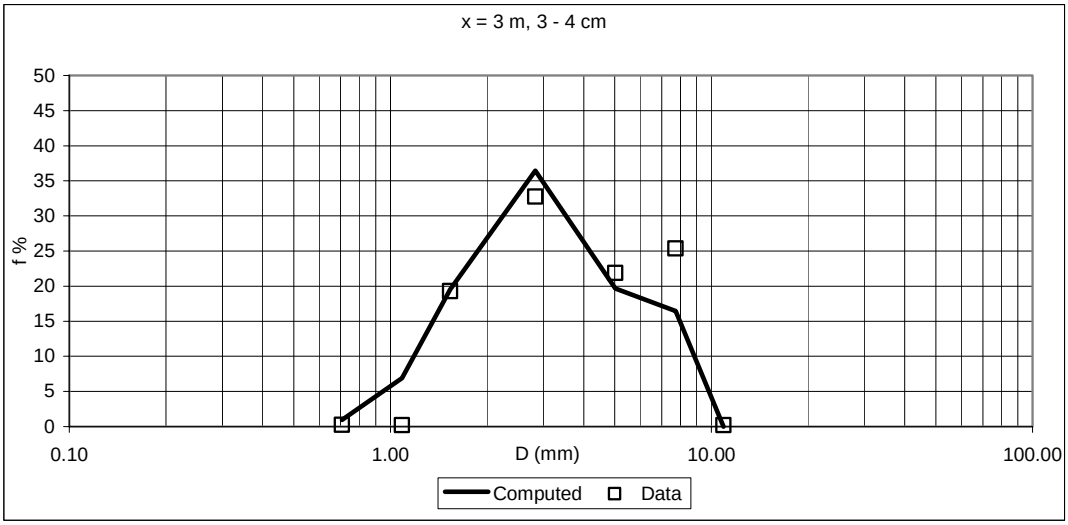
x = 3 m, 3 - 4 cm
50
45
40
35
30
25
20
15
10
5
0
f %
0.10
1.00
D (mm)
10.00
100.00
Computed
Data

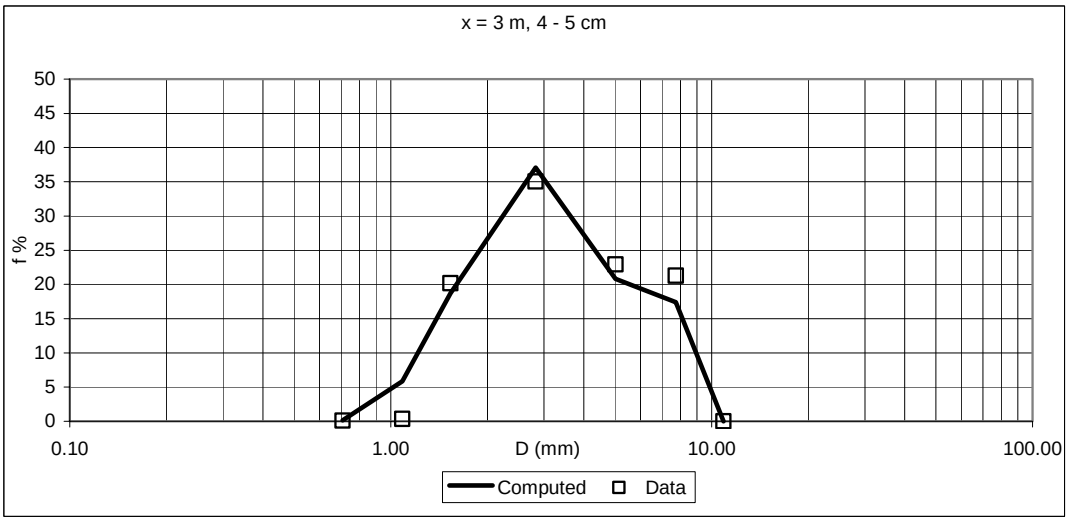
x = 3 m, 4 - 5 cm
50
45
40
35
30
25
20
15
10
5
0
f %
0.10
1.00
D (mm)
10.00
100.00
Computed
Data

x = 4 m								
First layer 0 -1 cm					Second layer 1 - 2 cm			
Computed		Data			Computed		Data	
Di (mm)	fi %	Di (mm)	fi %		Di (mm)	fi %	Di (mm)	fi %
0.707	0.219	0.071	0.099		0.707	0.230	0.071	0.117
1.086	5.694	0.707	0.214		1.086	6.772	0.707	0.130
1.536	17.889	1.086	0.393		1.536	20.990	1.086	0.363
2.828	35.196	1.536	22.859		2.828	40.126	1.536	21.712
5.020	21.133	2.828	32.735		5.020	18.237	2.828	36.388
7.736	19.847	5.020	19.773		7.736	13.633	5.020	22.919
10.897	0.022	7.736	23.928		10.897	0.012	7.736	18.371
		10.897	0.000				10.897	0.000
Third layer 2 - 3 cm					Fourth layer 3 - 4 cm			
Computed		Data			Computed		Data	
Di (mm)	fi %	Di (mm)	fi %		Di (mm)	fi %	Di (mm)	fi %
0.707	0.142	0.071	0.116		0.707	0.114	0.071	0.110
1.086	6.854	0.707	0.115		1.086	5.863	0.707	0.117
1.536	21.132	1.086	0.387		1.536	18.691	1.086	0.446
2.828	39.789	1.536	24.099		2.828	37.088	1.536	26.853
5.020	17.467	2.828	35.614		5.020	20.817	2.828	36.168
7.736	14.602	5.020	22.014		7.736	17.410	5.020	21.940
10.897	0.014	7.736	17.656		10.897	0.017	7.736	14.366
		10.897	0.000				10.897	0.000
Fifth layer 4 - 5 cm								
Computed		Data						
Di (mm)	fi %	Di (mm)	fi %					
0.707	0.114	0.071	0.100					
1.086	5.863	0.707	0.115					
1.536	18.691	1.086	0.418					
2.828	37.088	1.536	24.327					
5.020	20.817	2.828	34.520					
7.736	17.410	5.020	20.469					
10.897	0.017	7.736	20.050					
		10.897	0.000					

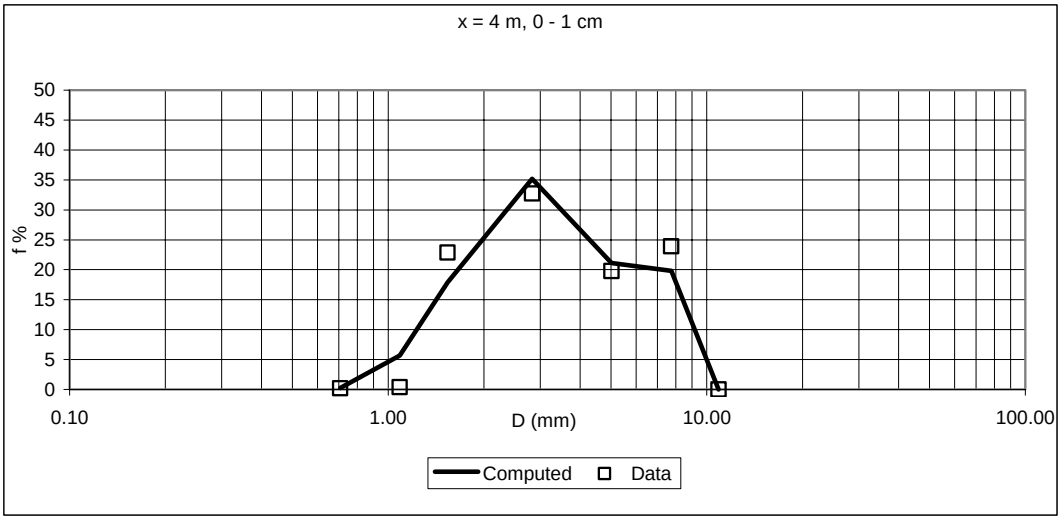
x = 4 m, 0 - 1 cm
f %
50
45
40
35
30
25
20
15
10
5
0
0.10
1.00
D (mm)
10.00
100.00
Computed
Data

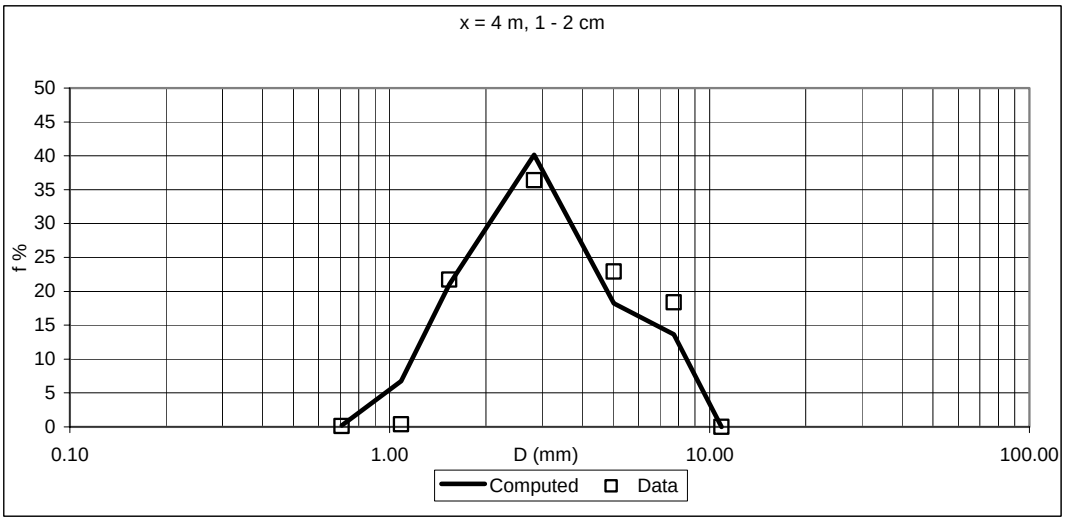
x = 4 m, 1 - 2 cm
f %
50
45
40
35
30
25
20
15
10
5
0
0.10
1.00
D (mm)
10.00
100.00
Computed
Data

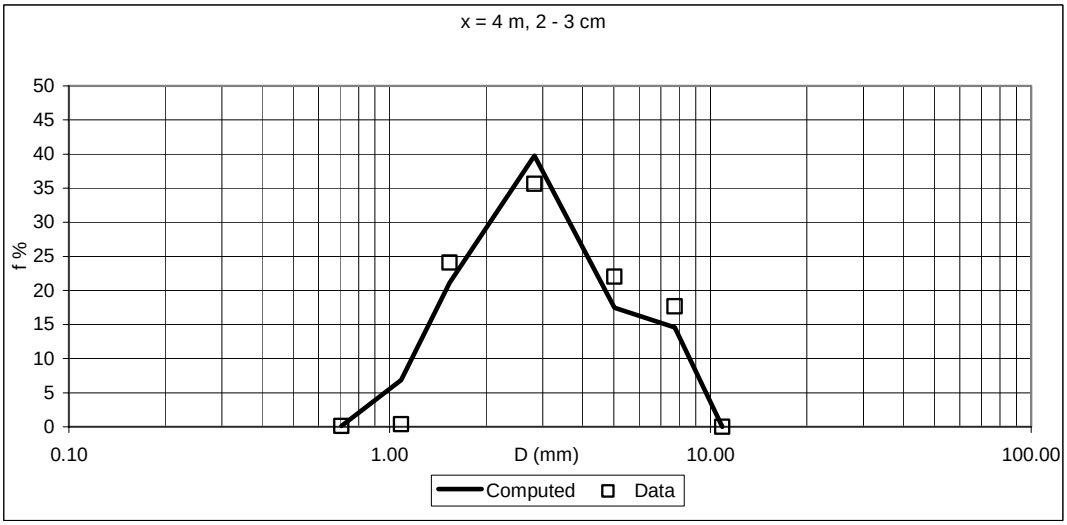
x = 4 m, 2 - 3 cm
f %
50
45
40
35
30
25
20
15
10
5
0
0.10
1.00
D (mm)
10.00
100.00
Computed
Data

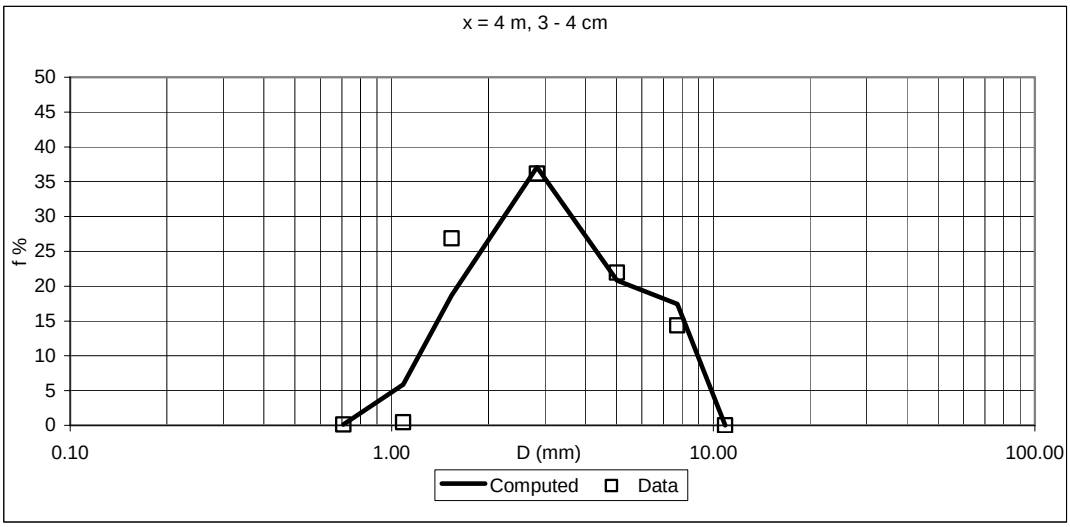
x = 4 m, 3 - 4 cm
f %
50
45
40
35
30
25
20
15
10
5
0
0.10
1.00
D (mm)
10.00
100.00
Computed
Data

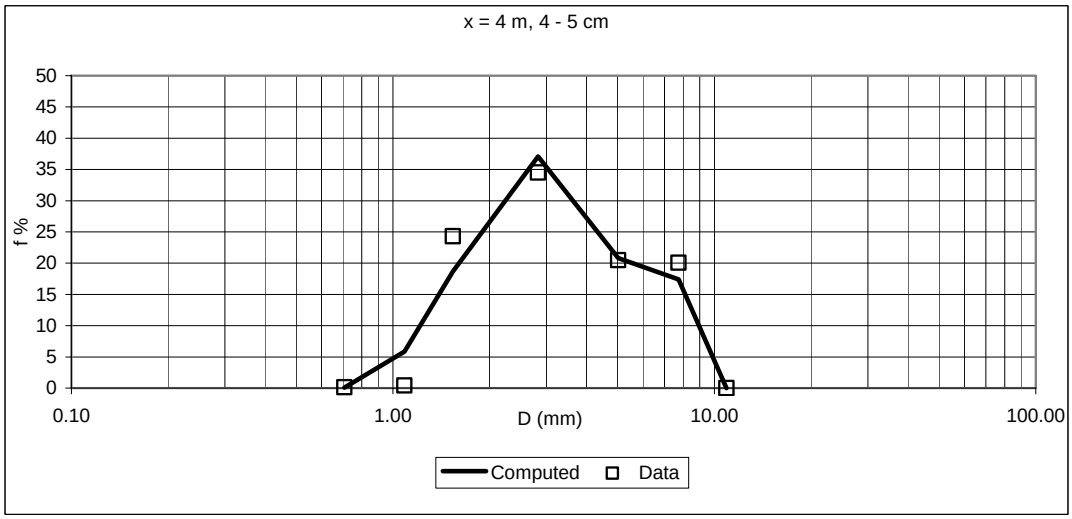
x = 4 m, 4 - 5 cm
f %
50
45
40
35
30
25
20
15
10
5
0
0.10
1.00
D (mm)
10.00
100.00
Computed
Data

x = 5 m								
First layer 0 -1 cm					Second layer 1 - 2 cm			
Computed		Data			Computed		Data	
Di (mm)	fi %	Di (mm)	fi %		Di (mm)	fi %	Di (mm)	fi %
0.707	0.217	0.071	0.056		0.707	0.178	0.071	0.085
1.086	5.636	0.707	0.164		1.086	7.135	0.707	0.126
1.536	17.714	1.086	0.319		1.536	22.277	1.086	0.322
2.828	34.911	1.536	17.945		2.828	42.766	1.536	17.033
5.020	20.679	2.828	28.981		5.020	15.969	2.828	30.892
7.736	20.817	5.020	23.971		7.736	11.665	5.020	25.004
10.897	0.026	7.736	28.564		10.897	0.011	7.736	26.537
		10.897	0.000				10.897	0.000
Third layer 2 - 3 cm					Fourth layer 3 - 4 cm			
Computed		Data			Computed		Data	
Di (mm)	fi %	Di (mm)	fi %		Di (mm)	fi %	Di (mm)	fi %
0.707	0.119	0.071	0.103		0.707	0.114	0.071	0.139
1.086	5.984	0.707	0.121		1.086	5.863	0.707	0.106
1.536	19.034	1.086	0.308		1.536	18.691	1.086	0.383
2.828	37.636	1.536	19.067		2.828	37.088	1.536	20.861
5.020	20.358	2.828	33.318		5.020	20.817	2.828	32.620
7.736	16.852	5.020	23.575		7.736	17.410	5.020	22.941
10.897	0.017	7.736	23.508		10.897	0.017	7.736	22.950
		10.897	0.000				10.897	0.000
Fifth layer 4 - 5 cm								
Computed		Data						
Di (mm)	fi %	Di (mm)	fi %					
0.707	0.114	0.071	0.102					
1.086	5.863	0.707	0.097					
1.536	18.691	1.086	0.344					
2.828	37.088	1.536	21.030					
5.020	20.817	2.828	35.309					
7.736	17.410	5.020	22.212					
10.897	0.017	7.736	20.906					
		10.897	0.000					

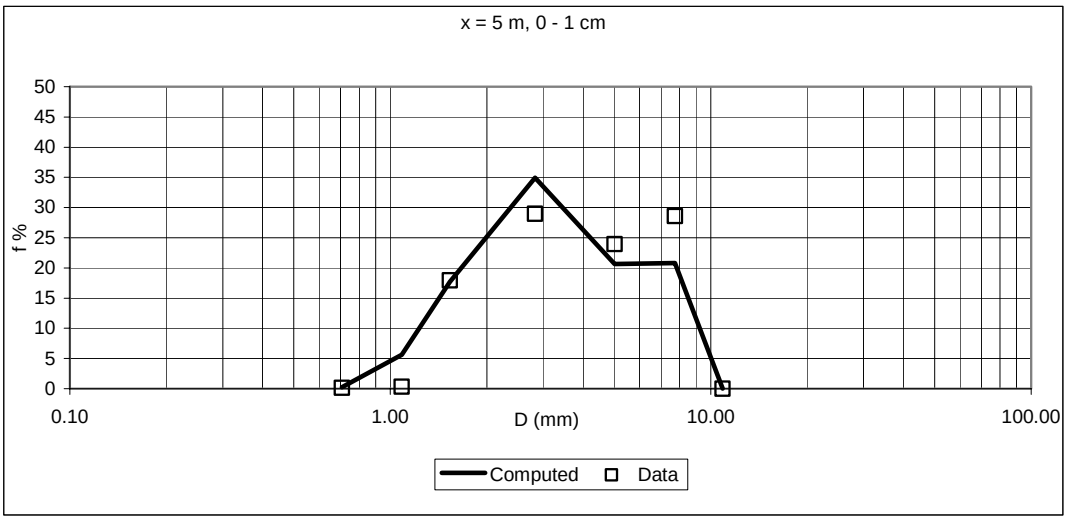
x = 5 m, 0 - 1 cm
f %
50
45
40
35
30
25
20
15
10
5
0
0.10
1.00
D (mm)
10.00
100.00
Computed
Data

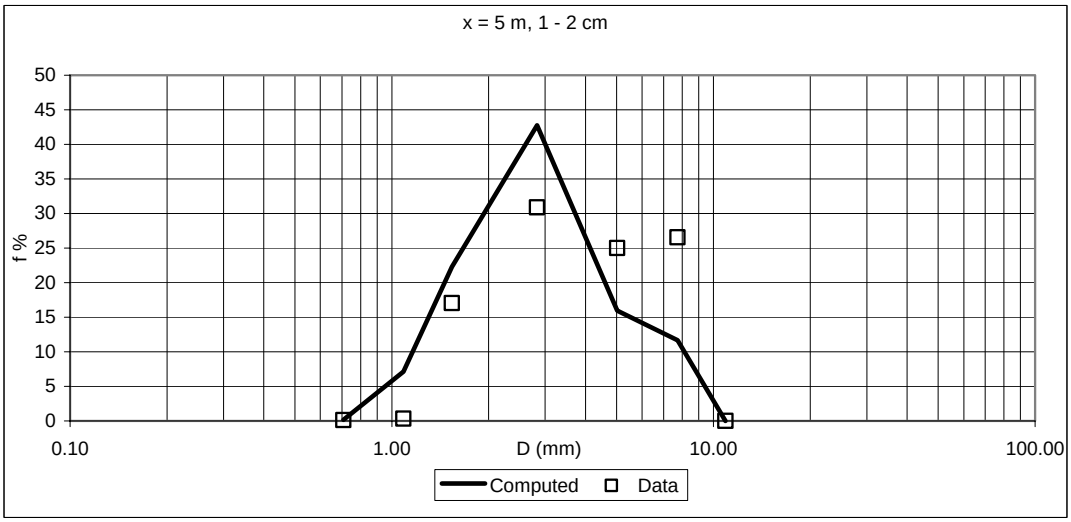
x = 5 m, 1 - 2 cm
f %
50
45
40
35
30
25
20
15
10
5
0
0.10
1.00
D (mm)
10.00
100.00
Computed
Data

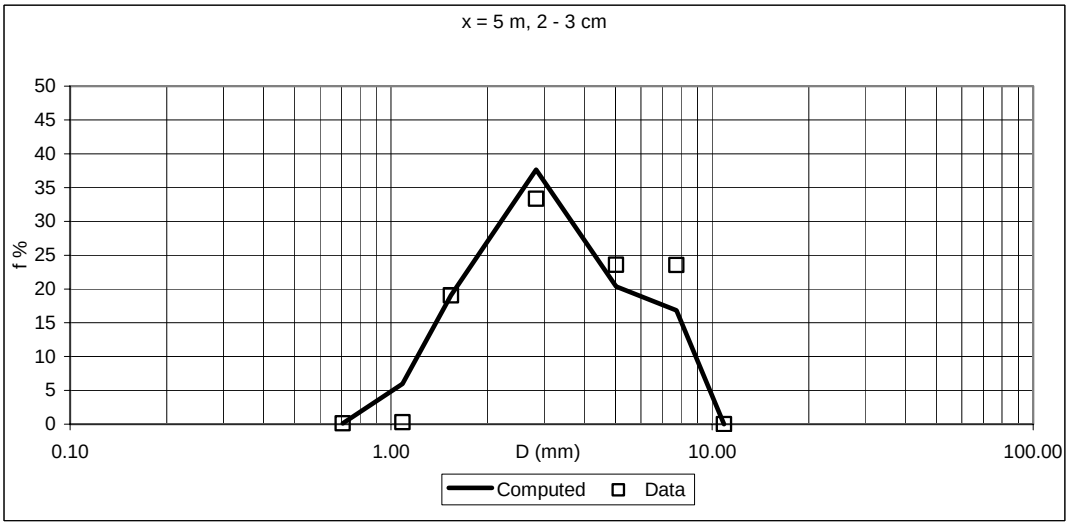
x = 5 m, 2 - 3 cm
f %
50
45
40
35
30
25
20
15
10
5
0
0.10
1.00
D (mm)
10.00
100.00
Computed
Data

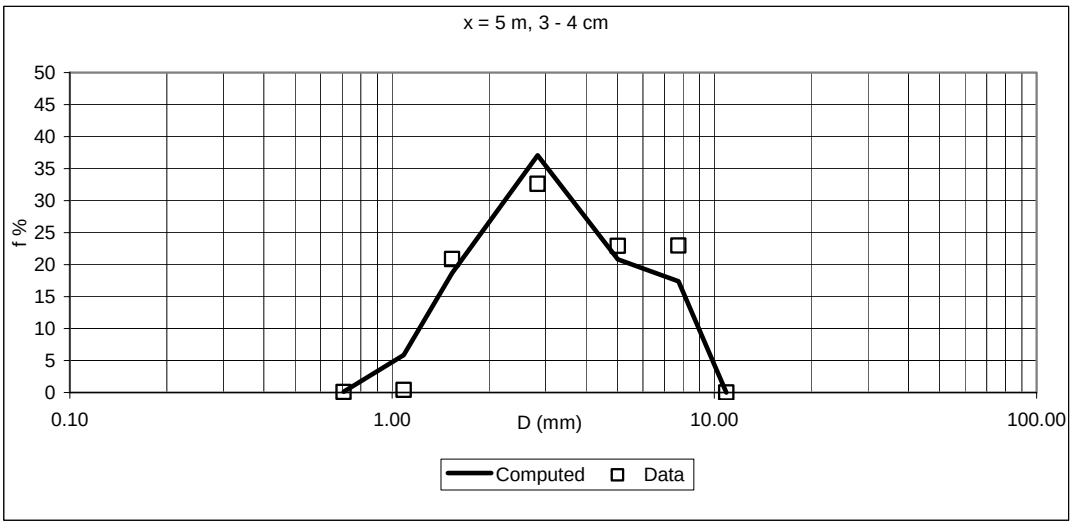
x = 5 m, 3 - 4 cm
50
45
40
35
30
25
20
15
10
5
0
f %
0.10
1.00
D (mm)
10.00
100.00
Computed
Data

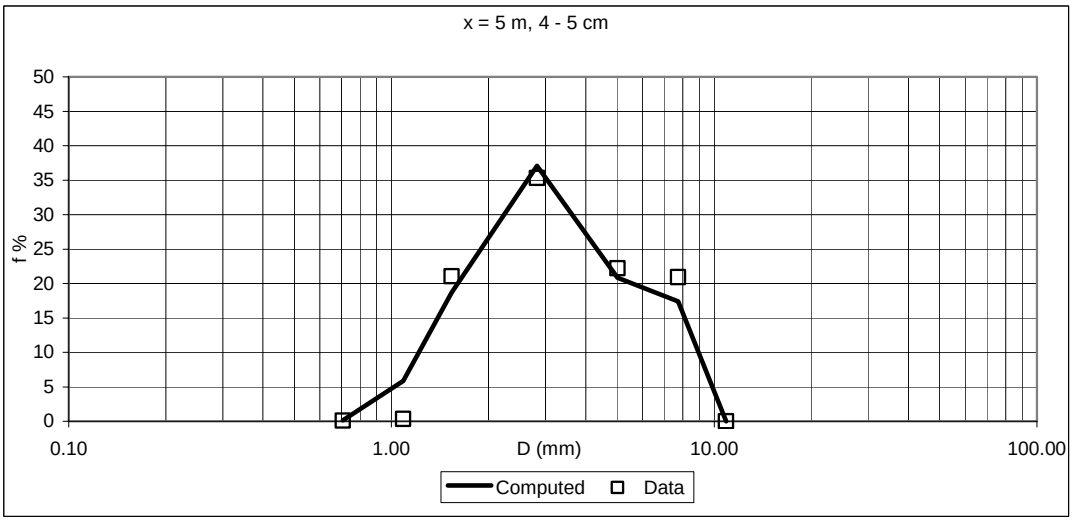
x = 5 m, 4 - 5 cm
50
45
40
35
30
25
20
15
10
5
0
f %
0.10
1.00
D (mm)
10.00
100.00
Computed
Data

x = 7 m								
First layer 0 -1 cm					Second layer 1 - 2 cm			
Computed		Data			Computed		Data	
Di (mm)	fi %	Di (mm)	fi %		Di (mm)	fi %	Di (mm)	fi %
0.707	0.206	0.071	0.086		0.707	0.164	0.071	0.096
1.086	5.498	0.707	0.209		1.086	5.968	0.707	0.142
1.536	17.324	1.086	0.422		1.536	18.895	1.086	0.364
2.828	34.255	1.536	20.939		2.828	37.184	1.536	19.923
5.020	19.670	2.828	32.395		5.020	21.260	2.828	33.773
7.736	23.015	5.020	21.532		7.736	16.515	5.020	22.251
10.897	0.032	7.736	24.417		10.897	0.013	7.736	23.452
		10.897	0.000				10.897	0.000
Third layer 2 - 3 cm					Fourth layer 3 - 4 cm			
Computed		Data			Computed		Data	
Di (mm)	fi %	Di (mm)	fi %		Di (mm)	fi %	Di (mm)	fi %
0.707	0.102	0.071	0.098		0.707	0.114	0.071	0.087
1.086	5.830	0.707	0.123		1.086	5.863	0.707	0.115
1.536	18.619	1.086	0.351		1.536	18.691	1.086	0.340
2.828	37.021	1.536	20.251		2.828	37.088	1.536	20.580
5.020	20.822	2.828	35.162		5.020	20.817	2.828	35.458
7.736	17.588	5.020	21.542		7.736	17.410	5.020	23.301
10.897	0.018	7.736	22.473		10.897	0.017	7.736	19.911
		10.897	0.000				10.897	0.209
Fifth layer 4 - 5 cm								
Computed		Data						
Di (mm)	fi %	Di (mm)	fi %					
0.707	0.114	0.071	0.094					
1.086	5.863	0.707	0.102					
1.536	18.691	1.086	0.358					
2.828	37.088	1.536	21.629					
5.020	20.817	2.828	34.718					
7.736	17.410	5.020	21.279					
10.897	0.017	7.736	21.626					
		10.897	0.194					

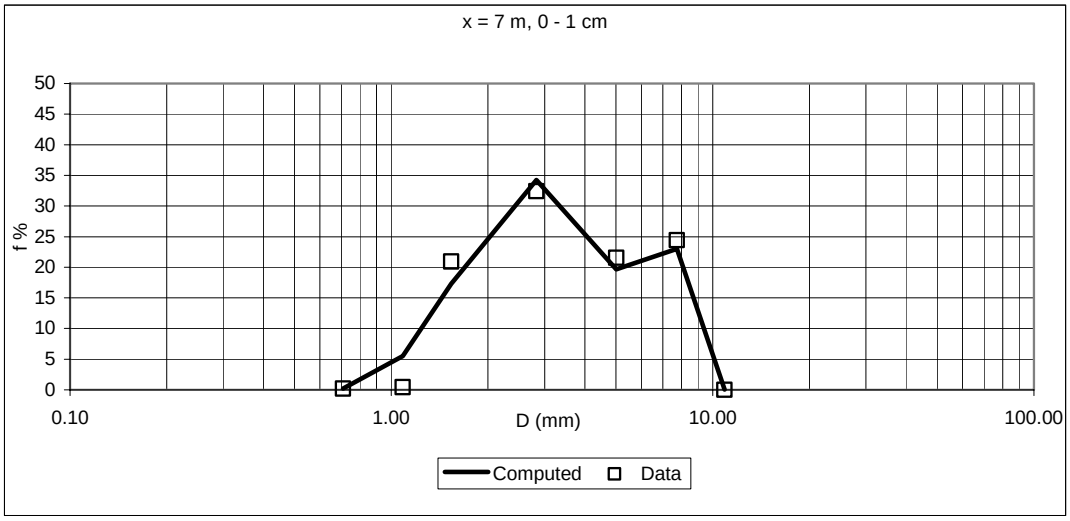
x = 7 m, 0 - 1 cm
f %
50
45
40
35
30
25
20
15
10
5
0
0.10
1.00
D (mm)
10.00
100.00
Computed
Data

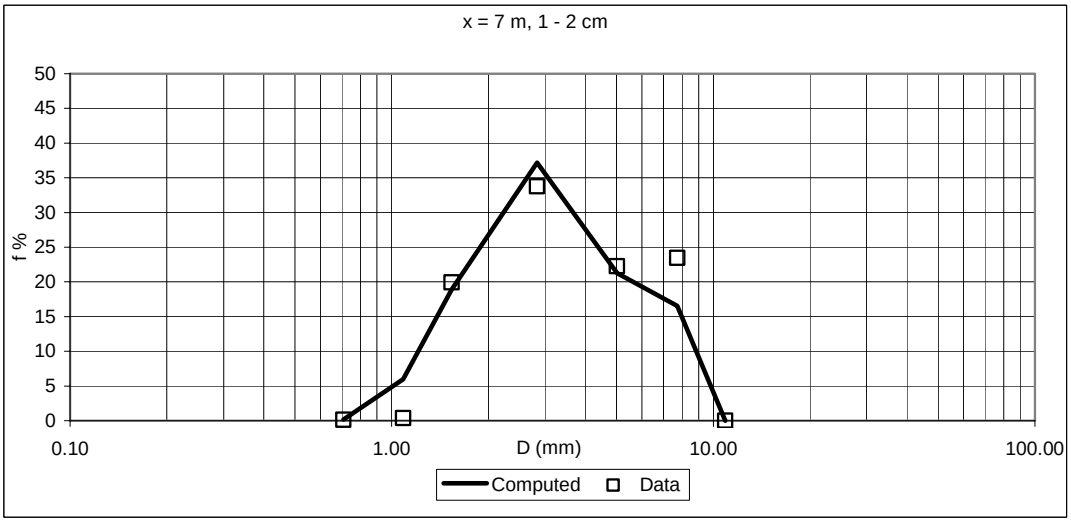
x = 7 m, 1 - 2 cm
f %
50
45
40
35
30
25
20
15
10
5
0
0.10
1.00
D (mm)
10.00
100.00
Computed
Data

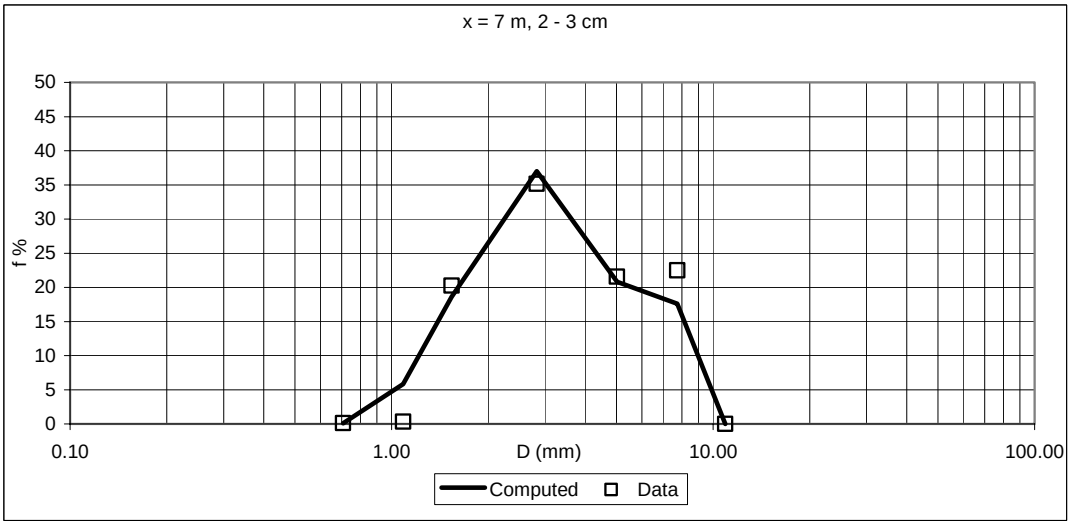
x = 7 m, 2 - 3 cm
f %
50
45
40
35
30
25
20
15
10
5
0
0.10
1.00
D (mm)
10.00
100.00
Computed
Data

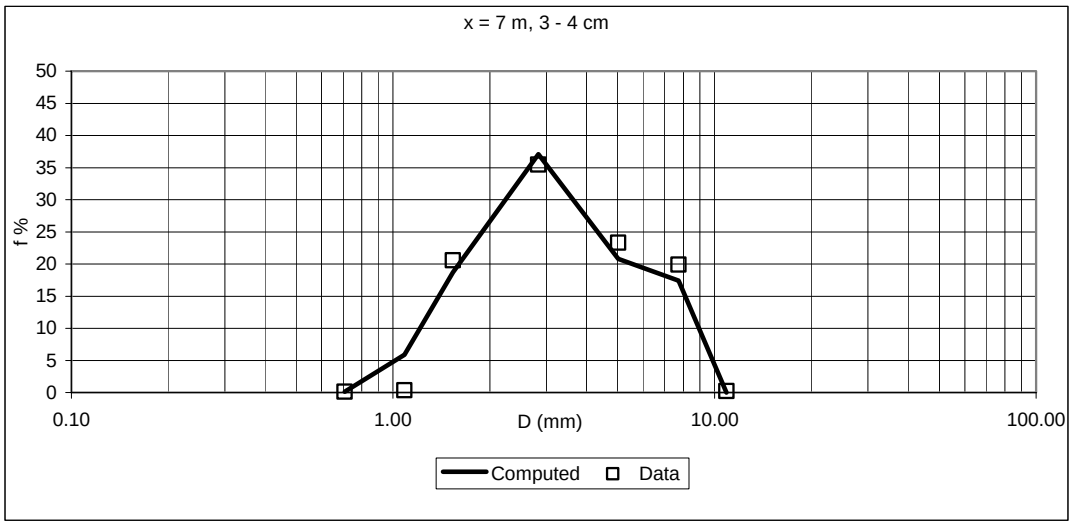
x = 7 m, 3 - 4 cm
f %
50
45
40
35
30
25
20
15
10
5
0
0.10
1.00
D (mm)
10.00
100.00
Computed
Data

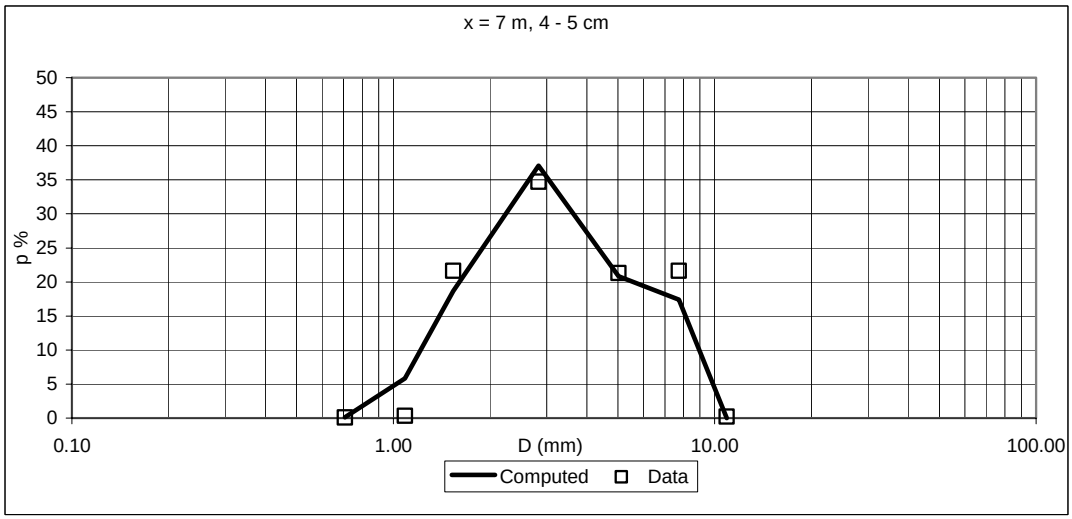
x = 7 m, 4 - 5 cm
p %
50
45
40
35
30
25
20
15
10
5
0
0.10
1.00
D (mm)
10.00
100.00
Computed
Data

x = 9 m								
First layer 0 -1 cm					Second layer 1 - 2 cm			
Computed		Data			Computed		Data	
Di (mm)	fi %	Di (mm)	fi %		Di (mm)	fi %	Di (mm)	fi %
0.707	0.199	0.071	0.035		0.707	0.160	0.071	0.070
1.086	5.424	0.707	0.136		1.086	6.122	0.707	0.146
1.536	17.131	1.086	0.320		1.536	19.353	1.086	0.354
2.828	33.797	1.536	19.219		2.828	37.998	1.536	21.131
5.020	20.088	2.828	35.187		5.020	20.357	2.828	35.408
7.736	23.333	5.020	20.767		7.736	15.994	5.020	21.715
10.897	0.029	7.736	24.002		10.897	0.014	7.736	21.176
		10.897	0.334				10.897	0.000
Third layer 2 - 3 cm					Fourth layer 3 - 4 cm			
Computed		Data			Computed		Data	
Di (mm)	fi %	Di (mm)	fi %		Di (mm)	fi %	Di (mm)	fi %
0.707	0.114	0.071	0.072		0.707	0.114	0.071	0.075
1.086	5.863	0.707	0.107		1.086	5.863	0.707	0.091
1.536	18.691	1.086	0.334		1.536	18.691	1.086	0.299
2.828	37.088	1.536	20.062		2.828	37.088	1.536	20.777
5.020	20.817	2.828	34.673		5.020	20.817	2.828	37.221
7.736	17.410	5.020	22.845		7.736	17.410	5.020	23.335
10.897	0.017	7.736	21.907		10.897	0.017	7.736	18.201
		10.897	0.000				10.897	0.000
Fifth layer 4 - 5 cm								
Computed		Data						
Di (mm)	fi %	Di (mm)	fi %					
0.707	0.114	0.071	0.065					
1.086	5.863	0.707	0.079					
1.536	18.691	1.086	0.304					
2.828	37.088	1.536	19.709					
5.020	20.817	2.828	35.654					
7.736	17.410	5.020	22.413					
10.897	0.017	7.736	21.775					
		10.897	0.000					

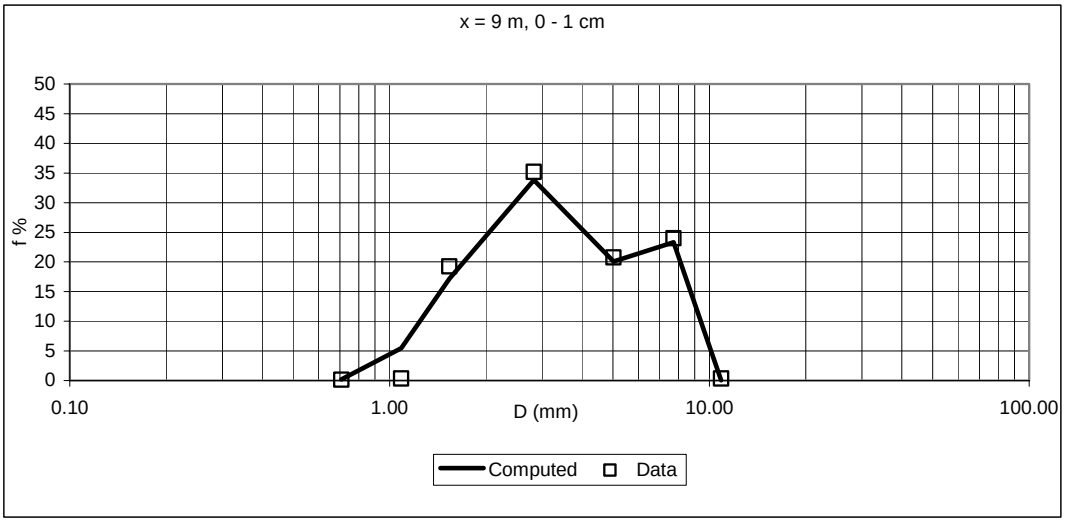
x = 9 m, 0 - 1 cm
f %
50
45
40
35
30
25
20
15
10
5
0
0.10
1.00
D (mm)
10.00
100.00
Computed
Data

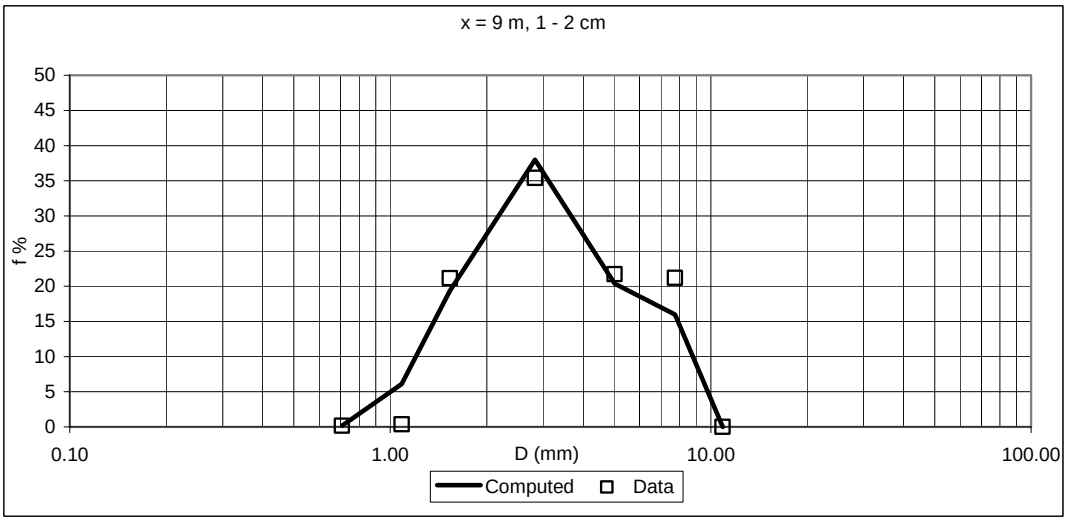
x = 9 m, 1 - 2 cm
f %
50
45
40
35
30
25
20
15
10
5
0
0.10
1.00
D (mm)
10.00
100.00
Computed
Data

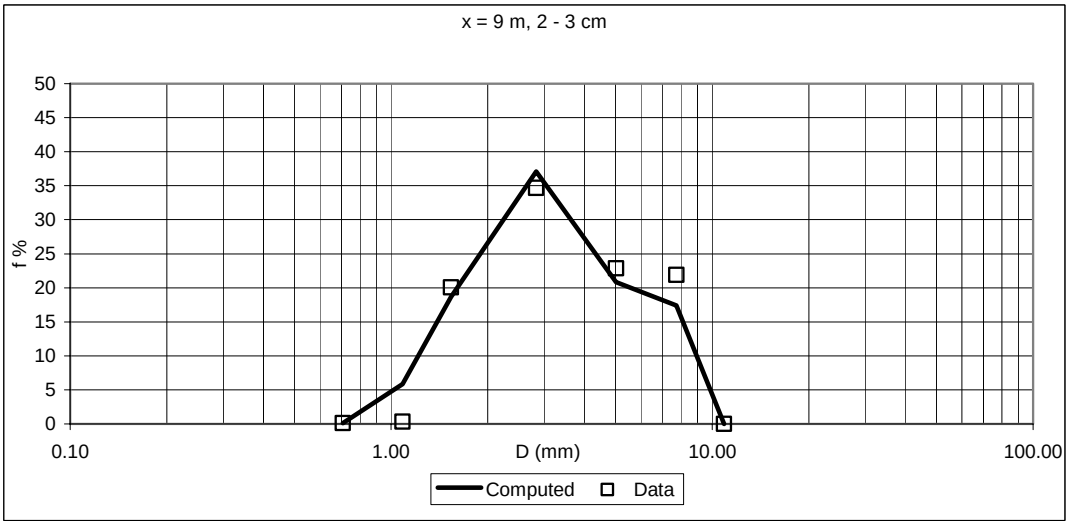
x = 9 m, 2 - 3 cm
f %
50
45
40
35
30
25
20
15
10
5
0
0.10
1.00
D (mm)
10.00
100.00
Computed
Data

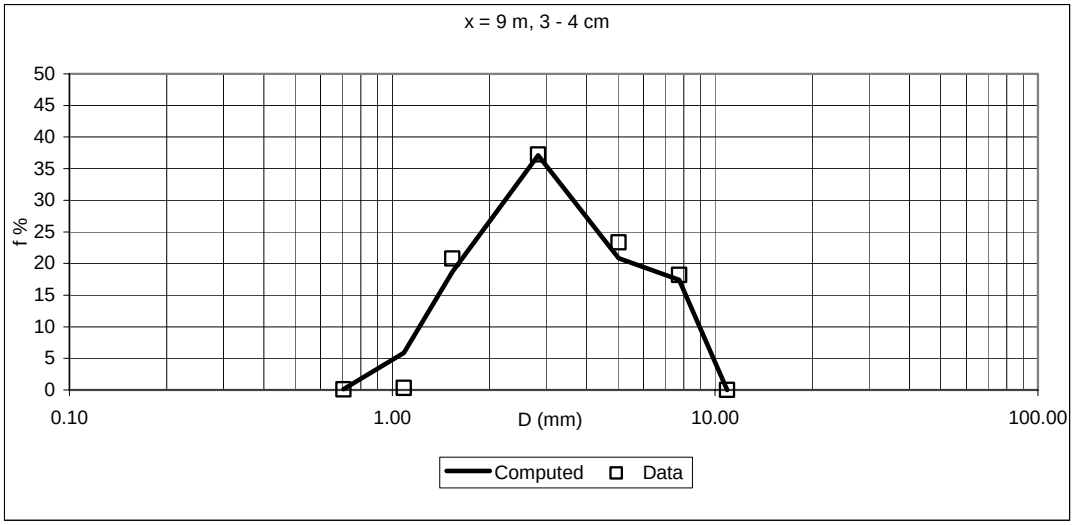
x = 9 m, 3 - 4 cm
f %
50
45
40
35
30
25
20
15
10
5
0
0.10
1.00
D (mm)
10.00
100.00
Computed
Data

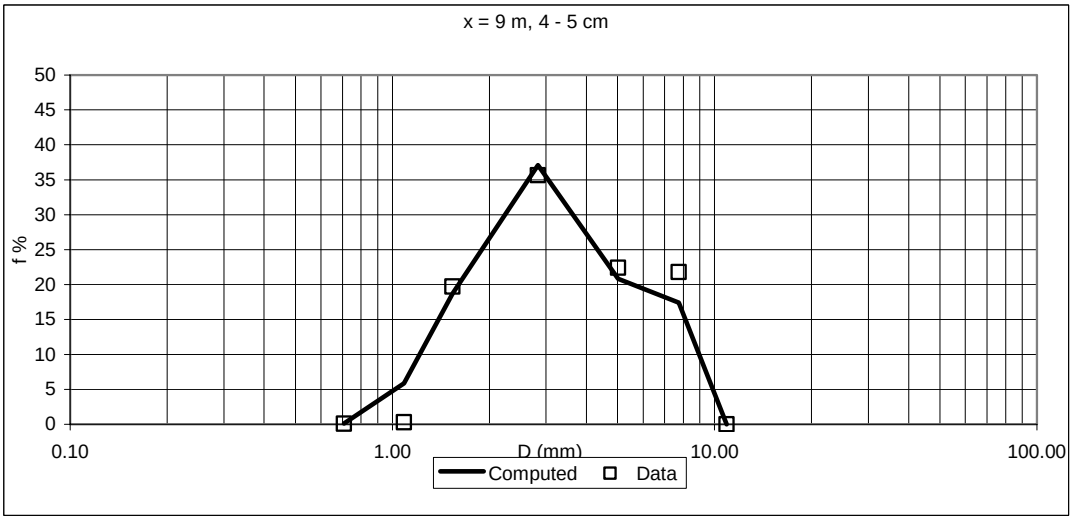
x = 9 m, 4 - 5 cm
f %
50
45
40
35
30
25
20
15
10
5
0
0.10
1.00
D (mm)
10.00
100.00
Computed
Data

VALIDATION OF THE MODIFIED PROCEDURE: THE FIRST ATTEMPT TO MODEL VERTICAL SORTING DUE TO A FRONT MIGRATING DOWNSTREAM

Longitudinal profile

RUN 1								RUN 2								RUN 3				
Computed			Data					Computed			Data					Computed			Data	
x (m)	η (m)	η (mm)	x (m)	η (mm)				x (m)	η (m)	η (mm)	x (m)	η (mm)				x (m)	η (m)	η (mm)	x (m)	η (mm)
0.000	0.224	224	2.5	205				0.000	0.225	225	2.5	206				0.000	0.234	234	2.5	208
0.100	0.223	223	2.9	201				0.100	0.225	225	2.9	203				0.100	0.233	233	2.9	204
0.200	0.223	223	3.3	202				0.200	0.224	224	3.3	200				0.200	0.232	232	3.3	196
0.300	0.222	222	3.7	202				0.300	0.223	223	3.7	196				0.300	0.231	231	3.7	195
0.400	0.221	221	4.1	197				0.400	0.223	223	4.1	199				0.400	0.231	231	4.1	195
0.500	0.221	221	4.3	196				0.500	0.222	222	4.3	195				0.500	0.230	230	4.3	194
0.600	0.220	220	4.5	196				0.600	0.221	221	4.5	194				0.600	0.229	229	4.5	194
0.700	0.219	219	4.9	194				0.700	0.221	221	4.9	192				0.700	0.228	228	4.9	190
0.800	0.219	219	5.3	188				0.800	0.220	220	5.3	188				0.800	0.227	227	5.3	188
0.900	0.218	218	5.7	188				0.900	0.219	219	5.7	186				0.900	0.226	226	5.7	185
1.000	0.217	217	6.1	182				1.000	0.219	219	6.1	184				1.000	0.226	226	6.1	182
1.100	0.217	217	6.5	180				1.100	0.218	218	6.5	179				1.100	0.225	225	6.5	178
1.200	0.216	216	6.9	178				1.200	0.217	217	6.9	178				1.200	0.224	224	6.9	177
1.300	0.215	215	7.3	175				1.300	0.217	217	7.3	176				1.300	0.223	223	7.3	173
1.400	0.215	215	7.7	172				1.400	0.216	216	7.7	173				1.400	0.222	222	7.7	171
1.500	0.214	214	8.1	169				1.500	0.215	215	8.1	167				1.500	0.221	221	8.1	165
1.600	0.213	213	8.5	169				1.600	0.214	214	8.5	165				1.600	0.221	221	8.5	162
1.700	0.213	213	8.9	166				1.700	0.214	214	8.9	161				1.700	0.220	220	8.9	158
1.800	0.212	212	9.3	161				1.800	0.213	213	9.3	157				1.800	0.219	219	9.3	155
1.900	0.211	211	9.7	160				1.900	0.212	212	9.7	155				1.900	0.218	218	9.7	152
2.000	0.211	211	10.1	158				2.000	0.212	212	10.1	152				2.000	0.217	217	10.1	148
2.100	0.210	210	10.5	153				2.100	0.211	211	10.5	150				2.100	0.216	216	10.5	145
2.200	0.209	209						2.200	0.210	210						2.200	0.216	216		
2.300	0.209	209						2.300	0.210	210						2.300	0.215	215		
2.400	0.208	208						2.400	0.209	209						2.400	0.214	214		
2.500	0.208	208						2.500	0.208	208						2.500	0.213	213		
2.600	0.207	207						2.600	0.208	208						2.600	0.212	212		
2.700	0.206	206						2.700	0.207	207						2.700	0.212	212		
2.800	0.206	206						2.800	0.206	206						2.800	0.211	211		
2.900	0.205	205						2.900	0.206	206						2.900	0.210	210		
3.000	0.204	204						3.000	0.205	205						3.000	0.209	209		
3.100	0.204	204						3.100	0.204	204						3.100	0.208	208		
3.200	0.203	203						3.200	0.204	204						3.200	0.207	207		
3.300	0.202	202						3.300	0.203	203						3.300	0.207	207		
3.400	0.202	202						3.400	0.202	202						3.400	0.206	206		
3.500	0.201	201						3.500	0.201	201						3.500	0.205	205		
3.600	0.200	200						3.600	0.201	201						3.600	0.204	204		
3.700	0.200	200						3.700	0.200	200						3.700	0.203	203		
3.800	0.199	199						3.800	0.199	199						3.800	0.202	202		
3.900	0.198	198						3.900	0.199	199						3.900	0.202	202		
4.000	0.198	198						4.000	0.198	198						4.000	0.201	201		
4.100	0.197	197						4.100	0.197	197						4.100	0.200	200		
4.200	0.196	196						4.200	0.197	197						4.200	0.199	199		
4.300	0.196	196						4.300	0.196	196						4.300	0.198	198		
4.400	0.195	195						4.400	0.195	195						4.400	0.197	197		
4.500	0.194	194						4.500	0.195	195						4.500	0.197	197		
4.600	0.194	194						4.600	0.194	194						4.600	0.196	196		
4.700	0.193	193						4.700	0.193	193						4.700	0.195	195		
4.800	0.192	192						4.800	0.193	193						4.800	0.194	194		
4.900	0.192	192						4.900	0.192	192						4.900	0.193	193		
5.000	0.191	191						5.000	0.191	191						5.000	0.192	192		
5.100	0.190	190						5.100	0.190	190						5.100	0.192	192		
5.200	0.190	190						5.200	0.190	190						5.200	0.191	191		
5.300	0.189	189						5.300	0.189	189						5.300	0.190	190		
5.400	0.188	188						5.400	0.188	188						5.400	0.189	189		
5.500	0.188	188						5.500	0.188	188						5.500	0.188	188		
5.600	0.187	187						5.600	0.187	187						5.600	0.187	187		
5.700	0.186	186						5.700	0.186	186						5.700	0.187	187		
5.800	0.186	186						5.800	0.186	186						5.800	0.186	186		
5.900	0.185	185						5.900	0.185	185						5.900	0.185	185		
6.000	0.184	184						6.000	0.184	184						6.000	0.184	184		
6.100	0.184	184						6.100	0.184	184						6.100	0.183	183		
6.200	0.183	183						6.200	0.183	183						6.200	0.182	182		
6.300	0.182	182						6.300	0.182	182						6.300	0.182	182		
6.400	0.182	182						6.400	0.182	182						6.400	0.181	181		
6.500	0.181	181						6.500	0.181	181						6.500	0.180	180		
6.600	0.180	180						6.600	0.180	180						6.600	0.179	179		
6.700	0.180	180						6.700	0.180	180						6.700	0.178	178		
6.800	0.179	179						6.800	0.179	179						6.800	0.178	178		
6.900	0.178	178						6.900	0.178	178						6.900	0.177	177		
7.000	0.178	178						7.000	0.177	177						7.000	0.176	176		
7.100	0.177	177						7.100	0.177	177						7.100	0.175	175		
7.200	0.176	176						7.200	0.176	176						7.200	0.174	174		
7.300	0.176	176						7.300	0.175	175						7.300	0.173	173		
7.400	0.175	175						7.400	0.175	175						7.400	0.173	173		
7.500	0.174	174						7.500	0.174	174						7.500	0.172	172		
7.600	0.174	174						7.600	0.173	173						7.600	0.171	171		
7.700	0.173	173						7.700	0.173	173						7.700	0.170	170		
7.800	0.172	172						7.800	0.172	172						7.800	0.169	169		
7.900	0.172	172						7.900	0.171	171						7.900	0.168	168		
8.000	0.171	171						8.000	0.171	171						8.000	0.168	168		
8.100	0.170	170						8.100	0.170	170						8.100	0.167	167		
8.200	0.170	170						8.200	0.169	169						8.200	0.166	166		
8.300	0.169	169						8.300	0.169	169						8.300	0.165	165		
8.400	0.168	168						8.400	0.168	168						8.400	0.164	164		
8.500	0.168	168						8.500	0.167	167						8.500	0.163	163		
8.600	0.167	167						8.600	0.166	166						8.600	0.163	163		
8.700	0.166	166						8.700	0.166	166						8.700	0.162	162		
8.800	0.166	166						8.800	0.165	165						8.800	0.161	161		
8.900	0.165	165						8.900	0.164	164						8.900	0.160	160		
9.000	0.164	164						9.000	0.164	164						9.000	0.159	159		
9.100	0.164	164						9.100	0.163	163						9.100	0.158	158		
9.200	0.163	163						9.200	0.162	162						9.200	0.158	158		
9.300	0.162	162						9.300	0.162	162						9.300	0.157	157		
9.400	0.162	162						9.400	0.161	161						9.400	0.156	156		
9.500	0.161	161						9.500	0.160	160						9.500	0.155	155		
9.600	0.160	160						9.600	0.160	160						9.600	0.154	154		
9.700	0.160	160						9.700	0.159	159						9.700	0.154	154		
9.800	0.159	159						9.800	0.158	158						9.800	0.153	153		
9.900	0.159	159						9.900	0.158	158						9.900	0.152	152		
10.000	0.158	158						10.000	0.157	157						10.000	0.151	151		
10.100	0.157	157						10.100	0.156	156						10.100	0.150	150		
10.200	0.157	157						10.200	0.156	156						10.200	0.149	149		
10.300	0.156	156						10.300	0.155	155						10.300	0.149	149		
10.400	0.155	155						10.400	0.154	154						10.400	0.148	148		
10.500	0.155	155						10.500	0.153	153						10.500	0.147	147		
10.600	0.154	154						10.600	0.153	153						10.600	0.146	146		
10.700	0.153	153						10.700	0.152	152						10.700	0.145	145		
10.800	0.153	153						10.800	0.151	151						10.800	0.144	144		
10.900	0.152	152						10.900	0.151	151						10.900	0.144	144		
11.000	0.151	151						11.000	0.150	150						11.000	0.143	143		
11.100	0.151	151						11.100	0.149	149						11.100	0.142	142		
11.200	0.150	150						11.200	0.149	149						11.200	0.141	141		
11.300	0.149	149						11.300	0.148	148						11.300	0.140	140		
11.400	0.149	149						11.400	0.147	147						11.400	0.139	139		
11.500	0.148	148						11.500	0.147	147						11.500	0.139	139		
11.600	0.147	147						11.600	0.146	146						11.600	0.138	138		
11.700	0.147	147						11.700	0.145	145						11.700	0.137	137		
11.800	0.146	146						11.800	0.145	145						11.800	0.136	136		

RUN 4								RUN 5								RUN 6				
Computed			Data					Computed			Data					Computed			Data	
x (m)	η (m)	η (mm)	x (m)	η (mm)				x (m)	η (m)	η (mm)	x (m)	η (mm)				x (m)	η (m)	η (mm)	x (m)	η (mm)
0.000	0.223	223	2.5	205				0.000	0.220	220	2.5	194				0.000	0.212	212	2.5	201
0.100	0.222	222	2.9	202				0.100	0.220	220	2.9	196				0.100	0.212	212	2.9	200
0.200	0.221	221	3.3	200				0.200	0.219	219	3.3	199				0.200	0.211	211	3.3	199
0.300	0.221	221	3.7	200				0.300	0.219	219	3.7	198				0.300	0.211	211	3.7	196
0.400	0.220	220	4.1	198				0.400	0.218	218	4.1	197				0.400	0.211	211	4.1	194
0.500	0.219	219	4.3	198				0.500	0.218	218	4.3	196				0.500	0.210	210	4.3	193
0.600	0.219	219	4.5	193				0.600	0.217	217	4.5	193				0.600	0.210	210	4.5	191
0.700	0.218	218	4.9	192				0.700	0.216	216	4.9	191				0.700	0.209	209	4.9	190
0.800	0.218	218	5.3	187				0.800	0.216	216	5.3	189				0.800	0.209	209	5.3	186
0.900	0.217	217	5.7	183				0.900	0.215	215	5.7	187				0.900	0.209	209	5.7	183
1.000	0.216	216	6.1	181				1.000	0.215	215	6.1	183				1.000	0.208	208	6.1	183
1.100	0.216	216	6.5	180				1.100	0.214	214	6.5	184				1.100	0.208	208	6.5	181
1.200	0.215	215	6.9	178				1.200	0.213	213	6.9	179				1.200	0.207	207	6.9	180
1.300	0.214	214	7.3	176				1.300	0.213	213	7.3	176				1.300	0.207	207	7.3	177
1.400	0.214	214	7.7	173				1.400	0.212	212	7.7	173				1.400	0.207	207	7.7	176
1.500	0.213	213	8.1	171				1.500	0.212	212	8.1	172				1.500	0.206	206	8.1	175
1.600	0.212	212	8.5	167				1.600	0.211	211	8.5	169				1.600	0.206	206	8.5	173
1.700	0.212	212	8.9	163				1.700	0.210	210	8.9	166				1.700	0.205	205	8.9	172
1.800	0.211	211	9.3	164				1.800	0.210	210	9.3	163				1.800	0.205	205	9.3	169
1.900	0.211	211	9.7	159				1.900	0.209	209	9.7	162				1.900	0.205	205	9.7	167
2.000	0.210	210	10.1	156				2.000	0.208	208	10.1	159				2.000	0.204	204	10.1	165
2.100	0.209	209	10.5	155				2.100	0.208	208	10.5	157				2.100	0.204	204	10.5	164
2.200	0.209	209						2.200	0.207	207						2.200	0.203	203		
2.300	0.208	208						2.300	0.207	207						2.300	0.203	203		
2.400	0.207	207						2.400	0.206	206						2.400	0.202	202		
2.500	0.207	207						2.500	0.205	205						2.500	0.202	202		
2.600	0.206	206						2.600	0.205	205						2.600	0.201	201		
2.700	0.205	205						2.700	0.204	204						2.700	0.201	201		
2.800	0.205	205						2.800	0.204	204						2.800	0.200	200		
2.900	0.204	204						2.900	0.203	203						2.900	0.200	200		
3.000	0.204	204						3.000	0.202	202						3.000	0.199	199		
3.100	0.203	203						3.100	0.202	202						3.100	0.199	199		
3.200	0.202	202						3.200	0.201	201						3.200	0.198	198		
3.300	0.202	202						3.300	0.200	200						3.300	0.198	198		
3.400	0.201	201						3.400	0.200	200						3.400	0.197	197		
3.500	0.200	200						3.500	0.199	199						3.500	0.197	197		
3.600	0.200	200						3.600	0.199	199						3.600	0.196	196		
3.700	0.199	199						3.700	0.198	198						3.700	0.196	196		
3.800	0.198	198						3.800	0.197	197						3.800	0.195	195		
3.900	0.198	198						3.900	0.197	197						3.900	0.195	195		
4.000	0.197	197						4.000	0.196	196						4.000	0.194	194		
4.100	0.197	197						4.100	0.196	196						4.100	0.194	194		
4.200	0.196	196						4.200	0.195	195						4.200	0.193	193		
4.300	0.195	195						4.300	0.194	194						4.300	0.193	193		
4.400	0.195	195						4.400	0.194	194						4.400	0.192	192		
4.500	0.194	194						4.500	0.193	193						4.500	0.192	192		
4.600	0.193	193						4.600	0.193	193						4.600	0.191	191		
4.700	0.193	193						4.700	0.192	192						4.700	0.191	191		
4.800	0.192	192						4.800	0.191	191						4.800	0.190	190		
4.900	0.191	191						4.900	0.191	191						4.900	0.190	190		
5.000	0.191	191						5.000	0.190	190						5.000	0.189	189		
5.100	0.190	190						5.100	0.190	190						5.100	0.189	189		
5.200	0.190	190						5.200	0.189	189						5.200	0.188	188		
5.300	0.189	189						5.300	0.188	188						5.300	0.188	188		
5.400	0.188	188						5.400	0.188	188						5.400	0.187	187		
5.500	0.188	188						5.500	0.187	187						5.500	0.187	187		
5.600	0.187	187						5.600	0.187	187						5.600	0.186	186		
5.700	0.186	186						5.700	0.186	186						5.700	0.186	186		
5.800	0.186	186						5.800	0.185	185						5.800	0.185	185		
5.900	0.185	185						5.900	0.185	185						5.900	0.185	185		
6.000	0.184	184						6.000	0.184	184						6.000	0.185	185		
6.100	0.184	184						6.100	0.184	184						6.100	0.184	184		
6.200	0.183	183						6.200	0.183	183						6.200	0.184	184		
6.300	0.182	182						6.300	0.182	182						6.300	0.183	183		
6.400	0.182	182						6.400	0.182	182						6.400	0.183	183		
6.500	0.181	181						6.500	0.181	181						6.500	0.182	182		
6.600	0.181	181						6.600	0.181	181						6.600	0.182	182		
6.700	0.180	180						6.700	0.180	180						6.700	0.181	181		
6.800	0.179	179						6.800	0.179	179						6.800	0.181	181		
6.900	0.179	179						6.900	0.179	179						6.900	0.180	180		
7.000	0.178	178						7.000	0.178	178						7.000	0.180	180		
7.100	0.177	177						7.100	0.178	178						7.100	0.179	179		
7.200	0.177	177						7.200	0.177	177						7.200	0.179	179		
7.300	0.176	176						7.300	0.176	176						7.300	0.178	178		
7.400	0.175	175						7.400	0.176	176						7.400	0.178	178		
7.500	0.175	175						7.500	0.175	175						7.500	0.177	177		
7.600	0.174	174						7.600	0.175	175						7.600	0.177	177		
7.700	0.174	174						7.700	0.174	174						7.700	0.176	176		
7.800	0.173	173						7.800	0.174	174						7.800	0.176	176		
7.900	0.172	172						7.900	0.173	173						7.900	0.175	175		
8.000	0.172	172						8.000	0.172	172						8.000	0.175	175		
8.100	0.171	171						8.100	0.172	172						8.100	0.175	175		
8.200	0.170	170						8.200	0.171	171						8.200	0.174	174		
8.300	0.170	170						8.300	0.171	171						8.300	0.174	174		
8.400	0.169	169						8.400	0.170	170						8.400	0.173	173		
8.500	0.168	168						8.500	0.169	169						8.500	0.173	173		
8.600	0.168	168						8.600	0.169	169						8.600	0.172	172		
8.700	0.167	167						8.700	0.168	168						8.700	0.172	172		
8.800	0.166	166						8.800	0.168	168						8.800	0.171	171		
8.900	0.166	166						8.900	0.167	167						8.900	0.171	171		
9.000	0.165	165						9.000	0.166	166						9.000	0.170	170		
9.100	0.165	165						9.100	0.166	166						9.100	0.170	170		
9.200	0.164	164						9.200	0.165	165						9.200	0.169	169		
9.300	0.163	163						9.300	0.165	165						9.300	0.169	169		
9.400	0.163	163						9.400	0.164	164						9.400	0.168	168		
9.500	0.162	162						9.500	0.163	163						9.500	0.168	168		
9.600	0.161	161						9.600	0.163	163						9.600	0.167	167		
9.700	0.161	161						9.700	0.162	162						9.700	0.167	167		
9.800	0.160	160						9.800	0.162	162						9.800	0.166	166		
9.900	0.159	159						9.900	0.161	161						9.900	0.166	166		
10.000	0.159	159						10.000	0.161	161						10.000	0.165	165		
10.100	0.158	158						10.100	0.160	160						10.100	0.165	165		
10.200	0.157	157						10.200	0.159	159						10.200	0.164	164		
10.300	0.157	157						10.300	0.159	159						10.300	0.164	164		
10.400	0.156	156						10.400	0.158	158						10.400	0.163	163		
10.500	0.156	156						10.500	0.158	158						10.500	0.163	163		
10.600	0.155	155						10.600	0.157	157						10.600	0.162	162		
10.700	0.154	154						10.700	0.156	156						10.700	0.162	162		
10.800	0.154	154						10.800	0.156	156						10.800	0.161	161		
10.900	0.153	153						10.900	0.155	155						10.900	0.161	161		
11.000	0.152	152						11.000	0.155	155						11.000	0.160	160		
11.100	0.152	152						11.100	0.154	154						11.100	0.160	160		
11.200	0.151	151						11.200	0.153	153						11.200	0.159	159		
11.300	0.150	150						11.300	0.153	153						11.300	0.159	159		
11.400	0.150	150						11.400	0.152	152						11.400	0.158	158		
11.500	0.149	149						11.500	0.152	152						11.500	0.158	158		
11.600	0.149	149						11.600	0.151	151						11.600	0.157	157		
11.700	0.148	148						11.700	0.151	151						11.700	0.157	157		
11.800	0.147	147						11.800	0.150	150						11.800	0.156	156		

RUN 7								RUN 8								RUN 9				
Computed			Data					Computed			Data					Computed			Data	
x (m)	η (m)	η (mm)	x (m)	η (mm)				x (m)	η (m)	η (mm)	x (m)	η (mm)				x (m)	η (m)	η (mm)	x (m)	η (mm)
0.000	0.219	219	2.5	198				0.000	0.213	213	2.5	201				0.000	0.226	226	2.5	201
0.100	0.218	218	2.9	202				0.100	0.212	212	2.9	200				0.100	0.225	225	2.9	201
0.200	0.217	217	3.3	199				0.200	0.212	212	3.3	199				0.200	0.224	224	3.3	199
0.300	0.217	217	3.7	198				0.300	0.211	211	3.7	199				0.300	0.224	224	3.7	198
0.400	0.216	216	4.1	196				0.400	0.211	211	4.1	196				0.400	0.223	223	4.1	196
0.500	0.216	216	4.3	195				0.500	0.210	210	4.3	197				0.500	0.222	222	4.3	196
0.600	0.215	215	4.5	192				0.600	0.210	210	4.5	196				0.600	0.222	222	4.5	194
0.700	0.215	215	4.9	190				0.700	0.209	209	4.9	192				0.700	0.221	221	4.9	191
0.800	0.214	214	5.3	187				0.800	0.209	209	5.3	189				0.800	0.220	220	5.3	188
0.900	0.214	214	5.7	185				0.900	0.208	208	5.7	187				0.900	0.220	220	5.7	186
1.000	0.213	213	6.1	182				1.000	0.208	208	6.1	186				1.000	0.219	219	6.1	183
1.100	0.212	212	6.5	180				1.100	0.207	207	6.5	184				1.100	0.218	218	6.5	180
1.200	0.212	212	6.9	179				1.200	0.207	207	6.9	184				1.200	0.217	217	6.9	181
1.300	0.211	211	7.3	175				1.300	0.206	206	7.3	182				1.300	0.217	217	7.3	176
1.400	0.211	211	7.7	173				1.400	0.206	206	7.7	179				1.400	0.216	216	7.7	172
1.500	0.210	210	8.1	172				1.500	0.205	205	8.1	176				1.500	0.215	215	8.1	168
1.600	0.210	210	8.5	171				1.600	0.205	205	8.5	173				1.600	0.215	215	8.5	166
1.700	0.209	209	8.9	170				1.700	0.205	205	8.9	171				1.700	0.214	214	8.9	165
1.800	0.209	209	9.3	168				1.800	0.204	204	9.3	171				1.800	0.213	213	9.3	160
1.900	0.208	208	9.7	165				1.900	0.204	204	9.7	168				1.900	0.213	213	9.7	158
2.000	0.207	207	10.1	160				2.000	0.203	203	10.1	166				2.000	0.212	212	10.1	158
2.100	0.207	207	10.5	158				2.100	0.203	203	10.5	165				2.100	0.211	211	10.5	153
2.200	0.206	206						2.200	0.202	202						2.200	0.211	211		
2.300	0.206	206						2.300	0.202	202						2.300	0.210	210		
2.400	0.205	205						2.400	0.201	201						2.400	0.209	209		
2.500	0.204	204						2.500	0.201	201						2.500	0.209	209		
2.600	0.204	204						2.600	0.200	200						2.600	0.208	208		
2.700	0.203	203						2.700	0.200	200						2.700	0.207	207		
2.800	0.203	203						2.800	0.200	200						2.800	0.206	206		
2.900	0.202	202						2.900	0.199	199						2.900	0.206	206		
3.000	0.202	202						3.000	0.199	199						3.000	0.205	205		
3.100	0.201	201						3.100	0.198	198						3.100	0.204	204		
3.200	0.200	200						3.200	0.198	198						3.200	0.204	204		
3.300	0.200	200						3.300	0.197	197						3.300	0.203	203		
3.400	0.199	199						3.400	0.197	197						3.400	0.202	202		
3.500	0.199	199						3.500	0.196	196						3.500	0.202	202		
3.600	0.198	198						3.600	0.196	196						3.600	0.201	201		
3.700	0.198	198						3.700	0.196	196						3.700	0.200	200		
3.800	0.197	197						3.800	0.195	195						3.800	0.200	200		
3.900	0.196	196						3.900	0.195	195						3.900	0.199	199		
4.000	0.196	196						4.000	0.194	194						4.000	0.198	198		
4.100	0.195	195						4.100	0.194	194						4.100	0.198	198		
4.200	0.195	195						4.200	0.193	193						4.200	0.197	197		
4.300	0.194	194						4.300	0.193	193						4.300	0.196	196		
4.400	0.193	193						4.400	0.192	192						4.400	0.195	195		
4.500	0.193	193						4.500	0.192	192						4.500	0.195	195		
4.600	0.192	192						4.600	0.191	191						4.600	0.194	194		
4.700	0.192	192						4.700	0.191	191						4.700	0.193	193		
4.800	0.191	191						4.800	0.190	190						4.800	0.193	193		
4.900	0.191	191						4.900	0.190	190						4.900	0.192	192		
5.000	0.190	190						5.000	0.189	189						5.000	0.191	191		
5.100	0.189	189						5.100	0.189	189						5.100	0.191	191		
5.200	0.189	189						5.200	0.189	189						5.200	0.190	190		
5.300	0.188	188						5.300	0.188	188						5.300	0.189	189		
5.400	0.188	188						5.400	0.188	188						5.400	0.189	189		
5.500	0.187	187						5.500	0.187	187						5.500	0.188	188		
5.600	0.186	186						5.600	0.187	187						5.600	0.187	187		
5.700	0.186	186						5.700	0.186	186						5.700	0.186	186		
5.800	0.185	185						5.800	0.186	186						5.800	0.186	186		
5.900	0.185	185						5.900	0.185	185						5.900	0.185	185		
6.000	0.184	184						6.000	0.185	185						6.000	0.184	184		
6.100	0.184	184						6.100	0.184	184						6.100	0.184	184		
6.200	0.183	183						6.200	0.184	184						6.200	0.183	183		
6.300	0.183	183						6.300	0.183	183						6.300	0.182	182		
6.400	0.182	182						6.400	0.183	183						6.400	0.182	182		
6.500	0.181	181						6.500	0.182	182						6.500	0.181	181		
6.600	0.181	181						6.600	0.182	182						6.600	0.180	180		
6.700	0.180	180						6.700	0.181	181						6.700	0.180	180		
6.800	0.180	180						6.800	0.181	181						6.800	0.179	179		
6.900	0.179	179						6.900	0.180	180						6.900	0.178	178		
7.000	0.179	179						7.000	0.180	180						7.000	0.178	178		
7.100	0.178	178						7.100	0.179	179						7.100	0.177	177		
7.200	0.177	177						7.200	0.179	179						7.200	0.176	176		
7.300	0.177	177						7.300	0.179	179						7.300	0.175	175		
7.400	0.176	176						7.400	0.178	178						7.400	0.175	175		
7.500	0.176	176						7.500	0.178	178						7.500	0.174	174		
7.600	0.175	175						7.600	0.177	177						7.600	0.173	173		
7.700	0.175	175						7.700	0.177	177						7.700	0.173	173		
7.800	0.174	174						7.800	0.176	176						7.800	0.172	172		
7.900	0.173	173						7.900	0.176	176						7.900	0.171	171		
8.000	0.173	173						8.000	0.175	175						8.000	0.171	171		
8.100	0.172	172						8.100	0.175	175						8.100	0.170	170		
8.200	0.172	172						8.200	0.174	174						8.200	0.169	169		
8.300	0.171	171						8.300	0.174	174						8.300	0.168	168		
8.400	0.171	171						8.400	0.173	173						8.400	0.168	168		
8.500	0.170	170						8.500	0.173	173						8.500	0.167	167		
8.600	0.170	170						8.600	0.172	172						8.600	0.166	166		
8.700	0.169	169						8.700	0.172	172						8.700	0.166	166		
8.800	0.168	168						8.800	0.171	171						8.800	0.165	165		
8.900	0.168	168						8.900	0.171	171						8.900	0.164	164		
9.000	0.167	167						9.000	0.170	170						9.000	0.164	164		
9.100	0.167	167						9.100	0.170	170						9.100	0.163	163		
9.200	0.166	166						9.200	0.169	169						9.200	0.162	162		
9.300	0.166	166						9.300	0.169	169						9.300	0.161	161		
9.400	0.165	165						9.400	0.168	168						9.400	0.161	161		
9.500	0.164	164						9.500	0.168	168						9.500	0.160	160		
9.600	0.164	164						9.600	0.168	168						9.600	0.159	159		
9.700	0.163	163						9.700	0.167	167						9.700	0.159	159		
9.800	0.163	163						9.800	0.167	167						9.800	0.158	158		
9.900	0.162	162						9.900	0.166	166						9.900	0.157	157		
10.000	0.162	162						10.000	0.166	166						10.000	0.157	157		
10.100	0.161	161						10.100	0.165	165						10.100	0.156	156		
10.200	0.161	161						10.200	0.165	165						10.200	0.155	155		
10.300	0.160	160						10.300	0.164	164						10.300	0.154	154		
10.400	0.160	160						10.400	0.164	164						10.400	0.154	154		
10.500	0.159	159						10.500	0.163	163						10.500	0.153	153		
10.600	0.158	158						10.600	0.163	163						10.600	0.152	152		
10.700	0.158	158						10.700	0.162	162						10.700	0.152	152		
10.800	0.157	157						10.800	0.162	162						10.800	0.151	151		
10.900	0.157	157						10.900	0.161	161						10.900	0.150	150		
11.000	0.156	156						11.000	0.161	161						11.000	0.150	150		
11.100	0.156	156						11.100	0.160	160						11.100	0.149	149		
11.200	0.155	155						11.200	0.160	160						11.200	0.148	148		
11.300	0.155	155						11.300	0.159	159						11.300	0.147	147		
11.400	0.154	154						11.400	0.159	159						11.400	0.147	147		
11.500	0.153	153						11.500	0.158	158						11.500	0.146	146		
11.600	0.153	153						11.600	0.158	158						11.600	0.145	145		
11.700	0.152	152						11.700	0.157	157						11.700	0.145	145		
11.800	0.152	152						11.800	0.157	157						11.800	0.144	144		

RUN 1

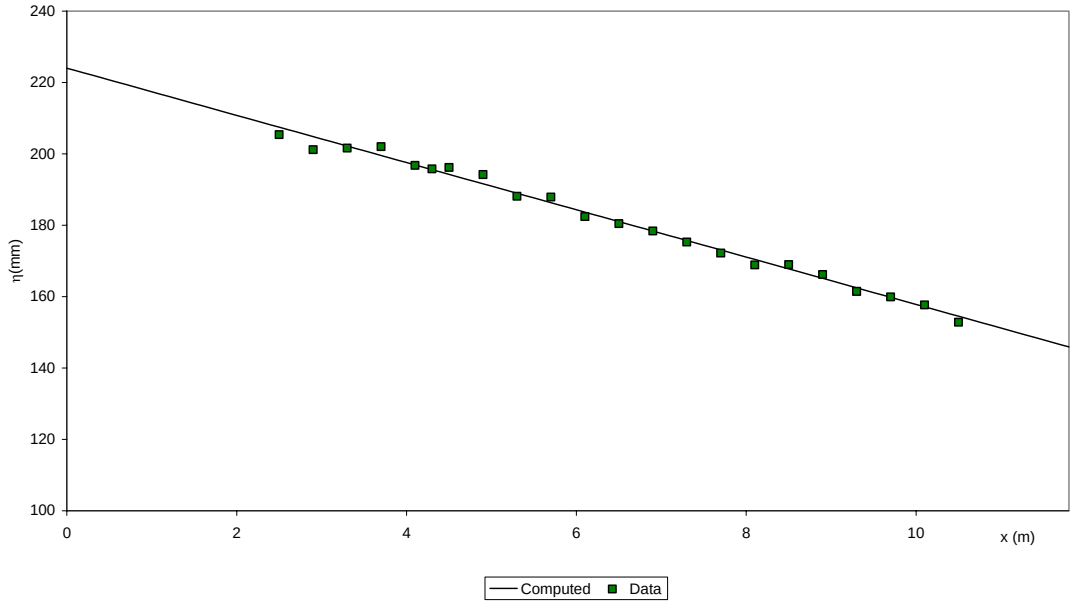
240
220
200
180
160
140
120
100
η(mm)
0
2
4
6
8
10
x (m)
Computed
Data

RUN 2

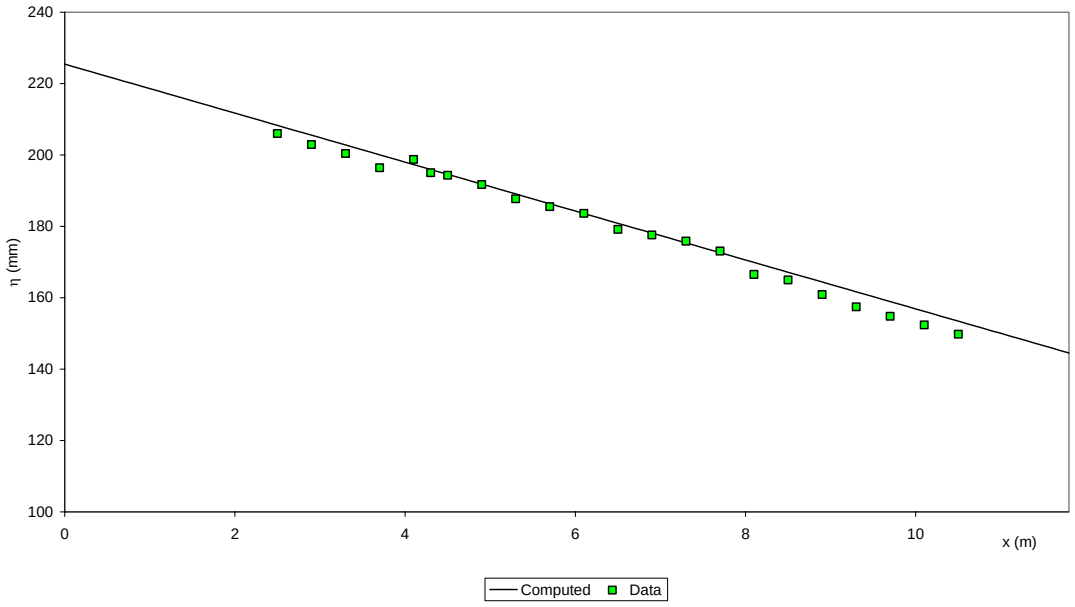
240
220
200
180
160
140
120
100
η (mm)
0
2
4
6
8
10
x (m)
Computed
Data

RUN 3

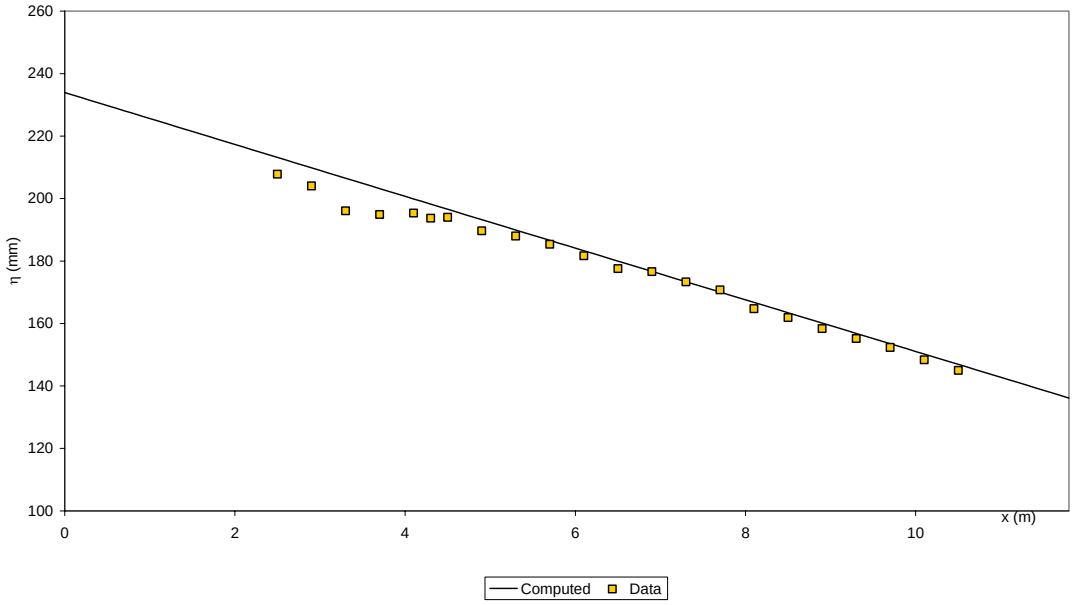
260
240
220
200
180
160
140
120
100
η (mm)
0
2
4
6
8
10
x (m)
Computed
Data

RUN 4

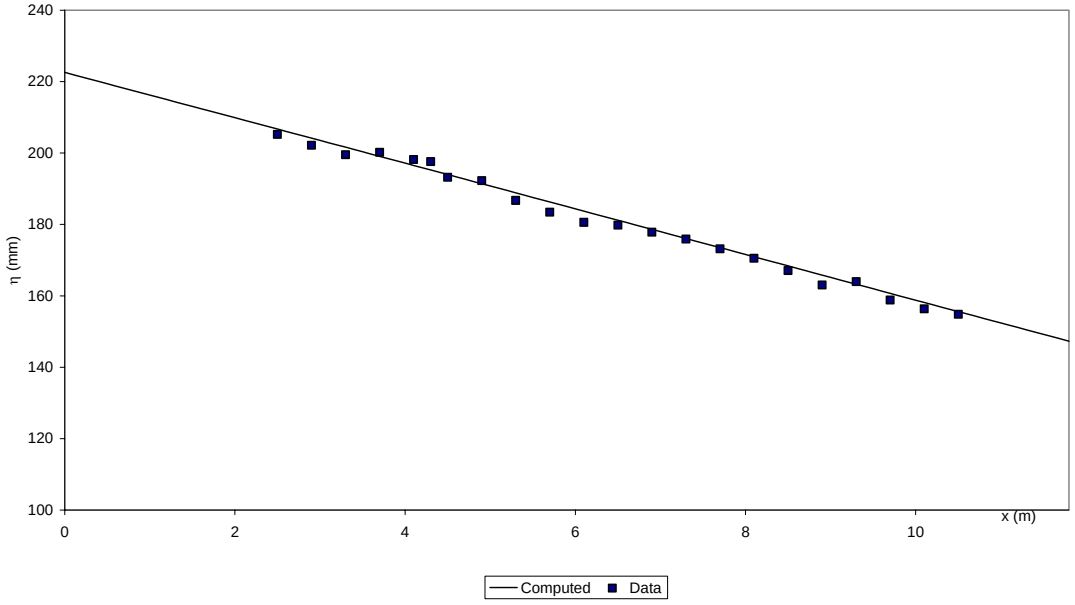
240
220
200
180
160
140
120
100
η (mm)
0
2
4
6
8
10
x (m)
Computed
Data

RUN 5

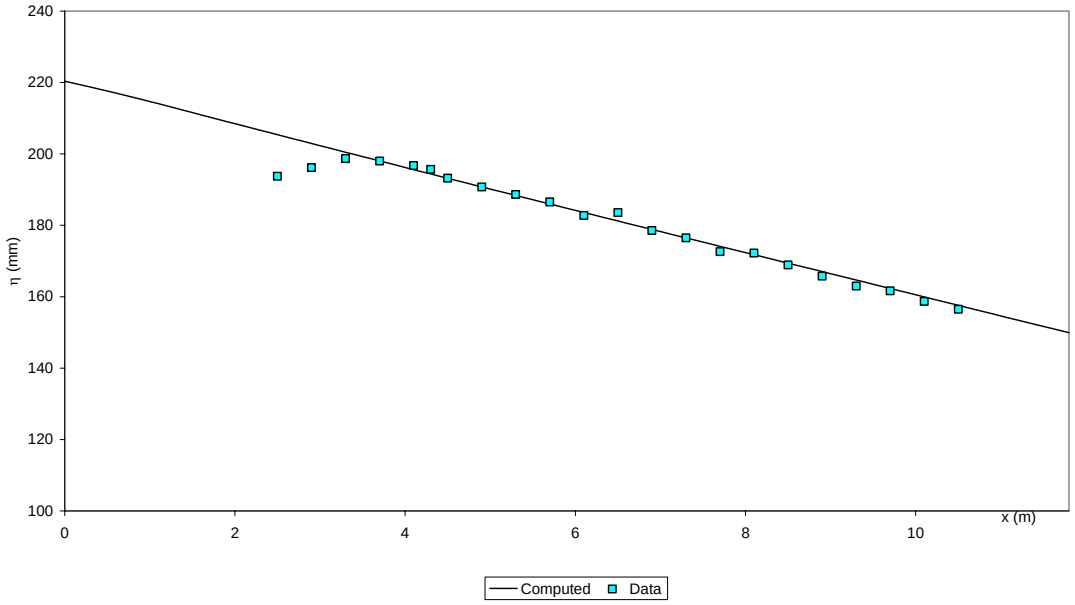
240
220
200
180
160
140
120
100
η (mm)
0
2
4
6
8
10
x (m)
Computed
Data

RUN 6

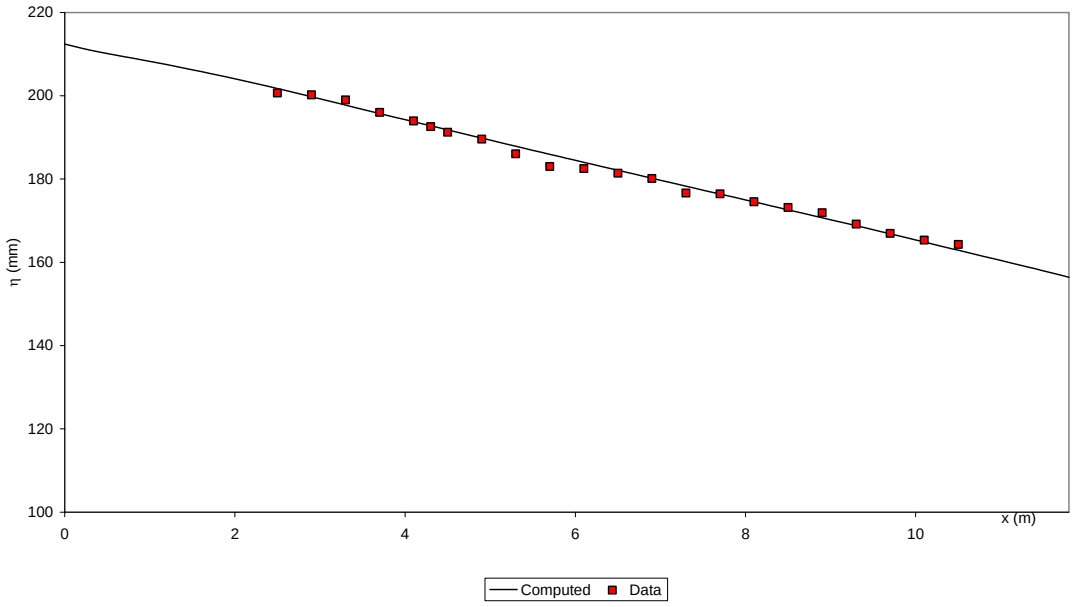
220
200
180
160
140
120
100
η (mm)
0
2
4
6
8
10
x (m)
Computed
Data

RUN 7

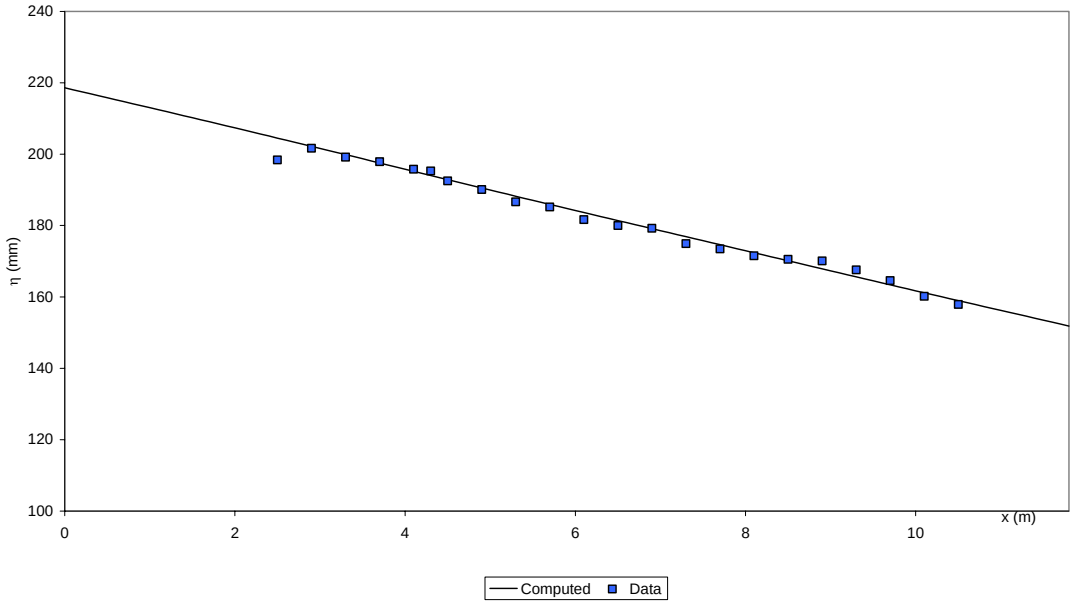
240
220
200
180
160
140
120
100
η (mm)
0
2
4
6
8
10
x (m)
Computed
Data

RUN 8

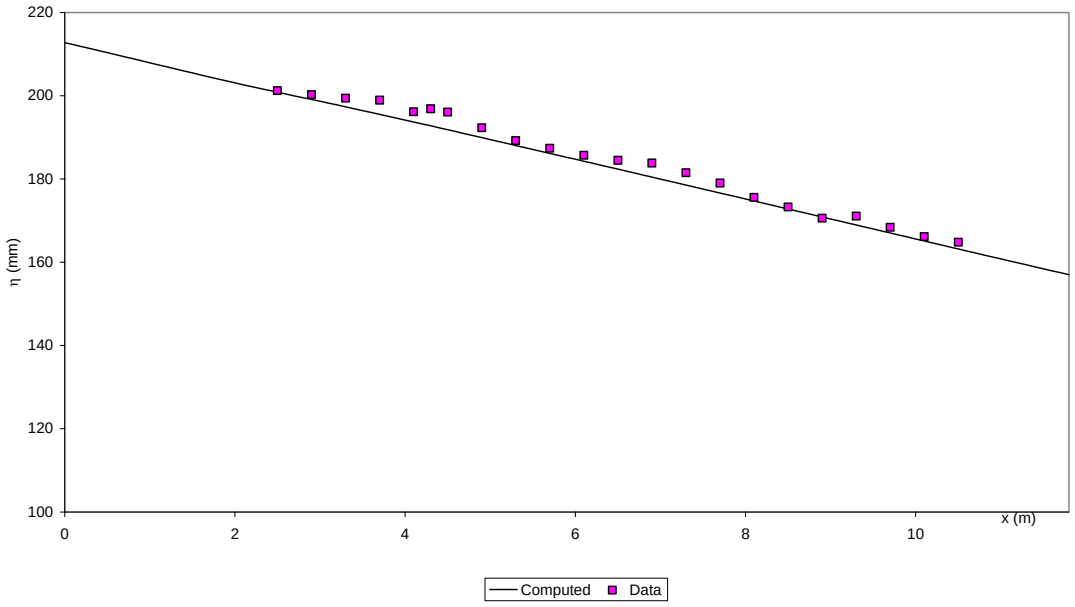
220
200
180
160
140
120
100
η (mm)
0
2
4
6
8
10
x (m)
Computed
Data

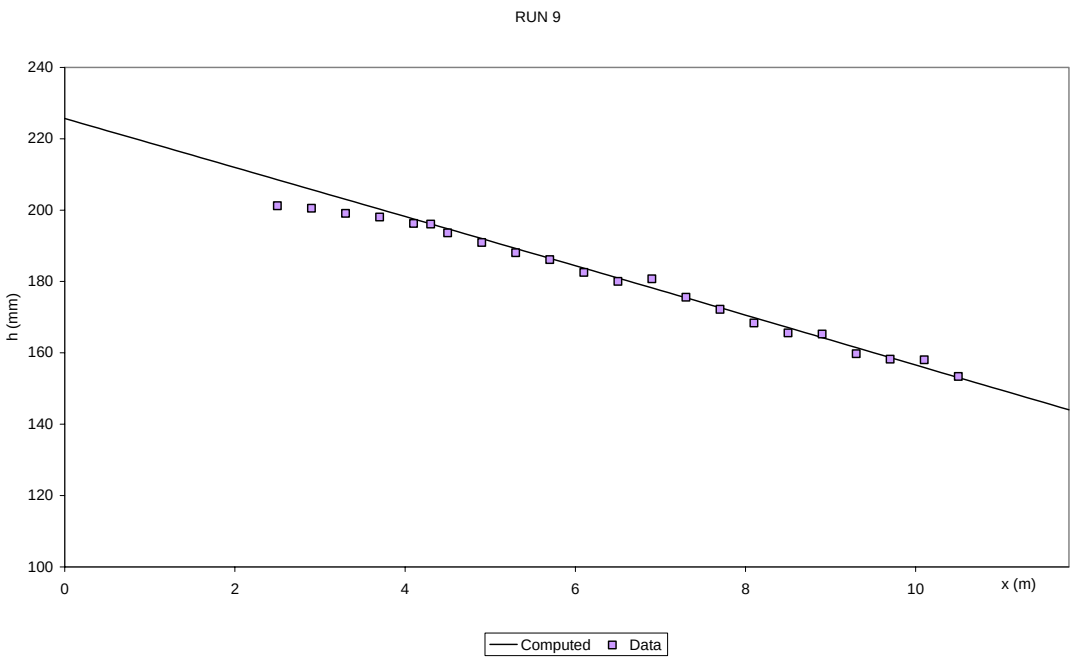
RUN 9
240
220
200
180
160
140
120
100
h (mm)
0
2
4
6
8
10
x (m)
Computed
Data

Water surface elevation

RUN 1								RUN 2								RUN 3				
Computed			Data					Computed			Data					Computed			Data	
x (m)	H (m)	H (mm)	x (m)	H (mm)				x (m)	H (m)	H (mm)	x (m)	H (mm)				x (m)	H (m)	H (mm)	x (m)	H (mm)
0.000	0.298	298	2.5	284				0.000	0.291	291	2.5	275				0.000	0.288	288	2.5	266
0.100	0.297	297	4.3	274				0.100	0.290	290	4.3	263				0.100	0.287	287	4.3	255
0.200	0.297	297	6.5	258				0.200	0.290	290	6.5	248				0.200	0.286	286	6.5	239
0.300	0.296	296	8.5	244				0.300	0.289	289	8.5	232				0.300	0.285	285	8.5	221
0.400	0.295	295	10.5	229				0.400	0.288	288	10.5	218				0.400	0.284	284	10.5	201
0.500	0.295	295						0.500	0.288	288						0.500	0.284	284		
0.600	0.294	294						0.600	0.287	287						0.600	0.283	283		
0.700	0.293	293						0.700	0.286	286						0.700	0.282	282		
0.800	0.293	293						0.800	0.285	285						0.800	0.281	281		
0.900	0.292	292						0.900	0.285	285						0.900	0.280	280		
1.000	0.292	292						1.000	0.284	284						1.000	0.279	279		
1.100	0.291	291						1.100	0.283	283						1.100	0.279	279		
1.200	0.290	290						1.200	0.283	283						1.200	0.278	278		
1.300	0.290	290						1.300	0.282	282						1.300	0.277	277		
1.400	0.289	289						1.400	0.281	281						1.400	0.276	276		
1.500	0.288	288						1.500	0.281	281						1.500	0.275	275		
1.600	0.288	288						1.600	0.280	280						1.600	0.275	275		
1.700	0.287	287						1.700	0.279	279						1.700	0.274	274		
1.800	0.286	286						1.800	0.279	279						1.800	0.273	273		
1.900	0.286	286						1.900	0.278	278						1.900	0.272	272		
2.000	0.285	285						2.000	0.277	277						2.000	0.271	271		
2.100	0.284	284						2.100	0.277	277						2.100	0.270	270		
2.200	0.284	284						2.200	0.276	276						2.200	0.270	270		
2.300	0.283	283						2.300	0.275	275						2.300	0.269	269		
2.400	0.282	282						2.400	0.274	274						2.400	0.268	268		
2.500	0.282	282						2.500	0.274	274						2.500	0.267	267		
2.600	0.281	281						2.600	0.273	273						2.600	0.266	266		
2.700	0.280	280						2.700	0.272	272						2.700	0.265	265		
2.800	0.280	280						2.800	0.272	272						2.800	0.265	265		
2.900	0.279	279						2.900	0.271	271						2.900	0.264	264		
3.000	0.278	278						3.000	0.270	270						3.000	0.263	263		
3.100	0.278	278						3.100	0.270	270						3.100	0.262	262		
3.200	0.277	277						3.200	0.269	269						3.200	0.261	261		
3.300	0.276	276						3.300	0.268	268						3.300	0.260	260		
3.400	0.276	276						3.400	0.268	268						3.400	0.260	260		
3.500	0.275	275						3.500	0.267	267						3.500	0.259	259		
3.600	0.274	274						3.600	0.266	266						3.600	0.258	258		
3.700	0.274	274						3.700	0.266	266						3.700	0.257	257		
3.800	0.273	273						3.800	0.265	265						3.800	0.256	256		
3.900	0.272	272						3.900	0.264	264						3.900	0.255	255		
4.000	0.272	272						4.000	0.264	264						4.000	0.255	255		
4.100	0.271	271						4.100	0.263	263						4.100	0.254	254		
4.200	0.270	270						4.200	0.262	262						4.200	0.253	253		
4.300	0.270	270						4.300	0.261	261						4.300	0.252	252		
4.400	0.269	269						4.400	0.261	261						4.400	0.251	251		
4.500	0.268	268						4.500	0.260	260						4.500	0.250	250		
4.600	0.268	268						4.600	0.259	259						4.600	0.250	250		
4.700	0.267	267						4.700	0.259	259						4.700	0.249	249		
4.800	0.266	266						4.800	0.258	258						4.800	0.248	248		
4.900	0.266	266						4.900	0.257	257						4.900	0.247	247		
5.000	0.265	265						5.000	0.257	257						5.000	0.246	246		
5.100	0.264	264						5.100	0.256	256						5.100	0.245	245		
5.200	0.264	264						5.200	0.255	255						5.200	0.245	245		
5.300	0.263	263						5.300	0.255	255						5.300	0.244	244		
5.400	0.262	262						5.400	0.254	254						5.400	0.243	243		
5.500	0.262	262						5.500	0.253	253						5.500	0.242	242		
5.600	0.261	261						5.600	0.253	253						5.600	0.241	241		
5.700	0.260	260						5.700	0.252	252						5.700	0.241	241		
5.800	0.260	260						5.800	0.251	251						5.800	0.240	240		
5.900	0.259	259						5.900	0.250	250						5.900	0.239	239		
6.000	0.258	258						6.000	0.250	250						6.000	0.238	238		
6.100	0.258	258						6.100	0.249	249						6.100	0.237	237		
6.200	0.257	257						6.200	0.248	248						6.200	0.236	236		
6.300	0.256	256						6.300	0.248	248						6.300	0.236	236		
6.400	0.256	256						6.400	0.247	247						6.400	0.235	235		
6.500	0.255	255						6.500	0.246	246						6.500	0.234	234		
6.600	0.254	254						6.600	0.246	246						6.600	0.233	233		
6.700	0.254	254						6.700	0.245	245						6.700	0.232	232		
6.800	0.253	253						6.800	0.244	244						6.800	0.231	231		
6.900	0.252	252						6.900	0.244	244						6.900	0.231	231		
7.000	0.252	252						7.000	0.243	243						7.000	0.230	230		
7.100	0.251	251						7.100	0.242	242						7.100	0.229	229		
7.200	0.250	250						7.200	0.242	242						7.200	0.228	228		
7.300	0.250	250						7.300	0.241	241						7.300	0.227	227		
7.400	0.249	249						7.400	0.240	240						7.400	0.226	226		
7.500	0.248	248						7.500	0.240	240						7.500	0.226	226		
7.600	0.248	248						7.600	0.239	239						7.600	0.225	225		
7.700	0.247	247						7.700	0.238	238						7.700	0.224	224		
7.800	0.246	246						7.800	0.237	237						7.800	0.223	223		
7.900	0.246	246						7.900	0.237	237						7.900	0.222	222		
8.000	0.245	245						8.000	0.236	236						8.000	0.222	222		
8.100	0.244	244						8.100	0.235	235						8.100	0.221	221		
8.200	0.244	244						8.200	0.235	235						8.200	0.220	220		
8.300	0.243	243						8.300	0.234	234						8.300	0.219	219		
8.400	0.242	242						8.400	0.233	233						8.400	0.218	218		
8.500	0.242	242						8.500	0.233	233						8.500	0.217	217		
8.600	0.241	241						8.600	0.232	232						8.600	0.217	217		
8.700	0.241	241						8.700	0.231	231						8.700	0.216	216		
8.800	0.240	240						8.800	0.231	231						8.800	0.215	215		
8.900	0.239	239						8.900	0.230	230						8.900	0.214	214		
9.000	0.239	239						9.000	0.229	229						9.000	0.213	213		
9.100	0.238	238						9.100	0.229	229						9.100	0.212	212		
9.200	0.237	237						9.200	0.228	228						9.200	0.212	212		
9.300	0.237	237						9.300	0.227	227						9.300	0.211	211		
9.400	0.236	236						9.400	0.226	226						9.400	0.210	210		
9.500	0.235	235						9.500	0.226	226						9.500	0.209	209		
9.600	0.235	235						9.600	0.225	225						9.600	0.208	208		
9.700	0.234	234						9.700	0.224	224						9.700	0.207	207		
9.800	0.233	233						9.800	0.224	224						9.800	0.207	207		
9.900	0.233	233						9.900	0.223	223						9.900	0.206	206		
10.000	0.232	232						10.000	0.222	222						10.000	0.205	205		
10.100	0.231	231						10.100	0.222	222						10.100	0.204	204		
10.200	0.231	231						10.200	0.221	221						10.200	0.203	203		
10.300	0.230	230						10.300	0.220	220						10.300	0.202	202		
10.400	0.229	229						10.400	0.220	220						10.400	0.202	202		
10.500	0.229	229						10.500	0.219	219						10.500	0.201	201		
10.600	0.228	228						10.600	0.218	218						10.600	0.200	200		
10.700	0.227	227						10.700	0.218	218						10.700	0.199	199		
10.800	0.227	227						10.800	0.217	217						10.800	0.198	198		
10.900	0.226	226						10.900	0.216	216						10.900	0.197	197		
11.000	0.225	225						11.000	0.215	215						11.000	0.197	197		
11.100	0.225	225						11.100	0.215	215						11.100	0.196	196		
11.200	0.224	224						11.200	0.214	214						11.200	0.195	195		
11.300	0.223	223						11.300	0.213	213						11.300	0.194	194		
11.400	0.223	223						11.400	0.213	213						11.400	0.193	193		
11.500	0.222	222						11.500	0.212	212						11.500	0.192	192		
11.600	0.221	221						11.600	0.211	211						11.600	0.192	192		
11.700	0.221	221						11.700	0.211	211						11.700	0.191	191		
11.800	0.220	220						11.800	0.210	210						11.800	0.190	190		

RUN 4								RUN 5								RUN 6				
Computed			Data					Computed			Data					Computed			Data	
x (m)	H (m)	H (mm)	x (m)	H (mm)				x (m)	H (m)	H (mm)	x (m)	H (mm)				x (m)	H (m)	H (mm)	x (m)	H (mm)
0.000	0.305	305	2.5	291				0.000	0.280	280	2.5	270				0.000	0.296	296	2.5	283
0.100	0.305	305	4.3	278				0.100	0.280	280	4.3	259				0.100	0.296	296	4.3	276
0.200	0.304	304	6.5	264				0.200	0.279	279	6.5	243				0.200	0.295	295	6.5	265
0.300	0.303	303	8.5	252				0.300	0.278	278	8.5	230				0.300	0.295	295	8.5	255
0.400	0.303	303	10.5	239				0.400	0.278	278	10.5	216				0.400	0.294	294	10.5	245
0.500	0.302	302						0.500	0.277	277						0.500	0.294	294		
0.600	0.301	301						0.600	0.276	276						0.600	0.293	293		
0.700	0.301	301						0.700	0.276	276						0.700	0.293	293		
0.800	0.300	300						0.800	0.275	275						0.800	0.292	292		
0.900	0.300	300						0.900	0.275	275						0.900	0.292	292		
1.000	0.299	299						1.000	0.274	274						1.000	0.291	291		
1.100	0.298	298						1.100	0.273	273						1.100	0.291	291		
1.200	0.298	298						1.200	0.273	273						1.200	0.290	290		
1.300	0.297	297						1.300	0.272	272						1.300	0.290	290		
1.400	0.296	296						1.400	0.271	271						1.400	0.289	289		
1.500	0.296	296						1.500	0.271	271						1.500	0.289	289		
1.600	0.295	295						1.600	0.270	270						1.600	0.288	288		
1.700	0.294	294						1.700	0.270	270						1.700	0.288	288		
1.800	0.294	294						1.800	0.269	269						1.800	0.287	287		
1.900	0.293	293						1.900	0.268	268						1.900	0.287	287		
2.000	0.293	293						2.000	0.268	268						2.000	0.286	286		
2.100	0.292	292						2.100	0.267	267						2.100	0.286	286		
2.200	0.291	291						2.200	0.267	267						2.200	0.285	285		
2.300	0.291	291						2.300	0.266	266						2.300	0.284	284		
2.400	0.290	290						2.400	0.265	265						2.400	0.284	284		
2.500	0.289	289						2.500	0.265	265						2.500	0.283	283		
2.600	0.289	289						2.600	0.264	264						2.600	0.283	283		
2.700	0.288	288						2.700	0.264	264						2.700	0.282	282		
2.800	0.287	287						2.800	0.263	263						2.800	0.282	282		
2.900	0.287	287						2.900	0.262	262						2.900	0.282	282		
3.000	0.286	286						3.000	0.262	262						3.000	0.281	281		
3.100	0.285	285						3.100	0.261	261						3.100	0.281	281		
3.200	0.285	285						3.200	0.261	261						3.200	0.280	280		
3.300	0.284	284						3.300	0.260	260						3.300	0.280	280		
3.400	0.284	284						3.400	0.259	259						3.400	0.279	279		
3.500	0.283	283						3.500	0.259	259						3.500	0.279	279		
3.600	0.282	282						3.600	0.258	258						3.600	0.278	278		
3.700	0.282	282						3.700	0.258	258						3.700	0.278	278		
3.800	0.281	281						3.800	0.257	257						3.800	0.277	277		
3.900	0.280	280						3.900	0.256	256						3.900	0.277	277		
4.000	0.280	280						4.000	0.256	256						4.000	0.276	276		
4.100	0.279	279						4.100	0.255	255						4.100	0.276	276		
4.200	0.278	278						4.200	0.255	255						4.200	0.275	275		
4.300	0.278	278						4.300	0.254	254						4.300	0.275	275		
4.400	0.277	277						4.400	0.254	254						4.400	0.274	274		
4.500	0.276	276						4.500	0.253	253						4.500	0.274	274		
4.600	0.276	276						4.600	0.252	252						4.600	0.273	273		
4.700	0.275	275						4.700	0.252	252						4.700	0.273	273		
4.800	0.275	275						4.800	0.251	251						4.800	0.273	273		
4.900	0.274	274						4.900	0.251	251						4.900	0.272	272		
5.000	0.273	273						5.000	0.250	250						5.000	0.272	272		
5.100	0.273	273						5.100	0.249	249						5.100	0.271	271		
5.200	0.272	272						5.200	0.249	249						5.200	0.271	271		
5.300	0.271	271						5.300	0.248	248						5.300	0.270	270		
5.400	0.271	271						5.400	0.248	248						5.400	0.270	270		
5.500	0.270	270						5.500	0.247	247						5.500	0.269	269		
5.600	0.269	269						5.600	0.246	246						5.600	0.269	269		
5.700	0.269	269						5.700	0.246	246						5.700	0.268	268		
5.800	0.268	268						5.800	0.245	245						5.800	0.268	268		
5.900	0.268	268						5.900	0.245	245						5.900	0.267	267		
6.000	0.267	267						6.000	0.244	244						6.000	0.267	267		
6.100	0.266	266						6.100	0.243	243						6.100	0.266	266		
6.200	0.266	266						6.200	0.243	243						6.200	0.266	266		
6.300	0.265	265						6.300	0.242	242						6.300	0.265	265		
6.400	0.264	264						6.400	0.242	242						6.400	0.265	265		
6.500	0.264	264						6.500	0.241	241						6.500	0.264	264		
6.600	0.263	263						6.600	0.241	241						6.600	0.264	264		
6.700	0.262	262						6.700	0.240	240						6.700	0.264	264		
6.800	0.262	262						6.800	0.239	239						6.800	0.263	263		
6.900	0.261	261						6.900	0.239	239						6.900	0.263	263		
7.000	0.261	261						7.000	0.238	238						7.000	0.262	262		
7.100	0.260	260						7.100	0.238	238						7.100	0.262	262		
7.200	0.259	259						7.200	0.237	237						7.200	0.261	261		
7.300	0.259	259						7.300	0.236	236						7.300	0.261	261		
7.400	0.258	258						7.400	0.236	236						7.400	0.260	260		
7.500	0.257	257						7.500	0.235	235						7.500	0.260	260		
7.600	0.257	257						7.600	0.235	235						7.600	0.259	259		
7.700	0.256	256						7.700	0.234	234						7.700	0.259	259		
7.800	0.255	255						7.800	0.233	233						7.800	0.258	258		
7.900	0.255	255						7.900	0.233	233						7.900	0.258	258		
8.000	0.254	254						8.000	0.232	232						8.000	0.257	257		
8.100	0.253	253						8.100	0.232	232						8.100	0.257	257		
8.200	0.253	253						8.200	0.231	231						8.200	0.256	256		
8.300	0.252	252						8.300	0.230	230						8.300	0.256	256		
8.400	0.252	252						8.400	0.230	230						8.400	0.255	255		
8.500	0.251	251						8.500	0.229	229						8.500	0.255	255		
8.600	0.250	250						8.600	0.229	229						8.600	0.254	254		
8.700	0.250	250						8.700	0.228	228						8.700	0.254	254		
8.800	0.249	249						8.800	0.228	228						8.800	0.254	254		
8.900	0.248	248						8.900	0.227	227						8.900	0.253	253		
9.000	0.248	248						9.000	0.226	226						9.000	0.253	253		
9.100	0.247	247						9.100	0.226	226						9.100	0.252	252		
9.200	0.246	246						9.200	0.225	225						9.200	0.252	252		
9.300	0.246	246						9.300	0.225	225						9.300	0.251	251		
9.400	0.245	245						9.400	0.224	224						9.400	0.251	251		
9.500	0.245	245						9.500	0.223	223						9.500	0.250	250		
9.600	0.244	244						9.600	0.223	223						9.600	0.250	250		
9.700	0.243	243						9.700	0.222	222						9.700	0.249	249		
9.800	0.243	243						9.800	0.222	222						9.800	0.249	249		
9.900	0.242	242						9.900	0.221	221						9.900	0.248	248		
10.000	0.241	241						10.000	0.220	220						10.000	0.248	248		
10.100	0.241	241						10.100	0.220	220						10.100	0.247	247		
10.200	0.240	240						10.200	0.219	219						10.200	0.247	247		
10.300	0.240	240						10.300	0.219	219						10.300	0.247	247		
10.400	0.239	239						10.400	0.218	218						10.400	0.246	246		
10.500	0.238	238						10.500	0.218	218						10.500	0.246	246		
10.600	0.238	238						10.600	0.217	217						10.600	0.245	245		
10.700	0.237	237						10.700	0.216	216						10.700	0.245	245		
10.800	0.236	236						10.800	0.216	216						10.800	0.244	244		
10.900	0.236	236						10.900	0.215	215						10.900	0.244	244		
11.000	0.235	235						11.000	0.215	215						11.000	0.243	243		
11.100	0.234	234						11.100	0.214	214						11.100	0.243	243		
11.200	0.234	234						11.200	0.213	213						11.200	0.243	243		
11.300	0.233	233						11.300	0.213	213						11.300	0.242	242		
11.400	0.233	233						11.400	0.212	212						11.400	0.242	242		
11.500	0.232	232						11.500	0.212	212						11.500	0.241	241		
11.600	0.231	231						11.600	0.211	211						11.600	0.241	241		
11.700	0.231	231						11.700	0.211	211						11.700	0.240	240		
11.800	0.230	230						11.800	0.210	210						11.800	0.240	240		

RUN 7								RUN 8								RUN 9				
Computed			Data					Computed			Data					Computed			Data	
x (m)	H (m)	H (mm)	x (m)	H (mm)				x (m)	H (m)	H (mm)	x (m)	H (mm)				x (m)	H (m)	H (mm)	x (m)	H (mm)
0.000	0.297	297	2.5	283				0.000	0.304	304	2.5	293				0.000	0.307	307	2.5	292
0.100	0.296	296	4.3	273				0.100	0.303	303	4.3	283				0.100	0.306	306	4.3	278
0.200	0.296	296	6.5	260				0.200	0.303	303	6.5	271				0.200	0.305	305	6.5	261
0.300	0.295	295	8.5	250				0.300	0.302	302	8.5	263				0.300	0.305	305	8.5	249
0.400	0.294	294	10.5	239				0.400	0.302	302	10.5	252				0.400	0.304	304	10.5	237
0.500	0.294	294						0.500	0.301	301						0.500	0.303	303		
0.600	0.293	293						0.600	0.301	301						0.600	0.303	303		
0.700	0.293	293						0.700	0.301	301						0.700	0.302	302		
0.800	0.292	292						0.800	0.300	300						0.800	0.301	301		
0.900	0.291	291						0.900	0.300	300						0.900	0.300	300		
1.000	0.291	291						1.000	0.299	299						1.000	0.300	300		
1.100	0.290	290						1.100	0.299	299						1.100	0.299	299		
1.200	0.290	290						1.200	0.298	298						1.200	0.298	298		
1.300	0.289	289						1.300	0.298	298						1.300	0.298	298		
1.400	0.289	289						1.400	0.297	297						1.400	0.297	297		
1.500	0.288	288						1.500	0.297	297						1.500	0.296	296		
1.600	0.287	287						1.600	0.297	297						1.600	0.296	296		
1.700	0.287	287						1.700	0.296	296						1.700	0.295	295		
1.800	0.286	286						1.800	0.296	296						1.800	0.294	294		
1.900	0.286	286						1.900	0.295	295						1.900	0.294	294		
2.000	0.285	285						2.000	0.295	295						2.000	0.293	293		
2.100	0.284	284						2.100	0.294	294						2.100	0.292	292		
2.200	0.284	284						2.200	0.294	294						2.200	0.292	292		
2.300	0.283	283						2.300	0.293	293						2.300	0.291	291		
2.400	0.283	283						2.400	0.293	293						2.400	0.290	290		
2.500	0.282	282						2.500	0.292	292						2.500	0.289	289		
2.600	0.282	282						2.600	0.292	292						2.600	0.289	289		
2.700	0.281	281						2.700	0.291	291						2.700	0.288	288		
2.800	0.280	280						2.800	0.291	291						2.800	0.287	287		
2.900	0.280	280						2.900	0.290	290						2.900	0.287	287		
3.000	0.279	279						3.000	0.290	290						3.000	0.286	286		
3.100	0.279	279						3.100	0.289	289						3.100	0.285	285		
3.200	0.278	278						3.200	0.289	289						3.200	0.285	285		
3.300	0.278	278						3.300	0.288	288						3.300	0.284	284		
3.400	0.277	277						3.400	0.288	288						3.400	0.283	283		
3.500	0.276	276						3.500	0.288	288						3.500	0.283	283		
3.600	0.276	276						3.600	0.287	287						3.600	0.282	282		
3.700	0.275	275						3.700	0.287	287						3.700	0.281	281		
3.800	0.275	275						3.800	0.286	286						3.800	0.280	280		
3.900	0.274	274						3.900	0.286	286						3.900	0.280	280		
4.000	0.274	274						4.000	0.285	285						4.000	0.279	279		
4.100	0.273	273						4.100	0.285	285						4.100	0.278	278		
4.200	0.272	272						4.200	0.284	284						4.200	0.278	278		
4.300	0.272	272						4.300	0.284	284						4.300	0.277	277		
4.400	0.271	271						4.400	0.283	283						4.400	0.276	276		
4.500	0.271	271						4.500	0.283	283						4.500	0.276	276		
4.600	0.270	270						4.600	0.282	282						4.600	0.275	275		
4.700	0.270	270						4.700	0.282	282						4.700	0.274	274		
4.800	0.269	269						4.800	0.281	281						4.800	0.274	274		
4.900	0.269	269						4.900	0.281	281						4.900	0.273	273		
5.000	0.268	268						5.000	0.280	280						5.000	0.272	272		
5.100	0.267	267						5.100	0.280	280						5.100	0.271	271		
5.200	0.267	267						5.200	0.279	279						5.200	0.271	271		
5.300	0.266	266						5.300	0.279	279						5.300	0.270	270		
5.400	0.266	266						5.400	0.278	278						5.400	0.269	269		
5.500	0.265	265						5.500	0.278	278						5.500	0.269	269		
5.600	0.265	265						5.600	0.277	277						5.600	0.268	268		
5.700	0.264	264						5.700	0.277	277						5.700	0.267	267		
5.800	0.264	264						5.800	0.276	276						5.800	0.267	267		
5.900	0.263	263						5.900	0.276	276						5.900	0.266	266		
6.000	0.262	262						6.000	0.275	275						6.000	0.265	265		
6.100	0.262	262						6.100	0.275	275						6.100	0.264	264		
6.200	0.261	261						6.200	0.275	275						6.200	0.264	264		
6.300	0.261	261						6.300	0.274	274						6.300	0.263	263		
6.400	0.260	260						6.400	0.274	274						6.400	0.262	262		
6.500	0.260	260						6.500	0.273	273						6.500	0.262	262		
6.600	0.259	259						6.600	0.273	273						6.600	0.261	261		
6.700	0.259	259						6.700	0.272	272						6.700	0.260	260		
6.800	0.258	258						6.800	0.272	272						6.800	0.260	260		
6.900	0.257	257						6.900	0.271	271						6.900	0.259	259		
7.000	0.257	257						7.000	0.271	271						7.000	0.258	258		
7.100	0.256	256						7.100	0.270	270						7.100	0.257	257		
7.200	0.256	256						7.200	0.270	270						7.200	0.257	257		
7.300	0.255	255						7.300	0.269	269						7.300	0.256	256		
7.400	0.255	255						7.400	0.269	269						7.400	0.255	255		
7.500	0.254	254						7.500	0.268	268						7.500	0.255	255		
7.600	0.254	254						7.600	0.268	268						7.600	0.254	254		
7.700	0.253	253						7.700	0.267	267						7.700	0.253	253		
7.800	0.252	252						7.800	0.267	267						7.800	0.253	253		
7.900	0.252	252						7.900	0.266	266						7.900	0.252	252		
8.000	0.251	251						8.000	0.266	266						8.000	0.251	251		
8.100	0.251	251						8.100	0.265	265						8.100	0.250	250		
8.200	0.250	250						8.200	0.265	265						8.200	0.250	250		
8.300	0.250	250						8.300	0.264	264						8.300	0.249	249		
8.400	0.249	249						8.400	0.264	264						8.400	0.248	248		
8.500	0.249	249						8.500	0.264	264						8.500	0.248	248		
8.600	0.248	248						8.600	0.263	263						8.600	0.247	247		
8.700	0.247	247						8.700	0.263	263						8.700	0.246	246		
8.800	0.247	247						8.800	0.262	262						8.800	0.246	246		
8.900	0.246	246						8.900	0.262	262						8.900	0.245	245		
9.000	0.246	246						9.000	0.261	261						9.000	0.244	244		
9.100	0.245	245						9.100	0.261	261						9.100	0.243	243		
9.200	0.245	245						9.200	0.260	260						9.200	0.243	243		
9.300	0.244	244						9.300	0.260	260						9.300	0.242	242		
9.400	0.244	244						9.400	0.259	259						9.400	0.241	241		
9.500	0.243	243						9.500	0.259	259						9.500	0.241	241		
9.600	0.242	242						9.600	0.258	258						9.600	0.240	240		
9.700	0.242	242						9.700	0.258	258						9.700	0.239	239		
9.800	0.241	241						9.800	0.257	257						9.800	0.239	239		
9.900	0.241	241						9.900	0.257	257						9.900	0.238	238		
10.000	0.240	240						10.000	0.256	256						10.000	0.237	237		
10.100	0.240	240						10.100	0.256	256						10.100	0.237	237		
10.200	0.239	239						10.200	0.256	256						10.200	0.236	236		
10.300	0.239	239						10.300	0.255	255						10.300	0.235	235		
10.400	0.238	238						10.400	0.255	255						10.400	0.235	235		
10.500	0.237	237						10.500	0.254	254						10.500	0.234	234		
10.600	0.237	237						10.600	0.254	254						10.600	0.233	233		
10.700	0.236	236						10.700	0.253	253						10.700	0.232	232		
10.800	0.236	236						10.800	0.253	253						10.800	0.232	232		
10.900	0.235	235						10.900	0.252	252						10.900	0.231	231		
11.000	0.235	235						11.000	0.252	252						11.000	0.230	230		
11.100	0.234	234						11.100	0.251	251						11.100	0.230	230		
11.200	0.233	233						11.200	0.251	251						11.200	0.229	229		
11.300	0.233	233						11.300	0.250	250						11.300	0.228	228		
11.400	0.232	232						11.400	0.250	250						11.400	0.228	228		
11.500	0.232	232						11.500	0.249	249						11.500	0.227	227		
11.600	0.231	231						11.600	0.249	249						11.600	0.226	226		
11.700	0.231	231						11.700	0.248	248						11.700	0.226	226		
11.800	0.230	230						11.800	0.248	248						11.800	0.225	225		

RUN 1

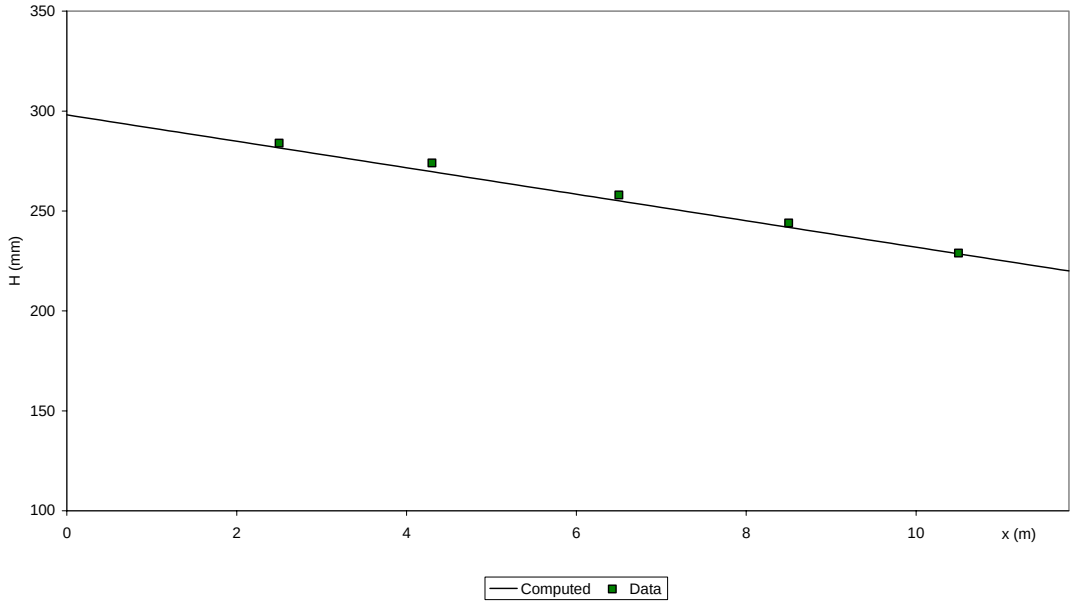
350
300
250
200
150
100
H (mm)
0
2
4
6
8
10
x (m)
Computed
Data

RUN 2

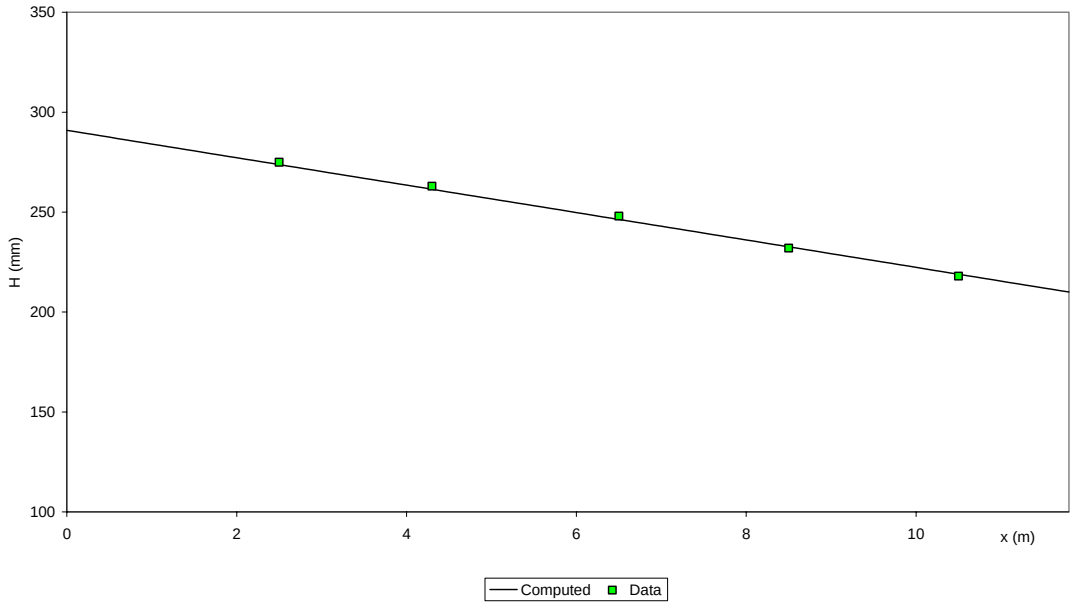
350
300
250
200
150
100
H (mm)
0
2
4
6
8
10
x (m)
Computed
Data

RUN 3

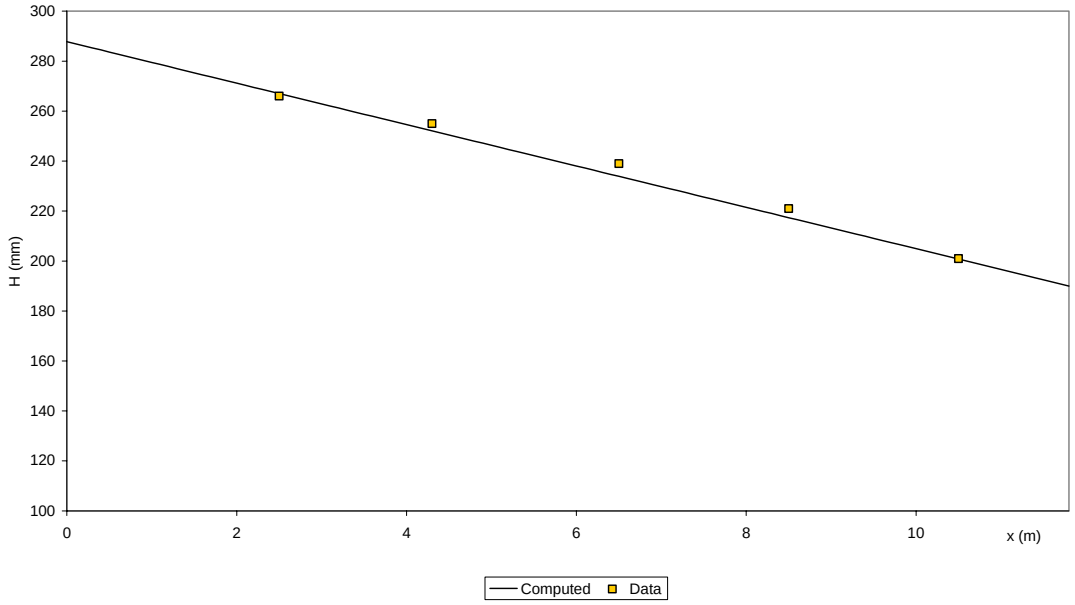
300
280
260
240
220
200
180
160
140
120
100
H (mm)
0
2
4
6
8
10
x (m)
Computed
Data

RUN 4

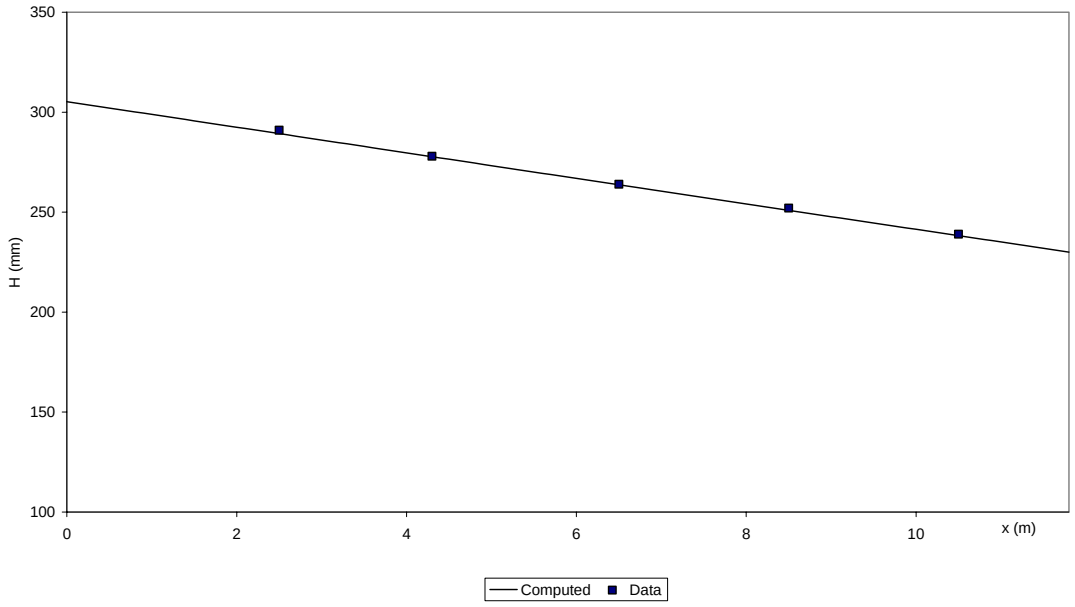
350
300
250
200
150
100
H (mm)
0
2
4
6
8
10
x (m)
Computed
Data

RUN 5

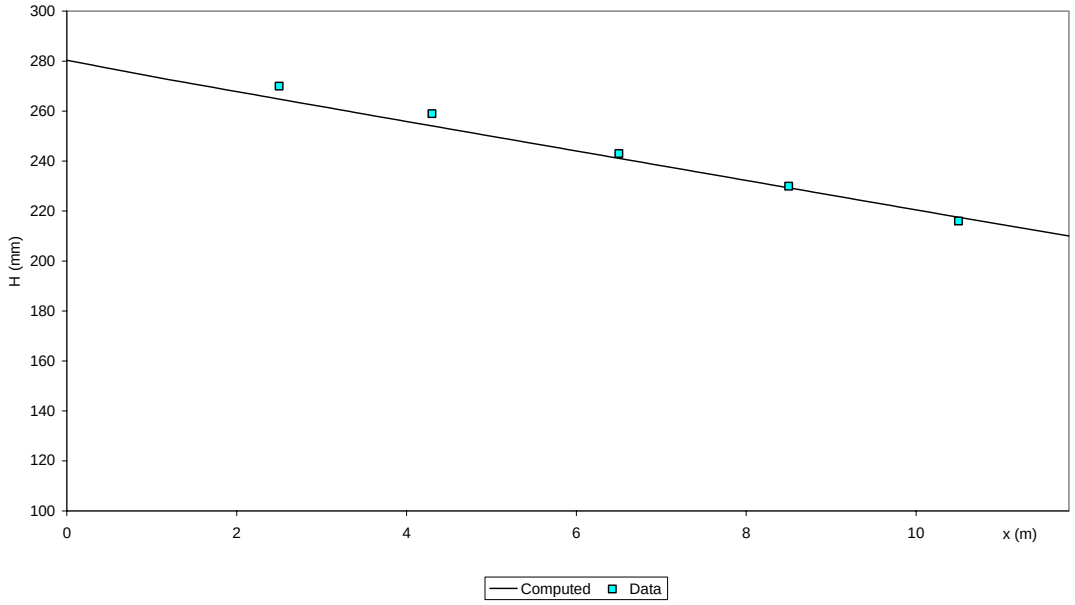
300
280
260
240
220
200
180
160
140
120
100
H (mm)
0
2
4
6
8
10
x (m)
Computed
Data

RUN 6

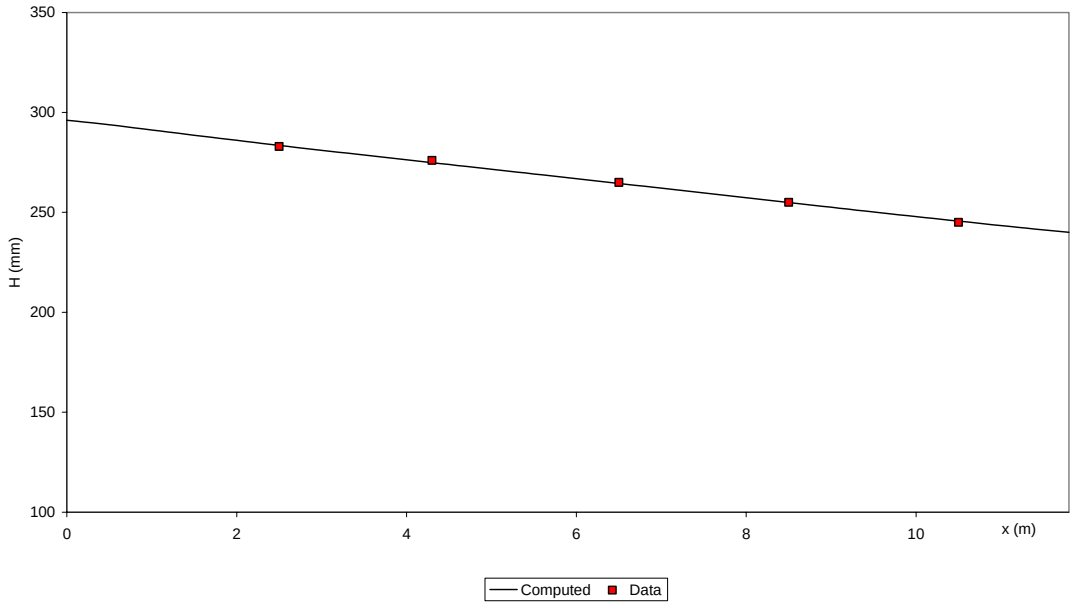
350
300
250
200
150
100
H (mm)
0
2
4
6
8
10
x (m)
Computed
Data

RUN 7

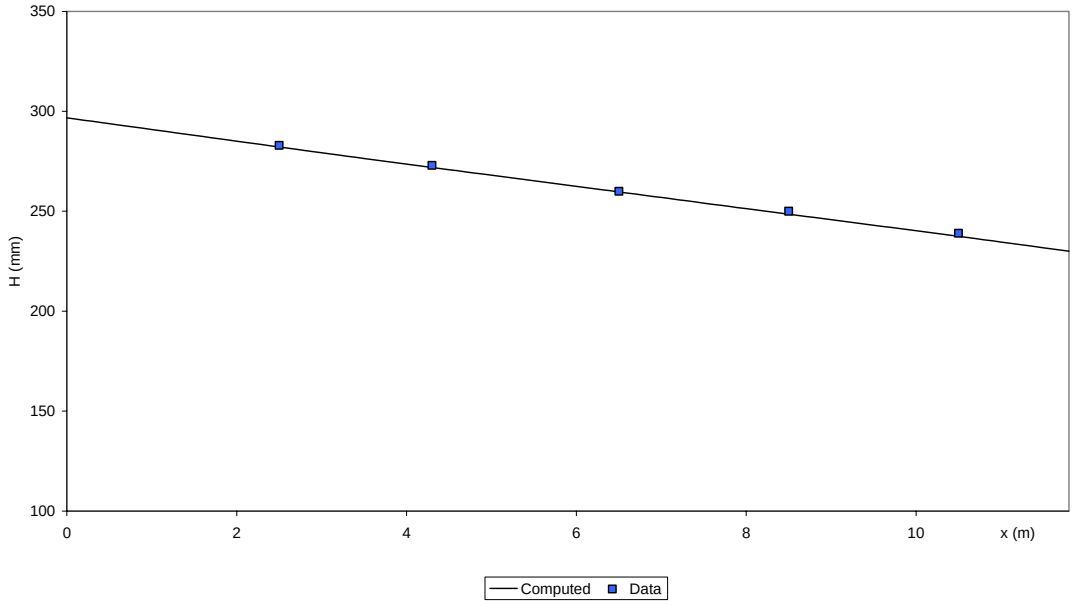
350
300
250
200
150
100
H (mm)
0
2
4
6
8
10
x (m)
Computed
Data

RUN 8

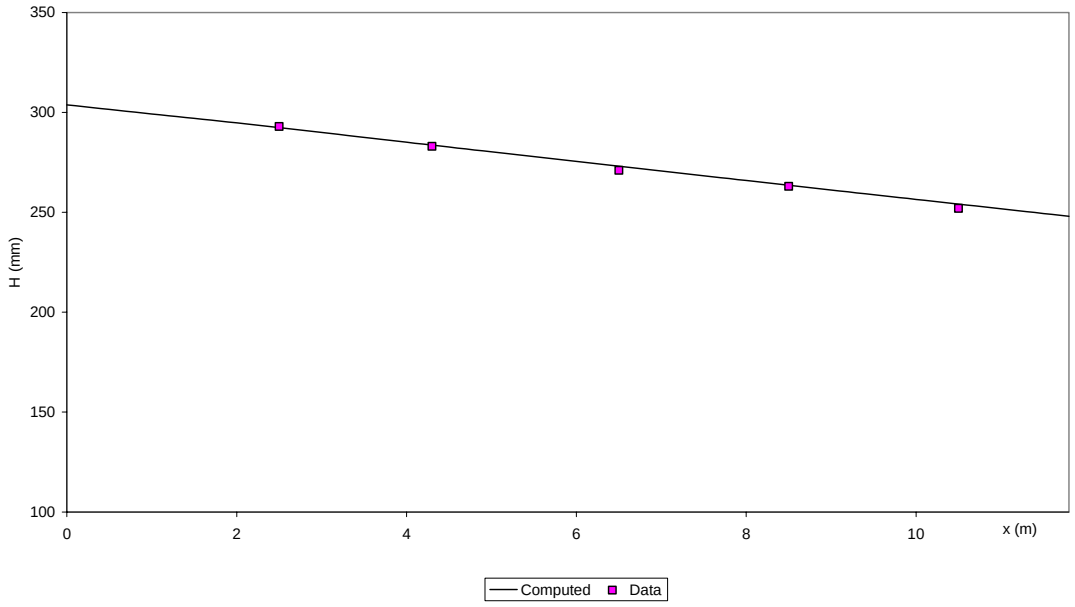
350
300
250
200
150
100
H (mm)
0
2
4
6
8
10
x (m)
Computed
Data

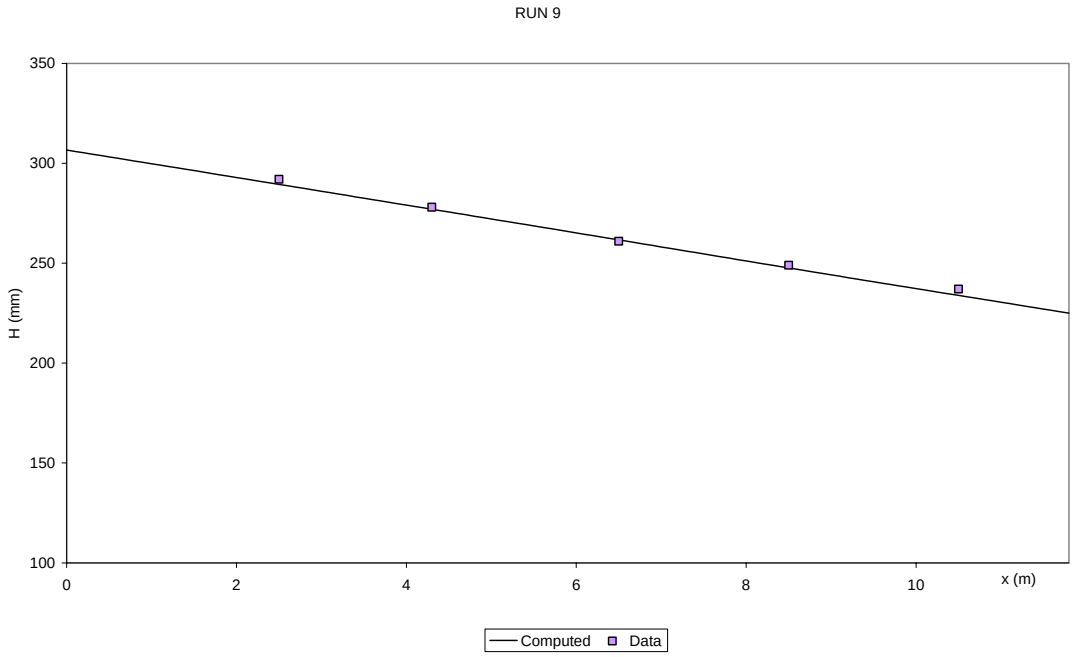
RUN 9
350
300
250
200
150
100
H (mm)
0
2
4
6
8
10
x (m)
Computed
Data

Bedload

RUN	G_s predicted (g/min)	G_s measured (g/min)
1	838	731
2	558	491
3	542	458
4	968	1432
5	68	54
6	103	64
7	240	371
8	147	151
9	841	1068

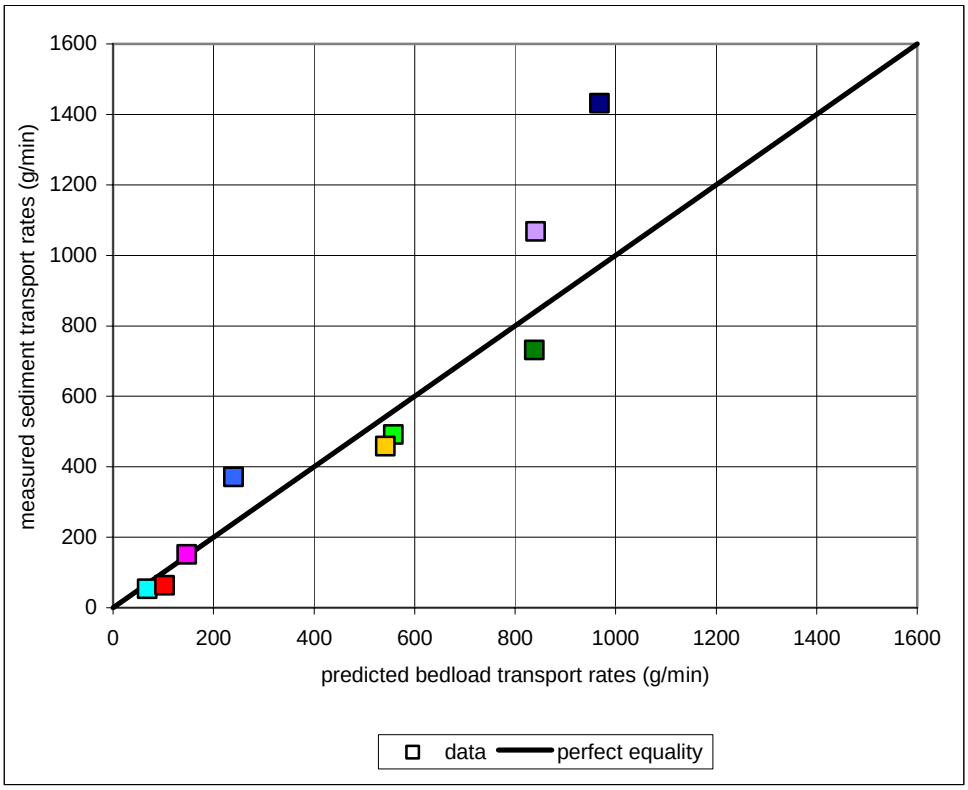

RUN 1

Computed		Data	
Di (mm)	**pi %**	**Di (mm)**	**pi %**
0.071	0.000	0.071	0.029
0.707	0.195	0.707	0.058
1.086	6.038	1.086	0.168
1.536	19.079	1.536	23.307
2.828	37.668	2.828	36.390
5.040	22.103	5.020	23.360
7.735	14.871	7.736	16.690
11.208	0.046	10.897	0.000

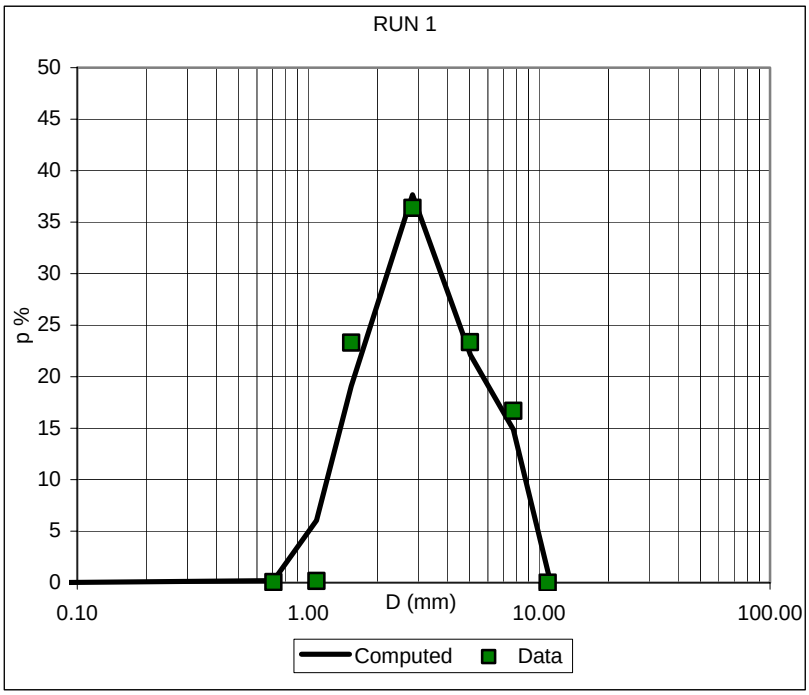

RUN 2

Computed		Data	
Di (mm)	**pi %**	**Di (mm)**	**pi %**
0.071	0.000	0.071	0.017
0.707	0.202	0.707	0.038
1.086	6.313	1.086	0.083
1.536	19.897	1.536	13.860
2.828	39.081	2.828	37.668
5.040	21.705	5.020	25.600
7.735	12.770	7.736	22.735
11.208	0.031	10.897	0.000

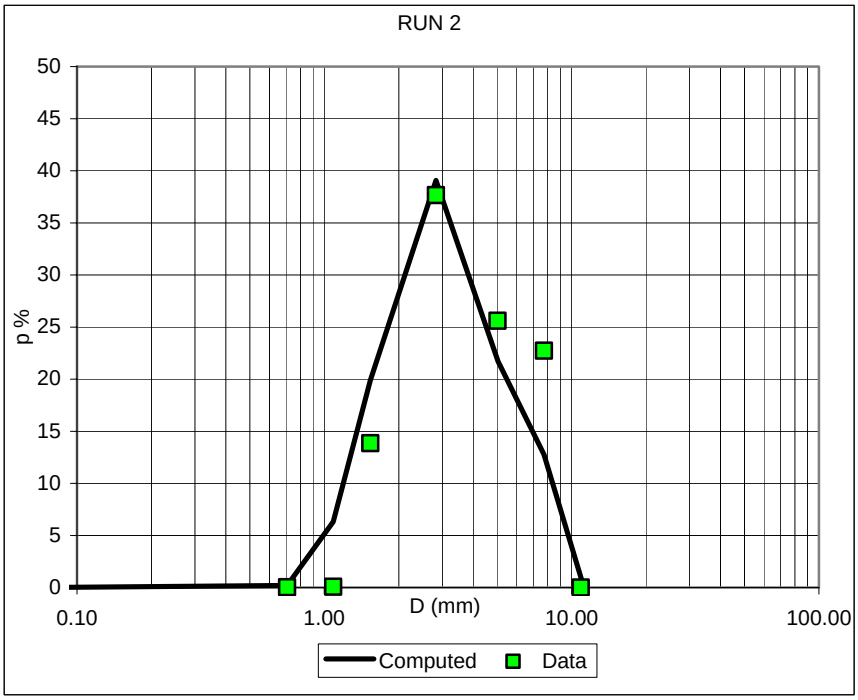

RUN 3

Computed		Data	
Di (mm)	**pi %**	**Di (mm)**	**pi %**
0.071	0.000	0.071	0.061
0.707	0.180	0.707	0.051
1.086	6.229	1.086	0.085
1.536	19.691	1.536	20.363
2.828	38.795	2.828	33.343
5.040	21.817	5.020	27.470
7.735	13.255	7.736	18.627
11.208	0.032	10.897	0.000

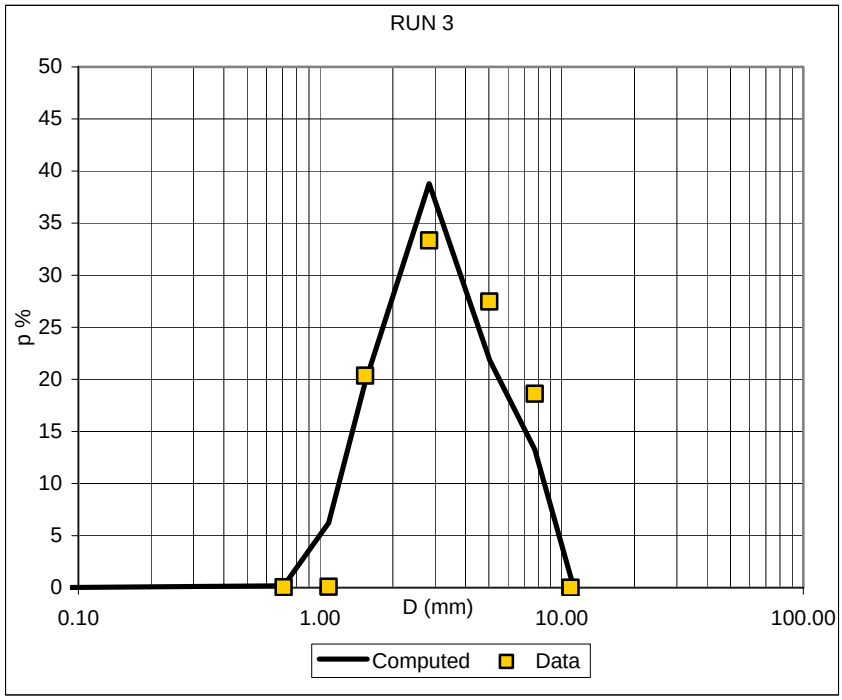

RUN 4

Computed		Data	
Di (mm)	pi %	Di (mm)	pi %
0.071	0.000	0.071	0.042
0.707	0.162	0.707	0.034
1.086	5.485	1.086	0.059
1.536	17.487	1.536	12.787
2.828	34.966	2.828	41.284
5.040	23.199	5.020	25.693
7.735	18.631	7.736	20.102
11.208	0.069	10.897	0.000

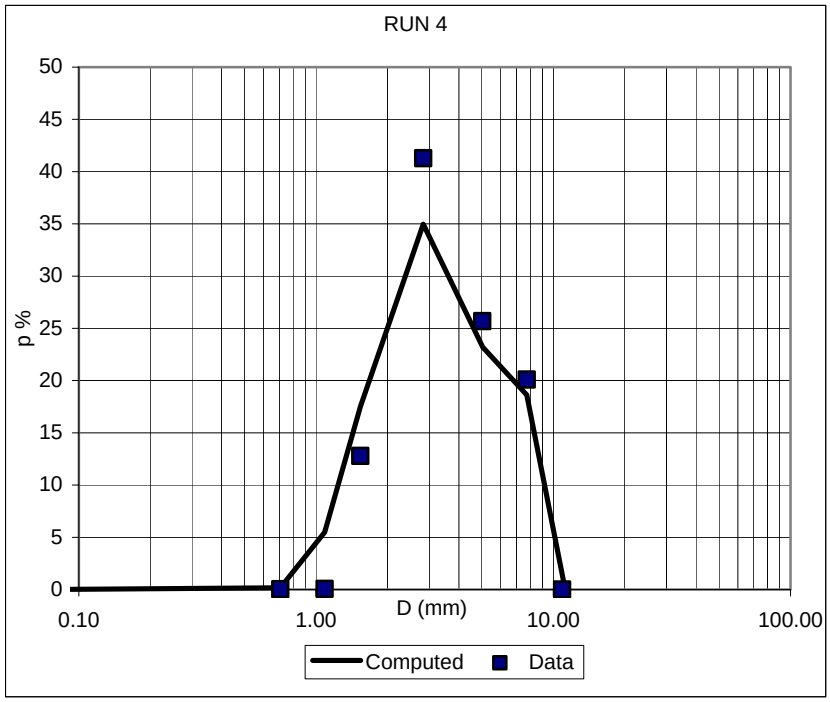

RUN 5

Computed		Data	
Di (mm)	pi %	Di (mm)	pi %
0.071	0.000	0.071	0.018
0.707	0.249	0.707	0.154
1.086	8.050	1.086	0.526
1.536	24.908	1.536	32.110
2.828	47.167	2.828	39.674
5.040	19.429	5.020	15.250
7.735	0.197	7.736	12.267
11.208	0.000	10.897	0.000

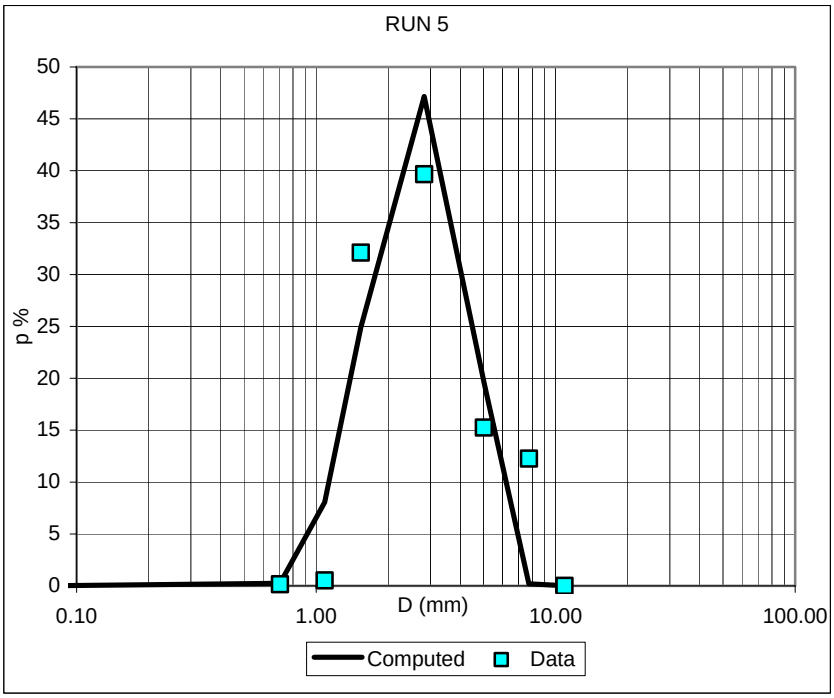

RUN 6

Computed		Data	
Di (mm)	pi %	Di (mm)	pi %
0.071	0.000	0.071	0.019
0.707	0.286	0.707	0.079
1.086	7.117	1.086	0.098
1.536	22.161	1.536	21.883
2.828	42.819	2.828	38.525
5.040	23.979	5.020	19.991
7.735	3.637	7.736	19.406
11.208	0.000	10.897	0.000

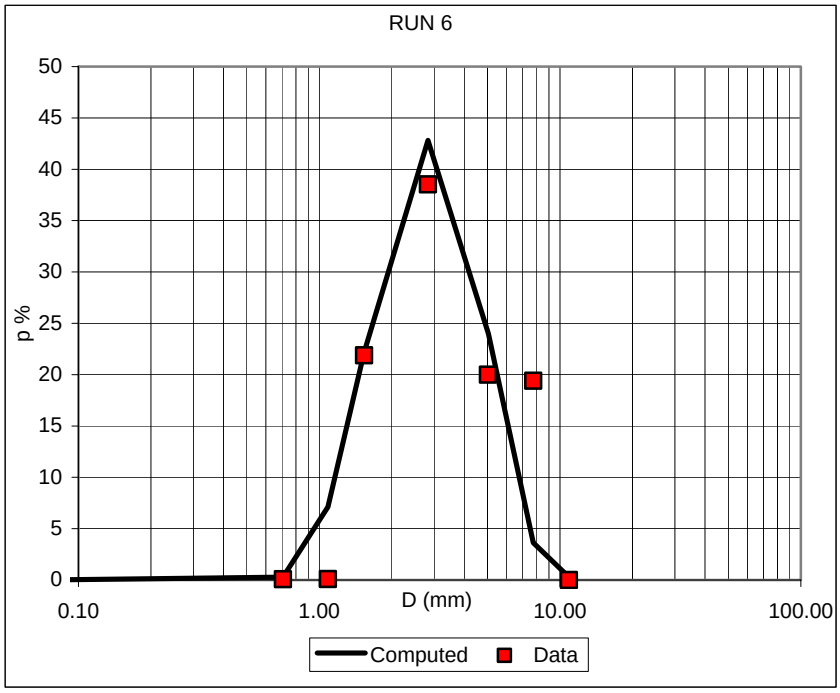

RUN 7

Computed		Data	
Di (mm)	**pi %**	**Di (mm)**	**pi %**
0.071	0.000	0.071	0.017
0.707	0.197	0.707	0.011
1.086	5.621	1.086	0.060
1.536	17.869	1.536	9.324
2.828	35.711	2.828	40.876
5.040	26.197	5.020	28.478
7.735	14.397	7.736	21.234
11.208	0.009	10.897	0.000

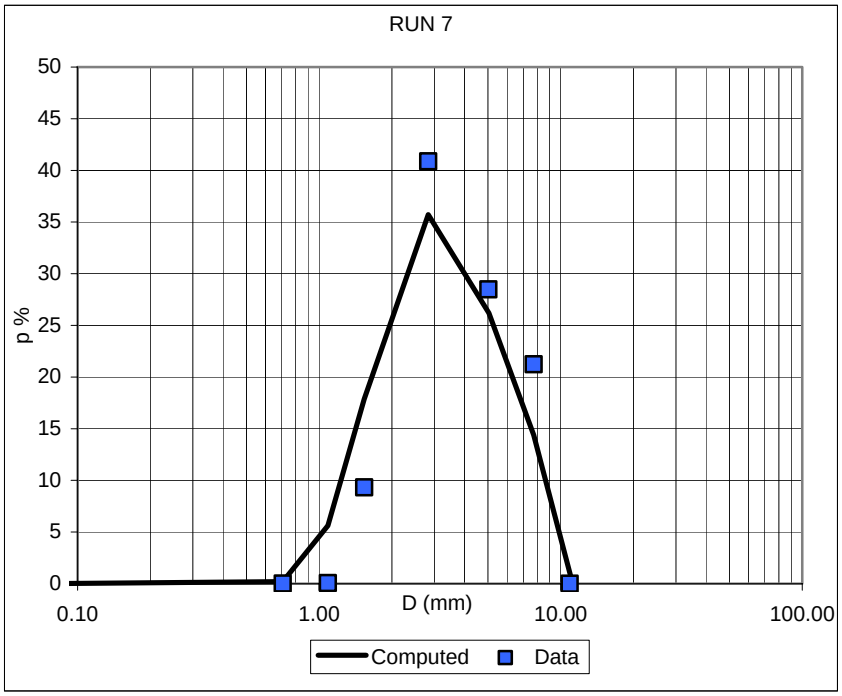

RUN 8

Computed		Data	
Di (mm)	**pi %**	**Di (mm)**	**pi %**
0.071	0.000	0.071	0.030
0.707	0.238	0.707	0.072
1.086	5.905	1.086	0.299
1.536	18.617	1.536	34.776
2.828	36.878	2.828	31.132
5.040	27.457	5.020	15.545
7.735	10.905	7.736	18.146
11.208	0.000	10.897	0.000

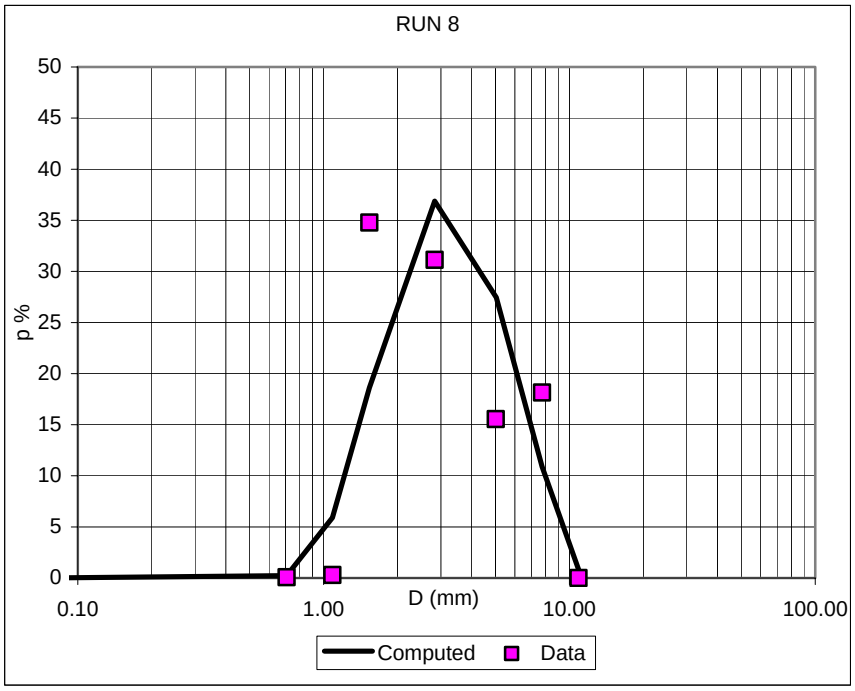

RUN 9

Computed		Data	
Di (mm)	pi %	Di (mm)	pi %
0.071	0.000	0.071	0.050
0.707	0.148	0.707	0.056
1.086	4.304	1.086	0.179
1.536	13.924	1.536	16.889
2.828	28.757	2.828	36.319
5.040	24.489	5.020	23.731
7.735	28.272	7.736	22.776
11.208	0.106	10.897	0.000

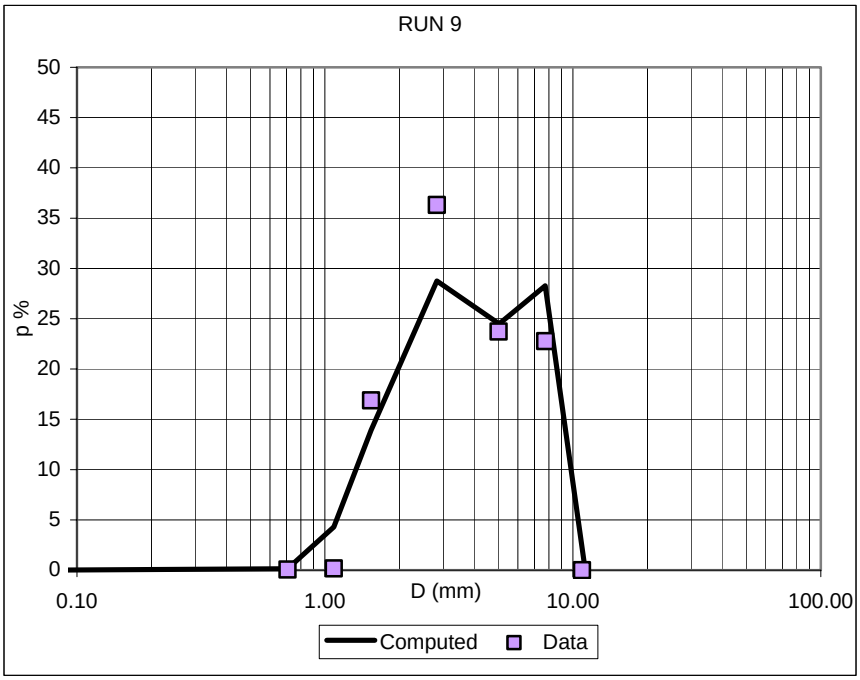

Bed surface

RUN 1

Section 1, x = 2.5 m

Computed		Data	
Di (mm)	Fi %	Di (mm)	Fi %
0.071	0.000	0.071	0.000
0.707	0.146	0.707	0.010
1.086	4.582	1.086	0.103
1.536	14.727	1.536	10.864
2.828	29.991	2.828	33.169
5.040	23.704	5.020	26.721
7.735	26.667	7.736	29.134
11.208	0.182	10.897	0.000

Section 2, x = 4.3 m

Computed		Data	
Di (mm)	Fi %	Di (mm)	Fi %
0.071	0.000	0.071	0.002
0.707	0.145	0.707	0.024
1.086	4.584	1.086	0.126
1.536	14.733	1.536	5.756
2.828	30.009	2.828	31.410
5.040	23.676	5.020	31.706
7.735	26.657	7.736	30.974
11.208	0.196	10.897	0.000

Section 3, x = 6.5 m

Computed		Data	
Di (mm)	Fi %	Di (mm)	Fi %
0.071	0.000	0.071	0.000
0.707	0.144	0.707	0.010
1.086	4.580	1.086	0.052
1.536	14.721	1.536	11.333
2.828	29.982	2.828	34.214
5.040	23.532	5.020	25.639
7.735	26.856	7.736	28.752
11.208	0.184	10.897	0.000

Section 4, x = 8.5 m

Computed		Data	
Di (mm)	Fi %	Di (mm)	Fi %
0.071	0.000	0.071	0.000
0.707	0.144	0.707	0.010
1.086	4.573	1.086	0.068
1.536	14.702	1.536	14.125
2.828	29.936	2.828	33.544
5.040	23.399	5.020	25.347
7.735	27.092	7.736	26.906
11.208	0.155	10.897	0.000

Section 5, x = 10.5 m

Computed		Data	
Di (mm)	Fi %	Di (mm)	Fi %
0.071	0.000	0.071	0.119
0.707	0.144	0.707	0.017
1.086	4.574	1.086	0.071
1.536	14.708	1.536	14.947
2.828	29.939	2.828	29.207
5.040	23.555	5.020	23.629
7.735	26.943	7.736	32.010
11.208	0.136	10.897	0.000

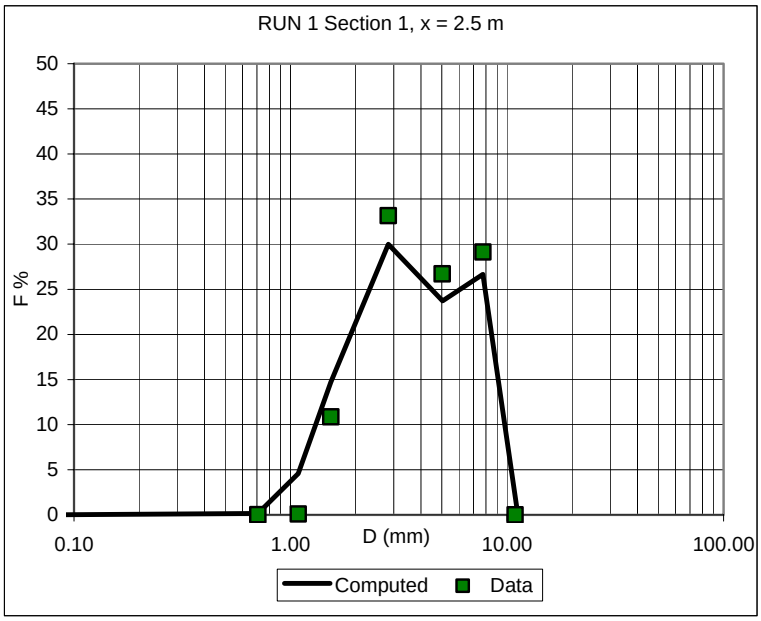
RUN 1 Section 1, x = 2.5 m
F %
D (mm)
0.10
1.00
10.00
100.00
Computed
Data

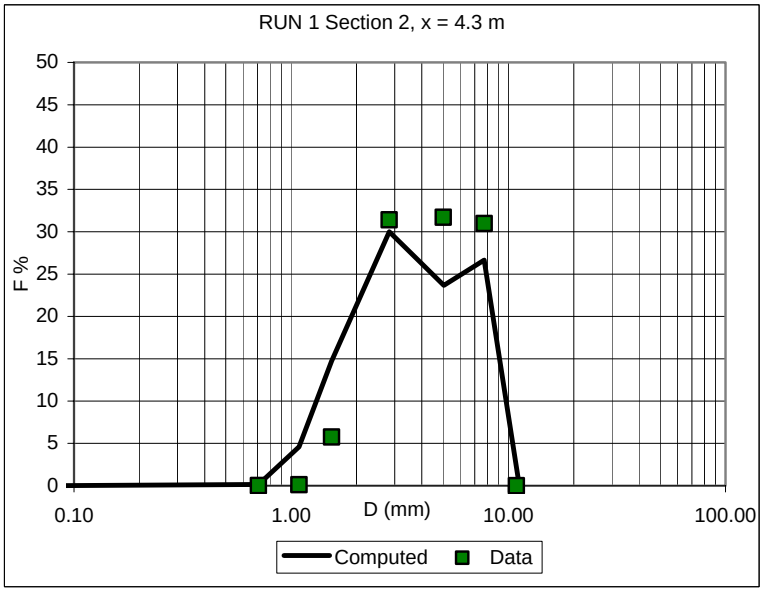
RUN 1 Section 2, x = 4.3 m
F %
D (mm)
0.10
1.00
10.00
100.00
Computed
Data

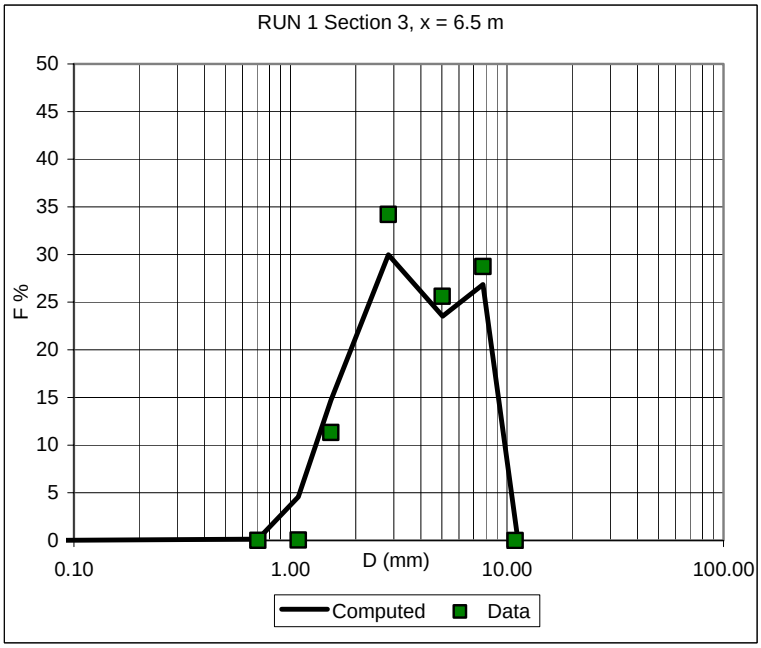
RUN 1 Section 3, x = 6.5 m
F %
D (mm)
0.10
1.00
10.00
100.00
Computed
Data

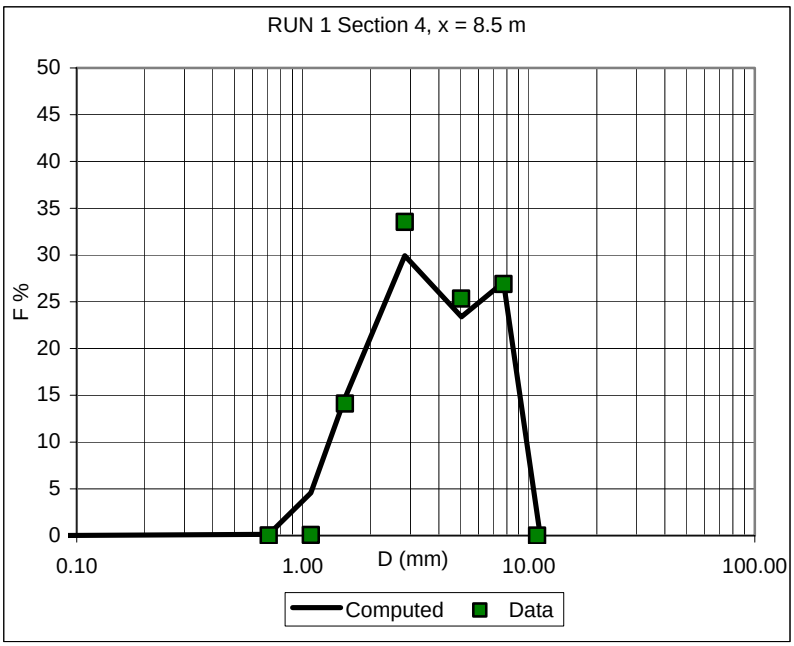
RUN 1 Section 4, x = 8.5 m
50
45
40
35
30
25
20
15
10
5
0
F %
0.10
1.00
D (mm)
10.00
100.00
Computed
Data

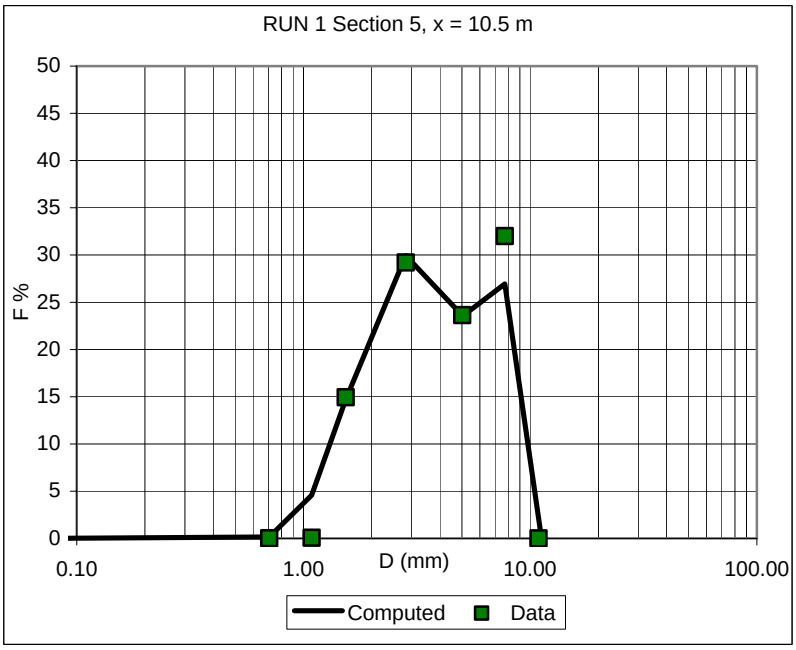
RUN 1 Section 5, x = 10.5 m
50
45
40
35
30
25
20
15
10
5
0
F %
0.10
1.00
D (mm)
10.00
100.00
Computed
Data

RUN 2

Section 1, x = 2.5 m

Computed		Data	
Di (mm)	**Fi %**	**Di (mm)**	**Fi %**
0.071	0.000	0.071	0.008
0.707	0.142	0.707	0.041
1.086	4.542	1.086	0.112
1.536	14.610	1.536	17.182
2.828	29.775	2.828	38.974
5.040	23.488	5.020	23.537
7.735	27.253	7.736	20.147
11.208	0.192	10.897	0.000

Section 2, x = 4.3 m

Computed		Data	
Di (mm)	**Fi %**	**Di (mm)**	**Fi %**
0.071	0.000	0.071	0.005
0.707	0.141	0.707	0.110
1.086	4.545	1.086	0.293
1.536	14.620	1.536	19.606
2.828	29.815	2.828	31.234
5.040	23.509	5.020	20.668
7.735	27.198	7.736	28.084
11.208	0.172	10.897	0.000

Section 3, x = 6.5 m

Computed		Data	
Di (mm)	**Fi %**	**Di (mm)**	**Fi %**
0.071	0.000	0.071	0.009
0.707	0.141	0.707	0.059
1.086	4.547	1.086	0.297
1.536	14.632	1.536	19.556
2.828	29.847	2.828	28.426
5.040	23.595	5.020	23.594
7.735	27.087	7.736	27.845
11.208	0.151	10.897	0.214

Section 4, x = 8.5 m

Computed		Data	
Di (mm)	**Fi %**	**Di (mm)**	**Fi %**
0.071	0.000	0.071	0.003
0.707	0.141	0.707	0.031
1.086	4.546	1.086	0.135
1.536	14.630	1.536	13.928
2.828	29.830	2.828	31.640
5.040	23.648	5.020	23.145
7.735	27.057	7.736	31.117
11.208	0.148	10.897	0.000

Section 5, x = 10.5 m

Computed		Data	
Di (mm)	**Fi %**	**Di (mm)**	**Fi %**
0.071	0.000	0.071	0.007
0.707	0.142	0.707	0.045
1.086	4.542	1.086	0.239
1.536	14.614	1.536	15.355
2.828	29.772	2.828	28.934
5.040	23.642	5.020	22.976
7.735	27.118	7.736	32.443
11.208	0.170	10.897	0.000

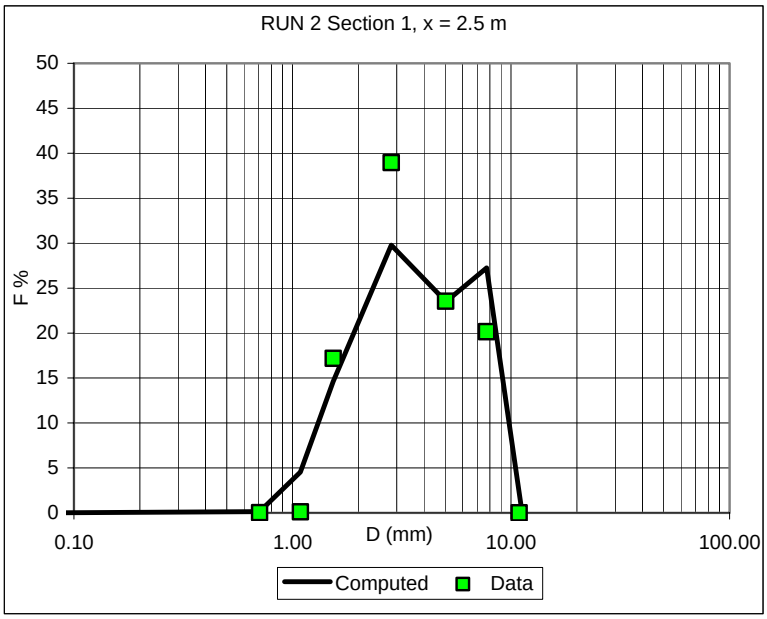
RUN 2 Section 1, x = 2.5 m
F %
D (mm)
0.10
1.00
10.00
100.00
Computed
Data

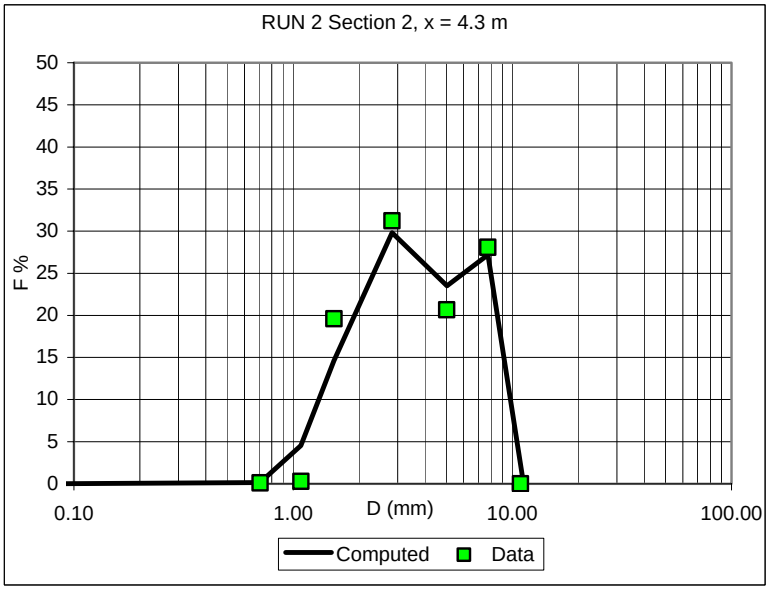
RUN 2 Section 2, x = 4.3 m
F %
D (mm)
0.10
1.00
10.00
100.00
Computed
Data

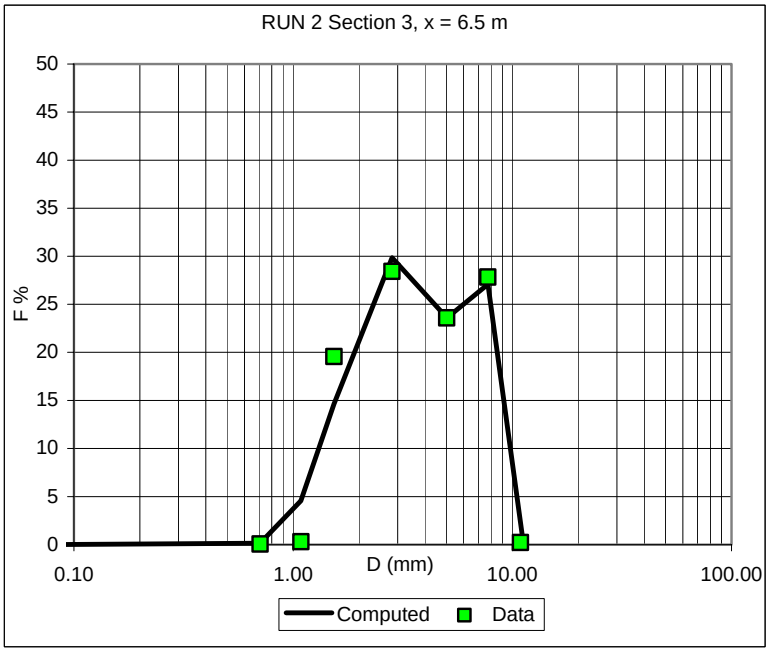
RUN 2 Section 3, x = 6.5 m
F %
D (mm)
0.10
1.00
10.00
100.00
Computed
Data

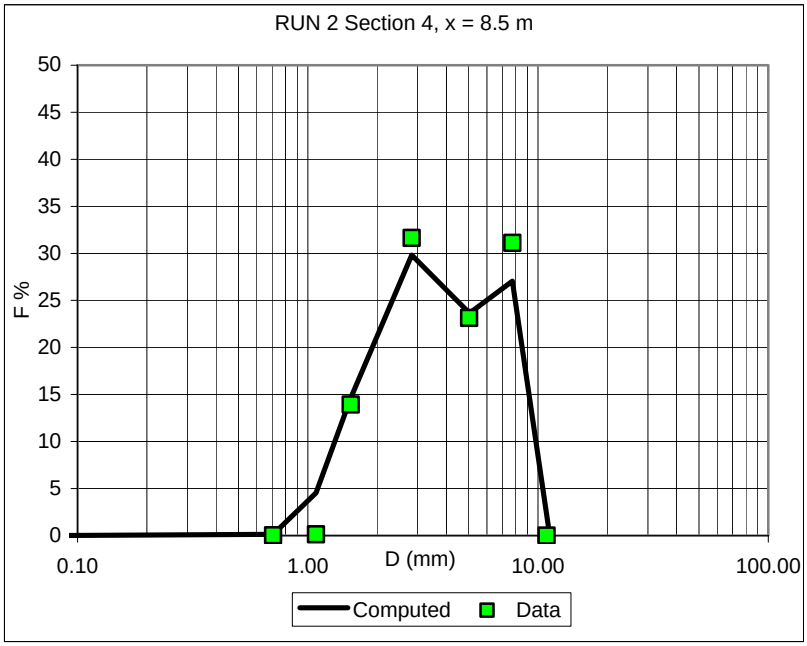
RUN 2 Section 4, x = 8.5 m
50
45
40
35
30
25
20
15
10
5
0
F %
0.10
1.00
10.00
100.00
D (mm)
Computed
Data

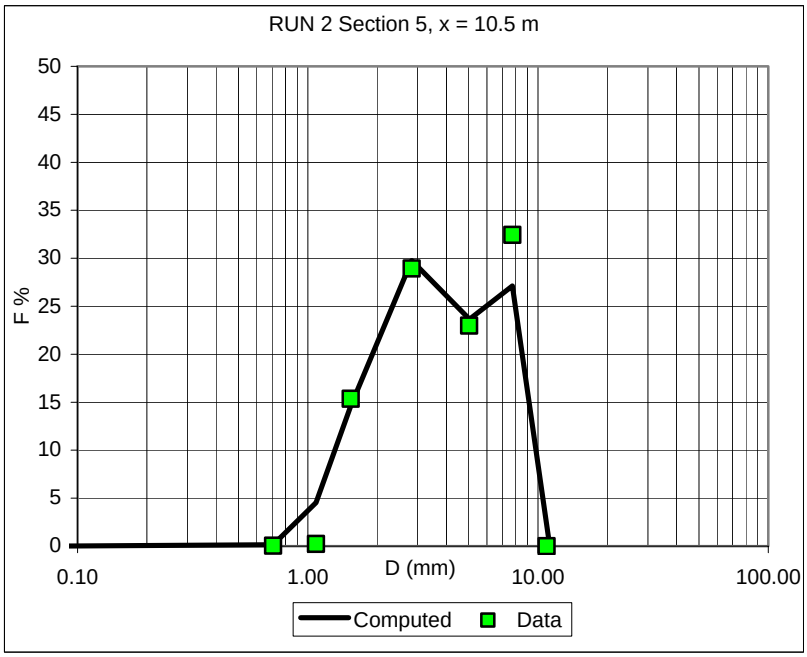
RUN 2 Section 5, x = 10.5 m
50
45
40
35
30
25
20
15
10
5
0
F %
0.10
1.00
10.00
100.00
D (mm)
Computed
Data

RUN 3

Section 1, x = 2.5 m

Computed		Data	
Di (mm)	**Fi %**	**Di (mm)**	**Fi %**
0.071	0.000	0.071	0.002
0.707	0.126	0.707	0.002
1.086	4.426	1.086	0.007
1.536	14.298	1.536	4.230
2.828	29.202	2.828	27.594
5.040	23.566	5.020	33.223
7.735	28.201	7.736	34.943
11.208	0.180	10.897	0.000

Section 2, x = 4.3 m

Computed		Data	
Di (mm)	**Fi %**	**Di (mm)**	**Fi %**
0.071	0.000	0.071	0.008
0.707	0.127	0.707	0.020
1.086	4.440	1.086	0.120
1.536	14.336	1.536	15.901
2.828	29.262	2.828	33.106
5.040	23.405	5.020	22.683
7.735	28.260	7.736	28.162
11.208	0.170	10.897	0.000

Section 3, x = 6.5 m

Computed		Data	
Di (mm)	**Fi %**	**Di (mm)**	**Fi %**
0.071	0.000	0.071	0.003
0.707	0.127	0.707	0.021
1.086	4.453	1.086	0.198
1.536	14.367	1.536	13.284
2.828	29.361	2.828	26.686
5.040	23.278	5.020	26.825
7.735	28.239	7.736	32.983
11.208	0.174	10.897	0.000

Section 4, x = 8.5 m

Computed		Data	
Di (mm)	**Fi %**	**Di (mm)**	**Fi %**
0.071	0.000	0.071	0.003
0.707	0.125	0.707	0.009
1.086	4.466	1.086	0.108
1.536	14.403	1.536	13.564
2.828	29.498	2.828	25.187
5.040	23.328	5.020	24.989
7.735	27.999	7.736	36.141
11.208	0.181	10.897	0.000

Section 5, x = 10.5 m

Computed		Data	
Di (mm)	**Fi %**	**Di (mm)**	**Fi %**
0.071	0.000	0.071	0.003
0.707	0.124	0.707	0.000
1.086	4.463	1.086	0.023
1.536	14.401	1.536	9.223
2.828	29.523	2.828	34.495
5.040	23.340	5.020	25.622
7.735	27.962	7.736	30.634
11.208	0.188	10.897	0.000

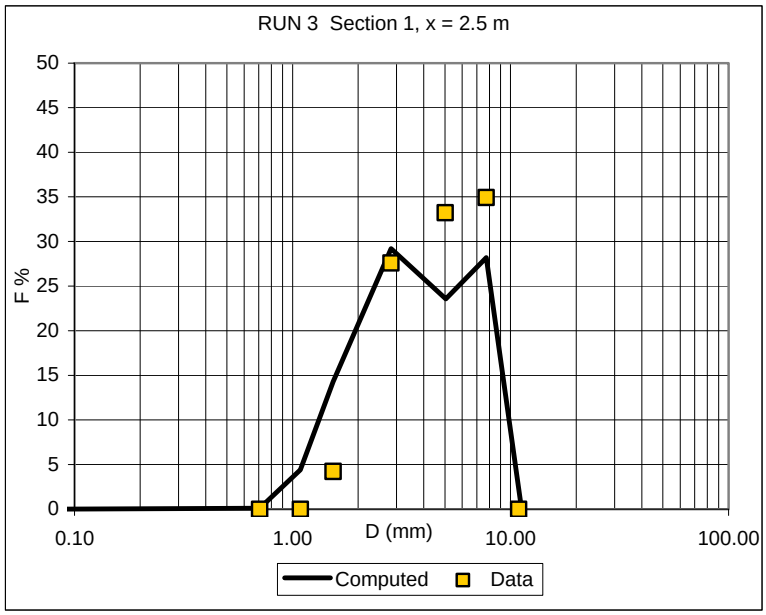
RUN 3 Section 1, x = 2.5 m
F %
D (mm)
0.10
1.00
10.00
100.00
Computed
Data

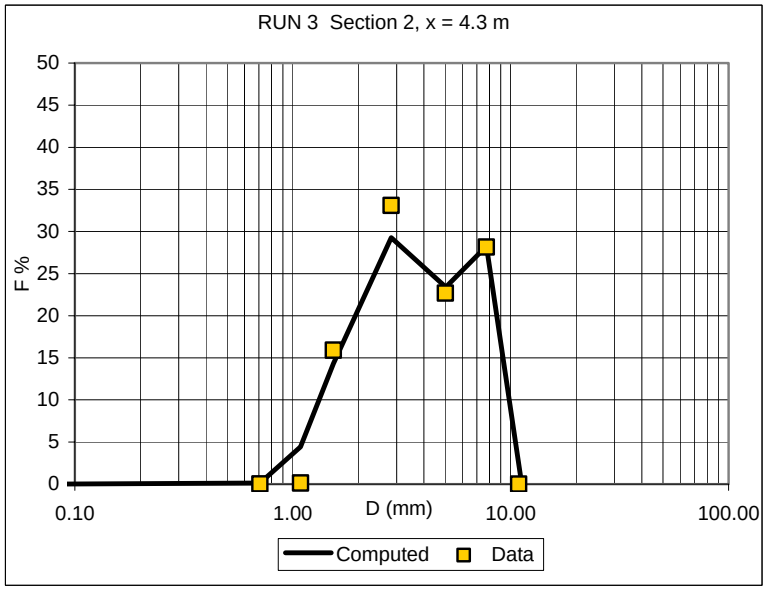
RUN 3 Section 2, x = 4.3 m
F %
D (mm)
0.10
1.00
10.00
100.00
Computed
Data

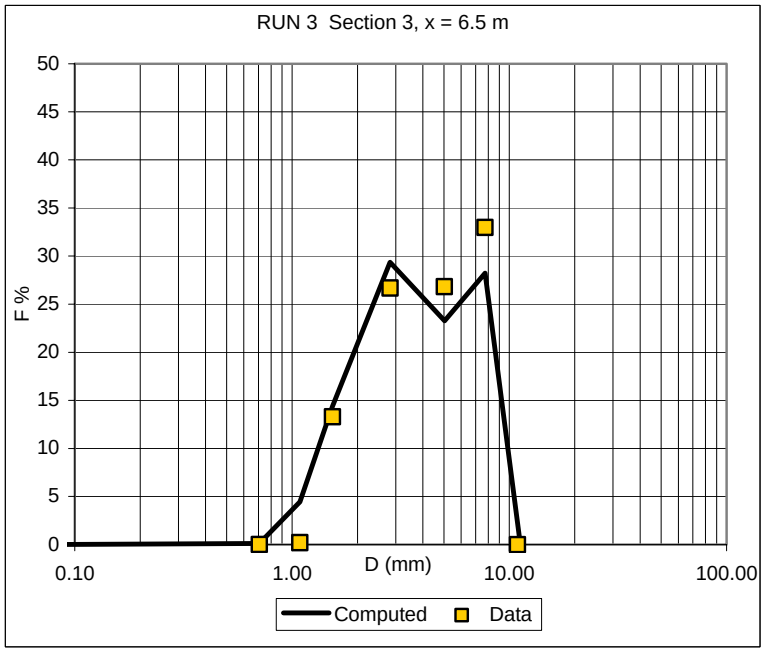
RUN 3 Section 3, x = 6.5 m
F %
D (mm)
0.10
1.00
10.00
100.00
Computed
Data

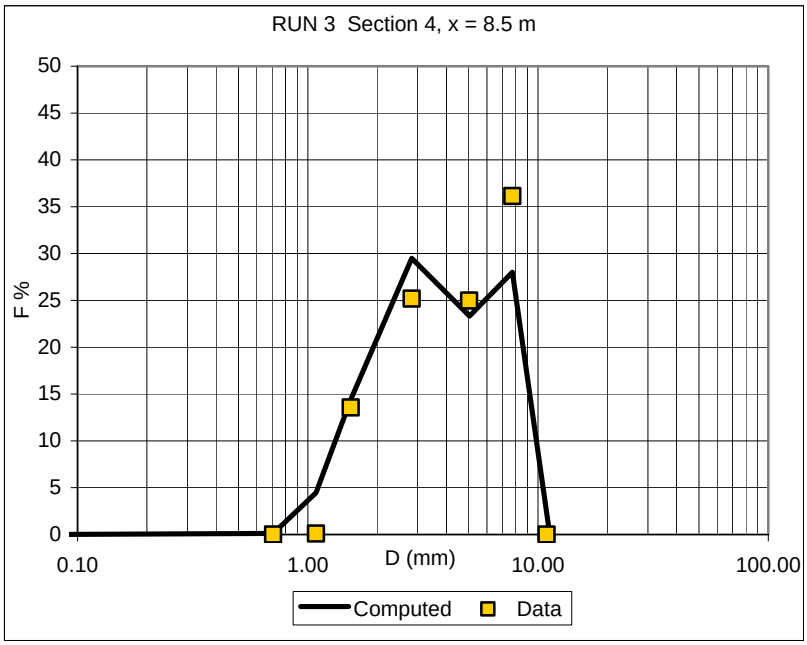
RUN 3 Section 4, x = 8.5 m
50
45
40
35
30
25
20
15
10
5
0
F %
0.10
1.00
10.00
100.00
D (mm)
Computed
Data

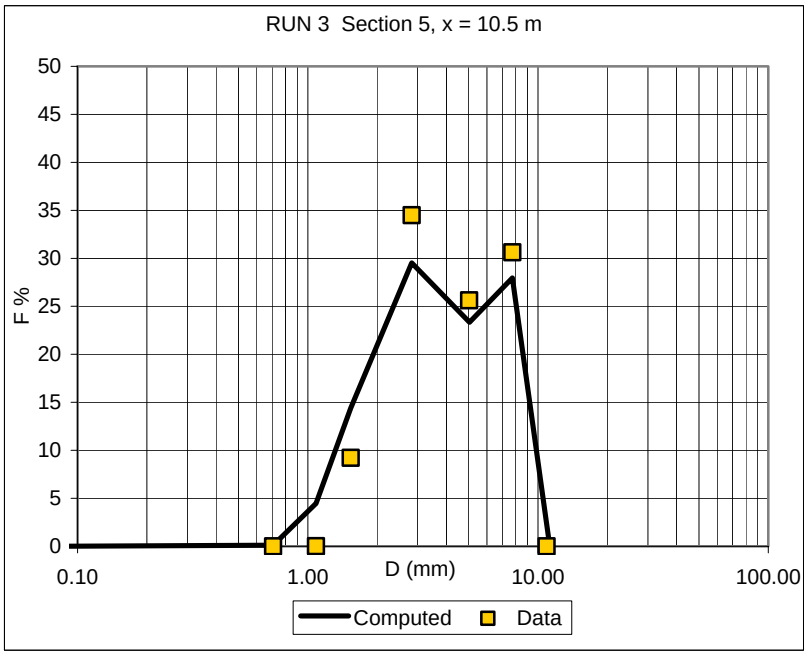
RUN 3 Section 5, x = 10.5 m
50
45
40
35
30
25
20
15
10
5
0
F %
0.10
1.00
10.00
100.00
D (mm)
Computed
Data

RUN 4

Section 1, x = 2.5 m

Computed		Data	
Di (mm)	**Fi %**	**Di (mm)**	**Fi %**
0.071	0.000	0.071	0.031
0.707	0.121	0.707	0.026
1.086	4.197	1.086	0.061
1.536	13.575	1.536	6.614
2.828	27.813	2.828	26.794
5.040	24.070	5.020	28.009
7.735	29.984	7.736	38.466
11.208	0.240	10.897	0.000

Section 2, x = 4.3 m

Computed		Data	
Di (mm)	**Fi %**	**Di (mm)**	**Fi %**
0.071	0.000	0.071	0.000
0.707	0.119	0.707	0.053
1.086	4.158	1.086	0.175
1.536	13.435	1.536	10.997
2.828	27.620	2.828	27.984
5.040	24.056	5.020	22.984
7.735	30.381	7.736	37.807
11.208	0.230	10.897	0.000

Section 3, x = 6.5 m

Computed		Data	
Di (mm)	**Fi %**	**Di (mm)**	**Fi %**
0.071	0.000	0.071	0.000
0.707	0.120	0.707	0.302
1.086	4.141	1.086	0.721
1.536	13.416	1.536	18.333
2.828	27.764	2.828	25.882
5.040	23.337	5.020	18.803
7.735	31.020	7.736	35.959
11.208	0.203	10.897	0.000

Section 4, x = 8.5 m

Computed		Data	
Di (mm)	**Fi %**	**Di (mm)**	**Fi %**
0.071	0.000	0.071	0.003
0.707	0.121	0.707	0.015
1.086	4.140	1.086	0.195
1.536	13.447	1.536	8.215
2.828	27.841	2.828	26.989
5.040	22.736	5.020	33.225
7.735	31.531	7.736	31.359
11.208	0.184	10.897	0.000

Section 5, x = 10.5 m

Computed		Data	
Di (mm)	**Fi %**	**Di (mm)**	**Fi %**
0.071	0.000	0.071	0.003
0.707	0.122	0.707	0.015
1.086	4.182	1.086	0.195
1.536	13.586	1.536	8.215
2.828	28.036	2.828	26.989
5.040	23.125	5.020	28.258
7.735	30.760	7.736	36.325
11.208	0.188	10.897	0.000

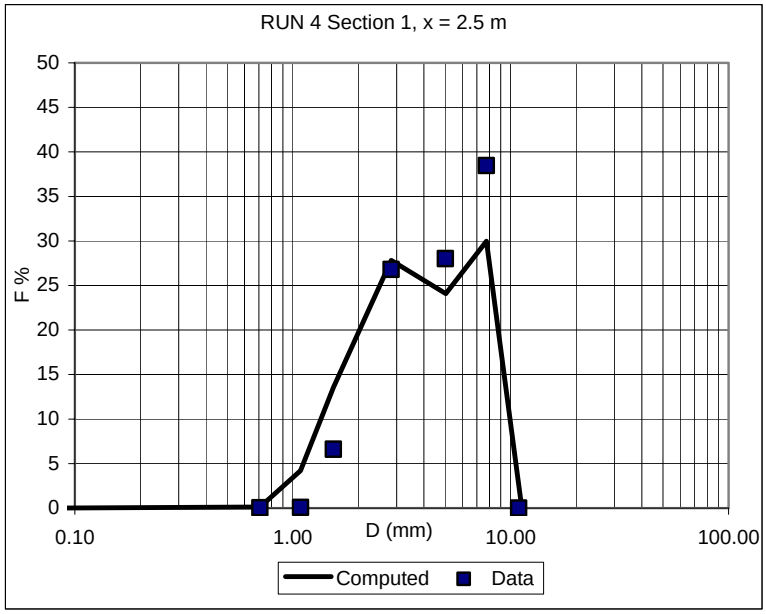
RUN 4 Section 1, x = 2.5 m
50
45
40
35
30
25
20
15
10
5
0
F %
0.10
1.00
10.00
100.00
D (mm)
Computed
Data

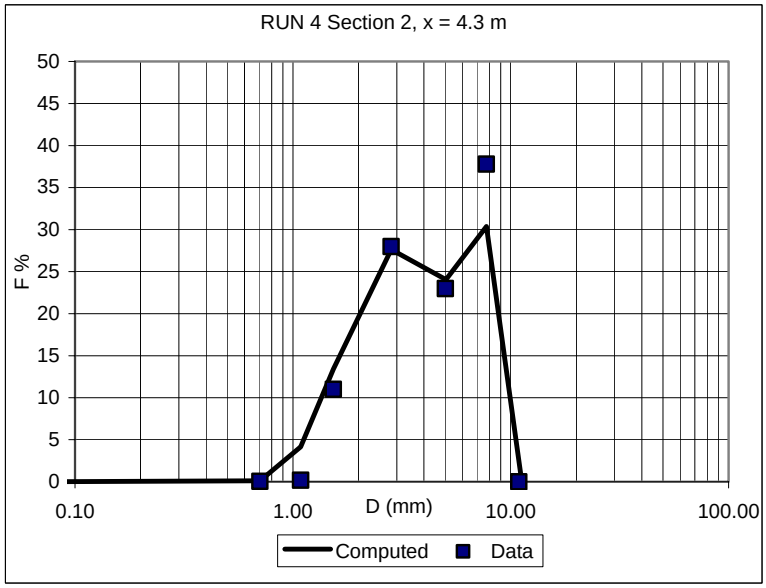
RUN 4 Section 2, x = 4.3 m
50
45
40
35
30
25
20
15
10
5
0
F %
0.10
1.00
10.00
100.00
D (mm)
Computed
Data

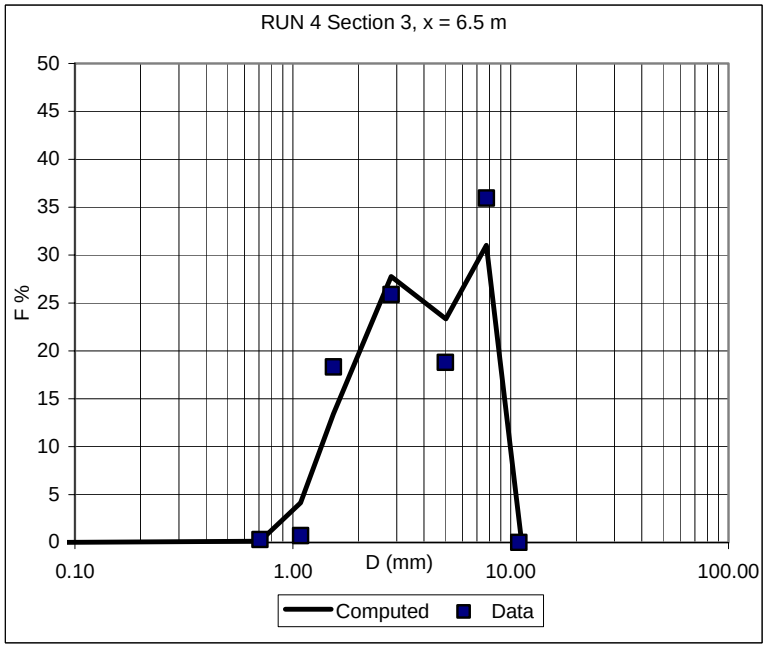
RUN 4 Section 3, x = 6.5 m
50
45
40
35
30
25
20
15
10
5
0
F %
0.10
1.00
10.00
100.00
D (mm)
Computed
Data

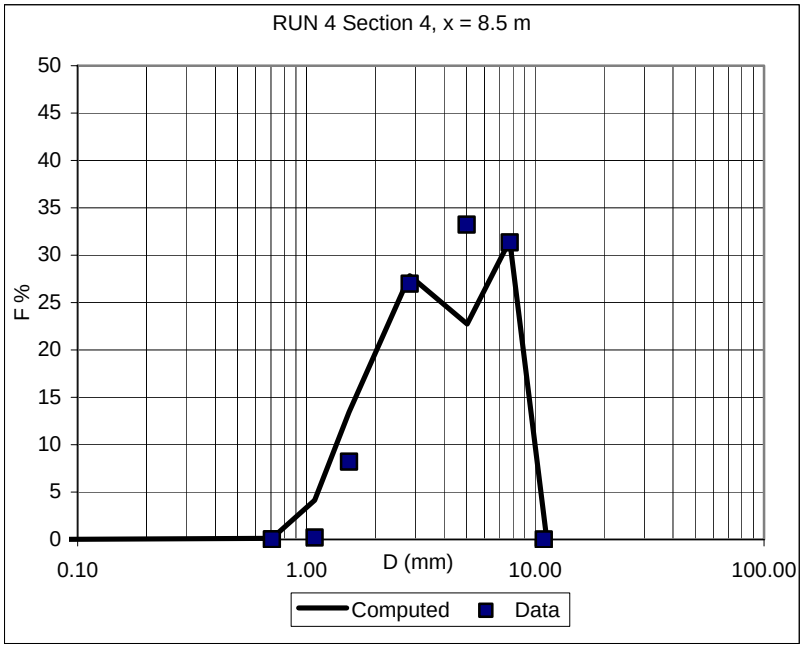
RUN 4 Section 4, x = 8.5 m
50
45
40
35
30
25
20
15
10
5
0
F %
0.10
1.00
10.00
100.00
D (mm)
Computed
Data

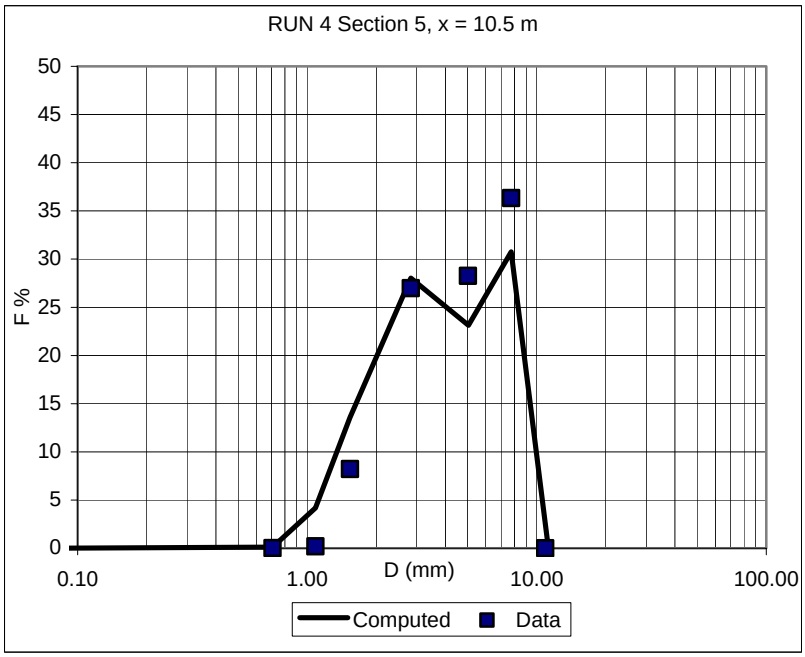
RUN 4 Section 5, x = 10.5 m
50
45
40
35
30
25
20
15
10
5
0
F %
0.10
1.00
10.00
100.00
D (mm)
Computed
Data

RUN 5

Section 1, x = 2.5 m

Computed		Data	
Di (mm)	**Fi %**	**Di (mm)**	**Fi %**
0.071	0.000	0.071	0.025
0.707	0.112	0.707	0.388
1.086	3.835	1.086	0.248
1.536	12.493	1.536	14.140
2.828	25.948	2.828	29.471
5.040	23.102	5.020	21.019
7.735	34.250	7.736	34.710
11.208	0.260	10.897	0.000

Section 2, x = 4.3 m

Computed		Data	
Di (mm)	**Fi %**	**Di (mm)**	**Fi %**
0.071	0.000	0.071	0.012
0.707	0.114	0.707	0.056
1.086	3.891	1.086	0.133
1.536	12.730	1.536	7.785
2.828	26.696	2.828	25.559
5.040	23.158	5.020	26.634
7.735	33.165	7.736	39.597
11.208	0.246	10.897	0.225

Section 3, x = 6.5 m

Computed		Data	
Di (mm)	**Fi %**	**Di (mm)**	**Fi %**
0.071	0.000	0.071	0.008
0.707	0.116	0.707	0.011
1.086	3.955	1.086	0.099
1.536	12.943	1.536	8.117
2.828	26.926	2.828	23.823
5.040	23.302	5.020	25.596
7.735	32.547	7.736	42.345
11.208	0.212	10.897	0.000

Section 4, x = 8.5 m

Computed		Data	
Di (mm)	**Fi %**	**Di (mm)**	**Fi %**
0.071	0.000	0.071	0.013
0.707	0.116	0.707	0.007
1.086	3.990	1.086	0.085
1.536	12.984	1.536	8.995
2.828	26.971	2.828	21.859
5.040	23.569	5.020	25.825
7.735	32.188	7.736	43.216
11.208	0.182	10.897	0.000

Section 5, x = 10.5 m

Computed		Data	
Di (mm)	**Fi %**	**Di (mm)**	**Fi %**
0.071	0.000	0.071	0.016
0.707	0.115	0.707	0.000
1.086	3.987	1.086	0.016
1.536	12.937	1.536	5.263
2.828	26.912	2.828	21.522
5.040	25.405	5.020	27.059
7.735	30.466	7.736	46.123
11.208	0.178	10.897	0.000

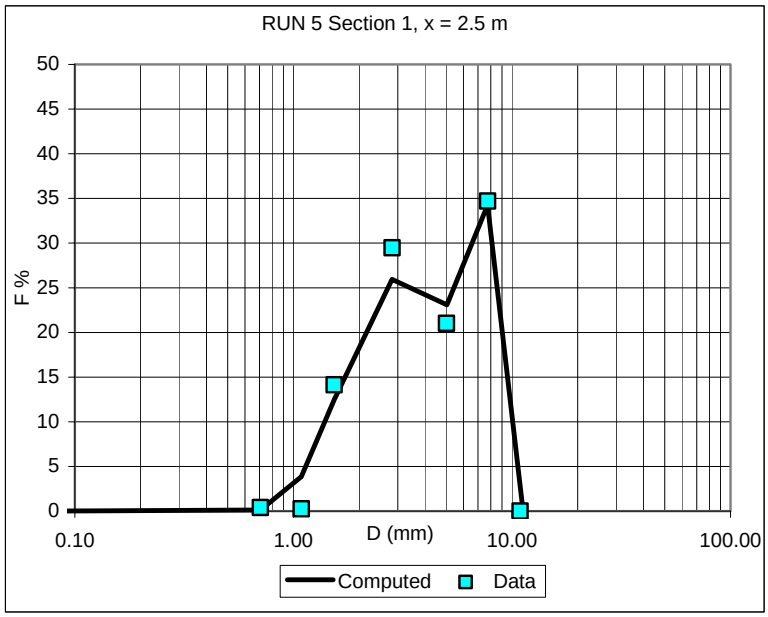
RUN 5 Section 1, x = 2.5 m
F %
D (mm)
0.10
1.00
10.00
100.00
Computed
Data

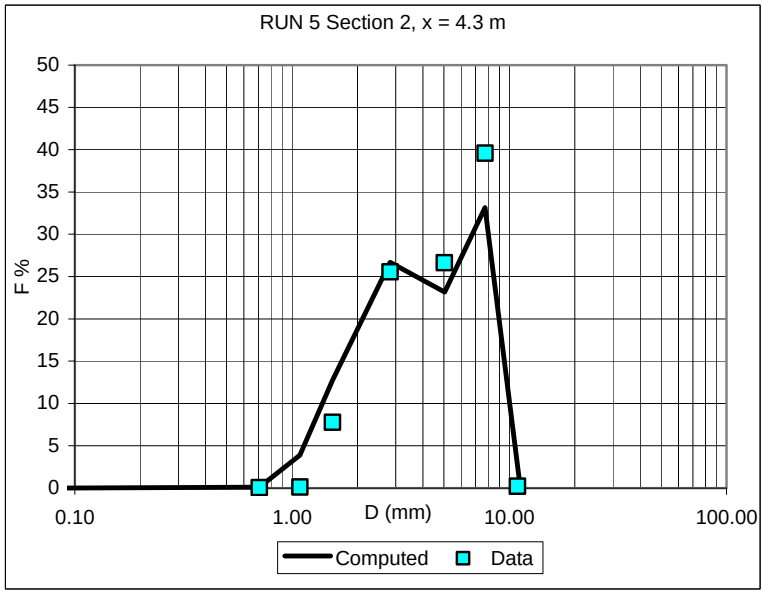
RUN 5 Section 2, x = 4.3 m
F %
D (mm)
0.10
1.00
10.00
100.00
Computed
Data

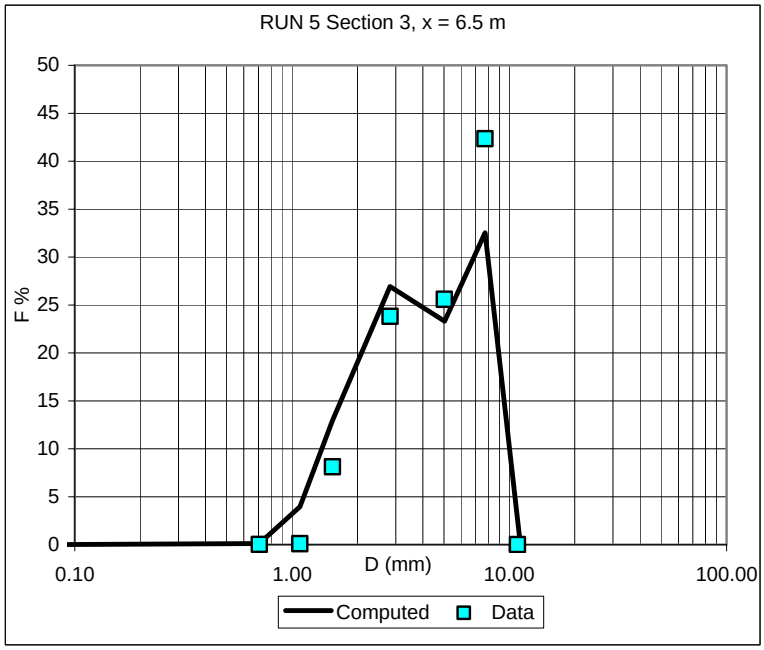
RUN 5 Section 3, x = 6.5 m
F %
D (mm)
0.10
1.00
10.00
100.00
Computed
Data

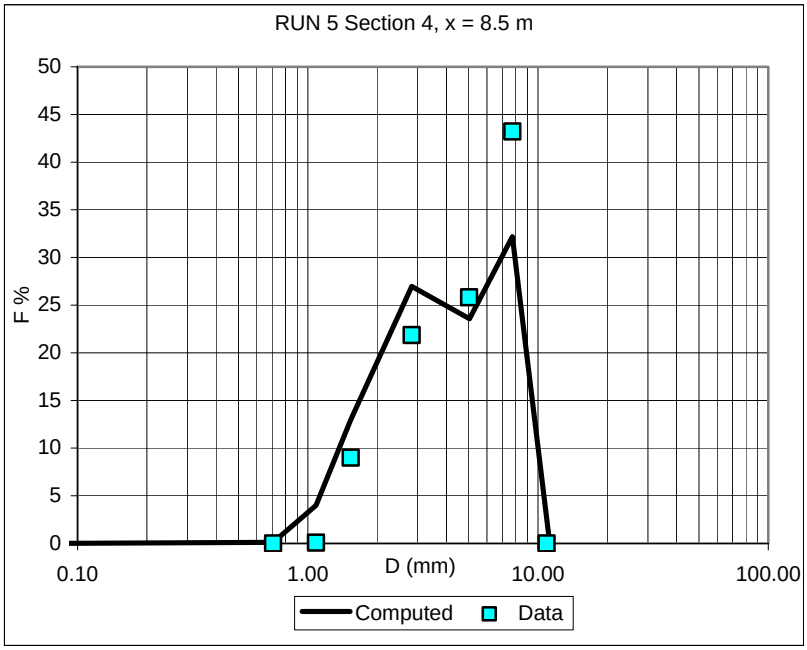
RUN 5 Section 4, x = 8.5 m
50
45
40
35
30
25
20
15
10
5
0
F %
0.10
1.00
10.00
100.00
D (mm)
Computed
Data

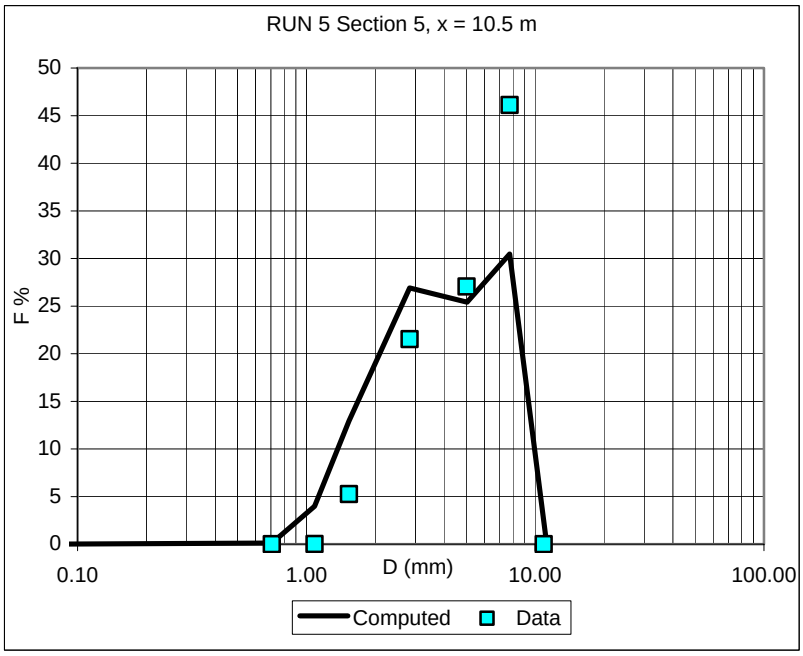
RUN 5 Section 5, x = 10.5 m
50
45
40
35
30
25
20
15
10
5
0
F %
0.10
1.00
10.00
100.00
D (mm)
Computed
Data

RUN 6

Section 1, x = 2.5 m

Computed		Data	
Di (mm)	**Fi %**	**Di (mm)**	**Fi %**
0.071	0.000	0.071	0.005
0.707	0.120	0.707	0.060
1.086	3.525	1.086	0.161
1.536	11.525	1.536	5.802
2.828	24.242	2.828	24.717
5.040	19.702	5.020	26.793
7.735	40.578	7.736	42.463
11.208	0.307	10.897	0.000

Section 2, x = 4.3 m

Computed		Data	
Di (mm)	**Fi %**	**Di (mm)**	**Fi %**
0.071	0.000	0.071	0.008
0.707	0.118	0.707	0.091
1.086	3.598	1.086	0.204
1.536	11.761	1.536	7.342
2.828	24.772	2.828	21.693
5.040	20.469	5.020	28.047
7.735	38.997	7.736	42.615
11.208	0.285	10.897	0.000

Section 3, x = 6.5 m

Computed		Data	
Di (mm)	**Fi %**	**Di (mm)**	**Fi %**
0.071	0.000	0.071	0.005
0.707	0.114	0.707	0.053
1.086	3.629	1.086	0.207
1.536	11.904	1.536	10.627
2.828	25.105	2.828	23.756
5.040	21.738	5.020	22.998
7.735	37.278	7.736	42.353
11.208	0.231	10.897	0.000

Section 4, x = 8.5 m

Computed		Data	
Di (mm)	**Fi %**	**Di (mm)**	**Fi %**
0.071	0.000	0.071	0.008
0.707	0.109	0.707	0.013
1.086	3.587	1.086	0.132
1.536	11.751	1.536	11.183
2.828	24.536	2.828	22.910
5.040	24.816	5.020	24.293
7.735	35.028	7.736	41.461
11.208	0.172	10.897	0.000

Section 5, x = 10.5 m

Computed		Data	
Di (mm)	**Fi %**	**Di (mm)**	**Fi %**
0.071	0.000	0.071	0.000
0.707	0.182	0.707	0.000
1.086	3.647	1.086	0.047
1.536	11.758	1.536	6.661
2.828	24.582	2.828	26.746
5.040	25.821	5.020	28.481
7.735	33.858	7.736	38.065
11.208	0.151	10.897	0.000

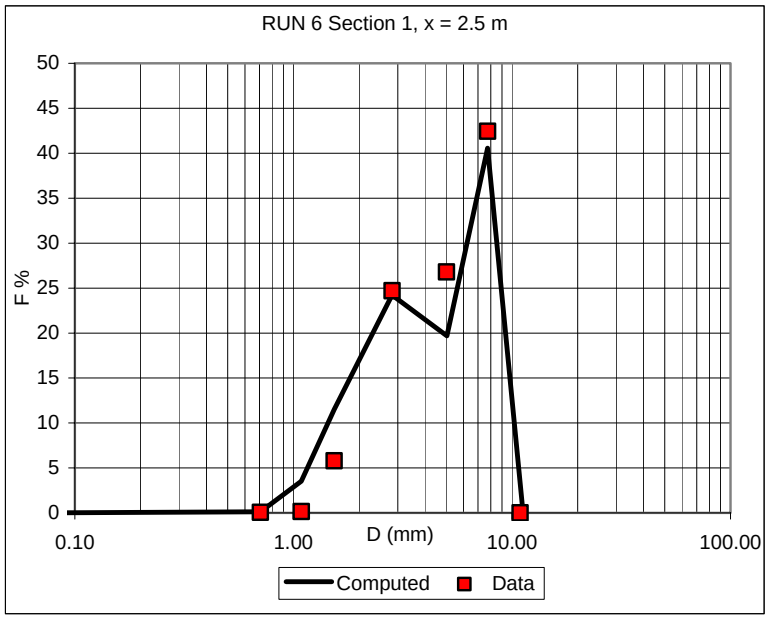
RUN 6 Section 1, x = 2.5 m
F %
D (mm)
0.10
1.00
10.00
100.00
Computed
Data

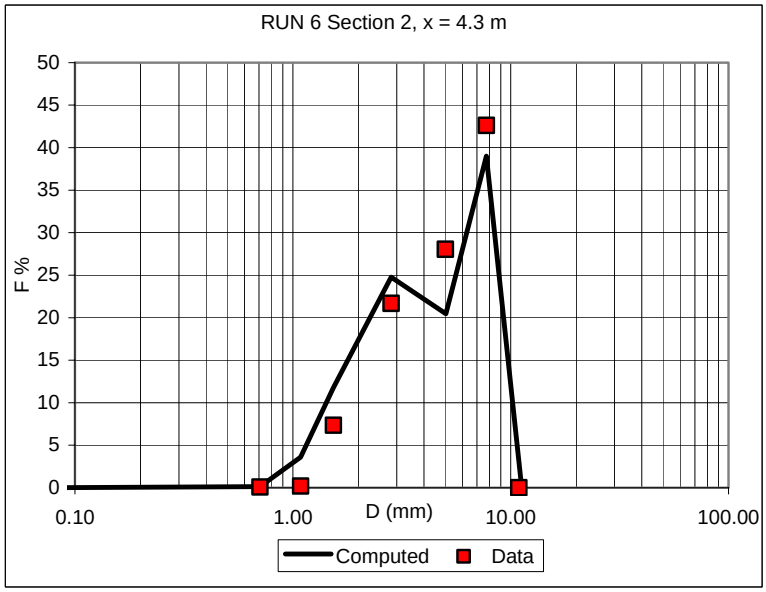
RUN 6 Section 2, x = 4.3 m
F %
D (mm)
0.10
1.00
10.00
100.00
Computed
Data

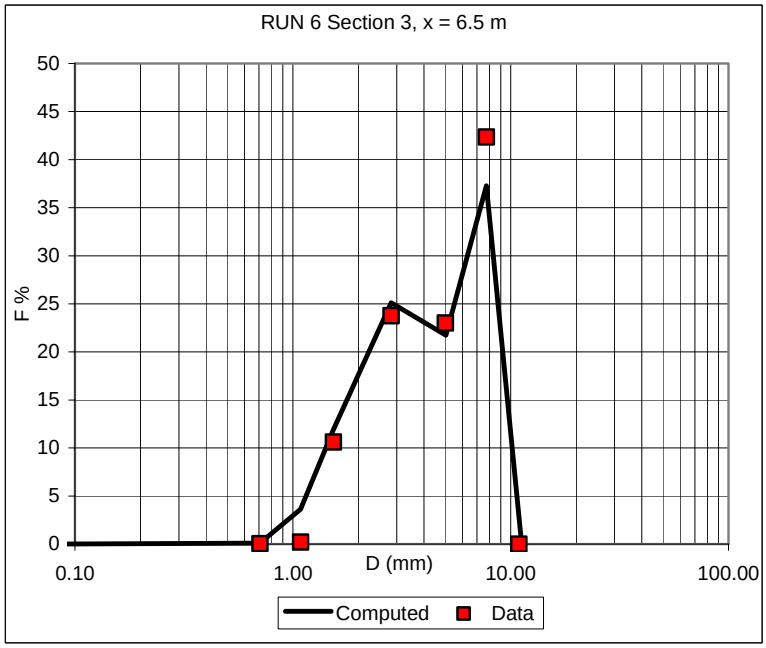
RUN 6 Section 3, x = 6.5 m
F %
D (mm)
0.10
1.00
10.00
100.00
Computed
Data

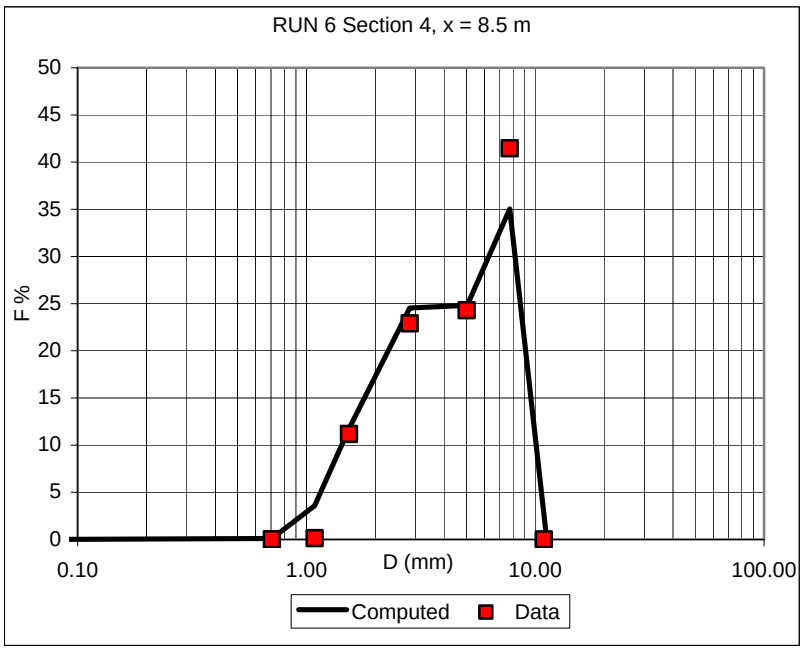
RUN 6 Section 4, x = 8.5 m
50
45
40
35
30
25
20
15
10
5
0
F %
0.10
1.00
10.00
100.00
D (mm)
Computed
Data

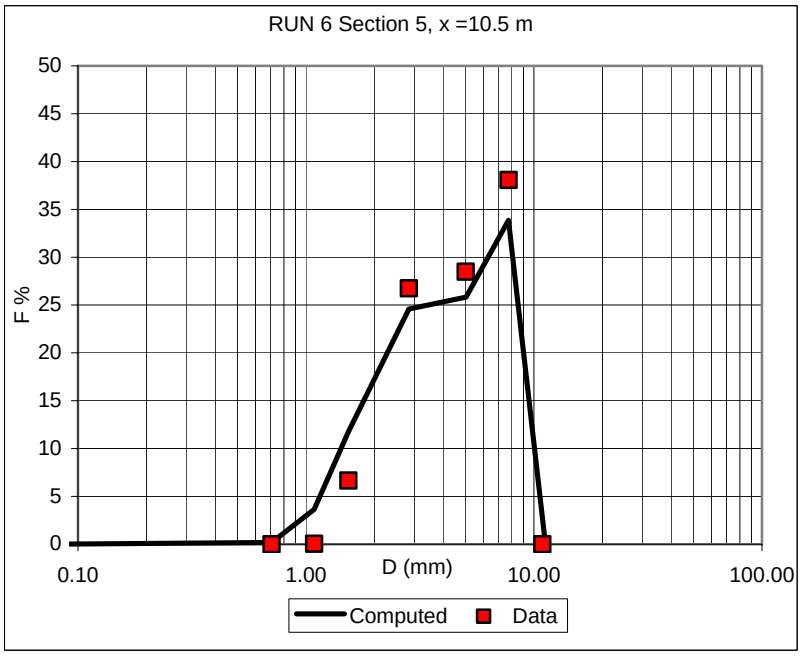
RUN 6 Section 5, x =10.5 m
50
45
40
35
30
25
20
15
10
5
0
F %
0.10
1.00
10.00
100.00
D (mm)
Computed
Data

RUN 7

Section 1, x = 2.5 m

Computed		Data	
Di (mm)	**Fi %**	**Di (mm)**	**Fi %**
0.071	0.000	0.071	0.010
0.707	0.104	0.707	0.020
1.086	3.289	1.086	0.057
1.536	10.789	1.536	9.775
2.828	22.875	2.828	29.884
5.040	22.255	5.020	27.837
7.735	40.385	7.736	32.417
11.208	0.304	10.897	0.000

Section 2, x = 4.3 m

Computed		Data	
Di (mm)	**Fi %**	**Di (mm)**	**Fi %**
0.071	0.000	0.071	0.011
0.707	0.111	0.707	0.011
1.086	3.298	1.086	0.027
1.536	10.848	1.536	6.750
2.828	23.272	2.828	32.305
5.040	21.912	5.020	27.163
7.735	40.270	7.736	33.732
11.208	0.288	10.897	0.000

Section 3, x = 6.5 m

Computed		Data	
Di (mm)	**Fi %**	**Di (mm)**	**Fi %**
0.071	0.000	0.071	0.021
0.707	0.125	0.707	0.025
1.086	3.365	1.086	0.118
1.536	11.086	1.536	10.344
2.828	23.622	2.828	24.818
5.040	22.631	5.020	26.242
7.735	38.898	7.736	38.433
11.208	0.273	10.897	0.000

Section 4, x = 8.5 m

Computed		Data	
Di (mm)	**Fi %**	**Di (mm)**	**Fi %**
0.071	0.000	0.071	0.013
0.707	0.121	0.707	0.011
1.086	3.414	1.086	0.063
1.536	11.219	1.536	8.064
2.828	23.722	2.828	30.618
5.040	23.428	5.020	26.525
7.735	37.857	7.736	34.706
11.208	0.238	10.897	0.000

Section 5, x = 10.5 m

Computed		Data	
Di (mm)	**Fi %**	**Di (mm)**	**Fi %**
0.071	0.000	0.071	0.012
0.707	0.115	0.707	0.015
1.086	3.447	1.086	0.139
1.536	11.292	1.536	11.336
2.828	23.786	2.828	24.754
5.040	24.833	5.020	26.170
7.735	36.308	7.736	37.573
11.208	0.219	10.897	0.000

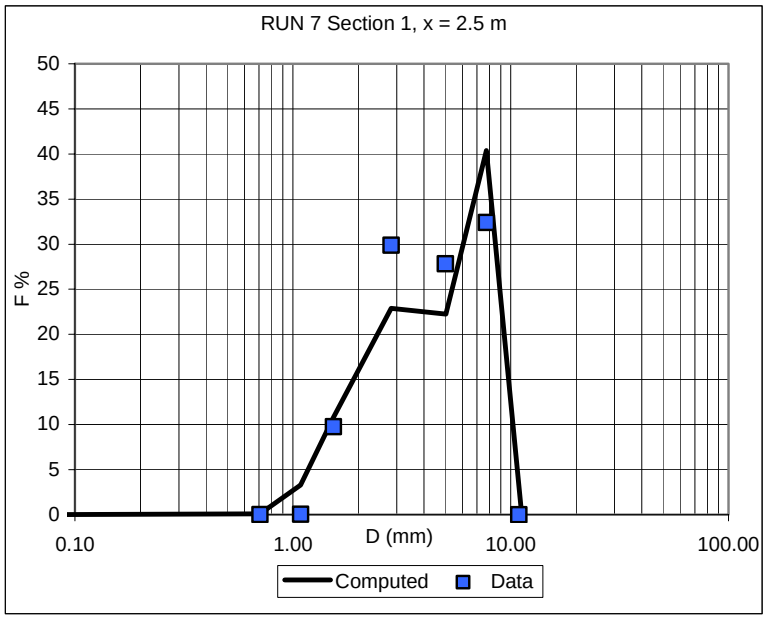
RUN 7 Section 1, x = 2.5 m
F %
D (mm)
0.10
1.00
10.00
100.00
Computed
Data

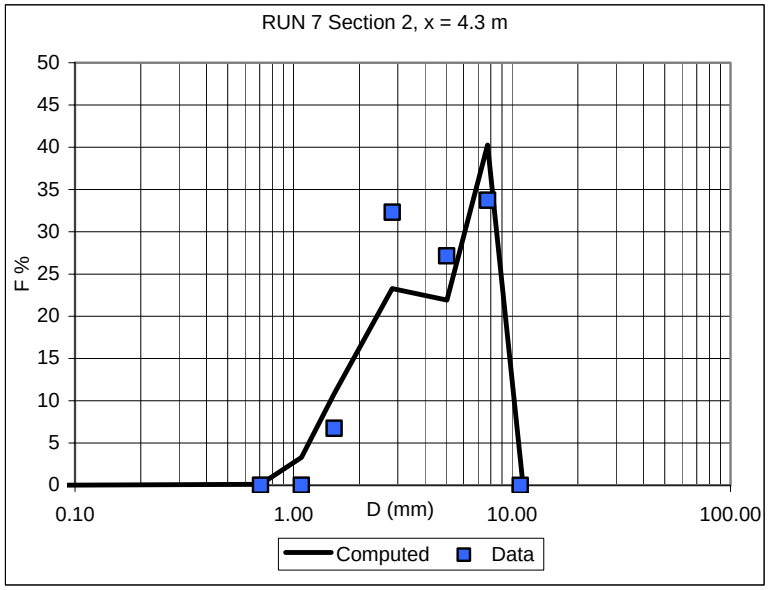
RUN 7 Section 2, x = 4.3 m
F %
D (mm)
0.10
1.00
10.00
100.00
Computed
Data

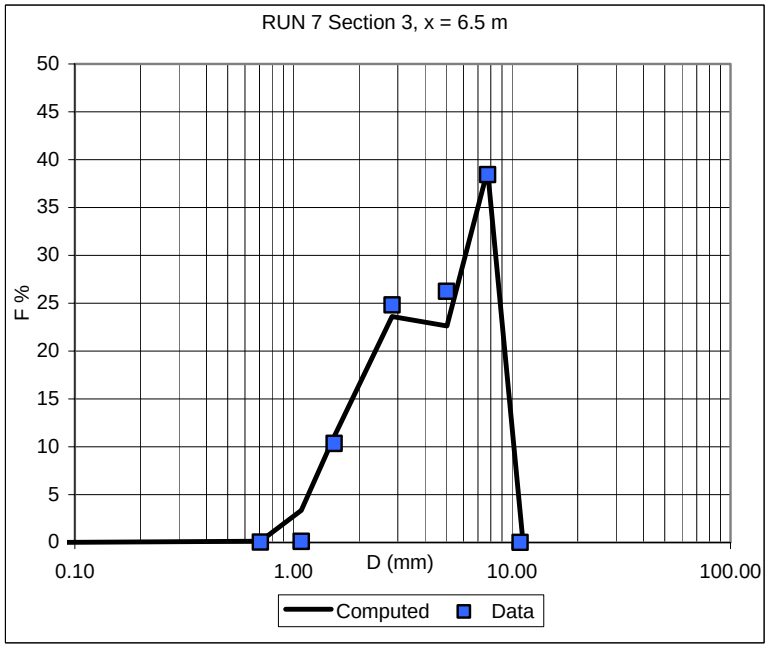
RUN 7 Section 3, x = 6.5 m
F %
D (mm)
0.10
1.00
10.00
100.00
Computed
Data

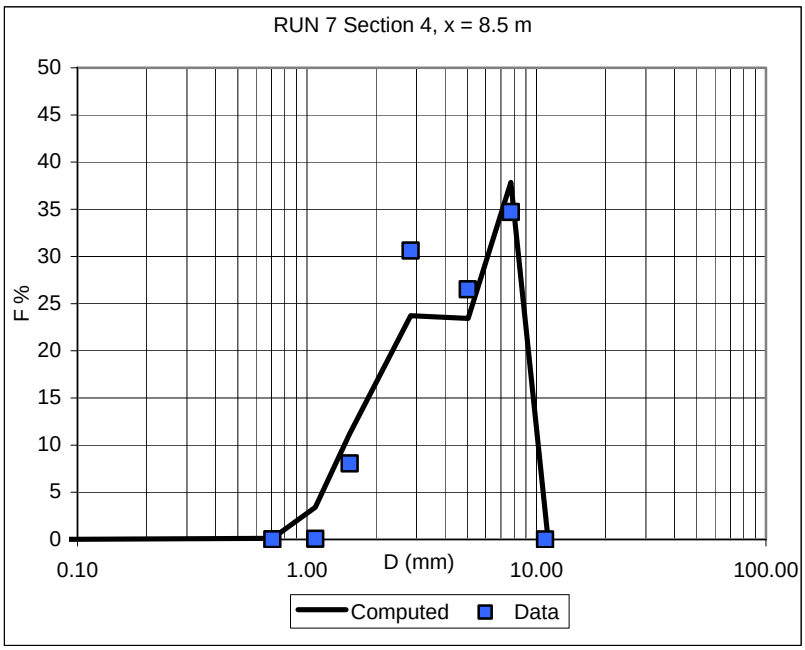
RUN 7 Section 4, x = 8.5 m
50
45
40
35
30
25
20
15
10
5
0
F %
0.10
1.00
10.00
100.00
D (mm)
Computed
Data

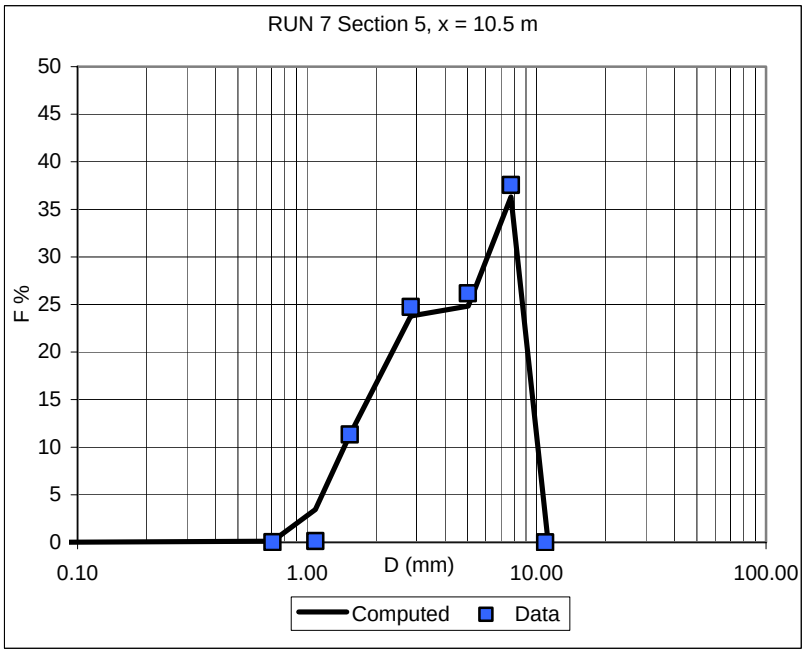
RUN 7 Section 5, x = 10.5 m
50
45
40
35
30
25
20
15
10
5
0
F %
0.10
1.00
10.00
100.00
D (mm)
Computed
Data

RUN 8

Section 1, x = 2.5 m

Computed		Data	
Di (mm)	**Fi %**	**Di (mm)**	**Fi %**
0.071	0.000	0.071	0.012
0.707	0.130	0.707	0.025
1.086	3.204	1.086	0.075
1.536	10.520	1.536	7.970
2.828	22.448	2.828	29.055
5.040	24.609	5.020	30.176
7.735	38.686	7.736	32.687
11.208	0.404	10.897	0.000

Section 2, x = 4.3 m

Computed		Data	
Di (mm)	**Fi %**	**Di (mm)**	**Fi %**
0.071	0.000	0.071	0.018
0.707	0.112	0.707	0.023
1.086	3.157	1.086	0.097
1.536	10.379	1.536	15.847
2.828	22.220	2.828	34.504
5.040	21.514	5.020	23.478
7.735	42.285	7.736	26.033
11.208	0.333	10.897	0.000

Section 3, x = 6.5 m

Computed		Data	
Di (mm)	**Fi %**	**Di (mm)**	**Fi %**
0.071	0.000	0.071	0.012
0.707	0.112	0.707	0.012
1.086	3.155	1.086	0.102
1.536	10.386	1.536	9.584
2.828	22.323	2.828	27.658
5.040	20.854	5.020	25.172
7.735	42.884	7.736	37.460
11.208	0.286	10.897	0.000

Section 4, x = 8.5 m

Computed		Data	
Di (mm)	**Fi %**	**Di (mm)**	**Fi %**
0.071	0.000	0.071	0.021
0.707	0.116	0.707	0.041
1.086	3.155	1.086	0.162
1.536	10.427	1.536	12.896
2.828	22.331	2.828	31.460
5.040	21.063	5.020	24.278
7.735	42.677	7.736	31.142
11.208	0.232	10.897	0.000

Section 5, x = 10.5 m

Computed		Data	
Di (mm)	**Fi %**	**Di (mm)**	**Fi %**
0.071	0.000	0.071	0.013
0.707	0.116	0.707	0.006
1.086	3.155	1.086	0.058
1.536	10.427	1.536	6.050
2.828	22.331	2.828	24.509
5.040	21.063	5.020	27.752
7.735	42.677	7.736	41.611
11.208	0.232	10.897	0.000

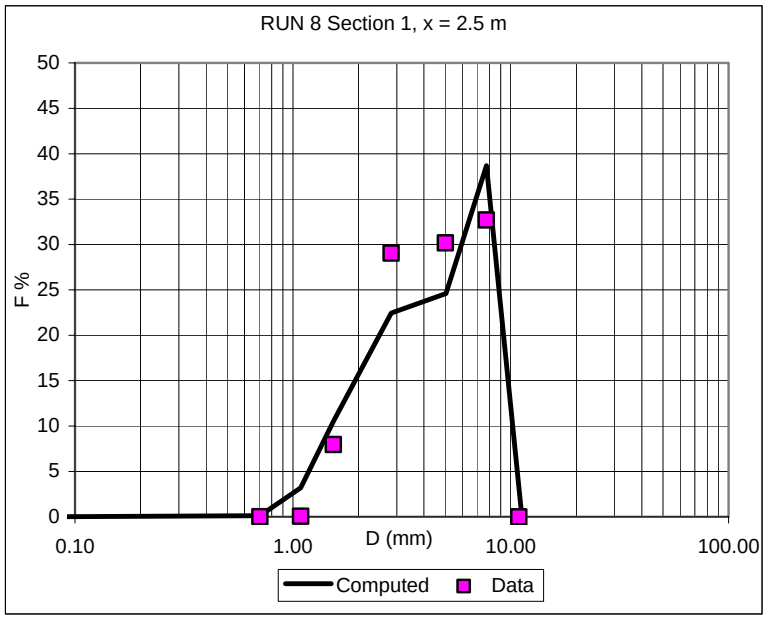
RUN 8 Section 1, x = 2.5 m
50
45
40
35
30
25
20
15
10
5
0
F %
0.10
1.00
10.00
100.00
D (mm)
Computed
Data

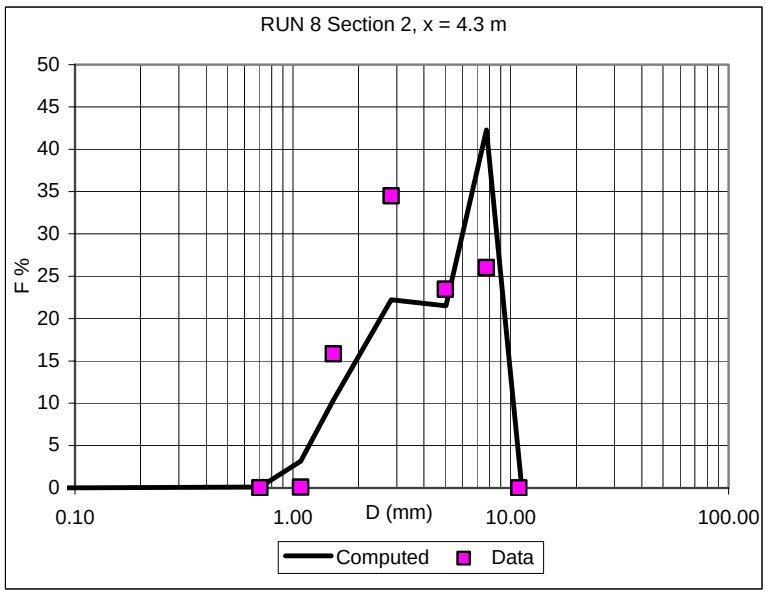
RUN 8 Section 2, x = 4.3 m
50
45
40
35
30
25
20
15
10
5
0
F %
0.10
1.00
10.00
100.00
D (mm)
Computed
Data

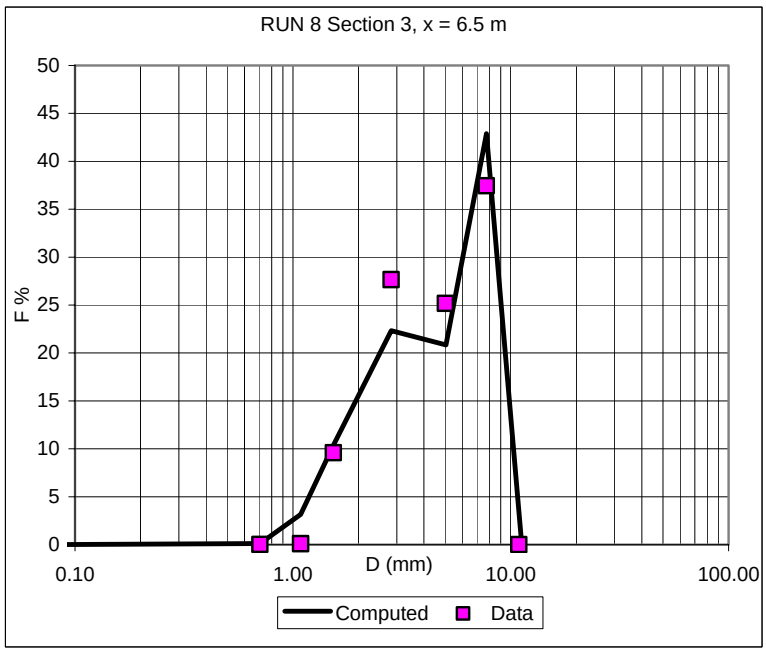
RUN 8 Section 3, x = 6.5 m
50
45
40
35
30
25
20
15
10
5
0
F %
0.10
1.00
10.00
100.00
D (mm)
Computed
Data

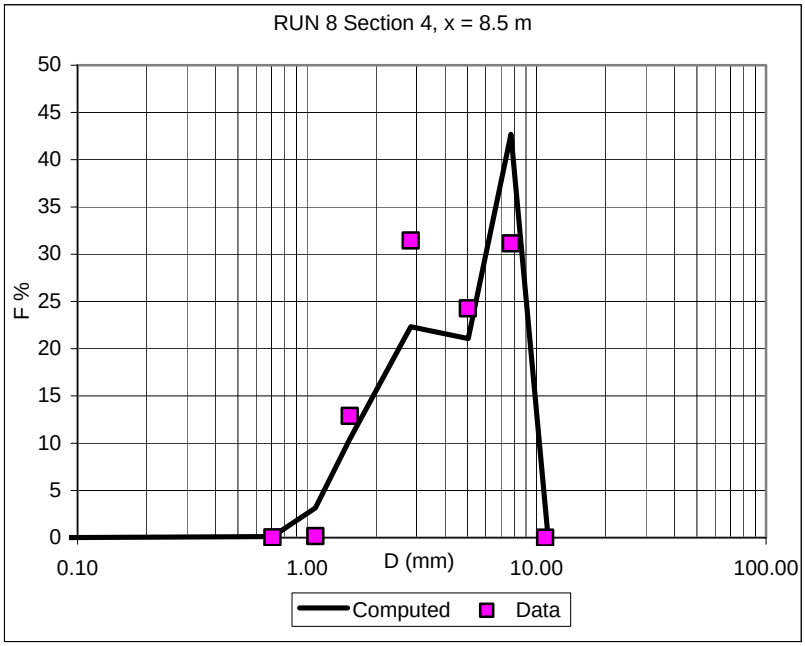
RUN 8 Section 4, x = 8.5 m
50
45
40
35
30
25
20
15
10
5
0
F %
0.10
1.00
10.00
100.00
D (mm)
Computed
Data

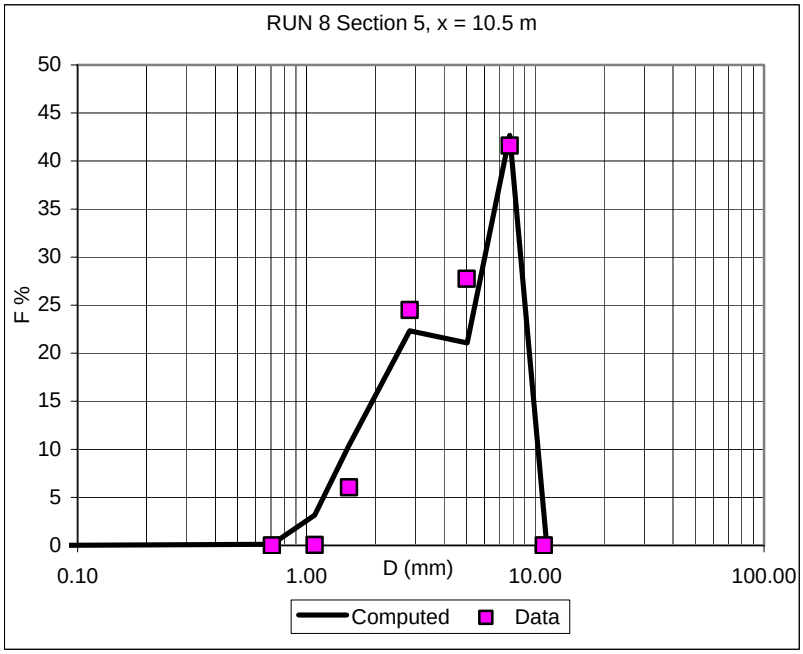
RUN 8 Section 5, x = 10.5 m
50
45
40
35
30
25
20
15
10
5
0
F %
0.10
1.00
10.00
100.00
D (mm)
Computed
Data

RUN 9

Section 1, x = 2.5 m

Computed		Data	
Di (mm)	**Fi %**	**Di (mm)**	**Fi %**
0.071	0.000	0.071	0.007
0.707	0.104	0.707	0.073
1.086	3.181	1.086	0.248
1.536	10.476	1.536	13.395
2.828	22.341	2.828	27.246
5.040	21.602	5.020	26.696
7.735	41.924	7.736	32.334
11.208	0.371	10.897	0.000

Section 2, x = 4.3 m

Computed		Data	
Di (mm)	**Fi %**	**Di (mm)**	**Fi %**
0.071	0.000	0.071	0.003
0.707	0.105	0.707	0.014
1.086	3.190	1.086	0.117
1.536	10.486	1.536	9.979
2.828	22.296	2.828	30.310
5.040	21.855	5.020	25.730
7.735	41.738	7.736	33.847
11.208	0.330	10.897	0.000

Section 3, x = 6.5 m

Computed		Data	
Di (mm)	**Fi %**	**Di (mm)**	**Fi %**
0.071	0.000	0.071	0.006
0.707	0.106	0.707	0.009
1.086	3.154	1.086	0.098
1.536	10.360	1.536	12.150
2.828	22.023	2.828	32.334
5.040	21.986	5.020	25.998
7.735	42.071	7.736	29.405
11.208	0.300	10.897	0.000

Section 4, x = 8.5 m

Computed		Data	
Di (mm)	**Fi %**	**Di (mm)**	**Fi %**
0.071	0.000	0.071	0.008
0.707	0.106	0.707	0.023
1.086	3.066	1.086	0.218
1.536	10.110	1.536	13.066
2.828	21.704	2.828	25.865
5.040	21.770	5.020	24.774
7.735	42.962	7.736	36.047
11.208	0.283	10.897	0.000

Section 5, x = 10.5 m

Computed		Data	
Di (mm)	**Fi %**	**Di (mm)**	**Fi %**
0.071	0.000	0.071	0.004
0.707	0.105	0.707	0.017
1.086	3.069	1.086	0.134
1.536	10.168	1.536	8.921
2.828	21.891	2.828	34.373
5.040	21.593	5.020	27.669
7.735	42.906	7.736	28.882
11.208	0.269	10.897	0.000

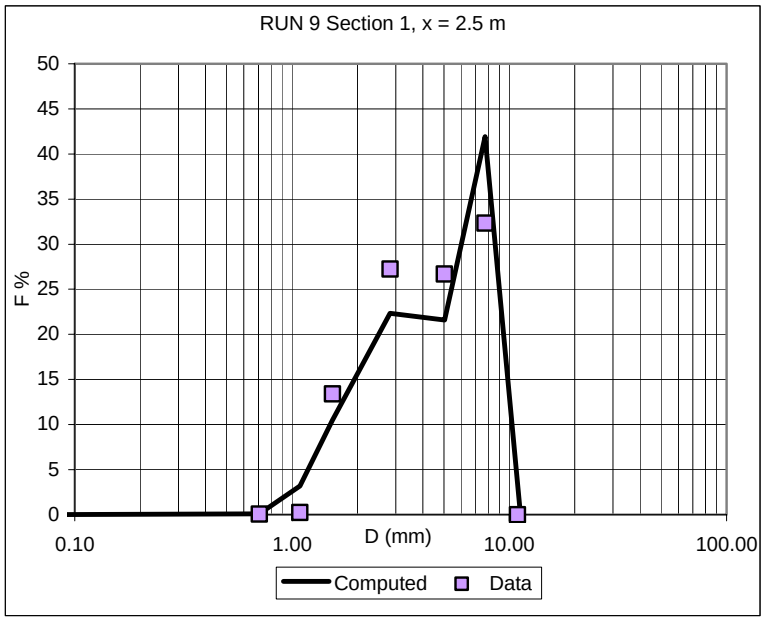
RUN 9 Section 1, x = 2.5 m
F %
D (mm)
0.10
1.00
10.00
100.00
Computed
Data

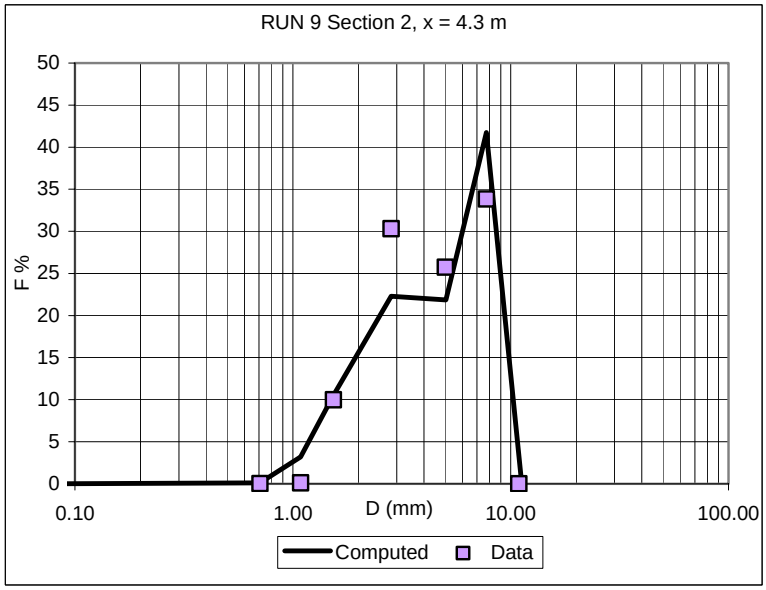
RUN 9 Section 2, x = 4.3 m
F %
D (mm)
0.10
1.00
10.00
100.00
Computed
Data

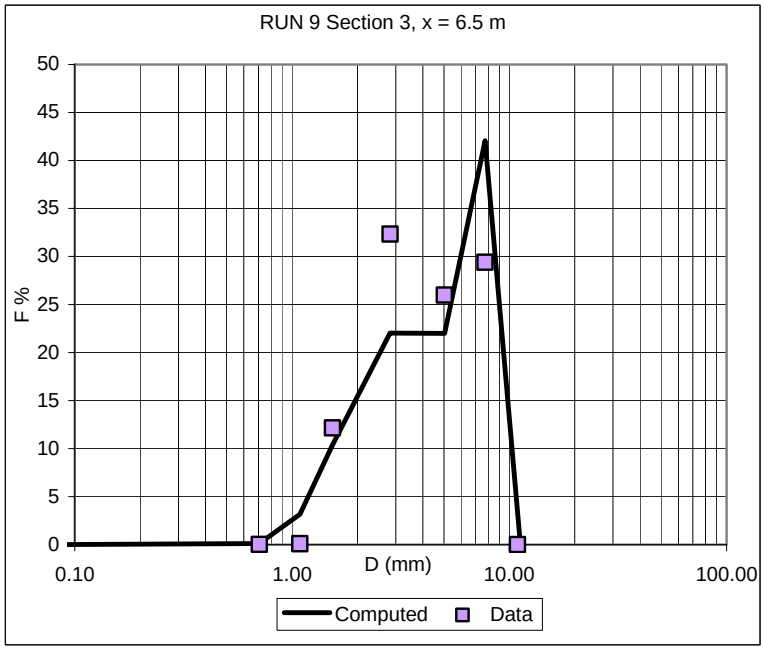
RUN 9 Section 3, x = 6.5 m
F %
D (mm)
0.10
1.00
10.00
100.00
Computed
Data

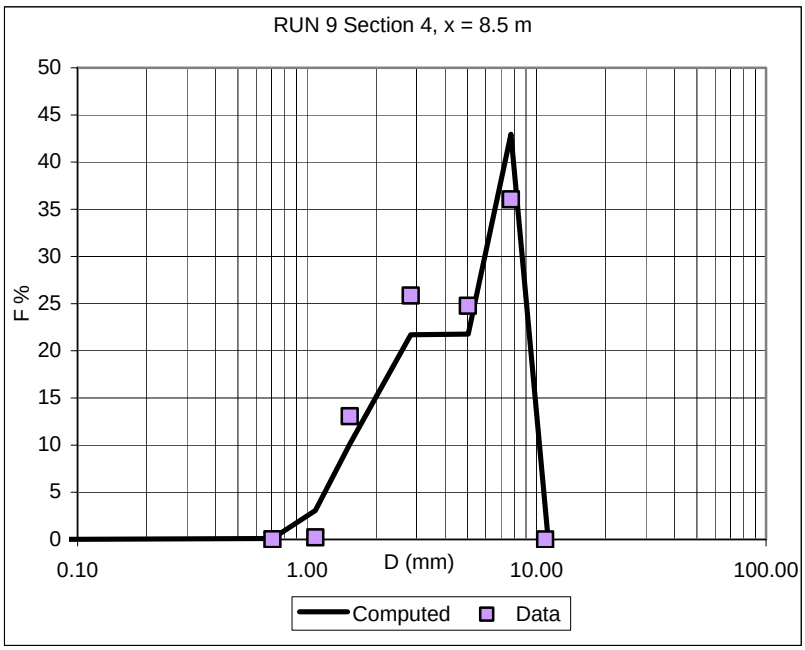
RUN 9 Section 4, x = 8.5 m
50
45
40
35
30
25
20
15
10
5
0
F %
0.10
1.00
10.00
100.00
D (mm)
Computed
Data

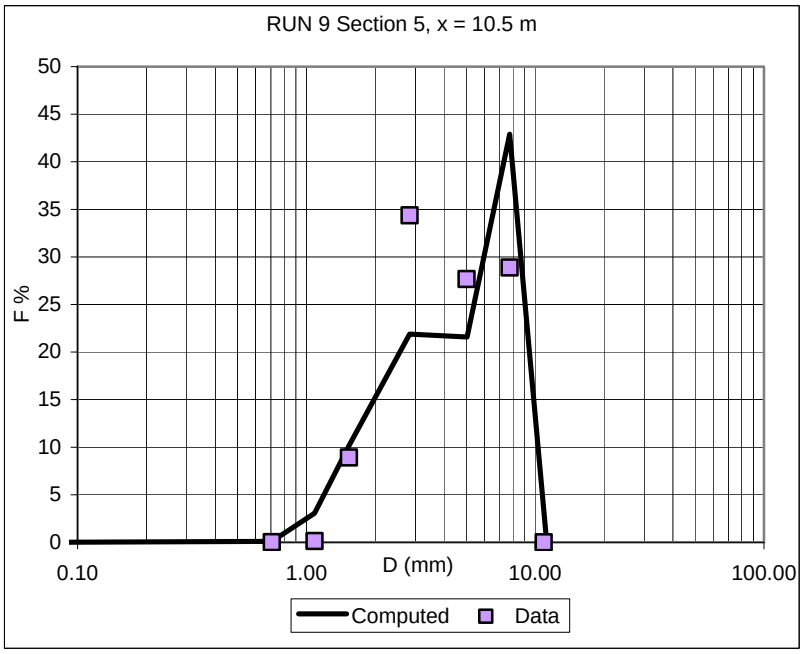
RUN 9 Section 5, x = 10.5 m
50
45
40
35
30
25
20
15
10
5
0
F %
0.10
1.00
10.00
100.00
D (mm)
Computed
Data

Substrate

x = 0.5 m								
First layer 0 -1 cm					Second layer 1 - 2 cm			
Computed		Data			Computed		Data	
Di (mm)	fi %	Di (mm)	fi %		Di (mm)	fi %	Di (mm)	fi %
0.707	0.105	0.071	0.107		0.707	0.133	0.071	0.356
1.086	3.144	0.707	0.437		1.086	3.254	0.707	0.396
1.536	10.384	1.086	0.496		1.536	10.626	1.086	0.424
2.828	22.206	1.536	22.195		2.828	22.519	1.536	22.301
5.040	21.645	2.828	31.045		5.040	24.604	2.828	33.847
7.735	42.191	5.020	21.661		7.735	38.503	5.020	20.169
11.208	0.324	7.736	24.059		11.208	0.362	7.736	22.508
	0	10.897	0.000				10.897	0.000
Third layer 2 - 3 cm					Fourth layer 3 - 4 cm			
Computed		Data			Computed		Data	
Di (mm)	fi %	Di (mm)	fi %		Di (mm)	fi %	Di (mm)	fi %
0.707	1.478	0.071	0.312		0.707	1.058	0.071	0.389
1.086	7.290	0.707	0.353		1.086	6.799	0.707	0.324
1.536	20.195	1.086	0.368		1.536	19.702	1.086	0.384
2.828	37.185	1.536	20.935		2.828	37.535	1.536	22.894
5.040	17.429	2.828	33.300		5.040	19.381	2.828	35.782
7.735	16.315	5.020	21.279		7.735	15.449	5.020	22.139
11.208	0.109	7.736	23.451		11.208	0.074	7.736	18.088
		10.897	0.000				10.897	0.000
Fifth layer 4 - 5 cm					Sixth layer 5 - 7 cm			
Computed		Data			Computed		Data	
Di (mm)	fi %	Di (mm)	fi %		Di (mm)	fi %	Di (mm)	fi %
0.707	0.243	0.071	0.280		0.707	0.114	0.071	0.238
1.086	5.974	0.707	0.241		1.086	5.863	0.707	0.177
1.536	18.783	1.086	0.429		1.536	18.691	1.086	0.362
2.828	37.090	1.536	21.467		2.828	37.088	1.536	21.819
5.040	20.995	2.828	36.161		5.040	21.179	2.828	34.716
7.735	16.834	5.020	22.768		7.735	16.983	5.020	20.836
11.208	0.081	7.736	18.654		11.208	0.082	7.736	21.851
		10.897	0.000				10.897	0.000

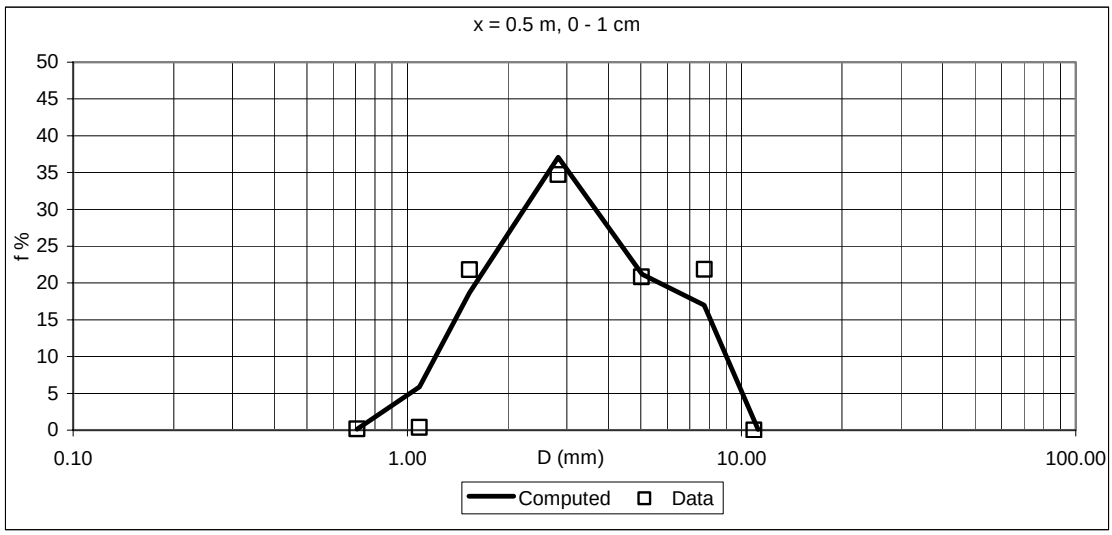
x = 0.5 m, 0 - 1 cm
f %
50
45
40
35
30
25
20
15
10
5
0
0.10
1.00
D (mm)
10.00
100.00
Computed
Data

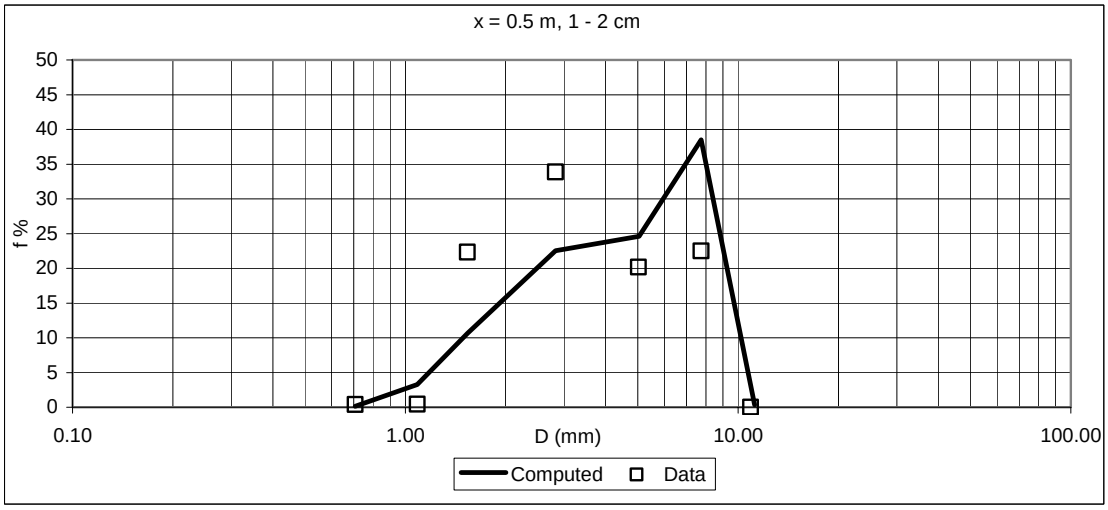
x = 0.5 m, 1 - 2 cm
f %
50
45
40
35
30
25
20
15
10
5
0
0.10
1.00
D (mm)
10.00
100.00
Computed
Data

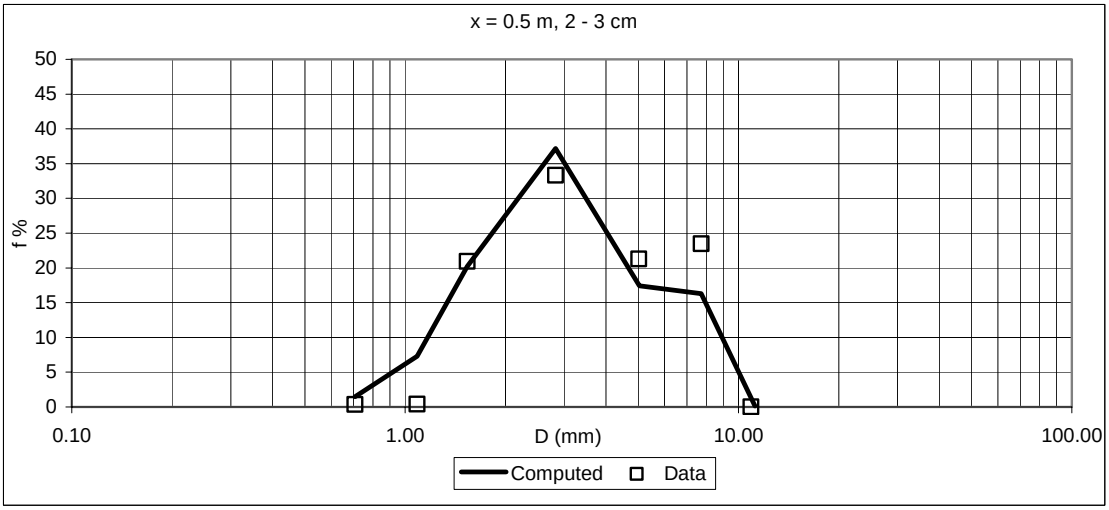
x = 0.5 m, 2 - 3 cm
f %
50
45
40
35
30
25
20
15
10
5
0
0.10
1.00
D (mm)
10.00
100.00
Computed
Data

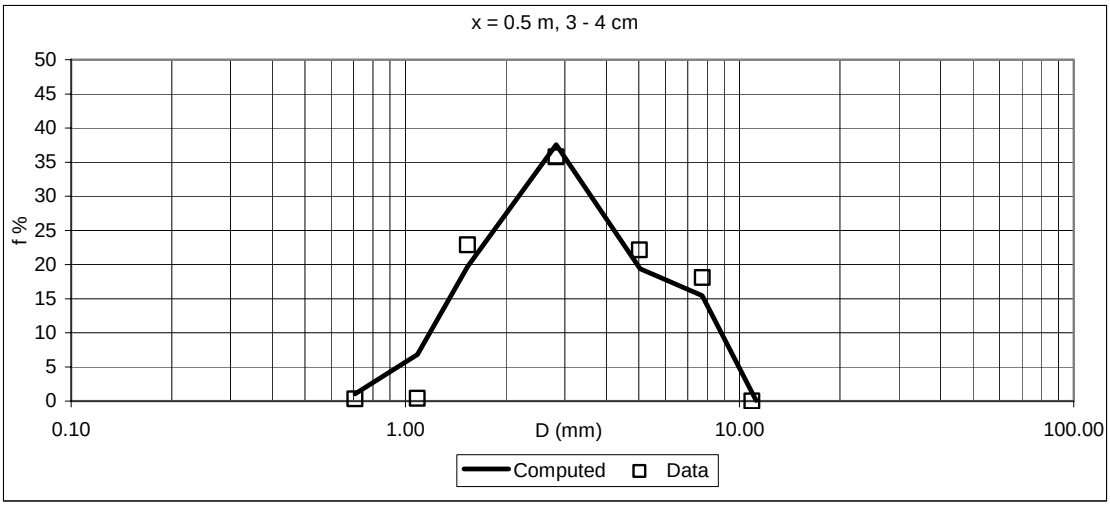
x = 0.5 m, 3 - 4 cm
f %
50
45
40
35
30
25
20
15
10
5
0
0.10
1.00
D (mm)
10.00
100.00
Computed
Data

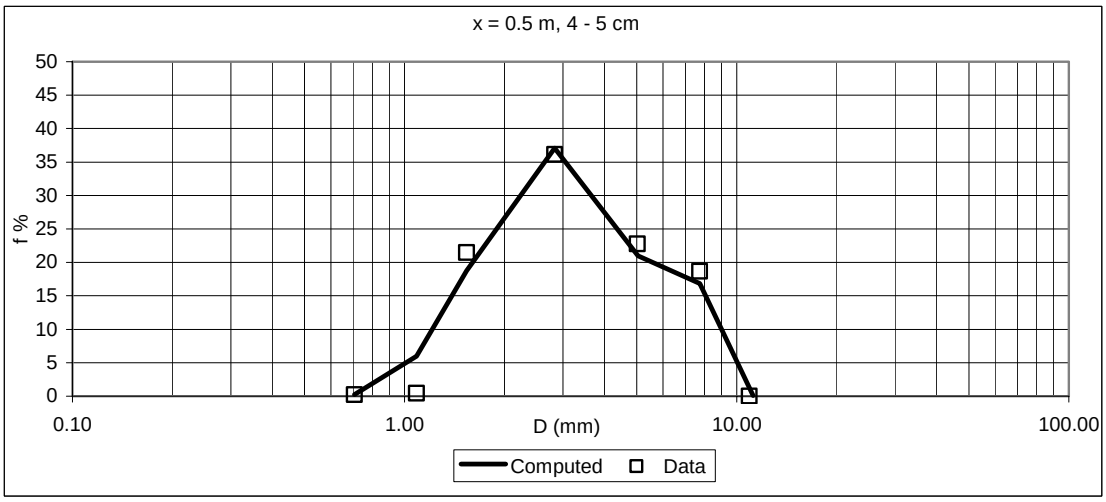
x = 0.5 m, 4 - 5 cm
f %
50
45
40
35
30
25
20
15
10
5
0
0.10
1.00
D (mm)
10.00
100.00
Computed
Data

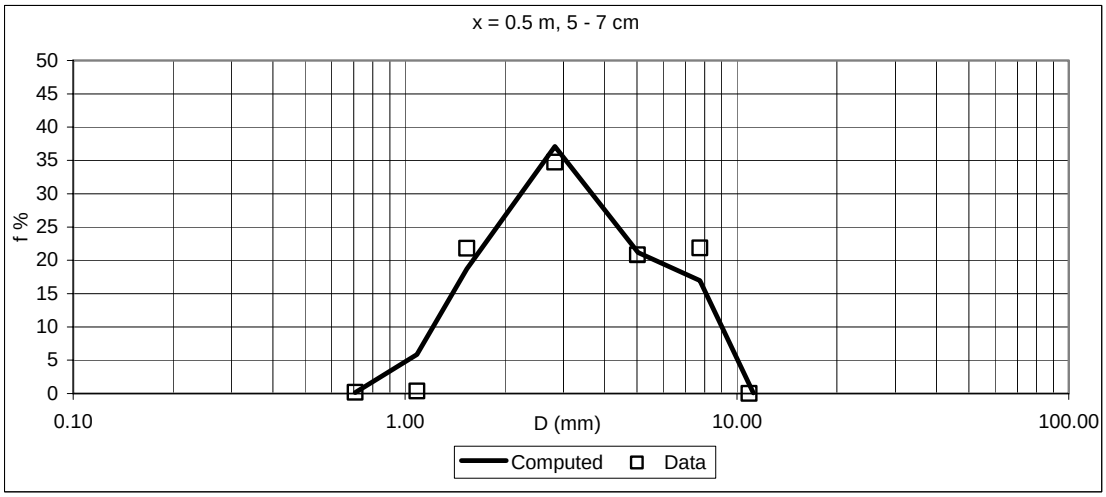
x = 0.5 m, 5 - 7 cm
f %
50
45
40
35
30
25
20
15
10
5
0
0.10
1.00
D (mm)
10.00
100.00
Computed
Data

x = 1 m								
First layer 0 -1 cm					Second layer 1 - 2 cm			
Computed		Data			Computed		Data	
Di (mm)	fi %	Di (mm)	fi %		Di (mm)	fi %	Di (mm)	fi %
0.707	0.108	0.071	0.238		0.707	0.267	0.071	0.481
1.086	3.157	0.707	0.449		1.086	3.604	0.707	0.398
1.536	10.410	1.086	0.369		1.536	11.546	1.086	0.312
2.828	22.244	1.536	16.866		2.828	23.903	1.536	15.306
5.040	21.848	2.828	30.960		5.040	23.855	2.828	26.940
7.735	41.875	5.020	23.926		7.735	36.466	5.020	33.484
11.208	0.359	7.736	27.192		11.208	0.360	7.736	23.079
		10.897	0.000				10.897	0.000
Third layer 2 - 3 cm					Fourth layer 3 - 4 cm			
Computed		Data			Computed		Data	
Di (mm)	fi %	Di (mm)	fi %		Di (mm)	fi %	Di (mm)	fi %
0.707	1.299	0.071	0.565		0.707	1.218	0.071	0.498
1.086	6.707	0.707	0.368		1.086	6.657	0.707	0.270
1.536	19.776	1.086	0.381		1.536	19.886	1.086	0.392
2.828	36.511	1.536	20.947		2.828	37.291	1.536	22.769
5.040	18.494	2.828	33.167		5.040	19.372	2.828	34.036
7.735	17.104	5.020	20.473		7.735	15.502	5.020	20.596
11.208	0.108	7.736	24.099		11.208	0.075	7.736	21.438
		10.897	0.000				10.897	0.000
Fifth layer 4 - 5 cm					Sixth layer 5 - 6 cm			
Computed		Data			Computed		Data	
Di (mm)	fi %	Di (mm)	fi %		Di (mm)	fi %	Di (mm)	fi %
0.707	0.114	0.071	0.399		0.707	0.114	0.071	0.315
1.086	5.863	0.707	0.176		1.086	5.863	0.707	0.155
1.536	18.691	1.086	0.379		1.536	18.691	1.086	0.350
2.828	37.088	1.536	21.495		2.828	37.088	1.536	21.389
5.040	21.179	2.828	34.838		5.040	21.179	2.828	35.925
7.735	16.983	5.020	20.785		7.735	16.983	5.020	21.792
11.208	0.082	7.736	21.928		11.208	0.082	7.736	20.074
		10.897	0.000				10.897	0.000
Seventh layer 6 - 7 cm								
Computed		Data						
Di (mm)	fi %	Di (mm)	fi %					
0.707	0.114	0.071	0.254					
1.086	5.863	0.707	0.138					
1.536	18.691	1.086	0.348					
2.828	37.088	1.536	21.660					
5.040	21.179	2.828	36.446					
7.735	16.983	5.020	22.181					
11.208	0.082	7.736	18.973					
		10.897	0.000					

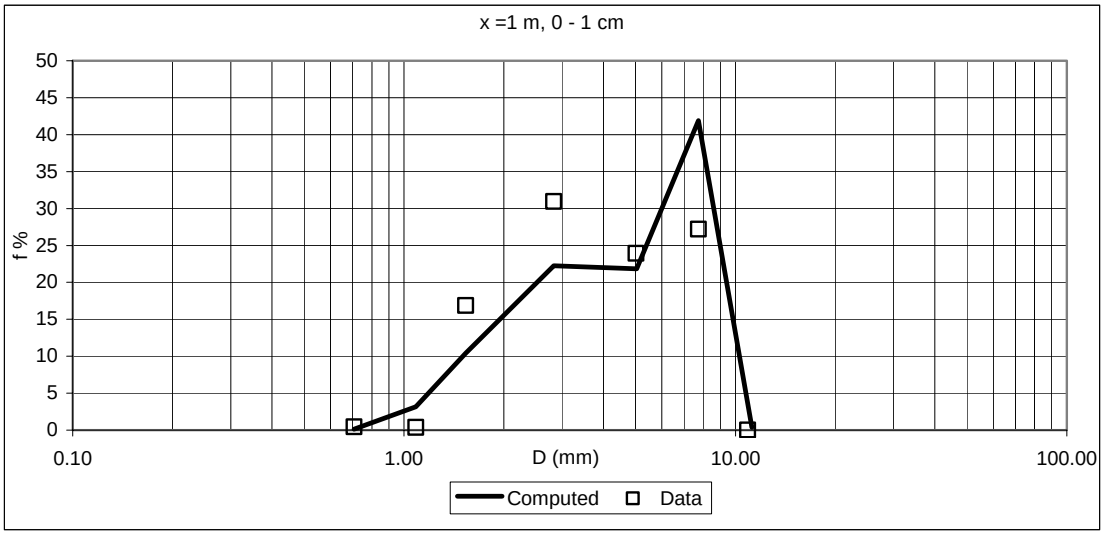
x =1 m, 0 - 1 cm
50
45
40
35
30
25
20
15
10
5
0
f %
0.10
1.00
D (mm)
10.00
100.00
Computed
Data

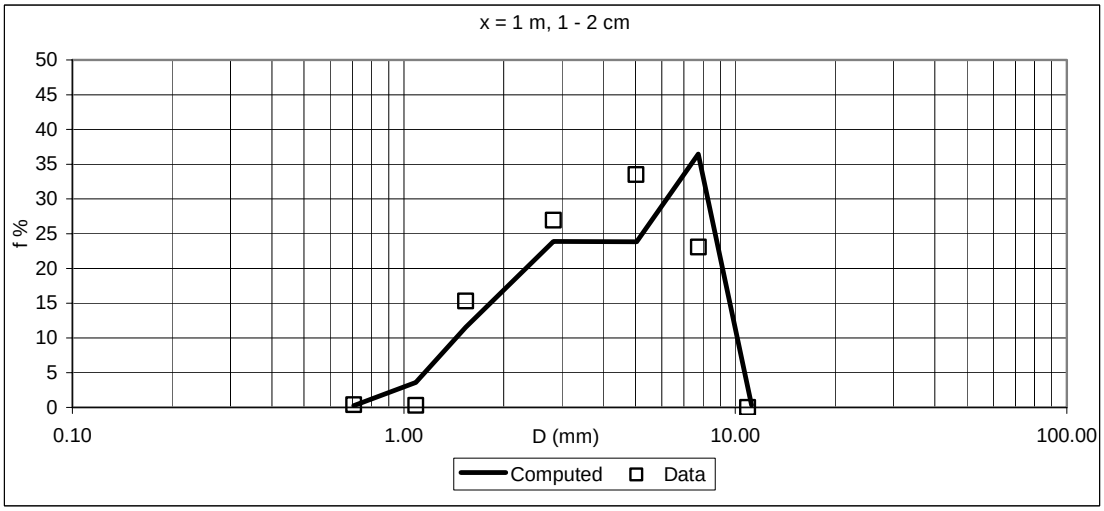
x = 1 m, 1 - 2 cm
50
45
40
35
30
25
20
15
10
5
0
f %
0.10
1.00
D (mm)
10.00
100.00
Computed
Data

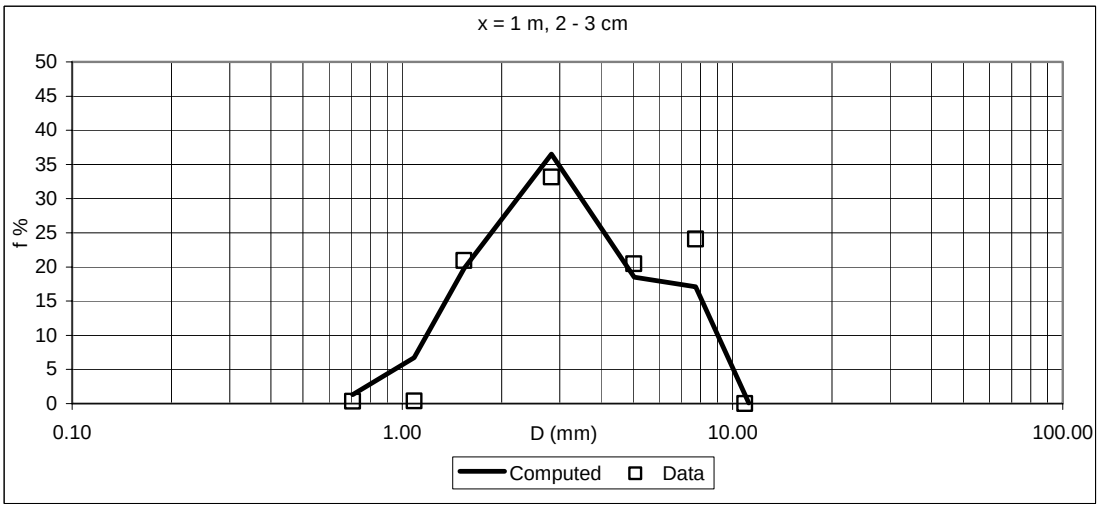
x = 1 m, 2 - 3 cm
50
45
40
35
30
25
20
15
10
5
0
f %
0.10
1.00
D (mm)
10.00
100.00
Computed
Data

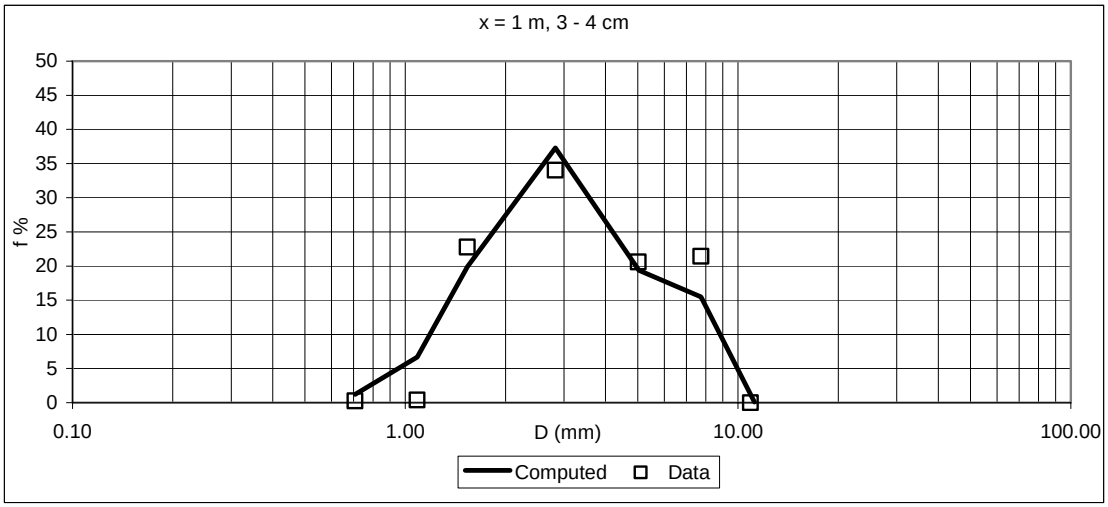
x = 1 m, 3 - 4 cm
f %
50
45
40
35
30
25
20
15
10
5
0
0.10
1.00
D (mm)
10.00
100.00
Computed
Data

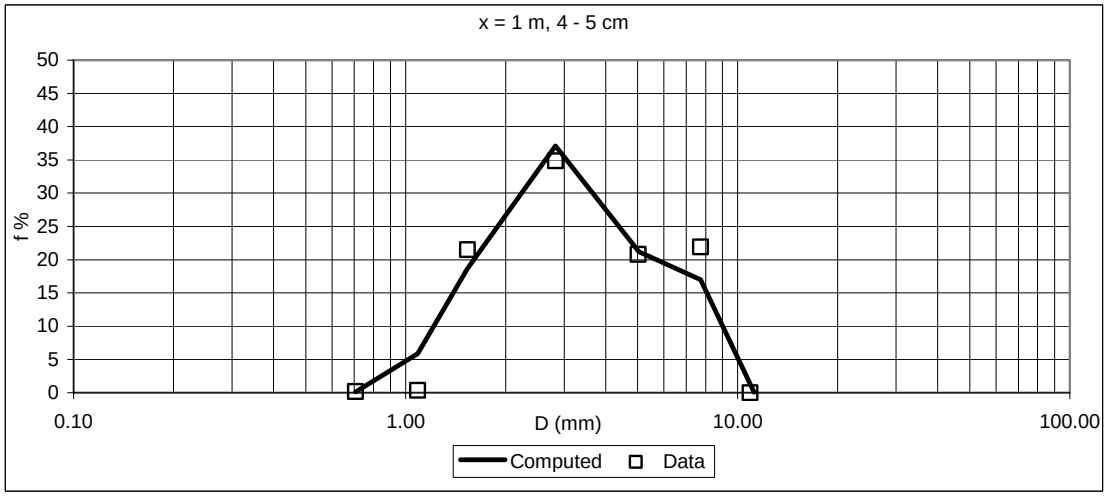
x = 1 m, 4 - 5 cm
f %
50
45
40
35
30
25
20
15
10
5
0
0.10
1.00
D (mm)
10.00
100.00
Computed
Data

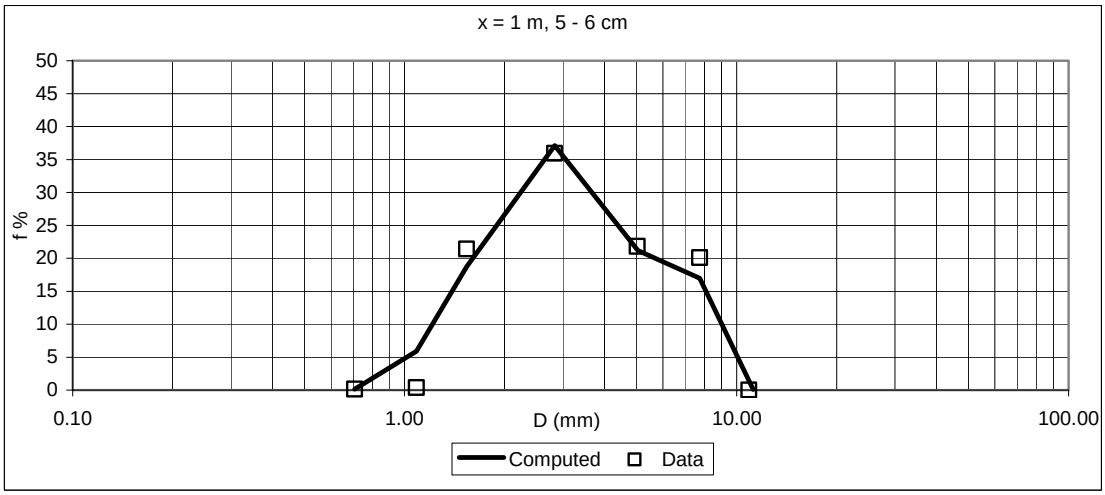
x = 1 m, 5 - 6 cm
f %
50
45
40
35
30
25
20
15
10
5
0
0.10
1.00
D (mm)
10.00
100.00
Computed
Data

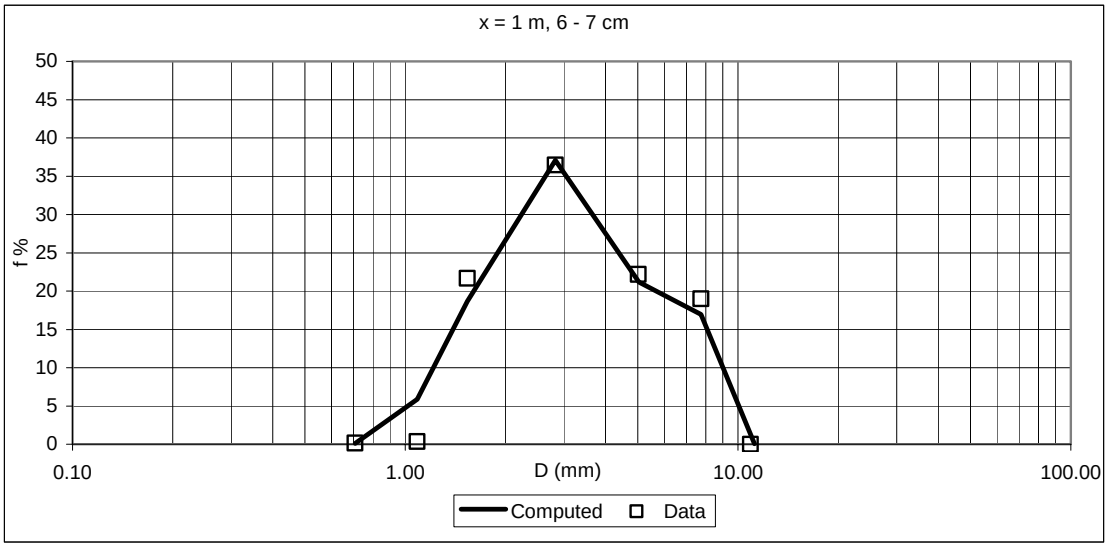
x = 1 m, 6 - 7 cm
50
45
40
35
30
25
20
15
10
5
0
f %
0.10
1.00
D (mm)
10.00
100.00
Computed
Data

x = 1.5 m								
First layer 0 -1 cm					Second layer 1 - 2 cm			
Computed		Data			Computed		Data	
Di (mm)	fi %	Di (mm)	fi %		Di (mm)	fi %	Di (mm)	fi %
0.707	0.107	0.071	0.235		0.707	0.232	0.071	0.461
1.086	3.164	0.707	0.438		1.086	3.837	0.707	0.296
1.536	10.430	1.086	0.406		1.536	12.206	1.086	0.355
2.828	22.273	1.536	21.199		2.828	25.142	1.536	19.881
5.040	21.846	2.828	36.052		5.040	23.223	2.828	35.393
7.735	41.809	5.020	20.363		7.735	35.041	5.020	22.770
11.208	0.372	7.736	21.307		11.208	0.319	7.736	20.843
		10.897	0.000				10.897	0.000
Third layer 2 - 3 cm					Fourth layer 3 - 4 cm			
Computed		Data			Computed		Data	
Di (mm)	fi %	Di (mm)	fi %		Di (mm)	fi %	Di (mm)	fi %
0.707	0.760	0.071	0.132		0.707	0.711	0.071	0.302
1.086	5.894	0.707	0.375		1.086	6.672	0.707	0.173
1.536	17.284	1.086	0.386		1.536	19.785	1.086	0.360
2.828	32.893	1.536	20.893		2.828	37.500	1.536	21.983
5.040	20.433	2.828	34.429		5.040	19.611	2.828	33.968
7.735	22.565	5.020	21.591		7.735	15.645	5.020	21.754
11.208	0.171	7.736	22.193		11.208	0.075	7.736	21.459
		10.897	0.000				10.897	0.000
Fifth layer 4 - 5 cm					Sixth layer 5 - 6 cm			
Computed		Data			Computed		Data	
Di (mm)	fi %	Di (mm)	fi %		Di (mm)	fi %	Di (mm)	fi %
0.707	0.114	0.071	0.247		0.707	0.114	0.071	0.224
1.086	5.863	0.707	0.165		1.086	5.863	0.707	0.145
1.536	18.691	1.086	0.376		1.536	18.691	1.086	0.360
2.828	37.088	1.536	22.015		2.828	37.088	1.536	21.784
5.040	21.179	2.828	35.809		5.040	21.179	2.828	36.193
7.735	16.983	5.020	22.385		7.735	16.983	5.020	21.601
11.208	0.082	7.736	19.002		11.208	0.082	7.736	19.694
		10.897	0.000				10.897	0.000
Seventh layer 6 - 7 cm								
Computed		Data						
Di (mm)	fi %	Di (mm)	fi %					
0.707	0.114	0.071	0.196					
1.086	5.863087	0.707	0.139					
1.536	18.69056	1.086	0.313					
2.828	37.08786	1.536	21.693					
5.040	21.17946	2.828	37.254					
7.735	16.98261	5.020	21.010					
11.208	0.08207	7.736	19.094					
		10.897	0.301					

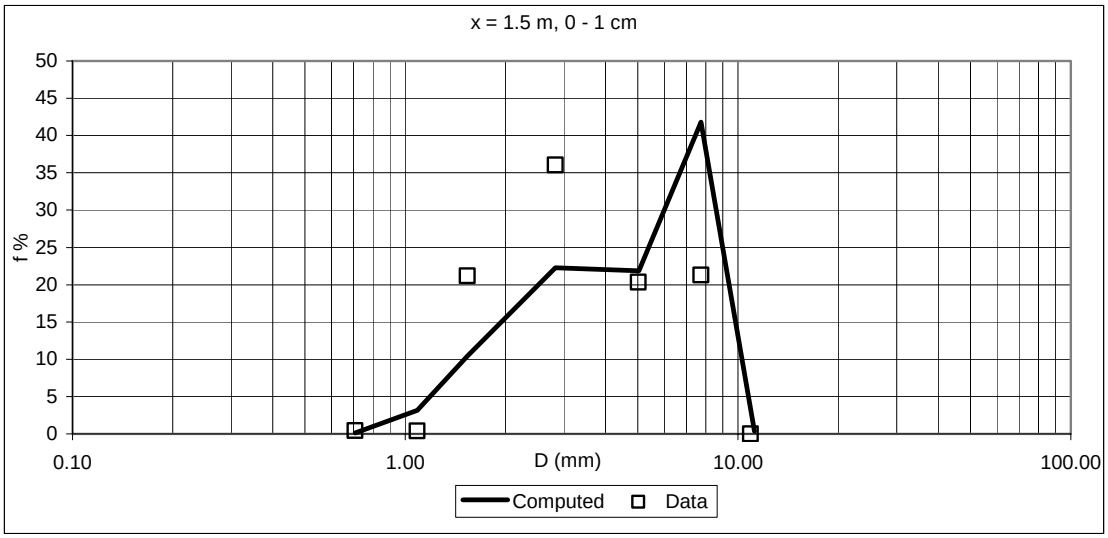
x = 1.5 m, 0 - 1 cm
f %
50
45
40
35
30
25
20
15
10
5
0
0.10
1.00
D (mm)
10.00
100.00
Computed
Data

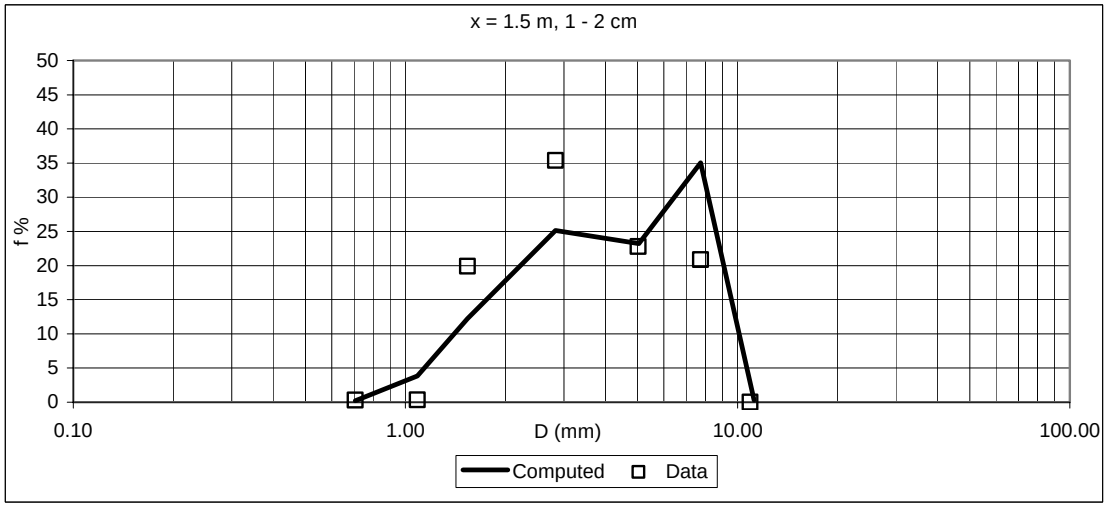
x = 1.5 m, 1 - 2 cm
f %
50
45
40
35
30
25
20
15
10
5
0
0.10
1.00
D (mm)
10.00
100.00
Computed
Data

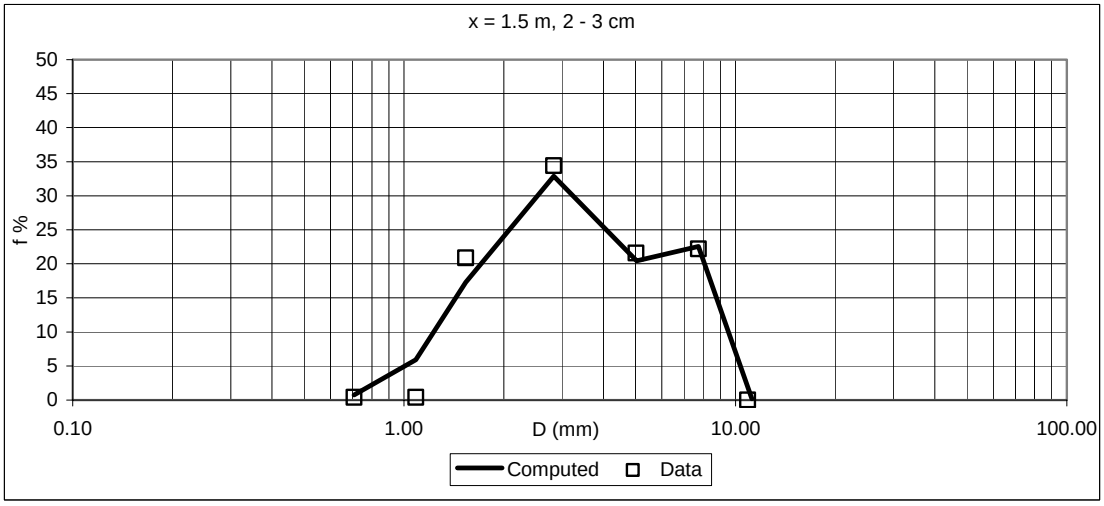
x = 1.5 m, 2 - 3 cm
f %
50
45
40
35
30
25
20
15
10
5
0
0.10
1.00
D (mm)
10.00
100.00
Computed
Data

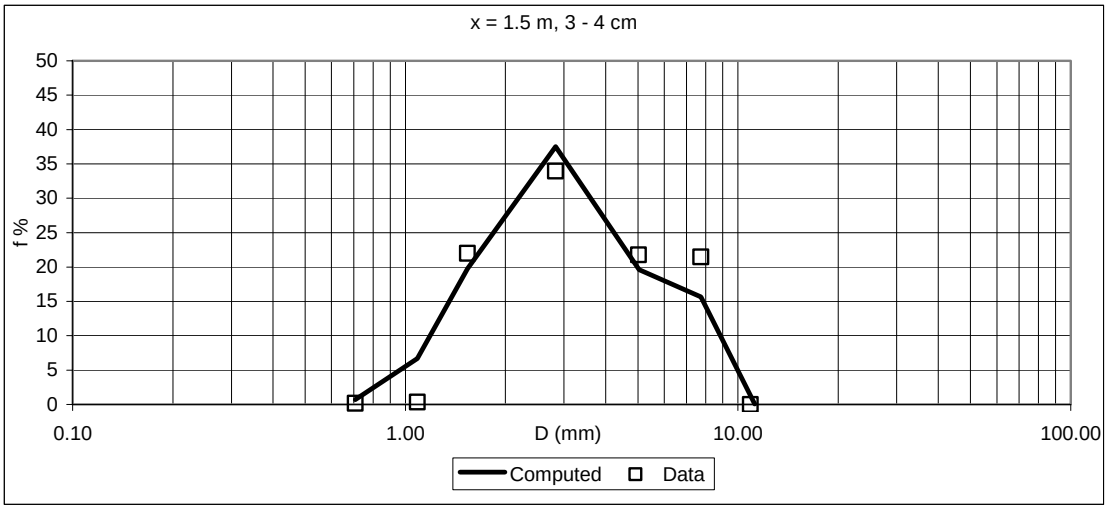
x = 1.5 m, 3 - 4 cm
f %
50
45
40
35
30
25
20
15
10
5
0
0.10
1.00
D (mm)
10.00
100.00
Computed
Data

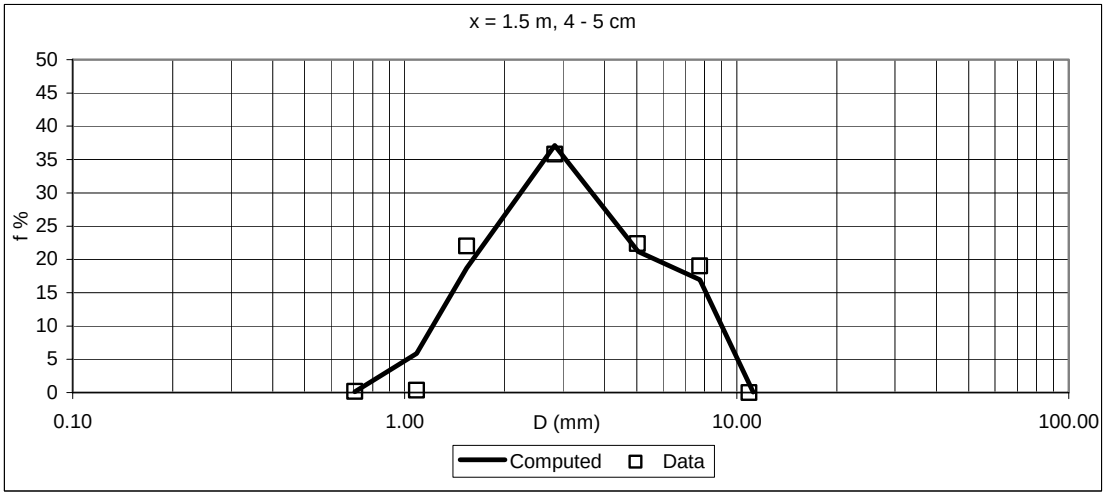
x = 1.5 m, 4 - 5 cm
f %
50
45
40
35
30
25
20
15
10
5
0
0.10
1.00
D (mm)
10.00
100.00
Computed
Data

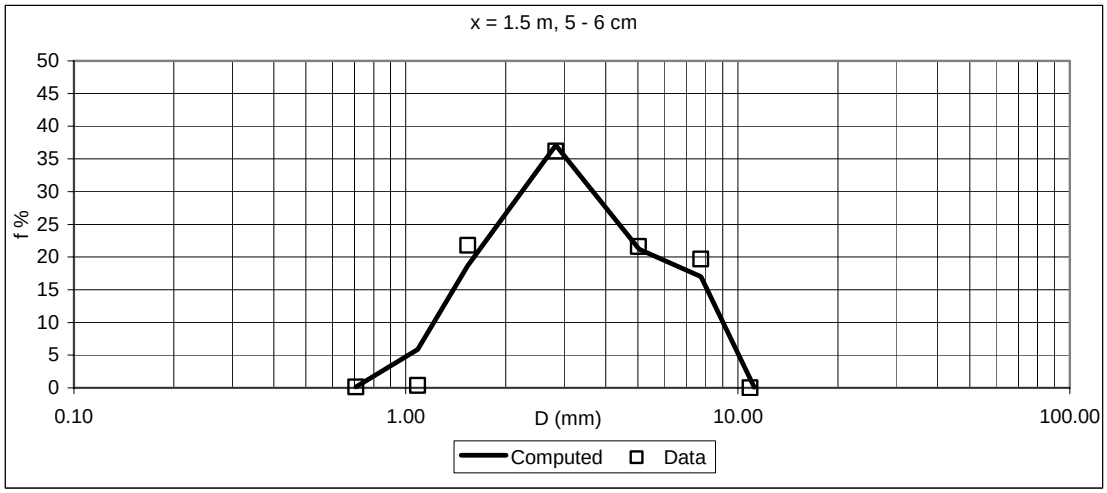
x = 1.5 m, 5 - 6 cm
f %
50
45
40
35
30
25
20
15
10
5
0
0.10
1.00
D (mm)
10.00
100.00
Computed
Data

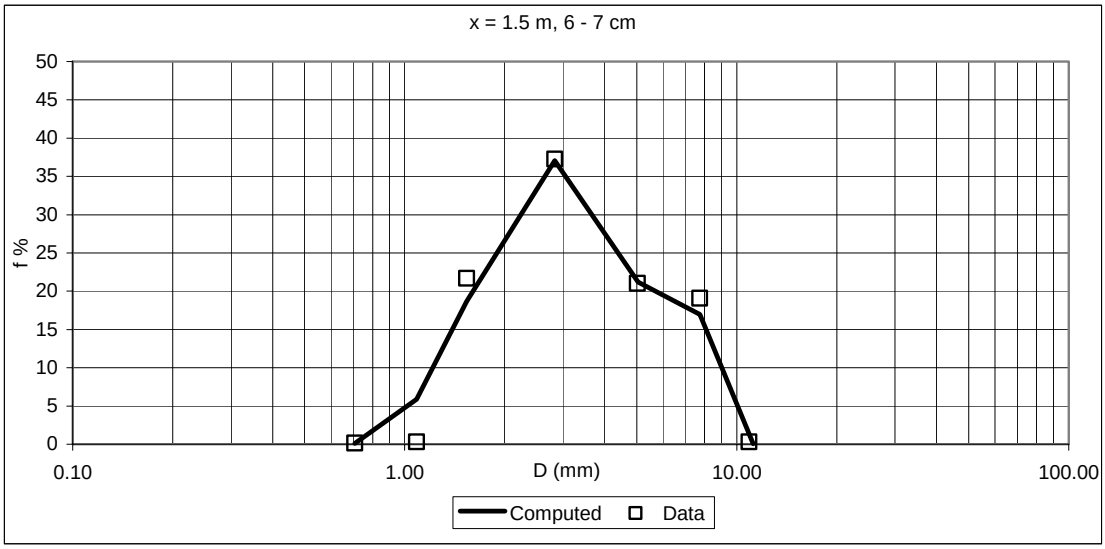
x = 1.5 m, 6 - 7 cm
50
45
40
35
30
25
20
15
10
5
0
f %
0.10
1.00
D (mm)
10.00
100.00
Computed
Data

x = 2 m								
First layer 0 -1 cm					Second layer 1 - 2 cm			
Computed		Data			Computed		Data	
Di (mm)	fi %	Di (mm)	fi %		Di (mm)	fi %	Di (mm)	fi %
0.707	0.105	0.071	0.236		0.707	0.168	0.071	0.328
1.086	3.168	0.707	0.350		1.086	3.590	0.707	0.220
1.536	10.442	1.086	0.222		1.536	11.609	1.086	0.262
2.828	22.283	1.536	17.337		2.828	24.291	1.536	17.046
5.040	21.760	2.828	33.119		5.040	23.716	2.828	34.314
7.735	41.867	5.020	23.003		7.735	36.294	5.020	24.096
11.208	0.374	7.736	25.607		11.208	0.333	7.736	23.735
		10.897	0.127				10.897	0.000
Third layer 2 - 3 cm					Fourth layer 3 - 4 cm			
Computed		Data			Computed		Data	
Di (mm)	fi %	Di (mm)	fi %		Di (mm)	fi %	Di (mm)	fi %
0.707	0.930	0.071	0.296		0.707	0.432	0.071	0.225
1.086	6.835	0.707	0.164		1.086	6.306	0.707	0.114
1.536	19.480	1.086	0.320		1.536	19.265	1.086	0.292
2.828	35.864	1.536	18.907		2.828	37.271	1.536	19.149
5.040	18.862	2.828	34.444		5.040	20.384	2.828	32.565
7.735	17.913	5.020	22.923		7.735	16.264	5.020	25.217
11.208	0.116	7.736	22.946		11.208	0.078	7.736	22.325
		10.897	0.000				10.897	0.114
Fifth layer 4 - 5 cm					Sixth layer 5 - 6 cm			
Computed		Data			Computed		Data	
Di (mm)	fi %	Di (mm)	fi %		Di (mm)	fi %	Di (mm)	fi %
0.707	0.144	0.071	0.219		0.707	0.114	0.071	0.185
1.086	5.889	0.707	0.127		1.086	5.863	0.707	0.114
1.536	18.706	1.086	0.291		1.536	18.691	1.086	0.338
2.828	37.065	1.536	20.983		2.828	37.088	1.536	21.188
5.040	21.153	2.828	35.390		5.040	21.179	2.828	33.778
7.735	16.961	5.020	21.384		7.735	16.983	5.020	22.394
11.208	0.082	7.736	21.428		11.208	0.082	7.736	21.629
		10.897	0.178				10.897	0.374
Seventh layer 6 - 7 cm								
Computed		Data						
Di (mm)	fi %	Di (mm)	fi %					
0.707	0.114	0.071	0.144					
1.086	5.863087	0.707	0.112999					
1.536	18.69056	1.086	0.340465					
2.828	37.08786	1.536	20.56001					
5.040	21.17946	2.828	33.03543					
7.735	16.98261	5.020	23.21916					
11.208	0.08207	7.736	22.47806					
		10.897	0.110064					

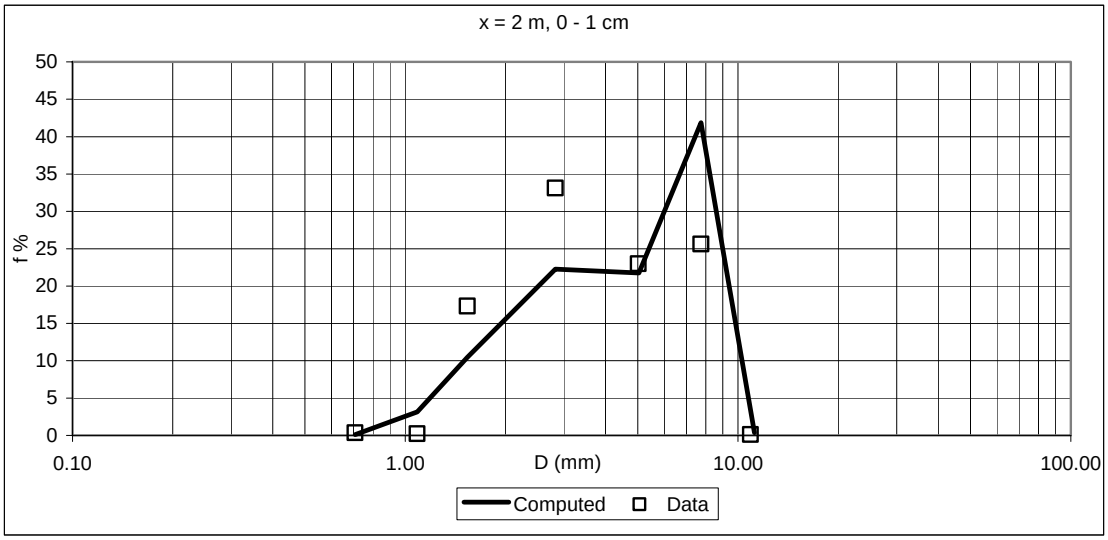
x = 2 m, 0 - 1 cm
f %
50
45
40
35
30
25
20
15
10
5
0
0.10
1.00
D (mm)
10.00
100.00
Computed
Data

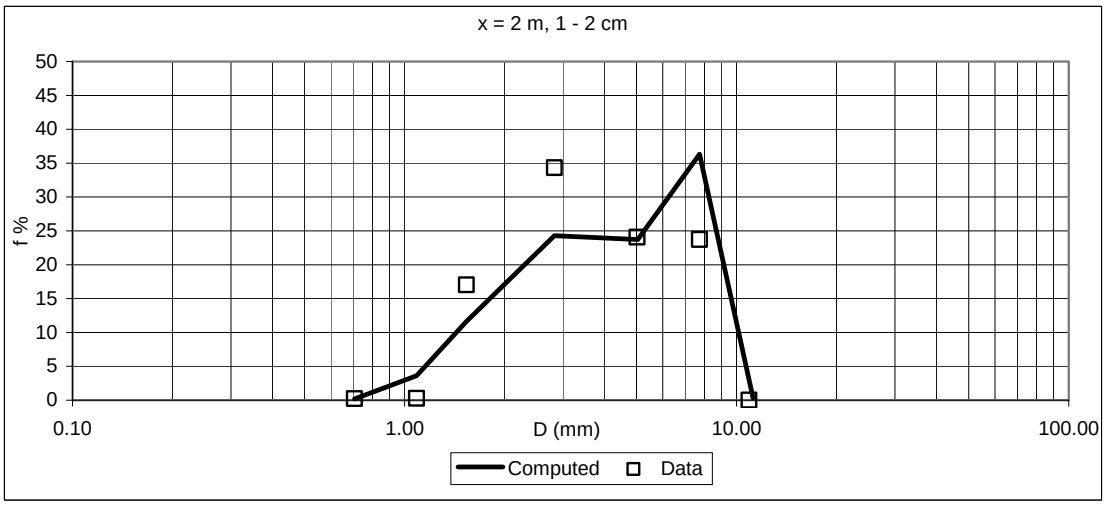
x = 2 m, 1 - 2 cm
f %
50
45
40
35
30
25
20
15
10
5
0
0.10
1.00
D (mm)
10.00
100.00
Computed
Data

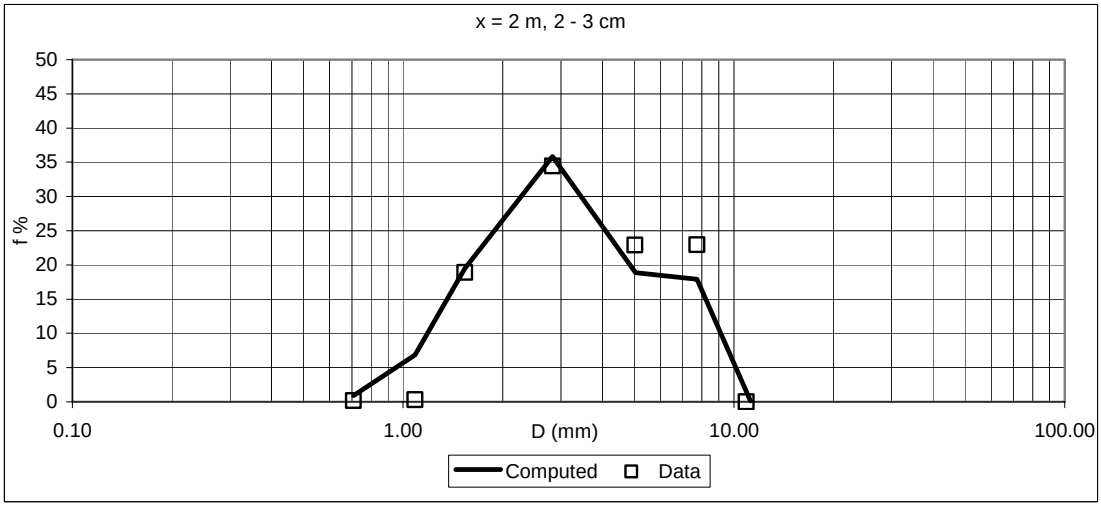
x = 2 m, 2 - 3 cm
f %
50
45
40
35
30
25
20
15
10
5
0
0.10
1.00
D (mm)
10.00
100.00
Computed
Data

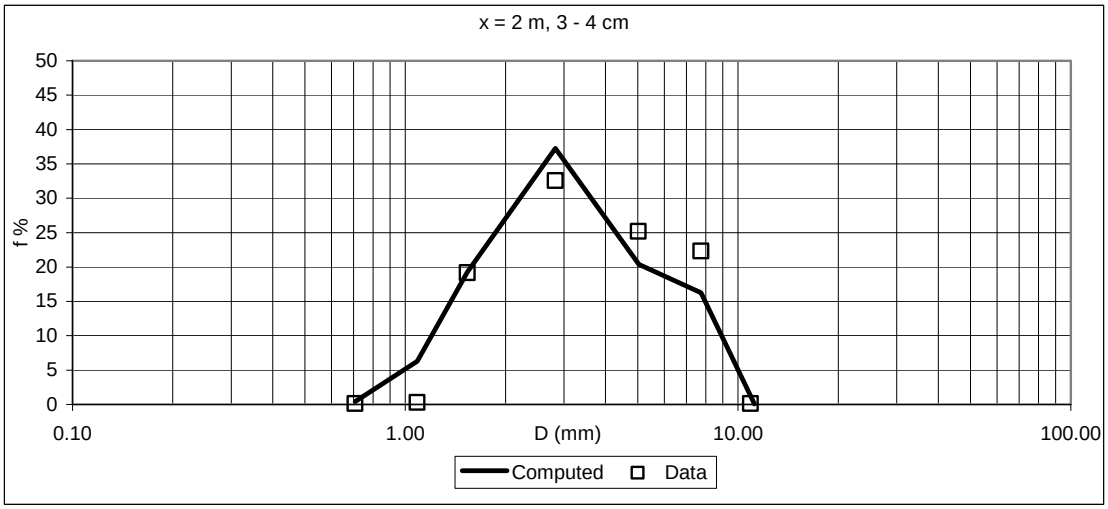
x = 2 m, 3 - 4 cm
f %
50
45
40
35
30
25
20
15
10
5
0
0.10
1.00
D (mm)
10.00
100.00
Computed
Data

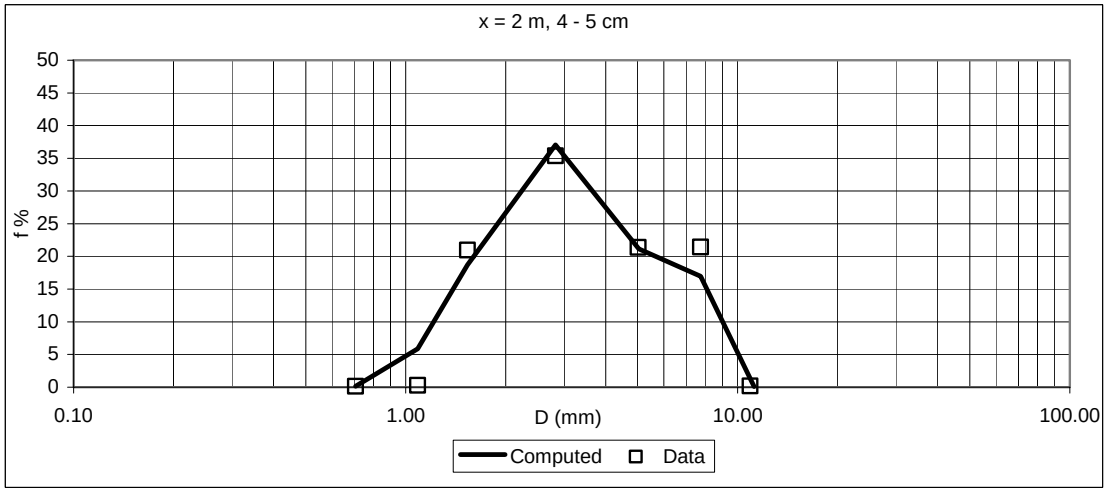
x = 2 m, 4 - 5 cm
f %
50
45
40
35
30
25
20
15
10
5
0
0.10
1.00
D (mm)
10.00
100.00
Computed
Data

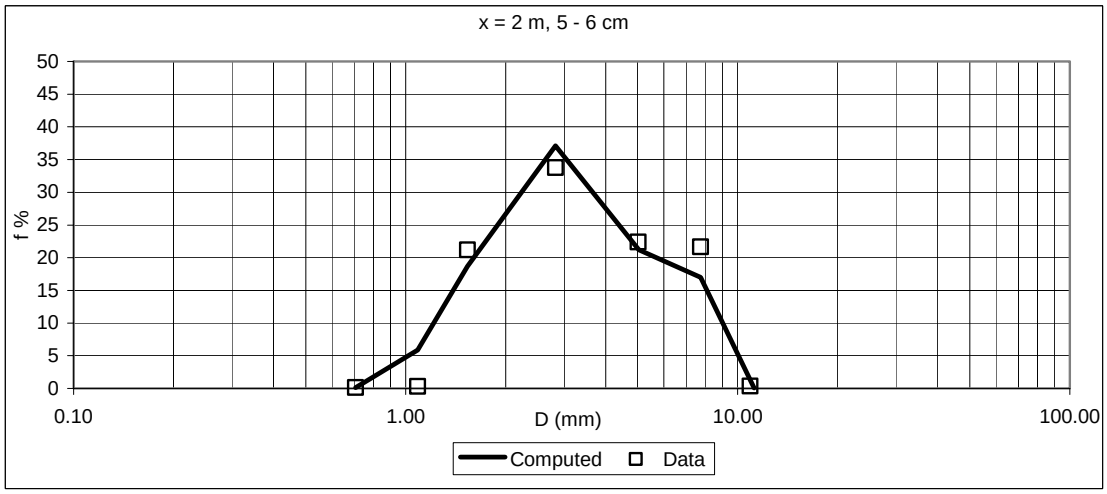
x = 2 m, 5 - 6 cm
f %
50
45
40
35
30
25
20
15
10
5
0
0.10
1.00
D (mm)
10.00
100.00
Computed
Data

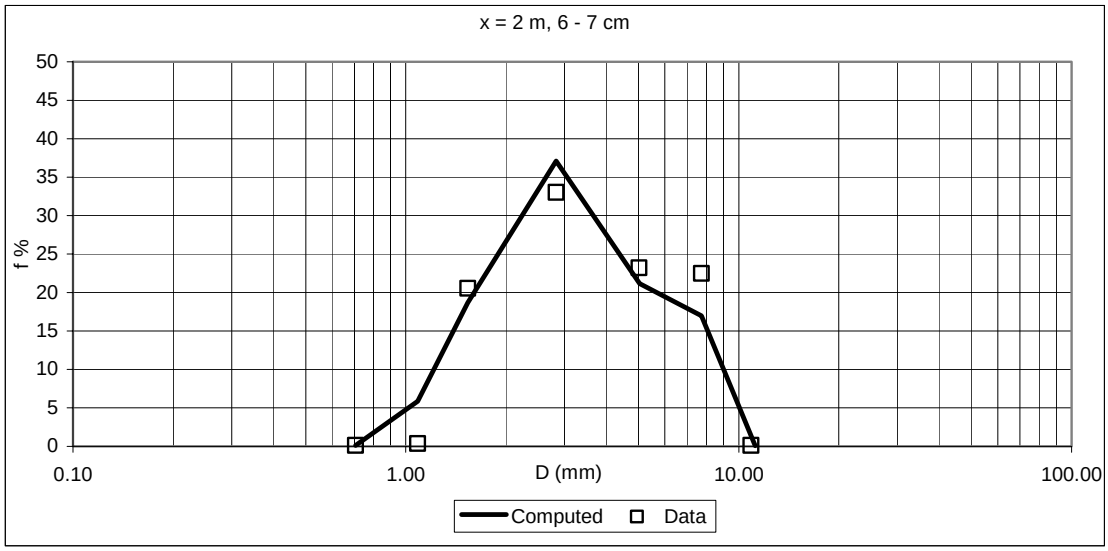
x = 2 m, 6 - 7 cm
50
45
40
35
30
25
20
15
10
5
0
f %
0.10
1.00
D (mm)
10.00
100.00
Computed
Data

x = 2.5 m								
First layer 0 -1 cm					Second layer 1 - 2 cm			
Computed		Data			Computed		Data	
Di (mm)	fi %	Di (mm)	fi %		Di (mm)	fi %	Di (mm)	fi %
0.707	0.107	0.071	0.185		0.707	0.131	0.071	0.216
1.086	3.194	0.707	0.300		1.086	3.830	0.707	0.208
1.536	10.514	1.086	0.313		1.536	12.324	1.086	0.272
2.828	22.410	1.536	17.398		2.828	25.347	1.536	18.336
5.040	21.907	2.828	34.805		5.040	22.941	2.828	34.280
7.735	41.497	5.020	22.940		7.735	35.109	5.020	23.101
11.208	0.370	7.736	24.059		11.208	0.318	7.736	23.410
		10.897	0.000				10.897	0.176
Third layer 2 - 3 cm					Fourth layer 3 - 4 cm			
Computed		Data			Computed		Data	
Di (mm)	fi %	Di (mm)	fi %		Di (mm)	fi %	Di (mm)	fi %
0.707	0.154	0.071	0.170		0.707	0.117	0.071	0.158
1.086	6.847	0.707	0.152		1.086	5.949	0.707	0.116
1.536	20.962	1.086	0.279		1.536	18.858	1.086	0.260
2.828	39.309	1.536	17.992		2.828	37.152	1.536	17.539
5.040	18.497	2.828	34.286		5.040	21.004	2.828	34.293
7.735	14.165	5.020	24.555		7.735	16.839	5.020	22.456
11.208	0.067	7.736	22.566		11.208	0.081	7.736	25.178
		10.897	0.000				10.897	0.000
Fifth layer 4 - 5 cm					Sixth layer 5 - 6 cm			
Computed		Data			Computed		Data	
Di (mm)	fi %	Di (mm)	fi %		Di (mm)	fi %	Di (mm)	fi %
0.707	0.114	0.071	0.156		0.707	0.114	0.071	0.162
1.086	5.863	0.707	0.105		1.086	5.863	0.707	0.116
1.536	18.691	1.086	0.303		1.536	18.691	1.086	0.303
2.828	37.088	1.536	20.186		2.828	37.088	1.536	20.425
5.040	21.179	2.828	34.748		5.040	21.179	2.828	34.694
7.735	16.983	5.020	23.611		7.735	16.983	5.020	24.315
11.208	0.082	7.736	20.890		11.208	0.082	7.736	19.805
		10.897	0.000				10.897	0.180
Seventh layer 6 - 7 cm								
Computed		Data						
Di (mm)	fi %	Di (mm)	fi %					
0.707	0.114	0.071	0.146					
1.086	5.863087	0.707	0.110					
1.536	18.69056	1.086	0.327					
2.828	37.08786	1.536	21.796					
5.040	21.17946	2.828	34.944					
7.735	16.98261	5.020	21.594					
11.208	0.08207	7.736	21.082					
		10.897	0.000					

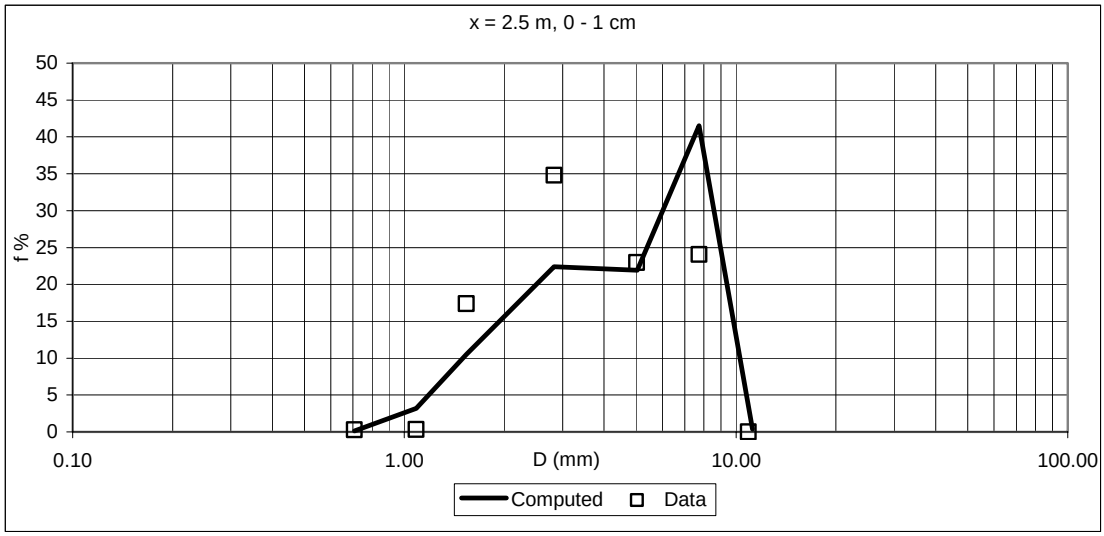
x = 2.5 m, 0 - 1 cm
f %
D (mm)
0.10
1.00
10.00
100.00
Computed
Data

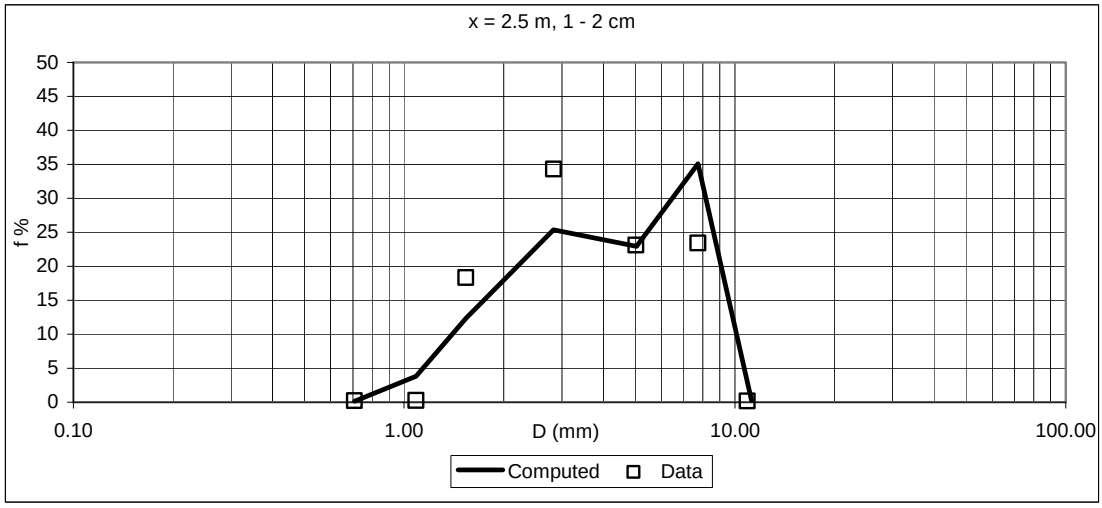
x = 2.5 m, 1 - 2 cm
f %
D (mm)
0.10
1.00
10.00
100.00
Computed
Data

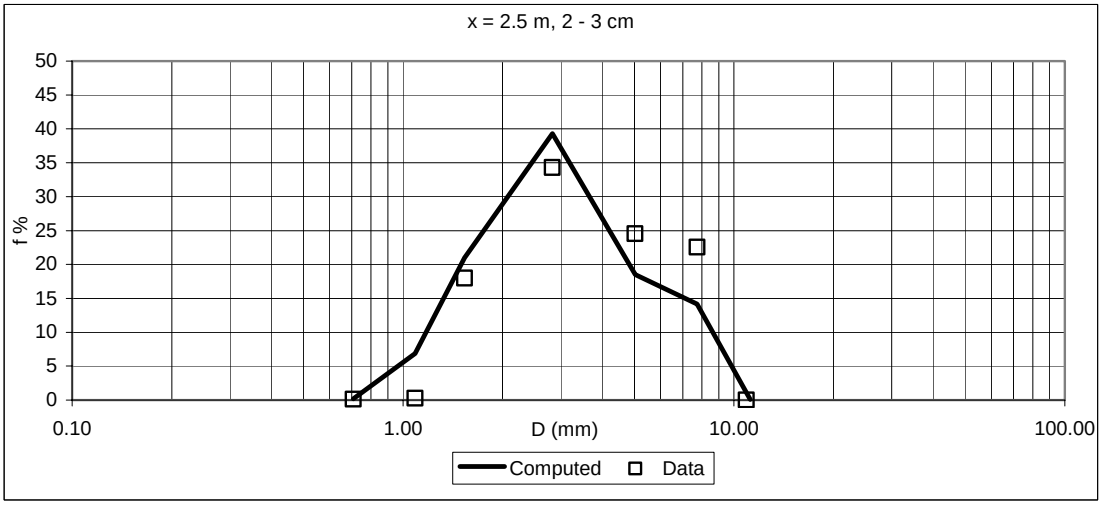
x = 2.5 m, 2 - 3 cm
f %
D (mm)
0.10
1.00
10.00
100.00
Computed
Data

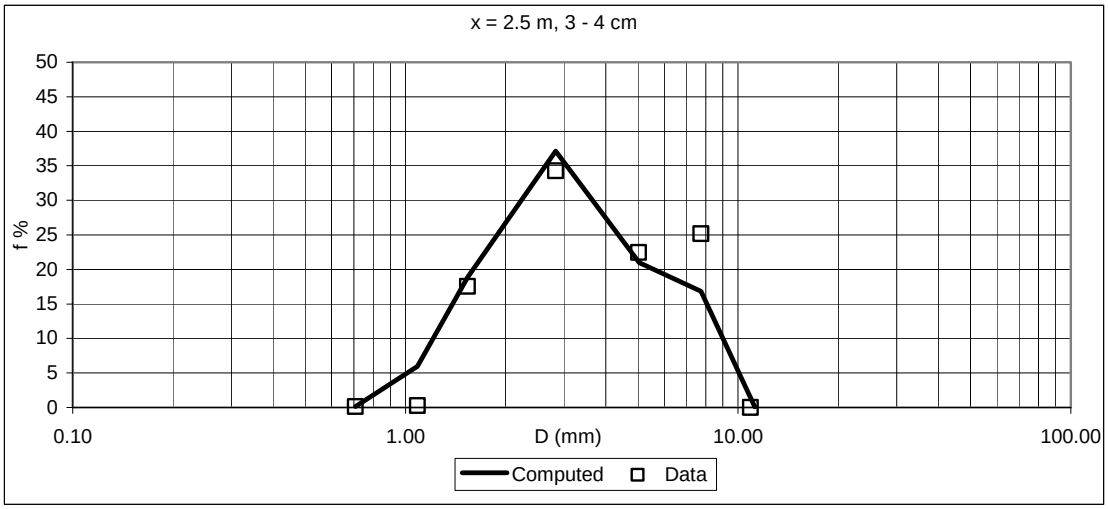
x = 2.5 m, 3 - 4 cm
f %
50
45
40
35
30
25
20
15
10
5
0
0.10
1.00
D (mm)
10.00
100.00
Computed
Data

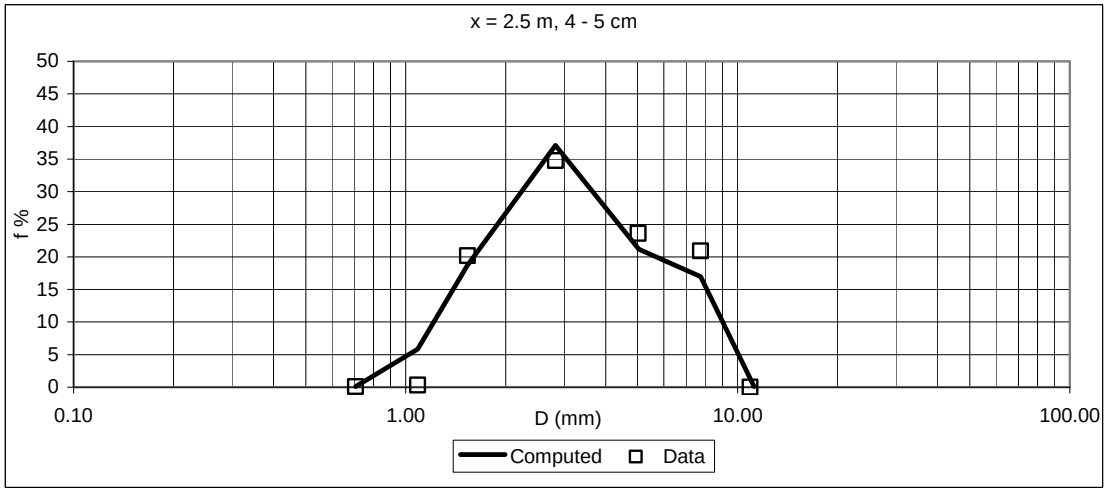
x = 2.5 m, 4 - 5 cm
f %
50
45
40
35
30
25
20
15
10
5
0
0.10
1.00
D (mm)
10.00
100.00
Computed
Data

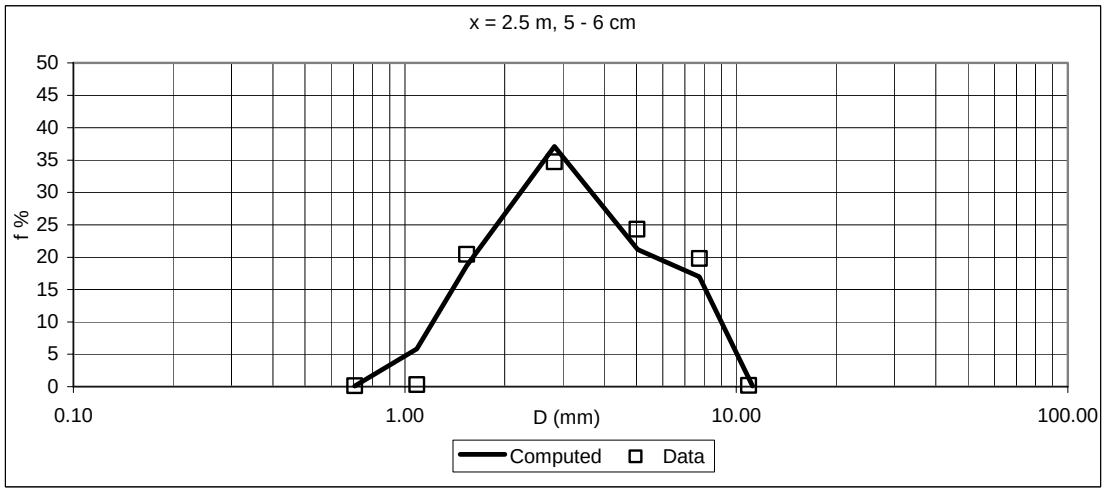
x = 2.5 m, 5 - 6 cm
f %
50
45
40
35
30
25
20
15
10
5
0
0.10
1.00
D (mm)
10.00
100.00
Computed
Data

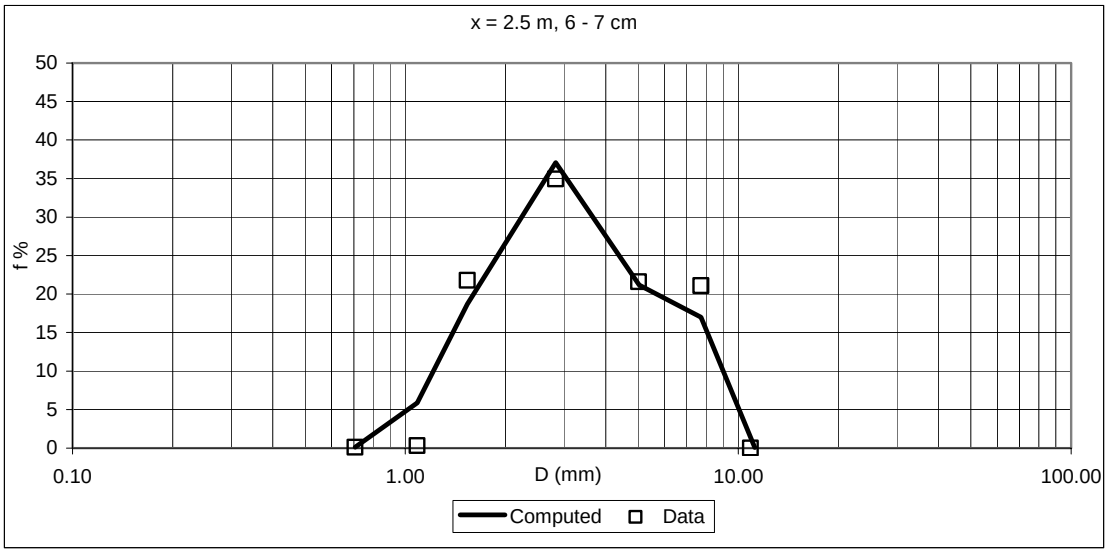
x = 2.5 m, 6 - 7 cm
50
45
40
35
30
25
20
15
10
5
0
f %
0.10
1.00
D (mm)
10.00
100.00
Computed
Data

x = 3 m								
First layer 0 -1 cm					Second layer 1 - 2 cm			
Computed		Data			Computed		Data	
Di (mm)	fi %	Di (mm)	fi %		Di (mm)	fi %	Di (mm)	fi %
0.707	0.107	0.071	0.129		0.707	0.135	0.071	0.176
1.086	3.177	0.707	0.235		1.086	4.685	0.707	0.166
1.536	10.459	1.086	0.337		1.536	14.972	1.086	0.344
2.828	22.300	1.536	19.320		2.828	30.202	1.536	20.253
5.040	21.951	2.828	34.082		5.040	21.783	2.828	34.391
7.735	41.642	5.020	23.464		7.735	27.992	5.020	22.305
11.208	0.365	7.736	22.432		11.208	0.231	7.736	22.364
		10.897	0.000				10.897	0.000
Third layer 2 - 3 cm					Fourth layer 3 - 4 cm			
Computed		Data			Computed		Data	
Di (mm)	fi %	Di (mm)	fi %		Di (mm)	fi %	Di (mm)	fi %
0.707	0.134	0.071	0.135		0.707	0.115	0.071	0.117
1.086	6.102	0.707	0.126		1.086	5.883	0.707	0.227
1.536	19.302	1.086	0.330		1.536	18.740	1.086	0.199
2.828	37.946	1.536	20.458		2.828	37.155	1.536	19.296
5.040	20.420	2.828	34.969		5.040	21.108	2.828	32.747
7.735	16.020	5.020	22.451		7.735	16.917	5.020	21.864
11.208	0.076	7.736	21.532		11.208	0.082	7.736	25.358
		10.897	0.000				10.897	0.191
Fifth layer 4 - 5 cm								
Computed		Data						
Di (mm)	fi %	Di (mm)	fi %					
0.707	0.114	0.071	0.157					
1.086	5.863	0.707	0.100					
1.536	18.691	1.086	0.322					
2.828	37.088	1.536	20.177					
5.040	21.179	2.828	35.067					
7.735	16.983	5.020	22.919					
11.208	0.082	7.736	21.257					
		10.897	0.000					

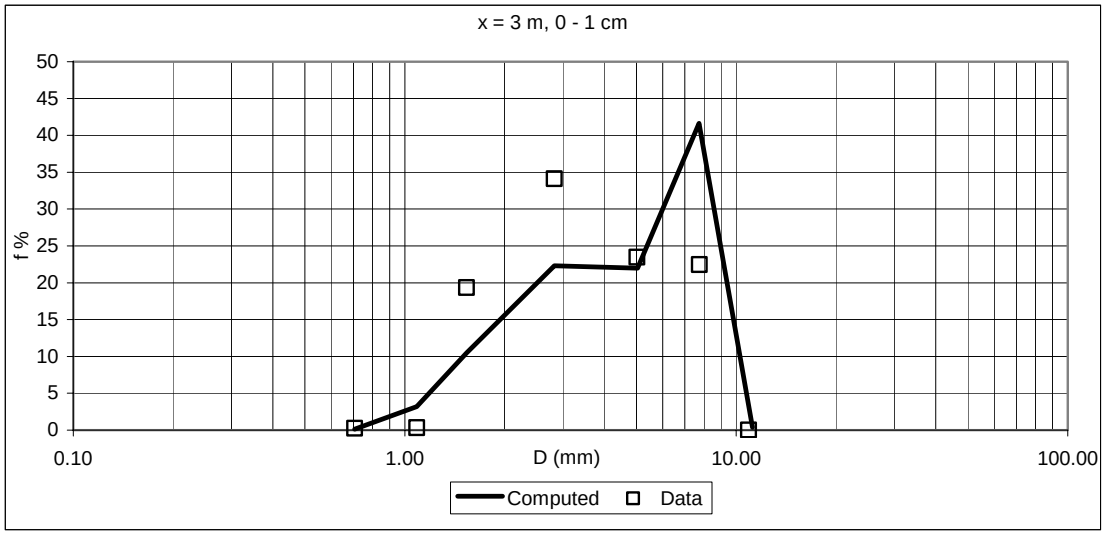
x = 3 m, 0 - 1 cm
f %
50
45
40
35
30
25
20
15
10
5
0
0.10
1.00
D (mm)
10.00
100.00
Computed
Data

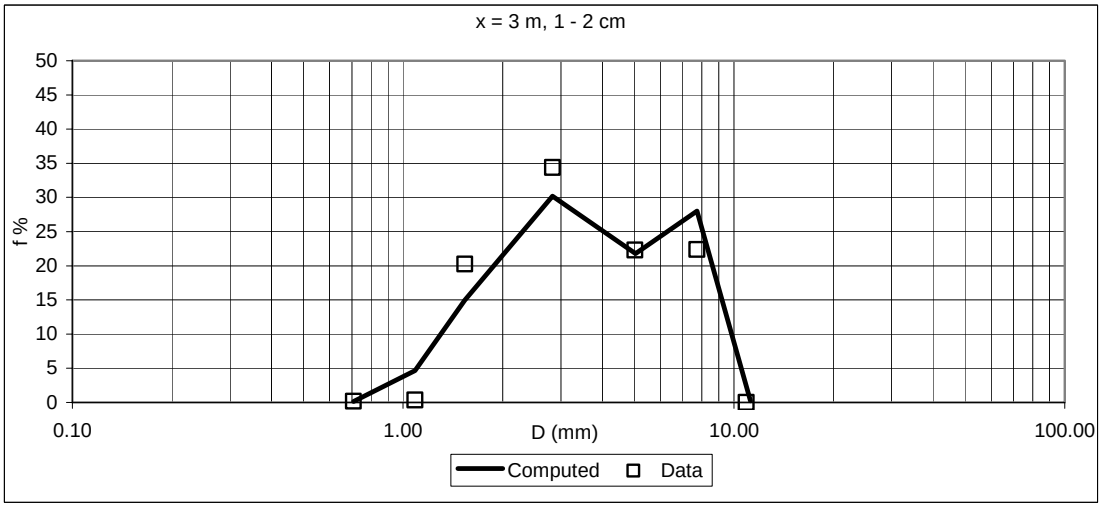
x = 3 m, 1 - 2 cm
f %
50
45
40
35
30
25
20
15
10
5
0
0.10
1.00
D (mm)
10.00
100.00
Computed
Data

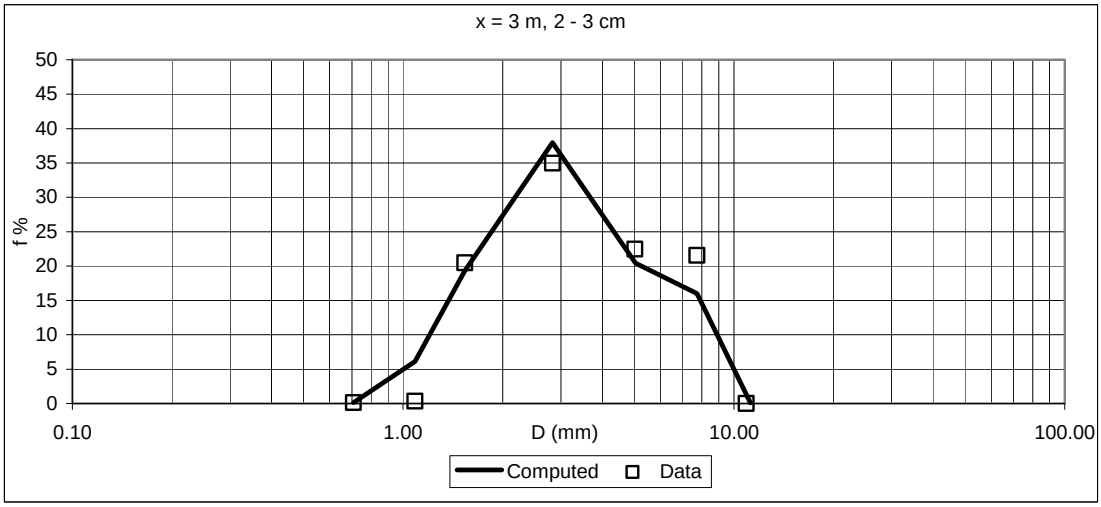
x = 3 m, 2 - 3 cm
f %
50
45
40
35
30
25
20
15
10
5
0
0.10
1.00
D (mm)
10.00
100.00
Computed
Data

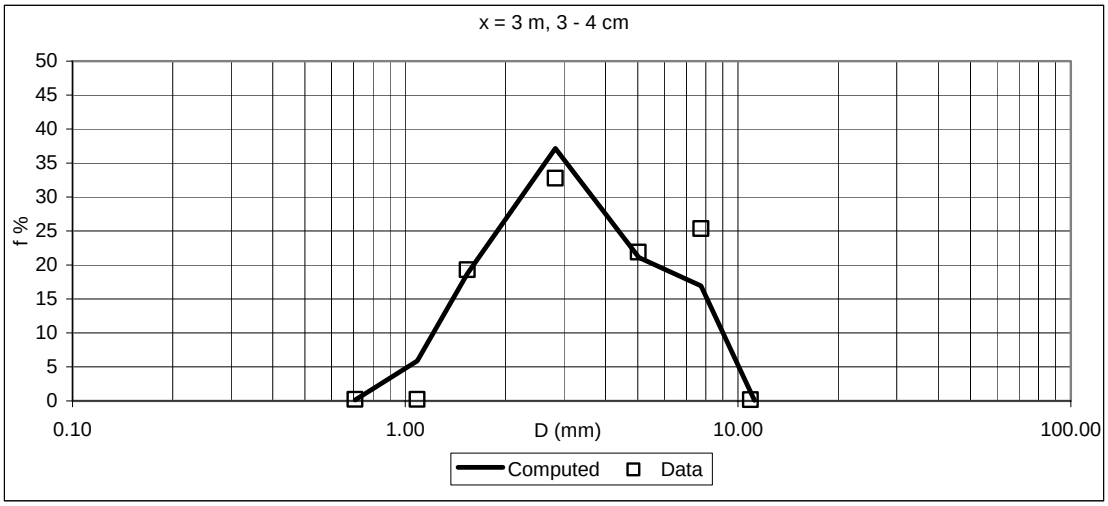
x = 3 m, 3 - 4 cm
50
45
40
35
30
25
20
15
10
5
0
f %
0.10
1.00
D (mm)
10.00
100.00
Computed
Data

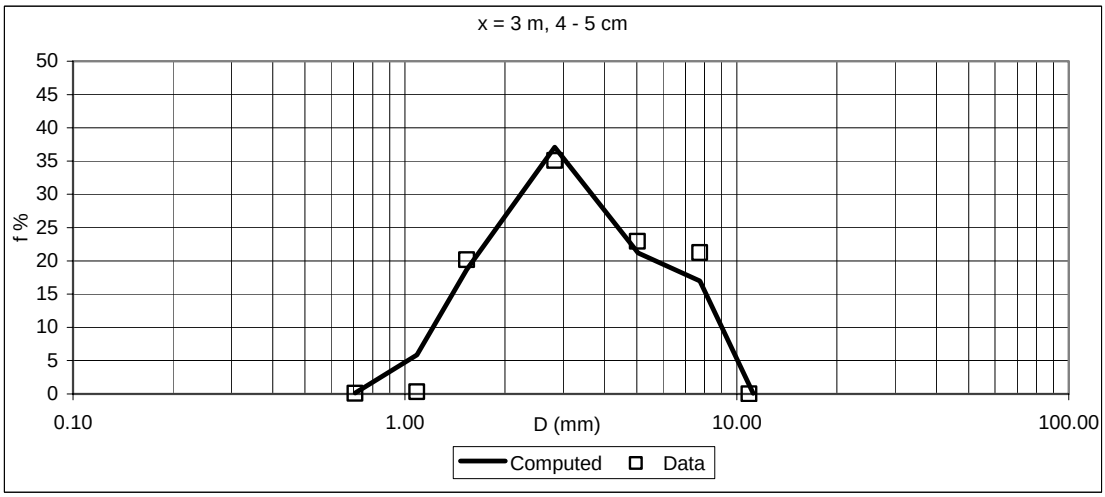
x = 3 m, 4 - 5 cm
50
45
40
35
30
25
20
15
10
5
0
f %
0.10
1.00
D (mm)
10.00
100.00
Computed
Data

x = 4 m								
First layer 0 -1 cm					Second layer 1 - 2 cm			
Computed		Data			Computed		Data	
Di (mm)	fi %	Di (mm)	fi %		Di (mm)	fi %	Di (mm)	fi %
0.707	0.108	0.071	0.099		0.707	0.125	0.071	0.117
1.086	3.247	0.707	0.214		1.086	3.988	0.707	0.130
1.536	10.664	1.086	0.393		1.536	12.935	1.086	0.363
2.828	22.644	1.536	22.859		2.828	26.790	1.536	21.712
5.040	21.893	2.828	32.735		5.040	22.343	2.828	36.388
7.735	41.112	5.020	19.773		7.735	33.577	5.020	22.919
11.208	0.332	7.736	23.928		11.208	0.243	7.736	18.371
		10.897	0.000				10.897	0.000
Third layer 2 - 3 cm					Fourth layer 3 - 4 cm			
Computed		Data			Computed		Data	
Di (mm)	fi %	Di (mm)	fi %		Di (mm)	fi %	Di (mm)	fi %
0.707	0.113	0.071	0.116		0.707	0.114	0.071	0.110
1.086	5.792	0.707	0.115		1.086	5.863	0.707	0.117
1.536	18.493	1.086	0.387		1.536	18.691	1.086	0.446
2.828	36.816	1.536	24.099		2.828	37.088	1.536	26.853
5.040	21.555	2.828	35.614		5.040	21.179	2.828	36.168
7.735	17.147	5.020	22.014		7.735	16.983	5.020	21.940
11.208	0.083	7.736	17.656		11.208	0.082	7.736	14.366
		10.897	0.000				10.897	0.000
Fifth layer 4 - 5 cm								
Computed		Data						
Di (mm)	fi %	Di (mm)	fi %					
0.707	0.114	0.071	0.100					
1.086	5.863	0.707	0.115					
1.536	18.691	1.086	0.418					
2.828	37.088	1.536	24.327					
5.040	21.179	2.828	34.520					
7.735	16.983	5.020	20.469					
11.208	0.082	7.736	20.050					
		10.897	0.000					

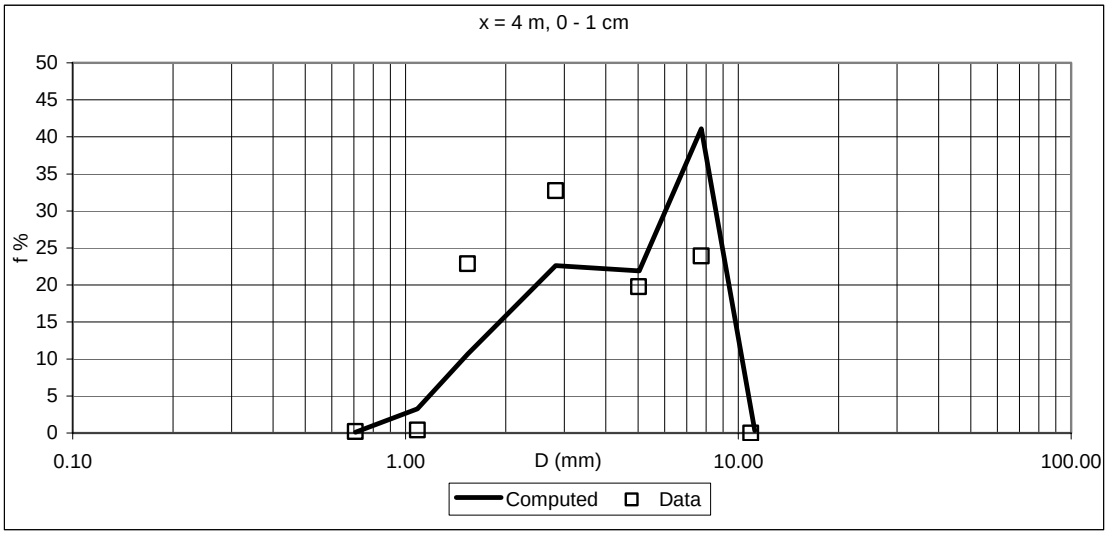
x = 4 m, 0 - 1 cm
50
45
40
35
30
25
20
15
10
5
0
f %
0.10
1.00
D (mm)
10.00
100.00
Computed
Data

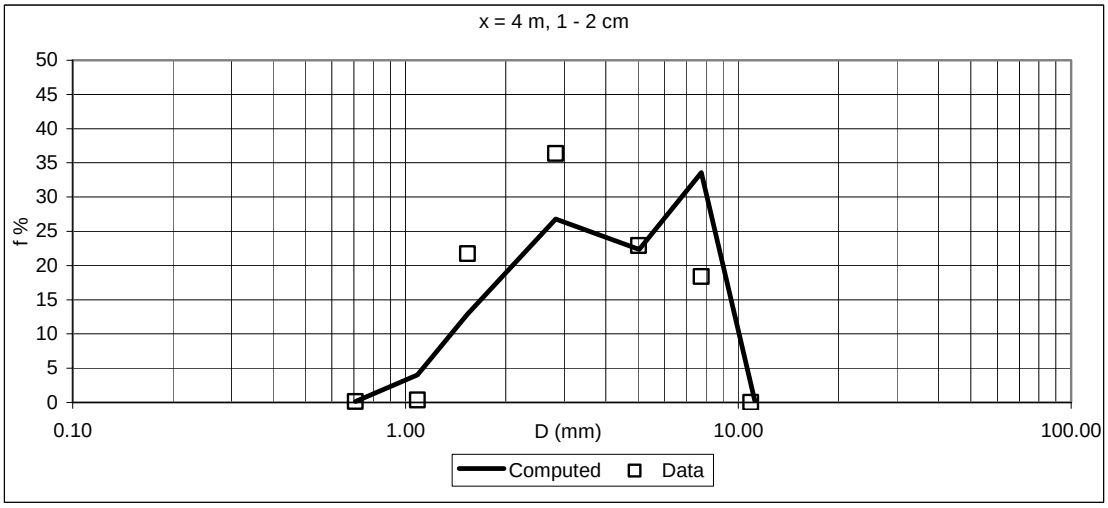
x = 4 m, 1 - 2 cm
50
45
40
35
30
25
20
15
10
5
0
f %
0.10
1.00
D (mm)
10.00
100.00
Computed
Data

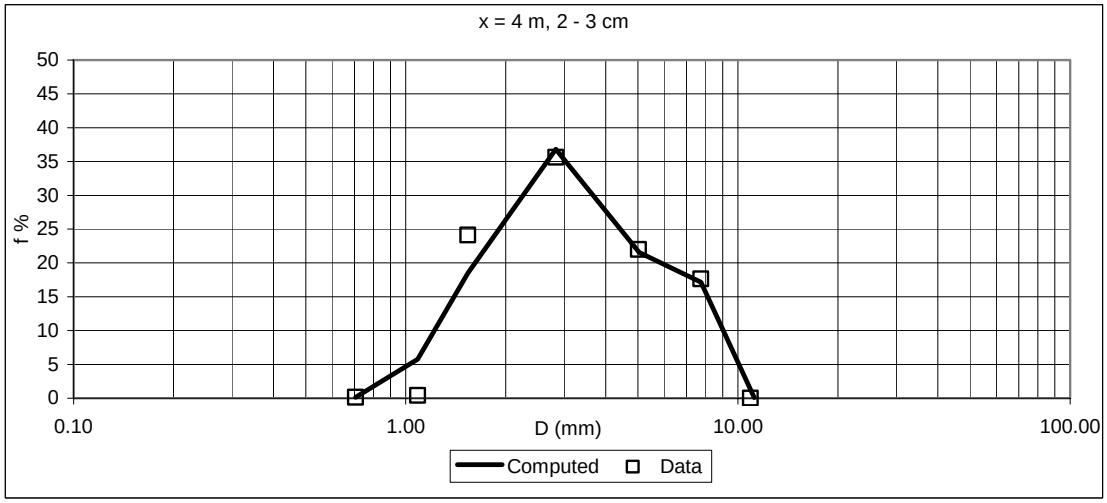
x = 4 m, 2 - 3 cm
50
45
40
35
30
25
20
15
10
5
0
f %
0.10
1.00
D (mm)
10.00
100.00
Computed
Data

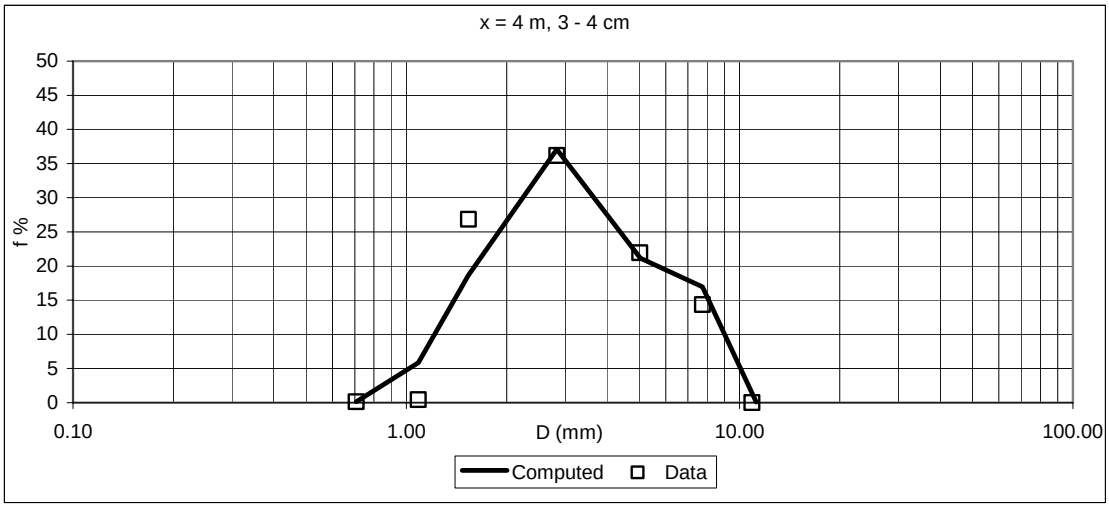
x = 4 m, 3 - 4 cm
50
45
40
35
30
25
20
15
10
5
0
f %
0.10
1.00
D (mm)
10.00
100.00
Computed
Data

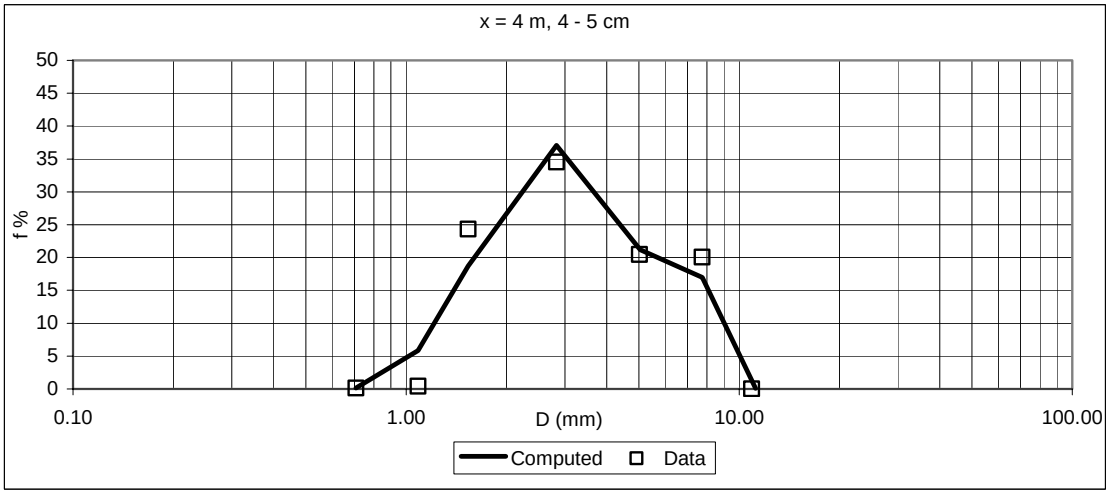
x = 4 m, 4 - 5 cm
50
45
40
35
30
25
20
15
10
5
0
f %
0.10
1.00
D (mm)
10.00
100.00
Computed
Data

x = 5 m								
First layer 0 -1 cm					Second layer 1 - 2 cm			
Computed		Data			Computed		Data	
Di (mm)	fi %	Di (mm)	fi %		Di (mm)	fi %	Di (mm)	fi %
0.707	0.106	0.071	0.056		0.707	0.110	0.071	0.085
1.086	3.170	0.707	0.164		1.086	5.145	0.707	0.126
1.536	10.425	1.086	0.319		1.536	16.533	1.086	0.322
2.828	22.175	1.536	17.945		2.828	33.360	1.536	17.033
5.040	21.929	2.828	28.981		5.040	22.556	2.828	30.892
7.735	41.871	5.020	23.971		7.735	22.169	5.020	25.004
11.208	0.323	7.736	28.564		11.208	0.127	7.736	26.537
		10.897	0.000				10.897	0.000
Third layer 2 - 3 cm					Fourth layer 3 - 4 cm			
Computed		Data			Computed		Data	
Di (mm)	fi %	Di (mm)	fi %		Di (mm)	fi %	Di (mm)	fi %
0.707	0.114	0.071	0.103		0.707	0.114	0.071	0.139
1.086	5.810	0.707	0.121		1.086	5.863	0.707	0.106
1.536	18.534	1.086	0.308		1.536	18.691	1.086	0.383
2.828	36.829	1.536	19.067		2.828	37.088	1.536	20.861
5.040	21.371	2.828	33.318		5.040	21.179	2.828	32.620
7.735	17.259	5.020	23.575		7.735	16.983	5.020	22.941
11.208	0.084	7.736	23.508		11.208	0.082	7.736	22.950
		10.897	0.000				10.897	0.000
Fifth layer 4 - 5 cm								
Computed		Data						
Di (mm)	fi %	Di (mm)	fi %					
0.707	0.114	0.071	0.102					
1.086	5.863	0.707	0.097					
1.536	18.691	1.086	0.344					
2.828	37.088	1.536	21.030					
5.040	21.179	2.828	35.309					
7.735	16.983	5.020	22.212					
11.208	0.082	7.736	20.906					
		10.897	0.000					

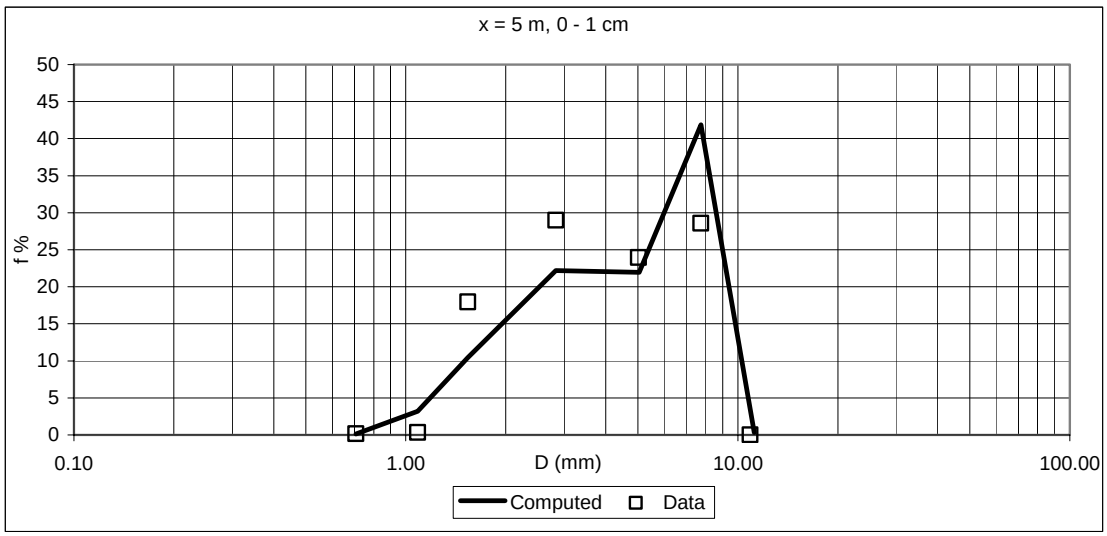
x = 5 m, 0 - 1 cm
f %
D (mm)
0.10
1.00
10.00
100.00
Computed
Data

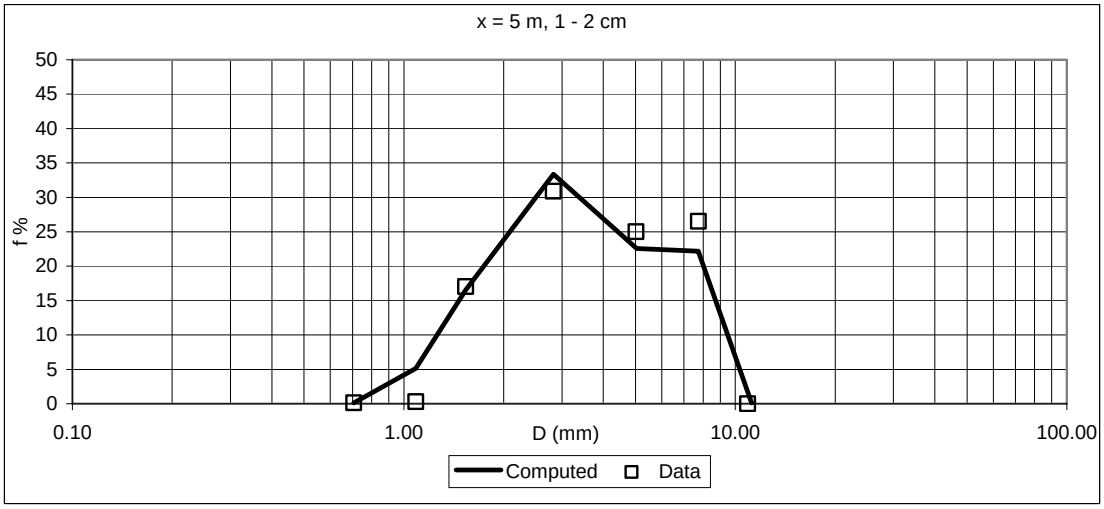
x = 5 m, 1 - 2 cm
f %
D (mm)
0.10
1.00
10.00
100.00
Computed
Data

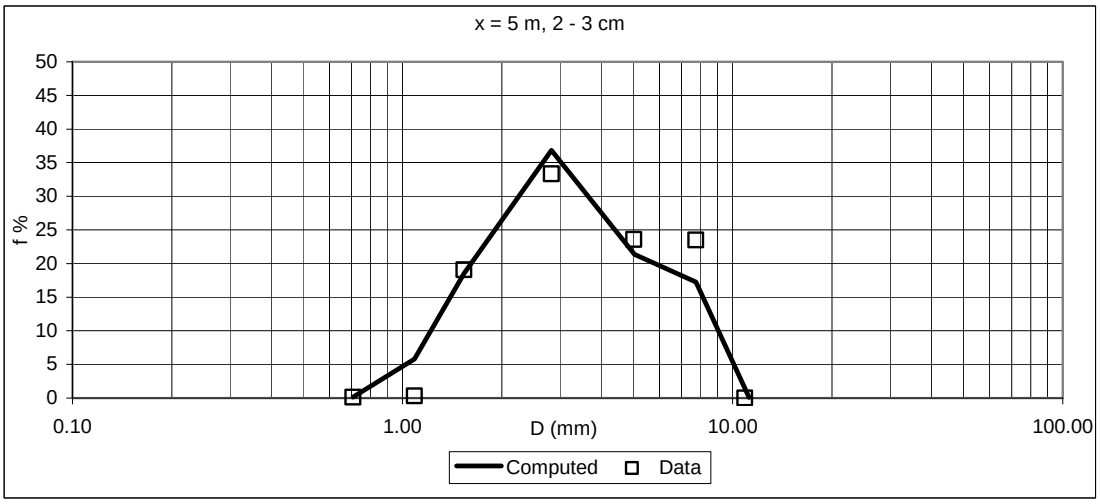
x = 5 m, 2 - 3 cm
f %
D (mm)
0.10
1.00
10.00
100.00
Computed
Data

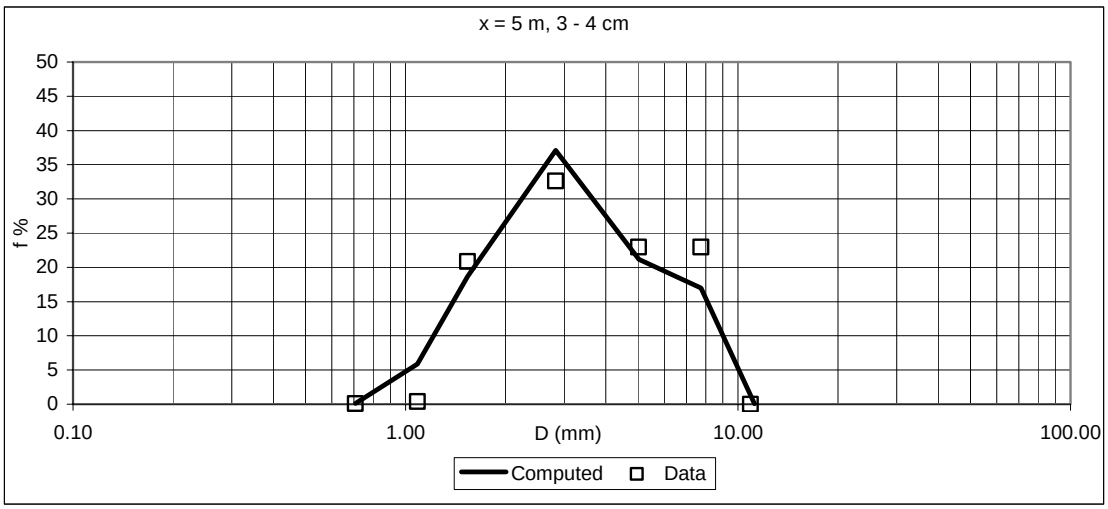
x = 5 m, 3 - 4 cm
50
45
40
35
30
25
20
15
10
5
0
f %
0.10
1.00
D (mm)
10.00
100.00
Computed
Data

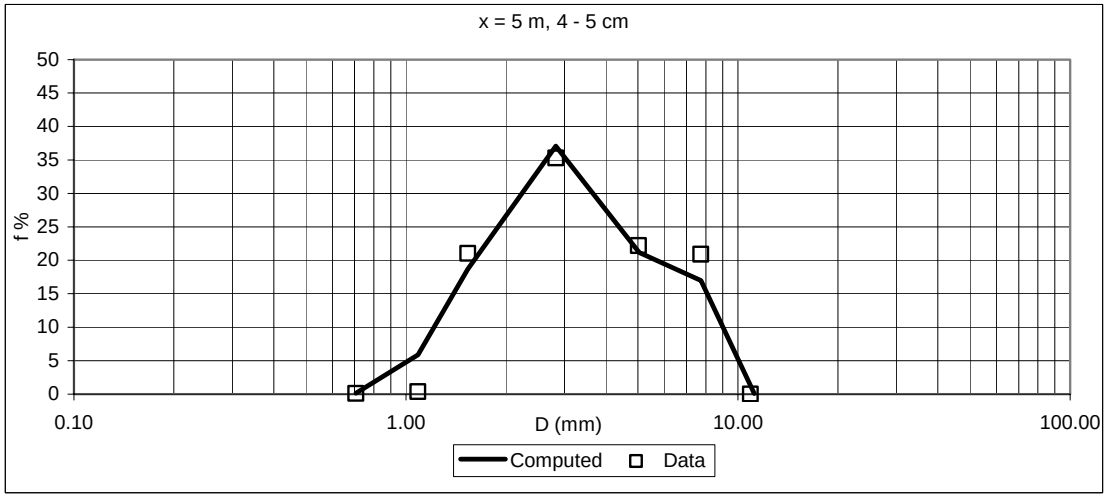
x = 5 m, 4 - 5 cm
50
45
40
35
30
25
20
15
10
5
0
f %
0.10
1.00
D (mm)
10.00
100.00
Computed
Data

x = 7 m								
First layer 0 -1 cm					Second layer 1 - 2 cm			
Computed		Data			Computed		Data	
Di (mm)	fi %	Di (mm)	fi %		Di (mm)	fi %	Di (mm)	fi %
0.707	0.108	0.071	0.086		0.707	0.119	0.071	0.096
1.086	3.347	0.707	0.209		1.086	4.965	0.707	0.142
1.536	10.955	1.086	0.422		1.536	15.935	1.086	0.364
2.828	23.120	1.536	20.939		2.828	32.150	1.536	19.923
5.040	21.993	2.828	32.395		5.040	21.960	2.828	33.773
7.735	40.199	5.020	21.532		7.735	24.722	5.020	22.251
11.208	0.278	7.736	24.417		11.208	0.149	7.736	23.452
		10.897	0.000				10.897	0.000
Third layer 2 - 3 cm					Fourth layer 3 - 4 cm			
Computed		Data			Computed		Data	
Di (mm)	fi %	Di (mm)	fi %		Di (mm)	fi %	Di (mm)	fi %
0.707	0.114	0.071	0.098		0.707	0.114	0.071	0.087
1.086	5.863	0.707	0.123		1.086	5.863	0.707	0.115
1.536	18.691	1.086	0.351		1.536	18.691	1.086	0.340
2.828	37.088	1.536	20.251		2.828	37.088	1.536	20.580
5.040	21.179	2.828	35.162		5.040	21.179	2.828	35.458
7.735	16.983	5.020	21.542		7.735	16.983	5.020	23.301
11.208	0.082	7.736	22.473		11.208	0.082	7.736	19.911
		10.897	0.000				10.897	0.209
Fifth layer 4 - 5 cm								
Computed		Data						
Di (mm)	fi %	Di (mm)	fi %					
0.707	0.114	0.071	0.094					
1.086	5.863	0.707	0.102					
1.536	18.691	1.086	0.358					
2.828	37.088	1.536	21.629					
5.040	21.179	2.828	34.718					
7.735	16.983	5.020	21.279					
11.208	0.082	7.736	21.626					
		10.897	0.194					

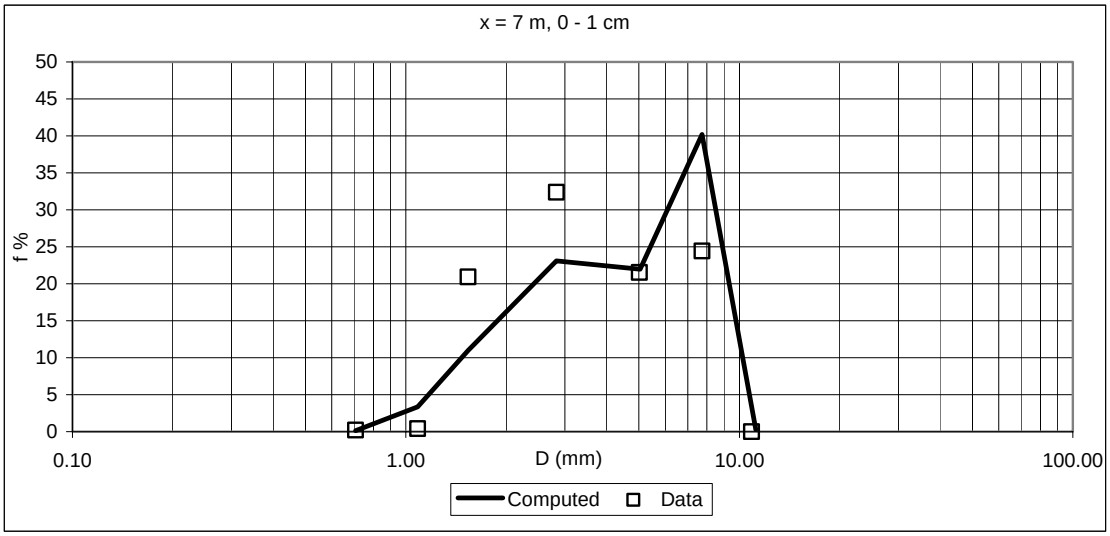
x = 7 m, 0 - 1 cm
50
45
40
35
30
25
20
15
10
5
0
f %
0.10
1.00
D (mm)
10.00
100.00
Computed
Data

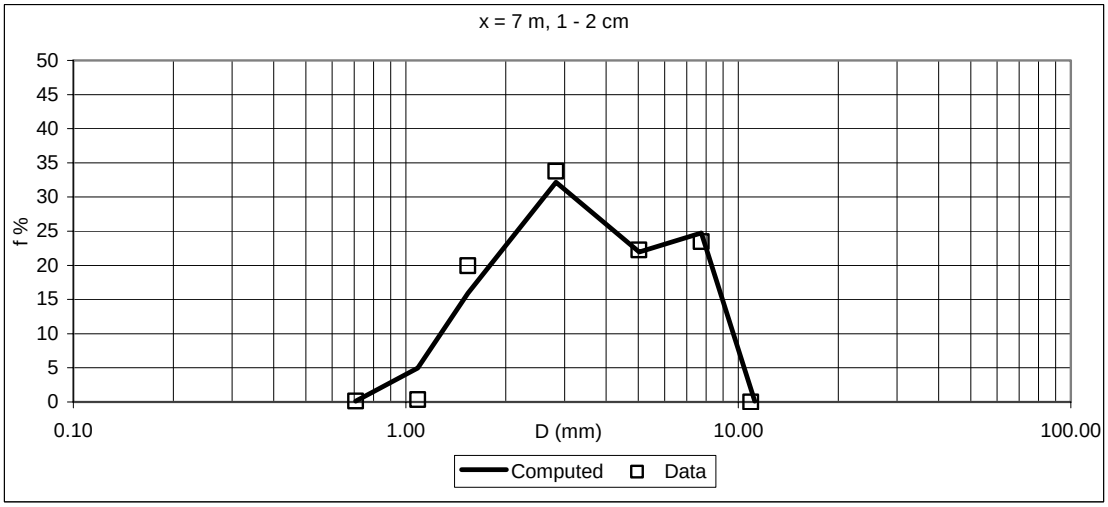
x = 7 m, 1 - 2 cm
50
45
40
35
30
25
20
15
10
5
0
f %
0.10
1.00
D (mm)
10.00
100.00
Computed
Data

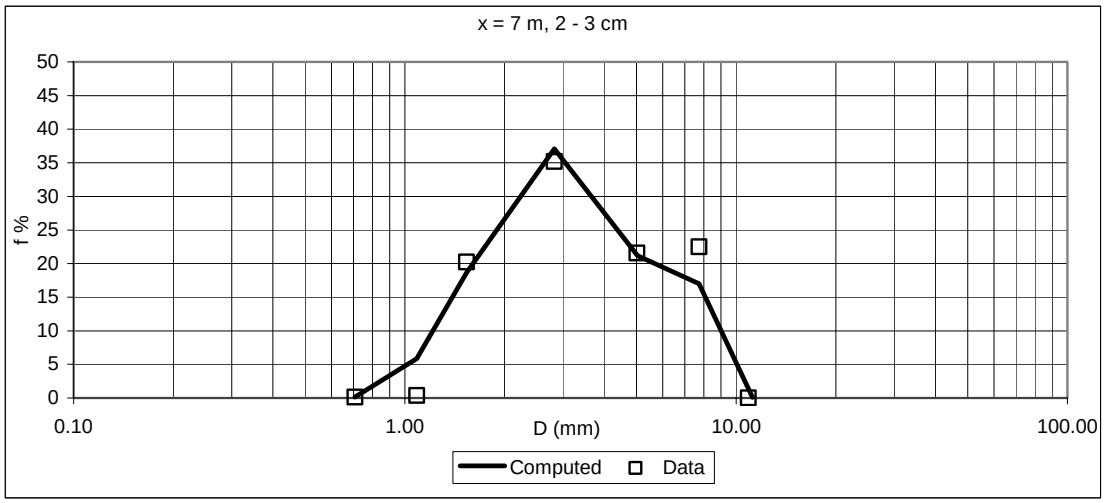
x = 7 m, 2 - 3 cm
50
45
40
35
30
25
20
15
10
5
0
f %
0.10
1.00
D (mm)
10.00
100.00
Computed
Data

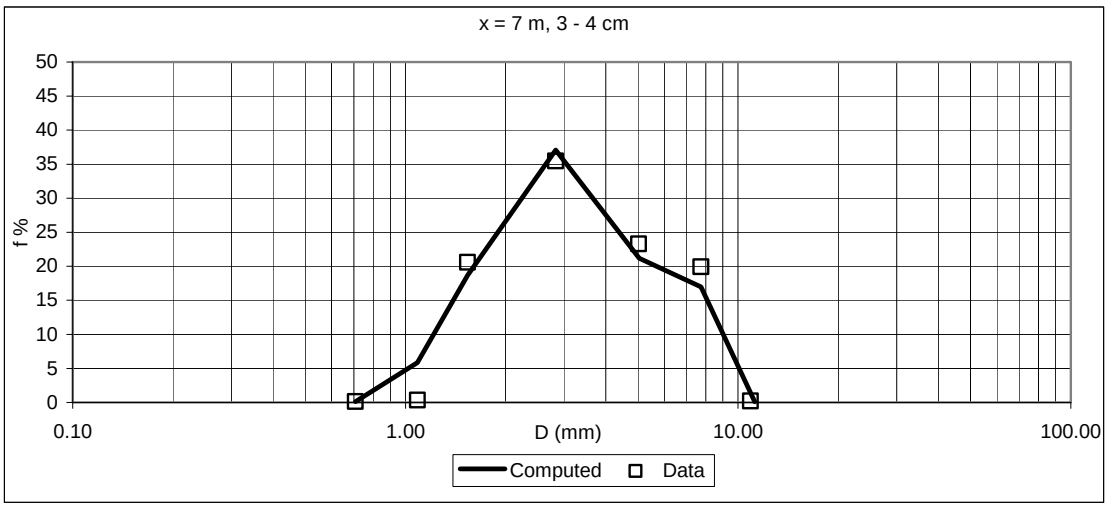
x = 7 m, 3 - 4 cm
50
45
40
35
30
25
20
15
10
5
0
f %
0.10
1.00
D (mm)
10.00
100.00
Computed
Data

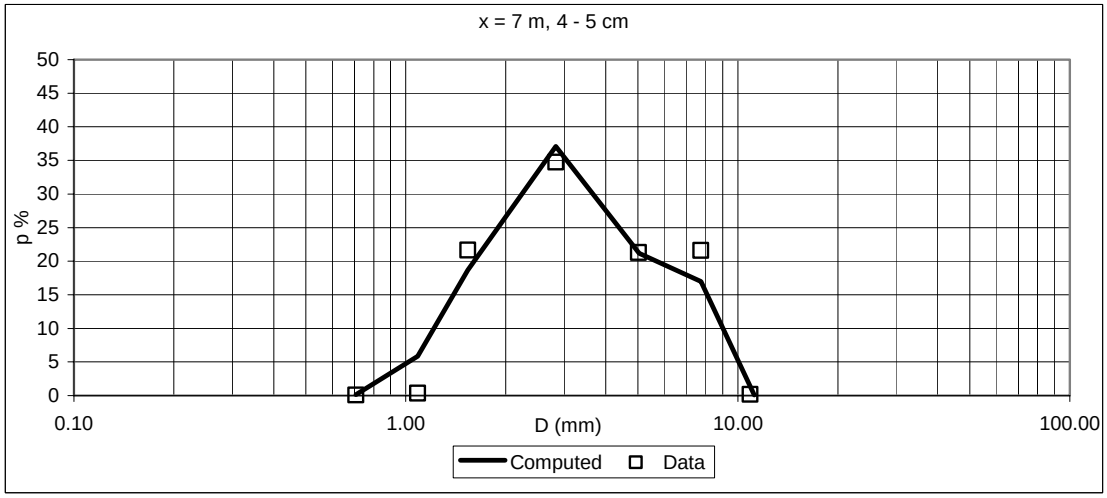
x = 7 m, 4 - 5 cm
50
45
40
35
30
25
20
15
10
5
0
p %
0.10
1.00
D (mm)
10.00
100.00
Computed
Data

x = 9 m								
First layer 0 -1 cm					Second layer 1 - 2 cm			
Computed		Data			Computed		Data	
Di (mm)	fi %	Di (mm)	fi %		Di (mm)	fi %	Di (mm)	fi %
0.707	0.107	0.071	0.035		0.707	0.116	0.071	0.070
1.086	3.170	0.707	0.136		1.086	5.164	0.707	0.146
1.536	10.446	1.086	0.320		1.536	16.553	1.086	0.354
2.828	22.347	1.536	19.219		2.828	33.270	1.536	21.131
5.040	21.902	2.828	35.187		5.040	21.863	2.828	35.408
7.735	41.759	5.020	20.767		7.735	22.906	5.020	21.715
11.208	0.269	7.736	24.002		11.208	0.129	7.736	21.176
		10.897	0.334				10.897	0.000
Third layer 2 - 3 cm					Fourth layer 3 - 4 cm			
Computed		Data			Computed		Data	
Di (mm)	fi %	Di (mm)	fi %		Di (mm)	fi %	Di (mm)	fi %
0.707	0.114	0.071	0.072		0.707	0.114	0.071	0.075
1.086	5.863	0.707	0.107		1.086	5.863	0.707	0.091
1.536	18.691	1.086	0.334		1.536	18.691	1.086	0.299
2.828	37.088	1.536	20.062		2.828	37.088	1.536	20.777
5.040	21.179	2.828	34.673		5.040	21.179	2.828	37.221
7.735	16.983	5.020	22.845		7.735	16.983	5.020	23.335
11.208	0.082	7.736	21.907		11.208	0.082	7.736	18.201
		10.897	0.000				10.897	0.000
Fifth layer 4 - 5 cm								
Computed		Data						
Di (mm)	fi %	Di (mm)	fi %					
0.707	0.114	0.071	0.065					
1.086	5.863	0.707	0.079					
1.536	18.691	1.086	0.304					
2.828	37.088	1.536	19.709					
5.040	21.179	2.828	35.654					
7.735	16.983	5.020	22.413					
11.208	0.082	7.736	21.775					
		10.897	0.000					

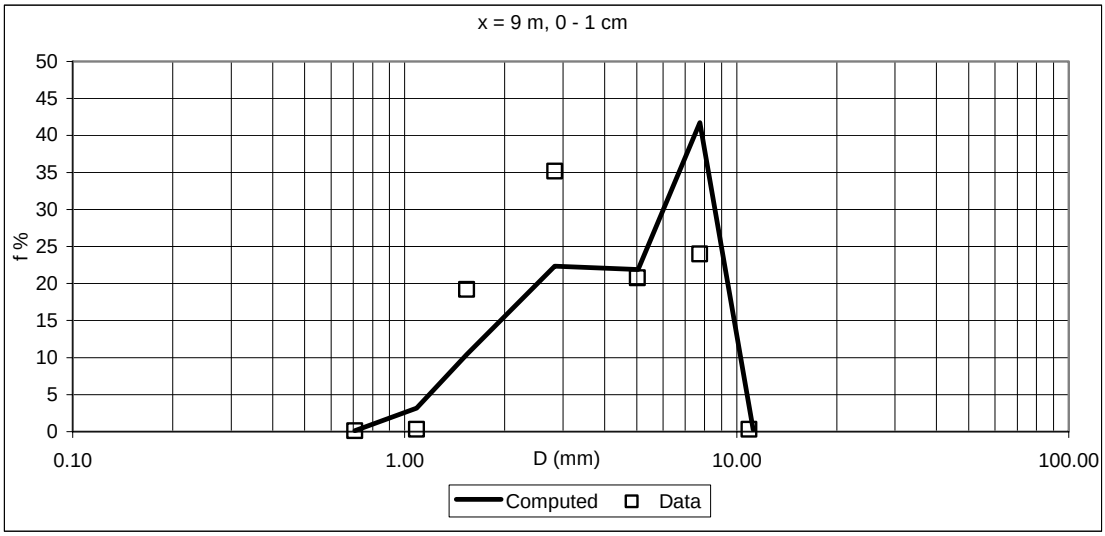
x = 9 m, 0 - 1 cm
f %
D (mm)
0.10
1.00
10.00
100.00
Computed
Data

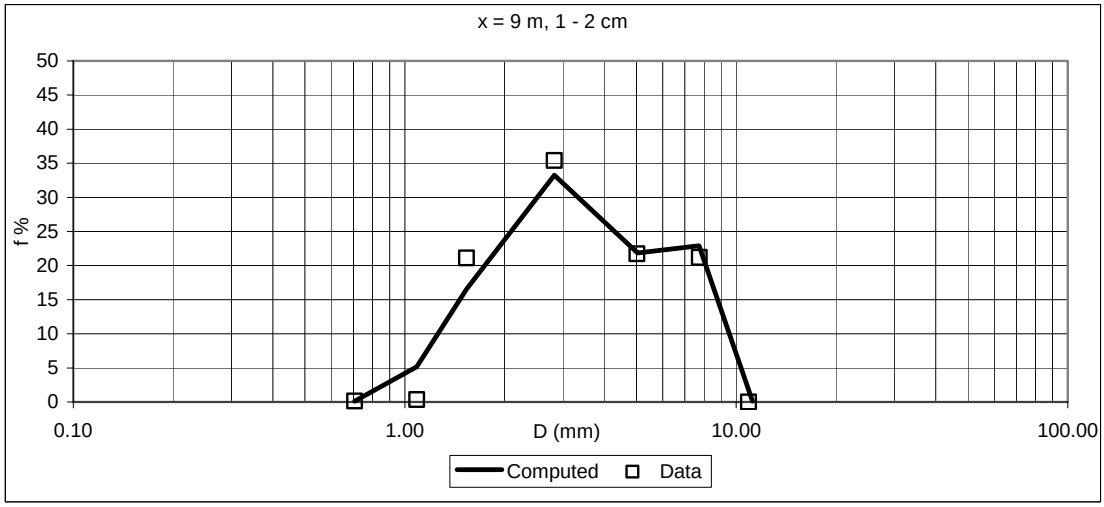
x = 9 m, 1 - 2 cm
f %
D (mm)
0.10
1.00
10.00
100.00
Computed
Data

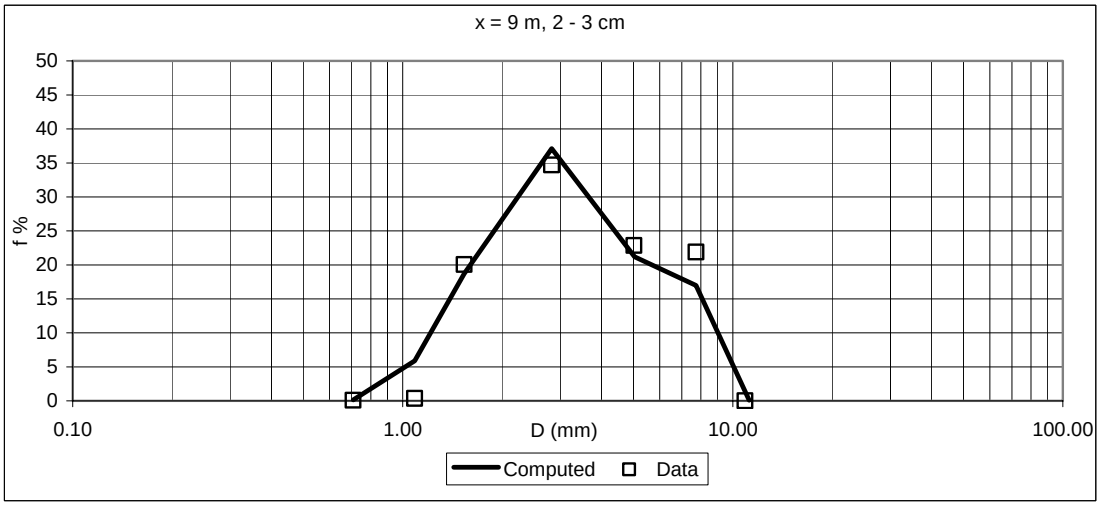
x = 9 m, 2 - 3 cm
f %
D (mm)
0.10
1.00
10.00
100.00
Computed
Data

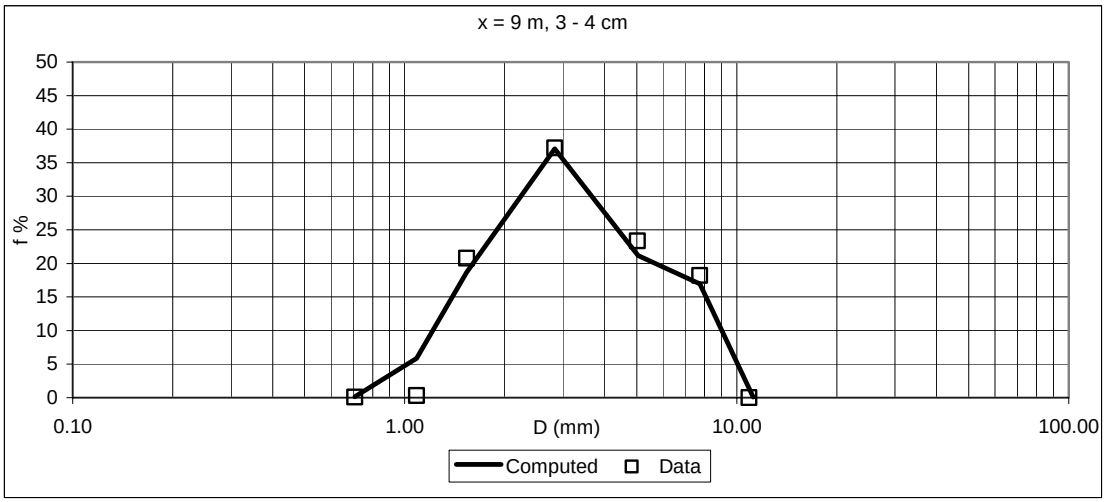
x = 9 m, 3 - 4 cm
50
45
40
35
30
25
20
15
10
5
0
f %
0.10
1.00
D (mm)
10.00
100.00
Computed
Data

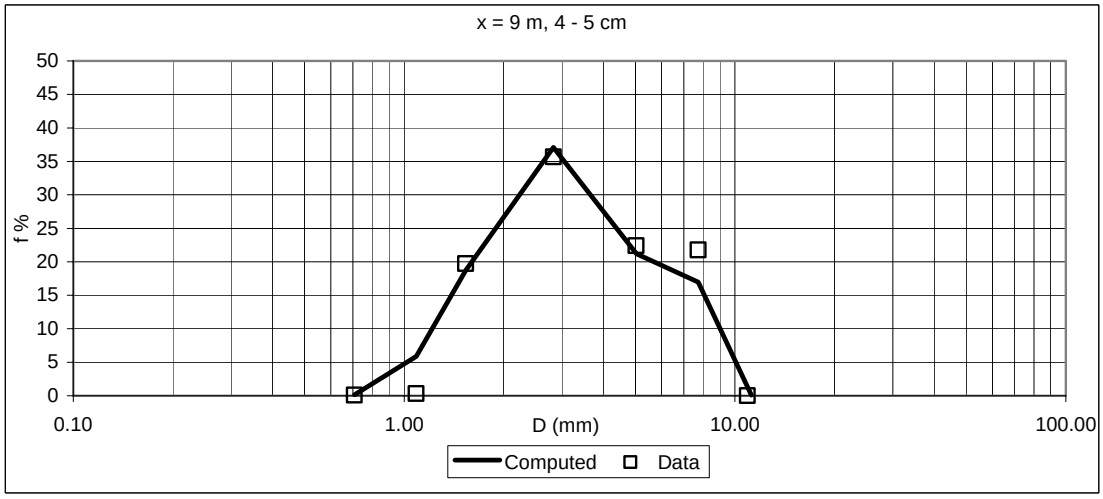
x = 9 m, 4 - 5 cm
50
45
40
35
30
25
20
15
10
5
0
f %
0.10
1.00
D (mm)
10.00
100.00
Computed
Data